The nature and significance of Late-Orogenic extensional structures in the Varsican Orogen of SW England and comparison to equivalent features from the Italian Apennines.

Adam James Styles

THE NATURE AND SIGNIFICANCE OF LATE-OROGENIC EXTENSIONAL STRUCTURES IN THE VARISCAN OROGEN OF SW ENGLAND AND COMPARISON TO EQUIVALENT FEATURES FROM THE ITALIAN APENNINES.

Adam James Styles
B.Sc. (University of Wales)

A thesis presented in partial fulfilment of the degree of Doctor of Philosophy at the Department of Geological Sciences, University of Durham, 1997.

To my parents

Copyright Declaration

No part of this thesis has been previously submitted for a degree at this university or any other university. The work described in this thesis is entirely that if the author, except where reference is made to previous published or unpublished work.

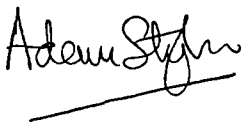

Abstract

Studies of Recent mountain belts suggest that major phases of extension can occur during and or subsequent to plate-collision. Such extensional events have subsequently been identified in some ancient orogenic belts. Authors have commonly hypothesised that the structures developed through changes in externally applied tectonic stresses or changes to the internal rheological properties of the orogenic welts.

This study was undertaken to clarify the typical structures associated with late-orogenic extension through systematic examination of the Variscides of SW England alongside a classic area of Tertiary late-orogenic extension (the Apuane Alps, Italy). A field-based approach was undertaken to provide a new, extensive structural database, to allow evaluation of such features without the evident bias of previous workers to explain extensional structures as localised peculiarities in a compression-driven architecture.

A descriptive methodology was applied to the study, examining the geometry of structures and applying shear-sense analysis. Apparent offset across faults was recorded to produce values for apparent extension. Stereographic analysis of structural elements alongside shear-sense criteria allowed the construction of kinematic models for deformation which, in turn, were considered in the context of the compressional framework from published works. Temporal constraints on deformation were provided by consistent superposition of structures across regions and were refined through integration with published geochronological data (whole-rock isochrons, fluid inclusion analysis in veins associated with structural phases). Microstructural and petrographic examination of samples from key localities allowed insight into style and P-T conditions during deformation.

In both Cornwall and the Apuane Alps, four structural associations are identified which disrupt pre-existing folds and fabrics related to crustal thickening: (1) distributed ductile shear at low-angles to pre-existing cleavage or bedding; (2) strain partitioned along shallow/moderately-dipping detachments (sometimes eroneously identified as thrusts in previous studies) which locally reactivate bedding or cleavage; (3) curviplanar, linked normal faults, which show synchronous movement on steep and shallow fault-planes; and (4) steep normal faults, which cross cut compressional fabrics and offset other extensional structures.

The magnitude of extension along extensional structures is variable and complex polyphase interference between phases make it difficult to assess with certainty. Distributed early extensional features and detachment faults appear to accommodate up to 120% extension (more typically 65%), linked extensional faults locally accommodate up to 50% layer offset and steep normal faults display 5-30% extension. The kinematics of extension show similarities, with hanging wall translation-sense down the dip of the dominant (compressional) anisotropy. Extension is directed away from structural highs and changes in extension direction occur across culminations in compressional architecture (e.g. the Padstow Facing Confrontation, Cornwall; the centre of the Apuane dome, Italy). Kinematic domains are locally separated by long-lived, transcurrent structures (e.g. Portnadler Fault, Cornwall) which may have reactivated pre-existing compressional structures.

Gravity appears to be the driving force of late-orogenic extension: (1) extensional structures show progressive embrittlement through time as predicted during exhumation; (2) structures show geometric similarity to slump folds (themselves gravity-driven); (3) structures conform to metamorphic, structural and geochronological criteria of crustal-scale extension; and (4) extension is directed down the dip of pre-existing compressional anisotropy (i.e. in the direction of maximum gravity-applied stress).

There rolls the deep where grew the tree,
O Earth what changes hast thou seen!
There where the long street roars, hath been
The stillness of the central sea.
The hills are shadows and they flow
From form to form and nothing stands;
They melt like mists, the solid lands
Like clouds they shape themselves and go.

Alfred Lord Tennyson (1809-1892)

Acknowledgements

This work has been jointly supervised by Dr Bob Holdsworth (Durham), Dr Robin Shail (Camborne) and Dr Rob Butler (Leeds). I would like to thank each for their assistance and patience and encouragement during the long, dark days of writing. Thank you to Bob for all his input during the write-up, for days spent in the field and for cajoling me into submitting in time. Thanks to Robin for introducing me to Cornish geology and BC's disco in Camborne, and thank-you to Rob for his careful guidance in the Italian Apennines. Thank-you also to Andy Alexander (Camborne) for his help, for discussion in the field, and for introducing me to HSD bitter (I still have the headache). This project was funded by NERC and I should like to thank them for ensuring that conference and fieldwork expenses were promptly and courteously dealt with.

During fieldwork in SW England I was fortunate to find fantastic lodgings with Phil and Lynn, Peter, Mark and Linda and at the Camborne School of Mines. I also wish to thank Trixie, Kate and Vicki for keeping me sane. In the course of field-study conducted in Italy I was greatly assisted by Professor Luigi Carmignani (Siena), and Drs Domenico Liotto, Marco Meccheri and Paolo Conti. Thank-you to each for pointing me in the right direction and their advice and geological discussion. I would also like to thank Domenico, Marco, Paolo, Niko and Paula for accommodation and showing me the sights of Italy and Sardinia.

Many thanks are due to my family and friends for all their encouragement and support. My heartfelt thanks to Ruth for getting me to work on time, for assisting on fieldwork, for typing in references and making the write-up survivable. I should also like to thank the postgraduate community and its extended family. Especial thanks to Wayne, Alun, Jonny, Jo, Caroline, Gail, Matt, Andy, Ziad, Sarah, Zoë, John, Jipper, Billy, Charlotte, Ackers, Alwin, the staff of the New Inn and anyone I have missed. Thanks to all the staff and technicians at Durham; to Jerry and Alan for photos, Julie and Ron for thin-sections, Carol and Claire in the office, Karen for her drafting advice, Dave Schofield, Dave Stevenson and Dave Asbery. A big thank-you to my friends and colleagues at Z&S Geology Ltd. who helped me during the final months, especially Nick, Vaughan and Caroline.

Finally, I thank my family and friends for their support during the past four years.

Contents

Chapter One: Introduction

Chapter Two: Palaeozoic evolution of SW England: Stratigraphic and structural history

Chapter Three : Late-Variscan evolution of the north Cornish Coast

Chapter Four : Late-Variscan evolution of the south Cornish coast

Chapter Five : Late-orogenic evolution of the Apuane Alps, Italy

Chapter Six : Synthesis and discussion

PART I

OVERVIEW

Chapter One - Introduction

CHAPTER 1 : INTRODUCTION

1.1 Introduction and aims

Extension of continental lithosphere is focused into rift-zones, but its importance within orogenic belts both during and after plate collision has only recently been identified (England 1983, Platt 1986, Dewey 1988, Behrmann 1988). Late-orogenic extension (i.e. recorded by structures postdating compressional features) appears to be driven more by the action of gravitational body-forces than by tectonic stretching and is often termed extensional collapse (Wheeler and Butler 1994). Collapse of the internal orogen is often balanced by simultaneous radial thrusting at the orogen margins (Dewey 1988).

Extensional collapse has been documented in many Recent mountain belts over the past quarter-century, with examples including the Basin and Range of North America (Davis *et. al.* 1980), the European Alps (Selverstone 1988; Tricart *et al.* 1994), and the Apennines of Italy (Carmignani and Kligfield 1990). Subsequent work has confirmed the importance of late-orogenic extension in ancient orogenic belts, notably the Caledonides (Larsen and Bengaard 1991; Fossen and Rykkelid 1992; Fossen 1992; Rykkelid and Andresen 1994, Holdsworth 1989), the Variscides of Western Europe (Rey *et al.* 1992; Faure and Becqgiraudon 1993), and more speculatively in Archaean shield regions of Canada (Kusky 1993) and China (Zhang *et al.* 1994).

Extension is today generally accepted as an integral stage of orogenic evolution and may help to explain many of the features of mountain belts, which remain enigmatic. These include: (1) the generation of 'post-orogenic' granite magmas (e.g. Caledonides; Dewey 1988); (2) the development of high-temperature, low-pressure metamorphic conditions which postdate compressional fabrics (e.g. Hercynian; Zwart 1967), (3) the surface exposure of high-pressure, low-temperature metamorphic rocks which escape re-equilibration during uplift (Platt 1986); and (4) the anomalously short timespan between deformation and post-orogenic marine sedimentation (e.g. Hercynian; Dewey 1988). Many local complexities of internal orogen architecture may more simply be explained through extension.

The relationship between extension and regions of anomalously high crustal thickness may reflect the increased gravitational potential in these zones, generating high vertical compressive stresses through isostatic compensation (Bott 1982). Bird (1979) suggested that delamination and sinking of dense orogen roots (*anchors*) may cause unloading of the lithosphere, rapid uplift and hence enhanced instability in the upper crust. The rebound of the crust may drive exhumation and hence produce high-temperature, low-pressure metamorphism and magmatism, further weakening the rheology of the orogen and making it more susceptible to extension (Platt 1986, Dewey 1988). The terms 'collapse' and 'late-orogenic' extension' are often used to describe the lateral attenuation of overthickened crust by body-forces (i.e. under the influence

of gravity) following cessation of compressive deformation. In contrast, post-orogenic extension relates to a change in boundary forces and hence to changes in plate motions (e.g. Pangaean break-up; Dewey 1988).

The basis for extension may be further investigated by applying the dynamic wedge models, in which orogens are considered to be macroscopically viscous, wedge-shaped prisms resting against their forelands and buttressed against rigid backstops (Platt 1986 *and references therein*). The shape of the wedge is considered to be controlled by a critical balance between a number of parameters including : the basal slope of the wedge (the sole thrust); the rheology of the wedge (its density, geothermal state, fluid properties, etc.); the longitudinal stress applied across the body (the convergent push); and the gravitational body forces generated within (Chappel 1978). In such a system, extension may be generated in many ways, for instance as a weakening in rheology or decrease in convergent stresses. Both of these changes are predicted in the final stages of convergence and therefore pervasive extension is predicted in the latter stages of orogenesis.

Despite the proliferation of such observations, many areas of classic geology await re-evaluation. The Variscides of SW England represents a region with a long history of orogen research and is worthy of examination in the light of recent advances. The aims of this research have thus been as follows :-

Regional objectives

1. To evaluate the importance of late-orogenic extensional structures within SW England.
2. To deduce the kinematics of extension and gain insight into the relationship between extensional tectonism and pre-existing orogenic architectures.
3. To estimate the magnitude of extension and its regional distribution.
4. To investigate the timing of extension and its relationship to the emplacement of the Cornubian granites.

Process specific objectives

1. To identify the typical structural assemblages relating to late-orogenic extension with reference to a classic Cenozoic example - the Alpi Apuane of northern Italy.
2. To compare and contrast extensional structures exposed in SW England with published case-studies and hence gain insight into the process of late-orogenic extension; its causes and significance to the interpretation of ancient orogens.

1.2 Recognition of extension

In general, the term 'extension' simply refers to the increase in length of material lines and as such must be defined further to ensure consistent usage. When applied to a field structure, extension is stated relative to layering such as bedding or veins. For example, a fault may be considered extensional if it is seen to cause omission of stratigraphy and an increase in the layer-parallel dimension of bedding. Several terms may be applied to extensional offsets across faults, according to the direction in which the linear dimensions are considered (i.e. relative to the slip direction; *displacement*, or relative to the horizontal; *heave*) (Figure 1.1).

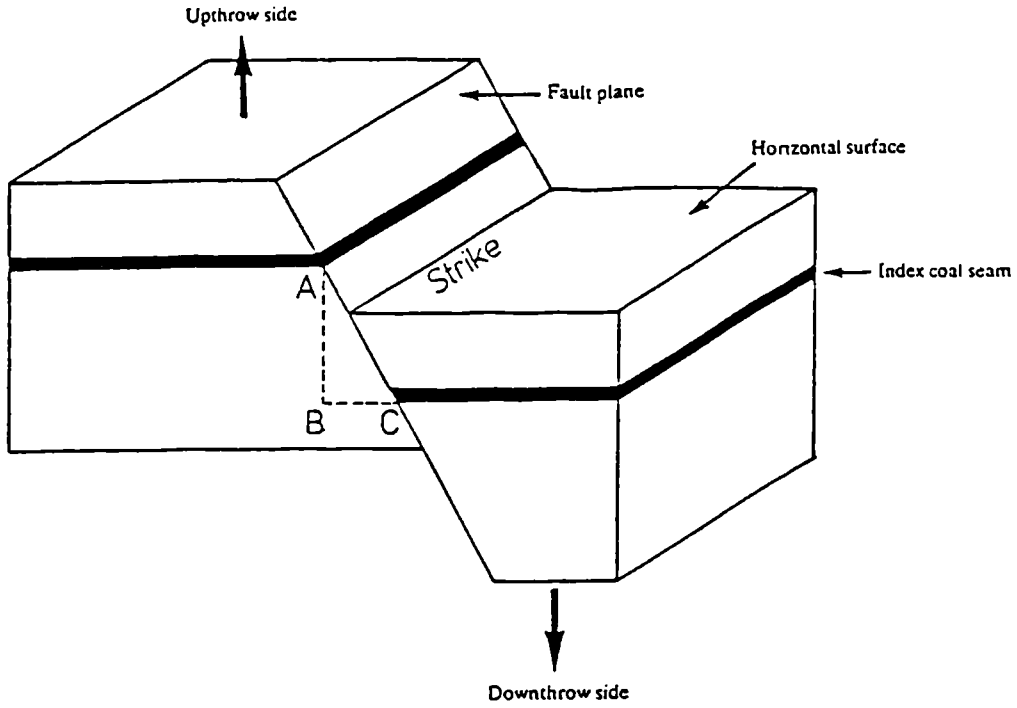

Figure 1.1 Fault terminology (Bolton 1989). A-B - throw (vertical displacement); B-C - heave (horizontal displacement); A-C – dip separation (displacement or slip if fault is normal dip-slip type).

Distinction must be made between extension of layering and extension of the crust itself, as the former considers movement sense relative to layering whilst the latter relates to movement sense relative to the present day surface. Wheeler and Butler (1994) note that some structures may shorten layering whilst causing extension relative to the surface, especially within orogens which have non-horizontal layering prior to proposed extensional deformation (Figure 1.2). The authors define several tests to relate field structure to crustal-scale deformation, which utilise several lines of evidence :-

***Structural** : If the shear zone (or fault) was related to crustal extension then, as it is followed in a direction opposite to that of hangingwall transport, it should ultimately intersect the Earth's surface as it was at the time of movement, even if the shear-zone (or fault) was later folded.*

***Metamorphic** : If the shear-zone (or fault) was related to crustal extension then the pressure recorded by rocks in the footwall should, (during movement), decrease faster than that recorded in the hangingwall.*

***Geochronological** : If the shear-zone was related to crustal extension, and isotherms paralleled the Earth's surface then, along part of its length, the shear zone would juxtapose rocks with old cooling ages in its hangingwall against rocks with younger ages in its footwall.*
(Wheeler and Butler 1994).

These authors argue that only when several criteria may be proved can structures be reliably correlated to a phase of crustal extension rather than localised reordering of the unit volume during compression.

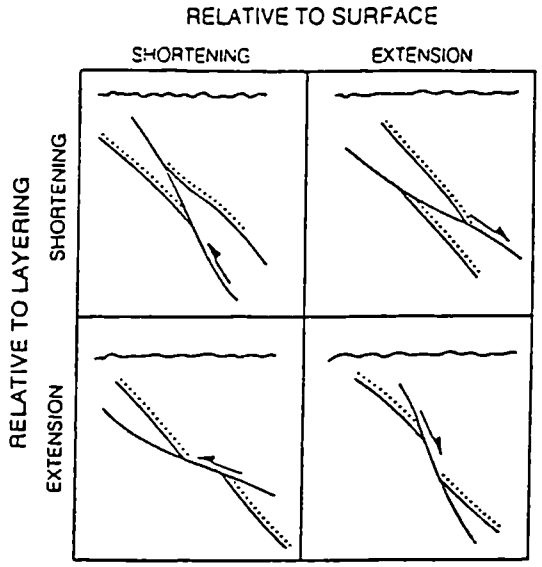

Figure 1.2 Sketches which demonstrate the ambiguity of layer-attenuation as an indicator of crustal extension (Wheeler and Butler 1994). Whilst extension or shortening of horizontal marker layers may reliably demonstrate extension or compression of the crust (respectively), this situation changes when layers are non-horizontal. When layering is steeper than the fault, which crosscuts it, shortened layers reflect crustal extension and extended layers reflect crustal compression.

1.3 Evaluation of shear-sense

Deducing the sense of movement of faults and shear-zones is an important stage in the construction of deformation models. In its most simple form, this is possible through correlation of marker layers across a structure and measurement of the displacement. More commonly, however, suitable markers are not available for study due to rock-type, outcrop quality, or the scale of exposure relative to displacement magnitude.

Shear-sense indicators are structures whose geometries allow the reliable inference of displacement-sense (Hanmer and Passchier 1991) and are developed in most tectonites on a variety of scales. In isolation many of the indicators are not sufficient to unambiguously define shear-sense, but when used together they can provide reliable information about the causative deformation.

The kinematic indicators preserved within specimens or outcrops are dependant upon bulk rheology and the level at which deformation was active. Accordingly, this section is divided into brittle (fault-related) and ductile (shear-zone-related) shear-sense indicators.

1.3.1 Brittle shear criteria

The main criteria used to constrain the sense of slip along brittle faults are; (i) offset of pre-extension markers, (ii) fault-surface lineations, (iii) secondary fracture orientations and (iv) drag-structures near the fault (Angelier 1994).

i. Offset of pre-fault motion markers. Normal fault separations are identified in plan where there is omission of strata or the lateral separation of marker layers (see also Section 1.3). For identification of the sense of slip, more rigorous criteria must be satisfied (Wheeler and Butler 1994; Section 1.2).

ii. Fault-surface lineations. Fault planes often host linear features, which trend in the direction of fault movement and comprise two main forms (Figure 1.3). Slickencrysts are formed by mineral growth within voids or in the strain shadows of irregularities of the movement surface. Within carbonates, the action of pressure solution causes stylolite-like dissolution features (slickolites). Fault striae are scratches and grooves scored into the movement plane by resistant protuberances. The description of fault-surface lineations follows the terminology of Means (1987).

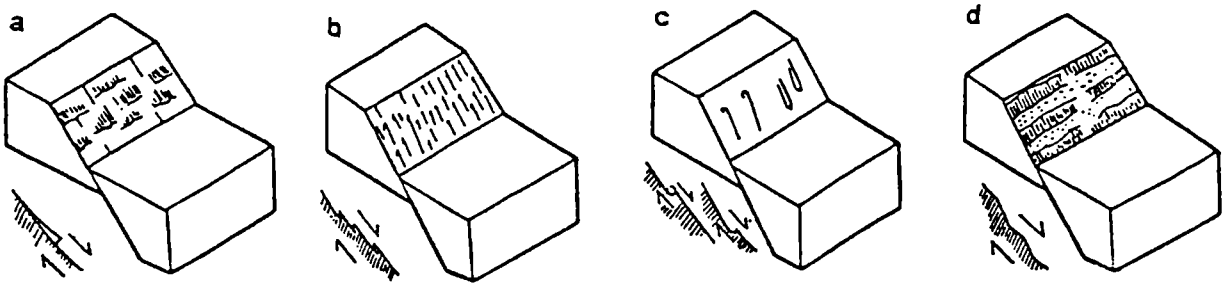

Figure 1.3 Fault-surface lineation types (Angelier 1994). Slickencrysts; (a) Accretion steps. (b) Slickolites in limestone lithology. Fault striae; (c) Tectonic tool marks. (d) Alternating polished and crushed or striated facets.

iii. Secondary fractures. Brittle faults are often accompanied by second-order fracture arrays with consistent angular relationships to the main fault plane. The four main types are : R-shears (Riedel), R'-shears (anti-Riedel), P-shears and T-fractures (Tensile fractures) (Figure 1.4). The fractures may further be classified according to their morphology, the development or absence of fault-surface lineations and their abundance relative to the strength of a mean fault plane (for nomenclature see Petit 1987).

iv. Drag-folding. The asymmetry of folds in the wall-rocks of faults must be used with caution and is discussed further in Section 1.3.3.

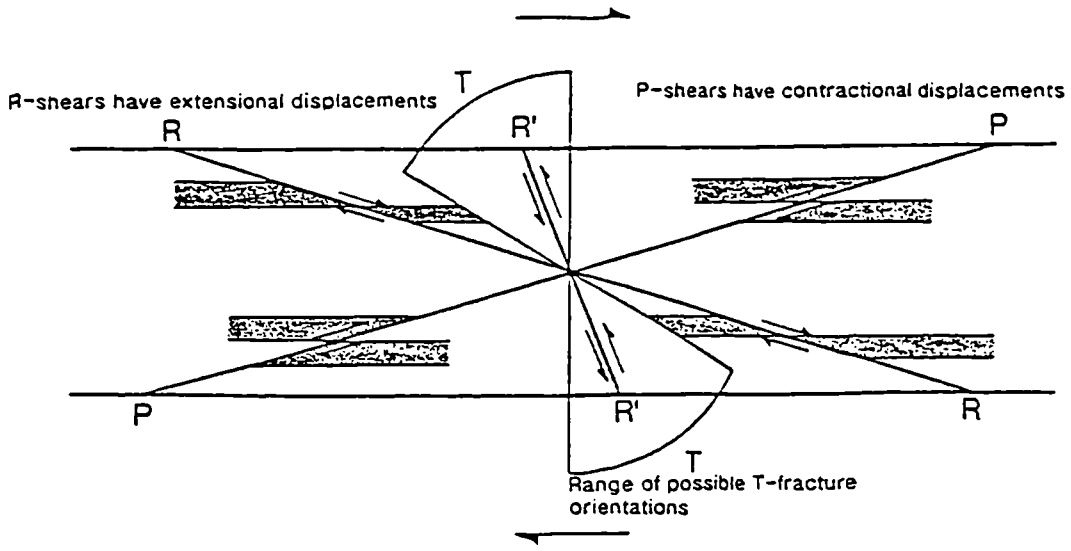

Figure 1.4 Secondary fracture orientations within a brittle shear-zone (Butler 1995; after Swanson 1988).

1.3.2 Ductile shear criteria

Ductile shear-zones commonly contain a variety of meso- and micro- scale criteria enabling the determination of shear-sense when considered alongside mineral lineation evidence and the orientation of fabric elements outside the shear-zone (Figure 1.5). Thorough reviews of such evidence have been published by White *et al.* (1986), Hanmer and Passchier (1991), Williams *et al.* (1994) and Passchier and Trouw (1996), and the reader is directed to these works for detailed discussion of terminology and usage. The three main categories of ductile shear-sense indicator are: (1) foliations; (2) rotated inclusions/appendages; and (3) veins (Hanmer and Passchier 1991). An evaluation of the use of fold vergence as a shear criterion is discussed in Section 1.3.3.

Foliations

Four distinct types of fabric commonly occur within shear-zones (Figure 1.5; 1.6); S-planes (Schistocity), C-planes (Cisaillement; shear), R-shears (Riedels, shear-bands, C'-planes, extensional crenulation cleavages) and inherited rotated fabrics (Williams *et al.* 1994). S-surfaces approximate to cleavage as they develop along the XY-planes of the principal strains within the shear-zone whilst C-planes lie parallel to the shear-zone boundary and partition the simple-shear component of the strain (Berthe *et al.* 1979). The fabrics are generally developed simultaneously to form S-C fabrics. Lister and Snoke (1984) recognise a

second type of S-C fabric developed in mica-rich rheologies, which is characterised by the development of mica fish through coaxial laminar flow along c-shears (Figure 1.5c,g).

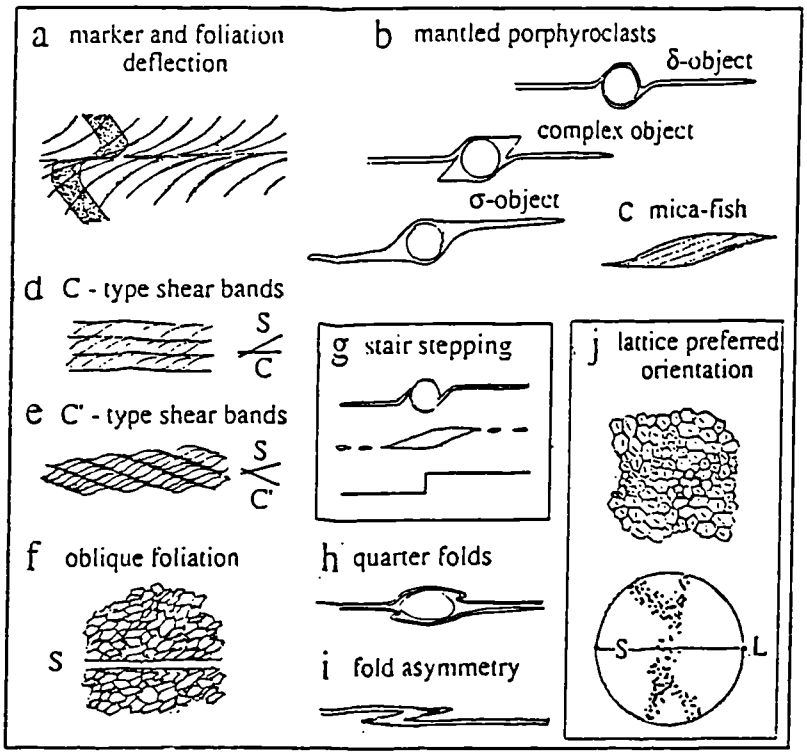

Figure 1.5 Shear-sense indicators in an ideal ductile shear-zone viewed in the XZ-plane (Passchier and Trouw 1996). Geometries are all indicative of top-to-the-right ductile shear.

Inclusions/appendages

Simple shear causes the rotation of material lines and as a consequence, objects entrained within a shear-zone are affected by this vorticity (Hanmer and Passchier 1991). Porphyroblasts are large grains that grow during metamorphism and simple shear (e.g. garnet, cordierite) and commonly contain inclusion trails, which record rotation of the growing crystal relative to the matrix.

Porphyroclasts are relict grains, which have undergone slower grain-size attenuation than the surrounding fine-grained material (e.g. feldspars, quartz or micas). They often develop mantles of fine-grained material ('wings'; Passchier and Simpson 1985; 'tails'; Simpson and Schmidt 1983) which is either produced through diffusive mass transfer of material from the margins of the clast parallel to the fabric and precipitation in strain-shadows, or from recrystallisation or cataclasis around the margins of the clast and/or its retrograde metamorphic product. The mantles form two geometric types; σ-porphyroclasts (clast is wrapped by

asymmetric fabric); and δ-porphyroclast systems (clast is rotated and causes drag on fabric) (for usage see Figure 1.7).

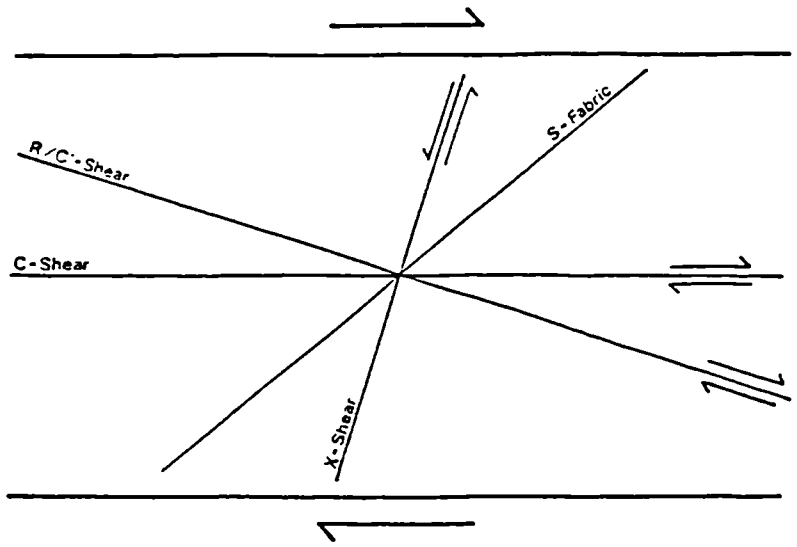

Figure 1.6 Planar fabric geometries produced during simple shear (after Shimamoto 1989).

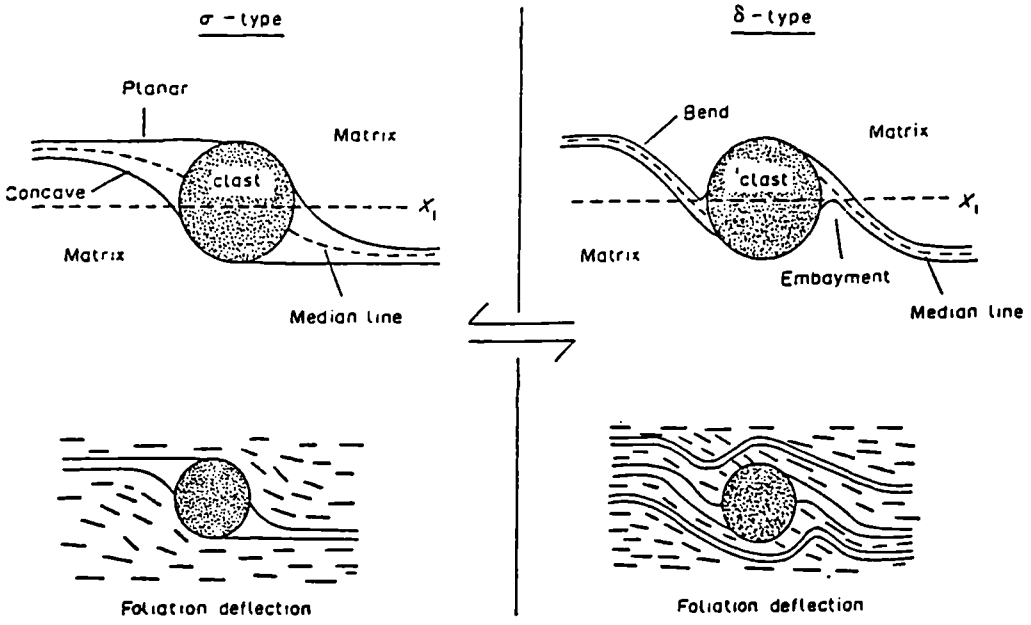

Figure 1.7 σ- and δ- type porphyroclast systems indicating sinistral shear. Both types show tail stepping above the reference plane X_1 in the direction of shear and are accompanied by rotation of matrix fabric towards the S-plane orientation (Williams *et al.* 1994, after Passchier and Simpson 1986).

The geometry of mica 'fish' and strain shadows mimic σ-porphyroclast systems in their stair-stepping shapes (Figure 1.5g) and may be used in a similar manner.

'Tiled', 'bookshelf' or 'domino' structures often develop when grains are fractured or sheared along a strong crystal cleavage (Figure 1.8). They may develop in a number of ways and consequently are not sufficient

alone to define shear-sense (Hanmer and Passchier 1991). The use of asymmetrical tail structures adjacent to blocks may help to interpret shear-sense.

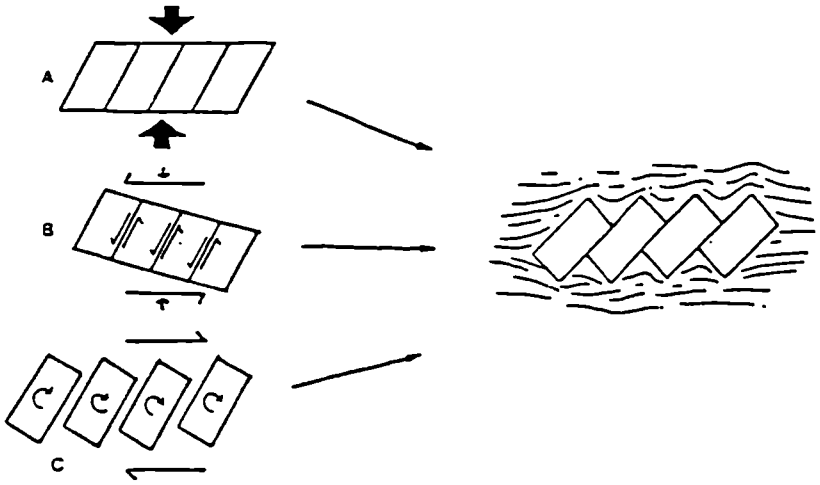

Figure 1.8 Formation mechanisms to produce tiled structures (with adaption from Ramsay and Huber 1987; Hanmer and Passchier 1991). (A) Coaxial pure shear acting upon favourably oriented anisotropies. (B) General non-coaxial sinistral shear causing sliding of weaknesses. (C) Dextral simple shear and rigid rotation of blocks. Note that the final product is common to all mechanisms.

Veins

Veins provide useful evidence of progressive shear kinematics in terms of their geometry, the nature and orientation of vein infill and their use as markers when subsequently deformed. For example, tension gash arrays develop through propagation of vein tips perpendicular to $\sigma 3$ whilst the older central portion of the gash undergoes rigid rotation towards parallelism with the shear-zone fabric. The orientation of fibres within dilational veins also tracks changes in the attitude of $\sigma 3$. The appearance of vein-infill is thus of extreme importance as a technique for investigating the nature and geometry of strain and is reviewed by White *et al.* (1986).

1.3.3 Fold vergence and shear-sense

"... 'drag folds' have long been used for determining sense of shear, and asymmetrical folds are probably one of the most reliable kinematic indicators if used with caution" (Williams *et al.* 1994, pp23).

Folds of consistent asymmetry are observed in many shear-zones, and may be used as a shear criterion if they have developed in response to flow vorticity. The vergence of asymmetric folds is defined as *'the horizontal direction within the fold profile plane, towards which the upper component of rotation is directed'* (Roberts 1974). This may provide the top sense of shear if they formed by rotation of the short limbs from a position now preserved by the longer limbs (Bell 1981).

In order to use this criteria with confidence, it must first be proven that the folds are related to fabric-parallel shear. This may be ascertained in the field through examination of the rock matrix for evidence of non-coaxial shear and by ensuring that the structures do not change vergence across large fold closures (i.e. that they are not parasitic buckle-folds; Figure 1.9). Next their geometries must be examined; if the fold-axes are curvilinear, care is needed because sheath folds provide unreliable indicators if cut oblique to the nosing direction. At high strains, fold axes are progressively rotated into parallelism with the transport direction, whilst at lower strains the axes may be plotted and the variation in trend bisected to ascertain the true shear-direction. Finally, folds may verge against the shear-direction if produced from marker bands, which dip at high angles in the direction of shear. A relative thickening of short limbs often indicates this 'antivergence' and attenuation of long limbs (Figure 1.10).

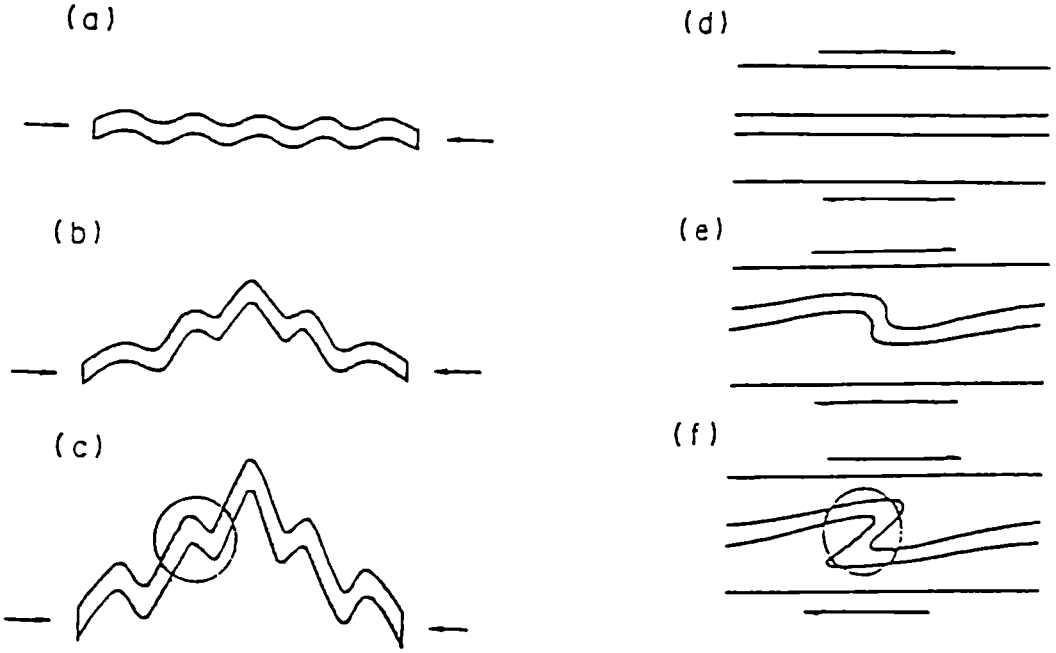

Figure 1.9 Models of the development of asymmetrical folds (Williams *et al.* 1994). (a-c) Buckle-fold development through layer-parallel shortening. Early symmetrical folding is followed by buckling of the contortions, amplifying some folds whilst reorienting others into asymmetrical parasitic features. (d-f) Shear-folding by rotation of short-limbs parallel to the long-limb plane. Note the geometrical similarity between products (c) and (f).

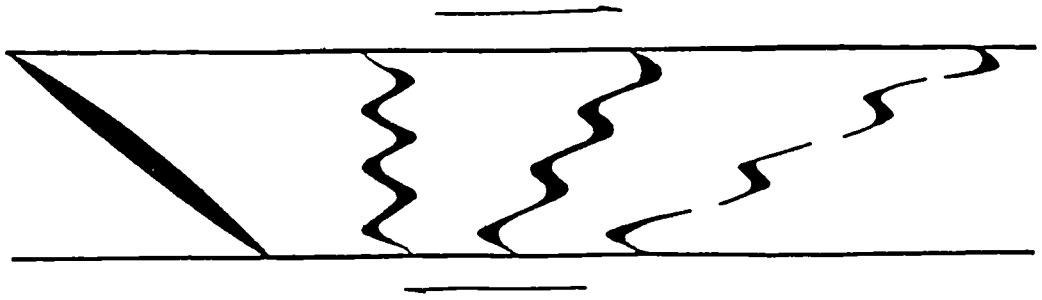

Figure 1.10 Model of the development of antivergent folds within an idealised dextral shear-zone (adapted from Williams *et al.* 1994). Successive stages of fold development are illustrated from left to right. Shear-zone margins shown by parallel black lines.

1.4 Estimation of extension magnitude

Extension and strain

The magnitude of extension may be quantified in most areas through measurement of the length of a given extended marker band and reconstruction of its original length prior to the deformation. Extension is thus synonymous with strain and may therefore be stated as :-

(1) $$e = \frac{(l - L)}{L}$$ Where e = strain, L = original length, l = final length

Thus where $e < 0$ the strain is compressive, and where $e > 0$ strain is extensional. The resultant value is commonly given as percentage extension by multiplying the value obtained by 100.

The value of extension obtained is a finite value where calculated for laboratory samples, but is rather subjective when estimated in the field. The method is one-dimensional whilst field situations are clearly three-dimensional (Lisle 1994), and thus results will vary according to the material line examined, the orientation of the line of calculation, the assumptions of original stratigraphic geometry and structural geometry and the length of deformation zone over which the calculation is made.

Estimating extension from fault geometry

To quantify extensional strains on the basis of fault geometry, it must first be assumed that fault-strikes are uniform, displacements are normal, and that change of length is accommodated wholly through displacements along fault segments in the line of section (Twiss and Moores 1992). If we assume constant bed-length and non-rotation of fault planes then the regional extension is equal to the sum of horizontal extensions on all faults (Figure 1.11A).

(2) $$e = \frac{\sum_{i=1}^{N} (l - L)_i}{\sum_{i=1}^{N} L_i}$$ Where N = number of fault segments

The trigonometric relationship between fault-geometry and layer-parallel length-change for each fault is as follows :-

(3) $$\Delta L = d \cos \phi$$ Where d = dip-slip displacement and ϕ = dip angle of fault

These equations may be manipulated to provide a relationship between extension (e), the dip of rotated bedding/marker layer (θ) and the dip of rotated fault-planes (ϕ) if the material line is assumed to be horizontal, faults are assumed to rotate with progressive displacements, and the faults have the same orientation, spacing and displacement (Figure 1.11B).

horizontal, faults are assumed to rotate with progressive displacements, and the faults have the same orientation, spacing and displacement (Figure 1.11B).

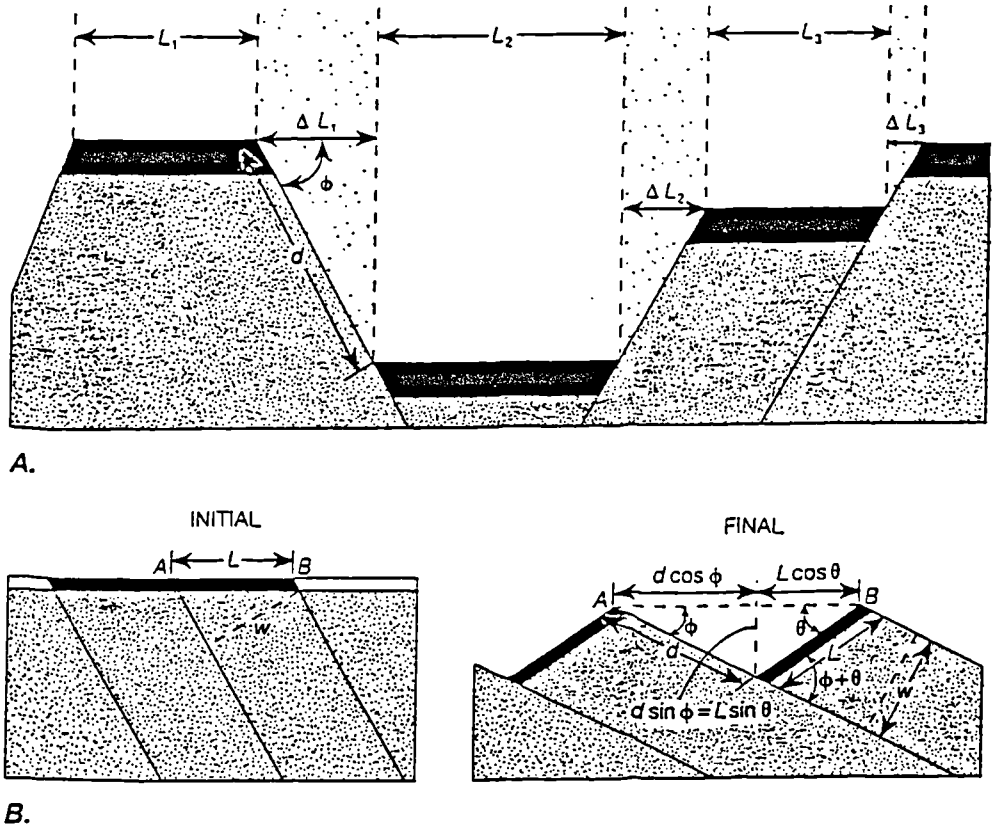

Figure 1.11 Models of normal fault geometry (Twiss and Moores 1992). (A) Non-rotating normal faults, where $l = L_1 + \Delta L_1$. (B) Geometric parameters for equally spaced, planar, rotating normal faults above a detachment fault.

(4) $$e = \frac{d}{L}\cos\phi + \cos\theta - 1$$ and (5) $$\frac{d}{L} = \frac{\sin\theta}{\sin\phi}$$

(6) $$\therefore \sin(\theta+\phi) = \sin\theta\cos\phi + \sin\phi\cos\theta$$

(7) $$e = \frac{\sin(\theta+\phi)}{\sin\phi} - 1$$

Clearly this equation is of limited use in previously deformed terranes, as it requires the presence of subhorizontal markers whilst compression largely reorientates horizontal material lines. The value obtained will thus provide a measure of layer-parallel extension rather than extension relative to the surface and requires further correction to arrive at an estimate of regional extension. The equations may be rewritten by

incorporating a correction factor to the chosen marker to orient it to the horizontal prior to the start of extension if its pre-extensional orientation can be evaluated.

To calculate the layer-parallel extension (e_{lp}), ϕ_r must be substituted into equation (7) in place of ϕ, and θ_r must be substituted in place of θ :-

$$\phi_r = (\theta - \theta_{pe})$$

$$\theta_r = (\theta - \theta_{pe})$$

Where ϕ_r= reoriented fault-dip, θ_r = reoriented marker dip and θ_{pe} = dip of pre-extension marker.

To convert this value back to horizontal extension requires simple trigonometry :-

(8) $$e = e_{lp} \cos \theta_{pe}$$

The value obtained by this method gives the best approximation to the amount of extension but is strongly dependant upon the orientation of the marker-layer used and the accuracy of assumptions. For this reason, the most suitable layers for examination are those which were formed late in the compressional deformation such as veins and cleavages.

Estimation of extensional strain from secondary features

In areas where extensional deformation is clearly present, but suitable marker offsets are not available for use in strain analysis, smaller-scale structures may provide minimum estimates. Suitable structures include extensional features such as attenuated fossils, boudins, bookshelf structures and shear-bands, and also compressional features such as folds developed through sticking along fault-planes. (Figure 1.12).

The use of such structures should be approached with caution and each feature should be evaluated in terms of orientation and style to ensure that it relates to extensional deformation rather than compressional events. A fundamental problem exists with the use of such strain markers: they are formed in response to competance contrast with the deforming matrix and consequently they do not provide a representative value for extension in the bulk of the rock (Lisle 1992). In each case, therefore, the value obtained is the *minimum* strain accommodated during the evolution of the strain marker. For example, drag-folds developed against faults may provide a measure of compression *during* sticking of that fault-plane but cannot provide any information on the amount of deformation which occurred prior to sticking or after the compressional feature was cut-out.

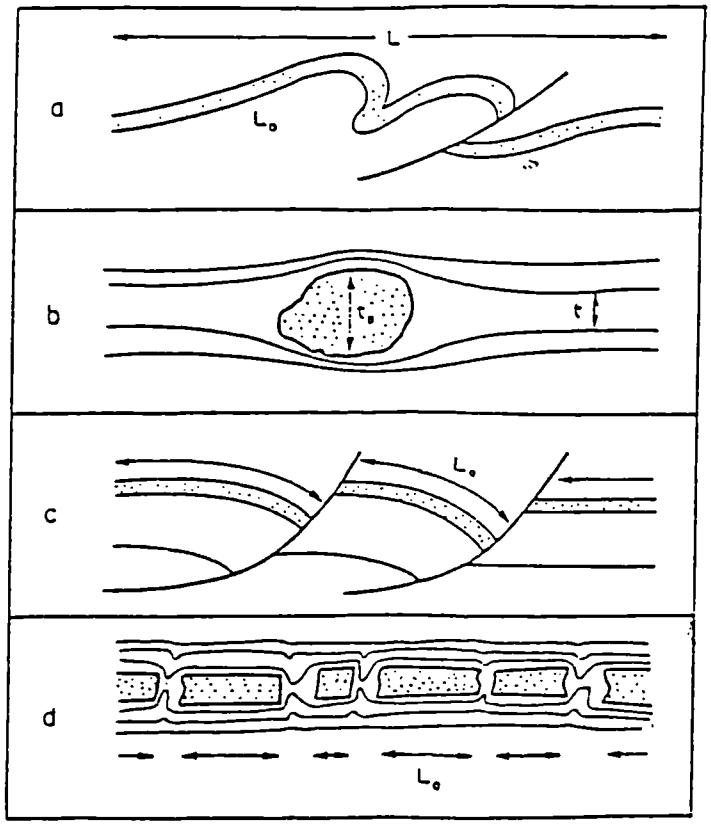

Figure 1.12 Strain markers (Lisle 1992). (A) 'Unrolling' folds. (B) Relative dimensions of strained pebbles or ovoids. (C) Bed-length reconstruction of minor faults. (D) Rejoining boudins.

1.5 Directional references and stereoplots

Where structural components are discussed in this work they conform to the following:

- Linear elements such as fold axes and slickenlines, are recorded as plunge and azimuth (i.e. a line oriented at 15°/135° plunges 15° towards the SE).
- Planar elements such as bedding, cleavage, fold axial planes and fault planes, are recorded as strike, dip and dip-direction (i.e. a plane oriented at 135°/20°NE strikes NW-SE and dips 20° NE).

Stereoplots throughout this work are Lower Hemisphere Schmidt projections. Planes are most commonly displayed as poles except where identifying mean orientations of planes which host lineations. Contouring of data is applied where a large amount of information is displayed. Contours represent the margins of data-density zones (1%), calculated upon a superimposed square grid.

1.6 Thesis outline

Part I : Overview

Chapter One provides an introduction into research on late-orogenic extension and outlines the nomenclature used in the description of deformation products and details the methods applied when assessing kinematics and the magnitude of extension.

Part II : Late-orogenic extension of SW England

Chapter Two reviews published works exploring the geology of SW England, outlining the stratigraphy and structural history with reference to geophysical models of the subsurface. Chapter Three details field observations made on the north Cornish coast whilst Chapter Four is concerned with deformation of the south Cornish coast. A final section (4.7) correlates structures across the peninsular with reference to papers of inland geology and summarises the extensional deformation.

Part III : Comparison with the Alpi Apuane, Italy

Chapter Five reviews the Alpi Apuane of northern Italy; an area which is widely considered to represent a collapsed dome within the northern Apennine belt. Previously published work is discussed alongside primary data collected during reconnaissance fieldwork.

Part IV - Synthesis and conclusions

Chapter Six examines the nature of late-orogenic extension through analysis of common features exposed in SW England and the Alpi Apuane and with reference to other published examples. The idealised geometries of post-convergent extensional features and their order of development are proposed and discussed in terms of timing, and kinematics. The controls upon deformation are considered and existing models examined in the light of field evidence. The final section concludes and states findings of the nature and significance of late-orogenic extension in SW England and its applications to ancient orogenic belts.

PART II

LATE-OROGENIC EXTENSION OF SW ENGLAND

Chapter Two - Palaeozoic Evolution of Southwest England : Stratigraphic and Structural Evolution

CHAPTER 2 : THE PALAEOZOIC EVOLUTION OF SOUTHWEST ENGLAND : STRATIGRAPHIC AND STRUCTURAL HISTORY.

2.1 Lower Palaeozoic plate tectonic setting

The British Isles straddles a complex section of the European plate which was consolidated in Lower Palaeozoic times. It owes its structural heterogeneity to two distinct orogenic cycles: the Caledonian and Variscan orogenies, which collectively resulted in the construction of the Pangaean supercontinent.

(a) The Caledonian Orogeny

The Caledonian Orogeny encompasses the early Ordovician to early Devonian convergence and consolidation of three plates; Laurentia, Baltica, and microplates of Gondwana (Figure 2.1; Soper and Hutton 1984; Ziegler 1982). The intra-plate sutures form a Y-shaped triple junction between the North Atlantic Caledonides (north/south trend), the North German - Polish Caledonides (east-northeast/west-southwest trend), and the Appalachians (northeast/southwest trend).

The docking histories of the three terrains have been constrained through palaeomagnetic, structural, stratigraphic, volcanogenic and faunal-province investigations (Soper and Woodcock 1990; Scotese and McKerrow 1990; Soper *et al.* 1992), and reveal a sequential collision with considerable transpression and plate-rotation during amalgamation. Baltica, Eastern Avalonia and Western Avalonia docked obliquely against Laurentia during the Silurian, producing significant sinistral transpression continuing into the Devonian (Figure 2.1). The newly-formed Laurussian landmass lay north of the Rheic Ocean, with the Gondwanan Craton beyond.

(b) Post-Caledonian extension

By early Devonian times, the British Isles lay on the southern margin of Laurussia, forming a spur to the Old Red Sandstone Continent (Selwood 1990). Whilst compression had largely ceased to the north of the suture zone, the translation of Gondwana continued further to the south through subduction along a trench south of the Ligerian - Moldanubian Cordillera (Figure 2.2; Barker and Gayer 1985). North of this arc-trench system, crustal extension led to the formation of a series of east/west trending basins and highs. In the northern Rhenohercynian domain, sedimentation began during the early Gedinnian with extension and subsidence continuing throughout the Siegenian, prompting the development of clastic-starved basinal conditions and progressive overstep of basin-margins (Ziegler 1990). During the Emsian, the continental margin failed in the Cornish and Rhenish Basins and began generating oceanic crust. Stable shelf conditions along the basin margins during Givetian times, gave way to a basin-wide regression during the Fammenian (Ziegler 1990).

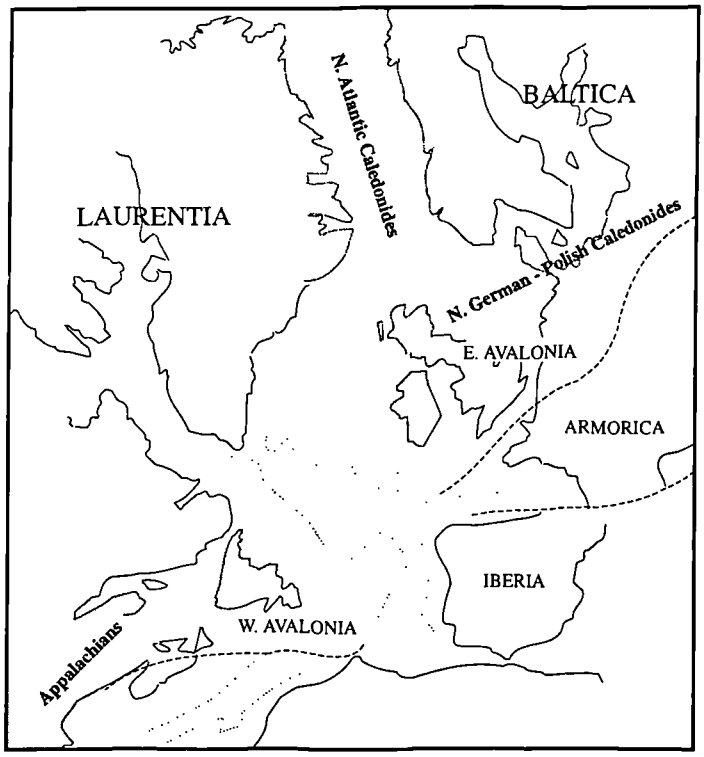

Figure 2.1 A pre-Atlantic reconstruction of Laurentia, Baltica, Gondwana and microplates involved in construction of the Pangaean supercontinent (Soper *et al.* 1987; Soper and Woodcock 1990).

The Armorican - Saxothuringian domain has a similar history to the Rhenohercynian Basin, with continuous sedimentation between the late Silurian and Givetian. Facies changes record the presence of a series of sub-basins and reflect the periodic emergence of structural highs through back-arc compression. Late Devonian transgressive deepening and renewed vulcanism preceded the onset of Variscan compression (Ziegler 1990).

(c) The Variscan Orogeny

Variscan orogenesis resulted from the closure of the Rheic Ocean, collision of Laurussia with Gondwana and formation of the Pangaean supercontinent. It generated a linear west-southwest/east-northeast trending composite fold-belt which today extends from the Ouachita and Alleghenian belts in North America, through the Mauritanian belt of North Africa to the Hercynian belt of Western Europe. Southern Britain marks the northern edge of the Variscides, whilst northern Britain lies within the sub-Variscan foreland (Figure 2.2).

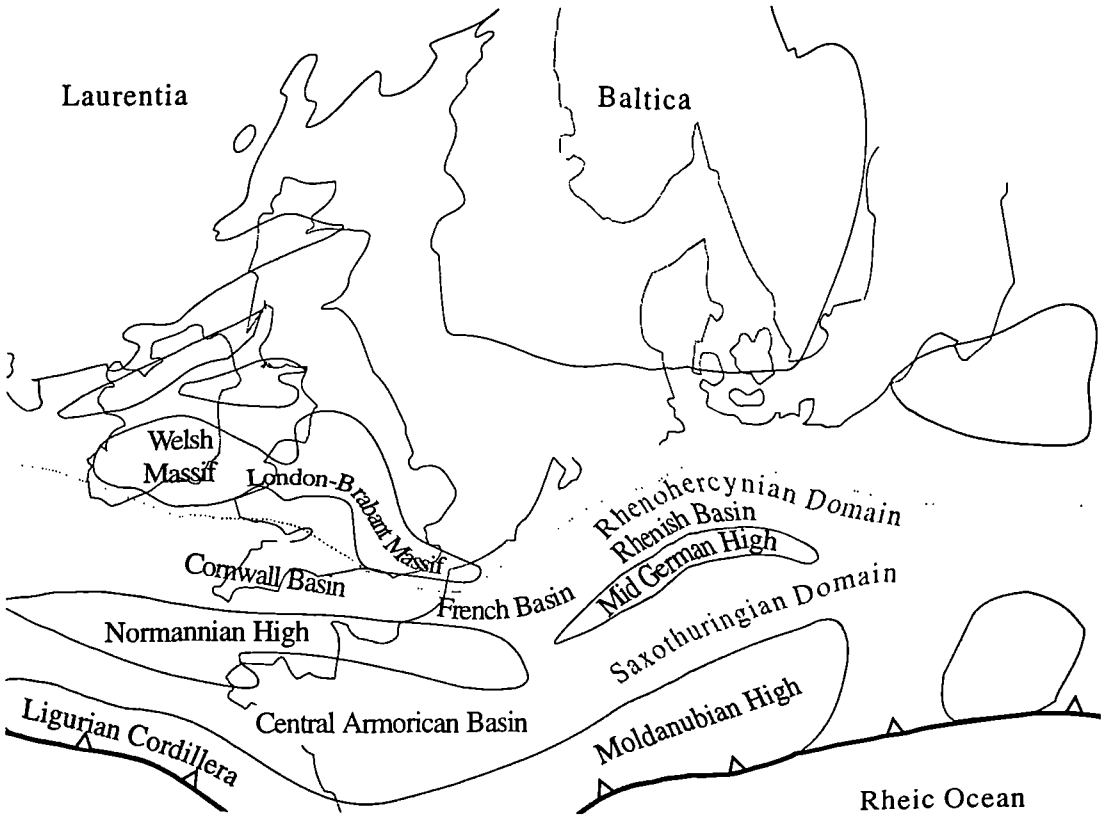

Figure 2.2 Structural components of Variscan deposition and deformation in western Europe (After Ziegler 1990). Shaded areas represent landmasses emergent during Variscan convergence whilst pale areas denote seas. Heavy barbed line represents subduction zone and stippled line follows the trace of the Variscan front (i.e. the northern limit of thrusting).

Plate convergence began in the Mid-Devonian and continued for a period of ~100 Ma, with the main collision between Laurussia and Gondwana during the late Viséan and late Westphalian (Ziegler 1990). Following waning of compression during the Stephanian, the tectonic regime became wrench-dominated as Europe underwent dextral translation with respect to Africa (Arthaud and Matte 1977; Ziegler 1990). This led to the generation of pull-apart basins with thick sedimentary infills across the Variscan foldbelt (eg. Oslo Graben, Wessex Basin; Storedvedt *et al.* 1978; Lake and Karner 1987). The mountain system experienced rapid disintegration during this time, accompanied by an increase in heatflow and steepening of the remnant subduction zone (Dewey 1986).

2.1.1 Geological overview of southwest England

A generalised geological map of southwest England shows a simple outcrop pattern of stratigraphic units (Figure 2.3). A broad east/west trending belt of Carboniferous rocks in north Cornwall and mid Devon is flanked to the north and south by Devonian rocks which become older outwards. The southern belt of Devonian rocks is overlain to the south by the overthrusted Lizard and Start metamorphic complexes. A series of late Carboniferous to early Permian granite bodies cut the Palaeozoic rocks along a northeast to east trending line. To the east of the region, deformed Palaeozoic rocks are unconformably overlain by shallowly dipping Permian and Mesozoic rocks (Hobson and Sanderson 1983). The arrangement of

Devono-Carboniferous rocks was at first thought to reflect a synformal structure (De La Beche 1839), but subsequent research into the stratigraphy reveals the presence of several sedimentary basins which control exposure pattern (Figure 2.3; Selwood 1990).

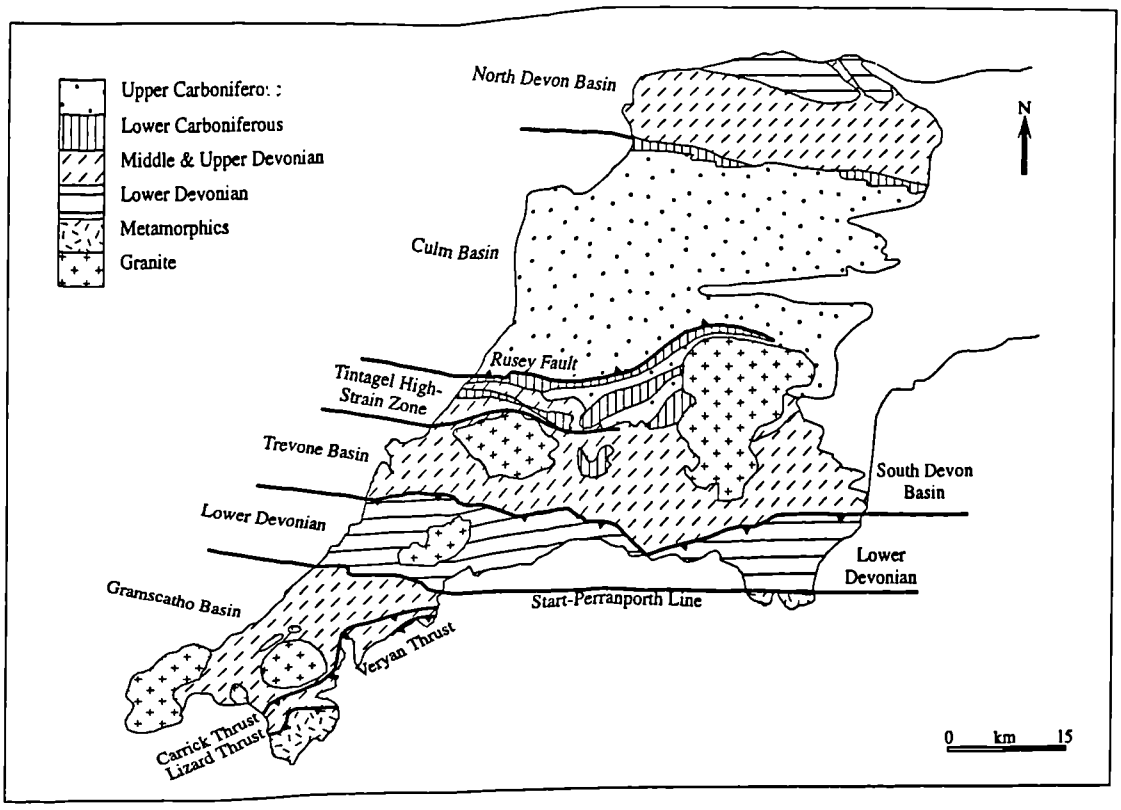

Figure 2.3 Tectonostratigraphic domains of southwest England (after Warr, Primmer and Robinson 1991). Barbed lines mark the traces of thrusts developed along basin-bounding faults during Variscan compression.

2.2 Stratigraphy

2.2.1 Pre-Devonian basement

The basement rocks of southwest England are not exposed. Where pre-Devonian rocks are preserved, they form clasts and xenoliths within Devonian formations; Upper Devonian olistostromes on the Roseland peninsular contain masses of fossiliferous Ordovician-Silurian limestone and quartzite (Bather 1907), whilst volcanic horizons within the Gramscatho Basin contain cataclastic granitoid xenoliths which yield late Proterozoic ages (Goode and Merriman 1987). Borehole and seismic refraction data support the presence of a Precambrian plutonised volcanosedimentary succession at depth, overlain by Lower Palaeozoic sediments which probably represent Eastern Avalonian basement similar to that exposed in Brittany (Freshney and Taylor 1980). Basement control during deformation may explain anomalous E-W

trending zones in the Cornish Variscides (eg. Start - Perranporth Line; Holdsworth 1989a), as Cadomian shear-zones in Brittany show similar trends (Shackleton 1984; Sanderson 1984).

2.2.2 Lower Devonian

The Lower Devonian Dartmouth and Meadfoot Groups outcrop along an east/west trending swathe of country 15 km wide and over 100 km long from Newquay in the west to Torbay in the east (Figure 2.3). Regional thickness and facies variations suggest that deposition occurred upon the southern shelf of the Old Red Continent (Selwood 1990).

The Dartmouth Group consists of finely variagated red, purple and green slates with subordinate thin sandstones, siltstones, occasional basic sills, tuff horizons and pebbly mudstones (Pickering 1986). A rich fauna of ostracoderms, corals, brachiopods, bryazoans, crinoids and plant remains is sporadically preserved, suggesting a Gedinnian to Siegenian age-range (Hendriks 1971; Evans 1981; Dineley 1986; Davis 1990). Palaeoenvironmental indicators are consistent with continental deposition interspersed with marine conditions which developed increasingly through time, allowing an influx of marine faunal assemblages and the presence of intrusive rocks and bimodal volcanics supports active rifting (Durrance 1985). Provenance studies (eg. Allen 1979) traditionally consider the Dartmouth Group a distal facies to the proximal clastics of south Wales despite a lack of direct evidence. However, recent correlations between Cornwall and east Devon show a westward decrease in grain-size and thus support an eastern provenance of clastic material and westerly transport along an east/west trending half graben (Shail *pers. comm.* 1996).

The Meadfoot Group (Bluck *et al.* 1988) comprises two formations; the Meadfoot Beds and the Staddon Grits. The older Meadfoot Beds are dominated by grey and grey-green mudstones, with inferior sandstones, basic volcanic sills and rare limestones (Shail 1992). Shallow marine brachiopods and corals are occasionally preserved and date to the Siegenian and Emsian (Evans 1981, 1985). Shallow marine conditions prevailed throughout deposition of the Meadfoot rocks, although the exact environment remains the subject of some contention (Richter 1967; Evans 1985; Selwood and Durrance 1982; Pound 1983). The Staddon Grits formed in similar conditions to the Meadfoot Beds but show increased coarse clastic input. Sandstones in the Plymouth area have been interpreted as fluvial and low wave-energy delta deposits (Pound 1983), whilst elsewhere they are consistent with storm-influenced shelf conditions.

2.2.3 Devonian to Lower Carboniferous basins

Continuing north/south extension led to the formation of sub-basins within the subsiding shelf which in turn caused a divergence of stratigraphic successions into distinct sequences (Figure 2.3). The stratigraphy of these troughs is briefly summarised:

2.2.3.1 Gramscatho Basin

The Gramscatho Basin is the most southerly basin and is unique within southwest Britain in having locally been floored by oceanic lithosphere (Isaac *et al.* in press). It developed outboard of the main shelf region during the Devonian, and displays facies associations which reflect the development of a deep marine rift. At the southern margin of the basin, two lithologically anomalous complexes occur which represent allochthonous components of the Gramscatho marginal sea. The Lizard Complex of south Cornwall shows MORB-type geochemistry (Floyd *et al.* 1993), and is therefore interpreted as an obducted remnant of oceanic crust, whilst the Dodman Phyllites appear to be metamorphosed equivalents of the Portscatho Formation to the southwest. Leveridge *et al.* (1984) subdivided the successions of the Gramscatho Basin into two units that were juxtaposed by NNW-directed thrusting along the Carrick Thrust (Figures 2.4, 2.5).

Parautochthonous succession

In the footwall of the Carrick Thrust, lithologies are mudstone dominated and were deposited at the centre of the Gramscatho Basin (Holder and Leveridge 1986b). The junction between Lower Devonian shelf-sediments and the basal greywackes of the Gramscatho Group is transitional, with apparent interleafing of mid-Emsian Meadfoot siltstones with coarse sandstones and conglomerates of the basal Porthtowan Formation (eg. Gamas Head, Pentewan [SW 025 473]; Shail 1992).

The coarse, thickly bedded (metre scale) Treworgans Sandstones grade upwards into the thick mud-dominated Porthtowan Formation (Frasnian; Leveridge *et al.* 1990). This in turn is succeeded by the Mylor Slate Formation, comprising grey and grey-green slates with subordinate horizons of sandstone, siltstone and dolerite, with olistolithic breccia at its top. The upwards change in palaeoenvironments is consistent with progressive deepening of a deep marine basin. The olistostromes of the Porthleven Breccias reflect mass-movement and instability ahead of an advancing nappe.

Allochthonous succession

The allochthonous succession in south Cornwall forms two distinct sequences (Leveridge *et al.* 1984, 1990); the Carrick and Veryan Nappes. The Carrick Nappe, bounded by the Carrick and Veryan Thrusts, crops out along much of the south Cornish coast. It consists solely of the Portscatho Formation; a thick sequence of alternating grey-green sandstones and grey slates with occasional siltstone bands. The presence of *Dadoxylon* plant debris, miospores and acritarchs support deepwater deposition during the Frasnian (Le Gall *et al.* 1985), whilst mineralogical and geochemical analysis of the sandstones suggest their derivation from a magmatic arc (Floyd and Leveridge 1987).

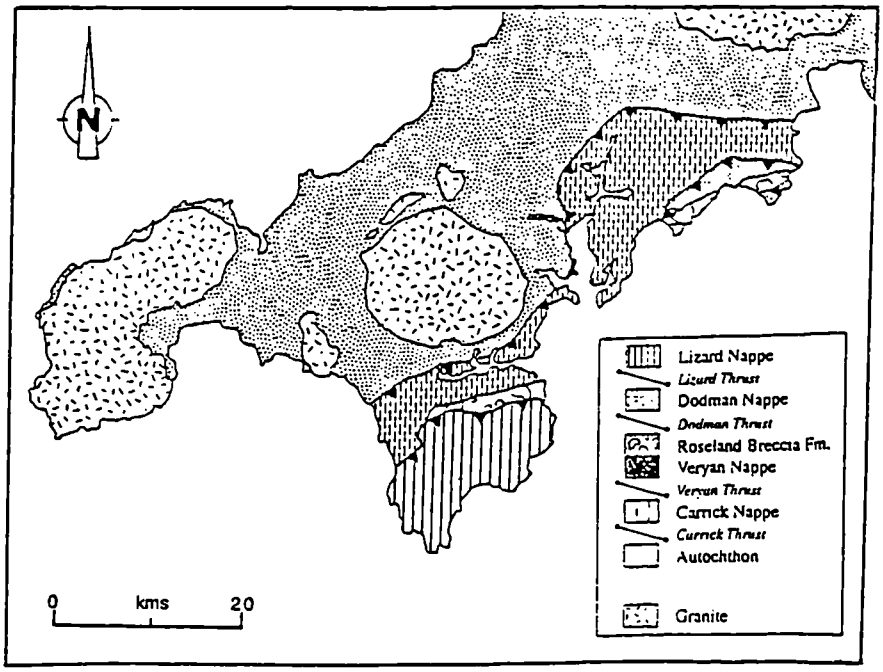

Figure 2.4 Tectonostratigraphic units in the Gramscatho Basin of south Cornwall (Leveridge *et al.* 1990).

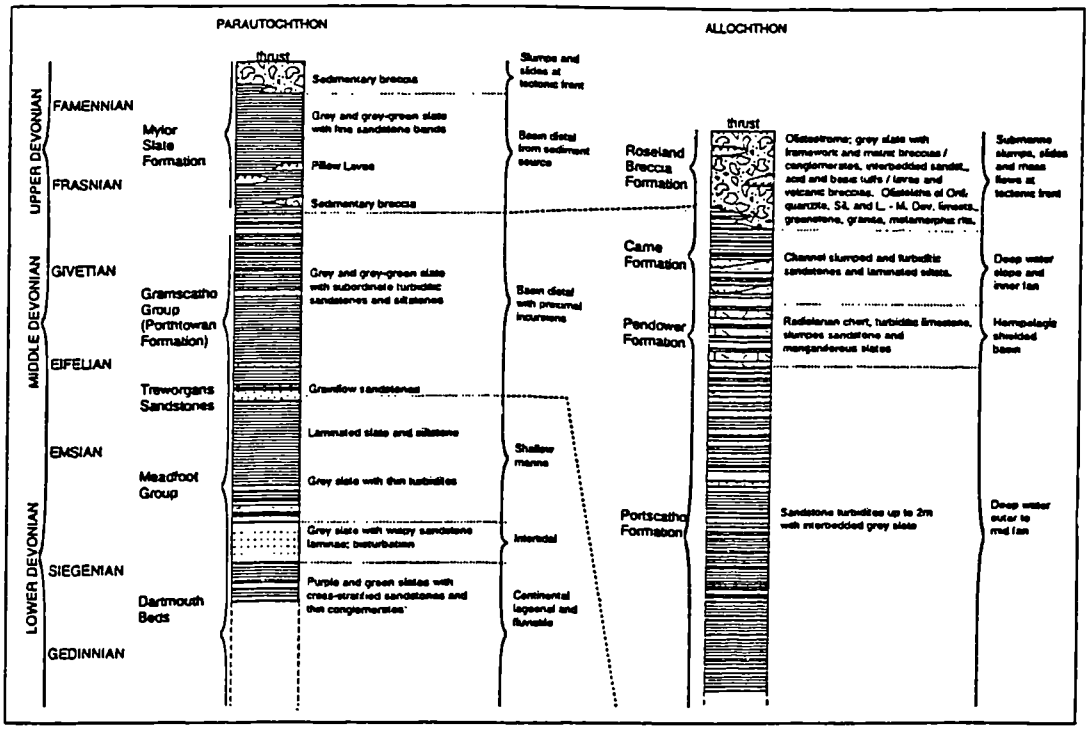

Figure 2.5 The lithostratigraphy of south Cornwall (Redrawn from Leveridge *et al.* 1990).

The Veryan Nappe is exposed on the coast around Veryan Bay, and is bounded by the Veryan Thrust below and the Dodman Thrust above. It contains rocks of three formations; the Pendower, Carne and Roseland Breccia Formations. The Pendower Formation at the base consists largely of mudstones (locally manganiferous), with interbedded sandstones, cherts and limestones of turbiditic origin. It is superceded by Carne Formation sandstones and laminated siltstones, and is overlain by the Roseland Breccia Formation;

an olistostrome unit enclosing clasts of sandstone, tuff, dolerite, Ordovician quartzite, Silurian to Devonian limestone and metamorphic rock within a grey slate matrix (Leveridge *et al.* 1990). The presence of cherts within the Pendower Formation is suggestive of restricted, deep-water hemipelagic sedimentation, whilst carbonaceous and sandy material indicate a proximal source of material to the south. The Carne Formation represents continental slope and fan deposits, whilst the Roseland Breccia Formation was generated during closure of the basin and mass-movement down the basin margins (Leveridge *et al.* 1990). Mid-Eifelian to Givetian faunal dates have been published for the nappe succession (Sadler 1973a; Barnes 1982).

Lizard Complex

The ultramafic and mafic metaigneous rocks of the Lizard Complex represent the most southerly-derived Variscan thrust-sheet exposed onshore. It locally shows a complete section through oceanic crust (Barnes and Andrews 1986), with peridotites, gabbros, amphibolites, basalts and paragneisses of amphibolite grade. It is separated from the Roseland Breccia Formation to the north by a gently-dipping thrust (now cut out by extensional faults) and shows internal imbrication into thin thrust-slices (Styles and Kirby 1980). Recent Sm-Nd and Rb-Sr isotope work suggests that formation and emplacement of the complex occurred during the middle to Upper Devonian (375±34 Ma; Davies 1984, 369±12 Ma; Styles and Rundle 1984). The three-dimensional geometry of the complex was investigated by borehole in 1978 by the BGS, and discovered to be a sheet less than 500 metres thick (cf. Doody and Brooks 1986), and this was later confirmed geophysically by Al-Rawi (1980). Both lithological and structural evidence thus indicate that the Lizard Complex represents an obducted ophiolite.

Dodman Nappe

The rocks of Dodman Point differ from those to the north as they comprise phyllites and strained sandstones with much stronger schistose fabrics than seen elsewhere. Holder and Leveridge (1986a) noted the similarity between the "Dodman Formation" and Portscatho Formation and its close association with outcrops of Roseland Breccia Formation. To explain these features, they invoked the presence of a Dodman Thrust at the northern boundary of the formation and utilised available deep seismic profiles to image the structure at depth (Day and Edwards 1983).

2.2.3.2 Trevone Basin

The Trevone Basin is an E-W trending, fault-bounded belt of mid Devonian to Namurian basinal rocks which crops out between Bedruthan Steps and Tintagel in north Cornwall and is traceable eastwards to the St Teath-Portnadler Fault. Its eastward continuation, the South Devon Basin (section 2.2.3.3), contains limestone-dominated lithologies which are though to have developed on horsts in the eastern side of a high, the Liskeard High, which divided the basin into two distinct sub-basins (Sanderson 1984). The trough contains mudstones and volcanics which thin northwards and show progressive northerly shallowing of facies (Warr 1991b). Two distinct and laterally equivalent successions are recognised in the southern part of the basin; the Bounds Cliff Succession and the Padstow Succession. On the northern margin, two Upper Devonian to Namurian slate units, the Boscastle and Tintagel successions outcrop. These were traditionally considered the basal part of the Crackington Formation (Ashwin 1958; Freshney *et al.* 1972; see section 2.4.1), but subsequent work by Selwood *et al.* (1985) favours their inclusion in the Trevone Basin (Figure 2.6).

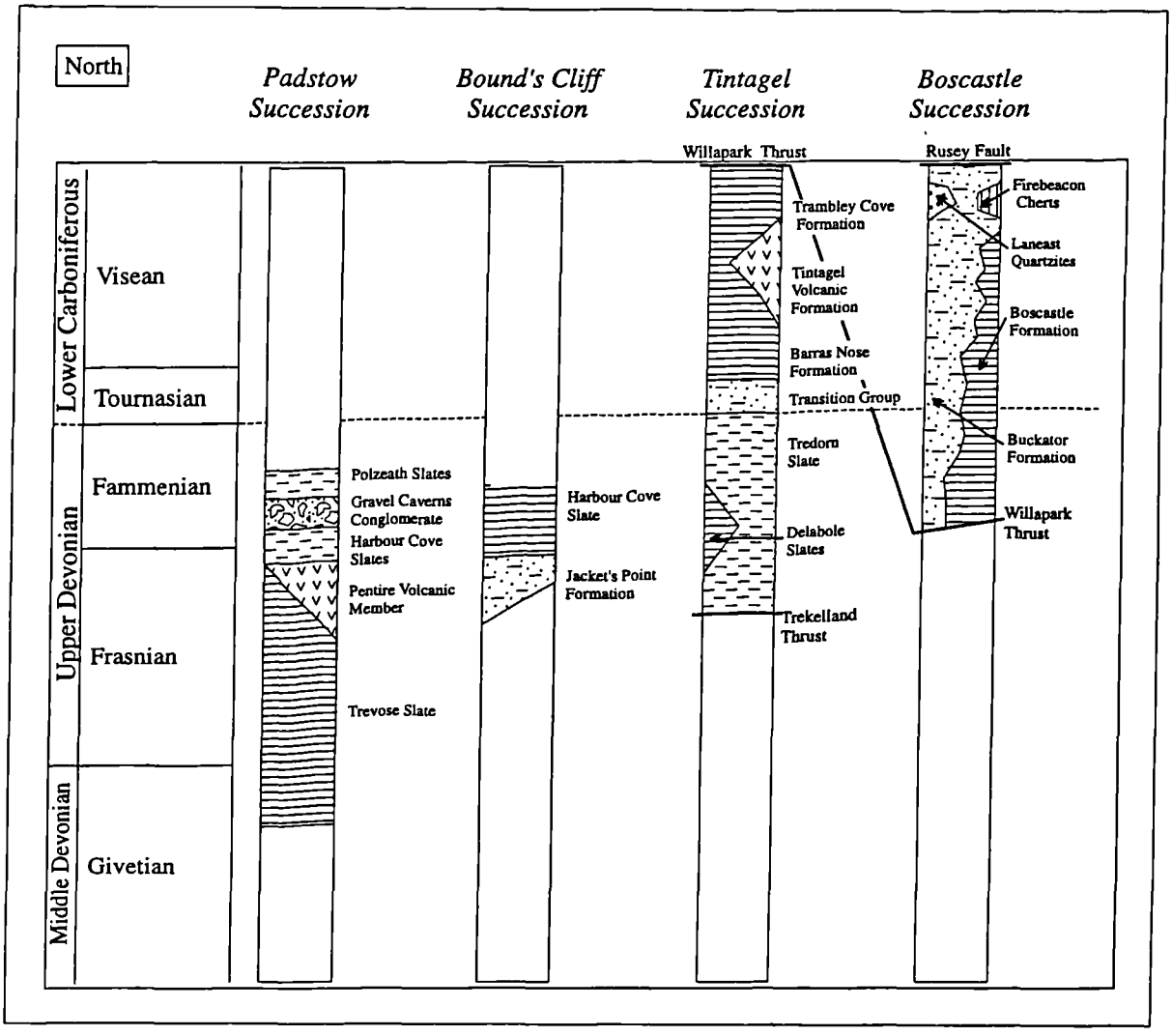

Figure 2.6 Successions of the Trevone Basin (adapted from Selwood and Thomas 1986a, Warr 1991a).

The Upper Givetian to Fammenian Padstow Succession occupies the southern part of the Trevone Basin, forming a thick sequence of Middle to Upper Devonian slates with conglomerates and intra-plate affinity volcanics towards the northern margin (Warr 1991a). The Frasnian to Lower Fammenian Bounds Cliff Succession comprises slates, siltstones, thin sandstones with common tuff horizons and rare intraformational conglomerates, deposited in a deep basin with sandstone influxes triggered by mass movement down the basin margins (Bluck *et al.* 1988). The Tintagel Succession preserves finer lithologies and higher volcano-sedimentary contents. Deposition occurred in a deep marine basin during the late Tournasian to late Viséan (Selwood *et al.* 1985). The Fammenian to Viséan Boscastle Succession preserves palaeoenvironmental indicators and fauna suggestive of shallow-water conditions during deposition except in the Uppermost Firebeacon Chert Formation, where deep water conditions are indicated (Selwood *et al.* 1985).

The origins of the Tintagel and Boscastle Successions are uncertain. Allochthon proponents (Selwood and Thomas 1986a,b; Isaac 1982) suggest that the successions are exotic thrust nappes on the basis of structural complexity and dissimilarities with rocks to the north and south, whilst fixists (eg. Sanderson 1984; Pamplin 1988; Andrews et al. 1988; Matthews 1977) emphasise that D1-structures are south-facing in all successions, and suggest that the units were in place prior to main Variscan compression. Conclusive evidence for either model is unavailable due to subsequent movement along the Rusey Fault and backthrusting of Culm rocks over the Trevone Basin boundary.

2.2.3.3 South Devon Basin

The middle to upper Devonian rocks of southeast Devon show few similarities to their temporal along-strike equivalents in the Trevone Basin (section 2.2.3.2), with limestones in place of slates as the dominant lithology (Figure 2.7). Facies variations are consistent with the Trevone-South Devon Basin consisting of a series of sub-basins and highs (Richter 1965, House *et al.* 1977 and Coward and McClay 1983). The Lowermost units exposed in the region are the Dartmouth and Meadfoot Groups (as discussed in section 2.2.2), which pass upwards into calcareous Eifelian shales and to the thickly bedded Torquay limestones (Givetian). The localised development of stromatoporoid banks and reefs led Scrutton (1977a,b) to interpret the limestones as shallow shelf deposits. The limestones pass upwards through a transitional facies into deep-water red pelagic shales yielding Frasnian to Fammenian goniatites (House 1963). Acid tuffs and lavas are common within middle Devonian rocks of the Ashprington and Kingsteignmouth areas, suggesting active vulcanism during extension.

Liskeard High

The stratigraphy of the inland region between the South Devon and Trevone basins is of great significance when modelling facies variation in the sub-basins. Despite poor inland exposure, Burton and Tanner

(1986) showed that the distribution of shallow-water deposits defines an elongate high which extends from Liskeard west-northwestwards to the Bodmin area and is bounded to both sides by dextral faults (Lane 1970). This high appears to have separated the Trevone Basin from the South Devon basin during the Emsian to Frasnian, restricting clastic sediment supply to the south and thus enhancing limestone development in the Torquay and Newton Abbot areas (Selwood and Durrance 1992).

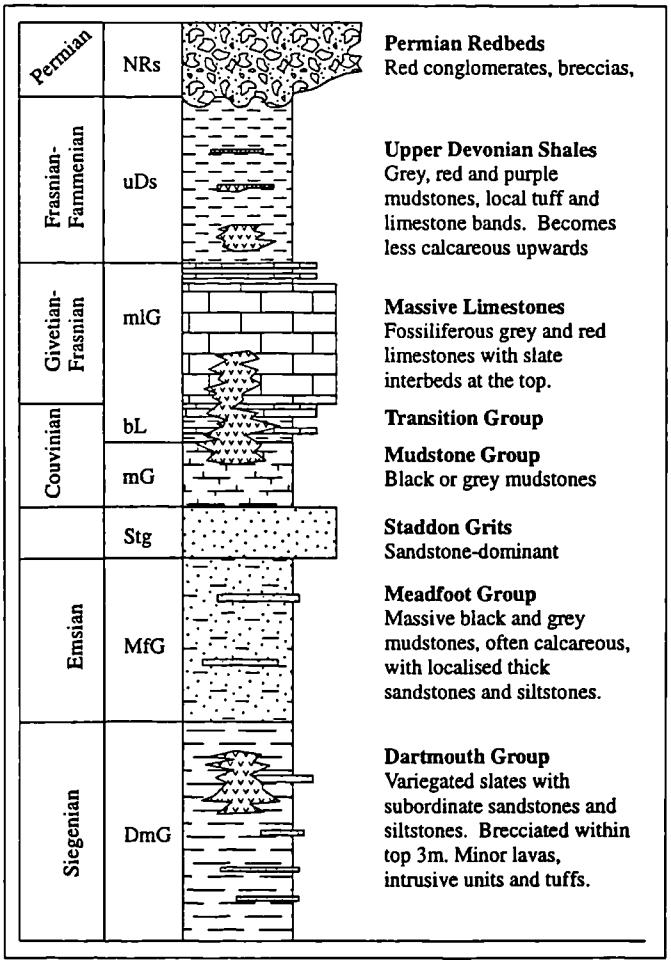

Figure 2.7 Stratigraphic succession in South Devon (after Richter 1968).

2.2.3.4 North Devon Basin

In north Devon, a thick sequence of Devonian to early Carboniferous alluvial and shallow marine sediments is exposed, bounded to the south by the Culm Basin and to the north by the Bristol Channel Fault Zone. The basin contains a thick post-Emsian succession (> 6 km; Figure 2.8; Brooks *et al.* 1983). Dewey (1982) suggested a regional β-factor of 2, although the absence of volcanic rocks suggests a lower value of attenuation.

The lowermost within the basin are the Lynton Beds; a group of sandstones and mudstones which display features indicative of deposition close to wave-base in a shelf environment (Bluck *et al.* 1988). The overlying Hangman Sandstone Grit Formation records an influx of alluvial clastic sediment from the north following late-Caledonian uplift of the south Wales region (Tunbridge 1986). The grits and sandstones form two units, separated by basinal muds. This cyclicity of sedimentation may record rejuvenation of the clastic source region through uplift along the Bristol Channel Fault-Zone (Tunbridge 1986). The superceding Ilfracombe Slate Formation yields Givetian corals, suggesting a rise in sea-level and flooding of the alluvial plains. They consist dominantly of mudstones with sandstones and locally developed thick bioclastic limestones, indicating an offshore shelf environment (Anderton *et al.* 1979). The Frasnian-Fammenian was a time of deepening in the basin, with the Morte Slates and Pickwell Down Sandstones recording delta development along the northern shore. The Upcott, Baggy and Pilton Beds at the top of the sequence show a return of fully marine conditions between the Fammenian and early Carboniferous. These siltstones, sandstones and shales are thought to have developed as coastal flat and nearshore deposits during the transgressive flooding of the southern margin of the Old Red Continent and migration of the shoreline towards south Wales (Bluck *et al.* 1988).

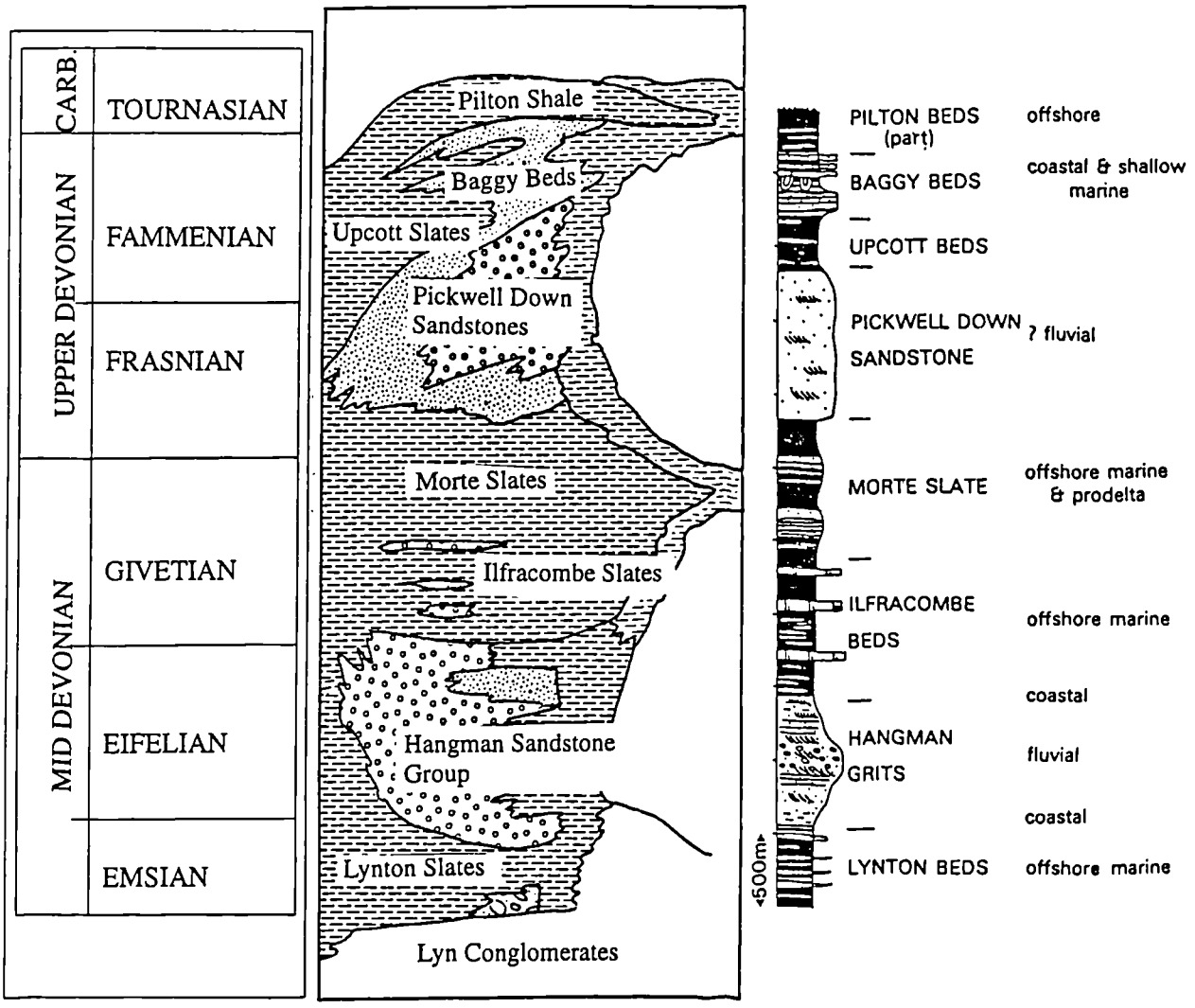

Figure 2.8 Generalised stratigraphy in North Devon (Anderton *et al.* 1979)

2.2.4 Foreland basins

The Carboniferous rocks of the Culm and South Wales Basins differ from adjacent basins in southwest England both in their facies associations and tectono-sedimentary history. They lie *"... between the front of a mountain chain and the adjacent craton"* (Allen *et al.* 1986) and thus represent foreland basins, developed in response to crustal flexure ahead of Variscan thrusting. The evidence for this interpretation is discussed within the following sections.

2.2.4.1 Culm Basin

The Upper Carboniferous rocks of north Cornwall and Devon mark the remains of an extensive east/west trending basin, the Culm Basin, which received sediments between the Lower Namurian and Westphalian C stage. It crops out on the coast between Rusey and Bideford, a distance of over 40 kilometers, and is recognised along strike to the east for over 70 kilometers as far as the Exeter area, where it passes beneath Permo-Triassic cover rocks (Figure 2.3).

The succession is dominated by turbiditic sandstones, siltstones and shales, and lies conformably upon deep-water mudstones and cherts of Dinantian age (Warr 1991b). From the southern margin of the basin, a thick basal sequence of distal turbidites (the Crackington Formation) passes northwards into more variable-grade turbidites (the Bude Formation) and is itself overlain by a shallow deltaic sequence (the Bideford Formation: Melvin 1986; Elliot 1976, Figure 2.9).

Thick sandstones found within the succession present sediment provenance problems, as no Namurian source region for the coarse material is as yet known. Palaeocurrent studies suggest that axial flow dominated during the deposition of the sandstones (Edmonds 1974), whilst the geometries of the bodies reveal no noticable thickening to either north or south and so prove inconclusive. Orthoquartzite debris is more likely to derive from an upfaulted mature source-region to the north rather than from the south (Selwood and Thomas 1986b). Geophysical survey findings (eg. Mechie and Brooks 1984) are consistent with emergence of a significant thrust in the Bristol Channel region which may have caused emergence of a source region, but late strike-slip motions on the Bristol Channel Fault-Zone and Rusey Fault have effectively destroyed all evidence of provenance (Warr 1991a).

The Culm Basin was traditionally considered to be extensional in origin, developing during the Upper Devonian in response to the regional extension or transtension (e.g. Sanderson 1984). At a time when the Culm Basin was thought to extend to the Tintagel area, workers cited the presence of alkali-basalts in the Tintagel area as evidence for crustal extension (e.g. Freshney *et al.* 1972). However, the reclassification of the Boscastle and Tintagel successions into the Trevone Basin (Section 2.2.3.2; Selwood *et al.* 1985) makes a foreland basin setting far more likely. In his review of the Rhenohercynian Zone, Warr (1991a)

convincingly presented evidence for a foreland basin origin. He noted that revised K-Ar dates after Dodson and Rex (1971) show that deformation within the Trevone Basin occurred synchronously with deposition of the Culm rocks, but with none of the vulcanism or mineralisation seen in the intrashelf basins to the south. Furthermore, the calculated geothermal gradient of 40°Ckm^{-1} compares favourably with heatflow recorded in present day foreland basins (Cornford *et al.* 1987; Warr 1991b).

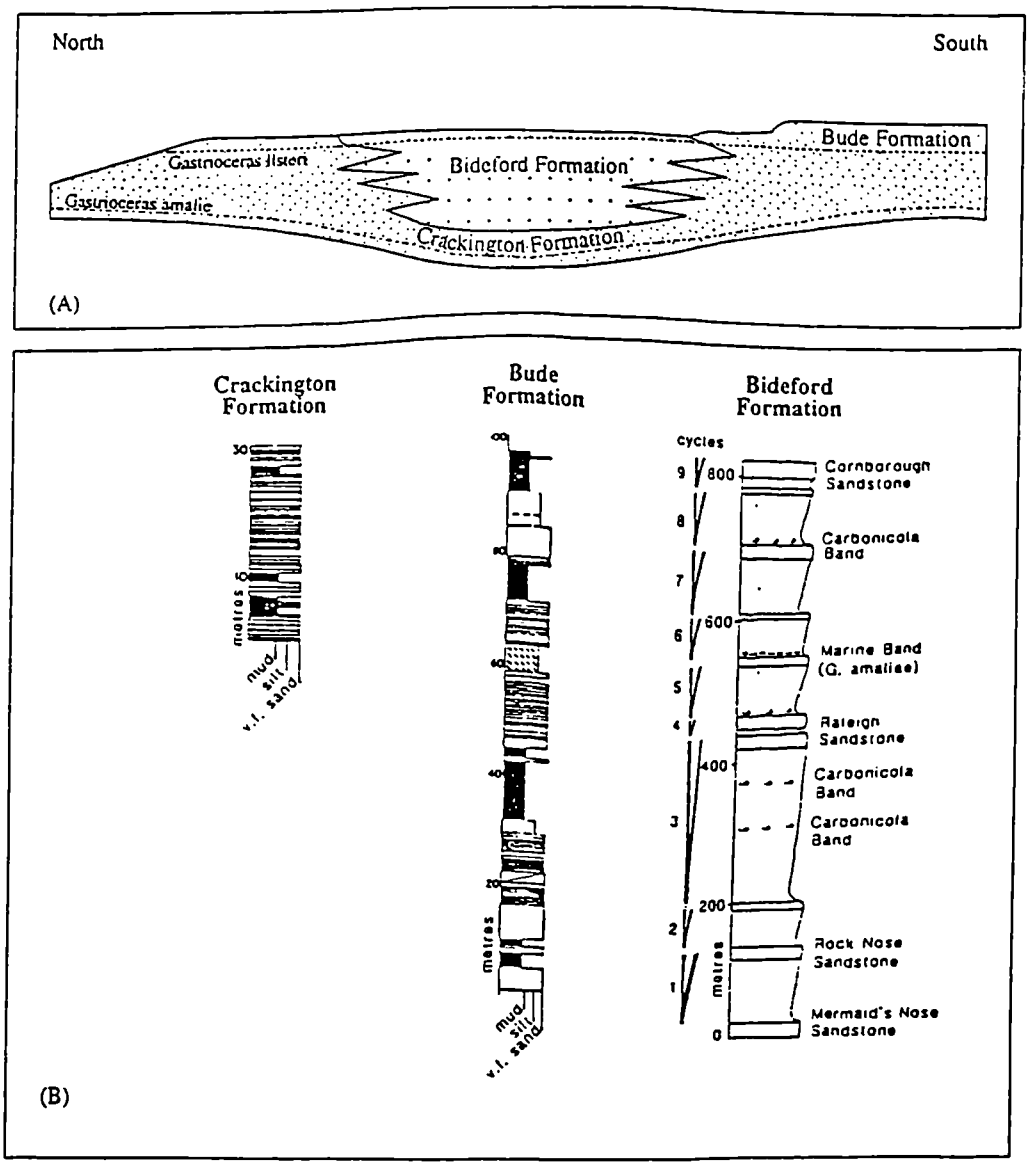

Figure 2.9 (A) Geometric relationship between formations of the Culm Basin (Warr 1991b); (B) Summary logs of the Crackington, Bude and Bideford Formations (Melvin 1986; Edmonds *et al.* 1979)

2.2.4.2 South Wales Basin

The South Wales Basin is over 30 kilometers wide and contains Upper Carboniferous strata of Namurian to Westphalian age (Owen and Weaver 1983). The pre-foreland basin rocks are bioclastic, oolitic and dolomitic limestones with thin calcareous shales developed at their base and top. They appear to have formed upon a carbonate platform after the end-Devonian transgression recorded in the Pilton shales

(Kelling and Williams 1966). Strong variations in thickness across the basin relate to differential subsidence controlled by fault movements to the south (Owen and Weaver 1983; Figure 2.3).

The Namurian rocks above show sudden facies change in response to the emergence of source regions to the north and east (Kelling 1988), with deposition of the Basal Grit Formation succeeded by dark goniatite-bearing shales and thin quartzites of the Shale Group. These formations represent the development of shallow marine and lagoonal conditions which continued into the Westphalian to deposit Coal Measures up to 3 kilometres thick (Swansea area; Owen and Weaver 1983). Coal seams occur within mudstones and sandstones and indicate marshy conditions on a coastal plain with clastic incursions from a northerly source (Hartley 1993). The Upper Westphalian corresponds to a change back a southerly provenance, with the Pennant Sandstones forming in response to uplift in the south along the Bristol Channel Fault (Hartley 1993).

Kelling (1988) identified two major stratigraphic cycles which appear tectonically controlled and may be accounted for by a foreland basin model. Kelling suggests that the Namurian to Westphalian B and Westphalian C to Stephanian intervals form two major tectonostratigraphic cycles which developed during two stages of nappe loading within the region, and that the Westpahlian C cambriense marks the inception of the second cycle.

2.2.5 Post-Carboniferous rocks

The youngest rocks affected by Variscan orogenesis are of Westphalian age and all younger rocks rest unconformably upon Variscan basement (Figure 2.3; Hobson and Sanderson 1983). Post-Variscan cover is most commonly Permo-Triassic and consists of conglomerates, breccias, sandstones and clays which are especially well exposed in southeast Devon. They are of molasse basin facies, with a red coloration which suggests that deposition occurred onland under hot conditions. Conglomeratic units contain clasts of Variscan material which represent scree and sediment fan deposits, whilst sandstones and clays display sedimentary structures diagnostic of aeolian or wadi deposits (Anderton *et al.* 1979). Their deposition coincides with a period of extension along north/south and east/west trending normal faults and reactivation of northeast trending Variscan thrusts and north-northeast trending transform faults, with redbeds occurring within fault-bounded troughs and as sedimentary dykes within fractures in the Upper Variscan surface (Richter 1966). Subsidence relating to this extension brought about the formation of sedimentary basins which locally contain a complete post-Carboniferous succession, including the Plymouth Bay, St. Mary's and Melville Basins to the south and the South Celtic Sea Basin to the north (Chadwick 1985; Evans 1990). In the Exeter region, early Permian redbeds are overlain by the vesicular lavas and olivine basalts of the Exeter Volcanic Series. They are basic in character and have a continental rift-type geochemical signature of incompatible elements, and are thus probably related to the phase of extension observed in the field

(Thorpe *et al.* 1986). K-Ar dating provides an age of 291±6 Ma for the series and hence rifting of the Cornubian platform (Thorpe *et al.* 1986).

2.3 Deformation history

The structure of SW England appears straight-forward upon initial examination with E-W to NNW-SSE striking formation contacts and thrusts. However, simplicity of outcrop pattern belies a very complex arrangement of folds and thrusts, with polyphase deformation structures often in parallism with one another. Structural overviews have been published by Hendriks (1937), Dearman (1971), Sanderson and Dearman (1973), Matthews (1977), Shackleton *et al.* (1982), Isaac *et al.* (1982), Selwood *et al.* (1982), Hobson and Sanderson (1983), Coward and Smallwood (1984), Sanderson (1984), Warr (1991a). The large-scale structure is shown in Figure 2.10 and is explained in this section.

2.3.1 Regional compression

Early models, (reviewed by Dearman 1971) invoke the presence of a continuous Lizard-Dodman-Start Thrust, whilst structural analysis of Devonian outcrops was thought to show two major antiforms [Truro and Watergate Bay - Dartmouth Antiforms]. Minor folds were thought to fan about the Bude area into isoclinal recumbent folds with a strong subhorizontal slaty cleavage in Devonian rocks to the north and south, with structures facing outwards and upwards. A change in facing and vergence was identified near Padstow with northwards-facing folds identified to the south (section 2.3.5).

Dodson and Rex (1971) used K-Ar dating to gauge the cooling age of syn-tectonic micas and discovered a general younging northwards, consistent with deformation caused by a northerly-advancing deformation front (Figure 2.11a). The oldest dates were found in south Cornwall (late Devonian), whilst central Cornwall and mid-Devon yielded Vìsean to Namurian ages and the Culm Basin provided end Carboniferous to early Permian dates. Areas of south Devon and north Cornwall yield Westphalian to Stephanian ages and which appear to have been reset during backthrusting (Coward and Smallwood 1984) or dextral shearing (Holdsworth 1989) along the Start-Perranporth Zone.

The first regional synthesis of deformation phases was complied by Sanderson (1973), with four phases of deformation encompassing compression and early extension across SW England . Sanderson and Dearman (1973) collated these ideas and divided Cornwall and Devon into twelve domains of consistent tectonic style on the basis of fold attitude, facing, number of phases present, age and cleavage (Table 2.1, Figure 2.11b). The zonation reflects the bulk structure after all phases of deformation, and so variation is due to both primary strain variations and later events. Subsequent work has highlighted the control which structural level exerts upon fold style (Sanderson 1979), with open folds generally thought to form high in

the nappe stack (eg. North Devon, Bude) whilst isoclinal folds and intense cleavage develop close to major thrusts.

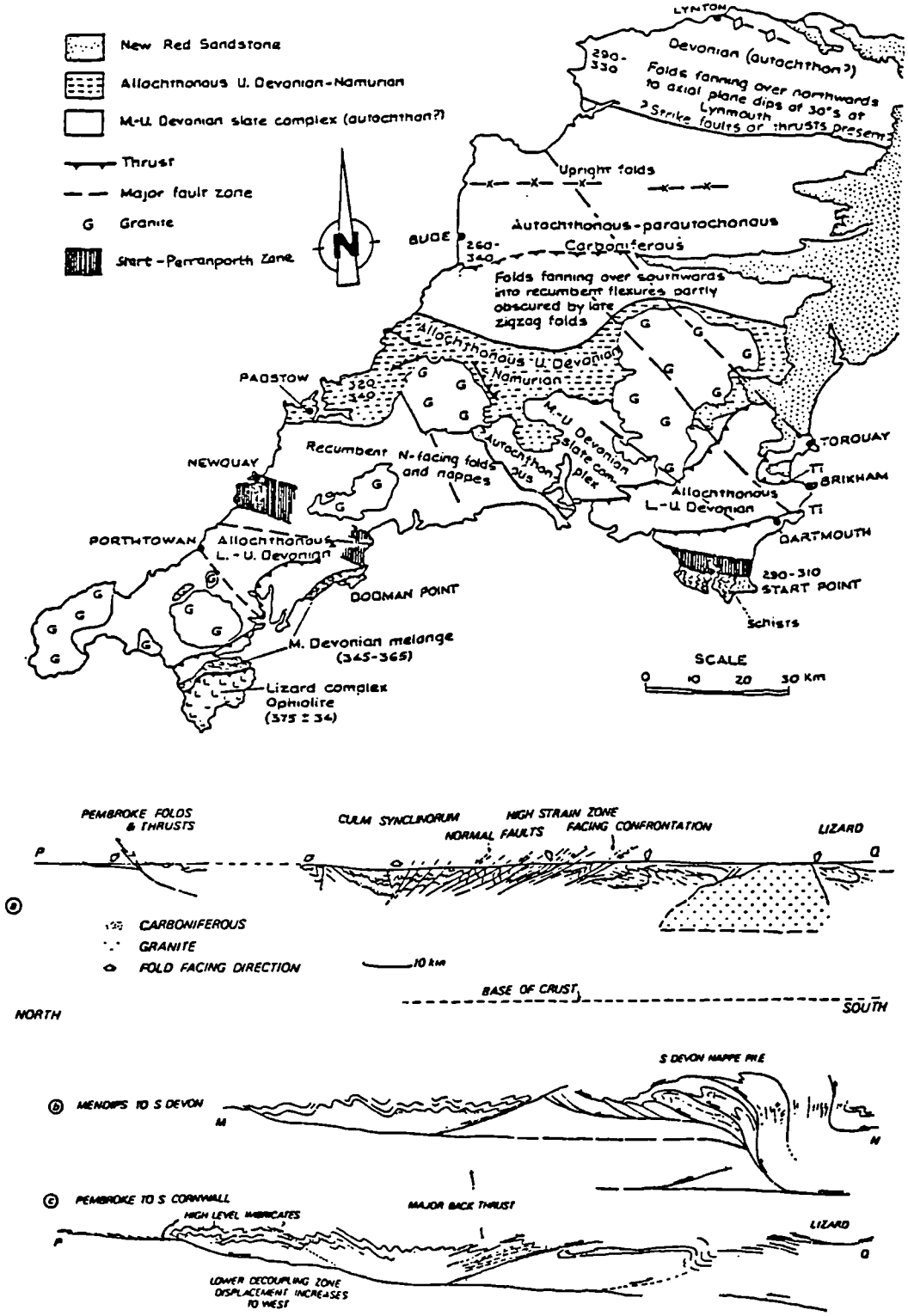

Figure 2.10 (a) Major strike features of SW England (Chapman 1986). (b) Synoptic cross-sections through SW England across regional strike (Coward and Smallwood 1984). Structural simplicity is largely due to scale of diagram.

The twelve tectonic zones form two groups. In the north, zones 1-6 form a structural fan about the upright structures of zone 2 and in the south (zones 7-12), folds generally verge north or northwest. The junction between these two domains lies along the Padstow Facing Confrontation Zone. Radiometric evidence from Dodson and Rex (1971) indicates that the southern zone was recrystallised (i.e. deformed *and* cooled) by ~340-320 Ma and the northern zone at ~300-280 Ma, thus supporting a diachroneity of deformation episodes.

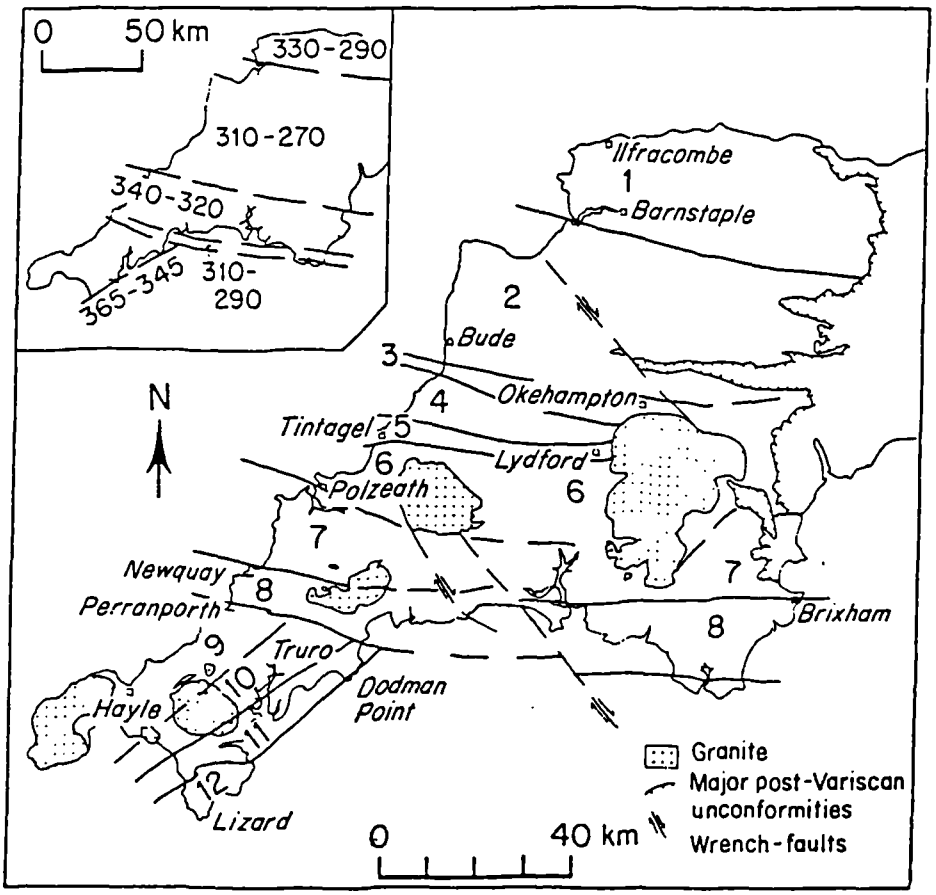

Figure 2.11 Structural zones of SW England (Hobson and Sanderson 1983). (a) K-Ar age zones, values in millions of years (after Dodson and Rex 1971). (b) Tectonic zones in SW England (Sanderson and Dearman 1973). For explanation see Table 2.1.

Investigation into thrust transport vectors was conducted through the use of several kinematic indicators, including mineral lineations, slickenlines, porphyroclasts, deformed markers, fold and thrust attitudes and vergence and the trend of strike-slip faults. Across south Devon, south Cornwall and the Tintagel region, transport is directed to the north-northwest and shows slight dextral obliquities.

(i) Thin-skinned model

Proponents of this model consider southwest England to be a typical foreland fold and thrust belt with deformation restricted largely to the upper crust above a basal dÈcollement (Coward and Smallwood 1984; Figure 2.10b). The presence of thrusts has been known from field study for over 100 years, but recent

advances in seismic profiling (section 2.6.1) have revealed their subsurface expression for the first time (Isaac et al. 1982; Coward and McClay 1983; Chapman *et al.* 1984; Meissner *et al.* 1981). Bright reflectors have been recorded to depths of 25 km, at which level they appear to sole into an infra-crustal decoupling zone (Brooks and Le Gall 1992). Estimates of shortening in Palaeozoic sediments of 150 km (50%; Shackleton *et al.* 1982) are unlikely to have been accommodated at depth as there is no evidence for the orogen attaining a great thickness (i.e. no high-grade metamorphic rocks; Coward and Smallwood 1984) but this may be under estimated at present if the amount of late-orogenic extension was more significant than is generally accepted.

Zone	*Location (Coastal)*	*Fold Attitude*	*Facing*	*Axial Trend*	*K-Ar Age / Ma*
1	North of Barnstaple	North Verging	N	E-W	330-290
2	Barnstaple-S. Bude	Upright	Up	E-W	310-270
3	Widemouth area	North Verging	S	E-W	310-270
4	Widemouth-Boscastle	Recumbent	S	E-W	310-270
5	Boscastle-Tintagel	Recumbent	S	Oblique	310-270
6	Tintagel-Polzeath	Recumbent	SSE	ENE-WSW	310-270
7	Polzeath-W'gate Bay	Recumbent	NNW	ENE-WSW	340-320
8	W'gate Bay-Perranporth	North Verging	NNW	WSW Plunge	?
9	Perranporth-Tregonning	Recumbent	NNW	ENE-WSW	?
10	Tregonning-Loe Bar	North-west Verging	NW	NE-SW	?
11	Loe Bar-Mullion Cove	North-west Verging	NW	Oblique	365-345
12	*Lizard, Dodman*	*Metamorphic Rocks*	-	-	-

Table 2.1 Tectonic zones of southwest England (After Sanderson and Dearman 1973).

(ii) Thick-skinned models

In this model, collisional thickening is thought to have involved the full thickness of the crust throughout basin development and closure (Figure 2.12; Badham and Halls 1975; Badham 1982; Sanderson 1984). Badham (1982) suggested that basins formed as dextral pull-aparts through back-arc processes and were sequentially deformed by a northwards-advancing compressional front through time. Whilst evidence for this transtensional model is confined mainly to the Gramscatho Basin and the Lizard Complex, Warr (1991) has suggested that transtension was important throughout the orogen (see also Holdsworth 1989).

A thick-skinned deformation model was also invoked by Sanderson (1984), who noted that deformation was concentrated into basins (which had the thinnest and hottest crust and thus weakest underlying lithosphere), and suggested that whole-crust thickening occurred synchronously with depression of the MOHO. He estimated compression as 40% through thrusting, underplating and dextral shear, and suggested that even at approximately 28 km, the crust was thick enough to cause partial melting and granite formation at a geothermal gradient of $30°Ckm^{-1}$.

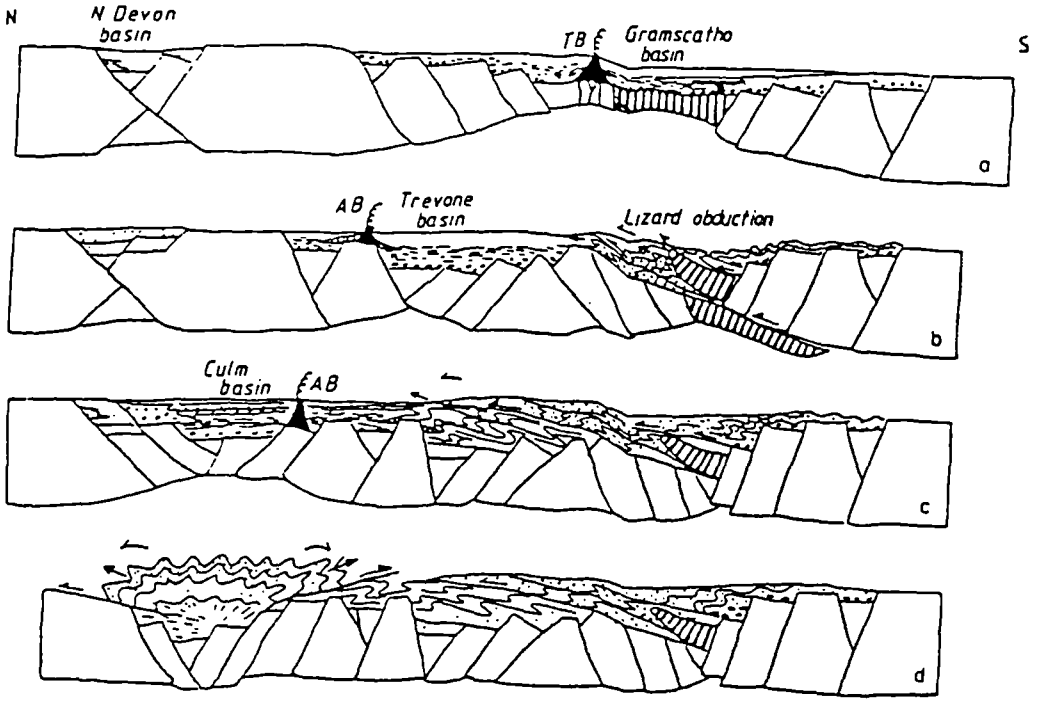

Figure 2.12 Thick-skinned model of tectonic evolution in southwest England (Sanderson 1984). Compare with thin-skinned model in Figure 2.10b.

To account for a dextral component to Variscan events, Scotese *et al.* (1979) suggested that collision between Europe and Africa was oblique. Turner (1986) emphasised the strike-parallel variation of structure and stratigraphy and suggested that this resulted from transtension and/or transpression above a basement which was cut by north-northeast/south-southwest fault-zones which may represent reactivated ancient lineaments, allowing rotation and vertical movements of crustal-blocks within a partitioned crust.

(iii) Basin inversion

Research into the deformation of previously attenuated crust has led to a hybrid model of deformation in SW England, in which both thick- and thin- skinned processes may have operated but were controlled by the inversion of individual basins and reactivation of their bounding faults (Butler 1989; Gayer and Jones 1989; Pamplin 1988; Powell 1989; Hartley and Warr 1990; Warr 1991a,b). Basin inversion in its simplest form considers that contraction perpendicular to the basin margin will cause the upward expulsion of the basin's contents through reactivation of bounding faults and buttressing against fault scarps (Figure 2.13; Hayward and Graham 1989; Cooper and Williams 1989).

Realisation of the importance of pre-existing basin architecture to the Cornish structure was made by Matthews (1977), who suggested that a number of deep east/west "fractures" were responsible for the changes in stratigraphic facies and thicknesses observed regionally, and that this variation may later have

controlled changes in fold style and facing. Powell (1989) noted that the South Wales Basin exhibited many of the criteria of inversion tectonics, including changes of mode along individual fault planes, the generation of shortcut faults through the footwalls of listric faults and accommodation backthrusts. Warr (1991b) applied a conventional basin inversion model to the Trevone and Culm basins of north Cornwall, suggesting that complex backfolds, backthrusts and dextral transpression zones could have developed by reactivation of and buttressing against marginal faults. Holdsworth (1989a) noted that the oblique inversion of east/west-trending basins through north-northwest directed compression should generate dextral transpressive strains, thus explaining the presence of the prolonged transpression along the northern margin of the Gramscatho and Start Basins.

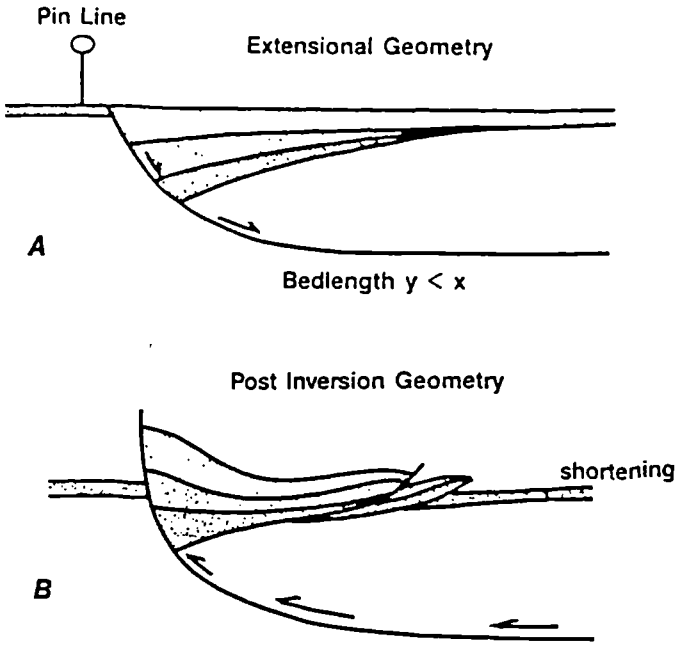

Figure 2.13 Basin inversion model for a half-graben. (A) Extensional geometry. (B) Post-inversion geometry (Hayward and Graham 1989)

The model is consistent with earlier thick-skinned hypotheses in that considerable amounts of compression would be partitioned into deforming syn-rift strata without requiring the development of far-travelled nappes, and thus whilst the surface expression of compression is of a fold and thrust-belt, it is likely that thick-skinned processes are important at depth (Warr 1991b).

The style and intensity of cleavage and strain has been considered by several authors during the early 1980s (Rattey and Sanderson 1982; Coward and McClay 1983; Hobson and Sanderson 1983; Coward and Smallwood 1984). Variation in intensity of deformation appears to relate to proximity to thrusts and folds and rheology of the deforming media. Strain is generally oblate (Coward and McClay 1983) as is consistent with volume loss or superimposition of several strains during deformation (Coward and Potts 1983). The regions of highest strain are located around Tintagel and Start, where aspect ratios of deformed

clasts reach values of 23:1 (Rattey and Sanderson 1982). Elsewhere, aspect ratios are commonly 2.5:1 (Coward and McClay 1983). Cleavages have formed through a combination of pressure solution, rotational recrystallisation and mechanical rotation of phyllosilicates, and this indicates that high volumes of fluid were present during deformation.

2.3.2 Regional extension

Much of the research into Variscan structure has focused on compressional features, despite extensional structures being present which have a strong influence upon regional trends. Several phases of extension are recorded and have occurred before, during and after the main phase of compression (e.g. Leveridge *et al.* 1990; Alexander and Shail 1995, 1996). Examination of primary thrusts (eg. Rusey Fault; Freshney 1965) also reveals a history of reactivation through low- and high-angle faulting. Whilst the magnitude of extension is largely unknown, previous estimates vary widely between 5% (Shackleton *et al.* 1982) and 30+% (Freshney 1965, Isaac *et al.* 1982).

Post-thrusting extension was reviewed by Coward and Smallwood (1984). In north Cornwall [Widemouth to Tintagel], workers have recognised east/west trending and moderately north dipping normal faults which cause block rotation and reorientation of earlier structures (Shackleton *et al.* 1982; Sanderson 1979). Further south [Tintagel to south of Polzeath], faults are often listric and join low-angle shears which reorient earlier fabric and become pervasive in the Tintagel High Strain Zone. Freshney (1965) and Isaac *et al.* (1982) suggest that this phase of extension is due to crustal doming during granite emplacement. Similar low-angle structures have been recorded between the Bodmin and Dartmoor granites (Isaac *et al.* 1982), north of the Dartmoor Granite (Dearman and Butcher 1959) and in Mounts Bay (Turner 1968; Rattey and Sanderson 1982; Alexander and Shail 1995), in each case being cross-cut by steeper normal faults. In SW Cornwall, minor extensional faults occur which are thought to be related to extrusion beneath the Lizard Nappe (Rattey 1980; Rattey and Sanderson 1982), but other workers favour their formation during the Permian opening of the English Channel (Stoneley 1982). Richter (1967, 1969) describes N-S and WSW-ENE trending normal faults in south Devon which formed during deposition of Permian redbeds, and less common NNE-SSW trending faults which clearly postdate all other structure.

The extensional structures of SW England are discussed at length in chapters 3 and 4.

2.3.3 Strike-slip faulting

North-northwest/south-southeast trending wrench faults produce several kilometers of dextral movement on stratigraphic boundaries and cumulative displacement of ~21 miles (33.6 km) across the region (Figure 2.14; Dearman 1963; Barton *et al.* 1993). When traced inland, the wrench faults are seen to cut the Dartmoor and Bodmin Moor granites thus suggesting significant post-Carboniferous movement. The

structures appear to be long-lived, as Tertiary reactivation is recorded in the Palaeocene Bovey Tracey Basin; a pull-apart structure along the Sticklepath-Lustleigh fault, and Recent movement is inferred from an earthquake in 1955 (Lane 1970).

The origin of the faults remain disputed. De Sitter (1956) examined the Portnadler Fault and noted a change in orientation from WNW to NNW inland. He suggested that the wrench fault passed laterally into thrusts of the main Variscan compression and thus represent primary lateral ramps. Dearman (1963) thought that the faults had initiated as Variscan extensional structures which had been rejuvenated during Alpine events, and tested this theory through construction of strain ellipses by inferring an Andersonian model and sinistral displacements along the Lizard-Start Fault (Figure 2.14).

Work on subsidiary fault-features by Lane (1970) and Barton *et al.* (1993) revealed conjugate dextral shears and east-northeast/west-southwest trending normal faults close to major wrench faults. Lane (1970) explained the change in fault-strike through two models. Either the structures either had an early history of wrenching synchronous to compression with deformation partitioned on either side of the fault, or the inland change in strike was initially formed by fault splays during the Variscan and were exploited and elongated by Alpine fault-systems. Subsequent research has led workers to support Lane's ideas, as detailed field studies show marked facies and structural changes across the faults. Arthaud and Matte (1977) examined wrench fault kinematics across the Variscan deformation belt and concluded that they form a dextral megashear system accommodating lateral components of plate motion. In such a model, the north-northwest/south-southeast trending dextral faults of southwest England may represent Riedel shears formed in the latter stages of Variscan collision. Matthews (1984) noted that NW-SE trending fractures are recorded throughout the southern Caledonides and thus they are likely to be Caledonian in their initiation, as Iapetan transform faults (Dewey 1982).

Coward and Smallwood (1984) analysed the orientation of the faults, and suggested that they lie sub-parallel to the direction of compressional transport because they initiated as transfer faults to the thrust-systems. Turner (1984) and Smythe (1984) accepted this model, but proposed that their reactivation was not Alpine but was a result of differential shear during gravity spreading of nappes during late-orogenic extension.

2.4 The Cornubian granitoids

At the close of the Variscan Orogeny, the deformed Palaeozoic sediments and volcanics of southwest England were intruded by a major granite batholith. Magmatism occurred over a timespan of approximately 20 Myrs, generating a suite of granitoids ranging from potassic lamprophyres and rhyolitic to rhyodacitic lavas to the main Cornubian Batholith. Crystallisation and cooling was accompanied by

hydrothermal mineralisation in the roof and margins of the plutons, producing the orefields which have been worked since the Bronze Age.

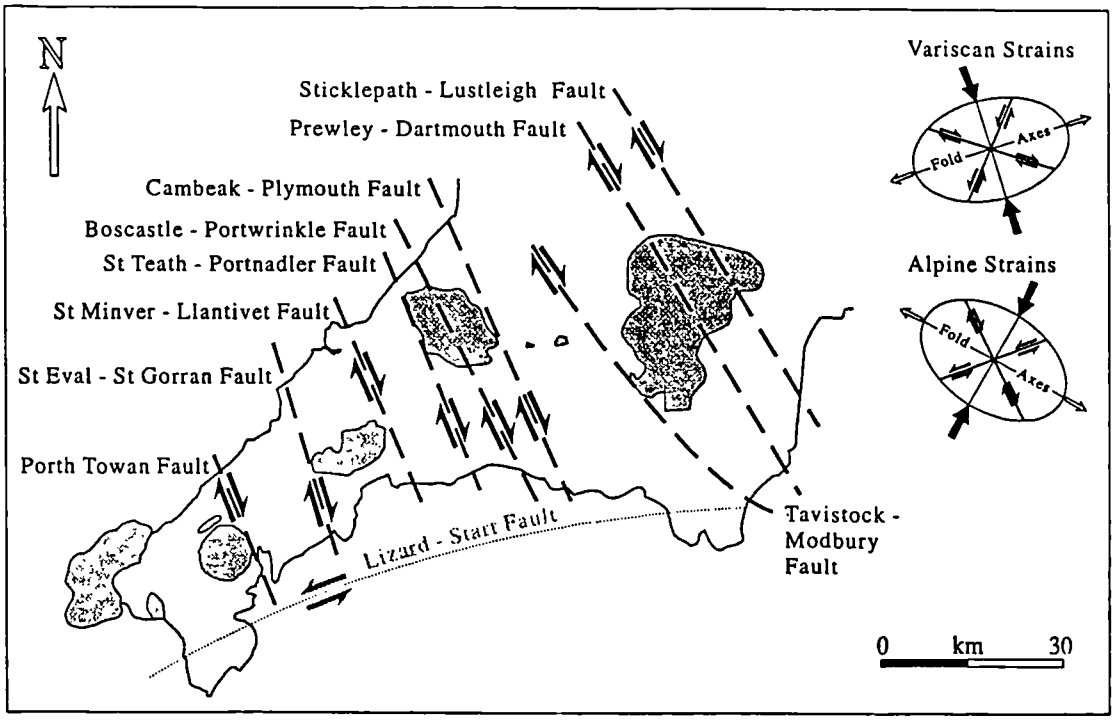

Figure 2.14 Dextral transcurrent fault-zones of SW England. Strain ellipses on the left display expected orientations of structures active / reactivated during Variscan and Alpine events (After Dearman 1963).

2.4.1 The Cornubian granite batholith

The Cornish granites are thought to represent S-type anatectic granitoids which are anomalous within the Rhenohercynian zone, being far larger and closer to the sub-Variscan foreland than all others (Chen *et al.* 1993). They are the surface expression of a large linear batholith, trending east-northeast/west-southwest for over 250 kilometers from Dartmouth to beyond the Isles of Scilly. Five main plutons (Dartmoor, Bodmin Moor, St Austell, Carnmenellis and Lands End) and several smaller satellite masses (Isles of Scilly, Tregonning, St Michaels Mount, Cligga Head; Figure 2.15) crop out. The Haig Fras granite, a second, smaller batholith, is exposed as an underwater reef 150 km west of Lands End. It also trends west-southwest/east-northeast and formed either as an en-echelon extension of the main batholith or may have been offset from the main axis by dextral strike-slip movement after emplacement (Darbyshire and Shepherd 1985).

Form

Whilst the granites form discrete outliers at the surface, it was long suspected that the outcropping bodies were linked at depth. This was confirmed by gravity and magnetic data (Bott *et al.* 1958) which reveal a deep bouguer anomaly low extending along the axis of the exposed granites and extending outwards from them, defining the Lower density of the intrusion. Whilst several three-dimensional models have been proposed since this time, the main features of the batholith remain consistent (Bott *et al.* 1958; Bott and Scott 1964; Willis-Richards and Jackson 1989):

1. All the major plutons are connected by ridges in the batholith roof which are seldom more than 2 kilometres below the surface.
2. The marginal contacts dip steeply outwards.
3. The batholith forms two distinct sub-areas when considered at the 2000 metre depth stratum-contour. Thus the St Austell, Bodmin Moor and Dartmoor Granites are separated from the Carnmenellis and Lands End Granites by a 3000 metre deep trough containing Gramscatho Group sediments.
4. The dissected shape of the St Austell pluton reflects post-emplacement strike-slip faulting.

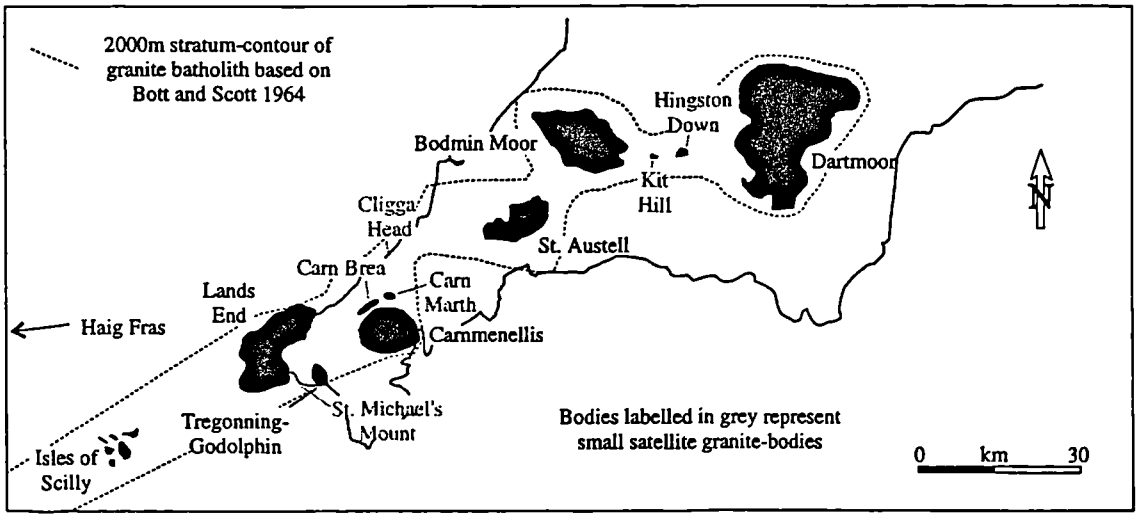

Figure 2.15 - Granite Bodies of SW England (adapted from Exley and Stone 1982).

The depth to which the batholith extends has been the subject of much investigation, with initial estimates of 10+ km subsequently refined to 9-16 km in the west and 12-22 km in the east with a gentle north-easterly dip to its base (*gravity;* Bott and Scott 1964; Brooks *et al.* 1983; *seismic;* Brooks *et al.* 1984).

Age of intrusion

Recent refined geochronological studies have demonstrated that emplacement of plutons was diachronous, with the oldest bodies having cooled and experienced hydrothermal mineralisation before emplacement of

the youngest (Table 2.2; Chen *et al.* 1993). There is no geographical trend in pluton ages, suggesting that the batholith is the result of several coalesced pulses of magma (Chesley 1993).

Origin, petrogenesis and emplacement

The Cornubian granites were intruded at the cessation of Variscan compression and are likely to have formed in response to melting of overthickened Variscan crust (Shackleton *et al.* 1982, Pearce *et al.* 1984). This would explain the peraluminous geochemical signature of the granites, and is consistent with a partial-melt generated from high-grade basement gneisses of Brioverian-type as found in Brittany (Charoy 1986).

Intrusion	Age / Ma	Method	Source
Carnmenellis	293.7 ± 3.4	U-Pb monazite	Chen *et al.* 1993
Bodmin	280.8 ± 0.4	U-Pb monazite	Chen *et al.* 1993
St Austell	278.4 ± 0.8	U-Pb monazite	Chen *et al.* 1993
Dartmoor G1	281.4 ± 0.8	U-Pb monazite	Chen *et al.* 1993
Dartmoor G2	285.7 ± 0.8		
Lands End	274.5 ± 0.7	U-Pb monazite	Chen *et al.* 1993
Tregonning-Godolphin	281.5 ± 1.6	Ar-Ar zinnwaldite	Clark *et al.* 1993
Isles of Scilly	286.4 ± 0.8	Ar-Ar muscovite	Chen *et al.* 1993

Table 2.2 Published Geochronology of Magmatism. Ages relate to a number of geochronological indicators with very different closure temperatures. The closure temperatures used are: monazite, 725 ± 25°C; muscovite, 320 ± 50°C (*cf.* sources above). The approximate time for cooling from emplacement (~800°C) to this temperature is estimated at ~ 5 Ma (Chen et al. 1996)

Alternatively, the granites may be the fractionated and crust-contaminated products of mantle-derived magmatism (Simpson 1979). A key argument in favour of this hypothesis is that crustal thickness at the end of orogenesis is unlikely to have been greater than 32 kilometres, insufficient to have provided enough radiogenic thermal energy to cause wholesale crustal melting (Watson 1984). Shackleton *et al.* (1982) suggested that melt was generated south of the region of final emplacement in thicker continental crust and was injected northwards along inactive thrust-planes. The process of fractional crystallisation from mafic mantle precursor to granitic magma would require downward gradation within the batholith into intermediate to basic rocks, and this is not evident in gravity, magnetic or seismic surveys (Willis-Richards and Jackson 1989).

A compromise between these two end-members was supplied by Leat (1987), who suggested that the source region for fusion was within the Lower crust, but that it was driven thermally by mantle underplating. This could provide the heat required for melting in a relatively thin collision zone whilst

explaining the longevity of magmatism and intrusion of potassium-rich lamprophyres synchronously with the granites (Huppert and Sparks 1988).

The mechanism of emplacement remains uncertain in southwest England. At the present level of unroofing, the granites appear to have stoped into their host, but the process at depth is less constrained. Recent advances in geochronological dating (eg. Chen *et al.* 1993) have shown that individual plutons were constructed from multiple magma pulses, and within crust experiencing an elevated geothermal gradient.

The cooling rate of granite plutons is proportional to the square of the pluton size divided by the thermal conductivity of the country rocks (Chesley *et al.* 1993; Willis-Richards and Jackson 1989). The Cornubian batholith is therefore predicted to have had a total cooling time of ~4-5 Ma, although repeated sourcing of magma (evidenced from the diversity of age-dates) would have prolonged this process. This is supported by radiometric evidence from the Carnmenellis pluton (Figure 2.16; Chen *et al.* 1996), where ages derived from monazites (closure temperature 725°C) and primary magmatic muscovites (closure temperature 320°C) show 5 Ma of primary cooling, with initial quenching of magma at a rate of ~ 80-100°C/Ma. Subsequent cooling is likely to have been much slower because of their high radiogenic mineral content.

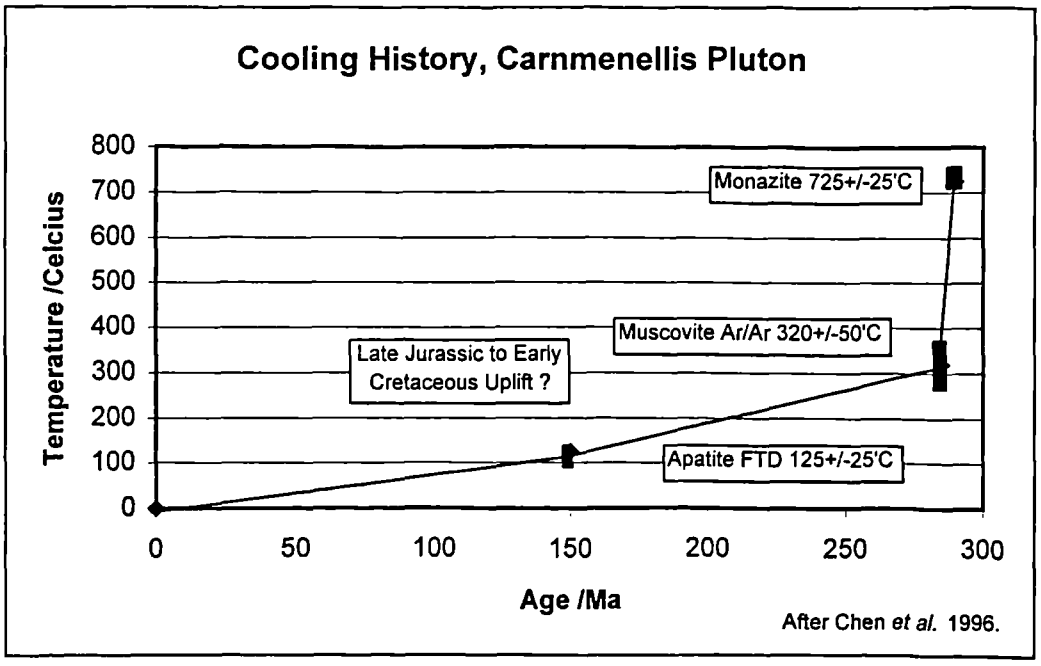

Figure 2.16 - Cooling history of the Carnmenellis pluton. Quenching is seen in rapid cooling between 290 and 285 Ma immediately following emplacement, and is succeeded by gradual cooling (Chen *et al.* 1996).

2.4.2 Elvans

Numerous quartz-feldspar porphyry-dikes (*elvans*) occur in swarms across southwest England, cross-cutting the main granites as well as the country rocks (figure 2.17). They occur as steeply dipping dykes ranging from a few metres to 10s of metres in width, and trend east-northeast/west-southwest, subparallel to the axis of the batholith. Alignment of megacrysts parallel to the margins is common, reflecting the laminar flow of viscous magma during intrusion (Leveridge *et al.* 1990). Both field relationships and radiogenic dating suggest that these dykes were intruded soon after emplacement of the main granites, locally being cross-cut by late-stage granite-pegmatite veins. Rb-Sr dates for elvans range from 290 to 270 Myrs, with the main phase of emplacement between 280 and 270 Myrs bp., immediately postdating pluton construction (Darbyshire and Shepherd 1985).

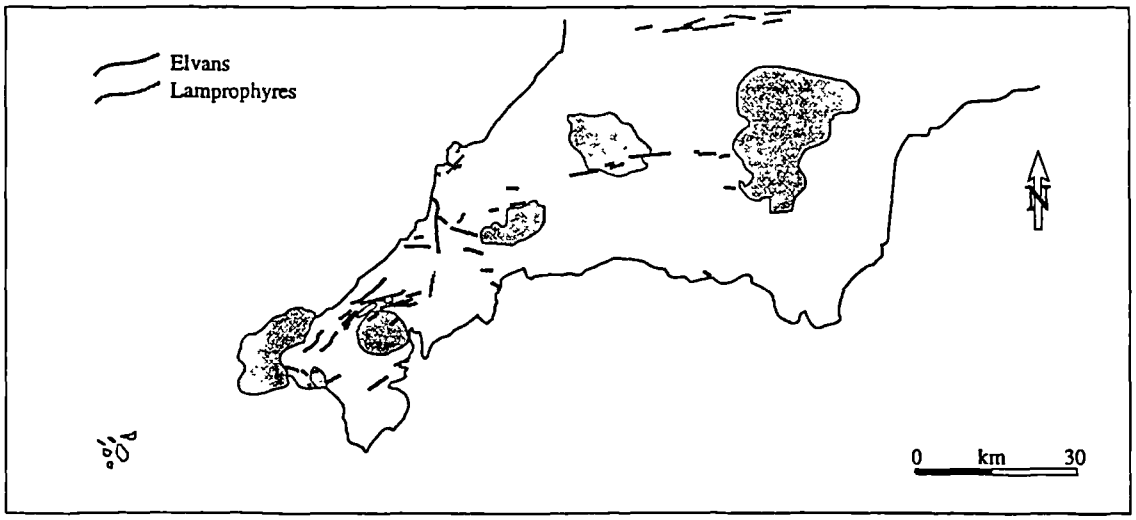

Figure 2.17 Sketch map of the distribution and trend of elvans and lamprophyres (Drawn from 1:250 000 solid geology maps 50°N-06°W and 50°N-04°W, British Geological Survey).

2.4.3 Lamprophyres

Lamprophyric dykes and sills form discordant sheets 1-15 metres thick (Figure 2.17). They are fine to medium-grained, reddish-brown porphyritic intermediate rocks which are petrographically minettes (i.e. biotite-orthoclase rocks). The mafic component is generally phlogopite or olivine and phlogopite when seen in fresh section, but exposures weather to chlorite, carbonate, iron oxides and clays (Exley and Stone 1982).

The sheets appear undeformed, suggesting that they are post-tectonic, but they have not been recorded within the granites or their thermal aureoles. Radiometric dates of individual lamprophyres yield values of 296 ± 5 Myrs (Hawkes 1981) and 292.9 ± 3.4 Myrs (Goode and Taylor 1988); ages which are similar to those of a suite of lamprophyres found in Brittany (Darbyshire and Shepherd 1985). They therefore

probably represent primitive mantle-derived magmas which partially predate the emplacement of the Cornubian batholith.

2.4.4 Mineralisation

Intense hydrothermal mineralisation characterises the region adjacent to the batholith, with lodes present in both the granites and country rocks. Base-metal species present include tin, copper, tungsten, arsenic, iron, zinc, silver and lead (Willis-Richards and Jackson 1989), with horizontal and vertical zonation of distribution (Figure 2.18).

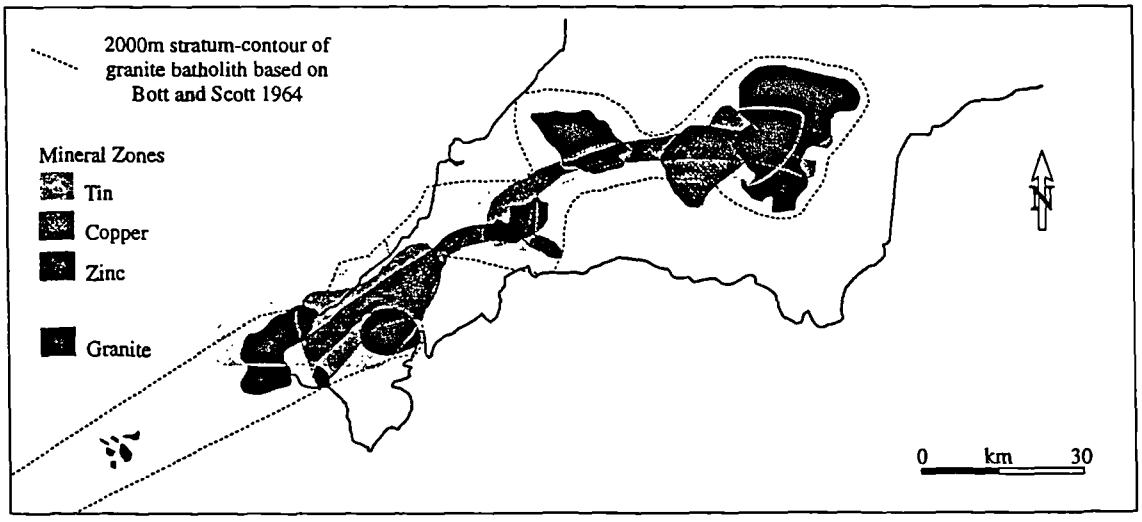

Figure 2.18 Zonation of mineral lodes above the Cornubian Batholith (from Stemprok 1995).

The source of the metals remains poorly constrained, although there is a close relationship both temporally and spatially between mineralisation and granite emplacement. The three most likely sources are; a) direct magmatic origin; b) scavenging of metals from Palaeozoic country-rocks by hydrothermal fluid cells; and c) assimilation of metal-enriched country rocks into the granites, with subsequent hydrothermal remobilisation (Leveridge *et al.* 1990). The tourmalinisation and greisenisation which affected several granites (eg. Roche Rock) require a magmatic fluid for formation and temperatures in excess of 500°C. Fluid inclusion studies of mainstage mineral veins have identified a basinal brine signature of NaCl and $CaCl_2$ concentration (Shepherd and Scrivenor 1987), supporting hydrothermal concentration. It therefore appears that mineralisation occurred through a combination of mechanisms through time, and this may explain the complex spatial distribution of metal-species.

Rb-Sr analyses of fluid inclusions within the South Crofty lode has yielded ages of around 270 Ma for the main phase of mineralisation (Darbyshire and Shepherd 1985) whilst Ar-Ar muscovite dating of the same lode yields an age of 286 Ma (Chen *et al.* 1993), a date coeval with granite emplacement. Jackson *et al.*

(1982) propose three further stages of base-metal mobilisation due to hydrothermal rescavenging at ~220 Ma, ~165 Ma and ~75 Ma.

2.4.5 Metamorphic aureole

Contact metamorphism of country rocks adjacent to outcropping granite is characterised by spotting in pelitic lithologies and the localised development of hornfelsic textures. Close to the granite-country rock boundary, mudrocks display andalusite (occasionally chiastolitic), biotite and white-mica assemblages whilst siltstones contain quartz, white-mica ± biotite, often within a penetrative fabric and psammites are unmodified. The outer aureole shows recrystallisation of chlorite and white-mica in pelitic lithologies (Leveridge *et al.* 1990). The contact aureoles of outcropping granites closely reflect their sub-surface forms; where the granite margins are steep, the aureole is restricted to 1-2 kilometres width, whilst regions of shallow boundary-dip show contact metamorphism over up to 10 kilometres (Bott *et al.* 1958).

2.5 Metamorphism

Regional metamorphism in the Variscides of southwest England is generally low-grade, ranging from diagenetic-level in the Upper Carboniferous rocks of the Culm Basin to Mid-Greenschist facies in the Tintagel area (Tilley 1925; Phillips 1964, 1966; Cooke *et al.* 1972; Barnes and Andrews 1981, 1984; Warr *et al.* 1991). In mudstone and sandstone units, the lower temperatures are reflected by rotational recrystallisation, intracrystalline fracturing of grains and development of pressure solution seams (Leveridge *et al.* 1990), whilst in volcanic and basic igneous rocks, it causes neomineralisation (Floyd 1983, Primmer 1985a).

The use of illite crystallinity techniques allowed the metamorphic pattern to be determined over large areas (Warr 1991b). In 1979, Brazier *et al.* looked at the characteristics of white micas along the north coast, and again identified an epizonal high in upper Devonian / lower Carboniferous rocks around Tintagel. Furthermore, he distinguished anchizonal rocks around Padstow and diagenetic-level rocks in the Culm basin, attaining a greater degree of clarity than previously possible. Ensuing work by Primmer (1985a,b,c), Warr (1991b; 1996), and Warr *et al.* (1992) covers almost all of Cornwall and south Devon (Figure 2.19).

On the basis of P-T-t paths, Warr (1991b) and Warr *et al.* (1991) have suggested two mechanisms which may explain the metamorphic pattern; diastathermal (basin subsidence controlled), and deformation-related (Warr *et al.* 1991). In this reinterpretation, the main primary metamorphism, M1, in the Culm Basin is due to sedimentary burial at a high geothermal gradient, whilst in the south it is due to thrusting and crustal thickening at a lower geothermal gradient. The Tintagel High Strain Zone displays a second phase of metamorphism, M2, due to underthrusting of the Culm Basin. There is no extensive regional overprint by

the contact aureoles surrounding the granite plutons of the area. The correlation between the position of the granites and of epizone rocks is thought to be due to updoming during emplacement.

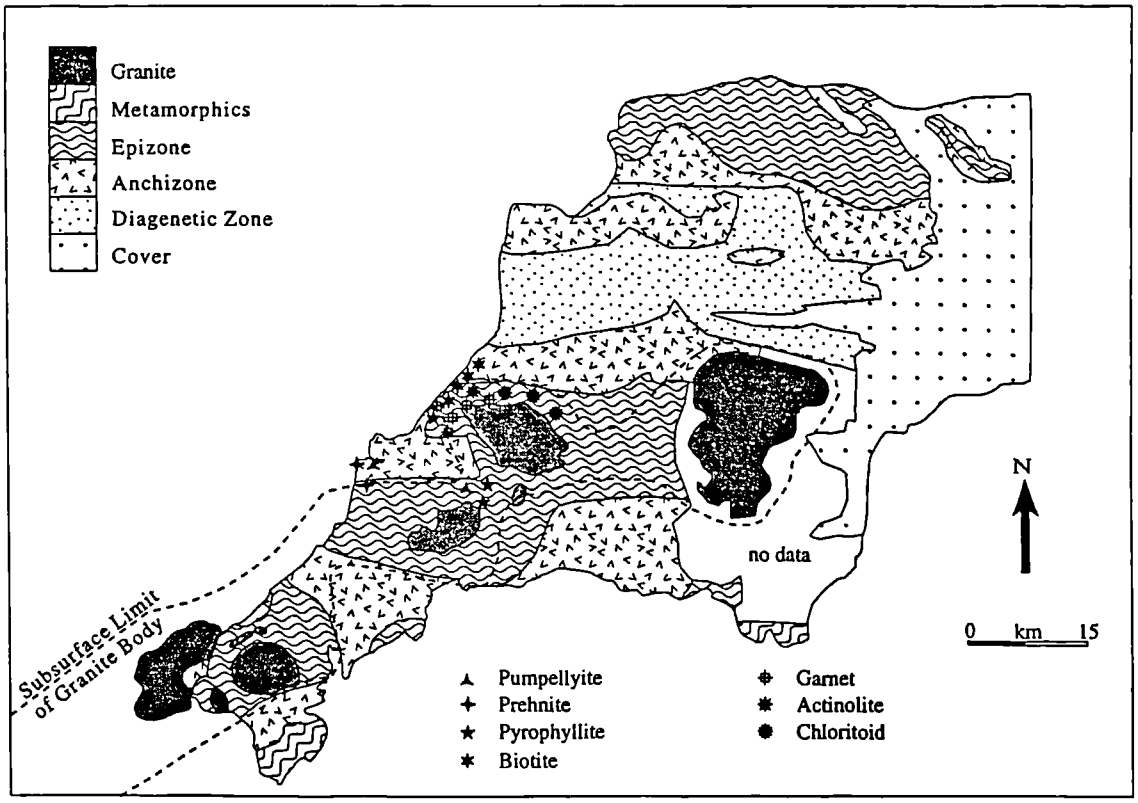

Figure 2.19 Illite Crystallinity Map of SW England with mineral localities added (adapted from Warr *et al.* 1991; Primmer 1985b).

The meta-igneous rocks of the Lizard Complex have anomalously high metamorphic grade, with peridotites, gabbros, amphibolites and basic dykes developed. The highest-grade rocks of Cornwall occur within two high-temperature mylonite zones, the Carrick Luz and Porthoustock shear-zones, in which schists and mylonites display mineral assemblages which suggest grades in excess of amphibolite facies (Kirby 1978). Goode and Taylor (1988) suggested that the elevated grades reflect the deep position of the Lizard within the thrust-stack during primary compression and apply the same argument to rocks of the Start and Eddistone areas. However, the presence of unaltered basaltic sheets of oceanic affinity indicate that high-temperature deformation occurred close to an oceanic spreading centre (Barnes and Andrews 1986; Gibbons and Thompson 1991), a model supported by anomalously old Rb-Sr age-dates in the area (Styles and Rundle 1984). The polyphase deformation in the Lizard Complex is thought to record the intra-oceanic amalgamation of hot thrust-slices (Vearncombe 1980) followed by cold obduction (Barnes and Andrews 1984) near to the top of the Variscan thrust-stack (Holder and Leveridge 1986) More recent geochemical work on the Start schists (Floyd *et al.* 1993) indicates that they are greenschists derived from Gramscatho protoliths.

2.6 Geophysical research into the deep geology of SW England

Seismic, magnetic and gravity techniques provide valuable information about subsurface structure with which to assess the validity of structural models proposed by field geologists. Southwest England and its surrounding waters have been the subject of geophysical investigation for over sixty years, the history of which is reviewed by Brooks *et al.* (1983, 1984) and Evans (1990).

2.6.1 Seismic surveys

The first seismic survey in the waters around SW England was conducted in 1938-9 (Bullard and Gaskin 1941), and by the 1970s, a good model of the subsurface geology had been constructed (Bott 1970; Holder and Bott 1971; Avedik 1975), depth to the MOHO was recorded at a constant 27 km and the form of the granites was documented. The involvement of petroleum companies in the seismic program prompted a great jump in the quality and coverage of seismic data and hence in understanding of Variscan structure.

Onshore seismic work has confirmed the presence of several major deep thrusts elsewhere in the Variscan belt which had previously suspected from surface geology (*Wiltshire* - Kenolty *et al.* 1981; *Rhenish Massif, Germany* - Meissner *et al.* 1981; *Southern England* - Chadwick *et al.* 1983). In Cornwall, three major (thrust?) reflectors at 8 km, 10-15 km and 27-30 km depth (Brooks *et al.* 1984; Edwards 1986) were imaged during the SWESE (South West England Seismic Experiment) program. The uppermost reflective layer is situated within the granite and is thought to reflect a transition between phases at depth, the second has a gentle southerly dip and is thought to be a late-Variscan thrust which forms the base of the granites, and the deepest reflector is consistent with other estimates of the Mohorovicìc Discontinuity (Edwards 1986).

Offshore studies in the Plymouth Bay Basin and Bristol Channel areas have been used to confirm the offshore continuation of a series of thrust sheets mapped onland. The east-northeast/west-southwest trending Lizard Thrust was identified in the Plymouth Bay Basin by Day and Edwards (1983) dissected by north-northwest/south-southeast trending dextral faults, whilst Doody and Brooks (1986) studied seismic velocity profiles beneath the Lizard and Start regions and proposed that they form thin sheets underlain by Devonian metasediments. Leveridge *et al.* (1984) identified south-dipping reflectors east of the Lizard which appear to form the offshore extension of the Carrick, Lizard and Dodman Thrusts (Figure 2.20; see also section 2.2.3.1), as supported by Edwards *et al.* (1989). Stratigraphic studies on the Roseland Peninsular have identified a further thrust (the Veryan Thrust) along the formation boundary of the Portscatho and Pendower Formations which has subsequently been confirmed from seismic profiles (Le Gall *et al.* 1985).

Deep seismic surveys have allowed study of the lower crust and upper mantle, and are important when constructing orogenic models (*South Western Approaches Traverse;* BIRPS and ECORPS 1986). Cheadle *et al.* (1986) picked out a bright reflector at 20 kilometers beneath the Bristol Channel and interpret it as the frontal thrust of the Variscan belt in Britain, whilst Hillis (1988) examined deep seismic data in conjunction with gravity data to construct contours to major Variscan thrusts (Figure 2.21) The SWAT lines reveal that Variscan thrusting to the south soles into an infra-crustal decoupling zone at 25 km depth (Brooks and Le Gall 1992). Northward dipping horizons imaged below the Culm Basin were identified by Brooks and Le Gall (1992) as Caledonian thrusts and they subsequently inferred that inherited basement structures exert a strong influence upon basin formation and deformation during Variscan orogenesis. Permian and Mesozoic basins surrounding the Cornish platform with up to 10 km of fill show an episodic history of rifting and inversion with reactivation of Variscan thrusts and transfer faults (BIRPS and ECORPS 1986; Evans 1990; Hillis and Chapman 1992).

2.6.2 Gravity surveys

Gravity surveying was first used on a large scale in southwest England by Bott *et al.* (1958), who published a regional Bouguer anomaly map (Figure 2.21). The most conspicuous feature of the map is a prominent -50 mgal trough around the outcropping granites; a result of mass deficiency of the granites relative to their hosts. Gravity surveying has subsequently been used to refine the form of the granites (Bott and Scott 1964; Day and Williams 1970; Al-Rawi 1980; Brooks *et al.* 1983; Edwards 1986; section 2.4.1).

The Start, Lizard and Dodman regions of the south coast are marked by a positive Bouguer anomaly. Advanced modelling techniques were employed by Al-Rawi (1980), who described the Start Complex as a wedge of metamorphic rock, down-faulted against the Start Boundary Fault and the Lizard as a thin (<1km) sheet underlain by Gramscatho or Mylor Group sediments. Surveying to the east of Start Point reveals a Bouguer low flanked to the south by a gravity high, revealing the presence of a Mesozoic Basin flanked by an uplifted ridge of Palaeozoic rock (Bacon 1975).

A 22 mgal drop seen from south to north across Exmoor on the Bouguer Anomaly map was initially explained by Bott *et al.* (1958) as a buried thrust between units of strongly differing density. Bott and Scott (1964) re-examined the feature and proposed northwards thickening of low-density Palaeozoic rocks as an alternative solution. Subsequent surveying in the Bristol Channel (Brooks and Thompson 1973) has revealed continued deepening of the Bouguer low to the north into a Mesozoic basin, and it may thus represent an overthrusted Upper Carboniferous Basin.

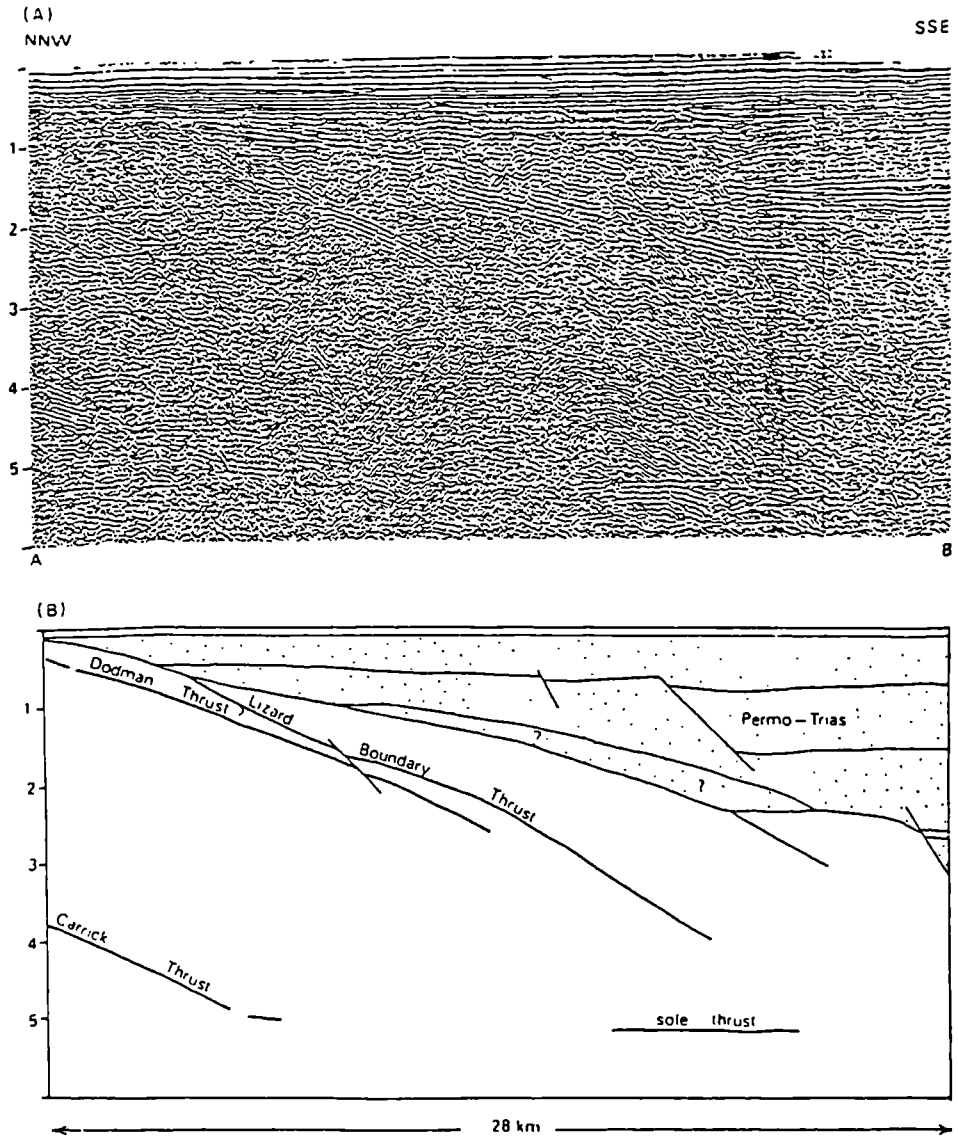

Figure 2.20 (A) Seismic section running NNW-SSE south of Dodman Point. (B) Interpretation of section (Leveridge *et al.* 1984).

2.6.3 Magnetic surveys

In his initial studies of the Plymouth Bay Basin, Allan (1961) saw that sharp anomalies associated with the Lizard ophiolite died out eastwards after a few kilometers. and suggested that it is faulted and dissected. A continuous Lizard-Dodman-Start thrust belt is not clear from the magnetic anomaly map (Institute of Geological Sciences 1965), although a change to a more uniform character is observed to the north of the Lizard-Start line. A large anomaly situated 27 km to the south of Eddistone Reef was explained by Allan

(1961) as a second Lizard-type body, but more recent seismic modelling discounts this possiblity (Brooks *et al.* 1983) and it is more likely to represent a buried Permian inselberg (Evans *pers. comm.* 1996).

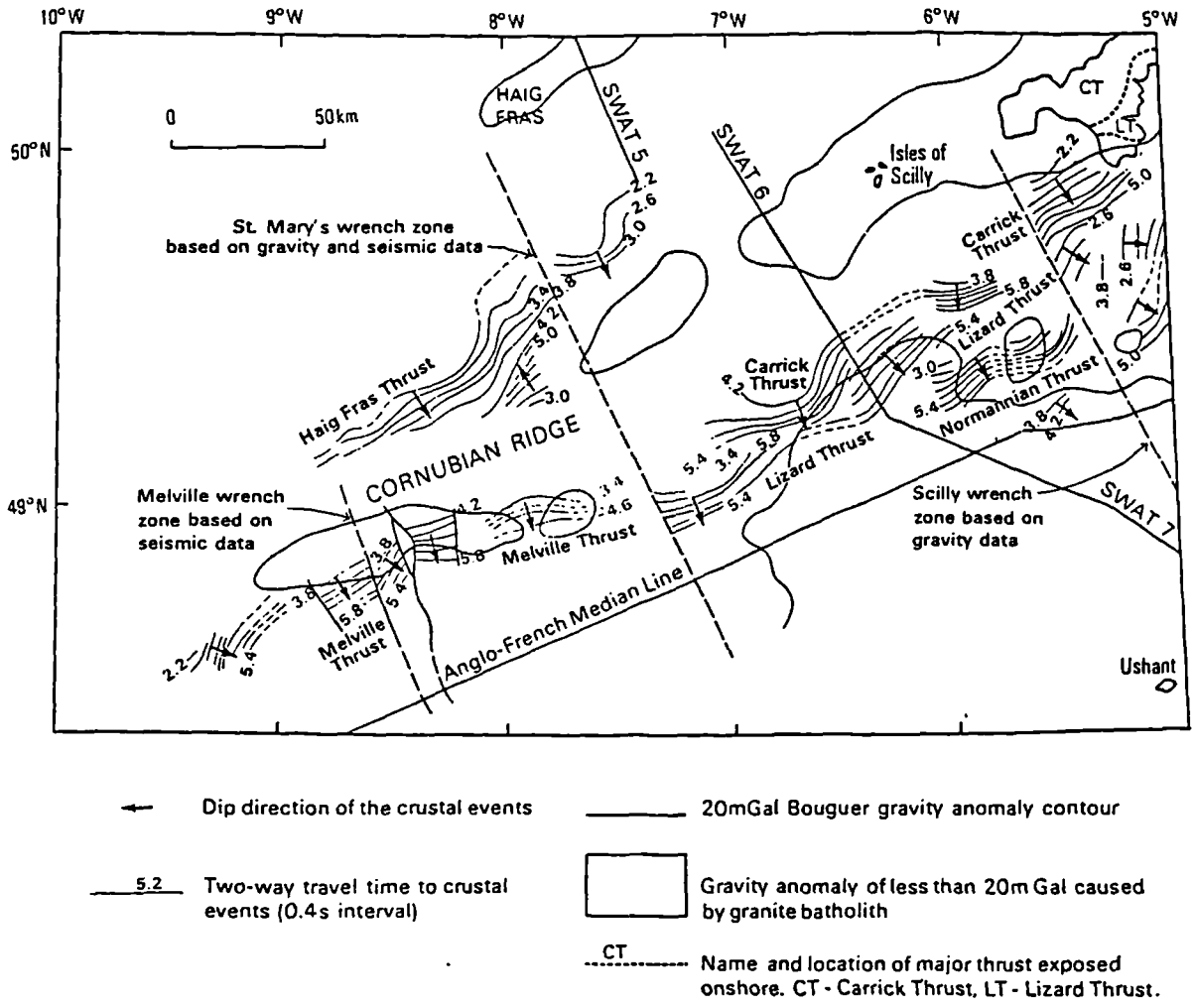

Figure 2.21 Deep crustal events in the Western Approaches (After Hillis 1988).

2.7 Summary

During the Gedinnian stage, southern Britain was part of the southern shelf of the newly consolidated Laurussian continent. Clastic sediment derived from the Caledonian mountain belt to the north was deposited upon a coastal plain to form the Dartmouth Group. A widespread transgression in the Siegenian and Emsian flooded the shelf to form a shallow sea in which the distal clastic and carbonate sequences of the Meadfoot Group developed. Fragmentation of the shelf and extension along E-W trending basement structures was active by the Emsian, with emergent horst blocks sourcing the Staddon Grits. As fragmentation and subsidence continued, deposition became focused into a series of E-W trending basins separated by rises (Table 2.3). The Gramscatho Basin developed first on the seaward edge of the shelf, where the crust was attenuated enough to generate oceanic crust. To the north and east, the Trevone and

South Devon basins developed restricted mudstone facies and limestones in areas of shallow water, whilst the north Devon area received coarse clastic material from the emergent Welsh Massif. Basic vulcanism was widespread throughout the Middle Devonian and has an intra-plate affinity consistent with extensional tectonics.

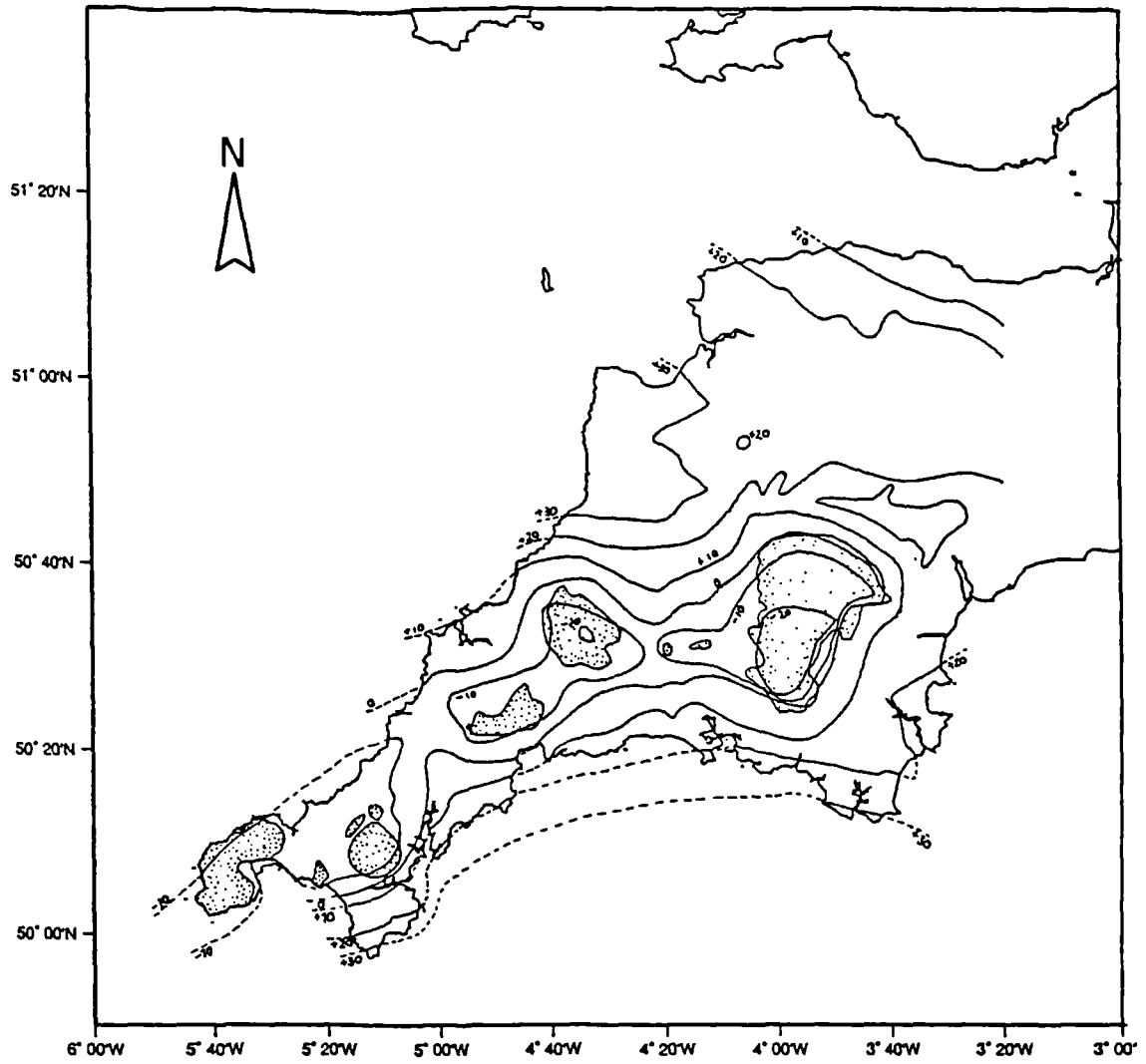

Figure 2.22 Bouguer anomaly map of SW England. Stippled areas represent granites at surface (after Bott *et al.* 1958).

The Upper Devonian marks the start of Variscan compression in southwest England. Thrusting to the south of the Gramscatho Basin produced uplift along the Normannian High, obduction of oceanic crust (the Lizard Complex) and coarse clastic input into the basin, whilst crustal flexure ahead of the nappes caused deepening of facies to the north and flooding of carbonate platforms in the South Devon Basin. Early thrusting is also recorded in the Roseland and Porthleven Breccia Formations (late Fammenian); olistolithic units formed from Palaeozoic material shed along the Normannian High.

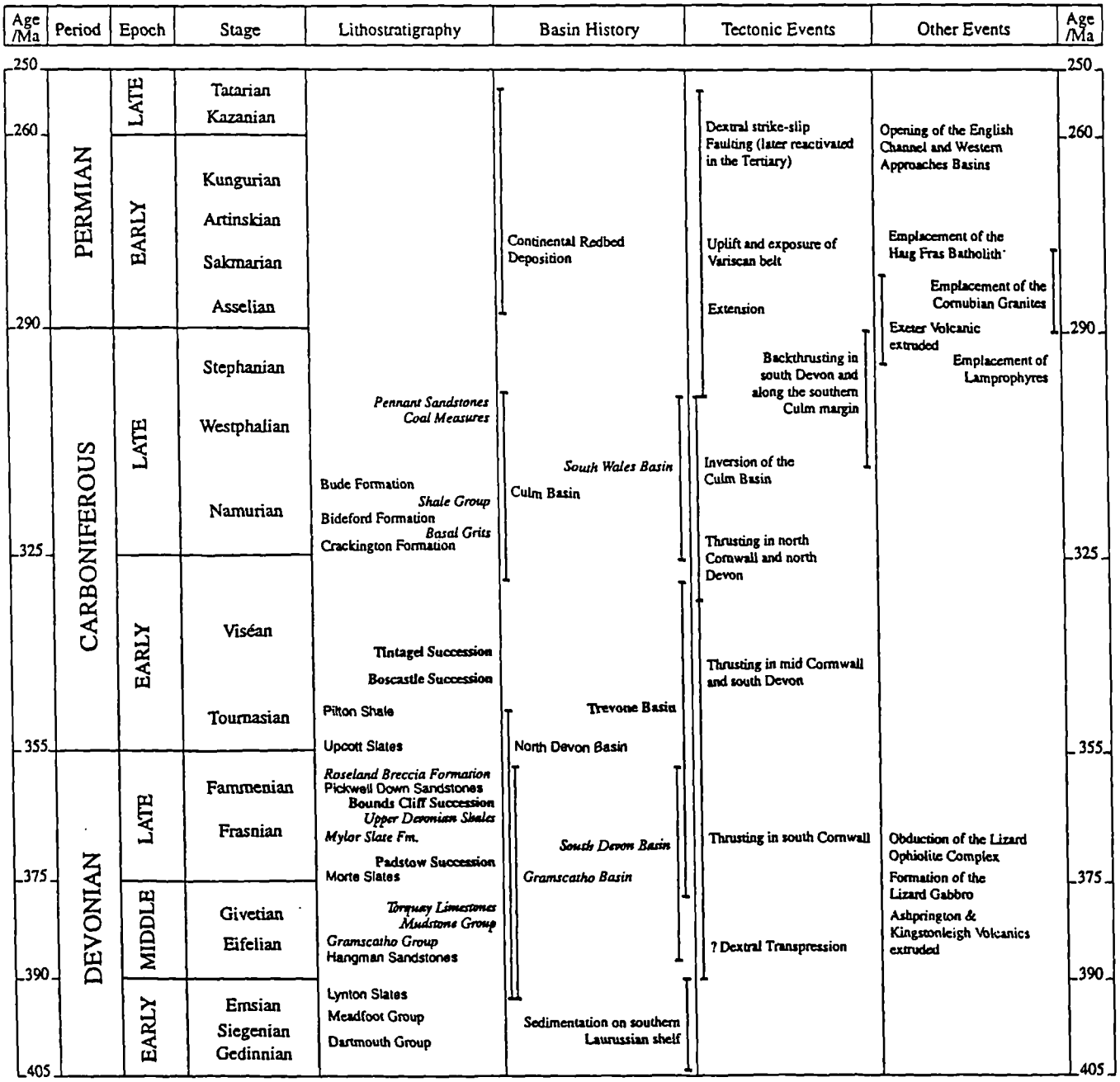

Table 2.3 Geological evolution of SW England (adapted from Evans 1990; timescale after Snelling 1985)

The thrust and fold belt migrated northwards through time until the late Westphalian, deforming the Devonian basins and transporting them northwards as thrust nappes. Backthrusting occurred along the northern margins of the Trevone and South Devon Basins, where basin-bounding thrusts acted as buttresses to the advancing nappes. The lithospheric loading of the thickening nappe stack resulted in downflexure to the north of the deformation belt and formation of the Culm and South Wales foreland basins, which were in turn inverted during compression. A further effect of crustal thickening was the generation of lamprophyres and the Cornubian Granites through partial melting of the depressed base of the crust.

The compressive stress-field which had characterised late Devonian to late Carboniferous times was replaced by extension during the Stephanian and Permian, resulting in the development of offshore sedimentary basins. Extension within the nappe-stack was facilitated by reactivation of compressional faults and fabrics, and its association with lamprophyre and granite magmatism suggests that it may record the collapse of previously thickened lithosphere. This phase of late-orogenic extension forms the subject of this work.

Chapter Three - Late-Variscan Evolution of the North Cornish Coast

CHAPTER 3 : LATE-VARISCAN EVOLUTION OF THE NORTH CORNISH COAST

3.1 Introduction

Chapters 3 and 4 present the results of fieldwork undertaken along the coast of southwest England in the period 1993-1996. Chapter 3 details field descriptions from the north coast of Cornwall whilst descriptions from the south coast of Cornwall are collected in Chapter 4. Field-mapping was conducted using 1:10 000 or 1:25 000 scale OS base maps, and hand drawn exposure maps. Mapping across such a large area presents considerable time constraints, and thus the study was restricted to coastal outcrop, concentrating on areas of high-magnitude extension identified from published works and areas identified during reconnaissance. Structural studies examine compressional and extensional features in order to evaluate the extent to which late orogenic deformation reactivates pre-existing orogen architecture. Descriptions are presented systematically from north to south across the structural grain towards more internal parts of the massif, and further divided into regions of consistent structure or sedimentation. Localities referred to in the text are accompanied by six- or eight- figure grid references with key areas shown in Figure 3.1. Correlation of extensional deformation between zones is discussed in sections 3.7 and 4.7, and implications of these findings are considered ir Chapter 6.

3.2 The Southern Culm Basin; Bude to Rusey Beach

Stratigraphy

The southern Culm Basin consists of the turbiditic Bude and Crackington Formations, which range in age from Namurian to Westphalian and represent the youngest units in SW England to have been affected by Variscan tectonism (Higgs 1991; Selwood and Thomas 1986a *and references therein*). To the north of the section, the Bude Formation comprises shales, siltstones and sandstones whilst to the south, the Crackington Formation is dominantly siltstone and shale (Section 2.2.4.1; Higgs 1991; Melvin 1986). The succession is generally right-way-up being inverted only in the short limbs of recumbent folds (Edmonds *et al.* 1979), and hence the older Crackington Formation is exposed in the cores of anticlines and on the southern margin of the basin (Freshney *et al.* 1972). The Culm rocks are truncated southwards by the Rusey Fault, a reactivated composite structure which records thrust-, normal- and transcurrent- movement episodes (Thomson and Cosgrove 1996).

Bulk structure

Structures exposed between Bude and Rusey Beach predominantly relate to D1 compression, evident in upright to recumbent chevron folds, north-dipping thrust-faults, north-dipping S1 cleavage and arrays of

east-west striking veins, tension gashes and joints (Figure 3.2). F1 folds are upright in the Bude region and fan over southwards, becoming recumbent and south-facing (Sanderson 1979) to the south of Wanson Mouth. They occur on a sub-metre to decimeter wavelength and appear to be parasitic to a major south-vergent D1 structure; the *Southern Culm Antiform* (Figure 3.2B; Ashwin 1958; Dearman 1962). The folds tighten southwards from interlimb angles of 60°-<30° (Sanderson 1979) and S1 foliation becomes more intensely developed and quartz-veining becomes more common in sandstone beds (Warr 1991b). D1 structures form zones 2-4 in the Sanderson and Dearman scheme (1973; outlined in Section 2.3.1).

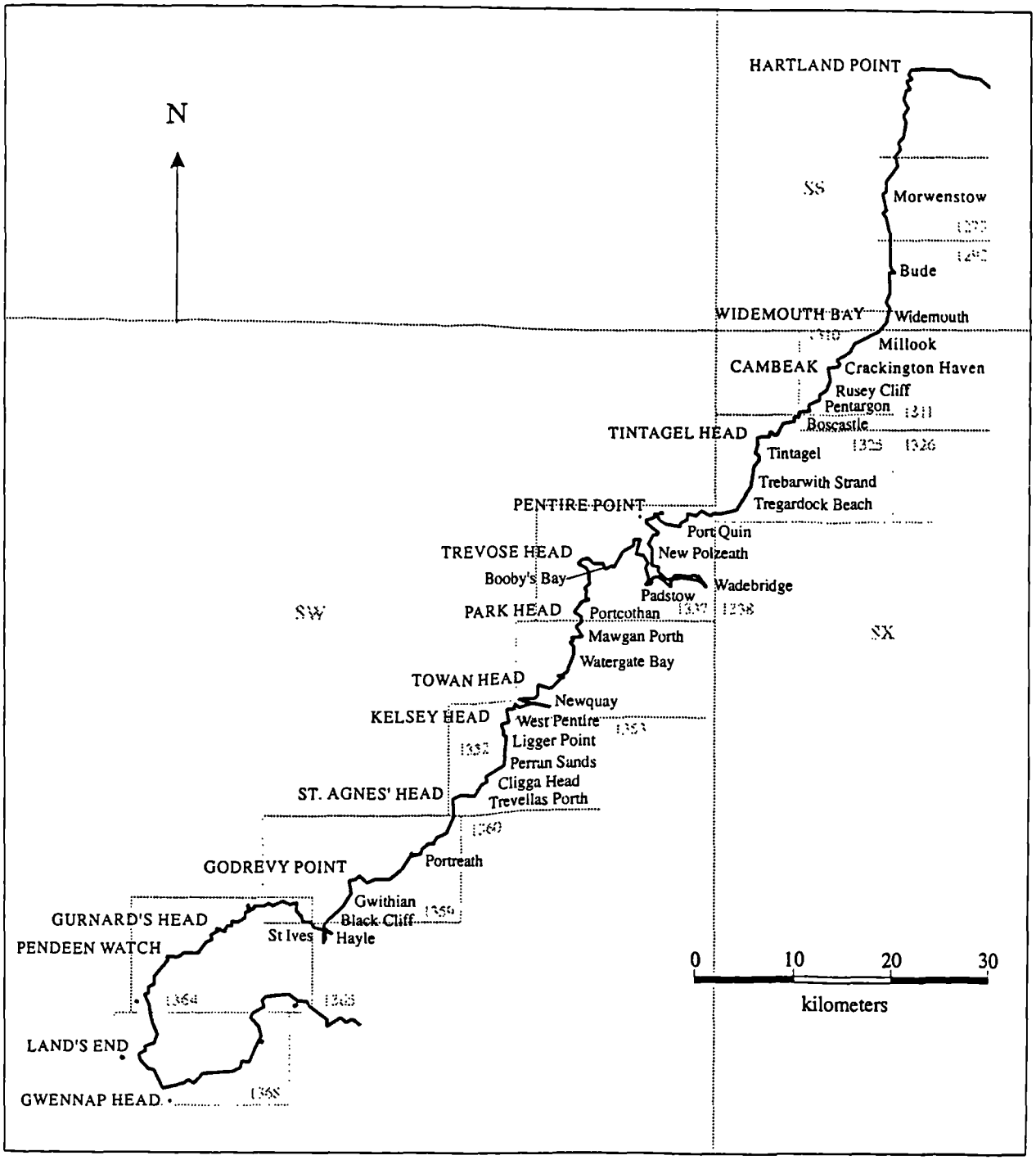

Figure 3.1 Locality map of the north Cornish coast, overlain with positions of 1:25 000 Ordnance Survey sheets.

Two groups of extensional structures are identified and appear to relate to separate events. The first (*D2*) is characterised by shallowly-dipping detachments which produced north-directed shear along bedding-planes and reactivation of T1 thrusts in extension. Such features are uncommon to the north of Millook Haven and are increasingly frequent towards Rusey Beach (Figure 3.2A). They may be traced inland by mapping of offset goniatite biozones (Freshney *et al.* 1972; Warr 1991b) and cause repetition of steeply-dipping strata which lies in the short limb of the Southern Culm Antiform (Figure 3.2B; Sanderson 1979). The second extensional event (*D3*) is represented by moderately- to steeply- dipping normal faults which crop out throughout the section. Downthrows are modally towards the north, although areas of conjugate faulting are seen, notably on the northern side of Crackington Haven. Both groups of faults are normally associated with quartz and/or calcite veining and sometimes D3 faults host lead, zinc and copper sulphides (e.g. Crackington Haven; Freshney et al. 1972). Steep (D3) faults consistently cut more shallowly dipping (D2) detachments.

Northwest to north-northwest trending dextral strike-slip and less commonly, normal oblique-slip faults are seen throughout the section, in all places cross-cutting D1-3 structures (Section 2.3.3; Figure 3.2). When traced inland, they displace the margins of the Bodmin Moor Granite (Dearman 1963) and are thus demonstrably post-Variscan in age. Faults are typically subvertical and associated with intensified fracturing within approximately 150 metres of main fault-planes The deformation zones comprise low-displacement dextral faults and subordinate antithetic sinistral faults, tension gashes, fibrous quartz veins and zones of rotated bedding and S1 cleavage.

3.2.1 Bude to Widemouth

Between Bude and Widemouth the coast is fully accessible although outcrop height is limited. Study was concentrated at Maer Cliff [SS 201 110], between Bude Haven and Compass Point [SS 2010 0950 - SS 2000 0639], and between Upton Strand and Widemouth Sand [SS 200 054 - SS 198 025] following the detailed description provided by Freshney *et al.* (1972).

Lithology

The Bude Formation crops out throughout the section and comprises moderate to thick sandstone beds (0.3-5.0 metres) with silt partings, separated by shale bands of mappable extent. Laminar and cross-stratified sandstone beds (Bouma B-C) may be traced across D1 structures, allowing accurate structural analysis along the foreshore (Freshney *et al.* 1972). Quartz veins are heterogeneously developed on the outer arcs of folds and restricted to within thick sandstone beds.

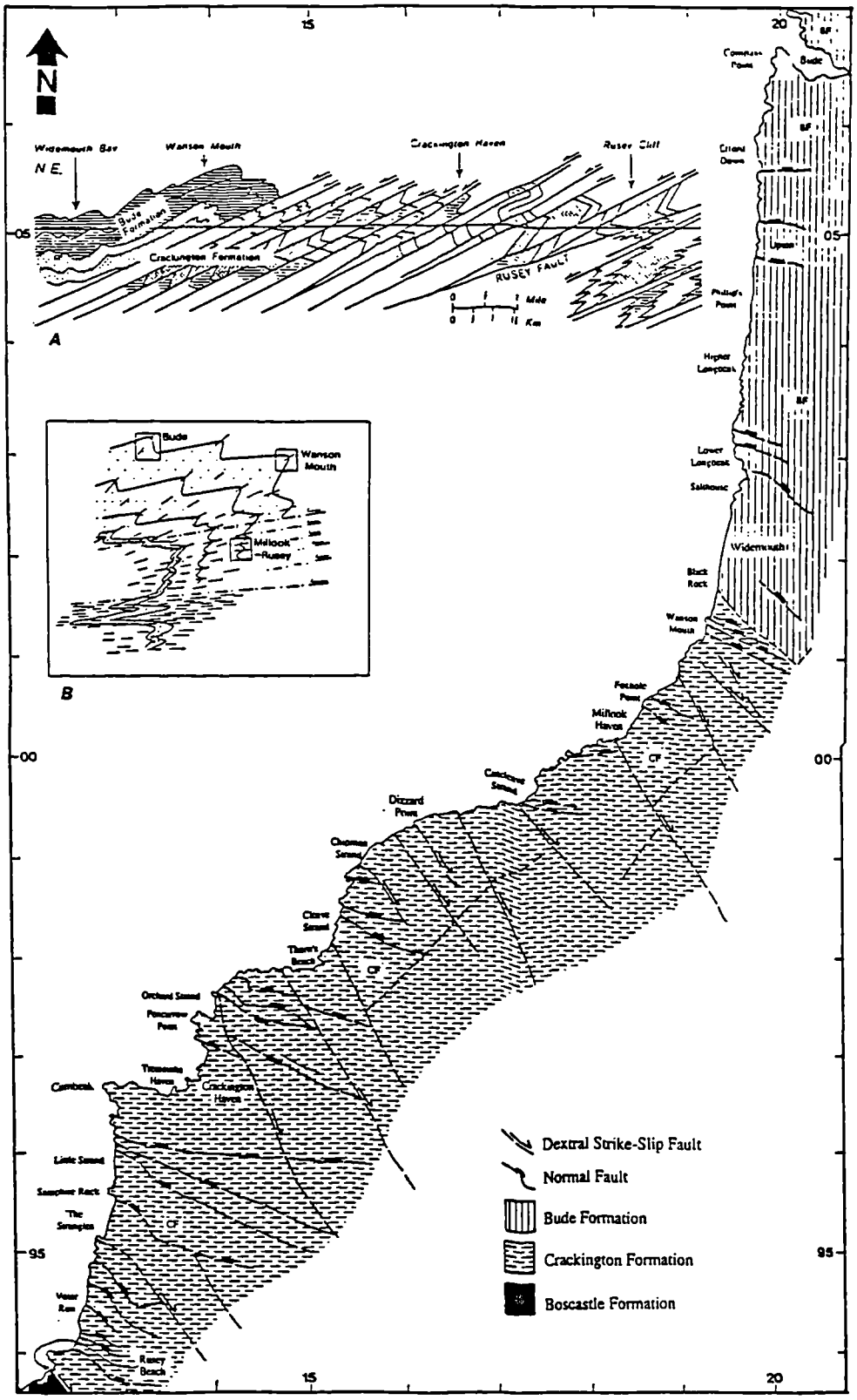

Figure 3.2 Generalised 1:50 000 solid geology map of the south Culm Basin (redrawn from BGS sheet 322 1" map; Freshney, Mc Keown and Williams 1969). Insets : (A) Interpretive cross-section between Higher Longbeak and Rusey Beach (Freshney, Mc Keown and Williams 1972). Ornament differentiates between goniatite subzones. (B) Restored (pre-extension) geometry of F1 fold structure of the South Culm Antiform with the position of Bude, Wanson Mouth and the Millook-Rusey section indicated (adapted from Sanderson 1979).

Compressional features

Bedding to the north of Bude dips moderately to the north or south and defines upright, angular F1 fold closures. S1 cleavage dips steeply north or south, and folds and cleavage face up to the north. (Figure 3.3) Fold-axes trend E/W and plunge shallowly westwards (2/271); a trend which continues as far south as Rusey Cliff (Sanderson and Dearman 1973). Thrust-faults are commonly developed along siltstone horizons and ramp through sandstone units. They steepen southwards into a zone of south-dipping reverse faults and pervasive S1 cleavage, resulting in the formation of thrust-stacks in which folds are highly disrupted (e.g. Crooklets Cove [SS 2010 0950]).

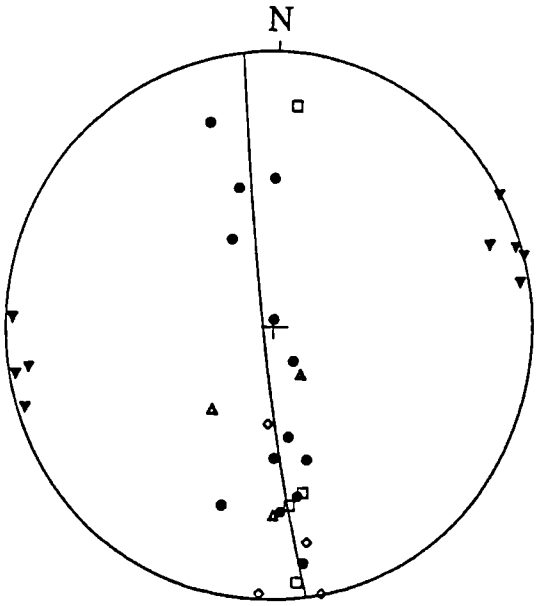

Figure 3.3 Stereoplot of compressional features, Maer Cliff to Compass Point [SS 201 110 - SS 200 064]. *Planes*; dots = S0 (13), squares = S1 (4), up-triangles = thrusts (3), diamonds = F1 axial planes (4). *Lineations*; down-triangles = F1 axes and L1 lineations (9). Girdle; 169/86W (suggesting that F1 axis = 4/079).

To the south of the Bude Canal, upright F1 folds with non-cylindrical geometries are exemplified by the doubly-plunging anticline at Whale Rock [SS 2000 0639] (Figure 3.4). S1 cleavage is pervasive and bed-parallel in slates, but occurs as spaced pressure solution seams refracted by up to 30° from bedding in sandstone beds. F1 axial planes steepen to the north and S1 forms divergent fans across fold hinges. Thrusts are exposed below the coastguard lookout (Figure 3.4), where they dip shallowly north-northwest and carry coarse sandstone beds in their hanging-walls.

Between Bude Haven and Widemouth Strand, a series of south-facing fold-pairs rotate bedding into moderately north-dipping normal limbs and more steeply north-dipping inverted limbs (Figure 3.5; King 1967; Freshney et al. 1972). Fold geometry appears closely related to lithology; with rounded fold hinges preserved in sandstones and cusped hinges in shales. Thrust and reverse faults are restricted to the hinges of folds and are less numerous than normal faults. At the southern end of the section, siltstones and thin sandstones exposed between Lower Longbeak and Salthouse preserve numerous south-facing folds and minor thrusts which are consistent with south-directed overthrusting (Figure 3.6; Plate 3.1).

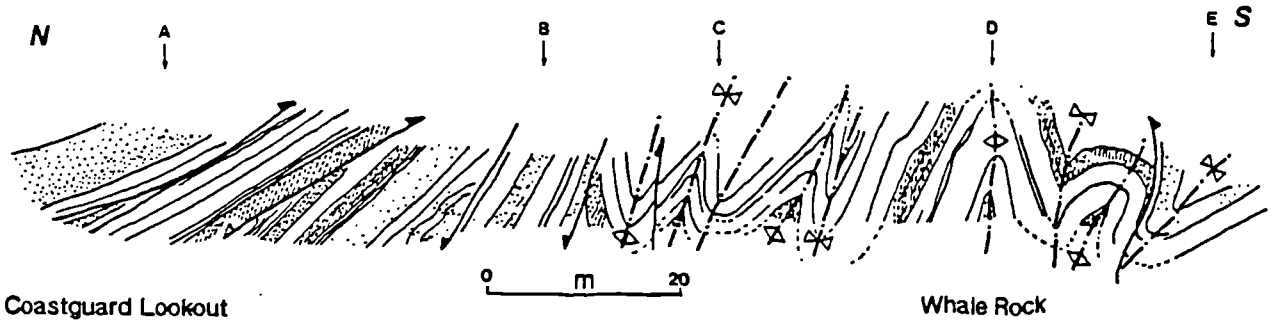

Figure 3.4 Interpretive sketch section to the south of Bude Haven : (A) Bedding-parallel T1 thrusts; (B) Steep normal faults (D3) with hanging-wall folds; (C) Close upright F1 folds; (D) Whale Rock antiform (exposed through foreshore); (E) F1 synform cut by folded reverse fault. D1 strain appears to increase towards the north, culminating in thrusting. D3 normal faults are concentrated away from F1 hinges.

Folds exposed on the foreshore are parasitic to kilometer scale folds evident from the distribution of marker beds such as the Black Rock Slumped Bed (Figure 3.2B; Warr 1991b). One such fold-pair with a wavelength of approximately 5 kilometers has its antiformal axis running through Lower Longbeak [SS 1964 0332] and its synformal axis running through Efford Ditch [SS 199 058] (Owen 1934; Figure 3.5).

Structural data collected between Upton and Lower Longbeak (Figure 3.7) shows that S1 dips modally towards the north. Bed dip-magnitude forms two clusters: (1) moderately to steeply north (long F1 limbs) and (2) shallowly north to steeply south (short F1 limbs). The S1 fabric is variably inclined (50°-75°N) reflecting the regional variation in axial planar dip. F1 axes and bedding-cleavage intersection lineations plunge shallowly to moderately east-northeast. Tectonic transport direction is estimted at between south and south-southeast on the basis of orientation, facing and vergence data.

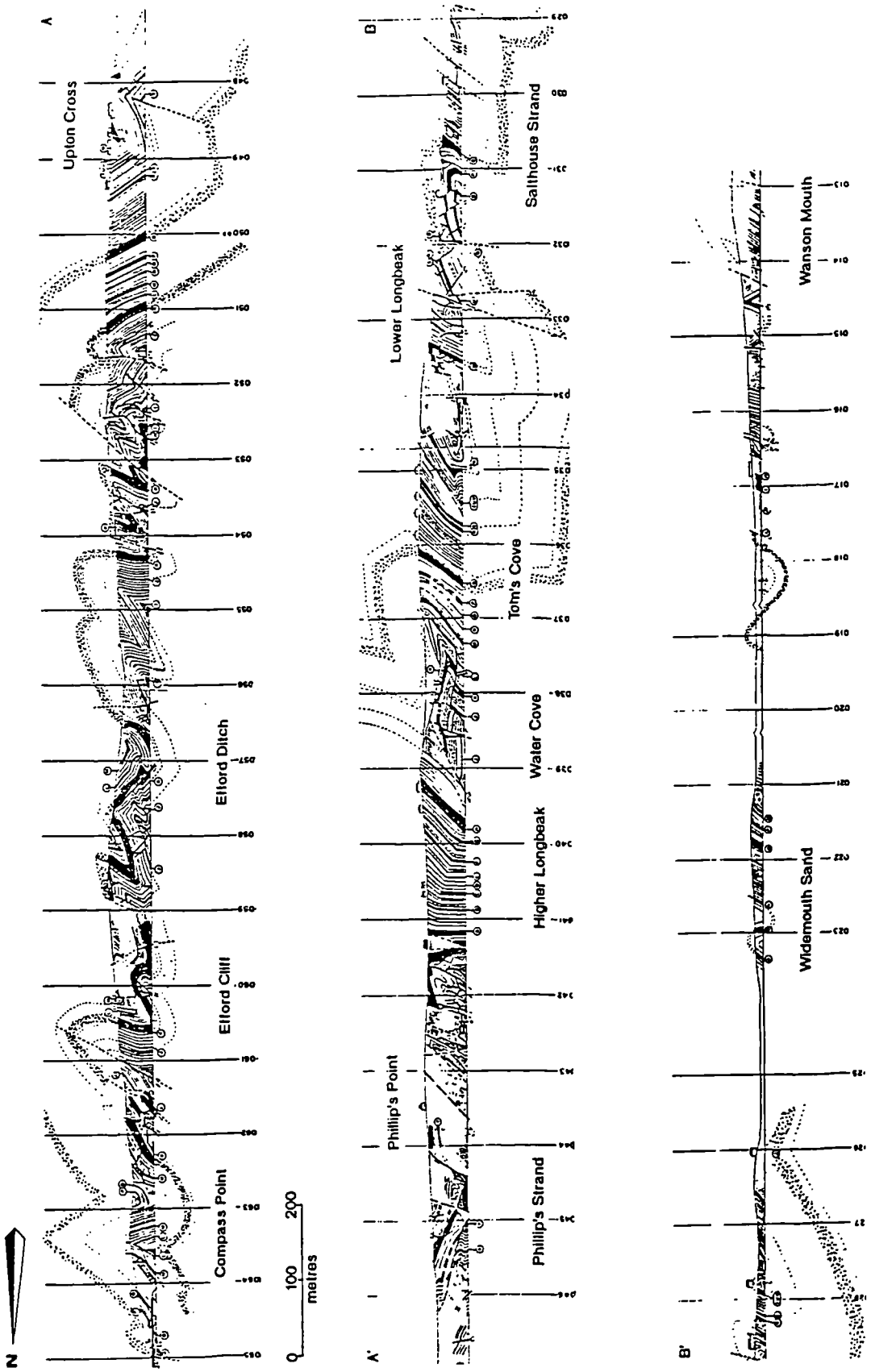

Figure 3.5 Interpreted sketch section of the cliffs between Compass Point and Wanson Mouth (adapted from Freshney *et al.* 1972). For regional context see Figure 3.2.

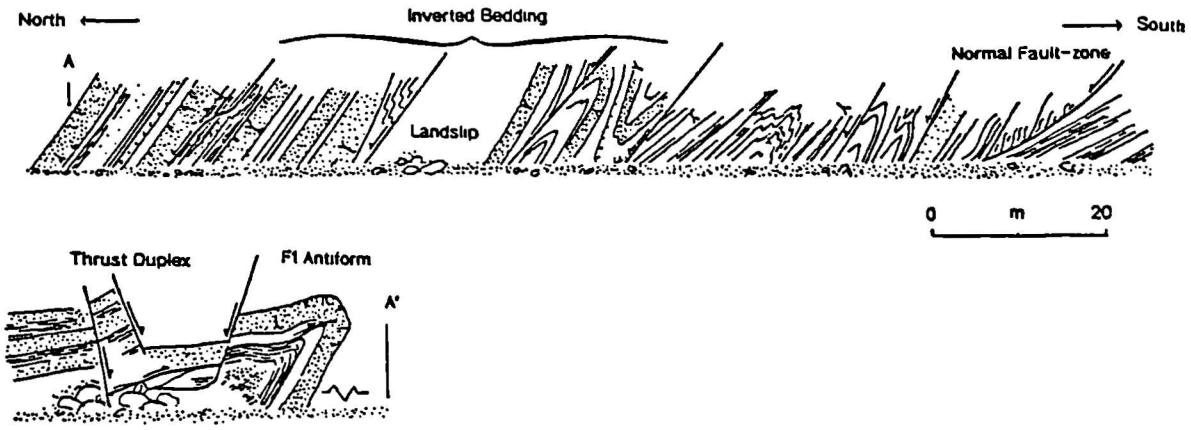

Figure 3.6 Interpreted cliff-section, Lower Longbeak. Heavy lines indicate faults, arrows denote sense of displacement. Note younging symbols (Y) change direction across fault-planes, indicating juxtaposition of fold-limbs across normal faults.

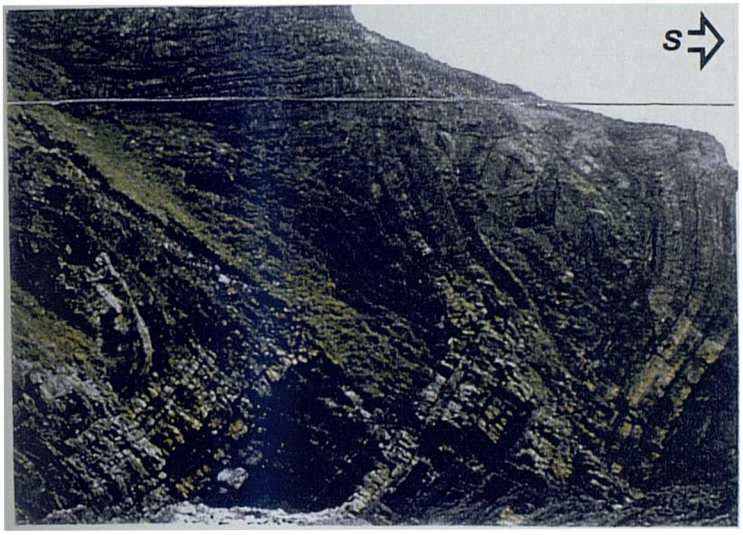

Plate 3.1 Crumpled south-verging chevron folds, Salthouse Cliffs.

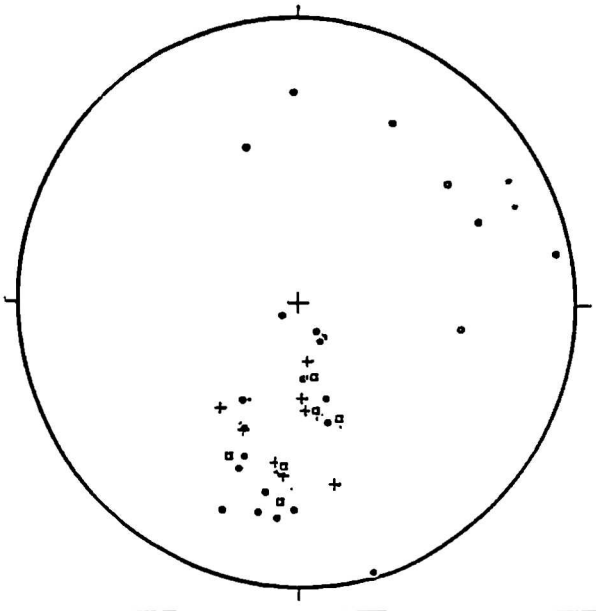

Figure 3.7 Stereoplot of compressional structure, Upton to Lower Longbeak. *Planes*; Dots = S0 (21), crosses = S1 (11), squares = F1 axial planes (6). *Lineations*; Stars = F1 axes (2), open dots = L1 lineations (4).

Extensional features

North of the Bude Canal, extension is expressed by north- and south- dipping conjugate normal faults. Slickenfibres plunge down the dip of the fault-planes or pitch slightly clockwise of maximum dip, suggesting a down-dip or dextral dip-slip sense of hangingwall translation. Between Bude Haven [SS 2013 0653] and Compass Point [SS 1992 0638], steep normal faults are developed in the north-dipping long limbs of upright F1 folds on an interval of approximately 50 metres. They typically have throws of 3 metres and are lined by fault-breccia. All features are associated with the second extensional phase (D3).

Steep east-west trending and north-dipping normal faults are common south of Compass Point (Figure 3.8). They truncate the normal limbs of large (400 metre wavelength) F1 folds and are commonly observed in shales within the southern limbs of F1 synclines. An east-west trending, steeply south-dipping normal fault crops out at the northern end of Upton Beach [SS 2000 0500] and displaces an F1 fold pair by over 15 metres (Freshney *et al.* 1972). Listric normal faults are seen immediately to the south, dissecting tight F1 folds.

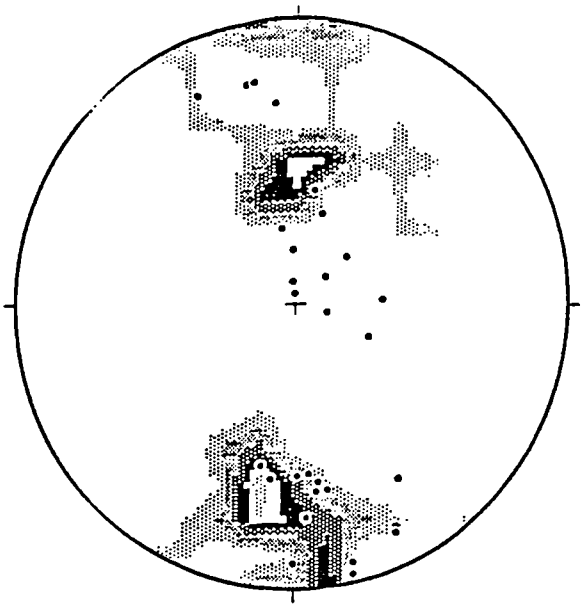

Figure 3.8 Stereoplot of extensional features, Upton to Lower Longbeak (*Contours*; Poles to fault-planes (51). *Dots*; Slickenlines (33). Note that faults dip either steeply north or less steeply south, demonstrating the influence of early fold limb orientation on later extensional surfaces. Clusters show the modal orientations of steep faults (D3), whilst secondary clusters against the primitive identify shallowly-dipping D2 detachments.

Phillip's Point [SS 1992 0436] is bounded on both sides by steeply north-dipping normal faults which have a cumulative downthrow of approximately 335 metres north (Freshney *et al.* 1972). The hangingwall of the northern fault is cut by north-northwest trending dextral faults. Smaller-displacement normal faults dip both north and south and record throws of up to a metre within a diffuse deformation zone agaist the high-displacement faults (Figure 3.8).

Extensional deformation is more intense south of Phillip's Point, where steep inverted bedding planes host normal slickenlines. Steeply north-dipping faults cross-cut thick sandstone beds and are most commonly

found in F1 hinges as seen at Tom's Cove [SS 1980 0360]. Thin sandstone layers within shale units are boudinaged and rotated above moderate-angle faults.

Normal faults occur at intervals of less than 50 metres between Upper and Lower Longbeak (Plate 3.2), dissecting F1 fold hinges (Figure 3.9) and cutting shallowly-north- dipping T1 thrusts at Water Cove which lie subparallel to bedding. Such thrusts sometimes focus extensional *D2* deformation which is evident from arrays of quartz tension-gashes which give a top to the northwest sense of shear. The southernmost end of the section preserves kink-bands which distort the S1 fabric. Their axial-planes dip shallowly east, and their modal westerly vergence suggest post-D1 west-directed compression.

Plate 3.2 Typical steep D2 normal fault, Higher Longbeak. Downthrow is approximately 4 metres southeast.

Thin Section Analysis

Siltstones and mudstones consist of detrital quartz, plagioclase and opaque minerals containing a strong schistosity defined by alignments of muscovite grains and represent a sub-greenschist assemblage. S1 cleavage shallowly transects iron-stained bedding and is formed of fine muscovite laths. Quartz grains have dusty margins, show little or no undulatory extinction and retain their detrital shapes, indicating low magnitude strain. Chlorite growth is noted in fault-rocks at Lower Longbeak replacing muscovite. It appears to have developed during fluid influx and shows no grain-scale morphological features indicating syn-tectonic growth.

A second group of deformation structures is characterised by brittle microstructure; kinks and fractures of muscovite laths within S1; bookshelf structures formed from feldspar grains and tensile quartz-veins at 90° to S1 fabric. In mudstone units, a type-I extensional crenulation fabric is locally developed, demonstrating

extensional (*D2/3*) deformation through more ductile mechanisms in finer grained units. Microstructures corroborate field evidence in indicating simple shear down the dip of S1 cleavage towards the north to northwest.

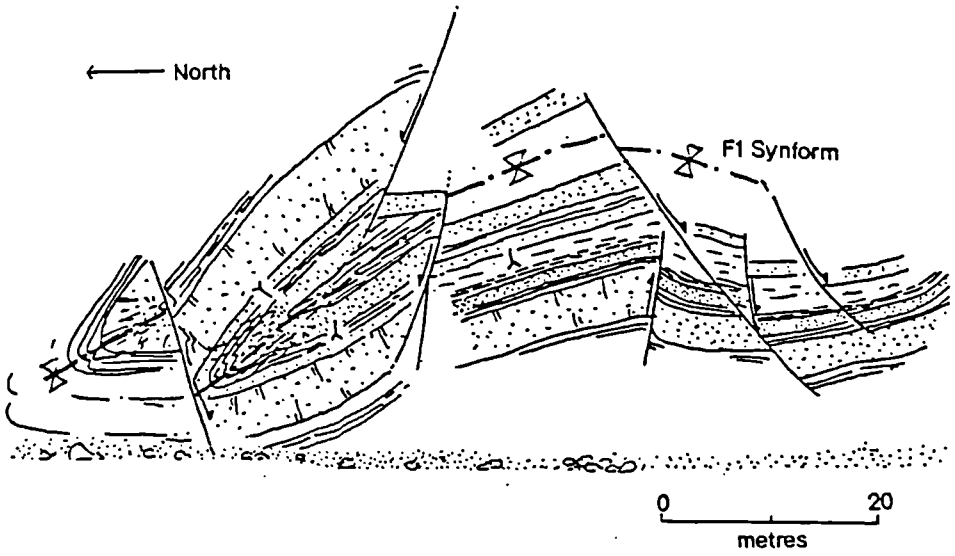

Figure 3.9 Faulted south-facing F1 synform cut by curviplanar north-dipping normal faults, Lower Longbeak.

3.2.2 Widemouth Sands to Millook Haven

Lithology

The boundary between the Bude and Crackington Formations forms the southern margin of Widemouth Sands, and lies immediately to the south of the west-northwest trending Widemouth South Fault (Figure 3.2). The Bude Formation comprises massive graded sandstones interbedded with impure sandstones, siltstones and black shales. It is locally repeated by F1 folds and (where beds are steeply dipping) by *D3* normal faults (Figure 3.2A). South of the boundary, indurated green-grey sandstones overlie pyritous grey shales with pink-grey sandstone interbeds (Crackington Formation). Pale-grey sandstone beds are exposed along the section at Saltstone [SS 191 009], Foxhole Point [SS 186 006] and Millook Haven [SS 184 001]. They range in thickness from 5 centimeters to 3 metres and vary in colour from grey-green or purple. Sandstones and purple slates exposed at Millook Haven contain abundant plant debris and a high muscovite content (Freshney *et al.* 1972).

Compressional features

The northern margin of Widemouth Sand [SS 197 020] exposes an east-plunging F1 antiform with black shale core. Outcrops in the backcliffs to the south contain a series of F1 folds with west-plunging axes and steeply south-dipping axial planes, whilst the southern foreshore is crossed by en echelon periclines with geometries consistent with their position on the southern limb of an F1 antiform (Figure 3.5).

At Wanson Mouth F1 axial planes dip 45° N and face south, their normal limbs often hosting T1 thrusts. Recumbent chevron-folds are well exposed at Foxhole Point and Millook Haven [SS 1865 0055, SS 1825 0010] (Plate 3.3). Their geometry suggests that they formed as upright folds through flexural slip and were progressively overturned towards the south by the action of south-directed subhorizontal simple shear (Sanderson 1979; Lloyd and Whalley *1997*). They have approximately 2 metres amplitude and 8 metres wavelength and plunge gently westwards, their long, inverted, north-dipping limbs commonly hosting T1 thrusts above which S1 is intensely developed.

Plate 3.3 Chevron fold cascade, Millook Haven.

Bedding is commonly inverted south of Wanson Mouth, and hence the section may represent the inverted limb of the Southern Culm Antiform whilst the Bude-Widemouth section forms its normal limb (Figure 3.2B; Freshney *et al.* 1972; Sanderson 1979). The interpretation of fold attitude in terms of position within the limbs of a major structure is somewhat simplistic, and up to three sub-phases within a progressive D1 deformation event may be present (Lloyd and Whalley 1997; Section 3.2.5).

Extensional features

The frequency of extensional faulting increases markedly into the Crackington Formation with shallowly north dipping D2 detachments seen increasingly south of Wanson Mouth. A north dipping normal detachment runs at beach-level around Bridwell Point [SS 1856 0023] with gouge and pods of cataclasite developed along its trace. It follows the interface between shale and sandstone beds, with synthetic Riedel shears cutting into the sandstones of the footwall. A dextral component of movement is evident from obliquely oriented quartz slickenlines. Intra-bed extensional movement may be significant as bedding surfaces contain stepped quartz slickenlines which recording two phases of shear in the direction of step

offset: the first with smooth profiles updip (thrust-sense or flexural slip during folding) and the second, overprinting set with smooth profiles downdip (indicative of extensional shear). Outcrops at Foxhole Strand [SS 1856 0040] are conspicuous for their F1 chevron folds but also preserve quartz tension gashes oriented parallel to Riedel shears which indicate a top-to-NNW sense of shear. Further south at Millook Haven, north-dipping D2 detachments are developed in mudstone beds and associated with centimetre-scale north-verging F2 folds (Figure 3.10). Where they cut thin siltstone beds the D2 detachments show horizontal separation of hangingwall beds by approximately 30 centimeters to the north or northwest. The magnitude of extension is difficult to establish in the field but may locally be as much as 35% on the basis of stratigraphic repetition (Freshney *et al.* 1972).

Low-displacement, north-dipping steep normal faults (*D3*) occur at intervals of approximately 100 metres, isolating F1 fold hinges and offsetting thick sandstone beds at Saltstone Strand [SS 1917 0086]. Application of the Wernicke and Burchfiel method (Section 1.4) indicates that *D3* faulting accounts for 22% of N/S extension, but the pattern of Namurian goniatite zone outcrop studied by Freshney *et al.* (1972) suggests that faults at Wanson Mouth and Foxhole Point may have northward downthrows of several hundred metres (Figure 3.2).

All extensional structures are crosscut by dextral faults at Wanson Mouth, Foxhole Point and Millook Haven (Figure 3.2; Freshney *et al.* 1972). Where the fault-planes are exposed (e.g. [SS 1869 0058]), they display sub-horizonal stepped quartz slickenlines trending NW-SE. Secondary dextral shear-zones are seen in mudstone units at Bridwell Point [SS 1835 0022] and NE-SW trending antithetic sinistral tension gashes are locally preserved.

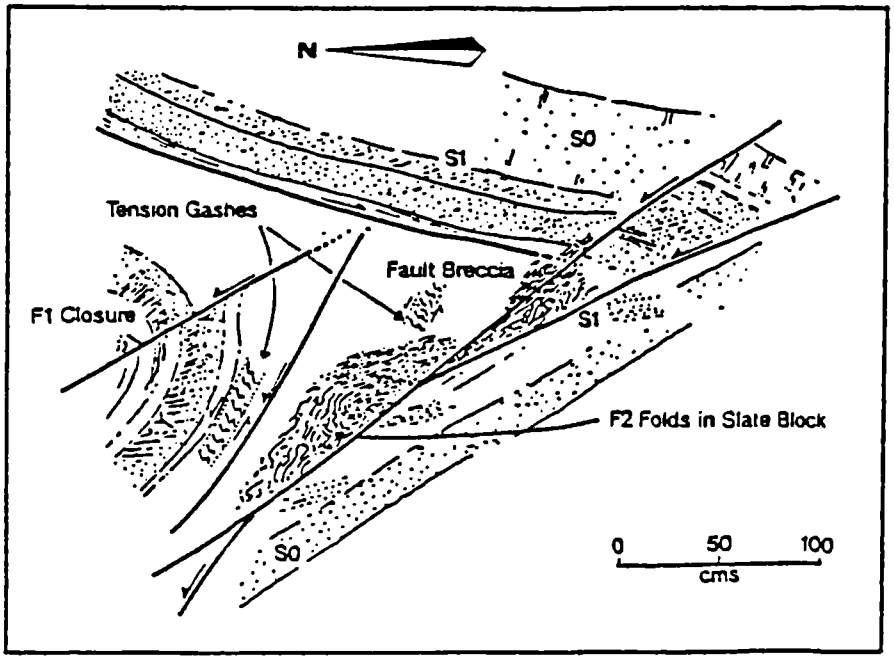

Figure 3.10 Normal faulting adjacent to core of F1 chevron fold, North Millook Haven. Note minor F2 down-dip vergent folds and fault-breccias developed against north-dipping detachment plane.

Thin section analysis

Samples were taken of sandstones and silty mudstones at both Widemouth and Millook Haven and show little variation in microstructure. The Widemouth samples of Bude Formation material are diagnostic of low-grade deformation, evident from quartz and plagioclase grains with speckled margins which preserve attrition pits and show no irregularity of extinction and hence no internal sign of deformation. A single cleavage is present in aligned muscovite and less commonly, chlorite laths accompanied by opaque-mineral shape fabric in fine mudstones. The thin-sections from Millook Haven (Crackington Formation) show evidence for heavy weathering and again contain muscovite laths which define slaty S1 cleavage and show no signs of quartz or feldspar deformation. Mica grains are not kinked and no other mineral alignment is observed.

Whilst there is no clear expression of extensional microstructures the existence of two groups of extensional macrostructure suggest that extension is only pervasive on a grain-scale in discrete zones that have not been sampled.

3.2.3 Millook Haven to Crackington Haven

Between Millook and Crackington Haven heavy landslippage and limited access from either end provided limited opportunity for study. Traverses around Millook Haven [SS 184 001] and from Pencannow Point to Tremoutha Haven [SX 137 974 - SX 134 965] were undertaken to characterise local extension.

Lithology

Remaining within the Crackington Formation, the coast between Millook Haven and Crackington Haven exposes grey slaty shales with laminar siltstone interbeds. Sandstone beds up to 50 centimeters thick are common throughout the succession, and massive, iron-stained, pink-grey or green-grey sandstones up to 1.2 metres thick crop out on the southern side of Millook Haven, at Pencarrow Point, Thorn's Beach and at the base of Long Cliff. The cliffs expose a strike section as far as Chipman Strand [SX 160 991], with stratigraphic variation occurring across NW-trending dextral wrench faults (Freshney *et al.* 1972). Outcrops are heavily iron-stained around wrench faults at Cancleave Strand, and contain plant-remains and goniatites.

Lithologies around Crackington Haven are highly variable from black slaty shales to coarse sandstones. with clear grading, grooved bases and rippled tops. Siltstone and shale units often show soft sediment structures where overlain by coarse sandstones. The sheet dip of bedding is moderately to the north and inverted indicating a position within the southern limb of the Southern Culm Antiform (Figure 3.2B).

Compressional features

Between Millook Haven and Sharnhole Point [SX 1713 9944], chevron folds with interlimb angles of 20°-30° (Figure 3.11; Freshney *et al.* (1966) dip shallowly north and dominate D1 structure. The folds continue to Orchard Strand [SX 1418 9754], where beds dip 45° north in inverted F1 limbs and 20° north in normal F1 limbs. Out-of-fold thrusts are observed in such F1 hinges, displacing thick sandstone units in F1 hinges and dying out into shale units in F1 limbs (Warr 1991b).

Uninverted bedding crops out from approximately 400 metres to the south of Pencannow Point until Crackington Haven, locating the short, common limb of an intermediate-scale D1 fold-pair (Figure 3.2 *Millook-Rusey*). Bedding-parallel thrusts present along the bases of coarse sandstone horizons in the normal limb are seen to ramp up succession and die out in shale units. Steep bedding on the southern side of Crackington Haven is inverted, indicating the presence of an F1 antiform with axial plane dipping approximately 30°N beneath the beach (Figure 3.12). A group of F1 folds with wavelengths of approximately 50 metres are exposed 70 metres to the southwest. Again, out-of-fold thrusts are present in sandstone fold-hinges, as seen at Bray's Point [SX 1397 9675].

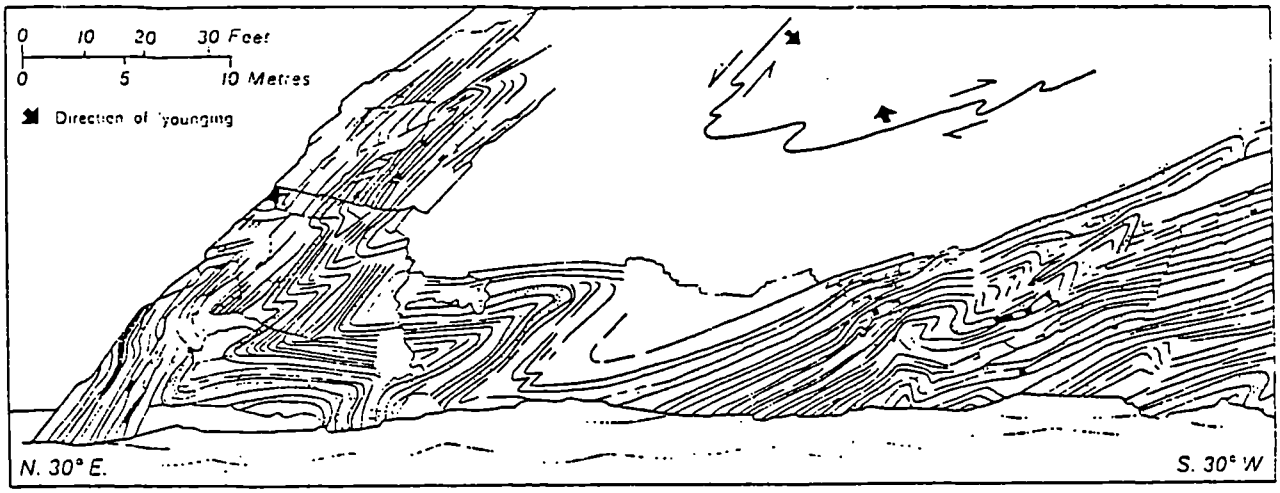

Figure 3.11 Closure of intermediate-scale F1 synform, Cleave Strand [SX 1541 9828]. Inset sketch illustrates parasitic folds and younging relationships (Freshney *et al.* 1966).

Bedding and S1 cleavage recorded around Crackington Haven dip moderately to shallowly northwards, and sometimes southwards in short F1 fold limbs (Figure 3.12; 3.13A). Variations in bed-dip thus reflect position within F1 folds or demonstrate rotation of primary fabrics by late normal faults (D3). F1 fold axes and bedding-cleavage intersection lineations plunge shallowly to the west or east, plotting close to the fold axis predicted from the girdle distribution of bedding.

Extensional structures

Extensional detachments (D2) trend east-west and dip at <35° north between Cancleave Strand [SX 1713 9944] and Dizzard Point [SX 1650 9930]. The detachments are associated with zones of north-verging and gently west to northwest plunging F2 folds and a south-dipping S2 crenulation cleavage. Both S2 cleavage- and F2 fold- vergence is down the dip of the respective detachments (i.e. to the north). Detachments are most commonly developed within fine-grained lithologies and hence their development may be dependant upon the presence and orientation of such lithologies. The relative age of D2 is demonstrated at Orchard Strand, where an intermediate-scale F1 antiform contains zones of downdip-vergent F2 folds in both of its limbs. The consistent vergence proves that the F2 folds formed after D1, *i.e.* they are not rotated about F1 folding (Freshney *et al.* 1966).

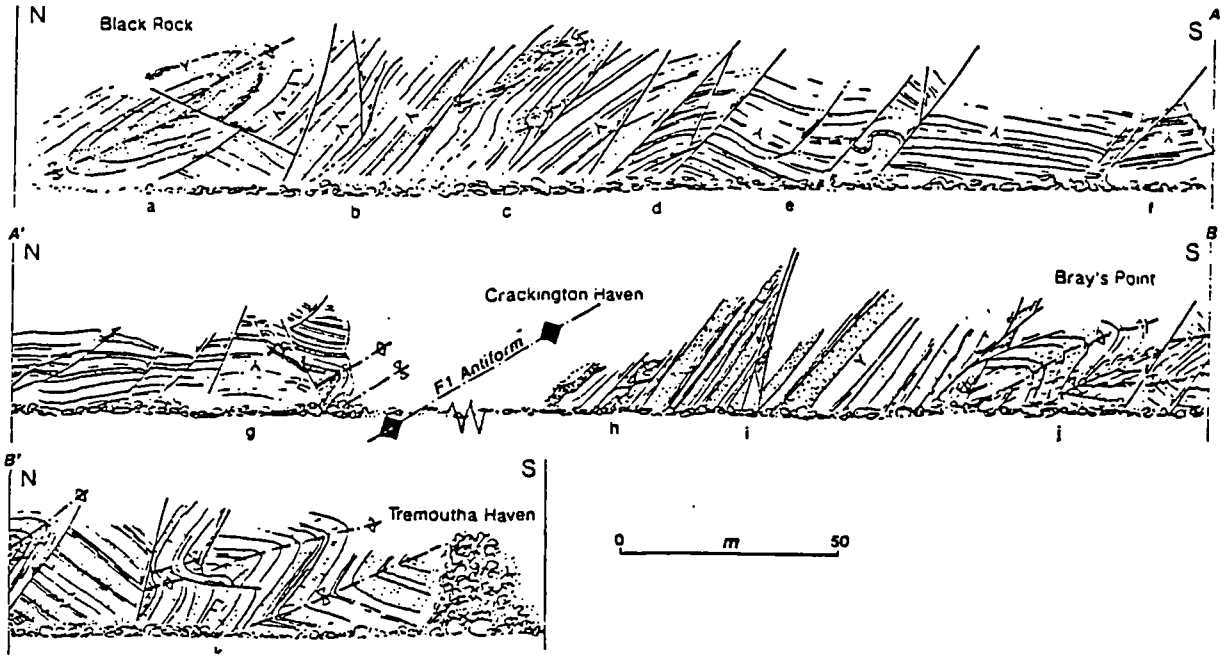

Figure 3.12 Cliff section from northern Crackington Haven to Tremoutha Haven. (a) Dissected F1 fold-pair. (b) Normal bedding transected by D1 thrusts. (c) Down-dip verging folds above normal fault-plane, formed through modification of parasitic s-folds in inverted F1 fold-limb. (d) NW-dipping normal faults. (e) Curviplanar normal faults. (f) Dextral oblique-slip faulting. (g) Conjugate faults accommodating 35% horizontal extension. (h) Heavy quartz-veining about normal faults. (i) Paired faults connected by Riedel shears. (j) Fanning S1 cleavage. (k) Out-of-fold thrusts reactivated as normal faults.

D2 detachments are again exposed at Black Rock [SX 1390 9719], 300 metres to the south of Pencannow Point. Shallowly north-dipping, quartz-veined normal faults with associated downdip-vergent asymmetric F2 folds are strongly developed in the footwall region of a primary thrust (Figure 3.12; *location a*). The folds verge down the dip of bedding and tension gash arrays again indicate top to the north simple shear. An S2 spaced pressure solution cleavage is present in mudrocks 50 metres to the south of the beach at Crackington Haven and dips moderately south-southwest, axial-planar to F2 folds exposed above a north-northeast dipping detachment (locality, Figure 3.12; *between i and j*). The detachment is curviplanar and is associated with strong quartz-veining and predominantly north-northeast plunging slickenfibres.

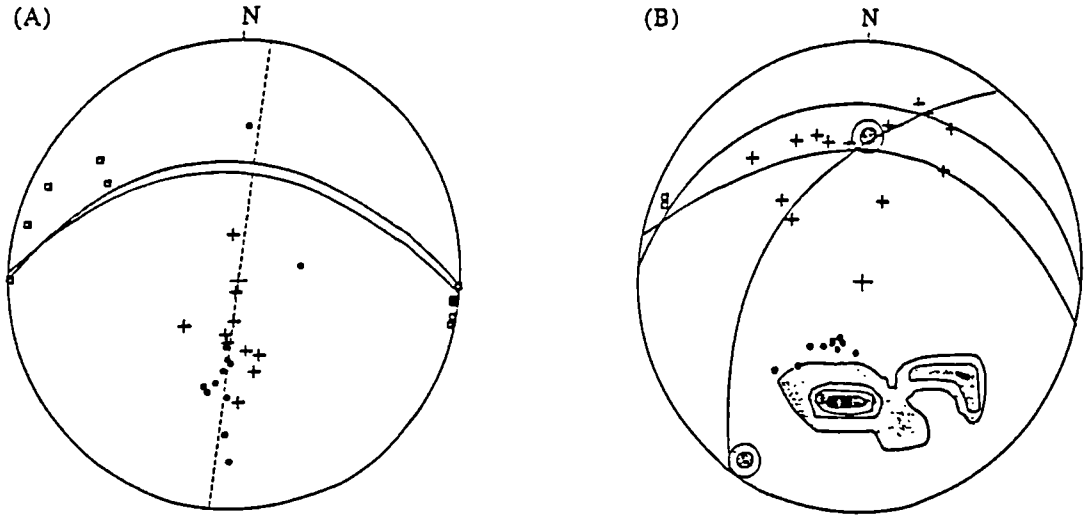

Figure 3.13 Stereoplots of structural elements, Crackington area. (A) Compression; *Planes*: dots = bedding (11), crosses = S1 cleavage (10). *Lineations* : squares = L1/F1 axes (8). *Great Circles*: S0 girdle (dashed) 008/89 W, mean S1 plane (grey) 099/44N, mean S0 plane (solid) 102/49 N. (B) Extension; *Planes*: 1% area contours = D2 fault-planes (9), dots = D3 detachments (10). *Lineations*: crosses = slickenlines (13; mean 39/354), squares = L2 lineations (2). *Great Circles*: mean fault planes (D2 : 105/42 N, 039/50 NW; D3 : 092/23 N).

D3 steep normal faulting disrupts F1 folds between Dizzard Point and Pencannow Point [SX 165 993 - SX 138 974], back-steepening bedding to near vertical in places through movement along curviplanar faults which allow back-rotation of hanging walls (e.g. [SX 1603 9910]; Freshney *et al.* 1972). Around Crackington Haven, steep normal faults again produce rotation of early fold-limbs in their hanging walls (Figure 3.12) across broad northwest-verging drag-folds. Conjugate east-west striking faults exposed to the northern side of Crackington Haven beach produce a value of 35% extension using the Burchfiel and Wernicke method (Section 1.4). Their movement planes preserve downdip-plunging normal slickenlines overprinted by horizontal slickenlines which suggest dextral reactivation following extension (Warr 1991b).

Stereographic analysis of extensional structures confirms that D2 faults dip moderately to steeply north and slickenfibres plunge downdip, parallel to the dip direction of bedding planes (Figure 3.13B). South-dipping antithetic D2 faults are developed to the south of Crackington Haven, but are subordinate to north-dipping faults. D3 detachments dip shallowly to the north and strike approximately 10° clockwise of D2 faults. Lineations formed at the intersection of S2 cleavage and bedding or S1 plunge shallowly towards 290°. The range of orientations displayed by bedding and S1 cleavage defines a common girdle (008/87 W; Figure 3.13A), the pole to which is parallel to the observed L2 lineation (3/098 *predicted*, 5/290 *observed*). F2 folds thus have a common ε_3 direction with and are coaxial to F1 folds.

Northwest-southeast trending strike-slip faults are again present throughout the section, with steeply-plunging dextrally-verging folds developed in shales to the west of Dizzard Point and the southwest of

Cancleave Strand. The trend of the dextral faults is approximately 140° (e.g. Barton Strand, 100 metres north of Crackington Haven). Steep dextral faulting is also observed on the southern side of Crackington Haven, where steep bedding-planes form the wall-rocks to a mineralised fault with subhorizontal slickenfibres (Freshney *et al.* 1972).

Thin section analysis

A sample of siltstone collected from the southern rocks of Crackington Haven reveals that the S1 foliation is defined by crudely aligned mica shards oriented subparallel to bedding. Quartz grains display unit extinction and retain a subangular sedimentary shape, suggesting that they have experienced little internal plastic deformation. A weak second fabric (S2) is observed where micaceous bands are offset towards the right by brittle microfractures oriented approximately 45° clockwise of S1 and indicative of downdip D2 shear.

3.2.4 Cambeak to Rusey Beach

Lithology

The Crackington Formation crops out along the whole section and comprises grey slates with thin, laminar siltstone and sandstone beds (See Figure 3.2). The promontory at Cambeak [SX 128 967] exposes sandstone beds up to 5 metres thick and of variable colour, locally containing ironstone nodules and rip-up clasts. They crop out for over a kilometer to the south due to repetition by low-angle and high-angle north-dipping normal faults (Freshney *et al.* 1972; Section 3.2.7). Slates, laminar siltstones and thin sandstones are exposed at Strangles Beach [SX 131 954] and sandstone beds reaching 0.6 metres thickness occur at Voter Run [SX 1262 9489]. Quartz and calcite veins are common and their wide variation of orientation and composition appear to relate to several episodes of deformation.

Compressional features

Recumbent F1 chevron folds with east-west trending axes and south-dipping overturned limbs typify the section. They face down to the south, again suggesting that they are parasitic within the inverted limb of the Southern Culm Antiform. Exposures between Cambeak and Northern Door [SX 1300 9611] best demonstrate the nature of D1, with angular to rounded, tight, recumbent F1 folds picked out by sandstone beds. The sandstone headlands of Voter Run [SX 1255 9400] and Lower Strangles [SX 128 951] again preserve recumbent F1 folds which are truncated by north and northeast dipping thrust-faults at Rusey Beach.

South-verging monoclines locally refold both normal and inverted F1 limbs and are associated with a patchy, north-dipping crenulation cleavage. They must therefore postdate D1 but are both kinematically inconsistent with, and offset by D2 detachments (e.g. Lower Strangles [SX 1288 9503]). These south-vergent folds are thus termed F1b, and are explained as the products of progressive D1 deformation (Freshney *et al.* 1972; Lloyd and Whalley 1997).

The orientation of compressional structures along the section is consistent with those around Crackington Haven (*compare* Figure 3.14A *with* Figure 3.13A). Bedding has maxima at 105/50N and 100/26N, indicating an F1 interlimb angle of less than 30°, whilst S1 cleavage subparallels bedding. The range displayed by bedding and S1 cleavage relates to reorientation due to F1b folding. F1 fold axes and bedding-cleavage intersection lineations plunge gently NW or WNW, and together with fold vergence and facing indicates south-directed shear during D1.

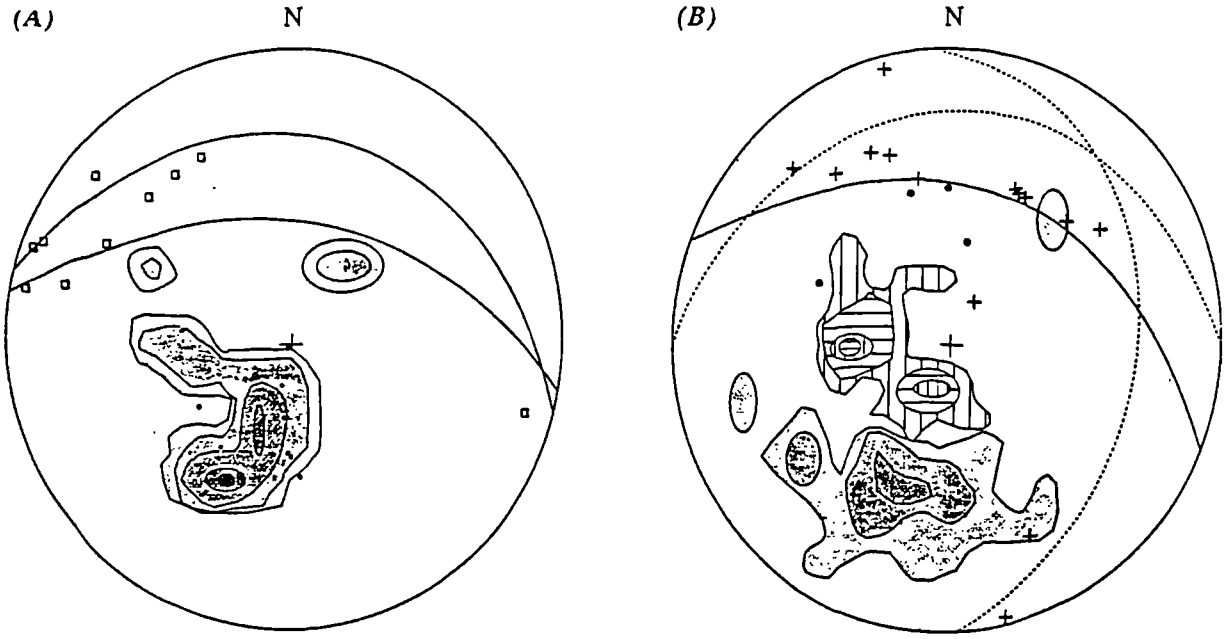

Figure 3.14 Stereoplots of orientation data, Rusey Beach. (A) Compression; *Planes*: contours = bedding (17), dots = S1 cleavage and F1 axial planes (9). *Lineations*: boxes = L1 lineations and F1 axes (10; a&b undifferentiated). *Great circles*: mean bedding planes (105/50 N, 100/26 N). (B) Extension; *Planes*: striped contours = D2 detachments (14), solid contours = D3 steep faults (16); dots = S2 cleavage and F2 axial planes (4). *Lineations*: crosses = slickenlines (14). *Great-circles*: dashed = D2 mean detachments (175/24 E, 092/19 N); solid = D3 mean fault (105/42 NNE).

Extensional Features

D2 low-angle detachments crop out in the foreshore between Cam Strand and Samphire Rock [SX 130 965 - SX 130 977], with quartz-veined movement planes developed along bedding planes dipping to the north or northwest at 15-35°. Down-dip vergent F2 folds commonly occur in the hangingwalls, whilst Riedel shears link detachments into a braided system of brittle-ductile shears. Low-angle D2 faults are again present at the Strangles and along Rusey Beach, with asymmetrical folds and domino-faults adjacent to the

detachments indicating down-dip extensional transport. A crenulation S2 cleavage is developed within fault-bounded lithons, dipping steeply southwards.

D3 faulting is again seen throughout the section, dipping moderately northwards in most cases. Anomalous east- and west- dipping faults are common between Tremouth Haven and Cambeak. A steep normal fault dipping 60° east-northeast separates massive sandstones of Great Cambeak from those of Little Cambeak [SX 1295 9662]. D2 detachments are consistently truncated by steeply north-dipping D3 normal faults to the south of Little Strand (Figure 3.15).

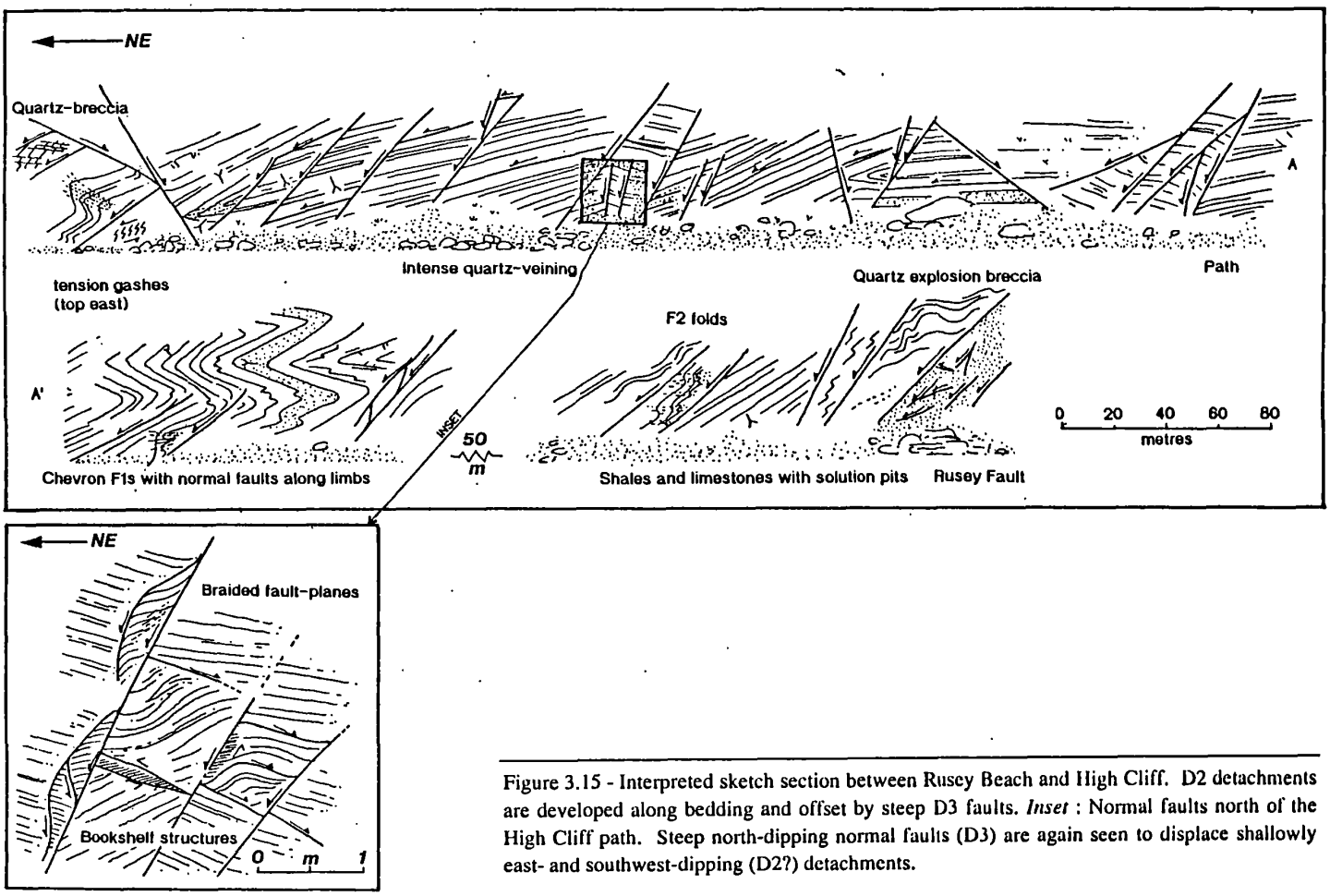

Figure 3.15 - Interpreted sketch section between Rusey Beach and High Cliff. D2 detachments are developed along bedding and offset by steep D3 faults. *Inset* : Normal faults north of the High Cliff path. Steep north-dipping normal faults (D3) are again seen to displace shallowly east- and southwest-dipping (D2?) detachments.

Extensional structures exposed between Cambeak and Rusey Beach are thus variable in form and orientation (Figure 3.14B). Shallowly-dipping detachments on average dip at 30° to the east or north and focus an S2 crenulation fabric which dips moderately south. Steeper D3 normal faults are strongly clustered about a maxima dipping 42° N. Slickenlines plunge to the north on all structures and hence ENE-dipping faults to the west of Tremoutha Haven accommodate strains related to dextral transfers.

A major post-D3, north-northeast trending dextral fault intersects the coast at The Strangles and is evident in subvertical quartz-veined movement surfaces which preserve subhorizontal slickenfibres (Figure 3.2). Minor strike-slip features are exposed close to the fault include synthetic dextral tension gash arrays, minor dextral shears, quartz-calcite veins with fibrous infill and antithetic east-northeast trending sinistral shears.

Thin section analysis

Cleaved siltstones sampled at Voter Run [SX 127 948] again show little evidence for grain-scale deformation : Aligned, unkinked muscovite crystals parallel compositional banding and quartz grains are sub-rounded and have unit extinction. A pervasive pressure-solution cleavage 10°-15° anticlockwise of the main S0/1 foliation is consistent with D1b strain, whilst pyrite cubes have strain shadows which indicate a northerly D2 transport direction. Calcite-quartz veins cross-cut bedding at 90° but show a massive rather than fibrous crystal nature and no internal deformation from which to constrain D2 strain.

3.2.5 Structural summary and discussion

The chevron folds which dominate compressional structure show a change from upright to recumbent attitude and neutral to south-facing direction towards the south. These changes are accompanied by the tightening of interlimb angles 60° to the north of Widemouth to <30° to the south of Strangles Beach (Sanderson 1979; Lloyd and Whalley 1997). Both Sanderson (1973, 1974) and Lloyd and Whalley (1986, 1997) interpret D1 structure in terms of a southwards increase in simple-shear strain. Empirical modelling indicates that steep and subhorizontal fold-limbs, were rotated into their current positions during post-buckling southerly-directed simple-shear formed in response to northwards progradation of the deforming thrust stack (Lloyd and Whalley 1986), and hence they record D1b deformation.

North-dipping normal detachments postdating folds and thrusts are common south of Wanson Mouth and striking between 065°-100°. Such faults are accompanied by F2 drag folds which verge down the dip of movement surfaces. Detachments reactivate bedding and sometimes appear to develop in the immediate vicinity of primary thrust-faults. They are not satisfactorily explained as secondary compressional features as they locally dominate structures and displace moderate-scale D1 structures (Warr 1991b). Later steep normal faults (D3) occur with a spacing of approximately 100 metres and displacement of 5-10 metres.

The magnitude of D2 and D3 extension has not been accurately calculated in previous work, but was thought significant by Freshney *et al.* (1972), who suggested that attenuation of the inverted limb of the Southern Culm Antiform by north-dipping normal faults explains the relatively large outcrop width of inverted rocks to the south of Widemouth Sand (Figure 3.2B). In this study, application of extension estimation techniques on offset marker layers suggest that up to 35% of extension occurred after the cessation of D1 compression.

3.3 The Tintagel High Strain Zone and Northern Trevone Basin

Stratigraphy

The Rusey Fault marks the southern limit of the Culm Basin, juxtaposing anchimetamorphic Crackington Formation turbidites against greenschist rocks of the Trevone Basin (Figure 3.16; Section 2.2.3.2; Selwood and Thomas 1985; Primmer 1985). The Trevone rocks form a 10 kilometer-wide unit of Namurian to Fammenian strata which belongs to the Boscastle and Tintagel Successions, comprising black laminar mudstones and dark-grey sandstones with an increasing volcanosedimentary content to the south (Selwood and Thomas 1985; Warr 1991b). Selwood (1990) suggests that the Boscastle Succession developed in a near-shore environment whilst the temporally equivalent Tintagel Succession developed in basinal conditions to the south.

Fine mudstones and volcaniclastic rocks of the Bounds Cliff Succession crop out to the south of Trebarwith Strand and range in age from Frasnian to Fammenian (Selwood and Thomas 1986b). Their facies association suggests that they developed on the outer northern shelf of the Trevone Basin. The pattern of outcrop may reflect the positions of major folds (Sanderson 1979), but more recent interpretations and field evidence suggests that the Boscastle Formation lies within a discrete nappe-sheet above the Willapark Thrust (Boscastle), whilst the Tintagel and Bounds Cliff Successions are incorporated into a more southerly nappe (Figure 3.16; Selwood and Thomas 1986b; Isaac *et al.* 1982).

Bulk Structure

The Rusey Fault is a composite fault-zone which has been active during several episodes of deformation. Field observations reveal shallowly north-dipping normal fault-planes offset by a steeply north-dipping dextral fault which shows some evidence of normal reactivation (Freshney *et al.* 1972). Its position between the Culm and Trevone Basins may suggest that it represents a long-lived basement feature which was active during basin formation, thrusting, extension and later wrenching.

South of the Rusey Fault, F1 fold-closures are isoclinal, fully recumbent, and often overprinted by an intense S1 cleavage. D1 structures continue to strike east-northeast and face south as far as Boscastle, and display strains that are considerably higher than before. The Tintagel High Strain Zone crops out between Boscastle and Tregardock Beach and characteristically displays intense bedding-parallel S1 cleavage, a strong, north-northwest plunging D1 mineral stretching lineation, oblique F1 fold-axes and attenuation of bedding into boudins (Sanderson 1979). Primary isoclinal folds continue to face south throughout the zone (Warr 1991b) and F1 axes trend NW/SE, subparallel to the mineral stretching lineation and hence the tectonic transport direction (Sanderson and Dearman 1973). The cause of intense compressional strains may be southwards overthrusting of the Culm Basin upon the Rusey Fault (Sanderson 1979; Section 3.7.7).

South of Tregardock beach, south-facing recumbent F1 folds with east-northeast trending axes are again ubiquitous. Strain magnitude decreases southwards into the Trevone Basin as seen in an increase in F1 interlimb angle to 40-100° (Andrews *et al.* 1988; Warr 1991b).

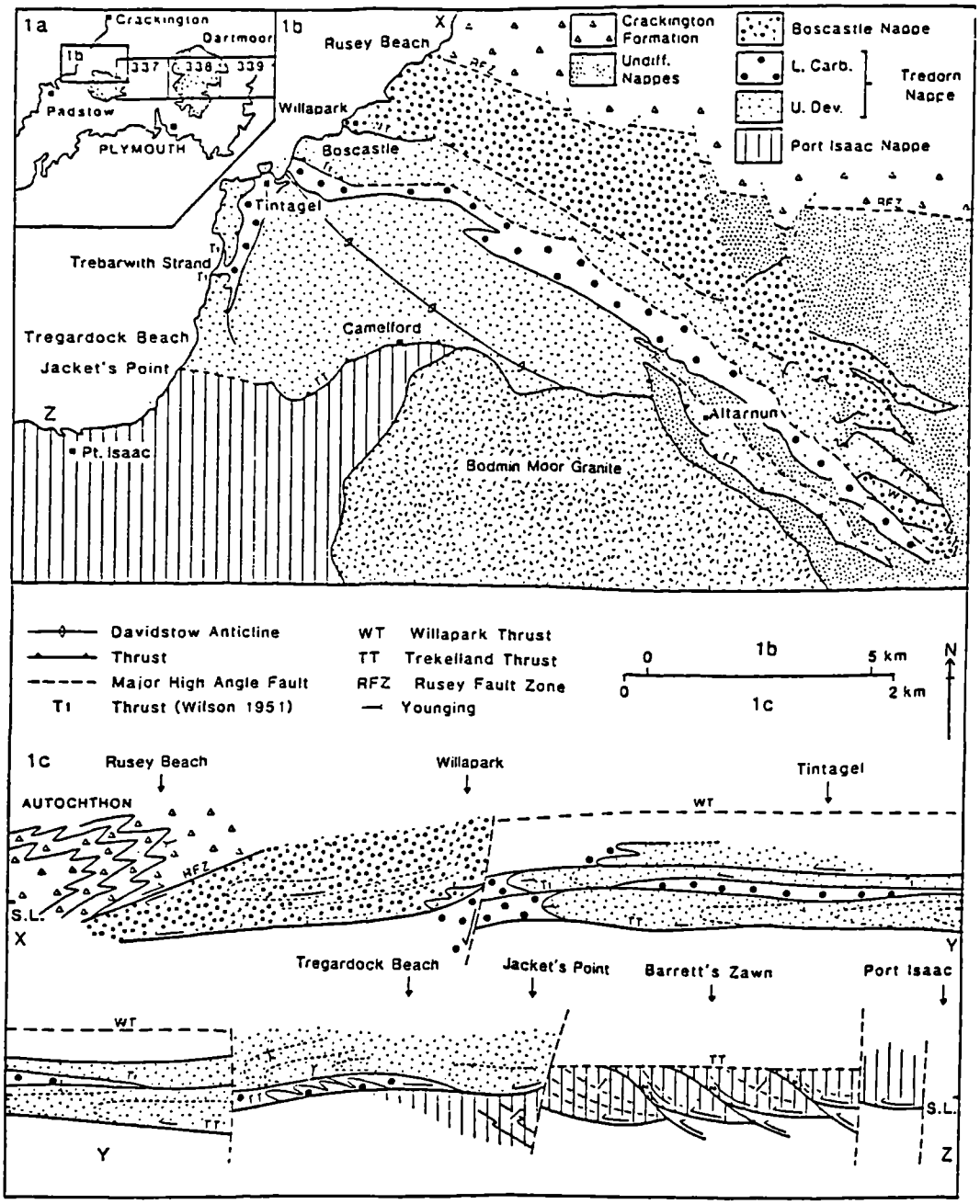

Figure 3.16 Geology of the section between Rusey and Port Isaac : (a) location map with positions of 1:50 000 BGS sheets. (b) Tectonostratigraphy of the section with locations of major localities. (c) northeast-southwest section interpreted for nappe-dominated D1 model.

Shallowly north-dipping D2 detachments are common throughout the high strain zone and decrease markedly in frequency to both north and south. Steeply north-dipping normal faults again crosscut detachments in most places but the presence of extensional duplexes locally suggests a synchronous movement history on both steep and shallow fault-planes.

A broad, late antiformal structure with a gently west-northwest plunging axis exposed between Boscastle and Tintagel is defined by the S1 fabric *(the Davidstow Antiform)*. It folds D2 detachments and has been variously attributed to granite emplacement and antiformal stacking during progressive north-directed thrusting (Section 3.3.7; Andrews *et al.* 1988 *and references therein*).

Major northwest-southeast trending dextral fault-zones are locally seen to reactivate earlier structures. The Rusey Fault itself is cut-out by a north-northwest trending dextral wrench fault and further dextral faults are present through Beeny Cliff, Boscastle Harbour, Firebeacon Hill, Trebarwith Strand and Tregardock Beach (Dearman 1963; Freshney *et al.* 1972).

3.3.1 The Rusey Fault

Lithology

The Rusey Fault [SX 1245 9349] is marked by a shallowly north-dipping zone of yellow-orange ochrous quartz-breccia approximately 30 metres thick, containing clasts of black shale, siltstone, sandstone and chert (Plate 3.4). The lithic fragments appear to derive from both the Crackington Formation (hangingwall) and components of Boscastle Formation (footwall). Within the breccias, bands of vein-quartz clasts cemented by radial growths of iron-stained quartz-spar define crude movement surfaces which are spaced at 30-50 cm intervals. The fault-rock suggests a history of repeated stick-slip movement as early bands of vuggy quartz are progressively brecciated and recemented into ordered zones parallel to more recent movement planes. Shales and thin sandstones crop out to the north of the fault and thick sandstone beds are exposed in the headland to the south.

Compressional Features

Exposed breccia-planes of the fault-zone contain slickenlines which record normal, dextral oblique-slip and dextral movement only, but the origins of the Rusey Fault may be in D1 thrusting on the basis of indirect evidence : (i) D1 strain increases southwards along Rusey Beach towards the fault-zone, from recumbent chevron hinges below the path to complex F1 fold geometries in limestones to the north of the fault (Figure 3.15; Figure 3.17A). Such strain-gradients are observed elsewhere on approaching larger thrust structures (e.g. Bude Haven; Section 3.2.1). (ii) Fault-planes preserved within the main fault-zone have a similar north to northeast dips to minor thrusts exposed on the foreshore which display south-dipping quartz

slickenfibres which step updip (Figure 3.17B). Thompson (1995) modelled the fault-zone on the basis of clast ordering, lithologies and fluid-type, and suggested that it formed within a dilational jog during underthrusting of a wedge of sandstones.

Plate 3.4 Rusey Fault. Breccias in fault-zone with quartz coronas and shale matrix. Lens cap diameter 52 mm.

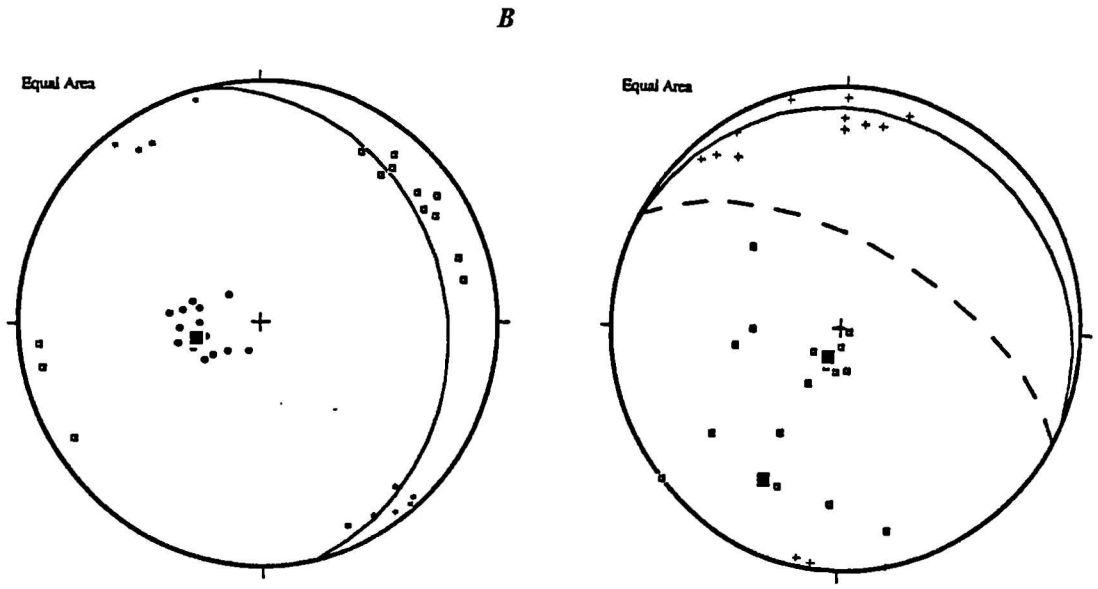

Figure 3.17 Stereoplots of structural orientations recorded within the Rusey Fault-Zone. (A) Compressional features: *planes*: dots = S1 cleavage (14), great circle = mean S1 cleavage orientation (166/23 E); *lineations*: squares = L1 lineation (13), stars = mineral stretching lineation (10). (B) Fault structures: *planes*: squares = fault planes (17); great circles = mean fault orientations (solid = D2 detachment planes, 111/11 N; dashed = dextral oblique-slip, 117/60 N); *lineations*: crosses = slickenlines (13).

Compressional structures enclosed within the fault-zone show anomalous trends (Figure 3.17A). The S1 cleavage dips shallowly to the east, 80° clockwise of their mean strike at The Strangles (Figure 3.14A). F1 fold axes plunge gently east-northeast or west-southwest and a well-developed mineral stretching lineation plunges north-northwest or south-southeast.

Extensional features

At present, the Rusey Fault [SX 1245 9349] appears to comprise a composite zone of normal and strike-slip detachments. The most prominent detachment exposed dips shallowly northeast and contains stepped quartz, calcite and gypsum slickencrysts which record normal overprinted by dextral movement. Rare (D2+) folds in slates immediately to the north of the fault trend northwest-southeast and plunge moderately to steeply southeast, defining a dextral sense of vergence.

To the south of the fault shallowly north-dipping D2 detachments are common and a north-dipping slaty S1 cleavage is present, whilst to the north D2 deformation is less common and S2 south-dipping cleavage only patchily developed. Detachments commonly reactivate bedding. Steep, north-dipping normal faults displace the breccia bands in the cliff, again suggesting the presence of a later steep faulting event (D3). Plots of structural orientation data show a wide scatter of fault attitudes but relatively consistent slickenfibre dips to the north and northwest (Figure 3.17B).

A northwest-southeast trending dextral strike-slip structure truncates the breccia bands and later steep normal faults on the southern side of Rusey Beach. The development of equant gypsum crystals along dextral fault planes suggests either that a reactivation episode occurred at low temperature, or that such structures were utilised as fluid pathways subsequent to tectonism (A. Peckett *pers. comm.*).

Thin Section Analysis

Microstructures within the fault rocks display a single grain-shape fabric with secondary deformation represented by veins with calcite and secondary quartz infill. Microfaults with quartz fill indicate top-to-the-east extension postdating D1 deformation. The abundance of vein quartz in the samples is consistent with high fluid volumes being present during movement episodes.

3.3.2 Firebeacon Cove to Buckator

A brief examination was made of the steep hogsback cliffs between Rusey and Buckator but landslipping of the poorly exposed Namurian mudrocks masks much of the structural detail. Consequently, interpretation largely follows findings in the BGS memoir 'Geology of the coast between Tintagel and Bude' (Freshney *et al.* 1972).

Lithology

Black pyritous slates with subordinate dark-grey siltstone and sandstone partings crop out along the section, with lithological variation occurring across low-angle normal detachments (Freshney *et al.* 1972). The rocks belong to the Boscastle Succession but bear a superficial resemblance to the partly diachronous Crackington Formation to the north (Figure 3.16). Green slates and fossilliferous limestones of the Buckator Formation (Section 2.2.3.2; Figure 2.6) crop out in the backshore at Buckator [SX 1181 9341] bounded both above and below by D2 detachment faults. A second fault-bounded limestone and green slate unit is exposed along the east-trending foreshore between Beeny Sisters and Buckator Beach, whilst medium-grained sandstones crop out at Firebeacon Point against a steep dextral fault.

Compressional features

D1 structure is disjointed and widely reactivated by low-angle normal detachments, characterised by a slaty S1 fabric which transposes bedding and dips shallowly to the north. F1 folds are isoclinal, semi-recumbent and south-facing. F1 chevron folds seen commonly to the north of Rusey are rarely preserved, but close examination of S1 microlithons reveals the hinge zones microfolds. Freshney *et al.* (1972) recorded southeast-facing F1 folds with northeast- plunging axes and shallowly north-dipping axial surfaces preserved in sandstone beds at Firebeacon Point. The long inverted limbs and z-profiles of the folds suggest that the succession continues to lie within the lower limb of a nappe-scale, recumbent fold.

Extensional Features

D2 shallowly-dipping detachments are often seen throughout the section and form lithological boundaries between subdivisions of the Boscastle Succession as described by Freshney (*et al.*) 1972. For example, Gull Rock [SX 1182 9339] exposes D2 detachments dipping 35°N which separate green-grey slates, marls and siltstones from dark-grey slates. The green unit is strongly veined (quartz-calcite) and deformed into decimetre scale north-northwest verging asymmetric folds, whilst black slates display extensional shear-bands and a moderately south-dipping S2 cleavage. Firebeacon Point [SX 1007 9282] again displays a change in lithologies across shallow north-dipping detachments, with the basal part of the Firebeacon Chert Formation defined by a normal fault-zone with ruck-folds plunging northeast or southwest and axial planes dipping shallowly south (Freshney et al. 1972). Subsidiary shear fractures and fold asymmetry consistently indicate top-to-the-north-northwest D2 shear.

Pelitic bands unaffected by detachment faulting commonly show L2 crenulation of S1 cleavage. The S2 crenulation fabric intensifies into transposing, bedding-parallel shear-zones (Figure 3.18). These zones of focussed D3 strain are seen only in fine-grained lithologies and hence reflect the partitioning of extensional strain into weak rheologies.

Steep D3 normal faults are developed sporadically along the section and downthrow D2 detachments by several metres to the north. A younger group of steep north-striking faults crop out at Buckator Beach and form a composite dextral fault-zone trending northwest-southeast and mapped by the BGS at Firebeacon Point (Freshney *et al.* 1972).

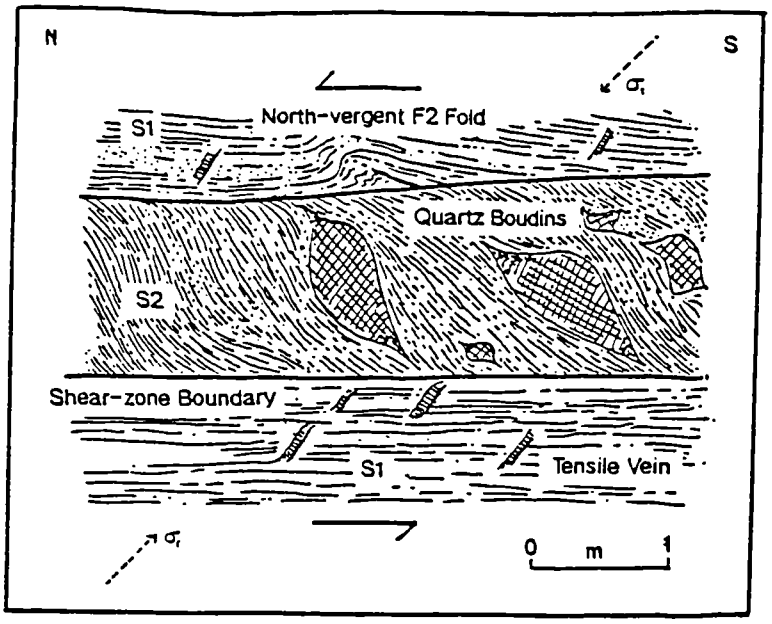

Figure 3.18 D2 shear-zone with margins parallel to S0/1 foliation in which S2 tranposes all earlier structure, Gull Rock [SX 1182 9339]. Shear is toward the north, as note in the sigmoidal S2 geometry, vergence of F2 folds, orientation of tensile quartz veins and the asymmetry of boudins.

3.3.3 Pentargon Cove to Boscastle

Slates and sandstones exposed at Pentargon Cove, Penally Head and Boscastle Harbour show intense D2 brittle-ductile extension superimposed upon high D1 strains (Figure 3.19).

Lithology

Dark-grey pyritous slates of the Boscastle Formation predominate between Boscastle and Pentargon, interbedded with thin grey siltstones. Intense quartz-veining is developed sporadically either parallel to the slaty cleavage or as boudinaged pods within fault-zones. Cross-laminated sandstone beds up to a metre thick are present locally in groups at Pentargon Cove [SX 0952 9161] and at the neck of Penally Point [SX 0945 9157]. Black pyritous slates are observed high in the cliffs on the southern side of Pentargon Cove, their position within a normal fault-zone suggesting that they represent a higher stratigraphic unit than is generally exposed elsewhere in the coastal section (Figure 3.19).

Compressional features

A primary slaty cleavage is present throughout the area, lying subparallel to bedding and dipping moderately to steeply to the north-northwest. It is refracted between layers of varying lithology and forms two modal orientations in the limbs of later folds. Isoclinal F1 fold closures with steeply northwest-dipping axial planes are well exposed at Penally Point [SX 0945 9157] where they are refolded and backsteepened by recumbent, north-verging F2 folds (Figure 3.24; Freshney *et al.* 1972). In the cliffs above Pentargon Cove [SX 1082 9134] recumbent F1 folds cause repeated changes in younging but long limbs remain inverted (Warr 1991b), thus indicating a position within the inverted limb of a large-scale F1 fold.

Structural orientation data from Pentargon Cove shows clustering of bedding and cleavage poles, demonstrating that they are subparallel and thus indicates that F1 folds are isoclinal (Figure 3.20). The cluster trends north-northwest, parallel to the mineral stretching lineation. This suggests that tectonic transport during D1 was to the north-northwest. Bedding-cleavage intersection lineations plunge shallowly east-northeast and west-northwest.

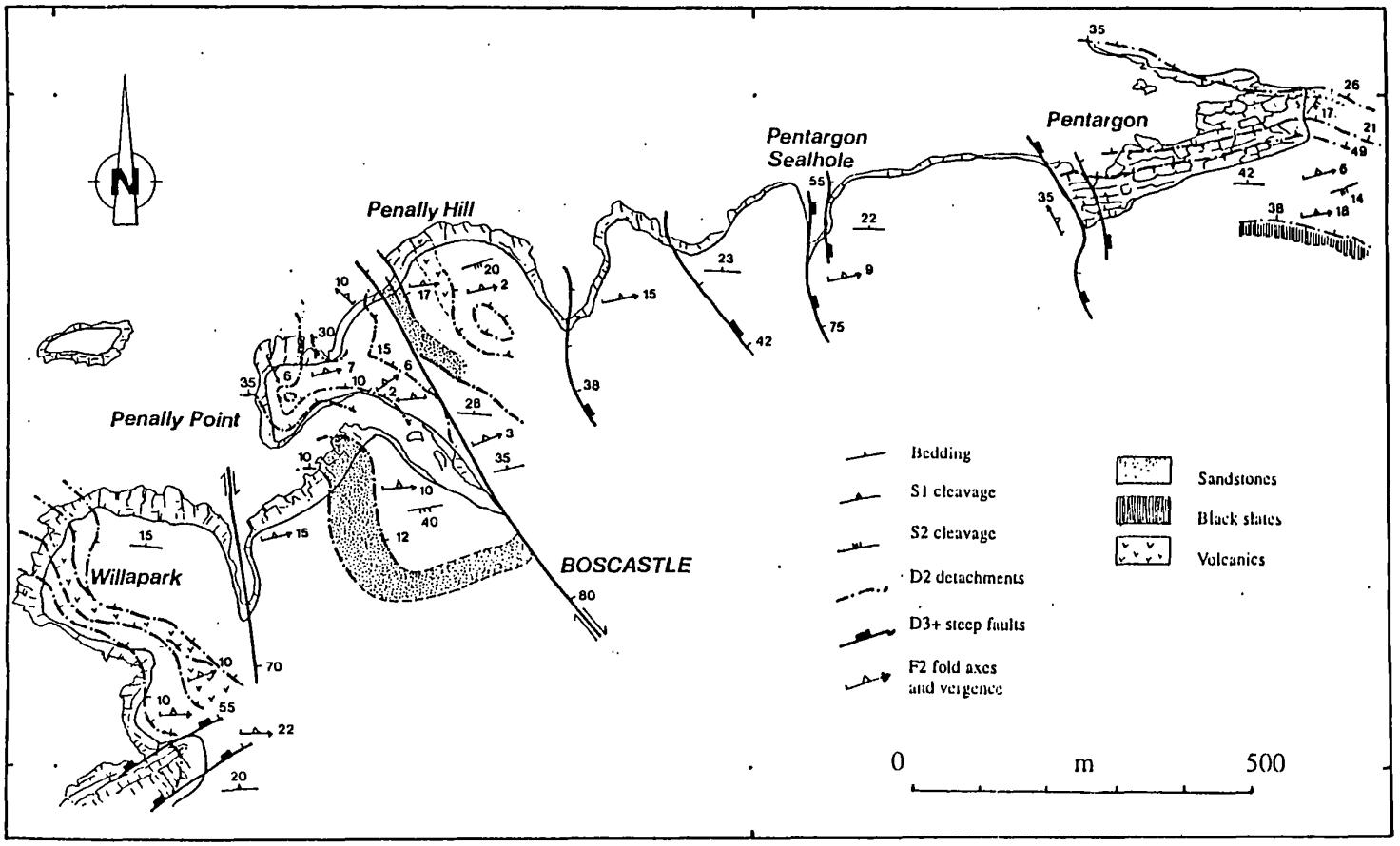

Figure 3.19 Structural map of the Pentargon-Boscastle section, showing the positions of significant low-angle normal fault zones. Adapted from field maps and BGS sheet 322 (Freshney *et al.* 1969).

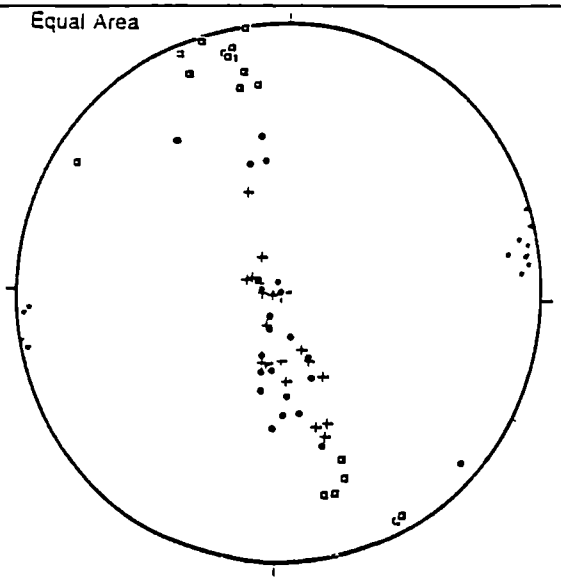

Figure 3.20 Stereoplot of structural orientation data of compressional features collected at Pentargon Cove. *Planes*: bedding = dots (24); S1 cleavage = crosses (14). *Lineations*: mineral stretching lineation = boxes (18); L1 lineation = stars (13).

To the south of Boscastle Harbour [SX 0947 9150], south-facing recumbent F1 isoclines locally record little post-D1 overprint. Bedding appears to be largely right-way up and hence a major F1 hinge must lie between Boscastle and Pentargon. Elongate pyrite crystals and mica aggregates plunge shallowly towards the north-northwest and are parallel to the L1 intersection lineation. The L1 lineation thus rotates into the tectonic transport direction between Pentargon and Boscastle, indicating high strain-rate and sheath F1 fold geometries. The switch in trends occurs abruptly across normal faults at Pentargon Cove (discussed in Section 3.3.7; compare stereonets in Figures 3.20 and 3.25).

Extensional features

A suite of post-D1 structures with apparent extensional geometries are exposed in the Boscastle-Pentargon region, including D2 detachments, ductile shear-zones, angular F2 folds and steep D3 faults (Figure 3.19). The first detailed geometrical analysis of the D2 structures was made by Dearman and Sanderson (1965), and an extensional origin was postulated in the Bude to Tintagel Geological Survey memoir on the basis of goniatite biozone distribution (Figure 3.2; Freshney *et al.* 1972).

Exposures of grey-green slate along the valley running inland from the northern side of Pentargon Cove [SX 1085 9200 - SX 1115 9208] contain bands of F2 asymmetric folds and S2 crenulation cleavage development, separated from the north-northwest dipping S1 cleavage by cleavage-parallel detachments (Figure 3.21; Plate 3.5). D2 deformation zones are up to three metres thick and their bounding detachments are commonly linked by Riedel shears which confirm top-to-the north or north-northwest movement. F2 fold axis azimuths are extremely variable, reflecting sheath and box geometries observed in the field (Figure 3.21A). The presence of sheath-folds indicates that strain was high during D2 and that shear was down the dip of pre-existing S0 and S1 fabrics (Figure 3.21i-iii). Towards the south, S0, S1 cleavage dip more shallowly northeast and the heterogeneous S2 fabric dips more steeply towards the southeast. This rotation must therefore postdate D1 and D2, and may relate to fault-block rotation across curviplanar D3 faults which crop out in the foreshore (Figure 3.19).

Plate 3.5 North-dipping D2 detachment developed in cherty mudstones, Pentargon Cove. Note domino-faulting in hanging wall, sheared fault rocks and late kink in foot wall.

Plate 3.6 F2 chevron folds, Penally Point Folds verge north and have a weak S2 cleavage in their hinges.

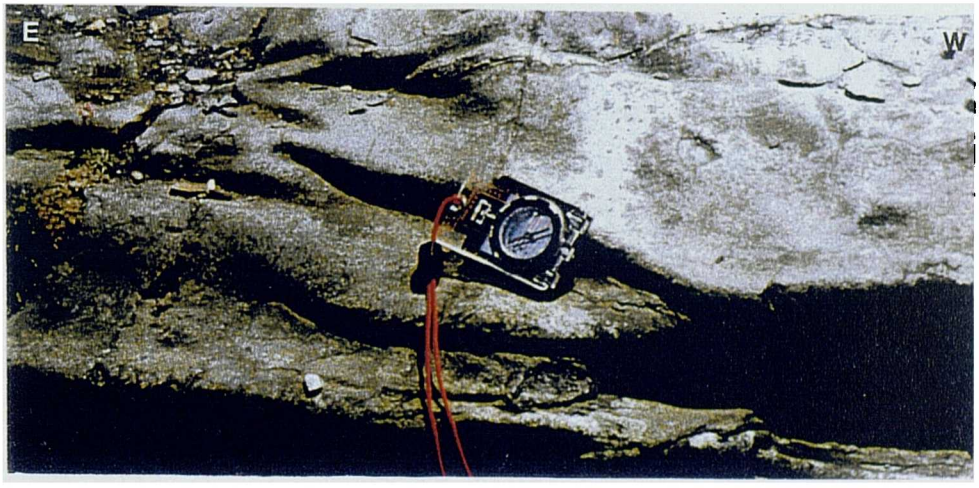

Plate 3.7 Plan view of F2 ruck-folds on S1 cleavage surface with sheath-styles. Folds verge downdip and overlie a north-dipping D2 detachment.

Pentargon Cove [SX 1082 9134] is bounded to the north and south by steep normal faults and from cliffs to the southwest. A system of braided normal faults and down-dip verging F2 folds are visible in the rear of the cove (Figure 3.22). Four large-scale, steep normal faults crop out in the cliff with a regular spacing of circa 100 metres, linked by low-angle north- and south- dipping detachments. North-dipping normal fault-planes are accompanied by subordinate antithetic faults which indicate shallowing of fault-plane dip at depth (Walsh and Watterson 1988). D2 detachments with shallow northerly dips splay into the steep faults and hence both steeply- and shallowly- dipping movement surfaces are assumed to have developed more-or-less synchronously. The magnitude of post-D1 extension across the steeper (D3?) faults is approximately 55% (Section 1.4) if offsets of a 2 metre thick S1-parallel quartz-vein are representative.

F2 folds are pervasive in the immediate hangingwall of detachments in the southern 300 metres of Pentargon Bay, tightening towards the movement planes. They verge down the dip of their associated detachment and their axes plunge shallowly towards 245° or 080° (Figure 3.22, stereonet 1). The variations in plunge relate to the curvilinear geometries of drag folds and the curviplanar nature of the detachments. Domino faults are locally observed in the immediate footwalls of D2 detachments and their offsets again indicate top-to-the north shear. S2 crenulation cleavage is widely developed in F2 fold hinges and dips shallowly to the south-southeast (Figure 3.22, stereonet 1).

D2 extensional structures are again exposed at Penally Hill [SX 0946 9172], Penally Point [SX 0937 9161] and along the banks of the River Bos [SX 094 914]. Detachments with intensely quartz-veined footwalls and ruck-folded hangingwalls can be traced from Penally Point into Eastern Blackapit [SX 0928 9129] (Plate 3.6), and have been recorded northwards to Firebeacon Point by Freshney *et al.* (1972). Movement surfaces are usually planar and are often seen to link to one another along ramps which exploit the S2 cleavage, indicating that they propagated in an overstep sequence. Detachments form a linked network of steeply- and shallowly- dipping movement surfaces across the cliff exposures (e.g. Penally Point), with detachments dying out laterally into F2 folds or offset by steeper normal faults.

Within detachment-bounded packages, D2 deformation produces a range of features which relate to variations in strain and/or strain rate (Figure 3.23). In pelitic units, semi-ductile deformation occurs with development of a strong S2 crenulation fabric and attenuation of markers into boudins and porphyroclasts (Figure 3.23a). Detachments are accompanied by north-vergent folds in many cases (Figure 3.23b,c) whose axes plunge to the southwest. In most cases, folds verge down the dip of their associated detachment, but where ramps link detachments, folds with updip vergence are observed (Figure 3.23c). A late phase of kink-banding is seen in slate units, with axial planes dipping steeply north (Figure 3.23d). They are sporadically developed throughout the slates of SW England (Mc Clay 1987), and may have formed during late dextral faulting (R. Holdsworth *pers. comm.*).

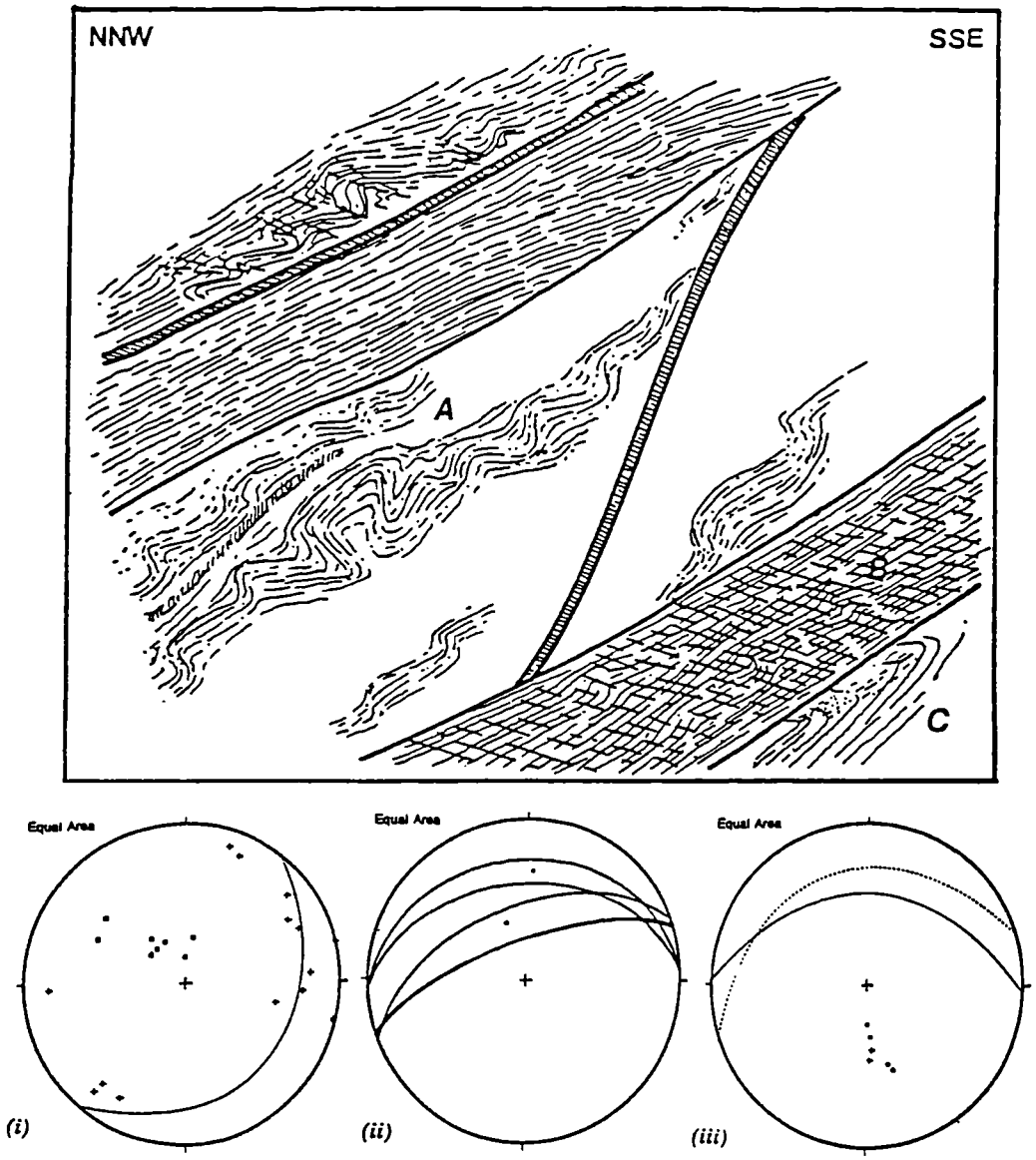

Figure 3.21 D2 structures developed in S1-parallel zones to the north of Pentargon Cove [SX 1090 9198] and stereoplots data within the zones. (A) F2 folds with down-dip asymmetry or box-geometries, (B) Locally transposed, pressure solution S2 cleavage in S1-parallel shear-zones forming a pencil cleavage where strain is low; (C).F1 fold hinge cut by D2 detachment. Stereoplots : (i) F2 folds: boxes = axial planes (8); crosses = axes (14); great circle = mean axial plane (047/25 SE). (ii) D2 fault orientations: great circles = slip planes (4); dots = slickenlines (2). (iii) D1 structure: dots = bedding (4); crosses = S1 cleavage (2); solid great circle = mean bedding; dashed great circle = mean S1.

Type-III refolds have are observed at Penally Point (Figure 3.24; Plate 3.7) whilst type-I refolds are reported by Freshney *et al.* (1972). Both geometries are predicted due to the sheath geometry of F2 folds. At Penally Point, F2 folds are seen to fold F1 isoclines and quartz boudins, and boudinage must therefore have occurred early in the D2 phase. The F2 folds are several metres in wavelength and amplitude, and appear to have formed above a curviplanar D2 detachment zone in a northwest directed D2 shear-sense is readily obtained.

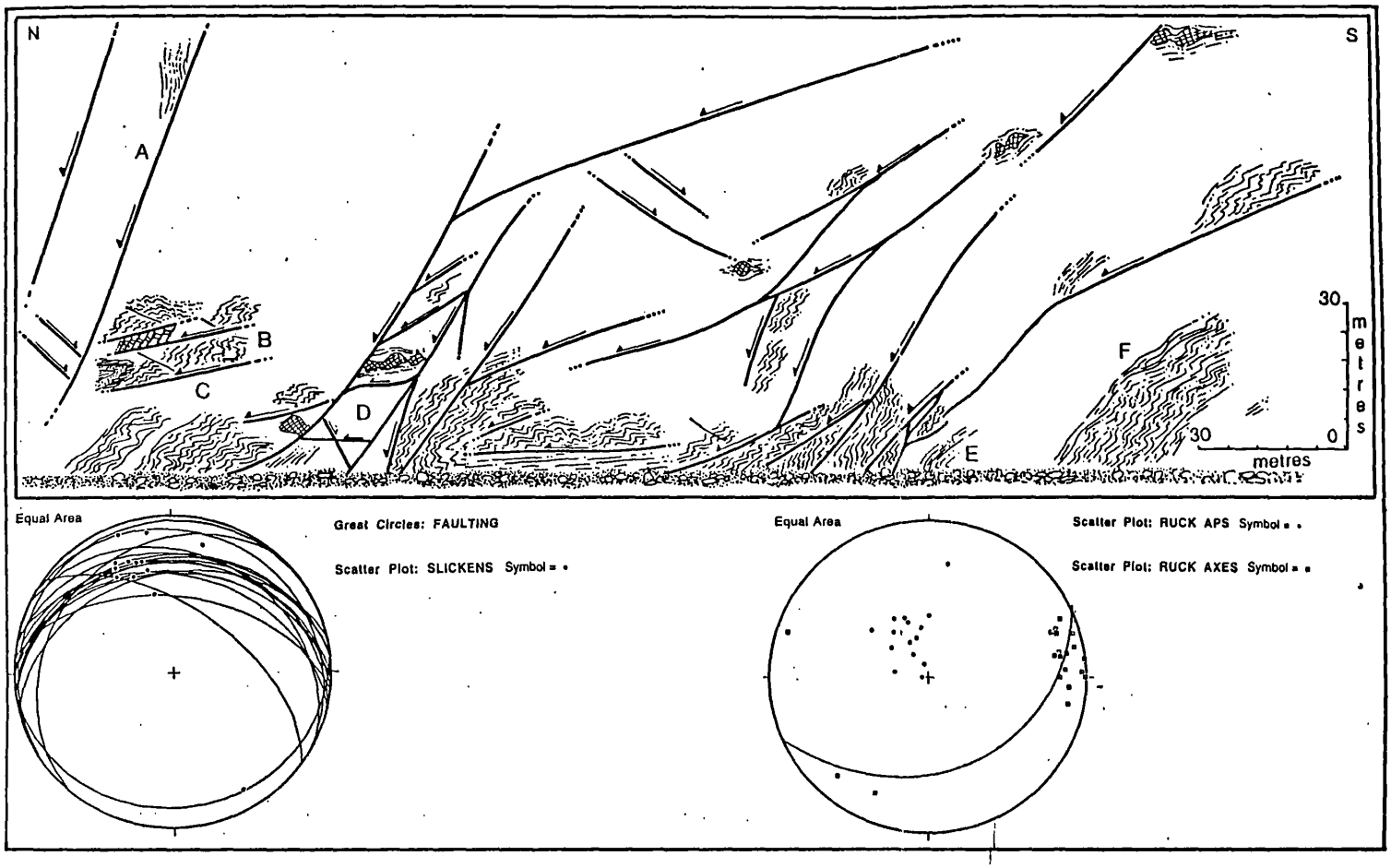

Figure 3.22 Sketch section of central Pentargon Cove [SX 1084 9191 - SX 1082 9202], showing a braided extensional fault-duplex. (A) Steep normal fault with F2-folds in hanging wall. (B) Low-angle (D2) normal fault-zone with hangingwall folds and P-shears, and footwall domino-faults (indicate top to the north shear) (C) North-verging chevron F2 folds. (D) Steep fault-zone containing conjugate fracture planes. (E) F1 closure (axis = 32/335). (F) F2 chevron folds of S0/1 fabric with pervasive D2 detachment planes. Stereoplots : (i) fault-planes (15) and slickenlines (13; top to the NNW) extension with slight sinistral slip component. (ii) F2 folds with NNW-vergence; dots = axial planes (15); boxes = axes (20). Mean axial plane great circle (072/22S).

Steep (D3) normal faults, dipping moderately to steeply northwest are observed in cliffs to the east of Penally Point. They appear unrelated to the curviplanar faults at Pentargon as they displace D2 deformation zones rather than run into parallelism with them, and imply that they post-date D2. North-

northwest trending dextral strike-slip faults which dissect the coast at Boscastle harbour and Eastern Blackpit and offset detachments and steep normal faults (Freshney *et al.* 1972).

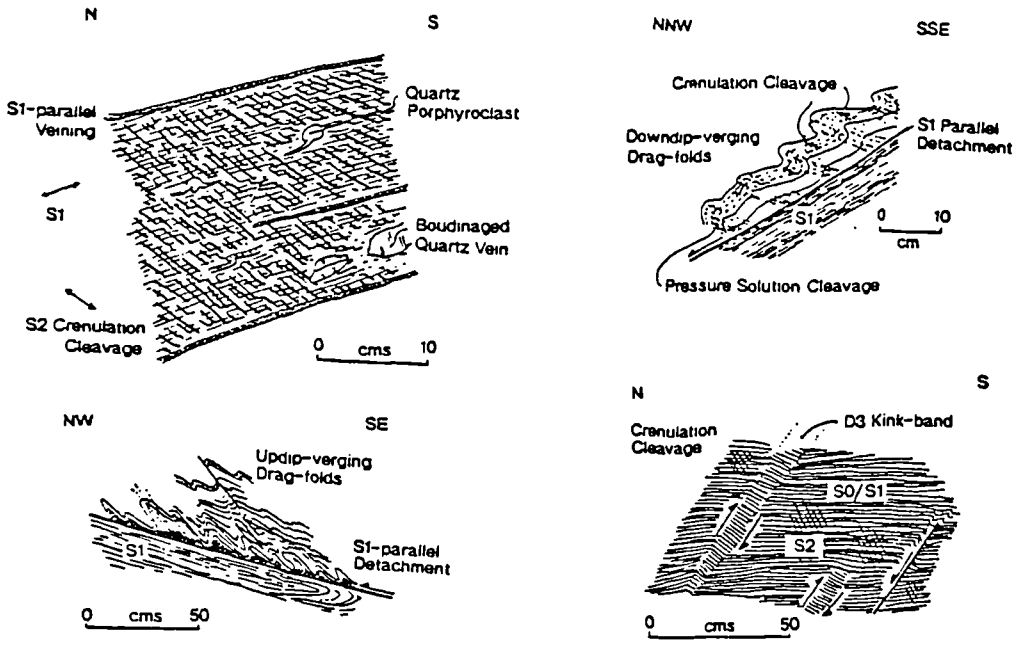

Figure 3.23 Small-scale extension-related features exposed around the River Bos. (a) Cleavage relationships and shear-sense indicators relating to the ductile compression in the THSZ. (b) Down-dip verging ruck-folds developed above a normal detachmane and their relationship with S2 cleavage. (c) Up-dip verging folds as locally seen adjacent to faults and along p-shears. First appearance is of thrusts, but they form sections of the anastomosing, north-transporting detachment system. (d) Late-stage kink-bands formed in response to layer-parallel compression.

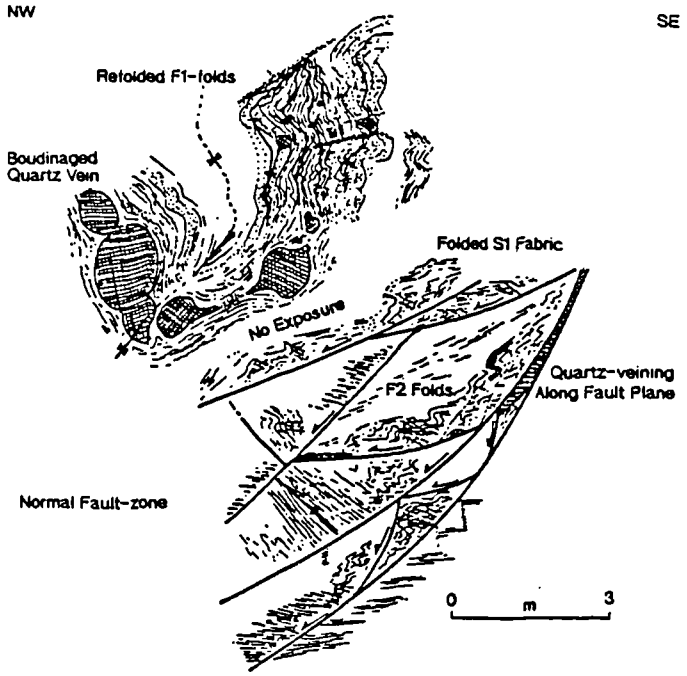

Figure 3.24 Refolded F1 folds, Penally Point East [SX 0937 9161]. F1 folds with steeply-dipping axial planes are refolded about F2 folds with subhorizontal axial planes. At this locality the interference is type-III, although coaxiality is not commonly observed.

Interpretation of stereoplots of D2 structures implies that they are associated with north-northwest directed shear (Figure 3.25A). F2 fold axes and L2 crenulation lineations plunge shallowly northeast and southwest, the wide scatter (ca. 65°) reflecting curvilinearity of fold-hinges as observed in the field. S2 cleavage and F2 fold axial-planes dip on average at 25° to the south or southwest. D2 detachments dip shallowly towards the north and preserve slickenlines plunging to the north-northwest (Figure 3.25B). Steeper normal faults are less common than D2 detachments, and dip steeply to the north-northwest.

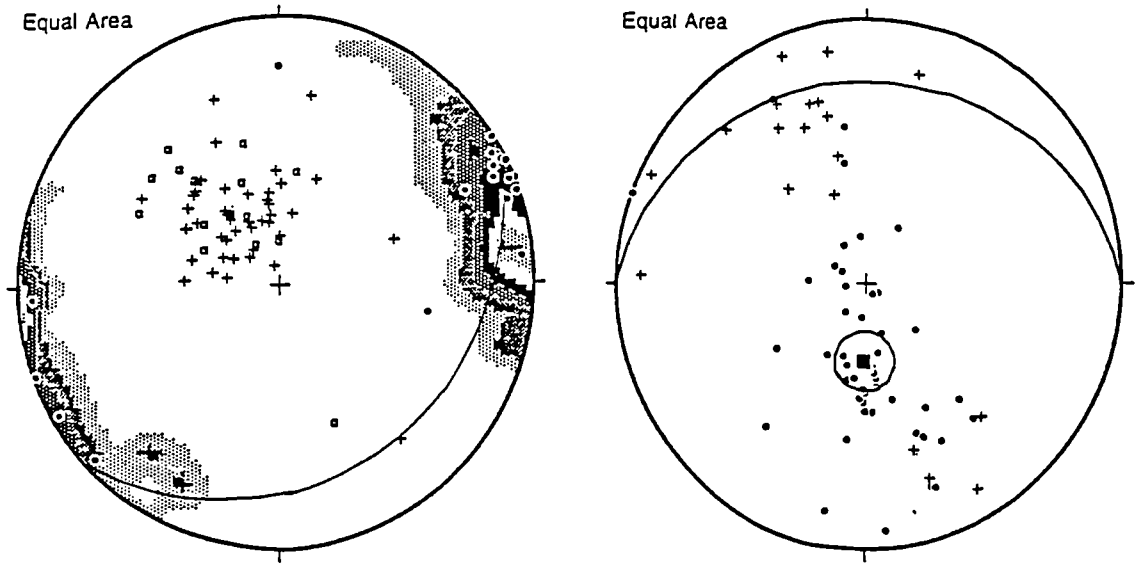

Figure 3.25 Stereographs of D2/3 structural orientations, Boscastle region : (A) D2 fabric elements : *Planes:* crosses = F2 axial planes (36); boxes = S2 cleavage (15). *Lineations:* contours = F2 axes (25); dots = L2 crenulation lineation (14). *Great circle:* mean S2/F2-axial plane orientation (056/31 SE). (B) Faulting (D2/3): *Planes:* dots = fault-planes (45). *Lineations:* crosses = slickenlines (20). *Great circle :* mean fault plane orientation (091/24 N).

Thin section analysis

Samples of black slate taken at southern Pentargon Cove are composed of muscovite and quartz with a minor component of chlorite and opaque minerals. The mineralogy is consistent with sub-biotite zone (lower) greenschist conditions. Siltstones within a D2 deformation zone on the beach below have a quartz-muscovite assemblage with minor opaque minerals and biotite, diagnostic of the lower biotite zone. Microstructure in the slates is dominated by an intense S1 schistosity formed of aligned muscovite laths (~0.25 mm long) and quartz ribbons, indicating that D1 was associated with crystal plasticity induced by abundant pore-fluids. Primary schistosity in the siltstones is a pressure solution and aligned mica fabric with slightly elongate quartz grains, supporting fluid-assisted diffusive mass transfer mechanisms.

D2 deformation is recorded in the black slates by crenulations and pressure solution seams which define a crude cleavage, the asymmetry of which is consistent with top-to-the west-northwest (298°N) shear. Further evidence for downdip-directed D2 shear are seen in the asymmetry of σ- porphyroclast-tail systems (quartz clasts with chlorite-muscovite tails), and the geometry of extensional shear-bands.

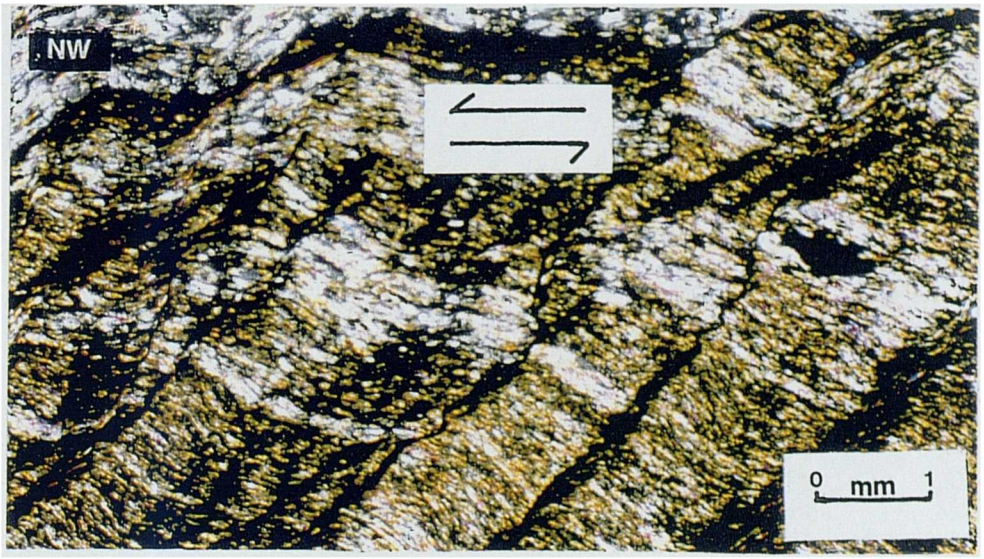

Plate 3.8 Photomicrograph of Boscastle Formation siltstones, with asymmetrical extensional shear bands developed indicative of general noncoaxial flow.

Slates from Boscastle Harbour have a quartz + muscovite ± chlorite ± biotite ± opaques ± cordierite ± staurolite assemblage indicative of greenschist conditions (Primmer 1985a). Metamorphic spotting is not seen in the field, but elongate voids < 1 mm long within grey slates may locate weathered spots of cordierite. A closely-spaced schistosity of aligned muscovite forms the dominant primary cleavage in each sample, with the most intense fabric developed in samples with above 40% mica content. A fluid assisted diffusive mass transfer origin to the fabric is inferred from ragged grain-margins and elongate shapes in quartz grains (Passchier and Trouw 1996). Quartz porphyroclasts with muscovite and chlorite recrystallised tails indicate southward shear during D1, consistent with macrostructural observations in the northern Trevone Basin (Warr 1991b).

Extensional shear-bands observed in samples from Boscastle Quay displace the slaty cleavage in an updip shear-sense. This is inconsistent with field observations of the D2 event and thus must be attributed either to progressive south-directed D1 shear or to anomalous strains within the D2 deformation system. Despite some kinematic ambiguity, the secondary microstructures continue to indicate extensional reactivation along the S1 fabric. Elsewhere, brittle separation of quartz and plagioclase and microfolds of the S1 fabric support top to the northeast shear and an element of cataclastic grain diminution. S2 cleavage from the hinge region of typical F2 folds is characterised by pressure solution seams with a sub-millimetre spacing.

Samples from siltstone and fine sandstone horizons have a quartz + feldspar + muscovite + iron oxide ± biotite ± chloritoid assemblage typical of biotite-zone greenschist conditions (i.e. temperatures in excess of 420°C). S1 cleavage is defined by braided pressure solution seams. In quartz-dominated bands amoebal grain-boundaries and rotational recrystallisation are typical of greenschist-grade microstructure. Quartz-veins oriented parallel to S1 or developed in the hinges of F1 folds are recrystallised and thus peak metamorphic conditions are likely to have persisted for some time after the primary deformation event.

3.3.4 Willapark to Tintagel

Between Boscastle Harbour and Tintagel, foreshore exposure is accessible at Willapark [SX 0920 9125], Rocky Valley [SX 0725 8950], Bossiney Haven [SX 0662 8937] and Tintagel Haven [SX 0513 8905] (Figure 3.26). Additional information is taken from Freshney *et al.* (1969, 1972), Fear (1984), Andrews *et al.* (1988) and Warr (1991b).

Lithology

The cliffs between Boscastle and Tintagel expose slates, siltstones and volcanic rocks of Dinantian to Upper Devonian age. Repetition of strata led Wilson (1951) to invoke the presence of three main thrust-sheets which Freshney *et al.* (1969) reinterpretated as low-angle north-dipping detachments (*D2 in this study*). The outcrop pattern may alternatively be explained through the presence of major refolded recumbent F1 isoclines as illustrated in Figure 3.26, but this is inconsistent with observations of formation boundaries in the field (Section 3.3.7).

Following the lithostratigraphy outlined in Section 2.2.3.2, black slates with thin grey siltstones interbeds of the Boscastle Succession crop out between Boscastle and Willapark [SX 0900 9130]. The southern cliff of Willapark exposes slices of Trambley Cove, Barras Nose and Tintagel Volcanic Formations; the three Formations which make up the Tintagel Succession. (Freshney *et al.* 1969, 1972; Figure 3.27). The Trambley Cove Formation (TCF) crops out as a thin sheet on the southern side of Trambley Cove [SX 0745 0930], and again at Willapark, Tintagel [SX 0630 8960], running inland to the southwest through Tintagel village. It comprises black and grey-green careous-weathering slates and is separated from the structurally overlying Boscastle Slates by a thick band of cataclasite and intensely folded slate.

The Tintagel Volcanic Formation (TVF) lies structurally below and is exposed in several discrete swathes between Trambley Cove and Gullastem, at Barras Nose, and on the foreshore of Tintagel Island. It comprises dark-grey slates and green-grey tuffs with black mineral spots. The margin between the TVF and TCF is often faulted and is boudinaged in many places (Figure 3.27; Freshney *et al.* 1972). Beneath the volcanics, the Barras Nose Formation (BNF) consists of green, purple and grey slates with thin limestone and tuff beds. It crops out as sheets on the neck of Barras Nose and Tintagel Island, inland from

Trewethet Gut and Saddle Rocks. In each case, the BNF lies within the hangingwall of shallowly north-dipping detachments (Freshney *et al.* 1972; Fear 1984).

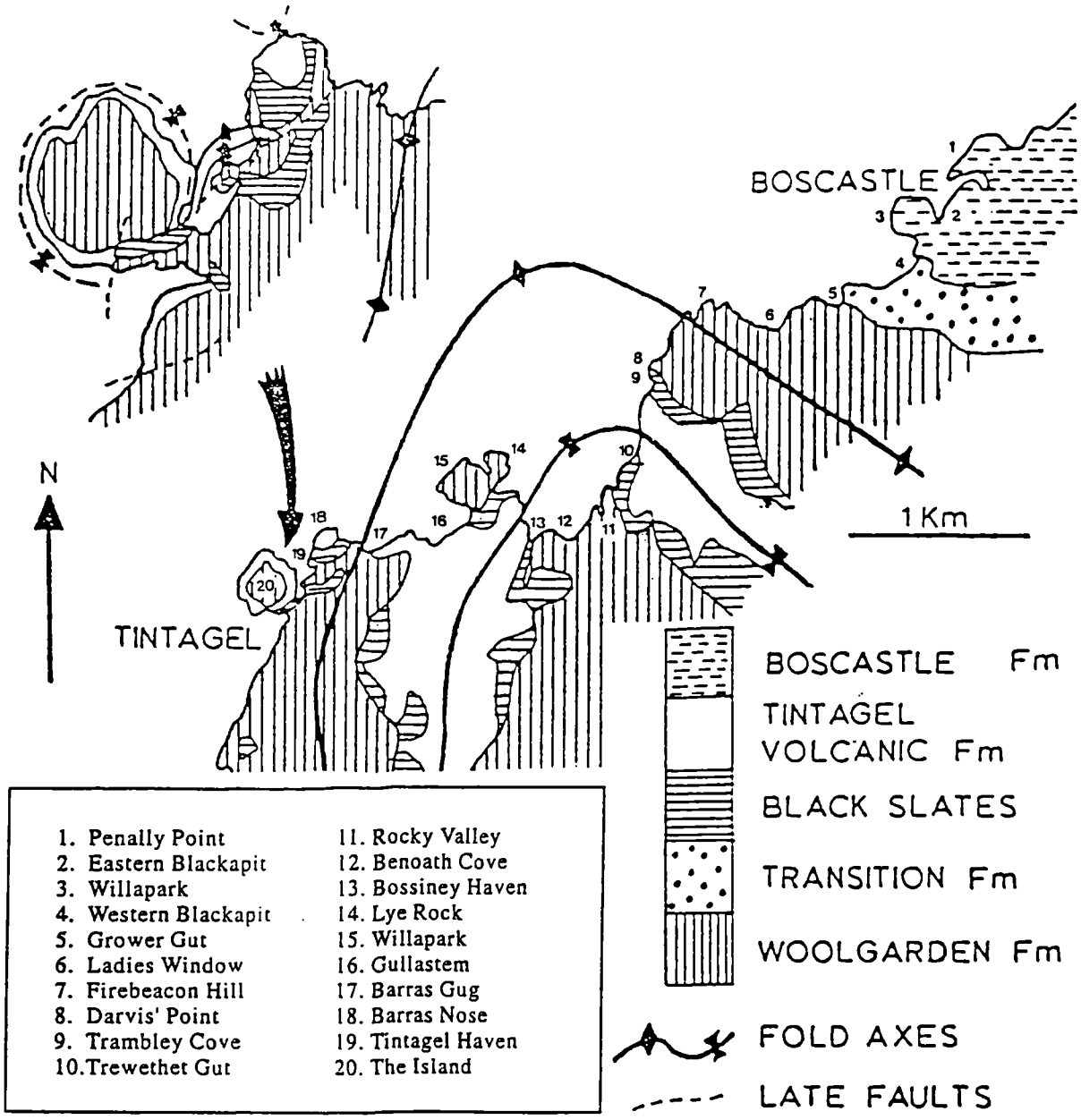

Figure 3.26 Simplified geological sketch map of the solid geology of the coast between Boscastle and Tintagel (adapted from Fear 1984; structure after Hobson and Sanderson 1975). Numbers locate key areas discussed in the text.

The Tintagel Succession structurally overlies Upper Devonian rocks of the Tredorn and Woolgarden Slate Formations. The two successions are separated by a transitional facies of pale-grey slates exposed in the sides of Western Blackapit [SX 0910 9100] and thus whilst the contact is faulted in most places, it appears that they also lie in stratigraphic sequence. The Tredorn Slate Formation is exposed between Western

Blackapit and Trambley Cove, and comprises rusty grey feldspathic slates and grey-green siltstones with visible pyrite cubes. The remainder of the section is composed of the older Woolgarden and Upper Delabole Slates, comprising grey-green slates and schists exposed clearly in the upper cliffs of Tintagel Island. Crags of metadolerites occur in the Tintagel area and appear to form a fault-bounded slice tectonically emplaced into the Upper Delabole Slate Formation.

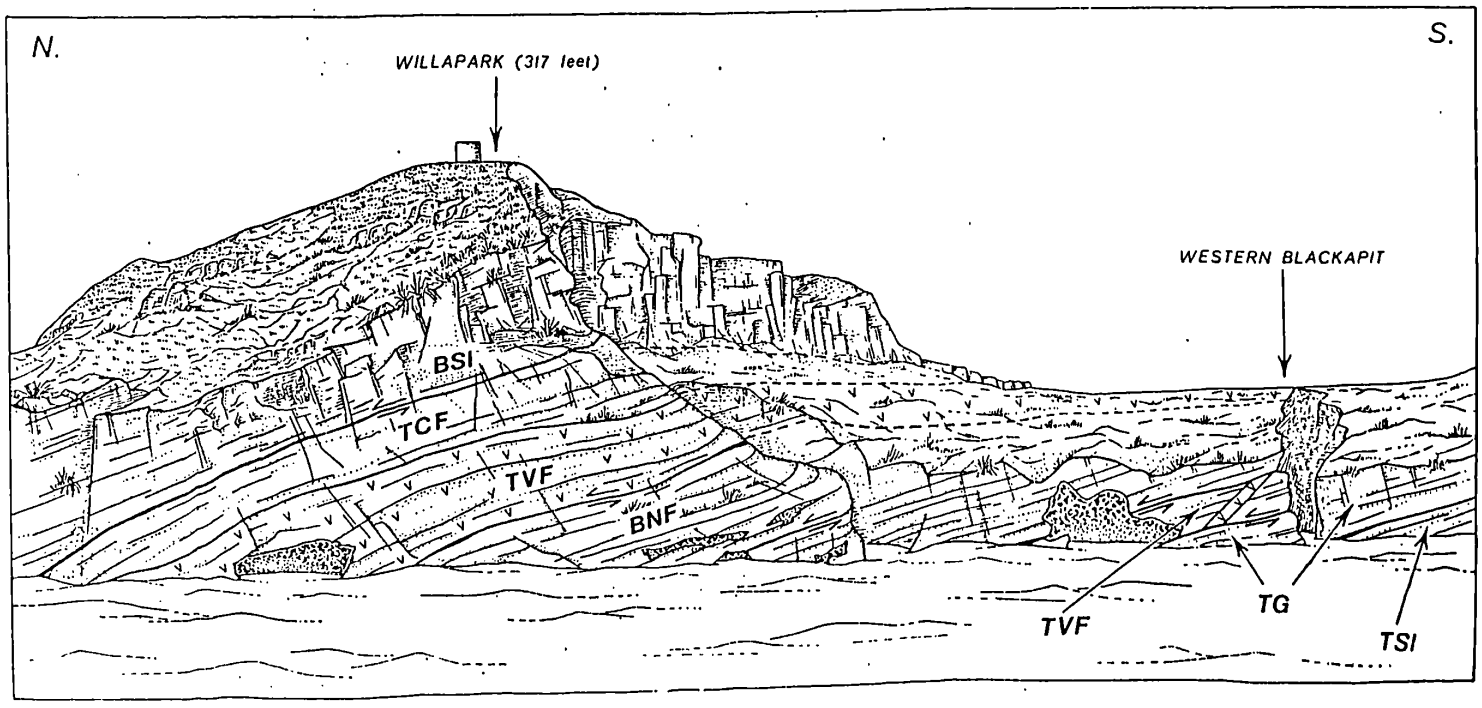

Figure 3.27 Sketch of Willapark and Western Blackapit from the sea showing tectonostratigraphy (Reproduced with minor amendments from Freshney et al. 1972). BSI Boscastle Slates, TCF Trambley Cove Formation, TVF Tintagel Volcanic Formation, BNF Barras Nose Formation, TG Transition Group, TSI Tredorn Slates

The relationships between the various units are best illustrated in north-south trending tracts of coast on the margins of Tintagel Island and Barras Nose. On the western side of the Barras Nose headland, distinct colour changes are observed from green-grey Delabole Slates close to the landing stage at Tintagel Haven, through approximately 60 metres thickness of dull grey slates with heavy quartz-veining (the Barras Nose Formation), and into a green, grey and black unit of Tintagel Volcanics. The boundaries between formations are seen on the coast to be low-angle fault-planes offset by moderate to steep north-dipping normal faults with small displacements.

Compressional Features

Between Boscastle and Tintagel the rocks show evidence for intense compressional deformation forming the northern part of the Tintagel High Strain Zone (Sanderson 1979, Andrews *et al.* 1988). Where strain is low, south- or east- facing F1 isoclines are preserved in a subhorizontal or shallowly north- dipping composite slaty cleavage (Figure 3.29). Such closures are common in black shales and grey siltstones around the bathing pool at Boscastle [SX 0944 9150] and show refolding of their attenuated limbs by north-verging D2 drag-folds. The S1 cleavage transects fold closures by approximately 10° clockwise, suggesting that a minor component of dextral shear is accommodated by parasitic F1 folds. Tight upright F1 folds are also seen about Boscastle Harbour where they are refolded above shallowly-dipping D2 detachments. F1 fold closures have been reported at Barras Nose [SX 0478 8930] by Freshney *et al.* (1972), where they face WSW.

The Tredorn Slates exposed to the west of Western Blackapit locally reveal bedding subparallel to S1 cleavage as a composite north-dipping fabric. The S0/S1 intersection lineation, where developed, plunges gently to the north-northwest at Grower Gut [SX 0869 9080]; an anomalous trend reflecting the rotation of linear D1 fabric elements into parallelism with the transport direction during high D1 strain, as observed in the formation of sheath folds (Dearman 1969; Cobbold and Quinquis 1980, Freshney *et al.* 1972). Further west at Trambley Cove, bedding dips swings from northeast to northwest across the *Davidstow Anticline* (Figure 3.28; Wilson 1951; Freshney 1965; Warr 1989); a broad flexure of S1 cleavage which coincides with the zone of anomalous L1 orientation. The antiform is, in fact, an antiformal syncline on the basis of stratigraphic ages (for discussion see Section 3.3.7).

High D1 plastic strains are indicated by the shapes of deformed tuff-bombs in the Tintagel Volcanic Formation, which form prolate to plane-strain ellipsoids defining a north-northwest plunging stretching lineation. Andrews et al. (1988) note that aspect ratios of 4.5:1:0.2 are not uncommon in the volcanics, and that these ductile features occur within the zone of increased in metamorphic grade (muscovite+chlorite+biotite+sericite±chloritoid ±actinolite in pelites; chlorite+muscovite+biotite±sericite in volcanics) reported by Robinson and Read (1981) and Primmer (1985c) (Section 2.5).

Boudins with b-axes trending both west-southwest and north-northwest are preserved within the section, with good examples seen at Grower Gut [SX 0869 9080] and Rocky Valley (Freshney *et al.* 1972) (Figure 3.29). At Rocky Valley, boudins of tuff are entrained within slates and thin limestones, their axes lying perpendicular to the mineral stretching lineation developed on the foliation. The orientation of their necks is problematic. In a typical nappe-stack, boudins form parallel to the trend of fold axes and thus should in this case be expected to trend west-southwest, perpendicular to tectonic transport (Coward and Potts 1982; Andrews *et al.* 1988). The zones in which anomalous north-northwest trending boudins necks are observed (to the west of Lye Rock; Figure 3.29) may therefore have formed either due to a localised strain

perturbation (e.g. lateral thrust ramp) which is not seen in other structural orientations, or through rotation of linear fabric elements during progressive diffuse D1 shear.

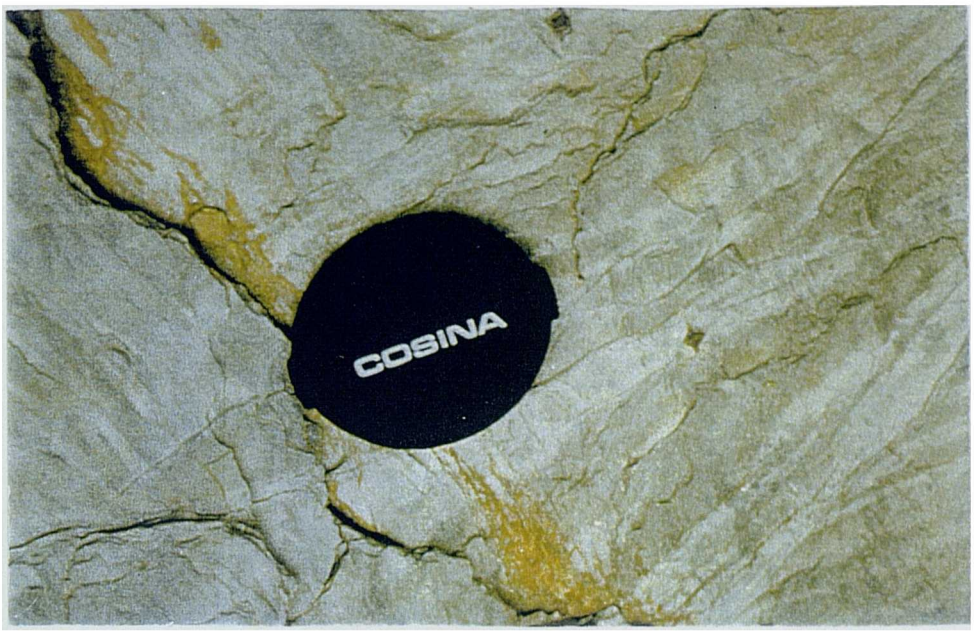

Plate 3.9 View southeast onto S0/1 composite fabric with strong NNW/SSE-trending mineral stretching lineation. Pyrite cubes with strain shadows also show NNW/SSE elongation. Late kink-bands which postdate D1 and D1 crenulate the foliation. Lenscap diameter 52 mm.

Stereoplots of D1 structure show a pronounced north-northwest trend of poles to planar fabrics, parallel to the tectonic transport direction (Figure 3.29). Bedding and S1 cleavage dip shallowly to the north-northwest or south-southeast, and the mineral stretching lineation plunges shallowly to the north-northwest or south-southeast (Plate 3.9). D1 fold axes plunge gently to the north-northwest and south-southeast, parallel to the mineral stretching lineation (i.e. they show anomalous orientations). The structural data collected from Tintagel Island shows complex bimodal orientations for boudin necks and F1 fold axes. This may reflect changes in strain magnitude (and hence variable rotation of linear fabric elements), or a localised phase of refolding relating to the detcahment structures pervasively developed in the area (Figure 3.29, Figure 3.30).

Extensional Features

D2 deformation zones comprising detachments, curvilinear ruck-folds and shear-zones with a transposing S2 cleavage are common within the Boscastle Formation (Figure 3.19, 3.30). D2 detachments are visible in the cliffs around Willapark [SX 091 912], where they form formation boundaries between the Boscastle Slates, Tintagel Volcanics, and Trambley Cove Slates (Figure 3.27). The detachments are described in detail by Freshney *et al.* (1972) and comprise quartz-calcite-dolomite breccias up to 3 metres thick along the movement planes, often overlain by F2 ruck-folds and shear-zones of S2 transposition.

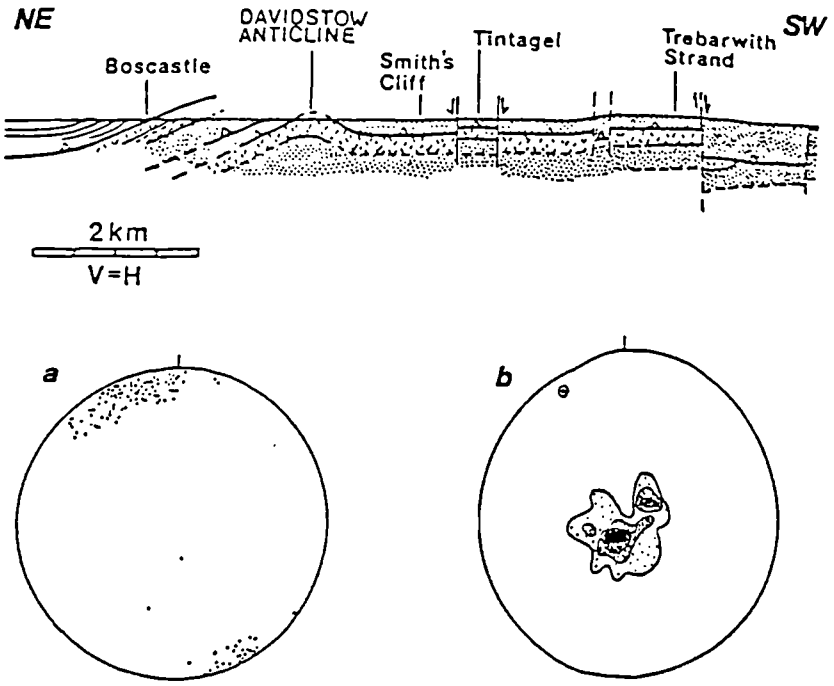

Figure 3.28 Sketch cross-section of the Tintagel High Strain Zone, locating the position of the Davidstow Anticline (Andrews *et al.* 1988). (a) Stereoplot of mineral stretching lineations across the Davidstow Anticline (n=76); (b) Contoured stereoplot of poles to S1 cleavage across the Davidstow Anticline (n=57; both from Warr 1991b).

F2 folds with curved hinge-lines plunging towards 215°-260° intensely deform the shallowly north-dipping long-limbs of F1 folds to the west of Boscastle. Between Western Blackapit and Trambley Cove patchy exposures of F2 folds and southeast-dipping S2 cleavage are seen along the cliff path. In the 1972 BGS memoir, Freshney *et al.* note that shallowly north-dipping thrust-faults emplace Upper Devonian Slates above Lower Carboniferous slates along the foreshore between Darvis's Point and Trambley Cove [SX 0743 9042 - SX 0740 9026], but ruck-folds in their hangingwalls verge downdip, and a south-dipping axial planar S2 cleavage is recorded, suggesting that the structure have experienced normal reactivation has occurred.

At Trambley Cove [SX 0734 9022], a quartz-calcite fault breccia up to 2 metres thick crops out in the cliffs (Figure 3.30). F2 Ruck-folds trend 215°-250°, verge to the northwest and are associated with a moderately southeast-dipping S2 cleavage, revealing the fault to be extensional. Marker bands cannot be traced across the fault and thus its extension magnitude is difficult to access. Hovever, the amount of shortening recorded by the faults (and hence minimum extension magnitude; Section 1.4) is between 30 and 40%.

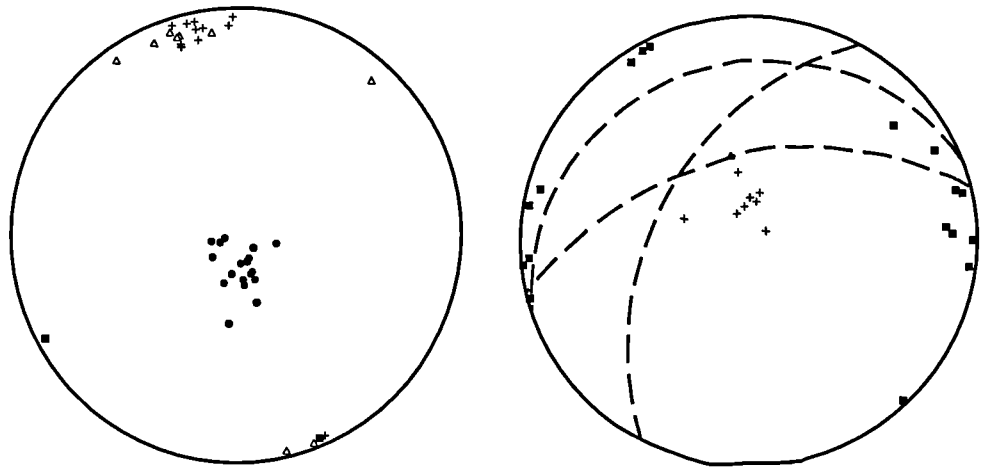

A. Rocky Valley to Lye Rock

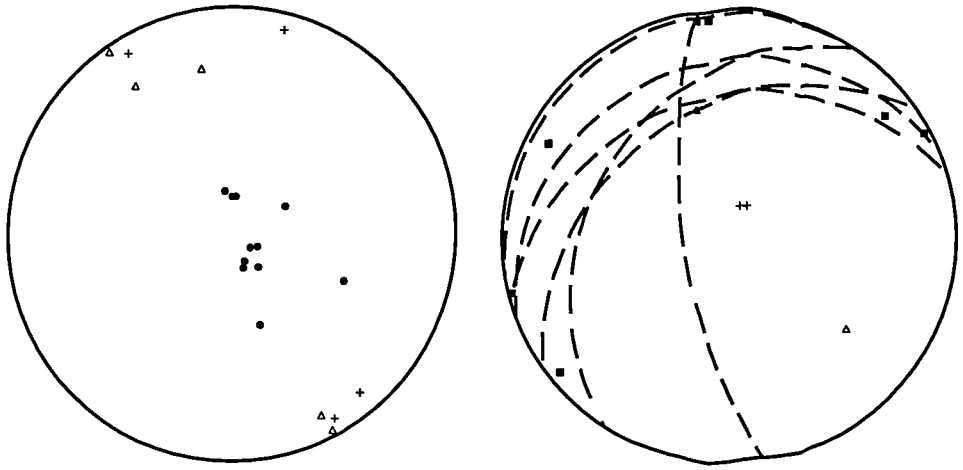

B. Gullastem to Barras Gug

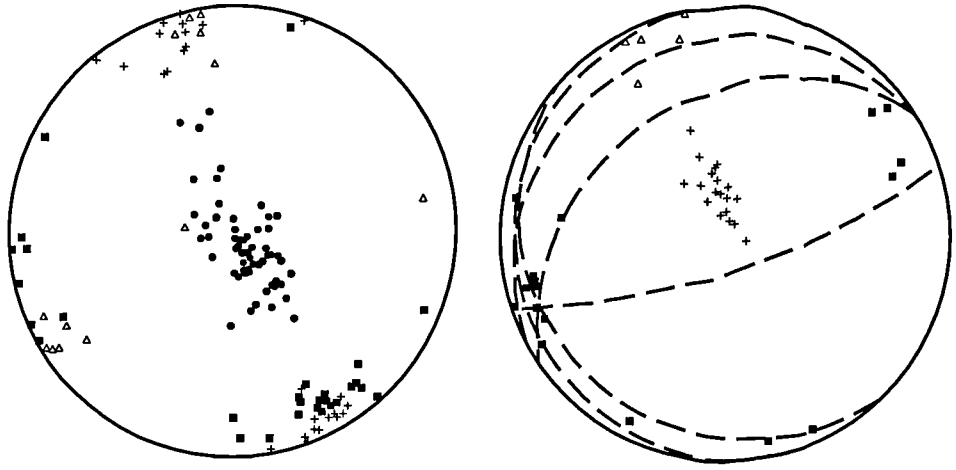

C. Barras Nose to Tintagel Island

Figure 3.29 Stereoplots of structural orientation data collected for three structural sections between Rocky Valley and Tintagel : (A) Rocky Valley to Lye Rock; (B) Gullastem to Barras Gug; (C) Barras Nose to Tintagel Island (for localities refer to Figure 3.26). D1 structures : *Planes:* dots = S1 cleavage. *Lineations:* triangles = F1 axes; boudin b-axes = boxes; mineral stretching lineations = crosses. D2 structures : *Planes:* crosses = S2; *(as great circles) :* fault-planes. *Lineations:* F2 axes = boxes; slickenlines = triangles.

Northwest-dipping detachments with associated decimeter-scale, north-vergent F2 folds are developed at the formation boundaries at Trewethet Gut and west Bossiney Haven and between Smith's Cliff and Barras Gug [SX 0560 8930 - SX 0552 8934] (Figure 3.30; Freshney *et al.* 1972). Shallowly- northwest-dipping faults dissect the headland at Barras Nose [SX 0522 8748], and were described as thrusts by Fear (1984). However, asymmetric fold kinematics, the age relationship of juxtaposed lithologies and secondary fracture orientations suggest that the faults represent D2 detachments which downthrow to the northwest (Figure 3.30). The western shore of The Island exposes low-angle detachments which separate Upper Delabole Slates, Tintagel Volcanics and Barras Nose Slates. Drag-folding, S2 cleavage orientation and subsidiary fault-planes along the detachments point to a top-sense of extensional transport toward the east-northeast (Figure 3.30).

Stereographs of D2 structure reveal a change in kinematics towards Tintagel (Figure 3.29). Between Trambley Cove and Lye Rock (Figure 3.29A), D2 detachments dip shallowly north or north-northwest and are associated with ruck-folds with shallowly east or west plunging axes and north vergence. S2 cleavage dips shallowly southeast throughout the area. F2 folds at Trewethet Gut show anomalous northwesterly plunges and west to southwest vergence which may be explained by : (i) generation in usual west-northwest-east-southeast axial trend and subsequent rotation to a northwesterly trend by localised deformation; or (ii) generation in anomalous orientation due to strain rotation above complexities within associated detachment systems (i.e. lateral ramps).

Between Gullastem and Barras Gug, D2 detachments dip shallowly northwest and F2 ruck folds verge north-northwest and plunge east-northeast or west-southwest (Figure 3.29B; Figure 3.30). S2 cleavage dips south more shallowly than further east, reflecting a flattening of fold attitudes. D2 folds with west to northwest vergence are infrequently observed above west-dipping detachments.

The orientation of D2 structure at The Island is complex, with north-northwest-dipping D2 detachments (parallel to S1 cleavage) and ruck-fold structures locally refolded about west-vergent folds and shallowly west-dipping D2 faults (Figure 3.29C). The west-vergent structures exposed between Tintagel and Gullastem are unlikely to have developed above lateral ramps in the normal fault system as they continue to show a down-dip rather than northwesterly shear direction. A third set of 'late' D2 features include broad northeasterly trending reverse kink-bands and southeast-dipping domino faults which record brittle southeast directed shear. The complexity of extensional kinematics at Tintagel suggests that deformation was long-lived, and that the pre-existing structural template was complex.

As elsewhere, north- to northwest-dipping normal faults with moderate to steep dips displace the low-angle deformation structures along the section, their frequency increasing towards the south. Late normal faults dipping steeply north-northwest cross-cut the shallowly-dipping decollément and are seen to back-rotate the shallower features at Saddle Rocks [SX 0735 9030], where throws of up to ten metres are observed.

They are often seen between Bossiney Haven and Trewethet Gut [SX 066 894 - SX 073 898], where faults strike parallel to the trend of the Davidstow Anticline. Further to the south at Rocky Valley, D3 faults are accompanied by quartz and calcite veins up to a metre thick. The headland at Barras Nose [SX 0522 8748] exposes a series of steeply northwest-dipping faults seen clearly when looking east from Tintagel Castle from changes in the colour of lithologies. In this locality they may be traced across the headland as low east-trending ridges.

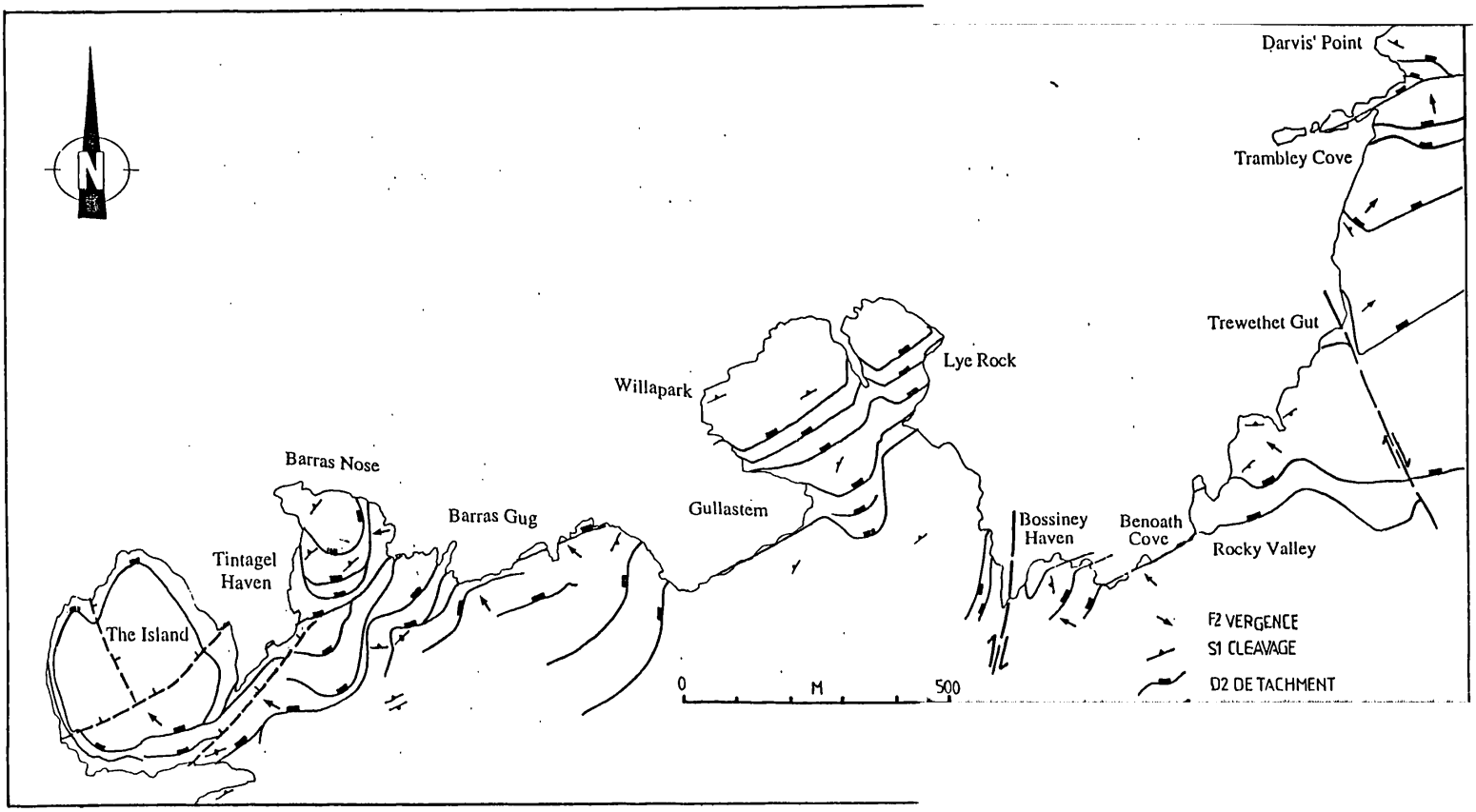

Figure 3.30 Map of major faults between Darvis' Point and Tintagel (adapted from Freshney *et al.* 1969).

A group of steep to moderately northwest-dipping normal faults run through the isthmus of The Island [SX 0515 8893], separating the Tintagel Volcanics, Upper Delabole Slates and Barras Nose Slates. They form a composite fault-zone which is well exposed on the western side of Tintagel Haven and contains a thin slice of Barras Nose slates with centimetre-scale quartz-veins parallel to the intense slaty cleavage (Plate 3.10). The veins define decimetre to metre scale updip verging angular ruck-folds within the fault-bounded wedge of slates whilst Riedel Shear orientations suggest that the fault formed in extension. The faults show many

of the features associated with D3 detachments, but the orientation of S1 is not locally oversteepened and thus they appear to have formed in this attitude. Although the vergence of drag-folds is generally taken to indicate the top sense of shear within each fault-zone, strain partitioning adjacent to sticking points at the margins of each fault-slice may cause backfolding. The nature of second-order structures suggests that the features formed as accommodation structures during the low-angle shear rather than during late brittle extension.

Dextral wrench-faults striking north-northwest are present at Gullastem [SX 061 895] where they displace a steeply northwest-dipping normal fault, and again at Trewethet Gut and immediately to the southwest of Western Blackapit (see Figure 3.26 for localities).

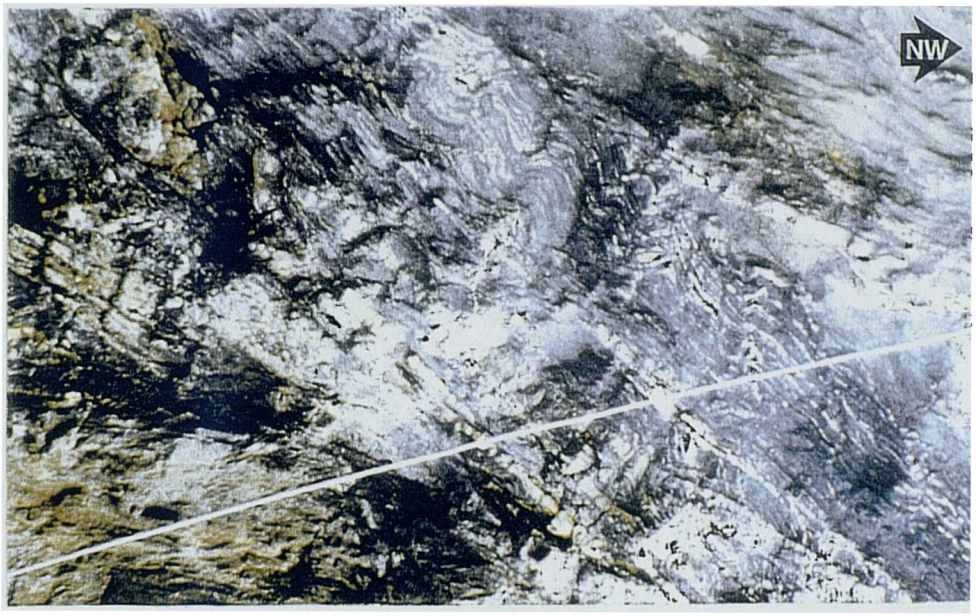

'ate 3.10 Detail of steep fault-zone, The Island. Black cherty slates represent a wedge of Barras Nose Formation entrained within buff Upper Delabole Slates. Ruck-folds verge updip whilst Riedel Shears indicate normal movement. Width of view 5 metres.

'hin section analysis

Samples of Upper Delabole Slate taken from Tintagel Island prove useful in characterising the late deformation due to colour variation and the presence of thin silt-grade planes. The dominant fabric is a micaceous cleavage subparallel to bedding formed from fine muscovite laths (d~0.04mm) aligned with chlorite sheets. Mottled brown iron oxides form masses parallel to the cleavage, suggesting that it was developed during the influx of Fe-rich fluids. Quartz-grain boundaries in silt bands are sutured and locally fractured, showing subgraining around their margins. D2 microstructure comprises crenulations of S1 schistosity and the formation of curviplanar microfaults and pressure solution seams approximately 80°anticlockwise of S1. The microfaults display extensional offsets directed towards 314° which die out in

parallelism with S1, and thus it appears that the D2 phase was accommodated by S1-parallel movement which caused compressional fabric development within the hinge zones of F2 folds formed in response to sticking along detachment surfaces.

3.3.5 South Tintagel to Trebarwith Strand

Lithology

Between Tintagel and Trebarwith Strand [SX 0514 8897 - SX0484 8641] the Upper Delabole Slates are extensively quarried. The slates are separated by sheets of the Tintagel Volcanic Formation and Barras Nose Formation tens of metres thick, juxtaposed across shallowly-dipping detachments (Figure 3.31). The southern shore of Tintagel Island exposes grey-green tuffs (locally cordierite-spotted), vesicular lavas and buff-weathering calcareous chloritic schists of the Tintagel Volcanic Formation, which overlie the older Delabole Slate Formation. To the south, the high ground exposes cleaved and indurated grey slates and black siltstones with occasional fossiliferous, chloritic slates and brown limestone with Upper Devonian brachiopod fauna (Upper Delabole Slate Formation; Freshney *et al.* 1972). A slice of Barras Nose Formation slates crops out at Dria Cove [SX 0485 8756] Dennis Scale [SX 044 862] and Glebe Cliff [SX 048 883]. Its boundary with the underlying Upper Delabole Slates is strongly sheared and cut out by low-angle normal faults (Freshney *et al.* 1972; Hobson and Sanderson 1975).

Rocks on the foreshore south of Bagalow Beach [SX 048 874] are formed of tuffs and vesicular lavas of the Tintagel Volcanic Formation, overlain subhorizontally by banded black slates and thin limestones of the Trambley Cove Formation. The junction between these two formations is strongly sheared and boudinaged and may be followed along the southwards along the shore as far as Vean Hole [SX 0489 8680].

Compressional features

Between south Tintagel Island [SX 0502 8900] and Bagalow Beach [SX 0502 8738], the S1 cleavage is pervasive and often obliterates bedding traces. S1 is flat-lying or shallowly west-dipping and appears to be parallel to bedding, Freshney *et al.* (1972) and Dearman *et al.* (1964) report isoclinal F1 fold closures at Tintagel Island and Hole Beach [SX 0510 8724] with axes plunging shallowly to 330°. To the south of Hole Beach, tuff and agglomerate beds contain elongate blebs of lava whose long axes trend north-northwest defining the D1 stretching lineation. S0 and S1 are again subparallel and dip shallowly west, northwest or southeast (Figure 3.33). The strain magnitude in this area appears to remain high, as rootless F1 isoclines are locally developed within the S1 cleavage plunging gently to the west-northwest.

Metre-scale sandstone boudins with gently eastnortheast plunging necks crop out at the contact between volcanics and slates at Vean Hole [SX 0492 8681] (Figure 3.32). Their necks are oriented perpendicular to

elongate strain markers (pebbles, clasts, brachiopods and reduction spots) in S1 cleavage planes, therefore appearing to have formed during the D1 deformation phase. The boudins may most simply be explained by flattening during development of the slaty cleavage (Warr 1991b) and thus appear to be D1 in age.

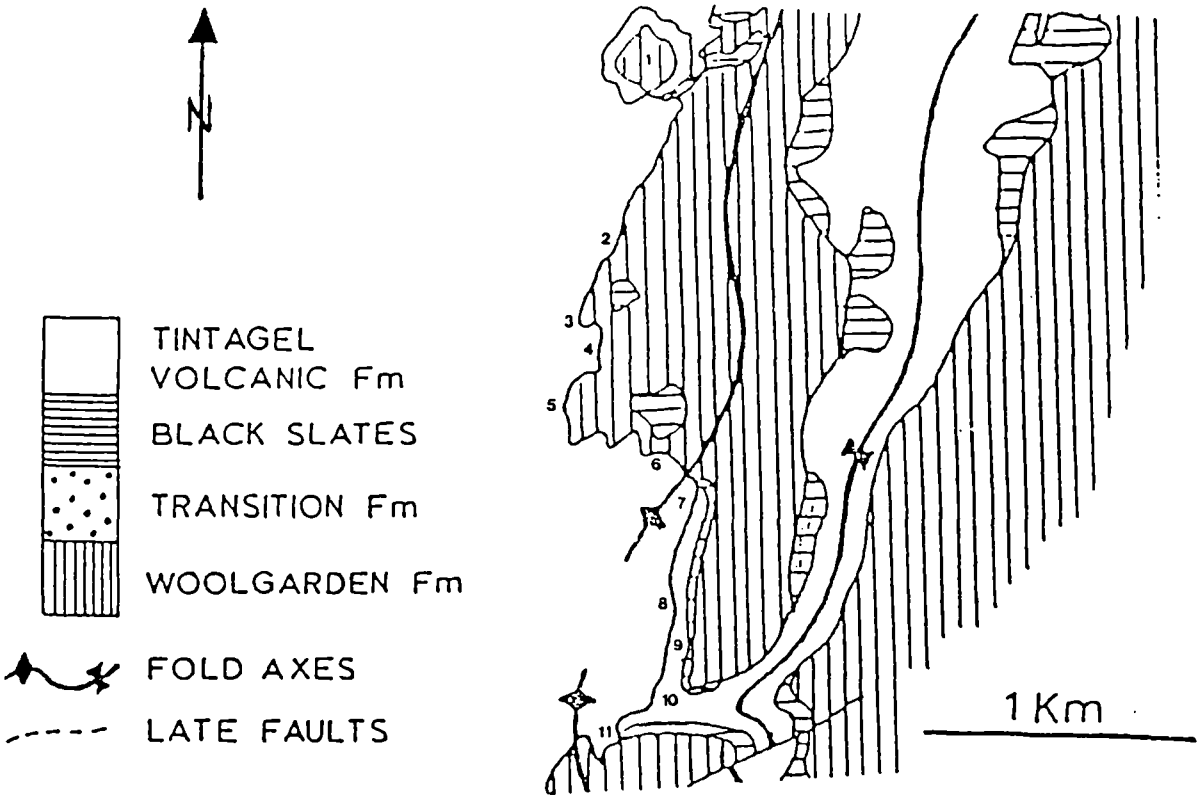

Figure 3.31 Geological sketch map of the coast between Tintagel and Trebarwith Strand (After Fear 1984). Numbers relate to key localities in the text.

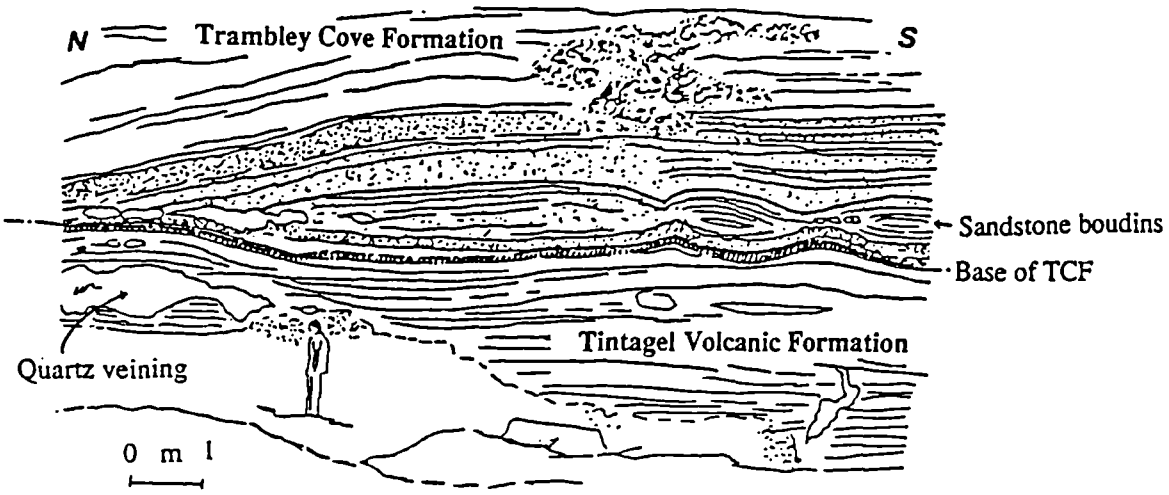

Figure 3.32 Elongate boudins at the base of the Trambley Cove Formation, Trebarwith Strand [SX 048 864]. Taken from Warr 1991a.

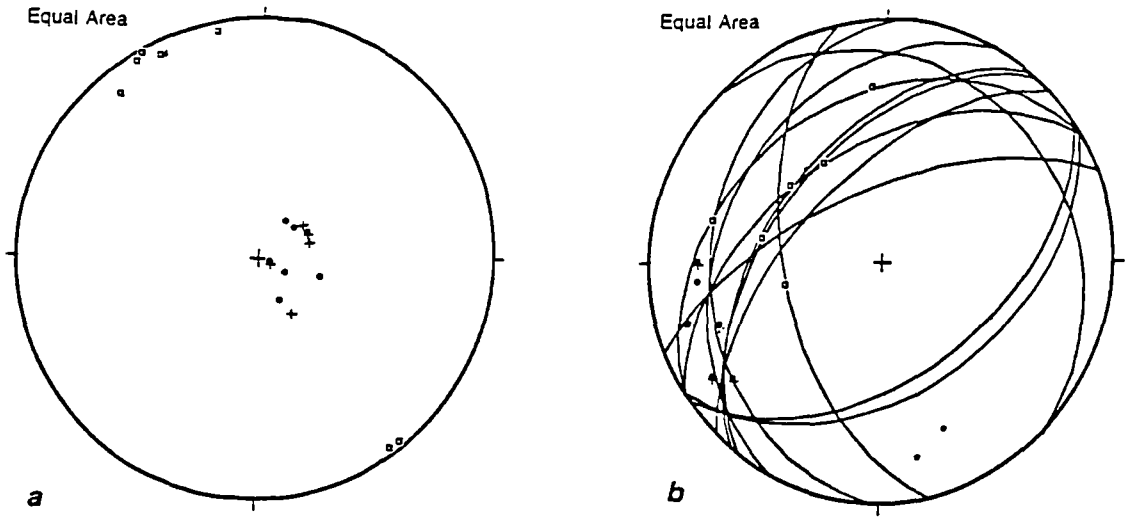

Figure 3.33 Stereoplots of structural orientation data, Trebarwith Strand to Bagalow Beach. (a) Compressional features: *Planes:* dots = bedding (7); crosses = S1 (5); *lineations:* boxes = stretching lineations (8). (b) Extensional features: *Planes:* great circles = faults (12); *Poles:* stars = kink axial planes (2); *Lineations:* boxes = slickenlines (6); crosses = fold axes (4); dots = kink axes (6).

Extensional features

Shallowly north-northwest dipping detachments are recorded by Freshney *et al.* (1972) between Tintagel and Trebarwith Strand, and are visible from the coastal path in quarry faces at Dunderhole Point, where they separate slates of different colour and grade. To the south of Hole Beach [SX 0507 8730], the junction between the Trambley Cove Formation and the Tintagel Volcanic Formation represents a shallowly west- to northwest-dipping D2 detachment. Its immediate hangingwall is intensely sheared and contains a southeast-dipping S2 crenulation cleavage. F2 sheath-fold vergence and Riedel Shear orientations indicate a top sense of shear toward the north-northwest. Sandstone boudins developed in the footwall rocks (Figure 3.32) have b-axes which parallel ruck fold axes, and where asymmetrical, show offsets compatible with top-to-the north-northwest shear. D2 detachments are again exposed in the backshore between Bagalow Beach and Trebarwith Strand, with quartz-veining defining movement planes dipping shallowly north along the S1 cleavage. Asymmetrical F2 folds distort the S1 cleavage into north-vergent folds which accommodate 35% of layer shortening (Figure 3.33b). Ductile D2 strain is partitioned along S1 cleavage, producing quartz σ-porphyroclasts and deforming S1-parallel quartz veins.

Locally developed post-D2 brittle kinks (λ ~40 cm) show the same north-northwest sense of shear if assumed to have formed through layer-parallel shear (Figure 3.33b). The kinks have linear hinge-lines, indicating a more brittle deformation style which may reflect : (i) extension at shallower structural level; or (ii) an increase in strain-rate. Both ruck fold-axes and kink-axes plunge shallowly west-southwest and verge north-northwest.

Steep northwest-dipping normal faults are common throughout the section and control coastal topography, forming northeast-striking cliffs on the northern side of inlets and headlands (Figure 3.33b; Bagalow Beach, Dria Cove, Lambshouse Cove). A throw of 38 metres is recorded across a high-angle fault by Freshney *et al.* (1972) on the northern side of Hole Beach, calculated by the stratigraphic offset across the structure. Faults are commonly paired at the south end of the section with secondary fracture planes separating mineralised wallrocks, or form braided systems of high and low angle movement planes. A major mineralised normal fault dips moderately northwest at Lill Cove [SX 0495 8662]. It has an ochrous breccia two metres thick containing pyrite, sphalerite and quartz, and its footwall contains steeply north-dipping tensile quartz veins. The development of polymetallic sulphide ores is not generally seen to the north of Trebarwith, and similar bodies in south Cornwall have been assigned radiogenic ages of 220, 170 and 75 Myrs (Halliday and Mitchell 1976). They may thus have been exploited as suitable conduits for fluid flow during after the Variscan.

Thin section analysis

A sample of interbedded tuff and marl collected in Lill Cove [SX 0490 8663] reveals high ductile strain along the intense foliation. The primary cleavage of biotite (d~1mm) and muscovite wraps around masses of magnetite and calcite to form symmetrical and σ-porphyroclasts with a top to the north or north-northeast sense of shear (Plate 3.11). The groundmass of the rock is very fine-grained and appears to be formed of dynamically recrystallised calcite and bands of cataclased feldspar and opaque minerals. Evidence of D1 southward shear is recorded in biotite fish, subordinate to down-dip directed shear indicators thought to indicate extensional shear. Quartz grains are subgrained and have recrystallised margins indicative of grain boundary migration recrystallisation at sub-greenschist temperature.

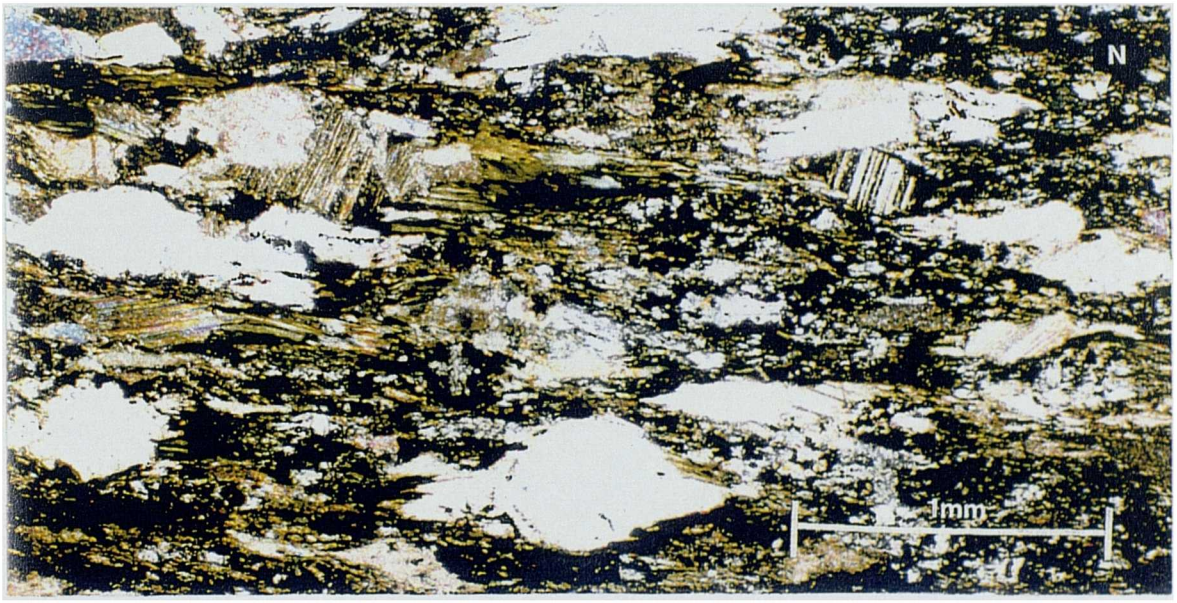

Plate 3.11 Photomicrograph of calcite porphyroclasts within the Tintagel Volcanic Formation, Trebarwith Strand. Clasts have calcite overgrowths and biotite tails, demonstrating shear along the S1 cleavage during greenschist metamorphism.

3.3.6 Port William to Port Isaac

Lithology

The coastal section south of Port William comprises Upper to Middle Devonian rocks of the Tintagel Succession (Figure 3.34; Section 2.2.3.2). Green and grey slates of the Tredorn Slate Formation overlie sheets of the Trambley Cove and Tintagel Volcanic Formations as far south as Tregardock Beach [SX 041 844], where a major east-striking normal fault downthrows the Tredorn slates to the south and thus they are exposed at sea-level (Andrews *et al.* (1988). Between Tregardock Beach and Trerubies Cove [SX 038 838] the green Tredorn slates grade into siltstones and marls of the Jacket's Point Formation (Selwood and Thomas 1986) and are again downfaulted towards the south by steep east-striking normal faults. Andrews *et al.* (1988) note that bedding is right-way-up and dips shallowly to the southwest between Tregardock Beach and Barrett's Zawn [SX 027 818], suggesting that the Jacket's Point Formation is younger than the Tredorn Slate Formation. A northwest-trending (southwest-dipping) reverse fault is exposed in caves on the western side of Tresungers Point [SX 0088 8120], placing Upper to Middle Devonian grey slates of the Pentire Slate Formation to the south over the Jacket's Point Formation to the north.

Compressional features

Between Trebarwith Strand and Tregardock Beach [SX 041 842], a pervasive S1 cleavage dips subhorizontally or shallowly southwest and contains the north-northwest trending stretching lineation seen elsewhere within the Tintagel High Strain Zone (Warr 1991b). At the northern end of the section, isoclinal F1 fold hinges are infrequently observed within the slaty lithologies due to the strength of S1 cleavage (and hence D1 strains). F1 folds plunges north-northwest, parallel to the stretching lineation. Observation of vesiculation in lavas at Port William [SX 0457 8631] suggests that rocks young towards the southwest and that F1 folds face down to the southwest.

In the derelict quarry at Backways Cove [SX 0431 8596] S1 dips shallowly southwest in slates of the Delabole Slate Formation. Dark grey colour bands plunging shallowly west appear to form an S0/1 intersection lineation (Warr 1991b), whilst strong mineral stretching lineations continue to trend north-northwest. The S1 cleavage faces down to the south in this locality (i.e. F1 folds face and verge down to the south). The stretching lineation trends east-west and its expression is weak at Portgaverne [SX 0006 8122]. Boudinage is rarely observed in the Devonian slates, perhaps as a result of the lack of sufficient competance contrast within the homogenous slates.

The change in orientation of F1 axes with respect to the regional stretching lineation to the south of Port William is of extreme importance, as it suggests a drop in strain. Where the D1 mineral lineation and F1 fold axes were subparallel, rotation of linear elements into parallelism with tectonic transport during D1

were invoked. If the mineral lineations and F1 axes are sub-perpendicular to the south of Port William Fault, strain may have fallen significantly. The Port William Fault may therefore juxtapose different structural levels in which strain is heterogeneous.

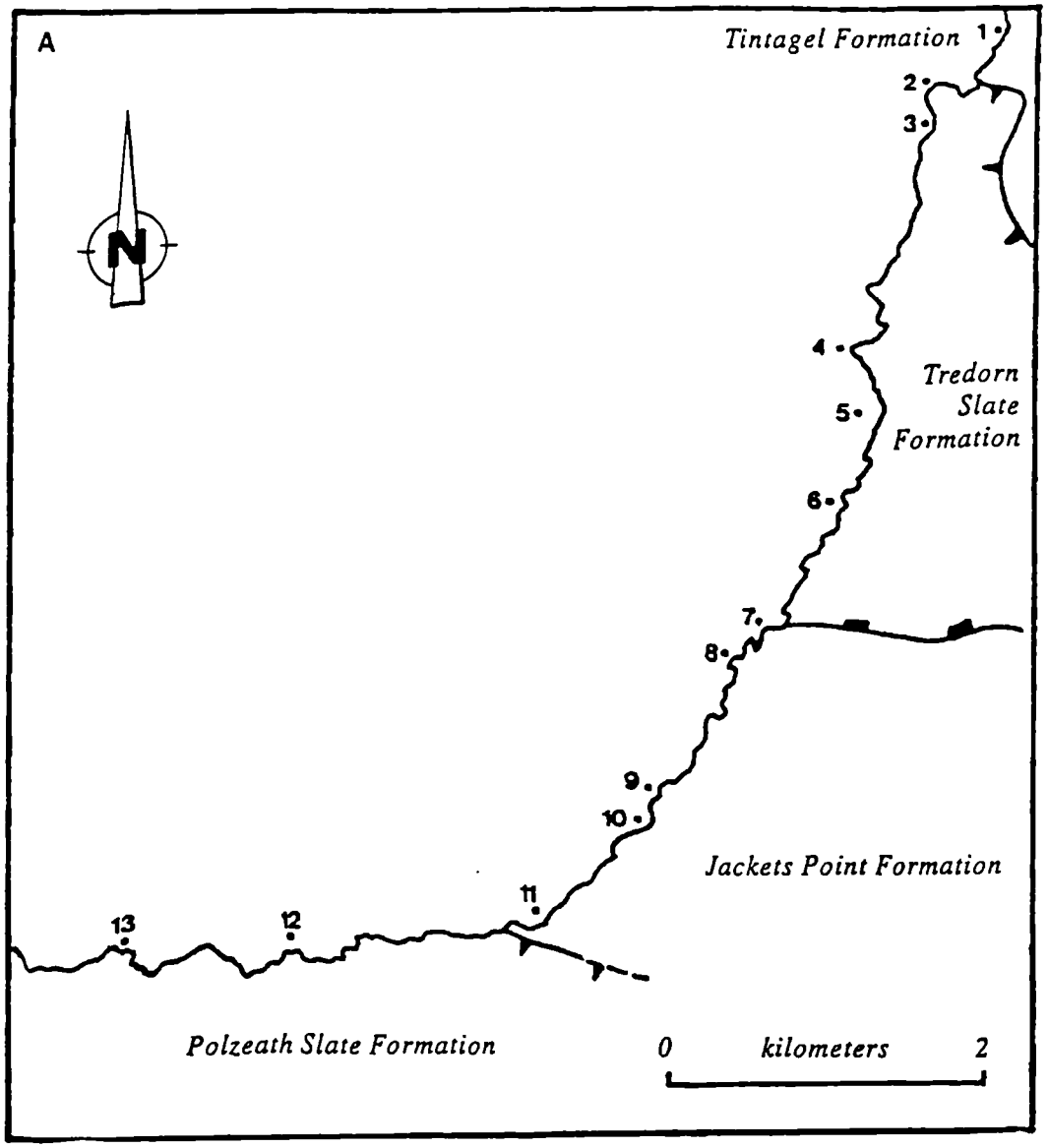

Key to localities : 1, Trebarwith Strand; 2, Dennis Point; 3, Backways Cove; 4, Tregonnick Tail; 5, Tregardock Beach; 6, Trerubies Cove; 7, Jackets Point; 8, Crookmoyle Rock; 9, Delabole Point; 10, Barretts Zawn; 11, Bounds Cliff; 12, Tresungers Point; 13, Port Isaac.

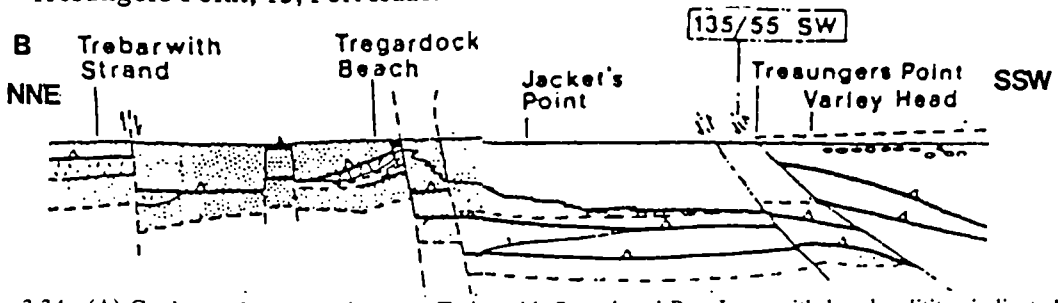

Figure 3.34 (A) Geology of the coast between Trebarwith Strand and Port Isaac with key localitites indicated (after BGS sheet 336, with adaption from Selwood and Thomas (1986) and Andrews *et al.* (1988). (B) NE/SW-trending structural section as illustrating stratigraphic relationships (Andrews *et al.* 1988).

The southernmost limit of the Tintagel High Strain Zone is generally accepted to be Tregardock Beach (Warr 1991b). South-facing F1 isoclines were reported by Hobson and Sanderson (1975), whilst Warr (1988) and Pamplin (1988) note folds facing both north and south, which they explain through north-directed thrusting in a second compressional event (prior to extension). The north-facing folds and south-dipping thrust structures are difficult to explain without a phase of northwest-directed compressional strain unless 'thrusts' represent ramps within an extensional system developed in a P-shear orientation. Between Tregardock Beach and Port Isaac, D1 structure is uniform (Warr 1991b; Figure 3.35). Bedding and cleavage are subparallel and subhorizontal or gently south- or southwest-dipping, the L1 (S0/S1 intersection) lineation plunges shallowly west and D1 mineral stretching lineation plunge south-southeast. F1 axes and S0/1 intersection lineations trend east-west but show some variation, perhaps reflecting the positions of T1 lateral ramps at depth. F1 folds face south or southwest, upwards between Trerubie's Cove and Jacket's Point [SX 039 838 - SX 0368 8343] (Warr 1991b). To the southwest of Crookmoyle Rock [SX 0319 8284], S1 cleavage and F1 folds face downward to the south. Changes in facing may indicate either that F1 folds are non-cylindrical, or reflect later folding and rotation of D1 structures.

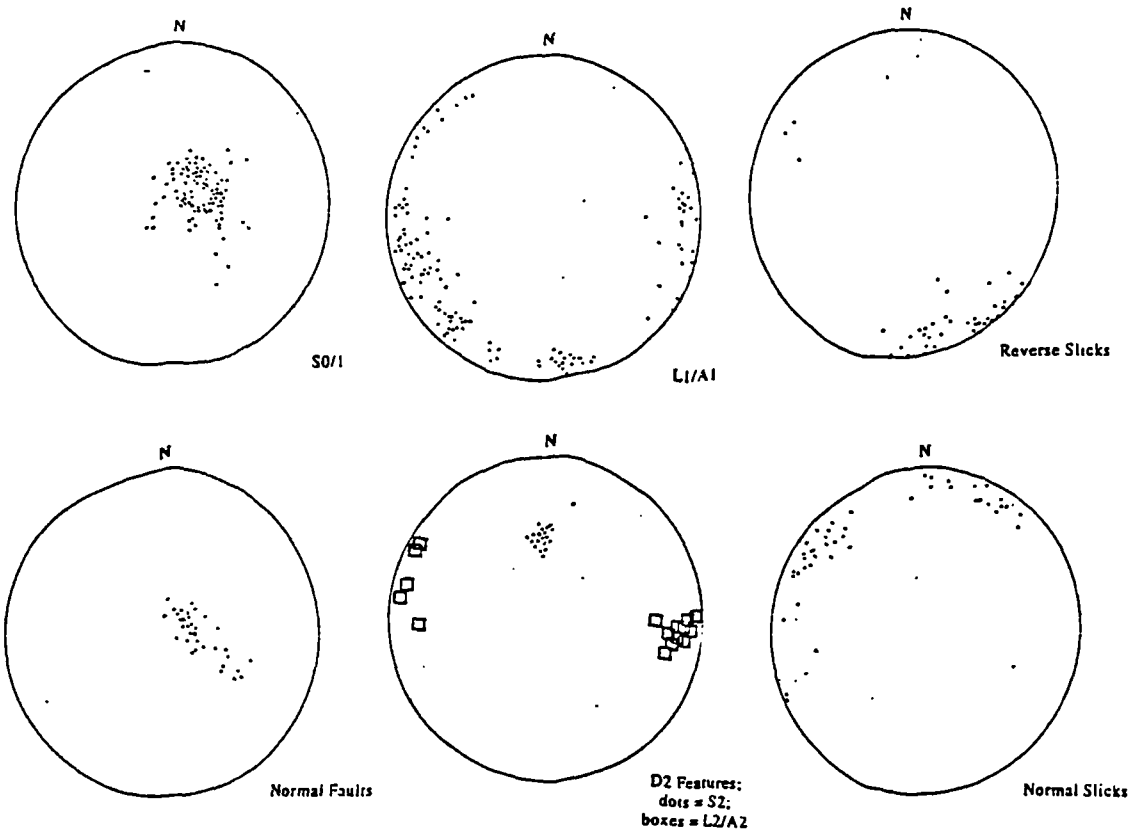

Figure 3.35 Stereographs of composite data-sets collected between Port William and Port Isaac by Warr (1991b). Planar data represented as poles.

Extensional features

At Port William, a shallowly northwest-dipping normal fault is exposed in the backshore, with downdip verging ruck-folds developed in its immediate hangingwall (Plate 3.12). The fault-plane is mineralised with quartz, pyrite, chalcopyrite and sphalerite in an explosion breccia 1.5 metres below the base of the folds. The folds have a weakly developed, south-dipping axial-planar crenulation cleavage which is exploited by quartz veins.

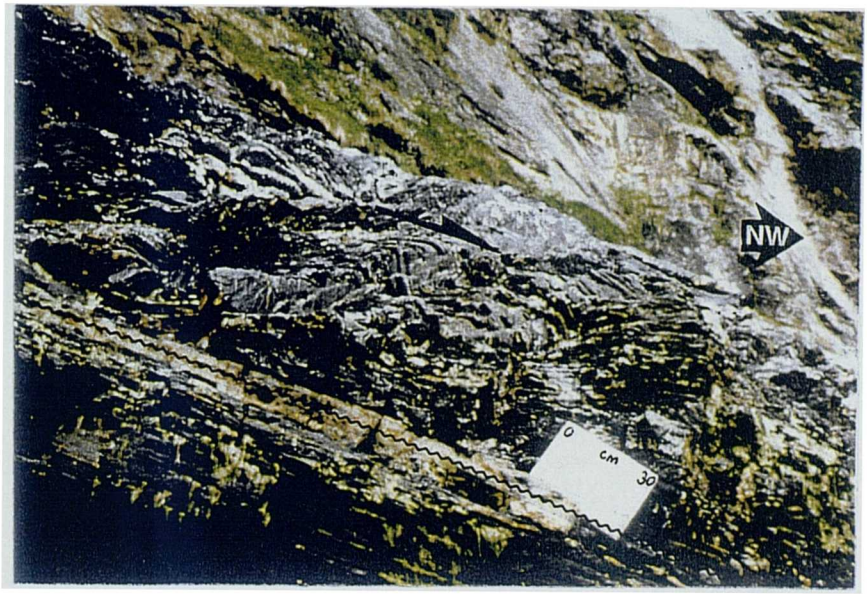

Plate 3.12 Downdip-verging asymmetric folds developed above veined D2 detachment, Port William

Further south at Tregardock Beach, slates of the Barras Nose, Delabole, Tredorn and Jacket's Point Formations are juxtaposed across shallowly north- to northwest-dipping normal faults with gouge up to a metre thick (Warr 1991b; Figure 3.36). The faults have curviplanar geometries which are concave upwards and their sense of offset confirms their extensional nature. The offset of the Delabole Slate-Tredorn Slate contact indicates up to 45% extension, although the curviplanar fault trajectories increase the degree of error to the figure (Section 1.4). Individual detachments record high lateral displacements, with lithostratigraphic boundaries offset by several hundred metres (Figure 3.36).

A southwest-dipping S2 crenulation cleavage is patchily developed at Tregardock Beach and Portgaverne [SX 0103 8119] (Warr 1991b) and is folded by F2 structures and overprinted by their related pressure solution cleavage. This early post-D1 fabric is attributed to north-directed thrusting by Warr (1991b), but may equally relate to early D2 extensional shear. Its anomalous orientation with respect to the later D2 fabric elsewhere may be explained through movement along oblique ramps at depth.

Linked high-angle normal faults are exposed on the southwestern face of Port William [SX 0459 8721], showing tectonic transport to the northwest and displacing units of agglomerate, tuff and slate. Steep

normal faults are common in the cliffs and dip at 43°-58° to the north causing offset of veined tuff bands by tens of metres. Steep normal faults are exposed at Tregardock beach, where they offset marker layers by as much as 40 metres (Warr 1991b). They dip uniformly to the northwest, and have brittle ruck-folds with northwest vergence developed adjacent to them. The development of folds along the fault-planes is more generally seen in D2 shallowly-dipping faults, but the faults at Tregardock Beach offset D2 detachments hence must postdate them. Steeply southwest-dipping normal faults are seen throughout the section and cause offsets which control the level of expose, notably between Tregardock Beach and Jackets Point (Figure 3.36).

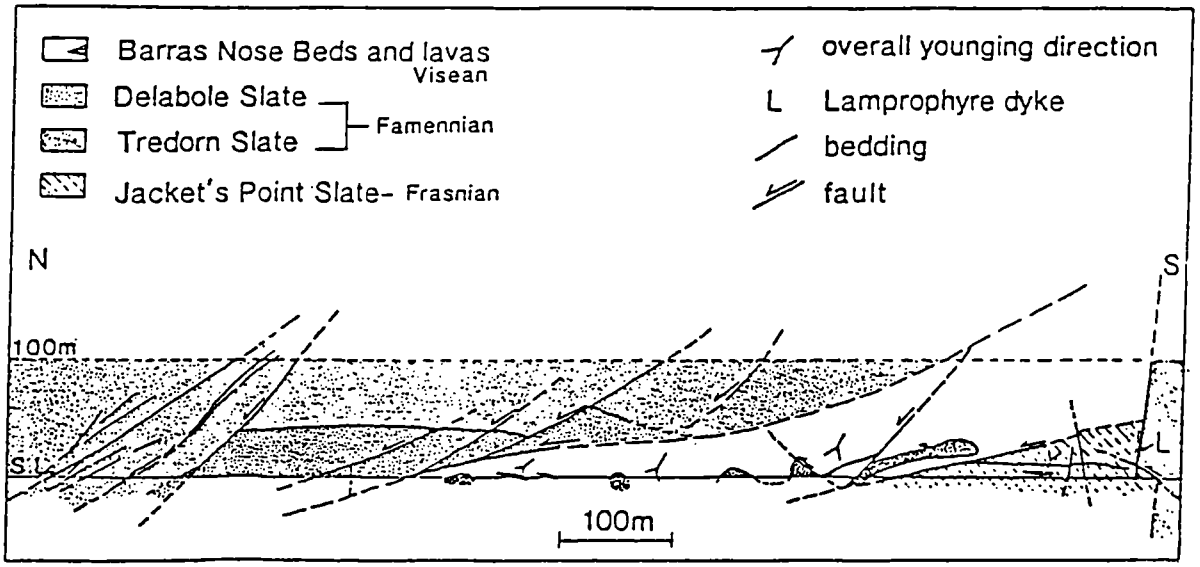

Figure 3.36 Structural section of Tregardock Beach, displaying northwest-dipping low-angle normal faults (Warr 1988; Figure 3.18).

Thin section analysis

Tuffs of the Tintagel Volcanic Formation which crop out below the Port William Fault, have a strong S1 foliation formed from aligned laths of chlorite. It entrains clasts of opaque minerals and calcite with muscovite and biotite tails which show ambiguous asymmetries. The development of clasts with a calcite composition indicates that they acted as the stronger component during low-greenschist non-coaxial flow, and as calcite is relatively weak rheologically in comparison to quartz or feldspar, the rock matrix must be extremely weak and prone to flow (Handy 1990). Calcite veins cross-cut the S1 foliation and are locally seen to crosscut porphyroclasts. They are recrystallised and crenulated by northeast-verging microfolds and truncated by pressure solution seams. The porphyroclasts must thus date to a deformation episode which occurred during greenschist facies metamorphism and prior to a crenulation event, indicating that they date to either a progressive D1 event or early D2 ductile shear event.

Siltstones from within the Port William Fault-Zone contain flattened quartz grains aligned with sericite laths to form the primary cleavage. Folds of coarser silt bands are ptygmatic and rootless, indicating an early phase of high ductile strain. Bands of muscovite and biotite mica wrap the fold hinges and form tails which indicate top to the southwest shear during the high-strain event. Quartz grains in the silts have annealed texture demonstrating ordering of grain boundaries through either a lowering of strain but maintenance of metamorphic conditions, or through increasing temperature through time. Pressure solution seams and large, aligned biotite crystals form an S2 fabric which dips more steeply southwest than bedding. Top to the northeast shear is evidenced by quartz porphyroclasts with muscovite tails. The porphyroclasts may have developed at the same time as S2 as they are not cross-cut by pressure solution seams and share a similar shear sense.

Within the fault breccias of D2 detachments, the S1 fabric warps euhedral pyrite crystals. The groundmass is speckled and grey-brown due to iron staining. Seams of cataclasite relating to fault movements are cemented by calcite and large cubic crystals of pyrite, and appear to have formed through hydrofracture. Further to the south at Backways Cove [SX 0446 8598], slates of the Upper Delabole Formation exposed in quarried faces are fine-grained with a matrix of fine sericite and clay minerals. Muscovite crystals are aligned to form the slaty schistosity, and wrap around fine pyrite cubes. Slates from Jacket's Point [SX 0335 8307] display purple and grey-green oxidation staining of a fine quartz-sericite matrix. In section, the slates have a phyllitic texture but appear to have experienced lower strain than seen in previous examples. Bedding is clearly distinguishable at low-angles to the slaty cleavage, and quartz grains show evidence for rotational recrystalisation. At Crookmoyle Rock [SX 0320 8282], northwest-dipping D2 detachments enclose bands of strongly deformed slate. Microscopic analysis shows that foliated mudrocks are entrained as clasts within a foliated cataclasite cemented by fine quartz crystals which have annealed textures. An S2 crenulation cleavage dips moderately towards the south-southeast, suggesting that the fault movement was towards the north-northwest.

3.3.7 Structural Summary and Discussion

The style of compressional and extensional deformation changes abruptly across the Rusey Fault, with metamorphic grade increasing from diagenetic to mid greenschist grade and F1 folds becoming recumbent and isoclinal. The style of D1 deformation changes abruptly towards Boscastle, as follows (Warr 1991b):

1. Rusey : F1 fold have ENE/WSW axial trends, face SSE, whilst S1 dips shallowly NNW and contains a downdip plunging mineral stretching lineation.
2. Pentargon : F1 axes (i.e. bedding-cleavage intersection lineations) trend NW/SE, parallel to the stretching lineation.
3. Port William/Backways Cove : stretching lineation and F1 axes show angular deviation of ~20°.
4. Tregardock Beach : F1 axes perpendicular to mineral stretching lineation.

This change in orientation was considered by Dearman and Freshney (1966) to have resulted from tergiversate folding during one phase of deformation; i.e. F1 folds face southwards and have sheath geometries due to intense southwards shear. Subsequent research has emphasised the importance of northward transport synchronous with greenschist facies metamorphism (Selwood *et al.* 1985; Andrews *et al.* 1988; Warr 1989a). In this model, F1 structures were generated in E W orientations and subsequently rotated (D2a; Andrews *et al.* 1988) during the formation of the Davidstow Anticline; an antiformal stacks above a blind ramp.

Field investigation supports early models of southwards-directed compression, and finds that the north-transporting features have a consistent transport sense, down the dip of the slaty cleavage. Early ductile strains attributed to D2a compression by Andrews *et al.* (1988) are heterogeneous and focused into discrete shear-zones which reactivate bedding and S1 cleavage. Subsequent semi-brittle detachment zones with apparent normal trajectories (D2b of Andrews *et al.* 1988; D2 in this study) were attributed to downsection-cutting thrusts by Selwood *et al.* (1985) and suggested to be roof thrusts to the Davidstow antiformal stack by Andrews *et al.* (1988), who argued that they have thrust geometries to the west of the antiform. This study does not see such a change in relationships and supports their generation as normal faults (Shackleton *et al.* 1982; Lloyd and Whalley 1986; Freshney 1965; Freshney *et al.* 1972; Isaac *et al.* 1982).

Extension of the North Trevone Basin is intense, with D2 north-northwest transportation along detachments accommodating moderate extension (~55%) between Boscastle and Tintagel, and extensional strain dropping to the south of Trebarwith Strand to below 40%. D2 detachments are associated with a range of secondary features which indicate northwest to north-northwest directed shear across most of the section, and minor west and southeast-directed shear events at Tintagel. The intense ductile shear may account for the presence of the Davidstow Anticline, as the action of low-angle normal faults is seen to cause decompression and upwarping of detachment zones in the Basin and Range of North America (Coney 1980).

A subsequent phase of D3 moderate to steep normal faulting crosscuts D2 detachments and again records top to the northwest downthrow. The strains associated with this event are lower than D2 but may locally accommodate above 30% extension.

3.4 The Central and Southern Trevone Basin

Stratigraphy

The stratigraphy of the section incorporates Givetian grey slates enclosing tracts of spilitic lavas, lying to the north and south of a 4 km wide, east-trending swathe of purple and green Polzeath Slates (Section 2.2.3.2). The Polzeath slates are Upper Devonian in age and form the core to the St Minver Synclinorium. Repetition of flattened pillow lavas at Kellan Head [SW 9700 8123] and Pentire Point [SW 923 805] allow way-up to be deduced and hence demonstrate the location of the subhorizontal limb of a south-facing F1 fold and that the across-strike section to the south exposes the inverted limb of the fold (Figure 3.37).

Bulk structure

Outcrops between Pentire Point [SW 923 805] and Daymer Bay [SW 928 775] expose a funadmentally important zone of D1 compression. The south-facing D1 structures recorded for over thirty kilometers to the north (Sections 3.2, 3.3) confront north-facing D1 structures developed to the south (Roberts and Sanderson 1971; Selwood and Thomas 1988; Andrews *et al.* 1988). Two D1 fabrics are preserved within this section and so as to avoid confusion, the cleavages are defined by their geographical distribution (Andrews *et al.* 1988). The first deformation north of the River Camel is named D1n and the first deformation south of the River Camel is denoted D1s.

The S1 fabrics to the north and south (S1n, S1s) never interfere in outcrop as both are penetrative in style. The north-facing structures apparently predate south-facing structures on the basis of their nature, intensity, facing and orientation (Roberts and Sanderson 1971; Pamplin 1988). K-Ar whole-rock ages support this hypothesis (Dodson and Rex 1971), showing older dates to the south of the River Camel (340-320Ma) than to the north (270-320Ma). Whilst structural evidence supports the generally accepted sequence of events, problems remain in modelling such polyphase deformations (Pamplin 1988). The fabrics investigated are overprinted by at least two further events and are thus ambiguous locally, as faulting and upright flexure reorients the structures and K-Ar whole rock isochrons must be treated with caution, as ages are likely to be in part reset during subsequent events. Pamplin and Andrews (1988) suggest that the only consistent criteria within the zone is shear-sense, as this is maintained even if structures are subsequently inverted.

In the absence of clear field relationships between the two sub-events, the supposition of a change in structural polarity has been discussed by several workers. Shackleton et al. (1982) accepted that D1 on the southern side of the Culm Basin faces south, although Selwood and Thomas (1986) disputed this and argued for consistent northwards thrusting throughout southwest England. Coward and Smallwood (1984) re-evaluated the facing confrontation in terms of thrusting, and suggested that the features seen may have formed through movement along a large, south-transporting backthrust.

Extensional structures have been little investigated despite the interest shown in the regional compressional structure. Brittle north-transporting detachments were noted in the area by Gauss (1973), but their significance has not been firmly established (Selwood and Thomas 1988).

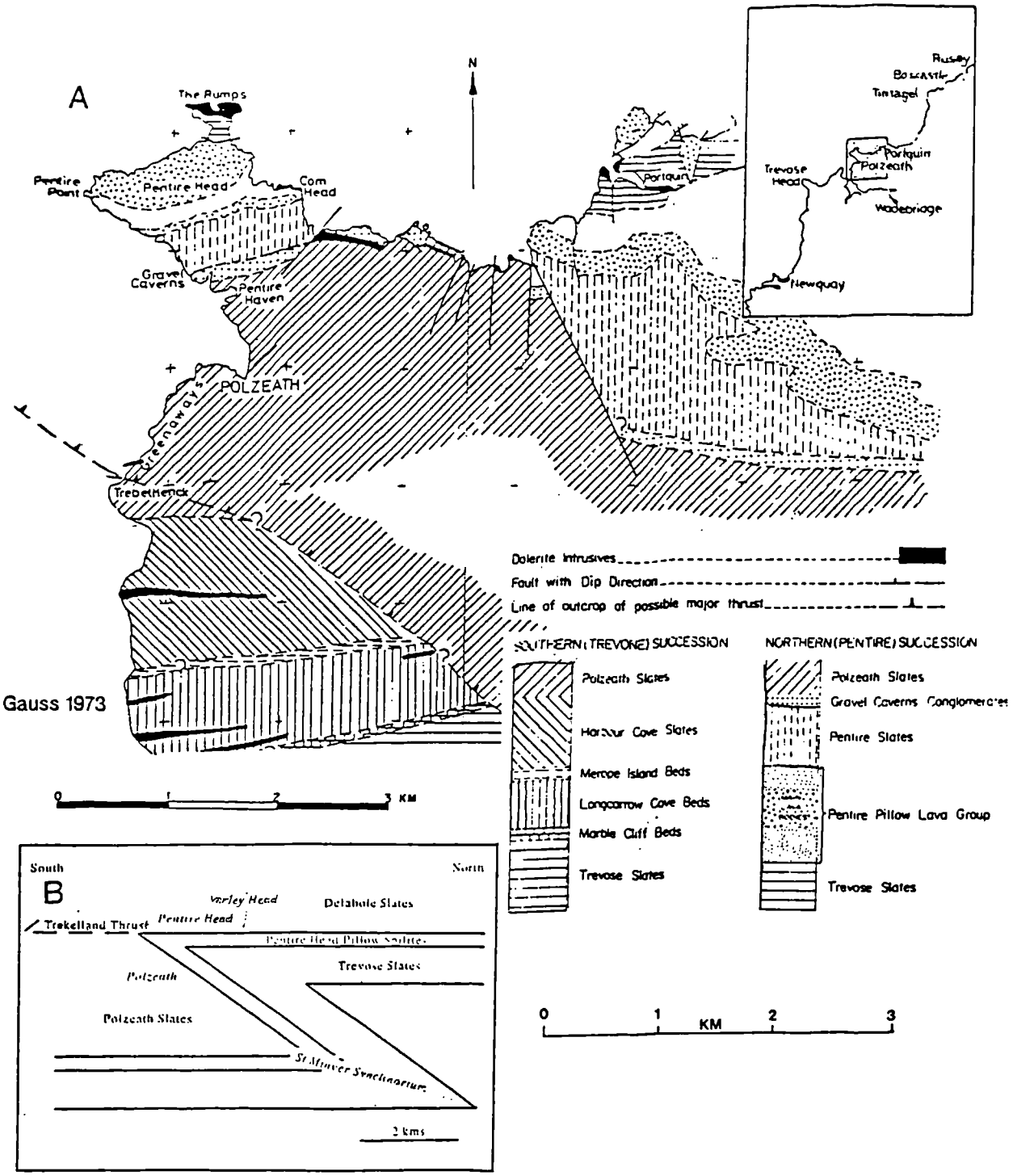

Figure 3.37 (A) Geology of the Central and Southern Trevone Basin. (B) Interpretation of the section between Rumps Point [SW 9302 8120] and Daymer Bay [SW 928 775], showing the positions of key localities (italics) within the stratigraphy (After Andrews et al. 1988).

3.4.1 Port Isaac to Pentire Point

Lithology

Grey Givetian slates, siltstones and sandstones of the Trevose Slate Formation crop out along the bulk of this section. They are typically featureless but are strongly laminated in discrete horizons. The northern sides of Lobber Point [SW 9932 8125] and Varley Head [SW 9869 8148] expose purple Delabole slates, down-faulted against the Trevose slates to the south. Steep cliffs of pillow lava and splilite occur at Scarnor Point [SW 9788 8118], Kellan Head [SW 9700 8124] and northern Port Quin [SW 9689 8070]. The pillow lavas appear to form the uppermost beds of the Trevose Slates but are often seen in faulted contact (e.g. Port Quin).

Between Port Quin [SW 9710 8050] and Pentire Point [SW 9229 8046], grey slates of the Trevose Slate Formation make up much of the coastal outcrop, punctuated by orange-brown spilitic pillow lavas at Doyden Point [SW 9694 8072], Trevan Point [SW 9606 8018] and around Pentire Point. Metadolerite bodies crop out at Port Quin, Lundy Bay [SW 957 799] and Rump's Point [SW 9302 8126]. The pillow lavas appear to lie at the top of the Trevose Slate Formation, but are down-faulted towards the north in a number of places (e.g. Doyden Point) by late steep structures.

Compressional features

A pervasive S1 fabric is developed throughout the section, dipping shallowly to moderately south-southeast. F1 folds observed where siltstone layers occur in the slates at Varley Head and Port Quin are open to close and most commonly face southwards, their axial planes parallel to the cleavage (Figure 3.38). The S1 fabric hosts a west-plunging mineral lineation of chlorite aggregates and stretched iron nodules.

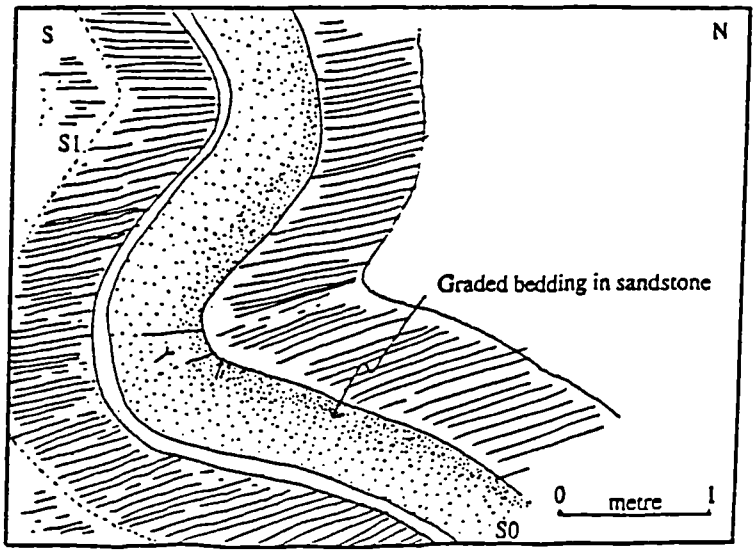

Figure 3.38 F1 folding, south Port Quin [SW 9695 8058]. Bedding youngs south and hence faces down to the south.

To the south of Port Quin, Warr (1991b) recorded both north and south- dipping S1 foliation, uniformly facing downwards to between the southeast and southwest. Bedding - S1 cleavage intersection lineations are subhoriontal and trend northnortheast and east-northeas. D1b compressional structures are common at Lundy Bay, where S1b crenulation cleavage and quartz-veins dip shallowly to the south. F2 fold axes plunge shallowly to the northwest or southeast, and verge northwards above minor thrusts. At Pentire Head, S0/S1 intersection lineations plunge southwest. Quartz-veining becomes less pervasive towards the south and faulting more infrequent.

A second compressional phase is recorded at Port Quin [SW 969 804] - south-dipping thrusts with tight north-verging folds in their hanging-walls, their axes plunging shallowly east-southeast represent D1b deformation. A steeply south-dipping crenulation cleavage occurs adjacent to the thrusts and axial-planar to the folds, causing transposition in some cases. Sandstone and splitic bands are boudinaged within this shear system and show northwards asymmetry consistent with north- to north-northeast directed thrusting (Warr 1991b). These structures must be viewed with caution, as the dominant anisotropy (S1n) dips south in this section - any continuation of the D2 extensional kinematics see to the north (e.g. Boscastle) would thus have thrust-like appearance.

Extensional Features

Shear-sense during the first extensional event, D2, is recorded by ruck fold vergence and the orientation of spaced steep shear-bands which indicate south-directed shear along bedding and/or S1 cleavage. Detachments are observed in bluffs on the eastern side of Greengarden Cove [SW 9941 8146] and at Port Quin [SW 9798 8067], where a steeply north-dipping S2 crenulation cleavage is developed within zones of intense ruck folding. The extensional structures appear to have developed through reactivation of D1b thrusts with quartz-haematite-ankerite mineralised movement planes. The vector of extension is to the south or east, as seen in irregular and curved slickenlines with dip-slip stepped quartz-calcite fibres overprinting oblique-slip grooves relating to thrusting.

Shallowly northwest-dipping detachments (D2) are exposed on the western side of Port Quin and again partition asymmetric folds and quartz-veins in their hangingwalls. They show extensional secondary fracture orientations and a semi-brittle deformation style, but are antithetic to the main group of D2 detachments. The two orientations of detachment are not seen to crosscut one another and thus appear to have developed synchronously.

Steep, north-striking normal faults occur in the western face of Port Quin and have concave-upwards geometries. Upright gentle flexures of the S1 cleavage appear to have formed through drag against the faults. The faulted base of the igneous rocks to the south of Kellan Head {SW 9675 8071] dips shallowly to north and displays metre-scale fault-offsets to the west across minor normal faults. Steep D3 normal

faults are common at the western end of the section, where they dip moderately to the north and are slightly curviplanar in cross-section. Warr (1991b) recorded moderately north-plunging slickenlines on the fault surfaces which are consistent with northerly downthrows.

Thin Section Analysis

A sample of slate taken below the slipway at Port Quin contains a strongly altered muscovite, quartz, clay- and opaque mineral groundmass which is strongly aligned to form the slaty schistosity. Metamorphic spots are conspicuous in both hand specimen and thin section, and appear to be heavily altered cordierite crystals which show internal inclusion alignments that imply that they formed synkinematically during D1 compression. The spots show a speckled pinate texture, having been retrogressed to quartz, sericite and chlorite (Plate 3.13). Despite this, the internal alignment of inclusions is clearly seen within the pseudomorph and two phases of their growth are recorded in a rim of darker alteration products around lighter core material. The geometry of chlorite-muscovite tails on the spots suggest shear following the mineral growth down the dip of S1 towards 113°. Convolute quartz-rich bands reveal close folding of bedding at high-angles to S1 and suggest that the sample is derived from the hinge of an F1 fold.
Metadolerites are strongly weathered but contain a basic mineralogy of olivine, feldspar, clinopyroxene, chlorite and opaque minerals. A fibrous grey-green mineral is present in patches and appears consistent with the character of pumpellyite. A crude foliation defined by aligned sericite grains cuts the rock where the groundmass is fine and recrystallised, but no overprinting microstructures are preserved.

3.4.3 Padstow Facing Confrontation; Gravel Caverns and New Polzeath

Lithology

The coast between Pentire Point and Daymer Bay exposes rocks of the Trevose slates, Harbour Cove slates and Polzeath slates (Section 2.3.2.2). They lie within the inverted limb of a kilometer-scale south-facing synform; the St. Minver Syncline and hence are inverted, younging down to the south (Figure 3.37).

Mid-grey slates, siltstones and tuffs of the Trevose Slate Formation are exposed in the western face of Pentire Point. They young southwards and in their upper part contain metadolerites and pillow lavas of the Pentire Volcanic Member (Warr 1991b). The pillows typically measure between 0.3 and 1.0 metres in diameter, and variations in the degree of vesiculation from base to top are useful way-up indicators. The lavas are heavily altered, their groundmasses formed of sericite, chlorite, plagioclase and albite. Amygdales and veins contain quartz, chlorite and calcite.

The Harbour Cove slates crop out over 400 metres of section to the southeast of Pentire Point. They are grey, dark grey or pale green and weather to a buff grey colour, but distinguishable from the older Trevose

slates to the north by the occurrence of ironstone and tuff beds. Above the grey-green slates, beds of poorly sorted conglomerate and gravel-grade greywacke surrounded by dark grey and green slates are exposed at Gravel Caverns [SW 9318 7982]. Clasts supported within the matrix include grey micritic limestone, slate, pyritous black mudstone and orange-weathering tuff, suggesting that they were sourced by the stratigraphically older Harbour Cove slates. Clasts are heavily sheared and are subrounded, and include metre-scale blocks of orange-weathering alkali-basalt pillow lavas exposed on the northern margin of Pentireglaze Haven [SW 9342 7970].

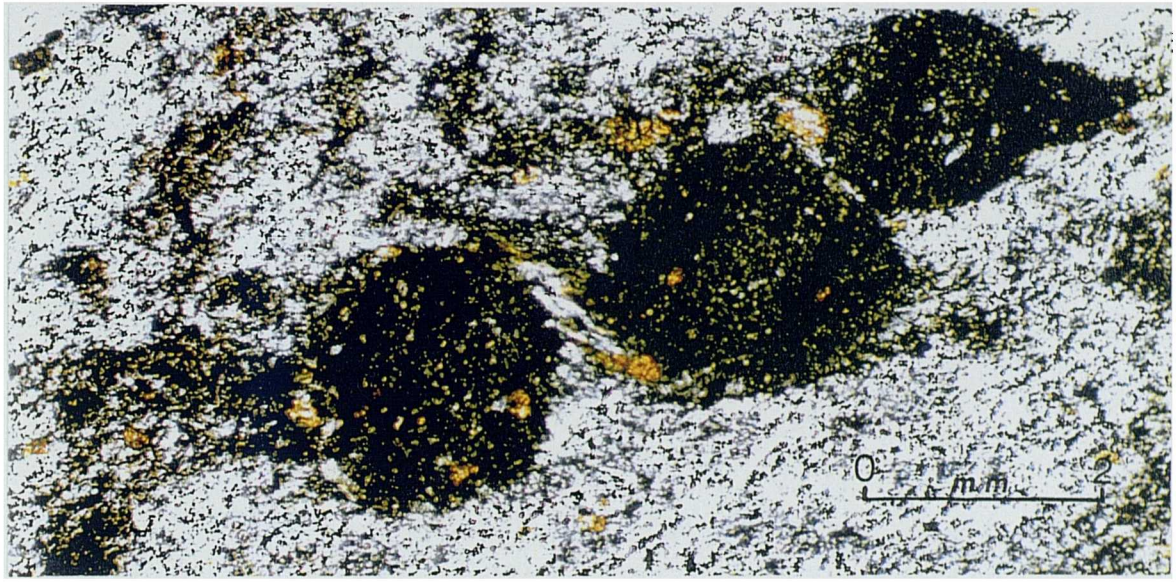

Plate 3.13 Photomicrograph of pinitised cordierite blasts, Port Quin. Note the development of biotite tails (shear-sense unclear), and dark internal striping of the blasts with consistent orientation at high-angles to the surrounding matrix.

The lithology changes on the northern side of Pentireglaze Haven [SW 9323 7968] to purple and green slates of the Polzeath Slate Formation. Colour variagation is diagenetic and masks bedding which may only be positively distinguished from bands of siltstone or occasional fossilliferous slate layers which provide a Fammenian age. They represent the youngest strata in this section and lie in the core of the St. Minver Syncline.

Compressional Features

The northern end of the mapped section (unnamed cove west of Pentire Farm [SW 9297 8005]) has a pervasive D1n foliation which is subhorizontal and varies between north and south dip directions across steep normal faults (Figure 3.39, 3.40). Bedding locally defines m- and s- shaped parasitic F1 closures which face down to the south. Moderately north-dipping thrusts (T1s; 45°NNW dip) partition a moderately south-dipping S1s cleavage locally (Selwood and Thomas 1988). S0/S1n intersection lineations are common and plunge gently to the northeast or southwest.

Traversing southwards toward Gravel Caverns [SW 9303 7996], the north-dipping S1n fabric continues to be pervasive but the intensity of S2 folding and cleavage development intensifies, manifested in a steepening of F1n fold axial planes and S1n fabric, and increased prevalence of a moderately south-dipping pressure solution S1s fabric. Selwood and Thomas (1988) proposed that this steepening of S1n orientation locates a short inverted limb to a north-verging F1s fold which refolds an F1n isocline.

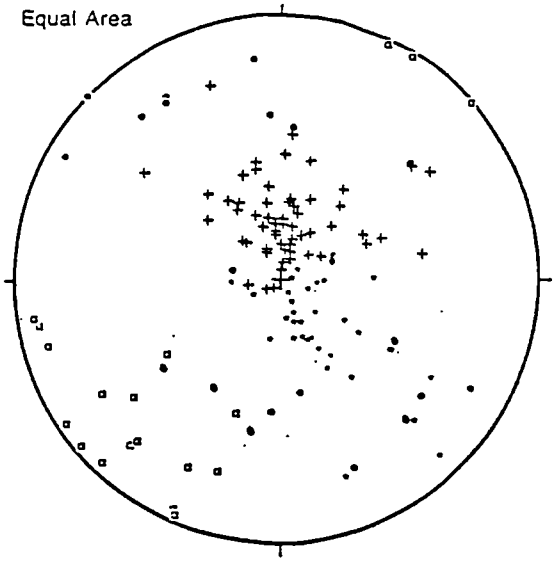

Figure 3.39 D1 structural components, New Polzeath. *Planes*: dots = composite S0/S1 fabric (22); crosses = S1n fabric (51); stars = S1s fabric (29); *lineations*: squares = F1 fold axes (19).

A conglomerate bed approximately 0.4 metres thick containing sub-vertically aligned clasts is exposed in the column between caves at Gravel Caverns [SW 9303 7995] (Figure 3.40). The clasts are contained within a steeply north-dipping pressure solution cleavage, again indicating post-D1n rotation through F1s or later folding. Minor F1 s-folds are seen to the west of the conglomerate band and m- and w- profiles are observed in the sides of the easternmost cave. A shallowly south-dipping S1n cleavage is present above the cave and obliterates evidence for previous fabrics (Figure 3.40)

Continuing south towards Tar Caverns [SW 9318 7980], a subhorizontal to shallowly south- dipping S1s cleavage forms low exposures, enclosing rootless isoclinal fold hinges with s- and m- profiles. Tracing the structures toward the cliffs, they steepen into a vertical S1s fabric which is overprinted by a spaced, south-dipping S1n cleavage (Figure 3.40). Selwood and Thomas (1988) identify this structure as the hinge of a F1n synform paired to the Gravel Caverns antiform to the north. Sedimentary structures indicate younging down to the south and hence the F1n synform faces south.

The Polzeath Thrust forms the boundary between the Gravel Caverns conglomerates and the Polzeath slates (Selwood and Thomas 1988). The thrust dips steeply south at Pentireglaze Haven [SW 9340 7965] but swings seaward and dips shallowly eastwards [SW 9301 7981]. The thrust disrupts bedding within the Polzeath slates over a thickness of ~ 15 metres and contains orange-weathering pillow lavas in its hanging-wall. Ductile S1s cleavages are preserved above the fault and stepped slickenfibres on the fault surface

indicate northward thrusting at Pentireglaze and westward thrusting at its seaward extent (Figure 3.43). Selwood and Thomas (1988) regard the structure as a T1s thrust folded about a north-verging F1n fold. This may have occurred if the quoted F1n fold is an s-fold from the inverted limb of a larger F1n structure, and the change in slickenfibre orientation along the thrust is inconsistent with the geometry being associated with a lateral ramp to the west.

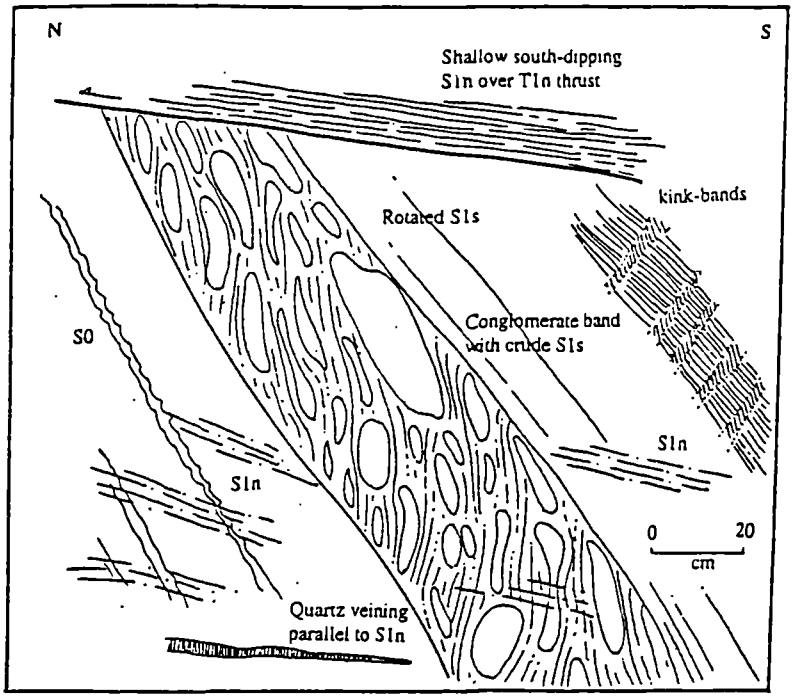

Figure 3.40 Field sketch of structural relationships at Gravel Caverns.

Between Slipper Point and New Polzeath Beach [SW 9342 7059 - SW 9367 7906], the dominant S1s fabric dips shallowly- to moderately southwards, its orientation affected by late open folds with north/south trending axes (post D2?) and north-vergent folds relating to the extensional event (Figure 3.43). Graded bedding continues to indicate southwards younging. The cleavage steepens at East Beach [SW 9371 7890] across angular F1n folds and is affected by a subhorizontal S1n pressure solution cleavage (Figure 3.41)

The coastal outcrops between Polzeath and Daymer Bay [SW 928 775] preserve four groups of structures (Pamplin 1988); D1n and D1s are recorded by flat-lying foliations which are usually mutually exclusive, and are axial planar to recumbent, east-west striking folds. S1n is often defined by spaced pressure-solution seams whilst S1s is pervasive. D1s folds and late D1s thrusts are overprinted by the D1n (north-dipping) cleavage in both limbs at Trestram Cove [SW 932 789] (Pamplin 1988), indicating that D1n is later than D1s at this locality. S1n is seen as crenulations and small-scale folds within the S1s fabric.

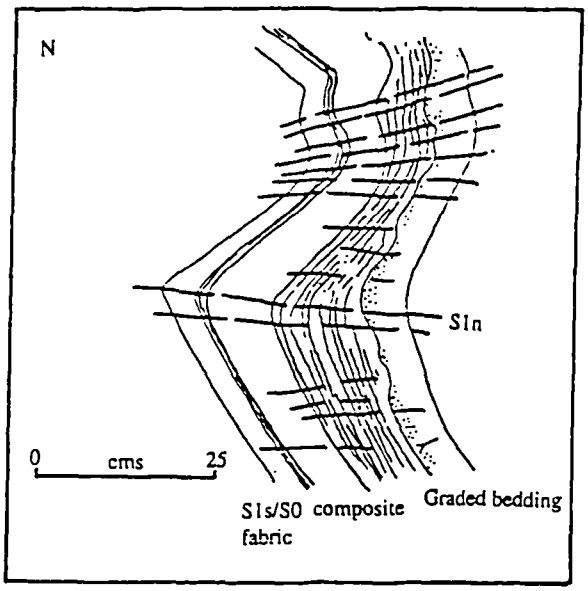

Figure 3.41 Vertical view through the steep short limb of south-facing and verging F1n fold, deforming S1s cleavage. East Beach, Polzeath.

Extensional features

In an area of such complex compressional structure, the nature of extensional tectonism is hard to assess with certainty. The most obvious extensional features throughout the section are steeply northwest-dipping normal faults (e.g. Gravel Caverns; Figure 3.42). The earlier, low-angle D2 detachments are difficult to distinguish from D1n/s thrusts. The bedding or dominant foliation is utilised by detachments during layer-parallel compressional and extensional shear. For instance, there are two sets of north-vergent minor folds at Slipper Point. The first fold bedding and are associated with axial-planar quartz-veining (D1n), whilst the second are associated with bedding-parallel movement surfaces which have secondary fracture orientations that indicate downdip shear. This second group are here denoted D2, and the orientation of F2 axes and axial planes are shown in Figure 3.43.

F2 ruck fold axial planes show a bimodal distribution of steeply southwest and northeast dipping planes and northeast and southwest-vergence, down the dip of S1n and S1s (Figure 3.43a). Fold axes plunge gently to the northwest or southeast, but show a wide range of azimuths. Curvilinear F2 fold axes are not generally seen, and thus the variation may reflect original differences in kinematics.

T1n thrusts show evidence of reactivation during D2 in the orientation of secondary fracture orientations which cut across S1n fabrics and veins, and in development of stepped quartz slickenfibres with normal displacement sense that overprint reverse slickenlines. North-dipping F2 fold-packages show shallowly east and east-northeast trending axes and downdip-vergent fold asymmetry

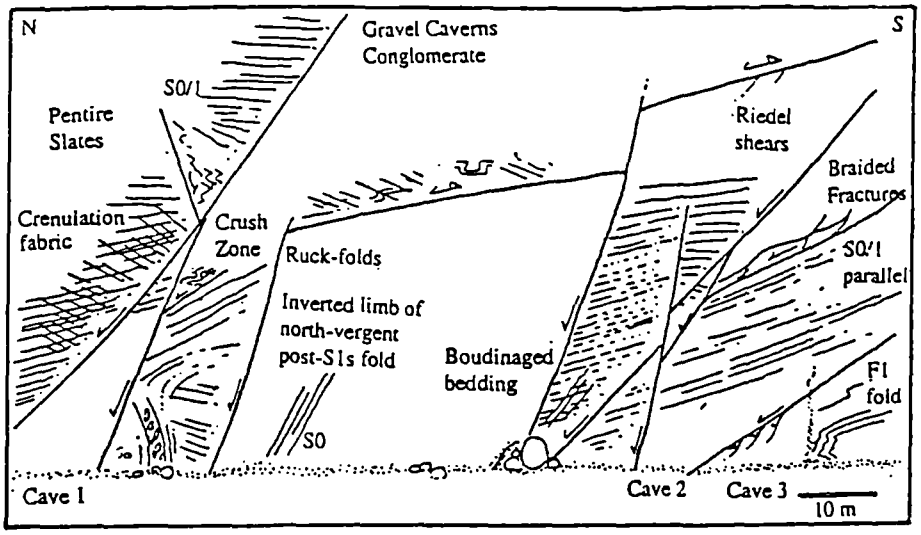

Figure 3.42 Extensional structures developed at Gravel Caverns. Shallowly north-dipping D2 detachments between caves 1 and 2 focus S2 cleavage and box-folding. Domino-faults, crenulation fabrics, Riedel Shears and ruck-folds suggest down-dip shear, whilst the formation of a transposing S1s fabric above the detachment in Figure 3.40 suggests that they may have initiated as thrusts.

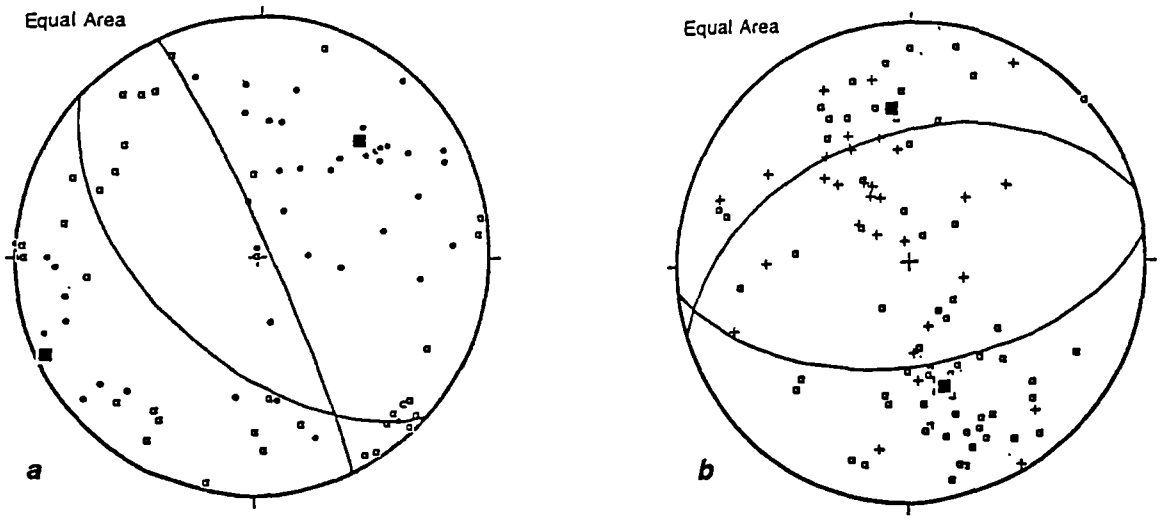

Figure 3.43 Extensional structure, New Polzeath section. (a) F2 ruck fold orientations: *Planes:* dots = S2 cleavage (42); great circles = mean S2 planes (132/54 S, 155/86 E). *Lineations:* squares = fold axes (30). (b) Fault orientations: *Planes:* boxes = faults (64); *lineations:* slickenlines = crosses (30); great circles = mean fault planes (073/45 N, 083/54 S).

Late steep faulting is common throughout the section with fault-planes dipping both to the northwest and southeast (Figure 3.43b). The northwest-dipping faults offset the southeast-dipping ones, and both sets offset D2 detachments. North and northwest trending vertical quartz veins are also associated with the steep faults. Upright open flexures (D3) with east-trending axes and steep quartz-veins developed along their axial planes occur adjacent to steep fault-planes. They do not appear to have been generated during

drag along the faults and thus may reflect buttressing against the faults during later renewed compression late in the regional structural history (e.g. during granite emplacement).

Thin Section Analysis

Slates from the Gravel Caverns Conglomerate Member were examined in section, and their muscovite ± chlorite + quartz + opaques + clays assemblage studied for microstructure. The phyllitic nature of the schistosity showed little evidence for a polyphase history. The dominant sense of shear deduced from tail asymmetry adjacent to ragged quartz-grains with undulose extinction is to to the south, indicating that the sample taken has a S1n foliation. A later overprint is evident in kinking of the muscovite laths, but such kinks have no clear asymmetry.

A number of samples from the Polzeath Thrust were collected in which a muscovite ± chlorite + quartz assemblage is noted, locally with the addition of biotite. Where samples come from outside the zones of extensional faulting and associated ruck-folding, they preserve a simple microstructure of fine sericitic D1 schistosity cross-cut at varying angles by second phase pressure solution seams (D1n?). The D2 extensional event is recorded by steeply east-dipping asymmetric shear-bands (Plate 3.14). It is developed axial planar to larger-scale F2 folds which appear to have formed through D2 reactivation of the Polzeath Thrust.

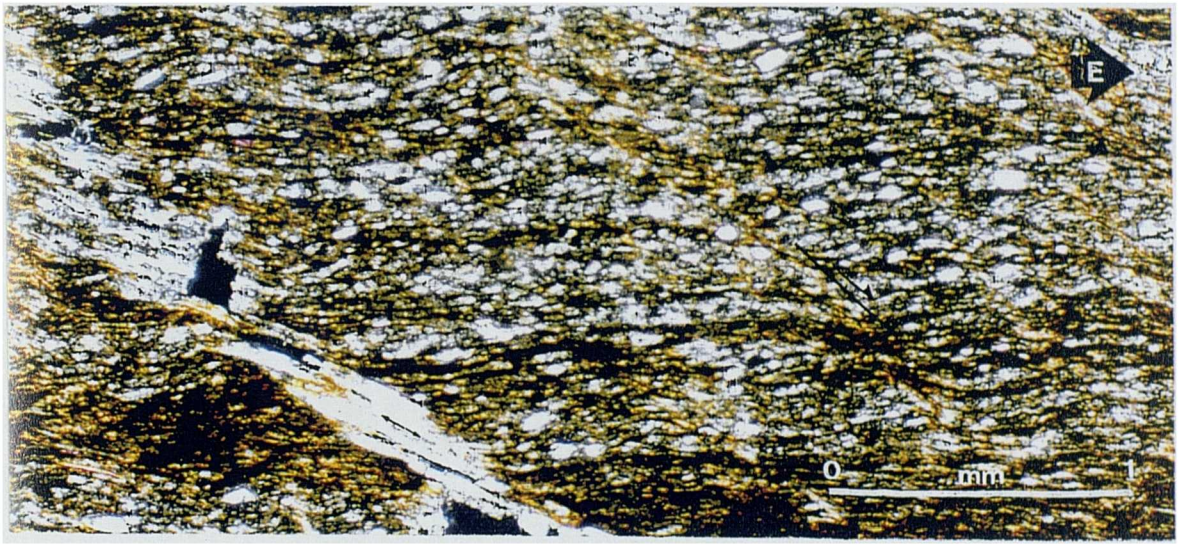

Plate 3.14 Photomicrograph of asymmetric extensional shear-bands of the S1s fabric, Pentireglaze Haven. Note conisitency of shear-sense between vein fibres and shear-bands.

Thin sections of north-vergent F2 ruck folds show microfolds of silt bands with both north-verging and box forms, whilst argillaceous layers have a pervasive crenulation cleavage. The foliation is subparallel to the long limbs of F2 folds rather than axial-planar, and encloses D2 veins of biotite and epidote. The biotite-

rich main foliation contains east-dipping asymmetric shear-bands in long fold limbs and shallowly north-dipping shear-bands in hinges.

3.4.5 Padstow to Mawgan Porth

Lithology

Polzeath Slates hosting extensive metadolerite sheets crop out on the southern shore of the River Camel, bounded to the south by purple, grey and green slates, grey siltstones, turbiditic and crinoidal limestones and green-weathering metabasites which represent subgroups of the Padstow Succession (Section 2.2.3.2) between the Polzeath Slates and the Trevose Slates (Gauss 1973). A prominent metadolerite band continues to the west of Trevone Bay through Cataclews Point [SW 8728 7620] and the northern side of Trevose Head, its course suggesting the presence of dextral wrench faults beneath the beach sands at Harlyn Bay and along the western flank of Mother Ivey's Bay. The Trevose Slates dominate the cliffs for 4 kilometers to the south, and comprise homogenous grey slates with buff-coloured and black interlayers.

The southern margin of the Trevose Slate Formation runs east through South Fox Cove [SW 8542 7300]. To the south, grey banded Eifelian slates of the Portcothan Slate Formation crop out until south Bedruthan Steps [SW 8481 6918]. Still further south lie the Staddon Grits and Meadfoot Beds (Section 2.2.2).

Compressional Features

D1s becomes the dominant compressional fabric to the west of the River Camel. Gauss (1973) identifies a large-scale recumbent syncline with south-southeast dipping axial plane between Padstow and Stepper Point (Figure 3.44; section a-a'). It contains Middle Devonian rocks in its overturned limb (i.e. Trevose Slates) and Upper Devonian rocks in its normal limb (i.e. Polzeath Slates) and faces and verges north. S1 dips shallowly toward the south or south-southeast, axial planar to isoclinal F1 folds which are parasitic to the larger synform. South-vergent meso-scale F1 folds are observed in much of the coastal section (Figure 3.44b-b'), representing z-folds on the inverted limb of the major synform. Detailed description of the bulk structure are provided by the works of Gauss (1973) and Pamplin (1988).

Bedding and S1 cleavage dip both north and south between Booby's Bay [SW 855 757] and Constantine Bay [SW 855 746] due to reorientation by late upright folds with axial planes striking east-west and across steep normal faults (Figure 3.45a). Bedding-cleavage intersection lineations plunge gently east-northeast or west-southwest, and south-dipping T1 thrusts confirm D1 transport towards the north. Further south at Portcothan [SW 8550 7221], D1 deformation is recorded by a pervasive S1 schistosity dipping shallowly south.

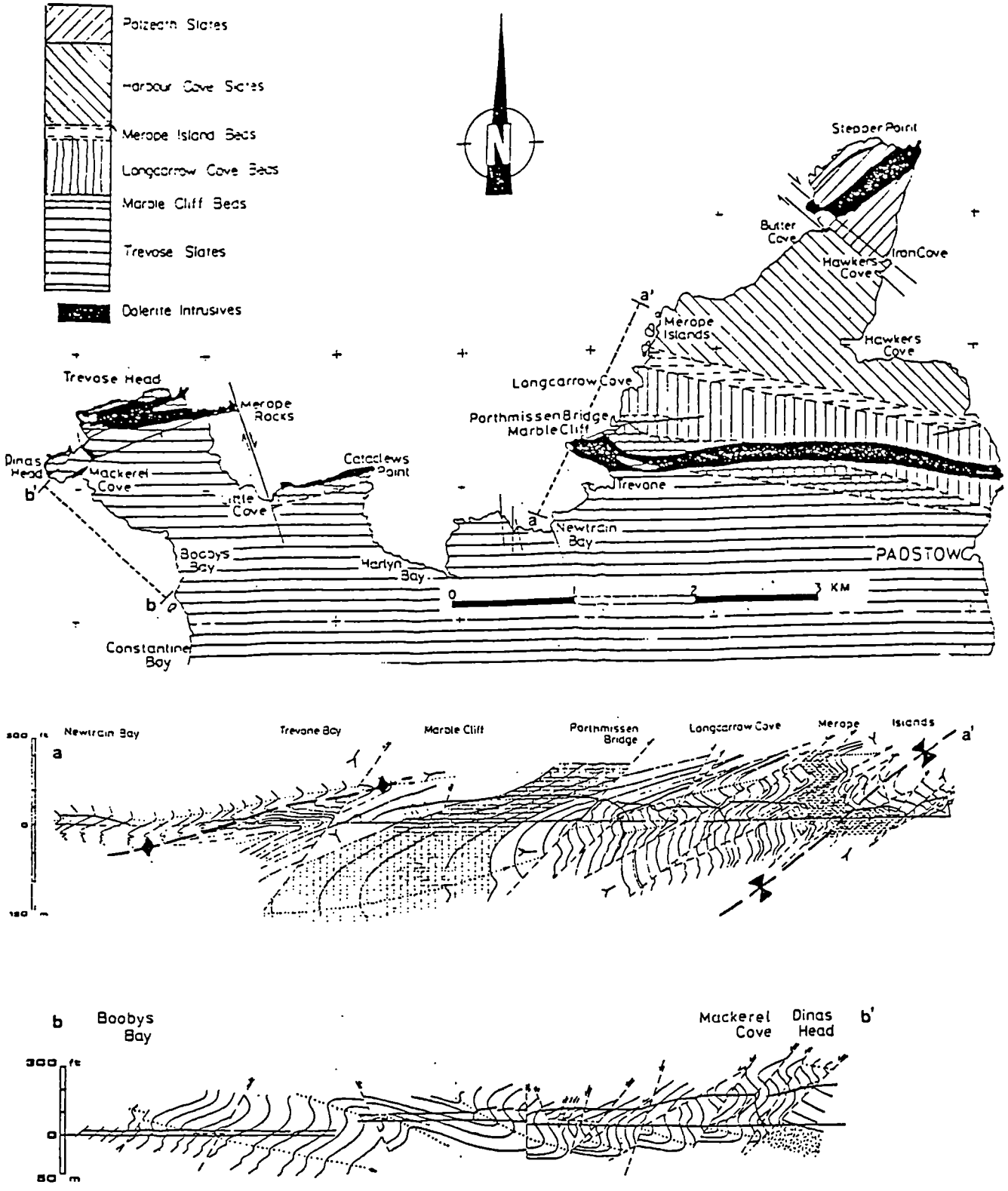

Figure 3.44 Geology of the section between Padstow and Trevose Bay (Gauss 1973). (a-a') Dip section west of Stepper Point showing section through Gauss' synformal structure (b-b'). Dip section south of Trevose Head. After Gauss 1973. (c) Explanatory sketch of sections within a larger context.

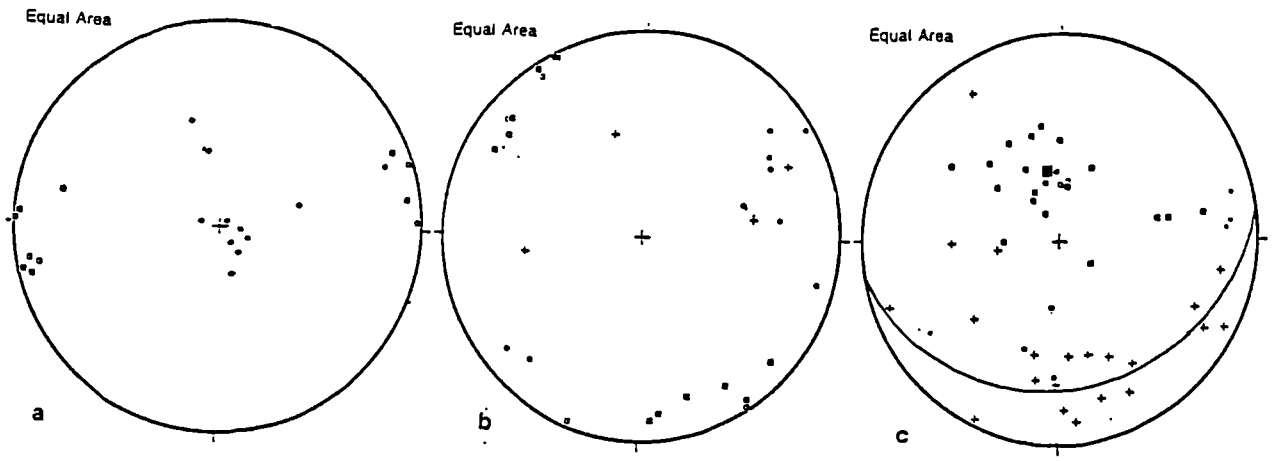

Figure 3.45 Stereographs of structural components, Booby's Bay. (a) D1 structure: dots = S1 and F1 axial planes (13); squares = L1 intersection lineations and F1 axes (11). (b) Late structures: dots = post-S1 foliations (9); squares = L2+ lineations (16); crosses = poles to veining (4). (c) Faulting and related structure: squares = fault planes (23); great circle = mean fault plane [080/28 S]; crosses = slickenlines (20); stars = ruck-fold axes (4); dots = ruck-fold axial planes (4).

Extensional features

Extension in the section is characterised by steep south-dipping normal faults (D3) which strike parallel to regional S1 strike (east-northeastwards). The fault-planes locally reactivate S1 cleavage surfaces and accommodate up to 50 metres of southerly displacement (Figure 3.44 section b-b'). The faults cut through F1 hinges (e.g. south Mackerel Cove [SW 8500 7618]) and offset of lithological boundaries and fold limbs. Displacements recorded in the field indicates in excess of 20% extension.

Normal faults exposed at Booby's Bay dip towards the south or south-southeast (Figure 3.45c). Primary cleavage planes often host slickencrysts which have consistent kinematics with fault-plane lineations, suggesting that they have been reactivated during the extensional event. The faults commonly consist of paired movement surfaces with interjoining secondary fracture planes, and thin breccia seams enclosing F2 ruck-folds with angular, chevron geometries of a more brittle style than to the north of Padstow. The folds verge down their associated fault-planes towards the south and their axes trend northwest-southeast (Figure 3.45b). An axial planar S2 crenulation cleavage is restricted to zones of F2 folding and dips moderately north. Dextral transtensile strains (post D3) are seen locally where oblique slickenlines overprint normal grooves on fault surfaces, in a suite of north striking subvertical quartz veins (parallel to the orientation of $\sigma 1$ during dextral movement of major northwest-southeast trending strike-slip faults), and in northwest striking dextral kink-bands.

Normal detachments reactivate S1 cleavage at Portcothan [SW 8541 7230], folding S1-parallel quartz-veins into southeast-verging F2 folds. The magnitude of extension is difficult to assess in the uniform slates at this locality, but estimation of shortening across F2 folds provides a value of ~15%. Northwest-southeast striking kink-bands at this locality show southwest-vergence which may be a component of D2 extensional strain which is preserved preferentially in the rheologically weak Portcothan Slates.

Thin section analysis

Trevose slate sampled at the northeast end of Booby's Beach contains a closely-spaced pressure solution S1 cleavage which contains quartz porphyroclasts and mica fish, the asymmetry of which relative to the fabric indicate shear along the foliation towards the north (i.e. progressive D1 strains). Calcite porphyroclasts are more ambiguous and offer little insight into extensional deformation mechanisms.

3.4.6 Structural summary and discussion

The compressional structures exposed in the southern Trevose Basin are bimodal, with F1n folds consistently facing southwards to the north of Polzeath and consistently facing north to the south of Polzeath (Roberts and Snaderson 1971). The two phases confront one another across an west-northwest-trending zone approximately 5 kilometers wide in which two convergence-related cleavages are developed and both field evidence and K-Ar radiogenic ages indicate that south-facing structures developed after north-facing structures (Andrews *et al.* 1988; Dodson and Rex 1971). The confrontation is thus seen by Andrews *et al.* (1988) and Pamplin and Andrews (1988) as a large-scale interference fold developed during renewed Carboniferous backfolding of earlier structures above a north-dipping backthrust beneath the Culm Basin. The zone may be somewhat more complex than this model suggests, as north-facing flexures reputedly of the early deformation event deform the main S1s cleavage (thought to be later) at Polzeath. This may reflect a progressive nature to D1 deformation in north Cornwall or simply locate parasitic F1s folds affected by the later backfolding event. D1n is not observed to the south of the River Camel, where north-facing recumbent F1s folds dominate structure.

Extensional deformation is again recorded by both D2 detachments and D3 normal faults which verge down the dip of S1 cleavage. Shallowly south-dipping detachments reactivate bedding and S1 cleavage to the north of Polzeath and localised north-directed detachment set are observed at Port Quin. The south-dipping (and transporting) detachments are the more common and are a continuation of structures exposed to the north as far as Rusey Beach. Steep normal faults dip moderately north and record small extensional offsets. In the Polzeath area, both north and south-transporting detachments are preserved, locally reactivating early thrusts. north to northwest-dipping steep faults crosscut south to southeast-dipping steep faults and thus two phases of post D2 extension are preserved. Steeply south-dipping normal faults dominate to the south of the River Camel, where they reactivate bedding in the inverted limb of a

recumbent north-facing syncline. South-dipping detachments and south-verging ruck-folds are locally observed and accommodate ~15% extension.

3.5 The Lower Devonian; Watergate Bay to Perran Sands

Stratigraphy

Between Mawgan Porth and Perranporth [SW 845 675 - SW 755 545], Lower Devonian rocks of the Dartmouth and Meadfoot slate Formations are arranged symmetrically about the Watergate Bay Antiform; a broad E/W-trending fold closure first identified by Reid and Scrivenor (1906). The older Dartmouth Beds comprise dark-grey, purple, buff and green slates and siltstones with a slaty S1 cleavage (Figure 3.46). Fish scales date the Formation to the middle Siegenian. The Meadfoot Beds exposed to the north and south are grey slates, marls and thin limestones with occasional green tuff bands. An intense slaty schistosity and increasingly abundant quartz veins to the south of Newquay reflect high compressional strains. The extreme north of the section preserves indurated quartzose sandstones and green micaceous slates of the Staddon Grits, the uppermost member of the Meadfoot Beds.

Bulk structure

The rocks exposed along this section are amongst the oldest on the north Cornish coast, and represent a basement high separating the Trevone and Gramscatho Basins. Sanderson and Dearman (1973) considered the section as a distinct structural domain in which F1 folds are north-verging, north-northwest facing and strike west-southwest. The Watergate Bay Antiform (Figure 3.46a) deforms the slaty S1 cleavage into a major north-facing recumbent antiform plunging eastwards. Hobson (1976a) considered it to be the westward expression of the Dartmouth Antiform and related it to progressive north-directed, subhorizontal simple shear. F1 folds are tight to isoclinal and have an intense axial planar slaty S1 foliation dipping shallowly towards the south. A second compressional phase (the local D2 phase) is seen in E/W-trending folds associated with a northerly-dipping cleavage which patchily refold D1 structures.

S1 steepens southwards from 45° southwards at Holywell Bay to subvertical at Perran Sands. The steep zone represents the western exposure of the Start-Perranporth Line; an east-west trending zone of long-lived dextral transpressive strain separating rocks of differing sedimentological, geochemical and metamorphic histories (Holdsworth 1989a; Shail 1992; Steele 1994). Rocks of the transpressional belt preserve shallowly south-dipping F1 folds which are progressively overprinted by moderately north-dipping S2 fabrics (Henley 1970, 1973; Sanderson 1971).

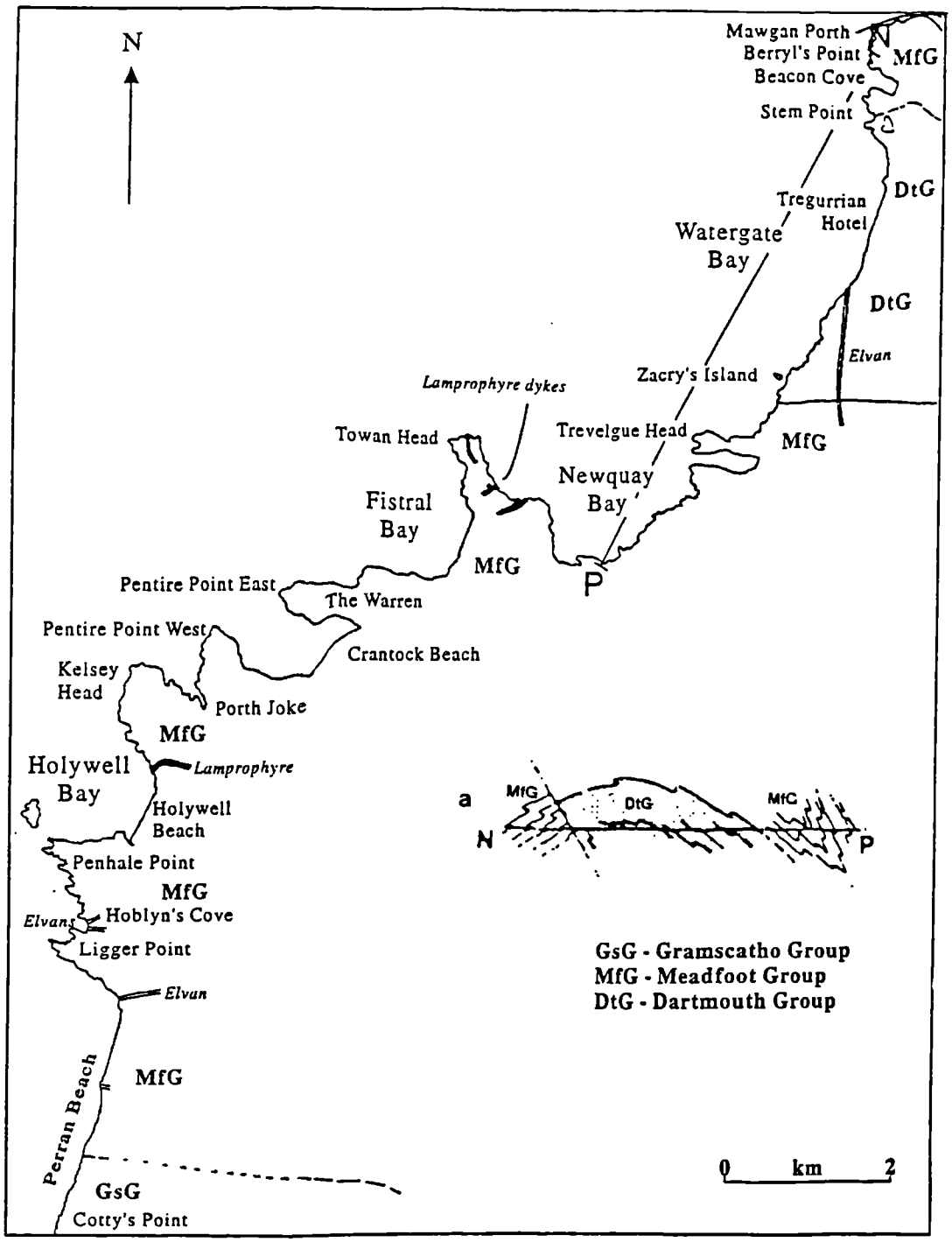

Figure 3.46 - Geological map of the coast between Mawgan Porth and Perran Sands. (a) Sketch section by Hobson (1976a) through the Watergate Bay Antiform (Redrawn from BGS sheet 346).

Toward the northern boundary of the Gramscatho Basin compressional structure becomes increasingly complex rocks and show increasing strains until the primary cleavage dips subvertically between Newquay and Perranporth. The reason for this change in attitude is contentious. Sanderson (1971) suggested that it represents the short limb of a large-scale monoclinal F2 fold which refolds primary isoclines, whilst Henley (1973) investigated younging directions within the zone and modelled the structure through the action of a post-D2 compressional event acting against a buttress now represented by the Perran Iron Lode.

Subsequent work by Hobson (1976a), Primmer (1985), Leveridge (1984), Holdsworth (1989a), Shail (1992) and Steele (1994) has invoked the generation of steep foliation through dextral transpressive reactivation of E/W-trending basement faults at depth. On the basis of these recent studies, it appears to have been generally accepted that the region marks remnants of a transpressive shear-zone developed during oblique syn- to post-D1 compression.

Recumbent south-verging folds and an axial planar crenulation cleavage were identified by Reid and Scrivenor (1906) and later confirmed by Sanderson (1971) and Henley (1973) as relating to D3 deformation. F3 folds become symmetrical where the compressional fabrics are steepened and form a subhorizontal crenulation fabric which indicates vertical, layer-parallel compression.

3.5.1 Watergate Bay to Newquay

The frequent sandy beaches and low rocky shores in this area provide excellent exposure. Detailed structural analysis was conducted on sections between Stem Cove and Horse Rock, Watergate Bay [SW 8417 6641 - SW 8362 6427], Cribbar Rocks and Fistral Beach [SW 7983 6302 - SW 8000 6232], Pentire Point East [SW 782 616], Pentire Point West [SW 776 608], and between Holywell Beach and Ligger Point [SW 7634 5926 - SW 7576 5813].

Lithology

At Stem Cove [SW 8417 6641], the northern junction between Dartmouth Slates and Meadfoot Beds crops out above abandoned mine adits within a thin green metabasite sill. To the south, the two formations may be difficult to differentiate as both weather to a buff grey colour, but the Dartmouth Beds are differentiated by the presence of ostracoderm scales to the north of the Watergate Bay Hotel [SW 8409 6497]. Black and dark-grey slates with thin pale-grey sandstone layers are the dominant lithology. Thin sandstones and intraformational conglomerates are sometimes seen and react when dilute hydrochloric acid is applied, implying high calcite content. Fault-breccias are predominantly quartz-cemented but often host sulphides (e.g. Stem Cove; chalcopyrite, pyrite and sphalerite).

Compressional features

The northern end of Watergate Bay exposes recumbent north-facing F1 isoclines with southeast-verging parasitic folds implying a position within the inverted limb of the Watergate Bay Antiform (Figure 3.46a). The S1 foliation is subhorizontal to shallowly north-dipping, and contains a north/south-trending micaceous mineral lineation. Second phase folds are not present, but east-west striking quartz-veins may relate to a second compressive event.

To the south at Fox Hole [SW 8430 6607], a group of thick sandstones crop out defining recumbent F1 fold closures. The cliffs between Fox Hole and the Watergate Bay Hotel locally preserve F1 hinges which are tight to isoclinal on a metre-scale but are more open and have rounded hinges when seen on a cliff-scale (Figure 3.47a). Fold axial planes and consequently the composite S0/1 foliation dip shallowly toward the north or south due to block rotation adjacent to normal faults. Fold facing is consistently northwards. Where discernable, F1 folds appear to verge south, thus placing them on the inverted limb of the Watergate Bay Antiform. Minor folds with wavelengths of less than two metres have s-profiles. An east-west trending mineral lineation is observed on S1 at the northern margin of the Bay, perpendicular to the regional mineral stretching lineation.

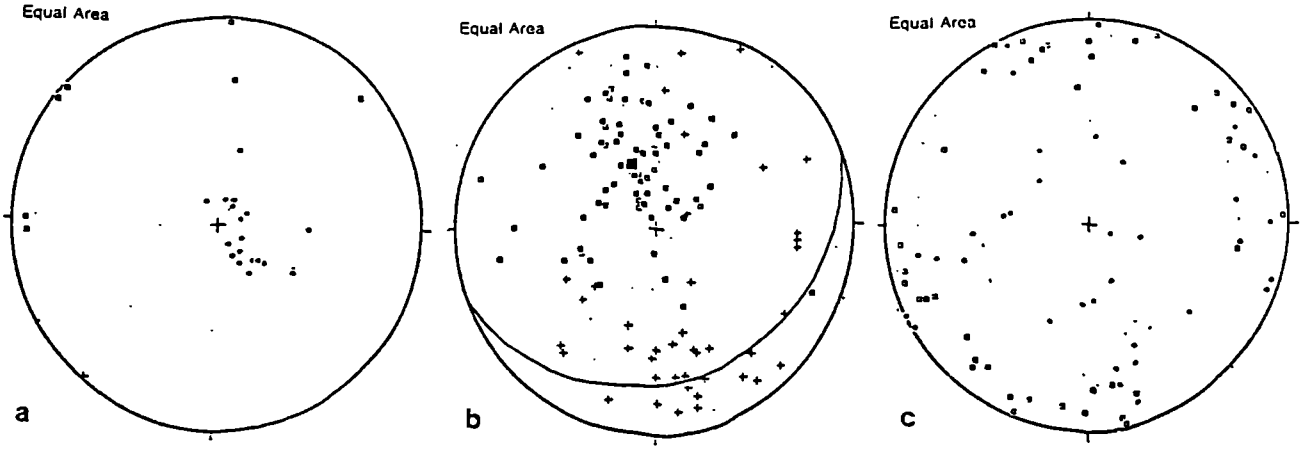

Figure 3.47 Stereoplots of orientation data for structural components, Watergate Bay. (a) D1 features: dots = S0/1 composite foliation (19); lineations; crosses = L1 bedding-cleavage intersection lineation (1); boxes = boudin necks (7). (b) Normal faults: boxes = fault-planes (41); great circle = mean fault-plane [069/27 S]; crosses = slickenlines (30). (c) Ruck-folding and kink-banding: grey symbols; boxes = ruck-fold axes/lineations (18); dots = ruck-fold axial planes/axial planar foliation (15); black symbols; boxes = kink axes/lineations (13); dots = kink axial planes/axial planar foliation (29).

South of the hotel at Tregurrian, the primary cleavage dips shallowly toward the north. Further minor F1 closures are seen in places and continue to indicate location in the inverted limb of the north-verging Watergate Bay Antiform. Further south at Tolcarne Beach, the slaty cleavage dips south at low angles and is affected by steep dextral shear-bands relating to the Start-Perranporth Zone (Steele 1994).

South-dipping T2 thrusts are locally exposed, distorting the S1 foliation in their hangingwalls. They locally site D3 domino-faulting and thus appear to have undergone normal reactivation (Plate 3.15).

Plate 3.15 T2 thrust structure with broad hangingwall flexure of S1 foliation against shallowly-dipping undeformed S1 foliation in footwall. Hangingwall is extended by south-dipping domino faults suggesting extensional reactivation. Stem Point, Tregurrian Beach.

Extensional features

Extension is partitioned along low-angle south-dipping normal faults (local D3) which are sometimes interlinked by and sometimes cut by steeper south-dipping normal faults (e.g. Stem Cove; Figure 3.47b; 3.48). Fault-planes are conspicuous as they are underlain in their immediate footwalls by networks of quartz-veins. Within low-angle fault-zones, south-verging ruck-folds with shallowly west-dipping axes occur alongside box-folds, south-dipping extensional shear-bands and chaotic buckle folds (Figure 3.47c). An S3 crenulation cleavage is heterogeneously developed axial planar to the asymmetric folds. It dips variably towards the north with shallow dips recorded above Riedel Shears and steep dips recorded above S1-parallel detachment 'flats'. The late (S3) foliation is seen only adjacent to detachments, suggesting that ductile deformation is partitioned into the fault-rocks whilst the intervening rocks rotate but remain internally undeformed.

Movement surfaces of steep faults within the cove contain dextrally oblique slickenlines where east/west-striking but become fully dextral as their strikes swing into parallelism with the tectonic transport direction. The faults thus have lateral ramps which show predominantly dextral movement, perhaps indicating a dextral transtensile component to extension locally.

Between Fox Hole and the Watergate Bay Hotel, normal curviplanar faults with south-dipping profiles are closely spaced and locally account for over 40% extension (Figure 3.48). Shallowly to moderately south-dipping D3 detachments separate zones of deformed from undeformed S1 fabric, forming linked systems of movement planes transporting down to the south or southwest (Figure 3.47b). Faults are joined by relay structures which step both up- and down- section, forming a braided composite displacement system. Low- to moderate- angle detchments are associated with intense veining in footwall rocks only, suggesting that the fault-planes acted as permeability barriers during movement.

The geometry of normal fault systems is complex, reflecting the influence of pre-existing anisotropy. Shallowly south-dipping D3 detachments commonly splay into Riedel fractures which link zones of faulting. North displacing shear-bands are also sometimes present in hanging-walls, their sense of shear broadly conjugate to the main extensional faults (R' orientation). The shear-bands may also accommodate a vertical coaxial component of pure shear in a bulk non-coaxial regime. In several places, notably at the northern end of Watergate Bay [SW 8430 6607], steep movement planes are seen to sole into low-angle south-dipping detachments which sometimes also steepen into ramp-sections (Figure 3.48A). Within the zones of D3 detachment, conjugate normal faults are sometimes developed and can accommodate up to 25% extension. They indicate a late component to the deformation which involves coaxial flattening of the deformation zones.

A range of fold-styles is associated with extensional shear along S1, reflecting variations in strain magnitude and embrittlement through time. Low-angle listric normal faults are typically overlain by fold-zones up to two metres thick in which long:short limb ratios are ~4:1 and fold hinges are angular (Figure 3.49). In such cases, folds verge towards the southeast or east-southeast, their axes plunging to the west-southwest or north-northeast and showing a degree of curvilinearity. With an increase in strain, the folds firstly tighten into chevrons and then become non-cylindrical and convolute, often forming box-folds or rootless hinges within breccias. This effect causes dispersion of data-points on stereographs of orientations (Figure 3.47c), with axes plunging at low angles across the northeast and southwest quadrants and foliations dipping north, south and locally east where oblique fault-ramps are developed.

The effects of D3 extension upon the D2 compressional structures are observed approximately 400 metres north of the Tregurrian Beach cafe [SW 8414 6492], where convolute folds are developed against a north-dipping normal fault, with north and east-vergent features present. In these zones steeply-dipping V1 quartz veins with close to tight angular F2 flexures form 'christmas tree' refolds (Plate 3.16), suggesting that the veins were initially steeply south-dipping, an orientation common for D2 across much of south Cornwall. In zones of such refolding, a steep south-dipping S2 fabric is developed adjacent to minor T2 thrusts which show evidence for later reactivation in extension.

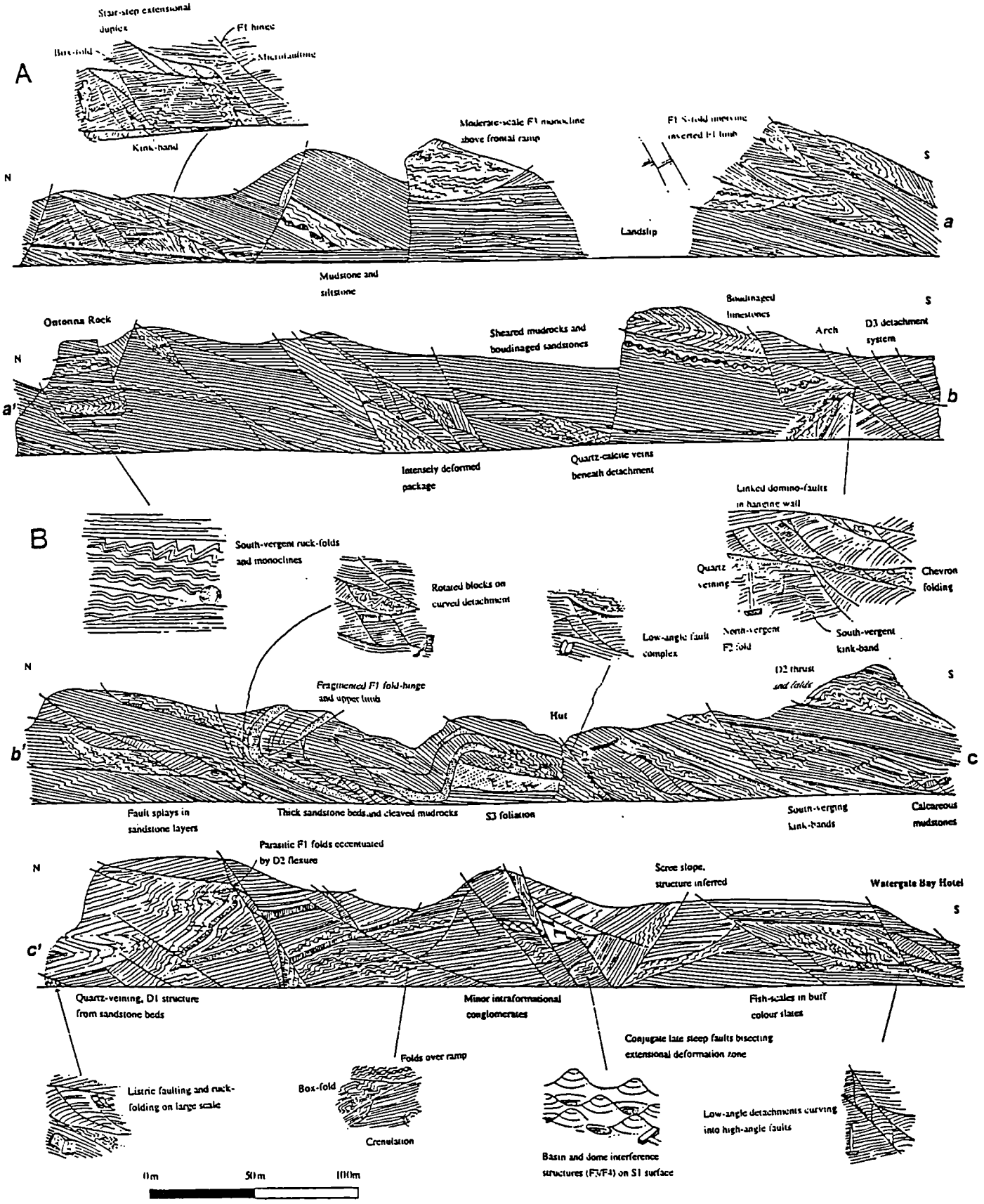

Figure 3.48 Across-strike section through northern Watergate Bay. (A) Fox Hole to North Trevarrian Cliff. (B) North Trevarrian Cliff to the Watergate Bay Hotel.

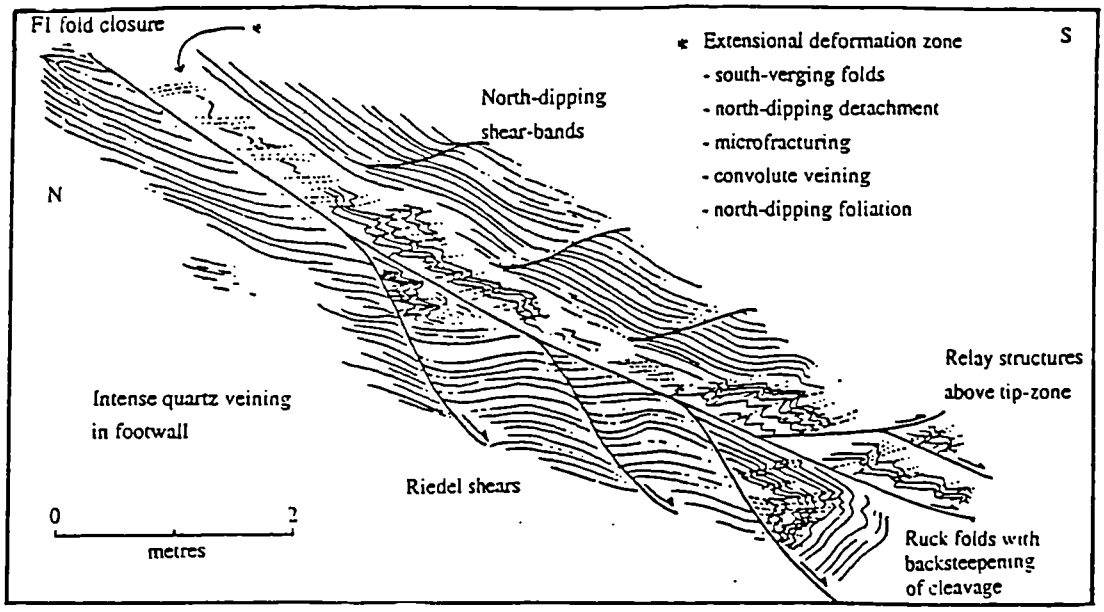

Figure 3.49 Characteristics of fault-bounded deformation zones, Watergate Bay.

S3 cleavage is seen as a crenulation of S1 in most areas, but in areas of higher strain, the S3 foliation intensifies and steepens until dipping moderately north and transposing the primary cleavage. In transposition zones, it is a closely spaced pressure solution seaming diagnostic of fluid assisted volume loss. Shear-senses deduced from slickenlines, subsidiary fault-planes, vein fibres, shear-bands. modal fold vergence and cleavage vergence along the central section of the beach all suggest top-to-the southeast tectonic transport.

Kink-bands are present across much of Watergate Bay, post-dating ruck-folds and locally cutting through their long limbs. The kinks consistently have south-vergent asymmetry and appear to be brittle expressions of continued low-angle D3 movement towards the south and east (Figure 3.42; Figure 3.43). Dextral (west-northwest trending) and less common sinistral (north-northeast striking) minor faults are laterally discontinuous and cross-cut extensional faults. They do not appear to have significant displacements along the mapped section.

To the south of the Watergate Bay Hotel, south-transporting D3 detachments continue to be commonplace and overprinted by north-south trending dextral kinks. Reconnaissance mapping of the Tocarne and Great Western Beaches confirms that south-dipping D3 extensional detachments continue to be present, with intense quartz-veining in their immediate hangingwalls.

Thin section analysis

A sample of rusty-weathering slate taken from the fault-zone at Ontonna Rock [SW 8428 6581] contains two fabrics; S1 cleavage is formed from aligned muscovite and chlorite laths and a secondary pressure solution cleavage dips more steeply to the south. On hand specimen scale, calcite σ-porphyroclasts are

seen within the primary cleavage recording D3 southerly-directed non-coaxial shear along the S1 foliation. Muscovite crystals of the S1 cleavage are kinked and show undulose extinction, suggesting brittle-ductile reworking during extension.

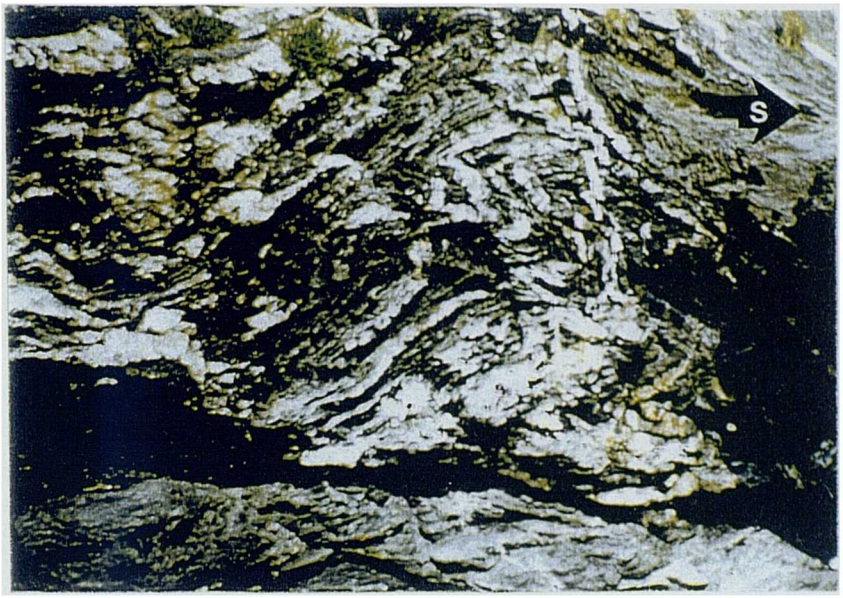

Plate 3.16 Upright F2 fold of V1 vein, refolded by F3 about subhorizontal axial planes. Field of view 1.5 metres. Beneath the Watergate Bay Hotel, Tregurrian Beach.

3.5.2 Fistral Bay (Newquay) to Pentire Point West

Lithology

To the south and west of Newquay, the Meadfoot Beds comprise pale grey siltstone bands and dark-grey slates with subordinate marls and thin recrystallised limestones. Indurated sandstones crop out at Towan Head [SW 8000 0630] and Pentire Point East [SW 7800 6157] interbedded with sandy grey slates. North to north-northeast lamprophyric dykes intersect the coast at Beacon Cove [SW 8044 6243], Spy Cove [SW 8010 6277] and Towan Head [SW 7991 6300]. Quartz-veining is concentrated into the hinges of F1 folds.

Compressional features

The foreshore on the western side of Towan Head exposes intensely cleaved slates dipping moderately the south or south-southeast (Figure 3.50). Tight to isoclinal F1 folds are discernible locally, suggesting that S0 and S1 form a composite, parallel foliation. To the west, at Nun Cove [SW 7992 6264], the foliation becomes moderately to steeply southwest-dipping and fold closures are not preserved, but cleavage vergence may be used to invoke the presence of F1 isoclines. In this region, younging is decipherable from graded bedding and suggests that early folds face up towards the north or northeast. The dip of foliations is variable across normal faults.

A dextral transpressive event is reflected in an east-west trending subhorizontal mineral stretching lineation defined by quartz and calcite aggregates and pressure shadows around sedimentary pyrite crystals. The slaty cleavage is deflected across steeply southwest-dipping dextral shear-bands. Kink-banding is common and comprises two orthogonal sets striking north or east. The north-striking set appear to predate or be an early component of the dextral transpressive event, whilst the east-striking set appear to have formed later than shear-band generation (i.e. post-D2).

At The Warren [SW 7815 6158 - SW 7801 6150], D1 is characterised by a south-dipping slaty cleavage and moderately west-plunging tight F1 folds associated with quartz-veining (Figure 3.51a). Close to the tumulus [at SW 7813 6163], the slaty S1 cleavage dips moderately to steeply southwards and the rocks are phyllitic. F1 folds have shallowly south-dipping axial planes and mullions with shallowly east-dipping axes are seen along boundaries between units of different competence. Transpression is recorded by dextral shear-bands which dip vertically and break the primary cleavage into lozenges. On the southern margin of the headland the intensity of dextral shear increases and an S2 crenulation fabric forms axial planar to dextral drag folds and is crosscut by dextral and subordinate sinistral shear-bands which reorient the early fabric (Plate 3.17a, 3.17b).

Moving southwards across Crantock Beach, a moderately south-dipping S1 cleavage is prevalent, in places preserving tight north-vergent F1 hinges. Dextral shears are developed in association with quartz-veining and appear dilational. The northern shore of Pentire Point West exposes a variably south-dipping S0/1 foliation disrupted by minor detachments. Isoclinal F1 folds are seen but their facing direction is unclear. Again, dextral shears and steep dextral (and second-order sinistral) oblique-slip detachments are common.

Extensional features

Extension at Towan Head is evident in moderately southwest-dipping normal faults which reactivate the early cleavage. Intense downdip-verging folds are often present in the immediate hanging-wall as are calcite crack-seal veins and tension gashes which suggest a dextral component to deformation (Steele 1994). A subordinate group of northeast-dipping normal faults and north-verging folds are developed. Kink-bands generally verge towards the southwest and dip shallowly toward the northeast, appearing to relate to late brittle movement down the early fabric. North-verging kink-bands are subordinate and accommodate a component of layer-perpendicular shortening. It is noted that the kink-bands reorientate the mineral stretching lineation and thus, if related to D2 transpression rather than D3 extension, must have developed relatively late during the D2 event. A late stage of deformation is preserved in north-northwest-trending dextral (and to a lesser extent, south-southeast-trending sinistral) steep faults associated with dextral drag-folds which deform all earlier structures.

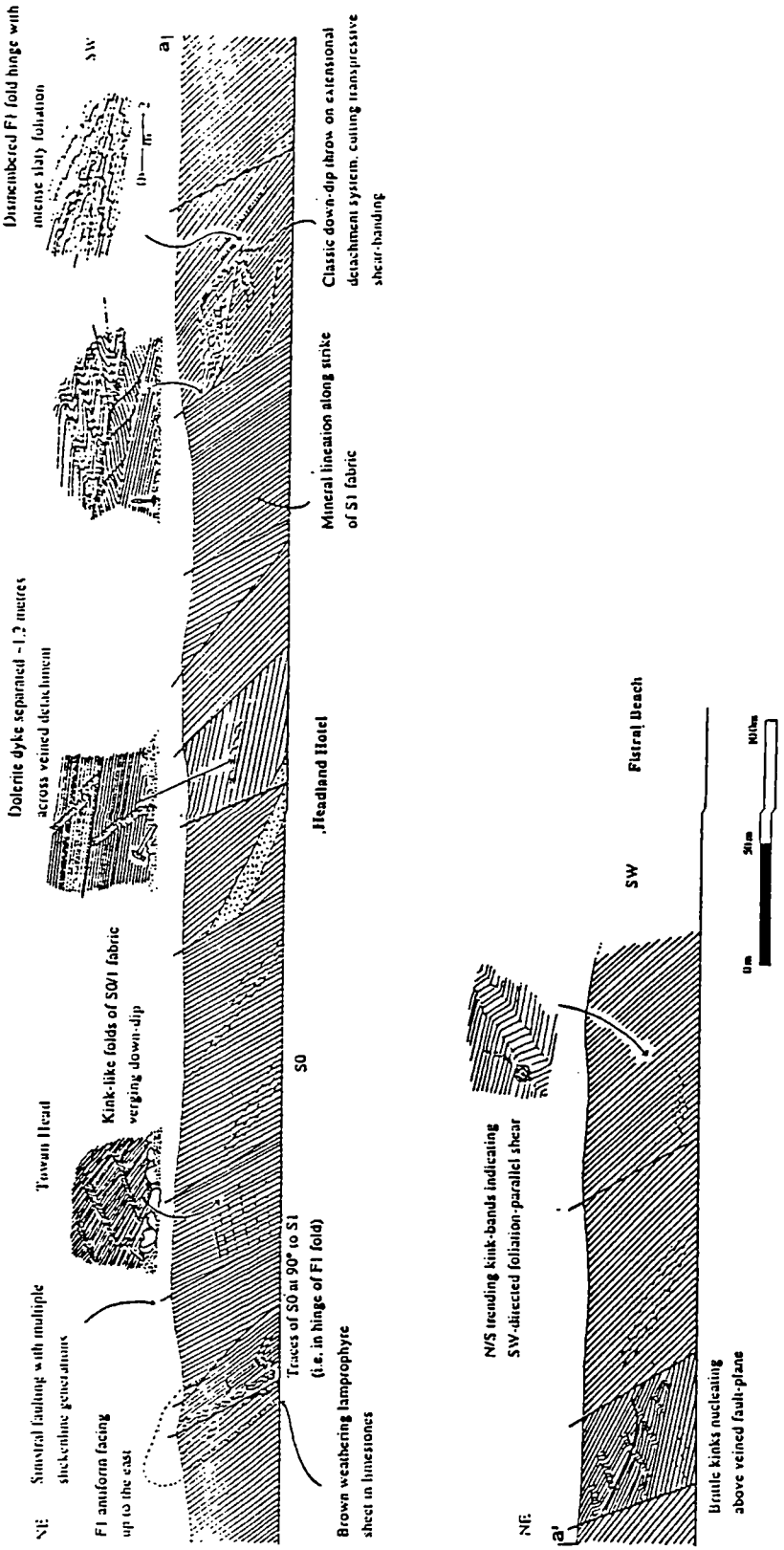

Figure 3.50 Dip section of the Towan Head - North Fistral Beach section (redrawn from field sketches).

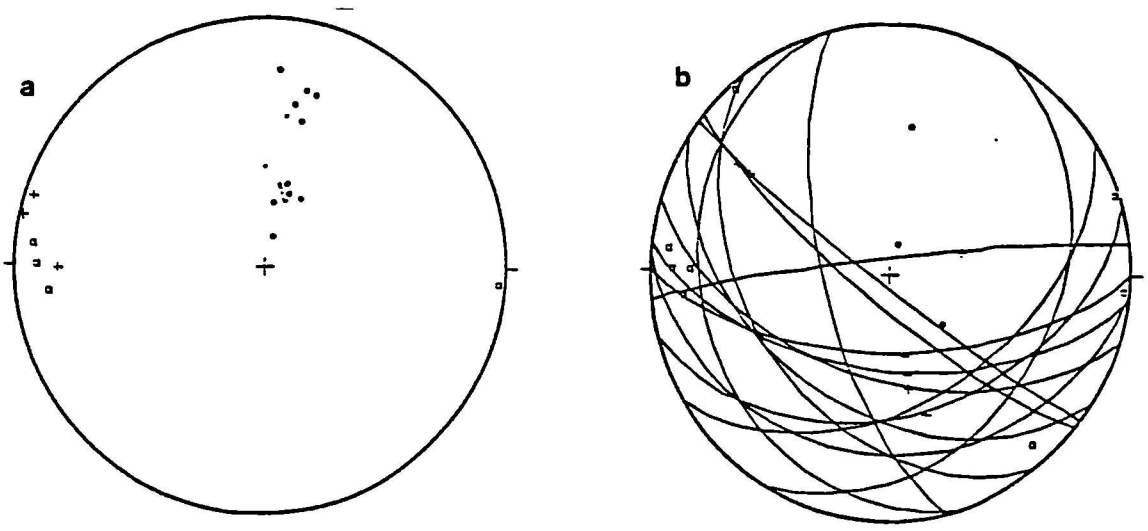

Figure 3.51 Structural data from the Warren, Newquay. (a) Compressional structure: *Planes:* S1 = dots (13); S2 = stars (3). *Lineations:* L1/F1 axes = crosses (3), L2 = boxes (4). (b) Extensional structure: *Planes:* S3 = dots (3). *Great circles:* normal faults (14). *Lineations:* L3/F3 axes = boxes (7), slickenlines = crosses (4).

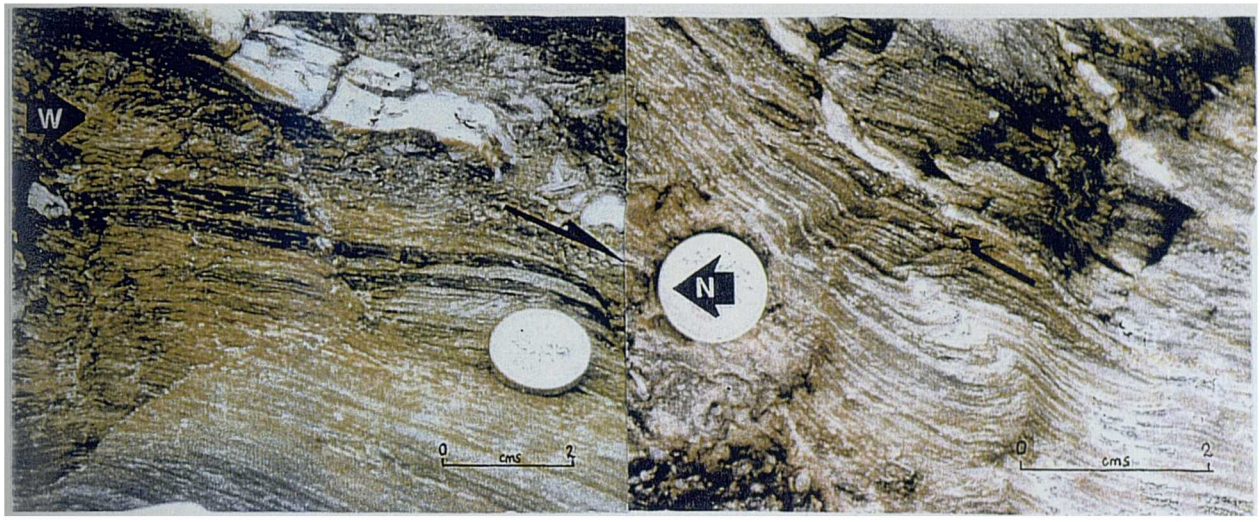

Plate 3.17a Dextral shear-bands exposed on subhorizontal surface, adjacent to quartz-vein with horizontal slickencrysts, the Warren (Slide 2.17, view south, right = west).

Plate 3.17b Sinistral F2 fold , the Warren (Slide 2.17, view east, left = north).

At The Warren, normal faults dip to the southwest and again display dextral oblique-slip histories (Figure 3.52b). Where the faults dip steeply southwards they are heavily quartz-mineralised and have normal slickenlines. At the end of Pentire Point East [SW 7801 6150], minor rucks are preserved in the S1 fabric on a mm- to cm- scale above D3 detachments.

Extensional tectonism intensifies at the end of the headland in the inverted limb of an open F1 synform (Steele 1994). Ruck-folding of the primary cleavage gives way to brittle north-verging kinks and an S-C fabric is increasingly developed. The extensional crenulation cleavage occurs on a large-scale, with shallowly south-dipping S1 cleavage overprinted by a moderately south-dipping set of C-planes allowing top-to-the south non-coaxial shear. A moderately south-dipping S3 cleavage is developed above the

detachments and crenulates S0/1 away from the faults, forming an L3/1 lineation which plunges gently southeast. The youngest structures present are poorly formed quartz tension gashes which have dextral asymmetry.

Foliation-parallel normal faults with second-order Riedel arrays are exposed at Pentire Point West (Figure 3.52c). The associated foliation is subparallel to detachments, indicating high strain magnitude and a component of vertical shortening. Braided oblique-slip movement planes are well formed and appear to pre-date extension but are partially reactivated as lateral ramps within a network of linked normal faults.

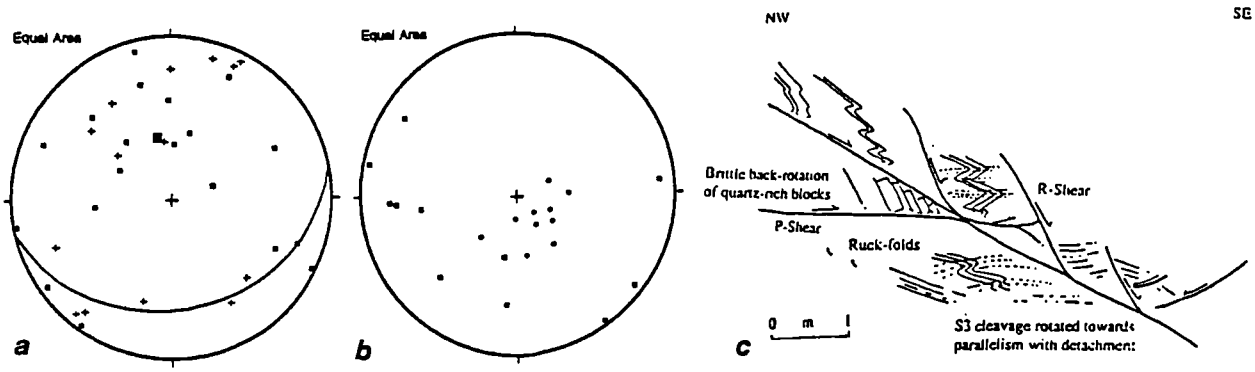

Figure 3.52 Extensional structure, north shore of Pentire Point East. (a) Stereoplot of extensional faults : *Planes*: squares = normal fault planes (15). *Great Circle :* mean fault plane (079/49 S). *Lineations:* crosses = slickenlines (13). (b) Stereoplot of D3 structures: *Planes:* dots = S3 foliation (10). *Lineations* : boxes = F3 fold axes (10). (c) Typical structures associated with extensional deformation.

Thin section analysis

Micro-scale study of the Meadfoot Beds from The Warren reveals a slaty cleavage of muscovite and clay minerals with green staining. On a sub-millimetric scale, the foliation wraps quartz clasts which record northerly shear, whilst on a larger scale, the foliation is crenulated by south-vergent semi-brittle folds. Muscovite crystals within the main fabric are kinked by this late (D3) event and locally are cross-cut by a moderately north-dipping pressure solution cleavage with quartz-veins formed parallel to it. Within finer grained slates, a crenulation is again present, perpendicular to the main foliation. The primary foliation has quartz-grains flattened into it whilst later crenulation are again axial planar to south-vergent microfolds. It thus appears that the extensional reworking in this area occurred through diffusive mass transfer at lower temperatures or higher strain-rates than initial compression.

3.5.3 Holywell Bay to Perran Sands

Lithology

Between Porth Joke and Penhale Sands [SW 7722 6060 - SW 7640 5740], slates of the Meadfoot Beds crop out as series of grey slates, thin graded sandstones and black, green and grey mudrocks. Buff-weathering metadolerite sills parallel to bedding are observed in many places and appear to act as weak layers during the late extensional phase. Boudinaged, irregular quartz-veins up to 50 cm thick are increasingly common towards the south. Between Ligger Point and Gravelhill Mine [SW 7569 5818 - 7641 5760], dark-grey slates are continuously exposed and contain thick dolerite sheets.

At the Gravelhill Mine, the north-northwest trending Perran Iron Lode crops out as a mineralised quartz-pyrite band tens of metres wide. South of the mine, sand-dunes cover exposures for over 500 metres until Carn Haut [SW 7602 5600], where pale grey sandstones and hornfelsic slates form the northernmost outcrops of the Gramscatho Group. Quartz-veining and iron-staining is intense and highlights steep normal fault-planes reactivating steep areas of bedding.

Compressional features

Between Kelsey Head and Holywell Bay [SW 7634 6082 - SW 7670 5968] a south-dipping S0/1 composite foliation dips shallowly to subvertically towards the south and southwest and primary isoclinal closures verge north and plunge gently east (Figure 3.53a). Southwest-dipping dextral shear-bands on a decimetre scale are ubiquitous, and appear to have been active during early movement on the normal faults. Steele (1994) noted open north-facing F1 folds of sandstone beds on the northern margin of Holywell Beach [SW 7652 6008], overprinted by centimetre-scale dextral shear bands. In zones of steep foliation, the S1 fabric appears to have been transposed by S2 cleavage to dominate exposures, and relationships between D1 and D2 are thus only discernible where lower D2 strains are developed (Steele 1994).

Both compressional and dextral strain is high to the south of Holywell Beach [SW 7641 5760], with bedding fully transposed by the primary cleavage and both oriented near-vertically and forming phyllonite and protomylonite shear-zones (Figure 3.54; Plate 3.18; Steele 1994). Strain is so intense that primary closures are not seen and consequently facing is not distinguishable. The steep south-dipping foliation is strongly crenulated by sub-horizontal planes with a spaced fracture or pressure solution cleavage attributable to vertical shortening.

The east-west trending coast approaching Penhale Point [SW 7560 5919] exposes the steep foliation which is intensely crenulated. Steeply plunging, dextrally-vergent folds and shear-bands are developed in grey-green phyllonites and attest to intense shear prior to extension. A steeply northeast-dipping fault

immediately to the east of the headland has a zone of phyllonites in its southern wallrocks over ten metres wide which contains σ- quartz porphyroclasts indicating dextral shear (Steele 1994). To the south, the the main foliation is subvertical and deformed into northeast-verging F2 folds with variable plunges (Steele 1994).

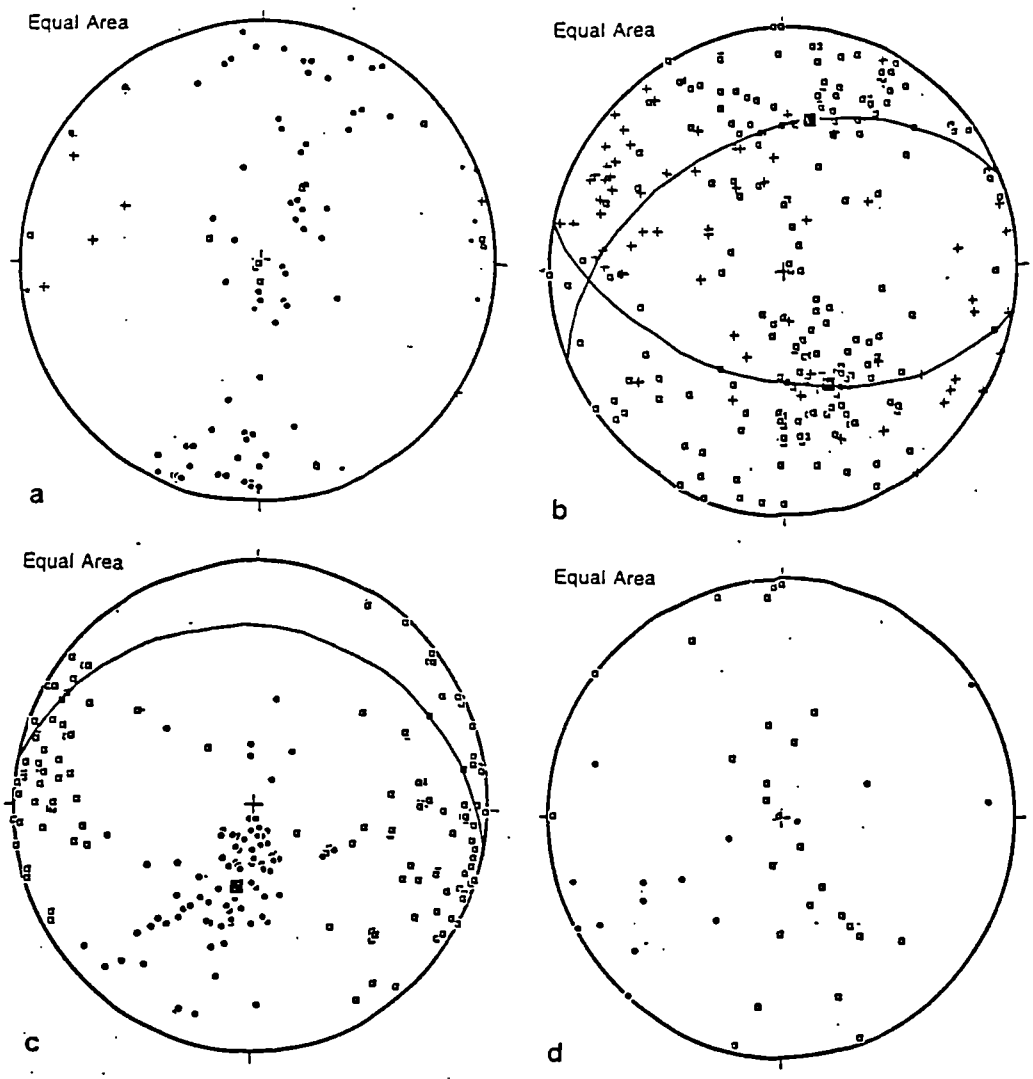

Figure 3.53 Structural orientation data for the section between Holywell Beach and Perranporth. (a) Compressional structure (poles; dots = S1 (67); grey dots = S2 (6); lines; crosses = L1 (5); grey crosses = L2 (7); boxes = mineral stretching lineations (3); stars = boudin b-axes (10). (b) Normal faults (poles; squares = fault surfaces (121); lines; crosses = slickenlines (34); great circle; mean fault planes 248/42 N, 101/53 S). (c) F3 folding adjacent to faults (poles; dots = S3 (75); lines; squares = L3 (88); great circle; mean S3 cleavage plane 281/28 N). (d) Post-D3 structures (poles; dots = S4 (14); lines; squares = L4 (27)).

Further south at Hoblyn's Cove [SW 7618 5820], the steep foliation hosts a ten-metre wide elvan. Adjacent to the felsitic intrusion, the foliation is crenulated by small-scale north-vergent folds, again attributed to D2 by Steele (1994). Continuing towards Perran Sands, the foliation remains steeply inclined and is strongly affected by steeply inclined F2 folds and locally overprinted by a northeast-dipping S2 cleavage.

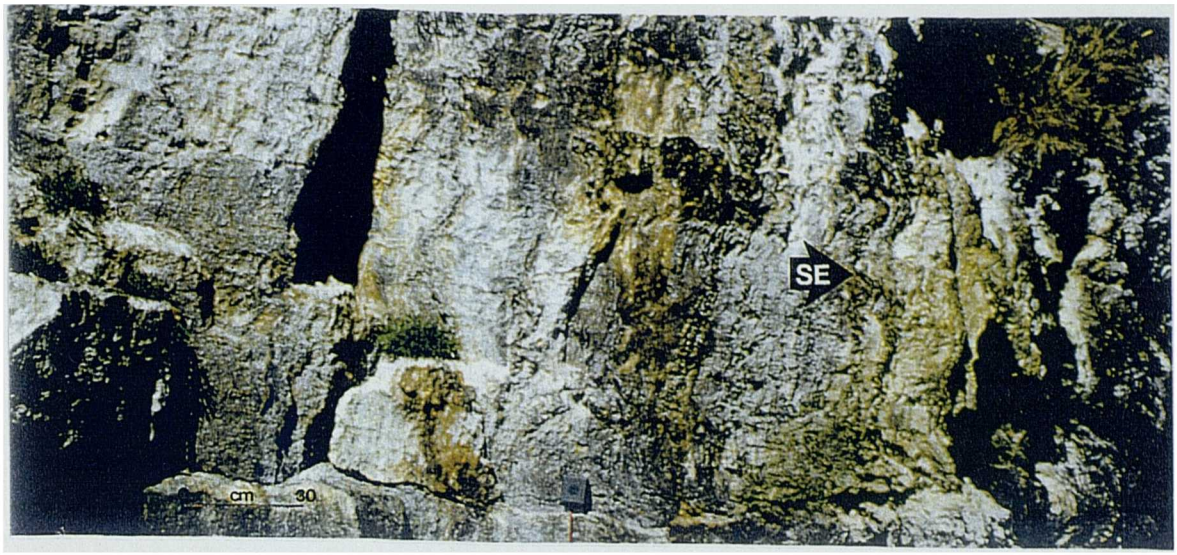

Plate 3.18 - Steep fabric diagnostic of the central Start-Perranporth Zone overprinted by flat-lying D3 crenulation.

Gramscatho Group sandstones and shales exposed in the centre of Perran Beach are strongly cleaved by have a subhorizontal fabric, which increases abruptly across the Perran Iron Lode. Two contractional phases are consistently identified along Perran Beach, their relationships being best demonstrated at the southern end of the beach [Figure 3.55; SW 7575 5490]. D1 is characterised by a variable south- to southwest- dipping foliation subparallel to bedding which changes inclination across a series of steep normal faults. V1 veins are subparallel to the foliation or at a slightly steeper dip, axial planar to F1 folds which verge northwest and face shallowly up or down to the north. D2 deformation is seen in south-inclined open to close angular folds developed in the upper limbs of F1 folds. F2 folds verge north and occasionally northeast, often appearing to be coaxial with the primary deformation.

At Cotty's Point [SW 7576 5508], the S1 foliation dips variably towards the south-southwest, west and north due to refolding by large-scale folds (local D2 age) which verge south and have tight synformal hinges (Steele 1994). This generation of folds is related to the development of a gently south-dipping foliation attributed to backthrusting by Leveridge et al. (1990), which Steele argues is an expression of extensional reactivation of T2 thrusts towards the southwest.

Stereoplots of the S1 fabric reveals a scatter of poles along a north-south trending axis (Figure 3.53a). The primary foliation varies between steep to the north of Gravelhills Mine to shallowly north or south dips in the south. Bedding-cleavage intersection lineations are uncommon and variable in both plunge between the west and east, reflecting the action of D2 compression and coaxial steepening of linear components. Mineral stretching lineations show no clear preferred orientation, suggesting that they may relate to several phases of the deformation and/or that they have been variably sheared and reoriented.

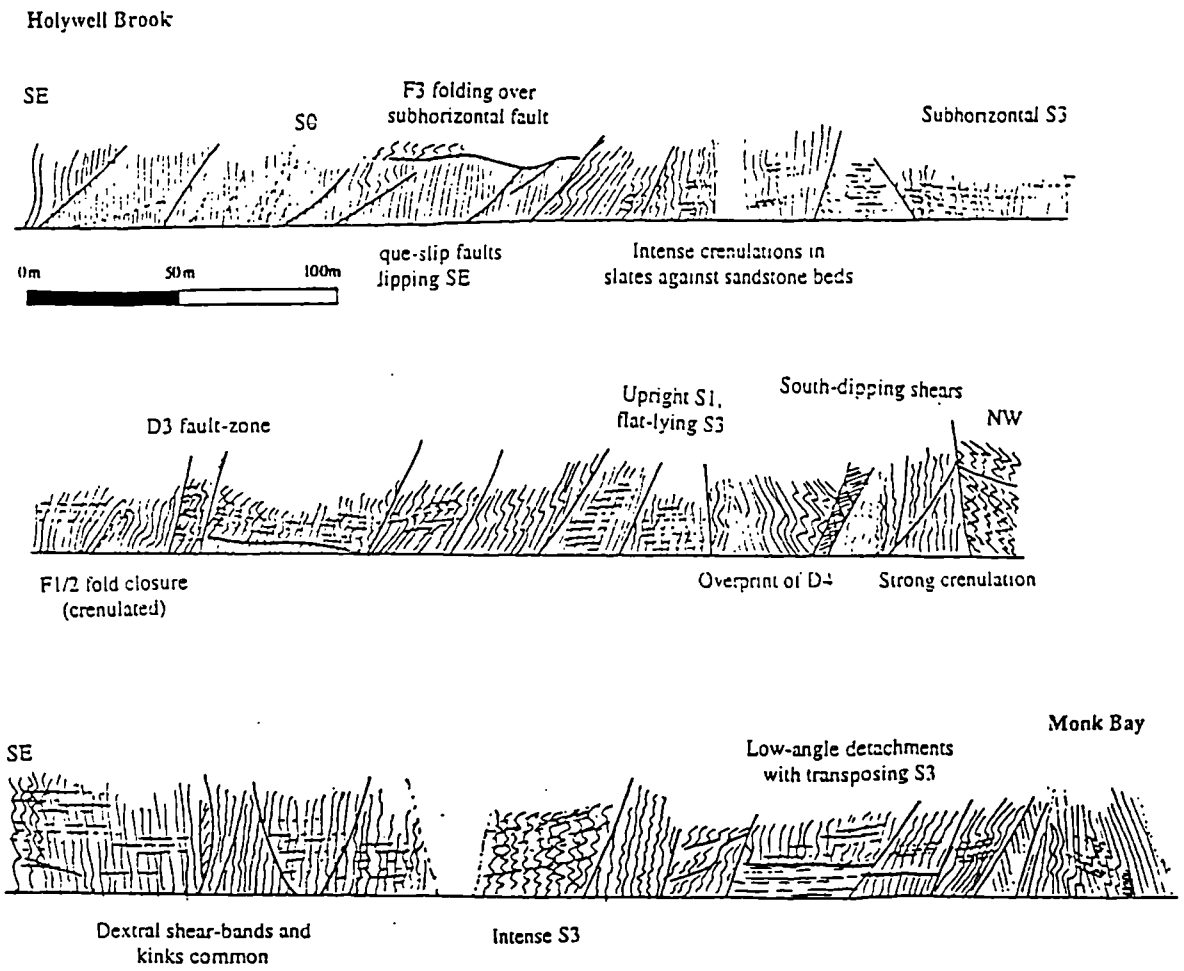

Figure 3.54 Sketch section across strike, south Holywell Beach.

Extensional features

In the area of steep S1 cleavage between Holywell Bay and Gravelhills Mine, the first extensional event (D3) is seen as concertina folds with subhorizontal axial planes reflecting bulk vertical compression (Figure 3.54). A related S3 foliation is a north to northeast-dipping crenulation or pressure solution cleavage developed axial-planar to south-verging sub-metre scale folds (Figure 3.53c). On a small-scale, south-vergent kinematics are reflected in a range of structures, from steep faults (Figure 3.53b) and related ruck-folds to S-C fabrics. Steeply south and north dipping normal faults cut the main foliation and bound zones of down-dip verging folds, reorienting the steep foliation and hence dating it to D2 age. Quartz-veins within the steep fabric are often boudinaged to form large augen, but as this is also noted in areas of phyllonite in which only dextral shear is recorded, boudinage is presumed to predate extension.

Exposures along Perran Sands (Figure 3.55) show a quite different style of deformation due to the much shallower inclination of the primary foliation. The outcrops are strongly attenuated by low-angle D3 detachments with steep splays, and by later steep normal faults which cross-cut shallower movement surfaces. Some faults partition semi-brittle folds in their immediate wall-rocks with gently west or east

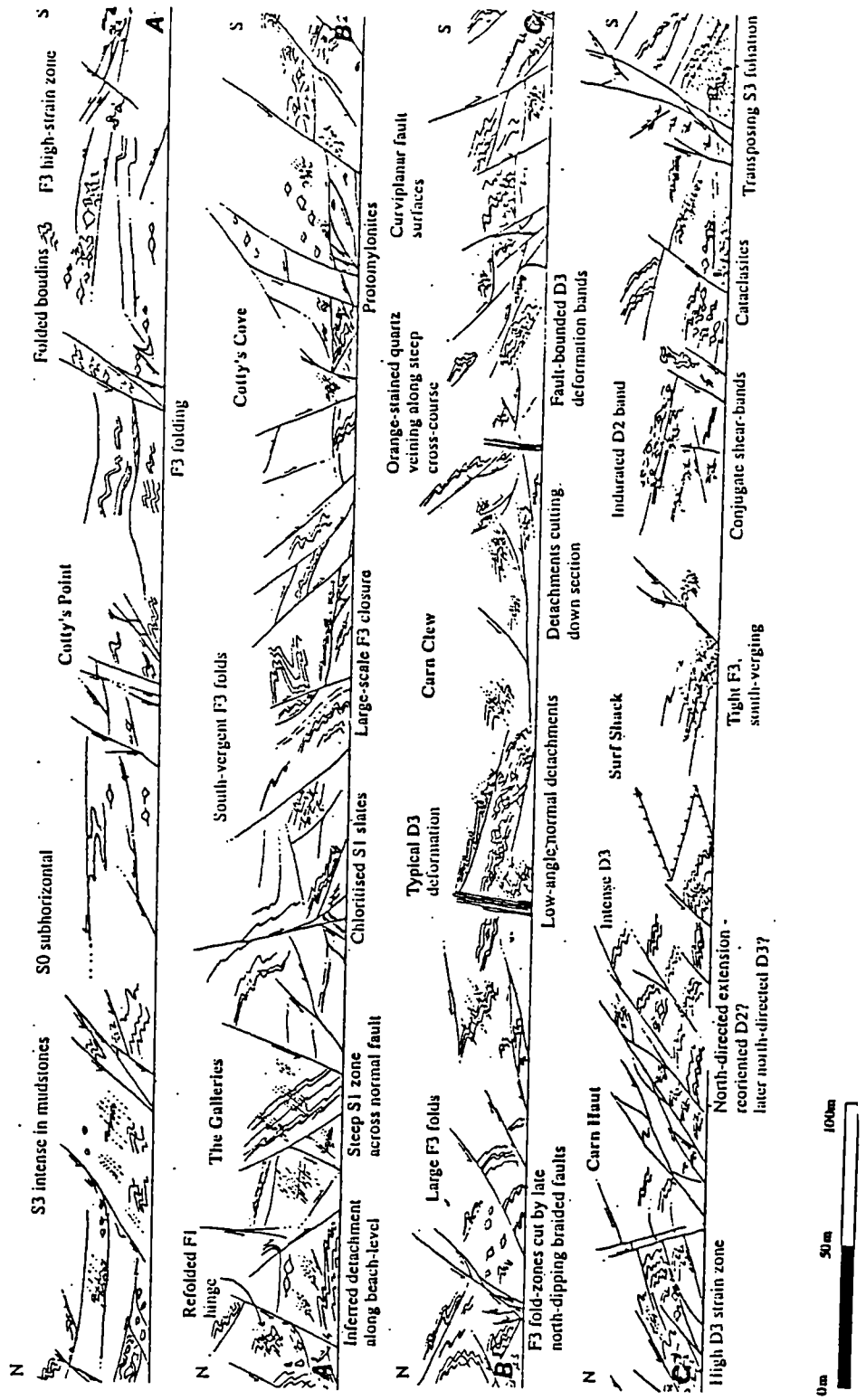

Figure 3.55 Sketch cliff-section, Perran Beach. Solid lines represent fault-planes (relative hangingwall translation direction indicated).

plunging axes and southerly vergence. An axial-planar S3 foliation dips shallowly north and locally transposes S0/1 fabrics (Figure 3.53b,c). The deformation chronology is sometimes difficult to ascertain due to the complexity of extensional kinematics. F3 folds are seen to refold F1/2 structures into type-III hook folds (e.g. south Cotty's Point [SW 7575 5490]). Most F3 folds are on a millimetric to decimetric scale, but in some places, monoclines with wavelengths of up to ten metres are preserved with north-vergent parasitic flexures on their steep limbs (e.g. 20 m north of Cotty's Cove [SW 7584 5523]). Detachments are often associated with synthetic domino-faults and zones of enhanced S3 cleavage. Microfaults have curviplanar geometries which dip southwards and sole into D3 detachments. Within zones of strong S3 fabric, quartz porphyroclasts locally indicate north-northwest directed non-coaxial flow.

Post-D3 deformation is recorded by moderately to steeply northeast-dipping spaced cleavage and north-trending steep kink-bands which overprint D3 detachments and ruck folds. The cause of this deformation is unclear as it does not appear to be related to steep normal faulting.

Thin section analysis

Along the beach section of Perran Sands, the main (S1) foliation is defined by fine aligned muscovite crystals in an opaque- and quartz- rich groundmass. Deformation appears to have been partitioned into detachments in this area, as lithons show no late overprint. Within the deformed zones, the primary cleavage is often highly contorted, with quartz and calcite veins folded and fractured and pressure solution seams developed. Quartz-veins often have subgraining around crystal margins, indicating rotational recrystallisation. Fine-grained siltstones from Cotty's Point have an intense primary cleavage formed from aligned muscovite crystals. A very fine grained groundmass of quartz and opaque minerals occurs in sub-millimetric bands. The sense of asymmetry in muscovite tails around quartz porphyroclasts indicate top-to-the-southwest shear along S3 planes, but no additional deformation is preserved.

3.5.4 Structural Summary and Discussion

A shallowly north or south-dipping S1 cleavage is seen in the northern part of the section which steepens to vertical between Perranporth and Holywell Bay due to the action of late D1 and D2 dextral transpression at the northern margin of the Gramscatho Basin (Holdsworth 1989b; Steele 1994). D2 deformation varies from shallowly south-dipping thrusts at Watergate Bay to upright to north-vergent folds and steep transposition fabrics at Holywell Bay.

Detachments of D3 age record southeast-directed tectonic transport and are well exposed at Watergate Bay, associated ruck folds and domino faults record over 40% extension. The structures swing clockwise in the Newquay area, where southwest-dipping normal faults reactivate the S1 cleavage and extensional crenulation cleavages record south-directed tectonic transport. In the steep S1 fabrics of the Start-

Perranporth Zone (Holdsworth 1989b), D3 deformation is largely restricted to subhorizontal crenulation fabrics and steeply north and south dipping normal faults which reactivate the S1 cleavage. At the southern end of the section, D3 detachments record noncoaxial southward shear, whilst steeper faults offset layers to both north and south.

3.6 The Gramscatho Basin; Perranporth to St. Ives

The coastline southwest of Perranporth provides a section along strike through the Gramscatho Basin, and forms the field area of Andrew Alexander (Camborne) who, in a parallel study, is looking into late orogenic structures and mineralisation in SW England.

Stratigraphy

Exposures along the section comprise metasediments of the Gramscatho Group and Mylor Slate Formation, and represent the basinal facies of the Gramscatho Basin (Figure 3.56; Section 2.2.3.1). These rocks have traditionally been considered to be parautochthonous Gramscatho lithofacies (Holder and Leveridge 1986), comprising sandstone-rich turbidites interbedded with siltstones, shales, thin limestones and metadolerites of MORB affinity (Floyd 1984). Remapping by Shail (1989) has defined areas of Mylor lithofacies in St Ives Bay, as exemplified by pelites, thin psammites, debrites and intra-plate affinity tholeiites. The two units are juxtaposed across north-dipping normal faults with throws in excess of ten metres.

Granites crop out between Perranporth and St Ives at Cligga Head, along the coast and inland to the west of St Ives. The Cligga Head Stock comprises kaolinised and greisenised muscovitic granite, whilst the Lands End Granite to the west consists of 80% coarse-grained megacrystic biotite granite and 20% megacrystic fine-grained granite. Both bodies are linked at depth to the Cornubian Batholith (Section 2.4; Chen *et al.* 1993; Hall 1971).

The Mylor Slates form the section to the east of St. Ives and are interspersed with metadolerite sills and bodies of pillow lava. The original mineralogy is heavily altered but evidence of sodic plagioclase, pyroxene and actinolite is preserved in a matrix of chlorite, epidote and ilmenite. Floyd (1976, 1982) found them to retain geochemical signatures of continental tholeiites and alkali basalts, hydrothermally altered during metasomatic fluid flux in the latter stages of granite emplacement.

Bulk structure

Early structures may be divided into two phases, both accommodating north-northwest directed contractional strain. The primary foliation, S1, is expressed as a penetrative slaty foliation parallel to bedding which dips shallowly to the southwest or south. Primary folds are sometimes seen, as tight to

isoclinal features with gently east-northeast or west-southwest plunging axes and north-northwest facing direction. The inverted limbs of the folds show intense non-coaxial shear attributed by Rattey and Sanderson (1984) to nappe-base processes operating during overthrusting. Increased strength of anisotropy ensures that later extension is partitioned into these areas.

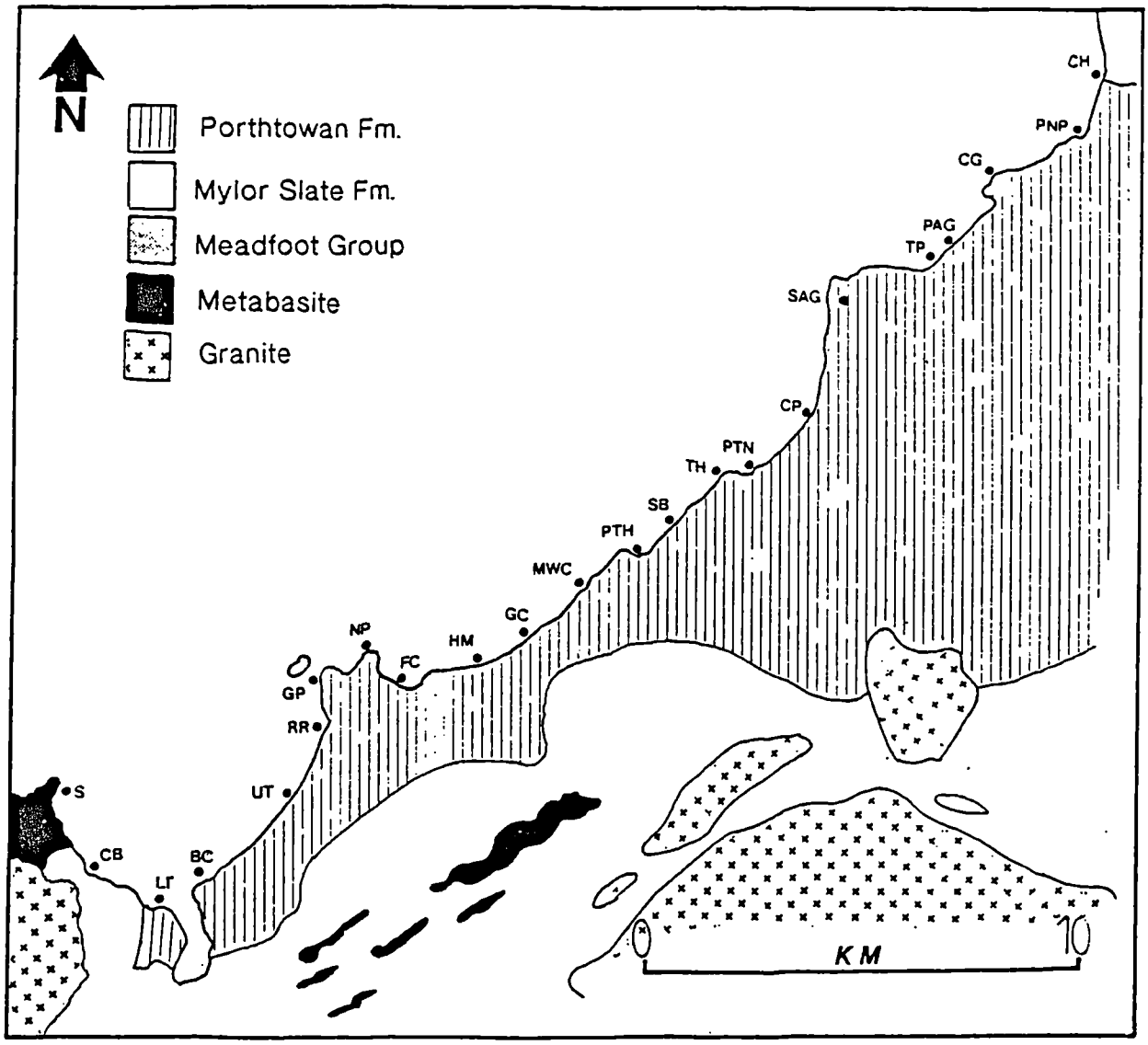

Key to Localities (Northeast to Southwest): CH, Carn Haut; PNP, Perranporth; CG, Cligga Granite; PAG, Pen-a-Grader; TP, Trevellas Porth; SAG, St. Agnes Granite; CP, Chapel Porth; PTN, Porthtowan; TH, Tobban Horse; SB, Sally's Bottom; PTH, Portreath; MWC, Mirrose Well Cove; GC, Greenbank Cove; HM, Hell's Mouth; FC, Fishing Cove; NP, Navax Point; GP, Godrevy Point; RR, Red River; UT, Upton Towan; BC, Black Cliff; LT, Lelant Towans; CB, Carbis Bay; S, St. Ives.

Figure 3.56 General Geological map of the coast between Carn Haut and St. Ives (redrawn from Shail 1992).

D2 is seen as open to tight north-northwest vergent monoclines or asymmetric flexures coaxial with D1 features. Fold axial planes and an associated crenulation cleavage dip moderately to steeply southeast. These structures occur with narrow high strain zones, and are particularly strongly developed at Godrevy Point [SW 580 433].

Extensional features form the local D3 phase and are directed down the dip of the earlier foliations towards the south or southeast. Structures range in style from shear-zones and fold packages to curviplanar normal fault systems, all reorienting D1 and D2 features. Anomalous areas of top-to-the-northwest displacing structures are developed to the south of Godrevy Point.

3.6.1 Perranporth to Godrevy Head

Lithology

This short section of steep cliffs comprises sandstones and slates of the Porthtowan Formation which comprise couplets of mud and sandstone of varying thicknesses. Exposures from Carn Haut to Godrevy Point are mudstone dominated with discrete groups of sandstone locally exposed. Shail (1992) describes the stratigraphy of this section at length, identifying areas of sandstone-dominated and mudstone-dominated facies which represent the Porthtowan and Mylor lithofacies of Holder and Leveridge (1986a). The metasediments are locally intruded by elvans (e.g. Trevellas Porth [SW 7237 5178]) and porphyry dykes (e.g. Wheal Coates [SW 6990 5026]), both of which are products of granitic magmatism.

The Cligga Head granite crops out at the northern end of the section as a kaolinised elliptical stock of granite-porphyry which is sited above a northerly projection of the Cornubian batholith at depth (Bott *et al.* 1958). It is a coarse, poorly megacrystic granite containing lithium mica which suggests that it evolved through alteration of a biotite granite (Floyd *et al.* 1993 *and references therein*). It is noted for tourmaline, topaz, quartz greisen veins which dip vertically and strike NW/SE, formed through the influx of fluorine-rich volatiles in late-stage cooling of the magmas (Floyd *et al.* 1993).

Compressional Features

A penetrative S1 foliation is ubiquitous, dipping gently southeast, subparallel to bedding . F1 closures, where retained, plunge gently east-northeast or west-southwest and verge north-northwest. Rattey and Sanderson (1984) noted that the lower limbs of F1 folds show intense shear typical of deformation at the base of nappe sheets during progressive thrusting. T1 thrusts are exposed in the foreshore at Bassets Cove [SW 6384 4420], where they reactivate bedding (Plate 3.19).

Coaxial F2 folds are sporadically observed in areas of a second, steeper southeast-dipping foliation, often where the lithology is psammitic. An upright F2 fold relating to this second event (Godrevy Antiform) was identified by Rattey and Sanderson (1982) on the basis of fold-vergence. Re-evaluation of the regional structure by Alexander and Shail (1995) discounted the need for the fold. The authors argue that south-verging folds used to infer a change in limbs are, in fact, related to later extensional shear.

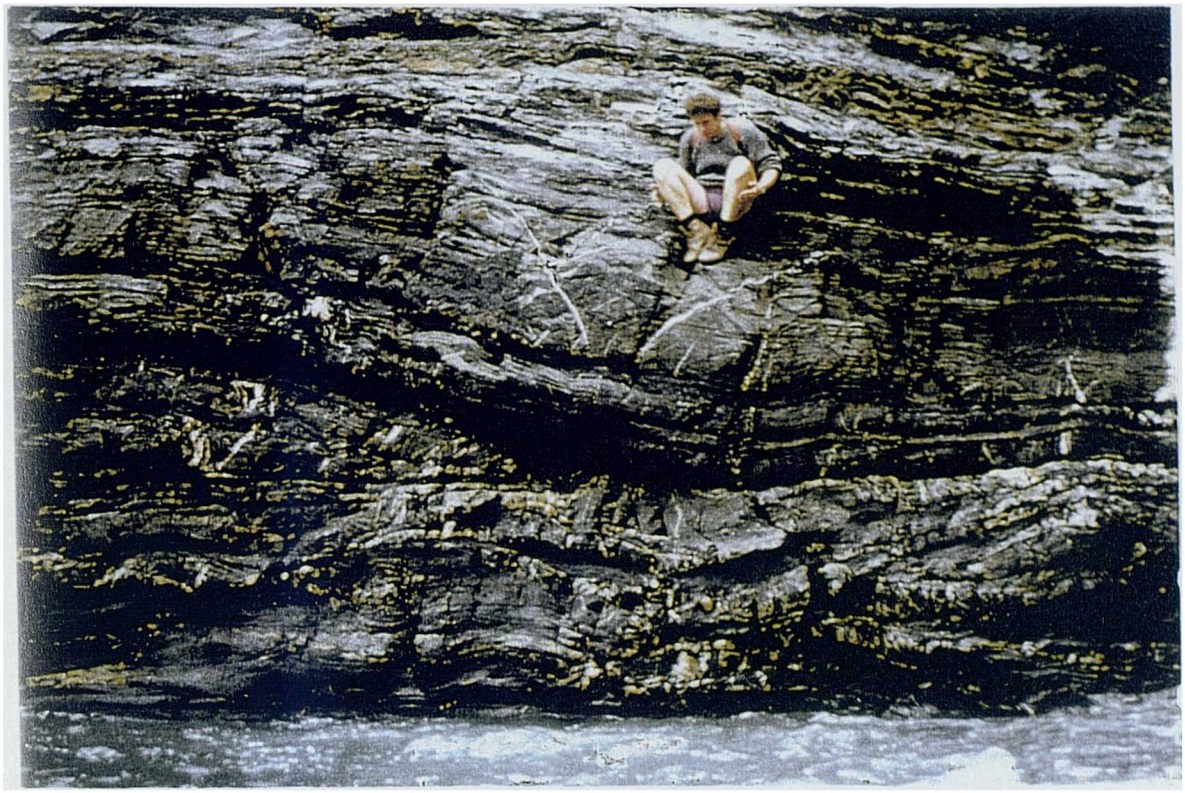

Plate 3.19 Lateral ramp structure of primary thrust, Portcadjack Cove.

A section through the Cligga Head Granite is exposed in the west-facing cliffs [SW 738 536]. Flat-lying joints within the stock define an antiform-synform pair which plunges shallowly WSW and is disputed by minor thrusts dipping both north and south (Figure 3.57). The structure clearly postdates D1/2 compression as its northern margin is irregular and cross-cuts the main cleavage, and is likely to have developed in response to magmatic stresses exerted by the granite magmas which became contractional during cooling (Moore and Jackson 1977).

Extensional features

Close to tight southeast-verging ruck-folds overlie S0/1-parallel D3 detachments between Chapel Rock and Droskyn Point. They are axial planar to a shallowly north to northeast dipping spaced crenulation cleavage and intensify and become sheathed when close to S1-parallel detachments. Quartz veins are focused into the detachments which appear to have acted as fluid conduits during movement along the foliation.

Normal faulting is seen within the Cligga Stock in the form of conjugate faults dipping steeply north and south, and late south-dipping steep faults which crosscut the folded joint set (Figure 3.57; Moore and Jackson 1977). The conjugate faults may have developed during cooling of the stock (Moore and Jackson 1977). At the northern margin of the stock, the igneous contact with Portscatho mudstones and thin sandstones is angular and crosscuts poorly developed D3 detachment features which must therefore predate

granite intrusion. The southern margin of the stock is intensely argillic and is faulted by a steeply north-dipping reverse fault (Moore and Jackson 1977). Conjugate normal faults are common in metasediments to the south and must postdate the granite intrusion as they cross-cut elvan dykes and host copper, tin and iron ores which were deposited at between 400°-240°C (Jackson *et al.* 1977).

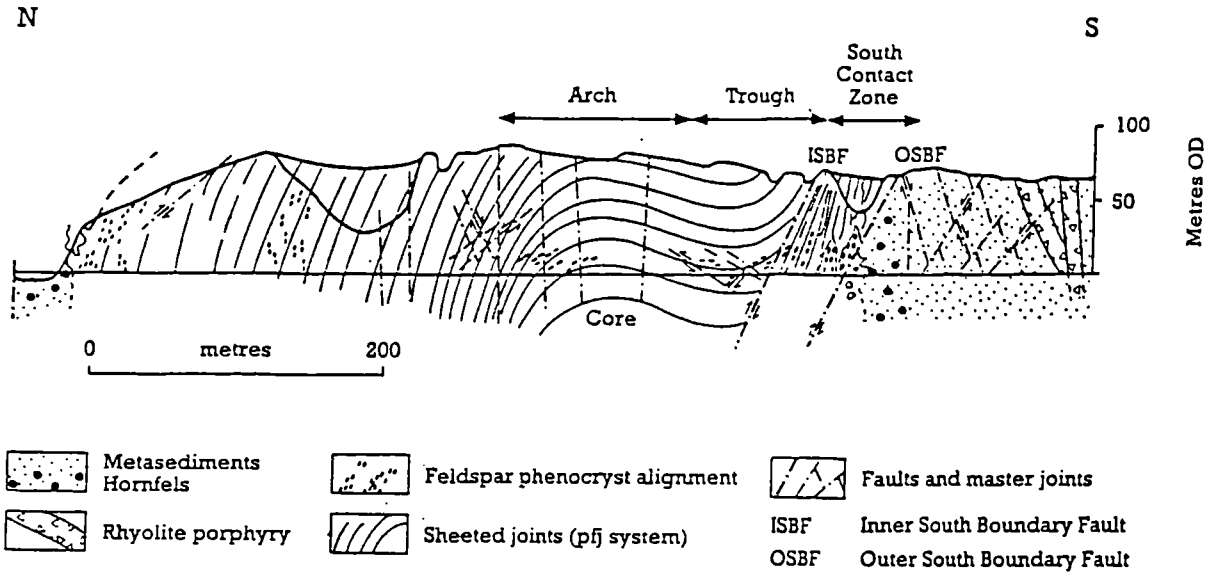

Figure 3.57 Structure of the Cligga Stock (Floyd *et al.* 1993).

A range of semi-brittle extension-related structures are developed and consistently verge towards the south or southeast, down the dip of the main foliation. Alexander and Shail (1995) sub-divided the structrures into three groups on the basis of their styles and geometries (Figure 3.58):

(A) Zones of distributed early D3 shear. Characterised by the southeast-vergent rucks and monoclines ranging in scale from tens of metres to millimetres with a weak crenulation to strong pressure solution S3 fabric. Strain magnitude is variable as illustrated by variation in fold interlimb angle and the intensity of late foliations. Such structures are characteristic of the section as far south as Porthtowan [SW 7514 5440 - SW 6908 4805] and to the west of Castle Giver Cove, east Godrevy Head [SW 5961 4300]. Deformation in these regions is accommodated through non-coaxial shear along the intense S1 foliation and fold structures are formed where slip planes ceased to move following strain hardening. The reason for such diffuse deformation rather than accommodation of strain into discrete planes may be the lithological homogeneity seen in the local stratigraphy.

(B) Zones of D3 detachment. Bedding and S1 parallel movement is common and again produces folds and cleavage above detachments. F3 folds have sheath geometries and produce a variably oriented axial planar S3 crenulation cleavage. These structures form a northeast trending band up to 1 kilometer thick which intersects the coastline west of Porthtowan as far south as Godrevy Head. The reason for such strain partitioning into discrete movement planes is unclear and discussed further in Chapter 6, but may reflect the

presence of mechanical anisotropy introduced by the presence of thick sandstone beds within the local sequence.

(C) Zones of brittle listric faulting (D4). Steep normal faults dip southeast and cross-cut shallower early structures. They crop out southeast of the detachment zone (described above) and are best exposed at Sally's Bottom [SW 6782 4688], Portreath [SW 6531 4532], and along Reskajeage Cliffs. The faults overprint the ductile southeast-directed extensional shear structures and consequently must postdate them.

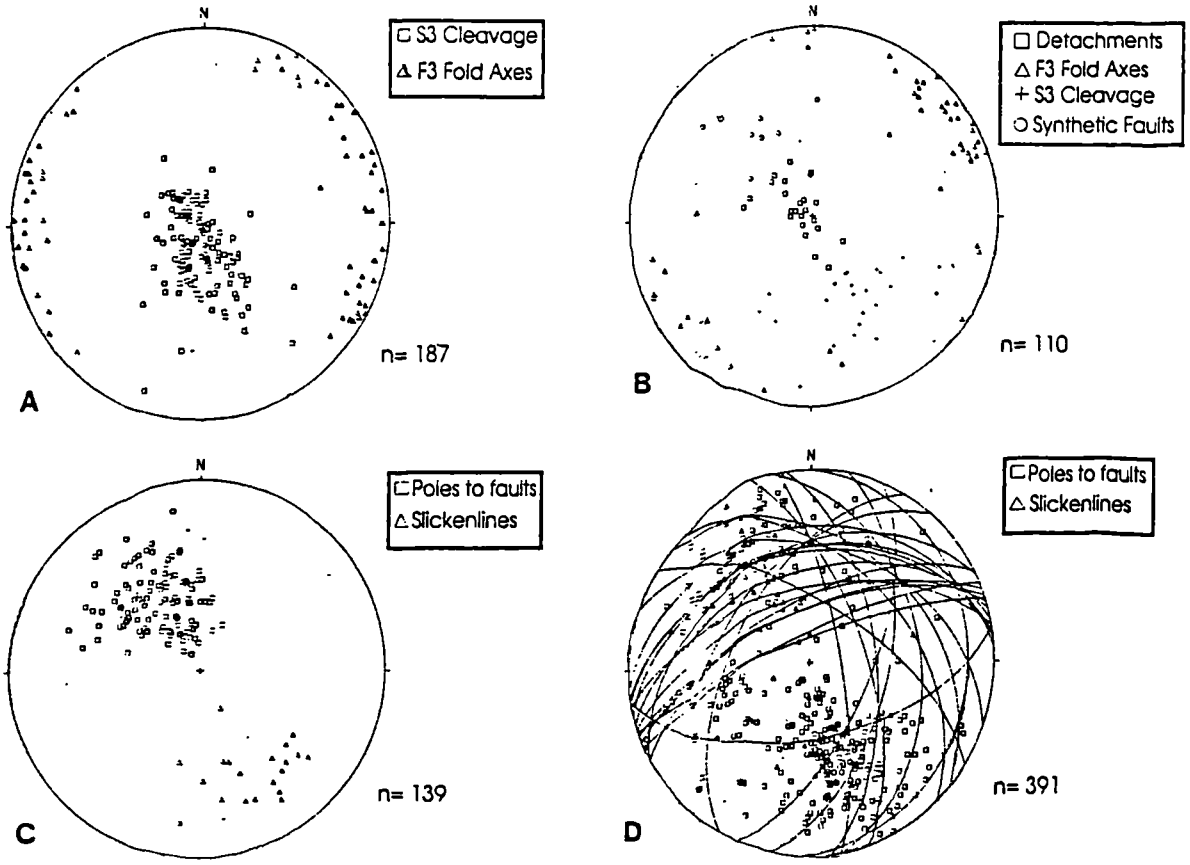

Figure 3.58 Stereoplots of structural orientation data for extensional features exposed between Perranporth and St. Ives (Alexander and Shail 1995). (A) Ductile D3 shear-zones. (B) D3 detachments. (C) Brittle listric faults. (D) Post-D3 faults.

Non-coaxial extensional shear id distributed in nature at Trevaunance Cove [SW 722 516], where shallowly south-dipping detachments are overlain by south-verging or boxed folds. The S3 cleavage is a crenulation or pressure solution fabric which dips moderately north and is most intense within shale layers. Later faults are steep, east-northeast trending and mineralised by orange-weathering main-stage quartz-iron lodes. North-dipping low and high angle normal faults consistently displace south-dipping normal faults.

Interactions between granite magmatism and extension may be examined at Trevellas Porth [SW 7237 5178], where wallrocks to a granite elvan are spotted with cordierite and preserve evidence of both the S1 and S2 fabrics (Plate 3.20). Emplacement of the felsite sheet appears to have occurred during or soon after D3 extension for a number of reasons. Firstly, the wallrocks are hornfelsed and hence unlikely to have

developed a crenulation cleavage once baked by the intrusion. Secondly, cordierite spots are elongate along the L3/1 intersection lineation, which must therefore have either existed prior to the thermal event in the aureole of the granite or grown along a pre-existing L3 lineation, and finally, the granite body is hosted within a shallowly northwest-dipping normal fault with domino-faulting in its immediate footwall. Hydrolytic explosion breccias with blebs of granite and aplite suggest forceful injection of magma, and faulting of the elvan is restricted to steeply north-dipping brittle faults.

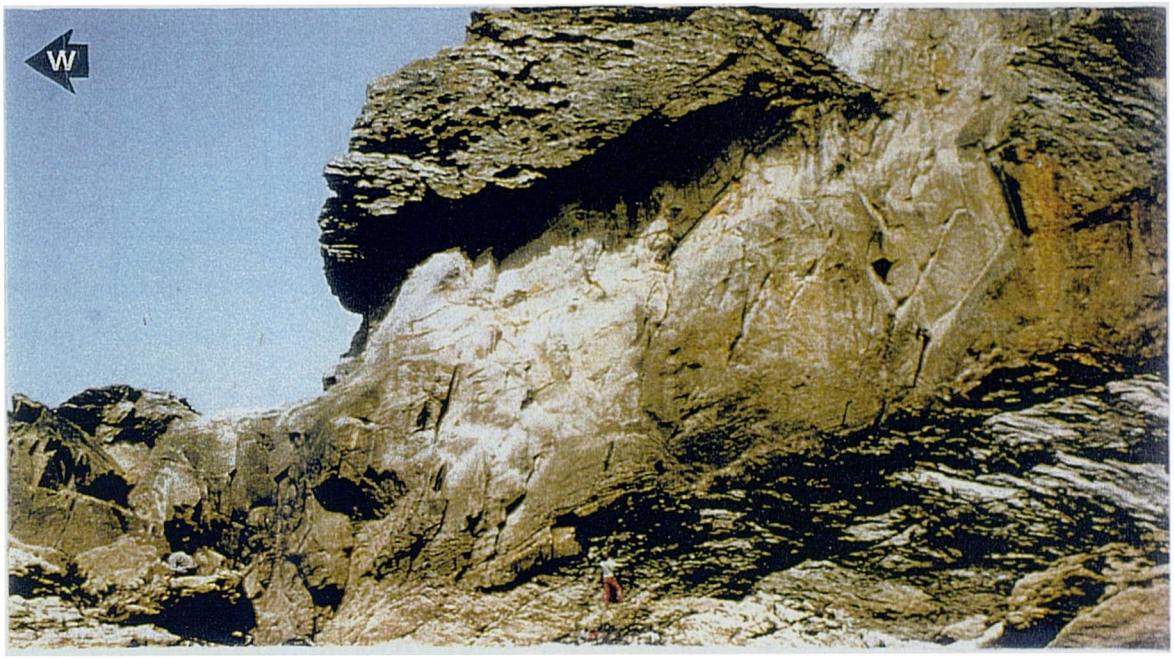

Plate 3.20 Elvan cutting foliation obliquely, with domino-faulting in its immediate footwall, Trevellas Porth [SW 7267 5224].

Iron-stained sandstones and shales are folded by small-scale monoclines at Wheal Coates, St Agnes Head [SW 6990 5026], indicating lower D3 strain than to the north. Towards the southeastern end of the locality, S3 cleavage dips gently to the northwest above a shallowly southwest-dipping normal detachment. Ten kilometers to the southwest at Portcadjack Cove [SW 6411 4469], low-angle normal detachments run parallel to bedding or cleavage. They dip north and contain second order minor folds which also verge north or northeast. The footwalls are commonly extended by shear-bands and domino faults, whilst the hanging walls are folded, the fold geometries relating to the geometry of the causative slip planes. The footwalls of D3 detachments contain networks of quartz-veins which do not cross the movement planes which may therefore have acted as permeability barriers during deformation.

3.6.2 Gwithian to St. Ives

Lithology

Backshore exposures of slates and siltstones with subordinate sandstones occur between Godrevy Point and West Hayle Inlet. The majority of the section exposes Mylor Slates, locally spotted with cordierite against metabasite sheets (Plate 3.21), and comprising turbiditic mudstones and siltstones, in places enclosing coarse turbiditic sandstones. Bedding is clearly visible due to variation in colour, and is disrupted by load and water-release structures formed prior to lithification of the sediments. In contrast, coarser sandstones with subordinate slates crop out several times along the section, at Godrevy Cove [SW 5808 4290], Peter's Point [SW 5775 4121] and Upton Towans [SW 5734 4052]. Mapping of lithofacies by Shail (1990) identified these coarser facies as Gramscatho Beds, downfaulted into the Mylor Slates by NW/SE and W/E trending steep normal faults.

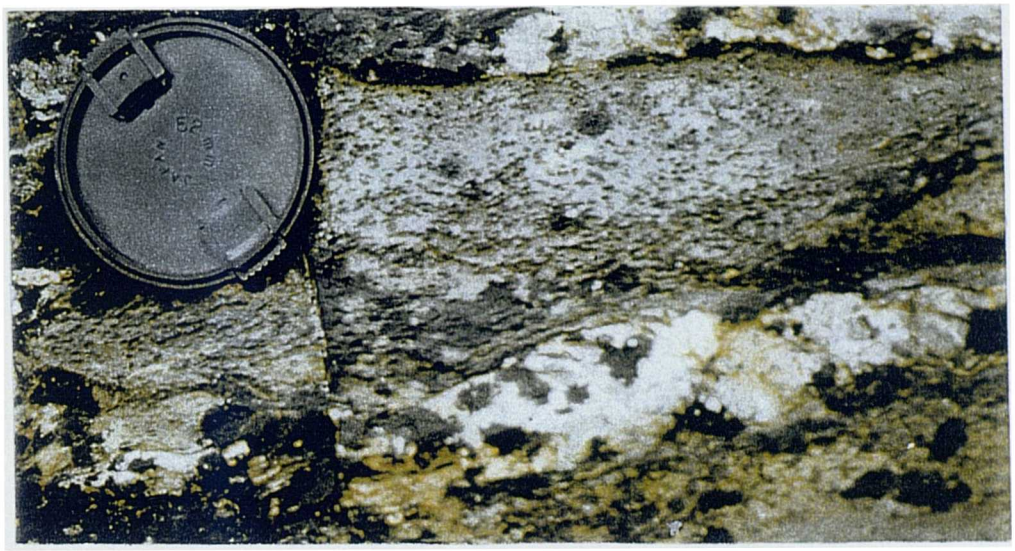

Plate 3.21 Spotted slates, Red River. Spots show elongation parallel to bedding and are restricted to fine-grained lithologies.

Exposures at Upton Towans are dominated by sandstones with scoured bases, rip-up-clasts of mudrock and sedimentary structures demonstrative of proximal turbidites of the Gramscatho lithofacies (Shail 1990). Sandstones continue across the Hayle estuary to its western side, where they revert to mudstones and distal facies at Carrack Gladden. The nature of transition between the two lithofacies in this area is unknown due a gap in exposure but variation in bedding orientation from gently southeast-dipping to subvertical suggests the presence of large folds which may cause repetition of the formation boundary.

At Carbis Bay, slates and thin sandstones of the Mylor Slates are exposed. At the east end of the beach [SW 5343 3887], the slates are recrystallised into a grey-green hornfels with rusty blastic spots

(?cordierite). Where present folded sandstone beds display divergent S1 cleavage fans. The spots increase in size to the west and grow to 4mm diameter. They are clearly elongate and in a west-northwest trend and surrounded by segregations of mica, forming a schistose S2 fabric which is heavily jointed. Red quartz-veins in the sequence have been mined for copper and tin as evidenced by the presence of adits. Proceeding eastwards, phyllonites are interbanded with recrystallised quartzites, with white weathered surfaces contrasting with pale-grey to black spots. At the western end of Barrepta Cove [SW 5242 3908], a group of metadolerite sills form massive dark grey-green exposures containing actinolite, and a crude primary foliation.

Compressional features

The juxtaposition of Mylor and Portscatho lithofacies has important implications for the early structure of the area (Shail 1992). The junction between the two lithologies is not clearly seen in this area, but is thought to be the Carrack Thrust, placing the Gramscatho Group (older), over Mylor Slates (younger). Inliers of sandy turbidites along the coastal section may thus form part of the allochthonous sheet, brought into contact with autochthonous rocks by steep normal faults (D4 age). The relationship between the Portscatho and Mylor rocks remains contentious as palynomorph data indicates a partial contemporaneity to their sedimentation (Knight and Wilkinson 1989).

The sequence of deformations is complex throughout this area and hence the primary structure is sometimes uncertain. However, the S1 foliation dominates most outcrops, dipping gently to the southeast. F1 folds are sometimes seen in the field, and appear to be isoclinal and recumbent with a northerly facing direction (Goode and Taylor 1988). Large wavelength F1 folds are present at Black Cliff, where the southwestern most exposures preserve inverted steeply dipping beds and to the northeast the beds dip gently to the southeast, and bedding-cleavage relationships suggest the presence of a decimetre-scale F1 synform. From Carrack Gladden westwards, the S1 foliation transposes bedding and is subhorizontal or shallowly southwest-dipping (Figure 3.59a). Fold closures are observed where sandstones are present, and bedding steepens westwards into the metadolerite outcrops where F2 refolding causes rotation of the primary fabric.

A second compressional event, D2, is well documented by Rattey (1980), who noted open to close north-northwest verging folds on the long limbs of F1 folds which cause coaxial refolding of F1 hinges (Godrevy Cove [SW 579 430] and Red River [SW 5821 4232]; Figure 3.60). A pressure solution S2 foliation dips steeply towards the south-southeast, with divergent fans formed in F2 hinge regions. The foliation shallows towards the southwest across the inferred Godrevy Antiform. To the southwest the second compressional phase is recorded along Carbis Bay by a set of north-verging folds of S1 and V1 veins. The resulting foliation is patchily developed and developed axial planar to F2 folds.

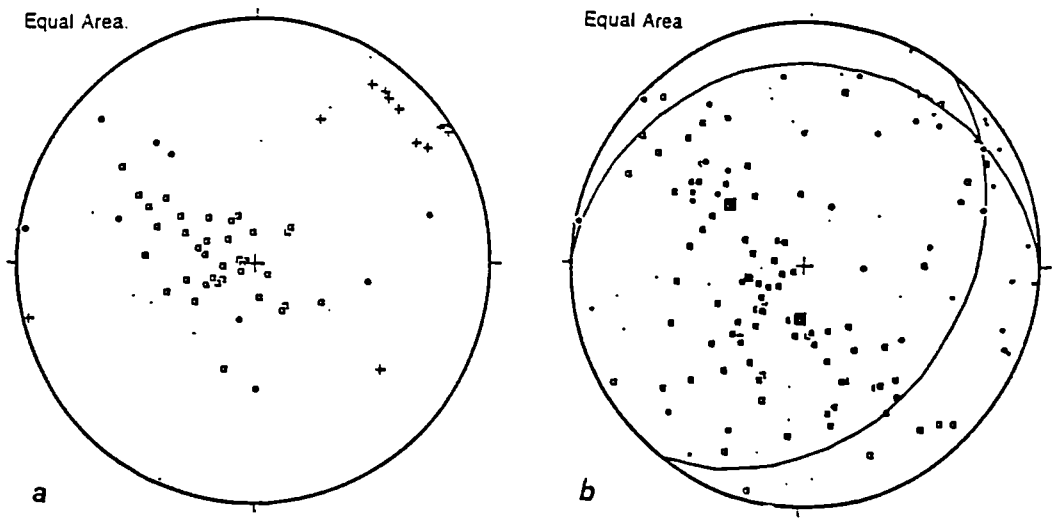

Figure 3.59 Stereographs of structural orientation data collected between Carbis Bay and Godrevy Head. (a) Compressional features (*poles;* dots = S0 (9), squares = S1 (29); *lines;* crosses = L1 lineation (12)). (b) Extensional features (*poles;* boxes = fault-planes; black = primary normal faults with SE-vergent ruck-folds (53); grey = secondary faults with northwest-vergent ruck-folds (19); white = late normal and dextral faults (18); *lines;* circles = slickenlines (17,2), colour relating to fault type (see previously); stars = down-dip verging fold axes (19).

Extensional features

Extensional structures are polyphase along this section. Early structures (D3a) include a group of shallowly southeast-dipping normal faults with ruck-folds and vein quartz concentrated along their traces. The faults occur along sandstone beds and along planes of rheological contrast (Figure 3.59). Asymmetric F3 folds verge southeast down the dip of the normal faults (and hence the S0/1 fabric), their axes plunging gently towards the northeast and southwest (Figure 3.59b). A shallowly northwest to west-dipping axial planar crenulation cleavage is heterogeneously developed in metre-scale shear-zones.

A second group of north-transporting extensional structures (D3b) cross-cuts the F3 folds and faults, locally offsetting them by several metres. Such features are well developed to the south of Peter's Point [SW 5775 4121], where moderately to steeply northwest and northeast-dipping normal faults with curviplanar profiles accommodate up to 50% extension of D2 veins. F4 northwest-verging folds are common and separable from the D2 structures by their concentration above normal fault-planes. The D4 event is more brittle in style than D3 in fold style and a more spaced fracture cleavage. At Carbis Bay, asymmetric ruck folds verge northwest and overlie northwest-dipping detachments. They occur within shallowly-dipping D3 shear-zones, and cause folding and boudinage of D2 quartz veins.

Thin section analysis

Exposures at the mouth of the Red River comprise slates and siltstones which host rusty cordierite blasts with yellow pleochroic haloes. The S1 foliation is defined by aligned biotite and muscovite laths in which the cordierite spots form σ-porphyroclasts with top-to-the southeast asymmetry (Plate 3.22). Down to the northwest shear-bands also deform the slaty foliation, recording the change in extensional kinematics late in D3 locally. Unspotted slates from the core of the F1 isocline at Magow Rocks, Red River (Figure 3.59) have a composite foliation of aligned muscovite crystals and pressure solution seams, with bedding clearly seen in colour variations.

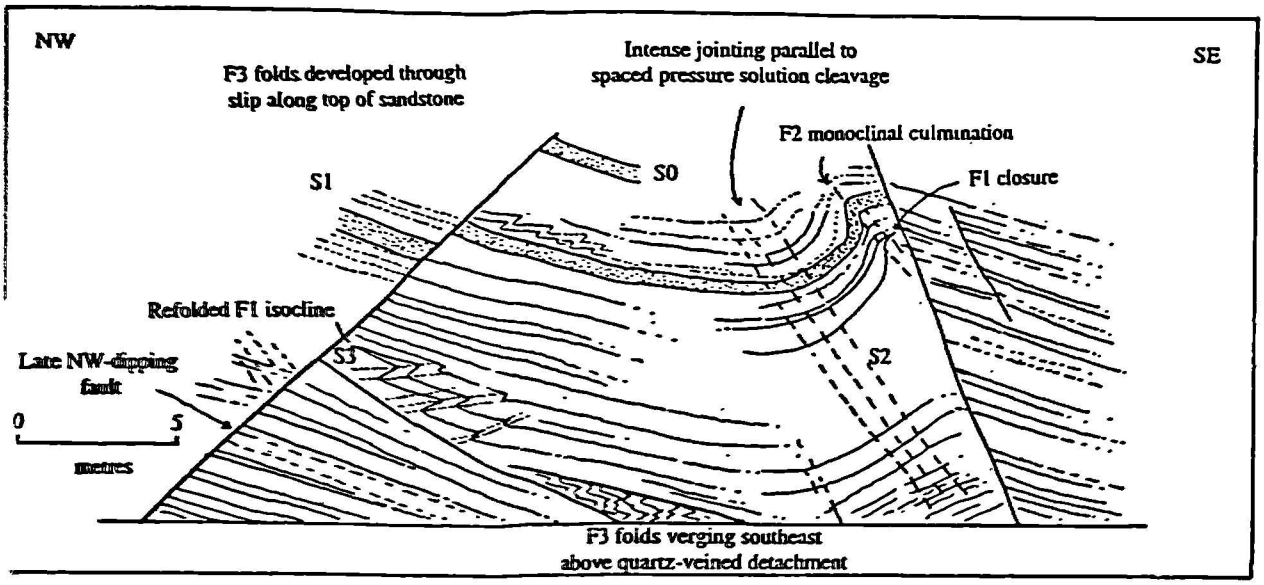

Figure 3.60 Refolding pattern, Red River [SW 5821 4232].

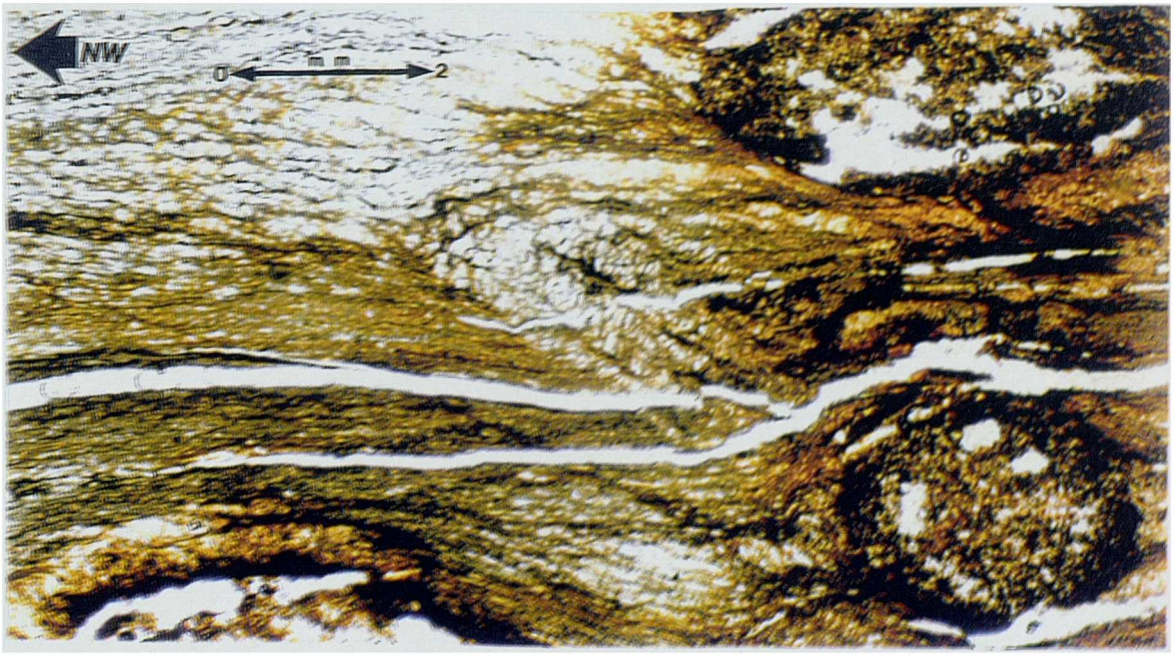

Plate 3.22 Photomicrograph of siltstones sampled at Red River, showing polyphase microstructures. Brown cordierite blasts have micaceous tails which confirm that they developed syntectonically with foliation-parallel shear

At Upton Towans siltstones preserve a pressure solution primary foliation cross-cut by features formed during two phases of extensional deformation. The first is represented by extensional shear-bands dipping north, whilst the second is recorded by asymmetric crenulations developing into pressure solution seams in places, relating to top-to-the-southeast shear. The two events are thought to be D2 and D3 respectively on the basis of their similarities of orientation to macrostructures. Where present, veins are quartz-infilled and folded into the primary foliation. Mudstones entrained along the northwest-dipping normal faults preserve northwest-vergent microfolds and are locally cataclastic, with entrained fragments of vein quartz and folds of the bedding fabric. Biotite mica is the dominant mineral in the dark mudrocks.

At Carrack Gladden [SW 5348 3882], mudrocks are composed of muscovite with a heavy iron stain. A phyllonitic texture of aligned mica and ultra-fine quartz and clay minerals has a mottled appearance which hinders interpretation, but the main foliation is due to the alignment of micas. A second, pre-existing foliation is revealed when viewed under sensitive tint, dipping more steeply to the south. It is defined by alignment of opaque minerals and muscovite. Overprinting this, fibrous biotite laths are developed with sygmoidal shapes which appear to have developed during fluid influx along hydrofractures. Late bands of sericite occur at high angles and appear to relate to D4 steep cleavage development. Elsewhere, chloritic bands of tuffaceous metasediment show alteration to needles of actinolite. The chlorites form large clumps with fibrous nature, overgrowing a very fine-grained sericitic and opaque-rich groundmass. A lack of preferred orientation indicates that metamorphism is thermal and thus that it may relate to emplacement of the granite to the west. Tourmaline crystals are present in the groundmass and have brittle offsets infilled with chlorite.

3.6.3 Structural summary and discussion

Compressional structure between Perranporth and St Ives is dominated by a southeast-dipping cleavage and tight NNW-vergent F1 folds. The cleavage changes orientation to horizontal or shallowly southwest-dipping to the west of Carrick Gladden. A second compressional event (D2) is heterogeneously developed as open to close NNW-vergent folds with an axial planar S2 pressure solution cleavage.

Extension is recorded by D3 detachments which dip southeast between Perranporth and Godrevy Head, and are overprinted by north-directed detachments with curviplanar profiles. Extension magnitude is variable but may reach 50% in places. Steep normal faults again have curviplanar profiles and modally dip to the southeast. They postdate the D3 detachment structures but show consistent kinematics with early D3 structures.

3.7 Discussion of extensional features of the north Cornish coast

3.7.1 Style

The geometries of fault-planes, folds of the S1/2 fabrics and of second-order structures allow their division into four main types :-

i. Ductile shear-zones - Regions in which early foliations have accommodated down-dip non-coaxial shear, expressed as ductile fabrics, small-scale folds and generation of porphyroclast-tail structures on a microscale. This group of structures occur within diffuse, broad shear-zones with sharp boundaries. Deformation is macroscopically ductile with strain accommodated through creep along anisotropies rather than movement along faults. Such structures are typically observed in weak rheologies with low variation in layer strength.

ii. Detachments - Zones in which deformation is focused into movement planes reactivating bedding and (more commonly) S1 cleavage. Such features have abundant shear-sense indicators developed during shear which include folds, Riedel fractures, bookshelf structures and porphyroclasts. Footwall veining is common along detachments, suggesting that the fault-plane acts as a permeability barrier during deformation. Detachments differ from group (i), in their partitioning of strain into discrete movement planes and the lower non-coaxial shear strain experienced in surrounding wall-rocks. Detachments are developed within zones of peak metamorphic grade in beds of lowest mean grainsize and may consequently reflect weak features prior to extension.

iii. Linked curviplanar normal faults - Extensional duplexes of interlinked normal fault-planes which allow moderate to high magnitudes of strain to occur in an anastomosing brittle form. Their ramp-flat geometry is reminiscent of thrust systems, but the combined evidence of vein offsets, shear-sense indicators and the anomalous orientations of the faults relative to identified D1 thrusts is consistent with their generation during extension.

iv. Brittle planar normal faults - Ubiquitous across the north coast, steep normal faults are locally intense and are seen to cross-cut and therefore postdate the other extensional assemblages. Folding is occasionally seen within fault-bounded blocks but is more angular than in types (i-iii).

3.7.2 Kinematic pattern

The top sense of extensional shear as inferred from analysis of kinematic indicators shows a basic pattern in which extension occurs down the dip of pre-existing foliations (Section 4.6). The major change in shear-direction is encountered around the Camel Estuary, where the Padstow Facing Confrontation separates

northwest- and southeast- dipping bedding and S1 cleavage. Late overprinting extensional features with diametrically opposed kinematics in extension are seen locally in the southwestern end of the section, indicating a change in the stress-field late in the extensional event.

Between Watergate Bay and Perranporth, additional complexity is observed at the western end of the Start-Perranporth Zone, with a dextral dip-slip component to movement on detachments. It thus appears that in this area the extensional stress-field was reoriented due to continual dextral movements along the recurrent basement structure inferred by Holdsworth (1989b). The reasons for this pattern are discussed in Chapter 6.

3.7.3 Magnitude

The areas of highest strain (as calculated by the Burchfiel and Wernicke method described in Section 1.4) occur within the Tintagel High Strain Zone, the Start Perranporth Zone, and again to the south of Godrevy Head. In each case, the dominant structures are types (i) and (ii), indicating semi-ductile conditions. Extensional strains drop off into the Culm Basin, which preserves steep normal faulting and hence displays a shallow level of exhumation in comparision to that south of the Rusey Fault.

Chapter Four - Late-Variscan Evolution of the South Cornish Coast

CHAPTER 4 : LATE-VARISCAN EVOLUTION OF THE SOUTH CORNISH COAST

4.1 Introduction

This chapter deals with structures exposed along the south coast of Cornwall, where mapping was conducted between Penzance and Plymouth (Figure 4.1). Structures observed on the south coast are summarised in Section 4.6 and correlated with structures observed along the north coast (Chapter 3) in Section 4.7.

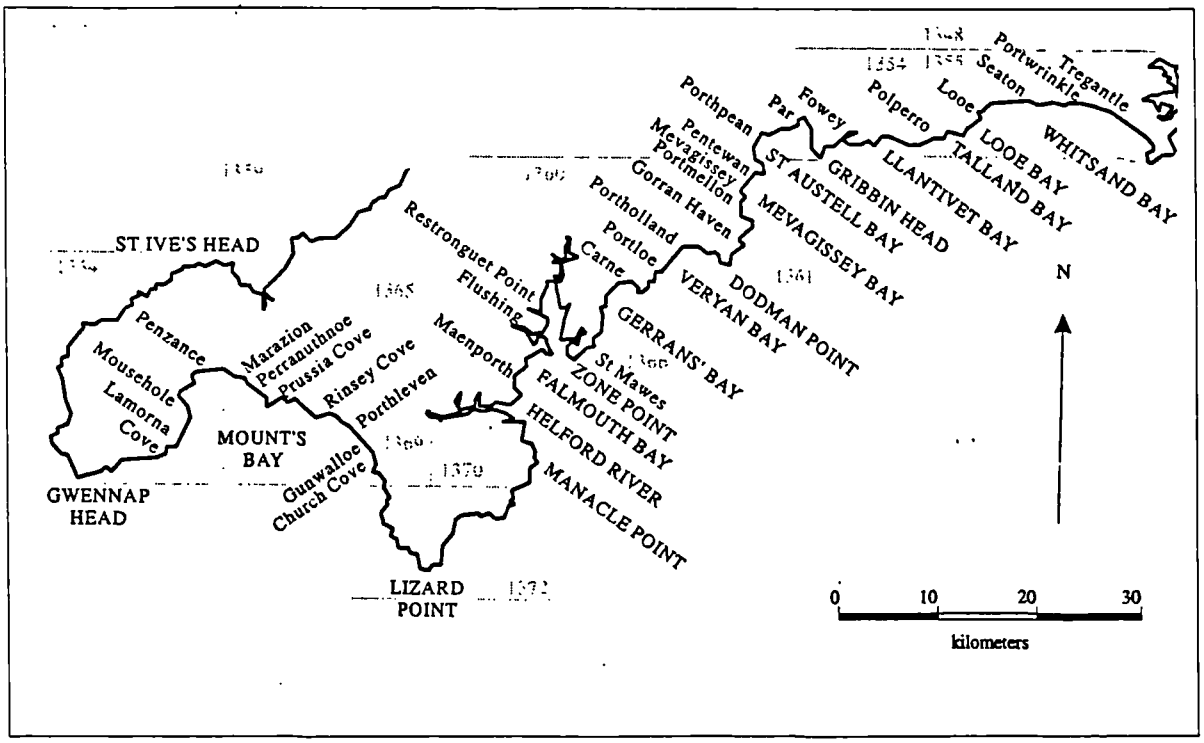

Figure 4.1 Locality map of the south Cornish coast, overlain with positions of 1:25 000 Ordnance Survey Sheets.

4.2 Mounts Bay; Lamorna Cove to Church Cove

Stratigraphy

Mount's Bay exposes an across-strike section through the Gramscatho Basin, exposing Devonian rocks of the Mylor Slate and Portscatho Formations. The bay is bounded to the west by the Land's End Granite and to the southeast by schists of the Lizard Nappe. The Gramscatho metasediments are punctuated by the St. Michael's Mount and Tregonning Godolphin stocks (Figures 2.4, 2.5; Leveridge *et al.* 1990; Figure 4.2).

Figure 4.2 Geological map of Mount's Bay, adapted from BGS 1:50 000 sheets 351, 358 and 359 with reference to Holder and Leveridge 1986 and Leveridge *et al.* 1990.

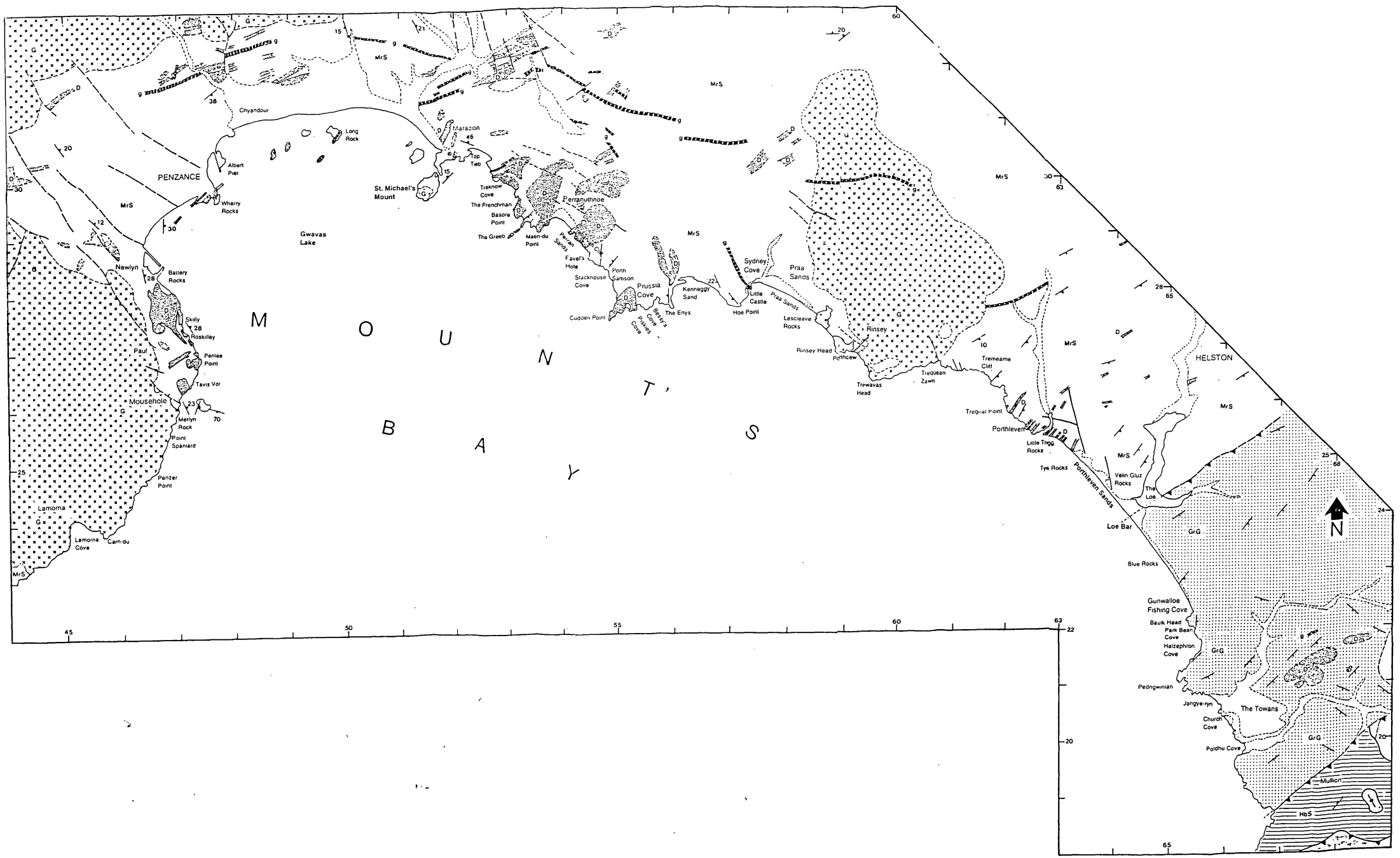
MOUNT'S BAY
PENZANCE
Albert Pier
Wherry Rocks
Chyandour
Long Rock
Marazion
Top Tieb
St. Michael's Mount
Treknow Cove
The Frenchman
Basore Point
The Greeb
Maen-du Point
Perranuthnoe
Perran Sands
Gwavas Lake
Newlyn
Battery Rocks
Skilly
Boskilley
Paul
Penlee Point
Tavis Vor
Mousehole
Merlyn Rock
Point Spaniard
Penzer Point
Lamorna
Lamorna Cove
Carn-du
Favel's Hole
Stacknouse Cove
Porth Samson
Prussia Cove
Cudden Point
Bessy's Cove
Pistols Cove
Kenneggy Sand
The Enys
Sydney Cove
Praa Sands
Little Castle
Hoe Point
Lescleave Rocks
Rinsey
Rinsey Head
Pollhcew
Trewavas Head
Trequean Zawn
Tremearne Cliff
Porthleven
Little Trigg Rocks
Tye Rocks
Porthleven Sands
Velin Gluz Rocks
The Loe
Loe Bar
Blue Rocks
Gunwalloe Fishing Cove
Baulk Head
Park Bean Cove
Halzephron Cove
Pedngwinian
Jangye-ryn
Church Cove
The Towans
Poldhu Cove
Mullion
HELSTON
MrS
GrG
HbS
N

The Mylor Slate Formation is exposed to the northwest of Loe Bar [SW 643 242], comprising interbedded slates, siltstones and fine sandstones indicative of deep basinal facies with distal turbidite influx (Section 2.2.3.1; Figure 2.5), and commonly enclose metabasic sheets (Figure 4.2). The upper part of the formation exposes the Porthleven Breccia Member, a bedded matrix-supported breccia indicative of mass flows from an active fault escarpment into the basin (Holder and Leveridge 1986a, Middleton and Hampton 1976). The Portscatho Formation exposed to the southeast of Loe Bar comprises grey to green-grey sandstones with intercollated mudstones and siltstones (Section 2.2.3.1; Figure 2.5). Sedimentary structures suggest that they represent proximal turbidites within a deep water fan system. Sediment provenance of the Mylor Slates and Portscatho Formation appears to be from an emergent region to the south (Figure 4.2; Leveridge and Holder 1985; Le Gall *et al.* 1985; Leveridge *et al.* 1990; Shail 1992). The metasediments are underlain at shallow depth by the main Cornubian batholith, the uppermost culminations of which are exposed in the Land's End, St. Michael's Mount, Tregonning-Godolphin and Carnmenellis stocks (Section 2.4.1).

To the south of Poldhu Point [SW 664 199], sandstones and slates are structurally overlain by hornblende and mica schists of the Lizard Complex. The boundary between the two formations is a southeast dipping normal fault along which metre-thick quartz-breccias are developed, but K-Ar ages and field relationships to the east (Porthallow [SW 796 233]) suggest that this is a late cut-out in the hanging wall of a large thrust (Dodson and Rex 1971; Holder and Leveridge 1986, Leveridge *et al.* 1990).

Bulk structure

The structural orientation of primary deformation products defines four domains (Sanderson and Dearman 1973): (1) West of the Tregonning Godolphin granite, primary folding is seldom observed due to intense late deformation. Where seen, it appears to be recumbent and north-northwest facing with ENE/WSW axial trends. (2) Between the eastern margin of the granite and Loe Bar, primary folds verge northwest and are inclined moderately southeast, producing shallowly southeast-dipping S1 cleavage and bedding. (3) Between Loe Bar and the Lizard boundary fault, fold axes plunge southeast within the gently southeast- to south-southeast dipping S1 cleavage, suggesting a degree of non-cylindricity to F1 folds or perhaps the effect of strong D2 refolding (Sanderson and Dearman 1973). (4) The Lizard schists have a distinct tectonic style preserving more ductile deformation products, as discussed recently by Alexander and Power (1996).

Two northwest-directed compressional phases are recognised regionally. The compressional structures are largely transposed by a late, subhorizontal crenulation foliation to the west of the Tregonning-Godolphin granite attributed to vertical compression above the upwelling granite bodies by several authors (*see discussion by* Hobson and Sanderson 1983). Compressional features are overprinted by ductile fabrics, faults and asymmetric folds thought to relate to regional extension. Late kink-banding and steep fabric development are locally important and appear related to movement on normal and wrench fault-zones.

4.2.1 Lamorna Cove to Newlyn

Lithology

Between Lamorna Cove and Merlyn Rock [SW 4502 2409 - SW 4698 2588] coarse-grained, megacrystic granite of the Land's End pluton crops out (Figure 4.2). A quartz, orthoclase, plagioclase, biotite and muscovite assemblage typical of Cornish granites is seen with apparent alignment of orthoclase phenocrysts into a north-northeast trending steep fabric which may relate to magmatic flow at the granite margins (Walton 1994). Sheets and pods of granite, aplite and pegmatite are observed within the main phase granite and are elongate along the north-northeast trend. Poorly foliated pegmatite sheets present at Carn-du [SW 4568 2380] contain enclaves of mica and cassiterite. A crude subhorizontal foliation is seen within the granite on nearing the margin with the Mylor Slates, reflecting increased strain close to the roof of the pluton and suggesting that it is exposed at a level close to its pre-erosional top.

The margin of the granite is exposed in the foreshore between Merlyn Rock and Mousehole [SW 4697 2590] and continues to the northeast across St Clement's Isle [SW 4740 2619]. It is irregular in geometry, with veins of aplite and hydrolytic explosion breccia fingering into the Mylor Slates and forming a network enclosing angular blocks of the host. Aplite veins commonly exploit the dominant subhorizontal foliation within the slates, thus suggesting that they were intruded after the fabric-forming event (see *Extensional features* for discussion).

The Mylor slates preserve multiple foliations and polyphase quartz-calcite veins, often defining decimetre-scale folds. Bedding is indistinct due to metasomatic alteration and pressure solution striping, but is occasionally seen in grainsize variation. Cordierite blasts up to 3 mm diameter occur close to the granite contact (e.g. Tavis Vor [SW 4719 2653]) The metasomatic spots are elongate and define a mimetic mineral lineation. This is likely to relate to preferred growth along the crenulation lineation which is seen away from the contact and thus predates granite emplacement.

Metadolerite sheets make up over 50% of the country rock to the north of Mousehole Harbour, with notable exposures ~100 metres to the northeast of the harbour [SW 4704 2662], at Penlee Point [SW 4738 2690], and to the north of Røskilley [SW 4716 2732]. They weather to a mid-grey colour but when broken reveal a structureless dark grey-green crystalline nature. A crude spaced cleavage seen in thick metadolerite sills north of Penlee Point and at Roskilley and folding of metadolerite-slate contacts indicates that they were intruded prior to the D1 compressional event.

The homogeneity of the metadolerites is broken by north-northeast striking aplite veins, north trending quartz veins in zones tens of metres wide and irregular early quartz-chlorite and calcite veins. East-dipping rafts of slate commonly break the continuity of thick metabasic sheets and show intense cordierite spotting.

The relative timing of this metasomatism is unclear; spotting is concentrated into the regions dominated by metabasite, and whilst this suggests that the spotting is related to metadolerite intrusion, the spotting may relate to later granite-related contact metamorphism and be preferentially developed due to the geochemistry of the metadolrites and their adjacent wallrocks.

Compressional features

The Land's End granite postdates compression and thus contains no internal features which could relate to compressional strain. At the granite-slate contact, the Mylor Slates contain a slaty composite foliation which dips shallowly south or east (Figure 4.3A). The L1 bedding-cleavage intersection lineation is largely obscured by cordierite growth and plunges shallowly toward the southeast or east. Bedding is identified tentatively in bands of fine-grainsize amongst siltstones which dip shallowly to the west and east.

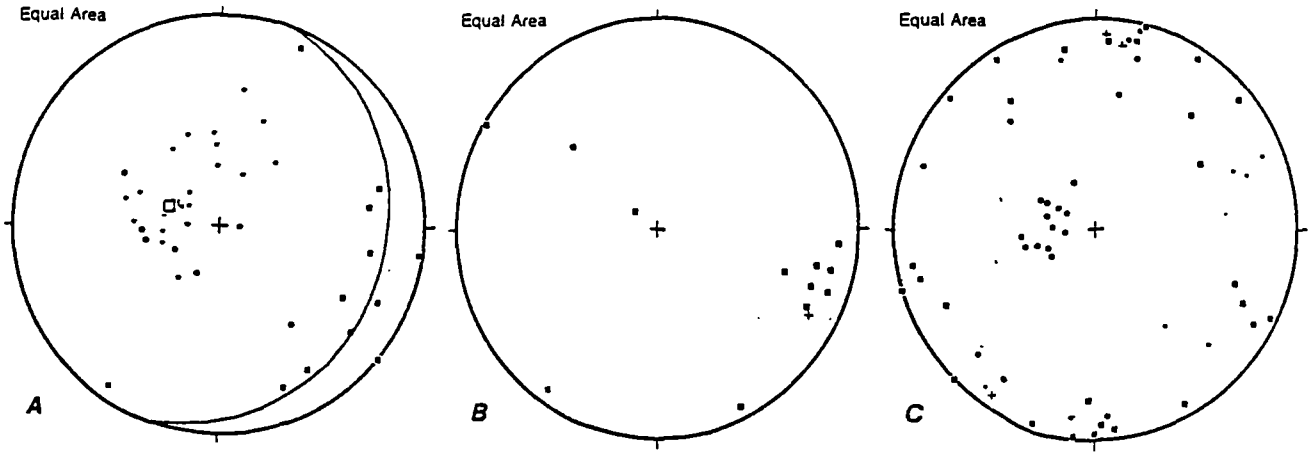

Figure 4.3 Stereoplots of structural orientation data for section 4.2.1; Lamorna Cove to Newlyn. (A) Compressional structure (• S0 (8); • S1 (22); ▪ L1 (12); *mean compressional foliation* 019/20 E). (B) Extensional fabric elements and faults (▫ L3 (9); ▪ normal fault (3); + normal slickenlines (1)). (C) Miscellaneous/late structure (• S4 (6); + L4 (3); • vein (10); ▪ joint (27); ○ igneous foliation (17)).

To the north of Mousehole bedding dips northeast and S1 foliation dips south. Variations in S1 dip appear to define north-vergent open F2 folds. Metadolerite foliations follow S1 fabric orientations or mimic the slate-metadolerite contacts (Figure 4.3C). At Penlee lifeboat station [SW 4731 2901], south-dipping ductile thrusts are picked out by quartz veins within the metabasites which record north-northwest directed D1 compressive strain.

Extensional features

Within the Land's End Granite, steep south- and southeast-dipping normal faults record metre-scale extensional offsets (Figure 4.3B). More significant throws (100s of metres to kilometers) are inferred from offsets of the granite margin, where faults strike northwest-southeast and downthrow to the northeast (Figure 4.2). In contrast, the Mylor Slates have experienced significant late shear prior to the emplacement

of the granite. At the granite-slate contact a shallowly west- to northwest-dipping crenulation cleavage transposes earlier fabrics and is focussed into S1-parallel bands.

Shallow to moderately southeast-dipping normal faults are present 80 metres to the south of Penlee Point [SW 4738 2682], with quartz-breccias developed along fault-planes which contain stepped quartz slickenlines. A weak, east to southeast plunging crenulation lineation is seen throughout the area, but shows no relationship to positively identified extensional structures such as drag-folds. F3 sheath-folds are likely to have developed locally and thus the lineation may be subparallel to the extensional transport direction.

Extension is not restricted to the slaty lithologies. Metadolerites to the north of Skilly [SW 4703 2760] are foliated by coarse amphibole-rich bands within a dark, glassy matrix. The coarse bands are attenuated by domino-faults indicating shear down to the east-southeast (Figure 4.4).

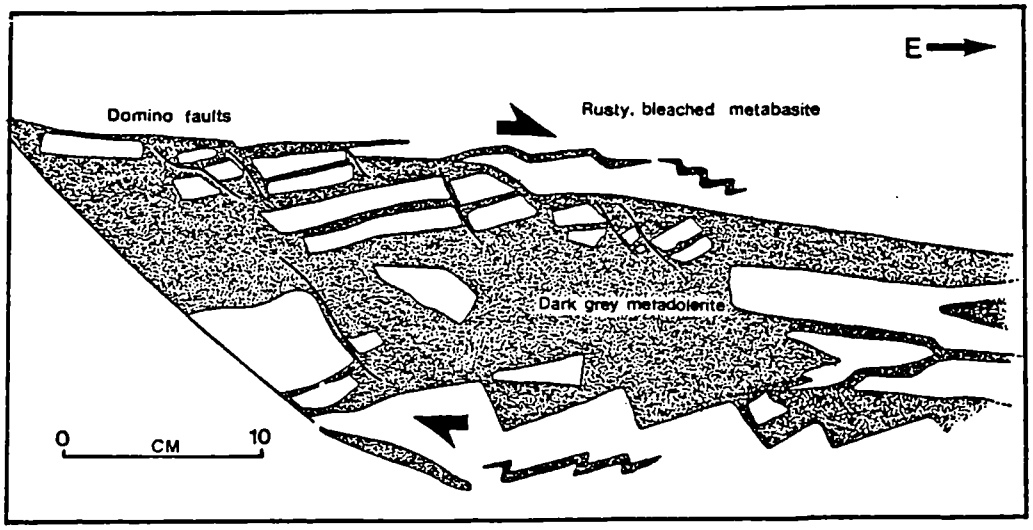

Figure 4.4 Field sketch of extensional structures within metadolerites to the east of Penlee Quarry [SW 4701 2790]. Pale compositional bands show layer-parallel attenuation along east to southeast-dipping domino faults/extensional shears. A moderately ductile nature to the deformation is attested to by east-vergent asymmetric minor folds in apophacies to dark-grey band.

Post D3 deformation is dominated by a steep, west-northwest striking late spaced cleavage observed at Tavis Vor and Roskilly. It intersects S3 and is axial planar to open upright F4 flexures (Figure 4.3C). An orthogonal joint-set is developed in the granites and larger metadolerite bodies with north, east-northeast and north-northwest striking steep planes, but these are likely to have formed in response to stress relaxation during uplift rather than a phase of tectonism.

Thin section analysis

The Land's End granite exposed at Carn-du [SW 4568 2380] has a two-mica mineralogy comprising quartz, orthoclase, plagioclase and intergrown biotite and muscovite. Metasomatic alteration in the presence of potassic fluid is inferred from the internal alteration of plagioclase to fine muscovite lathes. Biotite crystals are commonly altered to chlorite and have relict haloes surrounding zircon inclusions (Plate 4.1a). Metadolerite from north Mousehole [SW 4704 2662] is heavily altered and has a mineralogy of hornblende, sericite, clay minerals and muscovite.

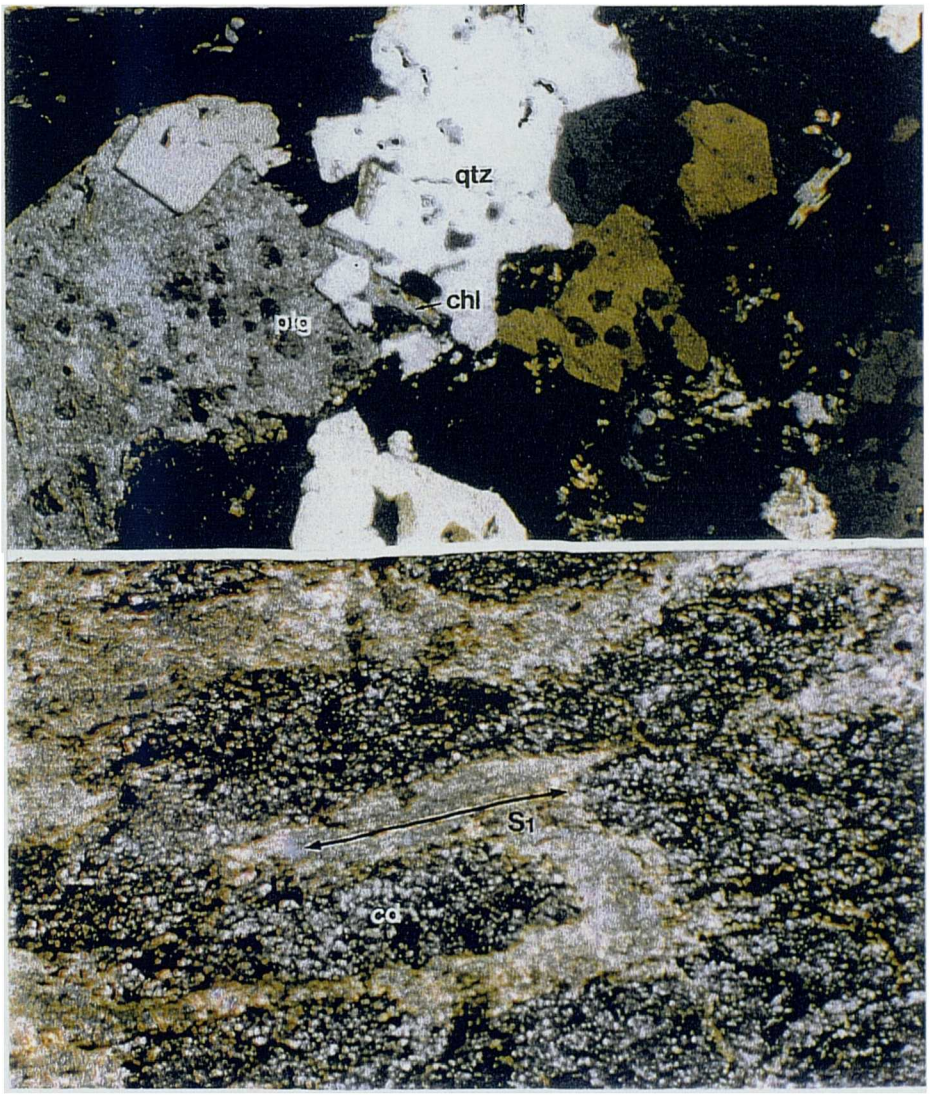

Plate 4.1 (a) Lands End Granite (x2, XPL). Note the presence of chlorite with zircon haloes suggesting its genesis as a biotite and subsequent alteration. (b) Mylor Slates, Tavis Vor (x2, XPL). Note mottled cordierite spots flattened into slaty S1 cleavage.

The Mylor slates between Mousehole and Roskilley [SW 4697 2608 - SW 4713 2721] are indurated and spotted, preserving a slaty foliation which obliterates bedding and is itself crenulated by a later foliation.

The spots comprise masses of muscovite, chlorite and talc, probably derived from the breakdown of cordierite. The altered cordierite pseudomorphs are flattened within the main foliation (Plate 4.1b) and contain aligned inclusions which suggest that they formed during a phase of applied tectonic (or magmatic) stress. Late upright crenulations at Roskilley are defined by needles of chloritoid.

Non-coaxial shear is evident along the dominant foliation in a set of sub-millimetric σ-porphyroclasts formed from recrystallised quartz masses. The clast-tail asymmetry suggests an eastwards sense of shear, down the foliation in an extensional sense. A moderately southwest-dipping crenulation cleavage is axial planar to minor drag folds, and is consistently cross-cut by steep north-dipping kink-bands.

4.2.2 Penzance to Cudden Point

Lithology

Mylor slates and sub-concordant metabasite bodies are exposed between Marazion and Cudden Point. The slates are grey-green to black in colour and contain thin partings of pale siltstone or fine sandstone which display metamorphic spots which appear to be pseudomorphs after andalusite (Plate 4.2). Olistostromic breccias are present at Stackhouse Cove [SW 547 283], where sheared lenses of sandstone, spilitic metabasite and siltstone occur within a dark grey slaty matrix. Pillow lavas are exposed at Temis Cove [SW 535 293] and between St. Michael's Mount and Marazion [SW 5165 3014], whilst metadolerite sills crop out at Maen-du Point [SW 5362 2911].

Granitic magmatism is restricted to a minor, steep-sided leucogranite body on the southern foreshore of St. Michael's Mount [SW 514 298] and an elvan dyke running inland from Little London [SW 5277 3028]. The St. Michael's Mount granite is cut by thin (<0.25 m) quartz veins with greisenised margins which extend into the slates for approximately 20 metres bearing of 060°-080°. Greisen mineralisation constitutes the main granite constituent minerals plus topaz, beryl, apatite and a number of polymetallic sulphides. Such minerals are typically formed during hydrothermal fluid-release into a joint system during volatile release from the cooling granites (Goode and Taylor 1988).

Compressional features

Bedding and primary cleavage are extremely variable in the foreshore between Marazion and Cudden Point due to the superposition of several phases of compressional and extensional deformation, and bedding is often difficult to distinguish due to the pervasive nature of S1 cleavage. The cleavage generally dips shallowly west, but dips moderately to steeply southeast in the inverted limbs of northwest-vergent F2 folds at Little London (Plate 4.2; Figure 4.5A). S2 dips moderately north, axial planar to downward-facing F2

flexures. The L1 intersection lineation plunges shallowly north-northeast, south-southwest or west-northwest due to F2 refolding.

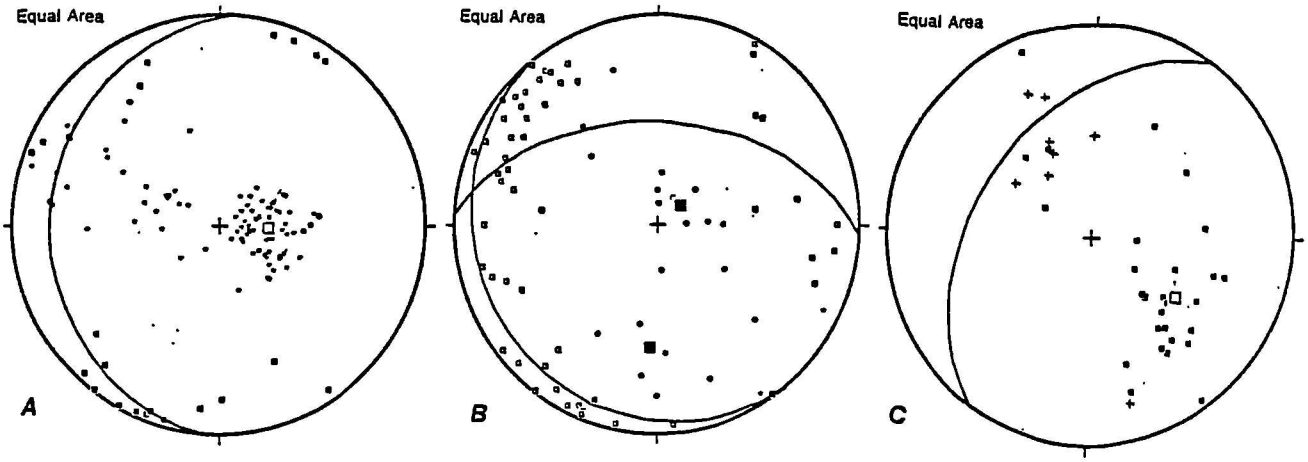

Figure 4.5 Stereoplots of structural orientation data for section 4.2.2; Penzance to Cudden Point. (A) Compressional structure (• S0 (6); • S1 (87); ▪ L1 (22); *mean compressional foliation* 183/19 W). (B) Extensional fabric elements (• S3 (20); ▫ L3 (51); • kink axial plane (2); ▪ kink axis (2); *mean extensional fabric* 093/46 N, 146/11 SW). (C) Faults and slickenlines (▪ normal fault (30); + normal slickenlines (8); *mean fault-plane* 034/43 W).

Plate 4.2 Interpreted photograph of main structural elements exposed in the foreshore at Little London [SW 5271 3042]. F1 isoclinal fold hinges indicated by lines with single dots, z- F2 fold traced are defined by lines with double dots, and the overprinting S3 crenulation cleavage is denoted by closely spaced lines.

In metadolerite bodies between Treknow Cove and Perran Sands [SW 5305 2992 - SW 5400 2918], a crude foliation is developed which encloses undeformed augen. The foliation is parallel to the S1 foliation and hence appears to be D1 in age. Rafts of slate preserved within the metabasites show an intense slaty S1 cleavage which is parallel to bedding.

To the east of Perran Sands the dip of S1 fabric swings from east to southeast and contains a spaced east-northeast trending intersection lineation related to D2 deformation. This change in orientation corresponds to an increase in the magnitude of D2 deformation. In Trevean Cove, S0 and S1 dip moderately northwest, again defining the inverted limb of a moderate-scale F2 fold. The southeastern end of the section is characterised by a shallowly west to southwest dipping S0/1 composite fabric with occasional isoclinal hinges retained. The fabric contains σ-porphyroclasts formed from disrupted quartz veins which suggest that north-directed shear has disrupted the fabric. D2 strains may thus be concentrated into the transposition fabric (Figure 4.6).

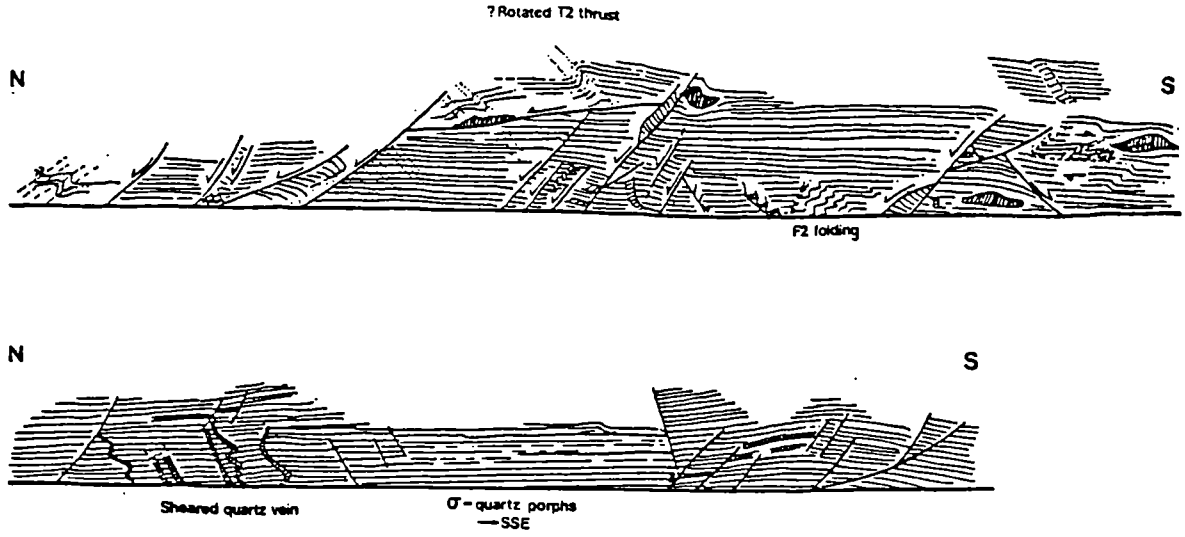

Figure 4.6 Sketch section of the cliffs at Stackhouse Cove [SW 5493 2845]. Subhorizontal composite S0/1 foliation is locally folded about north-vergent F2 folds or cross-cut by a moderately south-dipping S2 pressure solution fabric. Extension is recorded by southeast-dipping domino-faults and porphyroclasts within the main foliation, and by later moderate to steep northwest-dipping normal faults.

Extensional features

Extensional deformation (local D3 phase) is recorded by a shallow south- or north- dipping foliation which crenulates D1 and D2 structure (Plate 4.2). In areas of most intense S3 development, minor south-vergent F3 folds are seen. Such folds are seen at Top Tieb breakwater, in a region of southeast-dipping S0/1 fabrics, their down-dip vergence and geometries suggesting that the folds were generated through vertical compression. L3 crenulation lineations plunge shallowly northwest, southeast or south-southwest. Shallowly-dipping detachments are sometimes present, and hence the folds may have formed through drag on an obscured movement plane.

Southeast-dipping D3 shear-zones are developed at the southeast end of Basore Point and on the eastern side of Perran Sands [SW 5316 2941, SW 5411 2918], in which bookshelf structures and asymmetric folds of S0/1 fabric show a consistent downdip shear-sense. These extensional packages reactivate the contacts between metadolerite and slate, utilising planes of highest rheological contrast. Southeast-dipping detachments and shear-zones are subordinate to a group of moderately northwest-dipping fault-planes developed in both metabasites and slates (Figure 4.5C). These structures truncate shallowly-dipping normal faults and shear-zones and hence appear to postdate them.

The magnitude of extension appears to drop at the southeastern extent of the section. Semi-ductile non-coaxial shear is recorded in weak crenulation and occasional kinking of the S1 slaty cleavage. Southeast-vergent folds occur only in the immediate hanging wall of moderately south-dipping normal faults. These faults may accommodate large displacements as marker beds are not duplicated within the cliff-face.

Thin section analysis

Mylor Slate samples taken at Top Tieb Rocks [SW 5208 3050], East Perran Sands [SW 5413 2904] and West Trevean Cove [SW 5441 2873] all show an intense slaty cleavage (muscovite ± chlorite) parallel to compositional bands of silt-grade quartz-grains which sometimes form isoclinal closures (Plate 4.3a). Phyllitic samples taken close to the St Michael's Mount granite are intensely spotted with cordierite blasts. The spots are flattened along the main foliation, their long axes lying parallel to the pervasive crenulation lineation. The three-dimensional form of the spots appears to be controlled by mimetic growth along pre-existing fabrics rather than through deformation of cordierite spheres. A second compressive phase is recorded in siltstones and slates from West Trevean Cove [SW 5441 2873] and Stackhouse Cove [SW 5491 2824], with siltstone bands forming σ-porphyroclasts with top-to-the-east-northeast shear asymmetry, up the main cleavage during D2 compression.

The extension deformation event is recorded by crenulations normal to the primary cleavage and axial planar to centimeter-scale folds of the local S1 fabric. Thin quartz veins are developed parallel the main fabric (Plate 4.3a) and enclose siltstone boudins, indicating that the matrix was deformed by layer-normal compressional strains and layer attenuation. Fibrous veins of intergrown phengite, muscovite, chlorite and calcite are sometimes present and appear to be the latest features to have developed (Plate 4.3c).

Metadolerite samples taken at Top Tieb [SW 5260 3038] and Cudden Point [SW 5488 2750] have a plagioclase +quartz + chlorite + opaques ± actinolite ± muscovite assemblage. Chlorite and actinolite occur as rosette-like growths and appear to overprint an ophitic clinopyroxene texture. Opaque minerals are pulled apart and cemented by chlorite. The micas show no preferred orientation, but fibres are sometimes kinked.

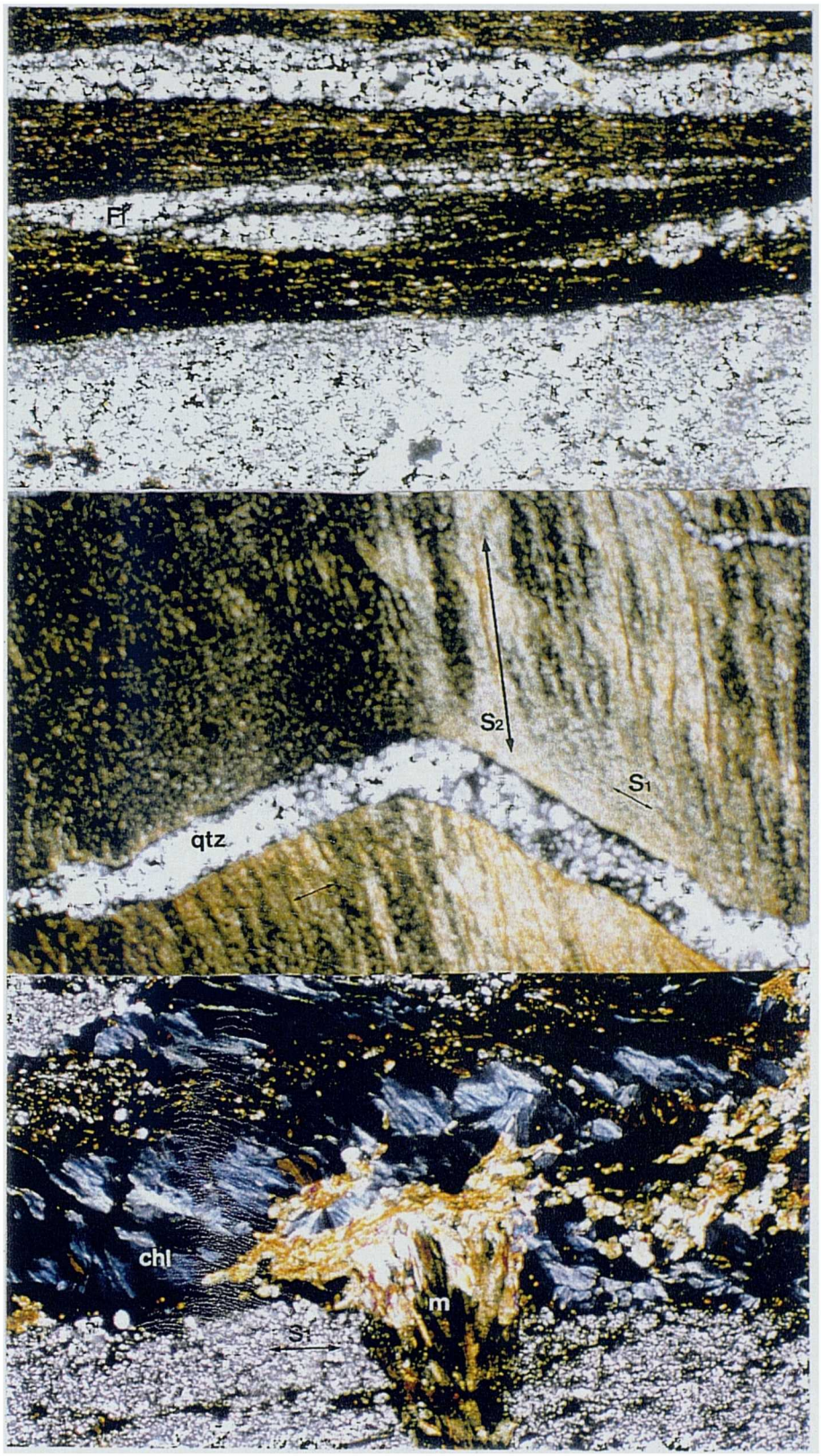

Plate 4.3 (a) Silty Mylor Slate, Samson Cove (x2, XPL). Quartz-rich bands preserve rootless isoclinal fold closures (F1) showing the intensity of bulk deformation regionally. (b) Section of crenulated Mylor Slate, Marazion (x2, XPL). Primary foliation is crenulated about asymmetric microfolds defined in V1 quartz-veins. This style of deformation is typical of the extensional phase in this area. (c) Chlorite-muscovite veins in Mylor Slates, Perranuthnoe (x4, XPL). Such minerals locally make up a moderate proportion of the rock and demostrate the abundance of fluids following the emplacement of the granites.

4.2.3 Piskie's Cove to Trewavas Head

Lithology

The Mylor Slate Formation in this area comprises black, grey and grey-green slates with thin siltstone partings. Bands of sedimentary breccia are present at Bessy's Cove [SW 5561 2791] and at the western end of Keneggy Sands [SW 5592 2809]. Siltstone, fine sandstone and metabasic clasts are enclosed within a muddy matrix, attesting to periodic soft-sediment deformation (Goode and Taylor 1988).

The proportion of metabasite intruding the Mylor Slate Formation is much lower than seen previously (Figure 4.2), with only minor bodies exposed at Piskie's Cove [SW 5542 2775] and a thicker metadolerite sheet in the backshore at the western end of Keneggy Sands [SW 5598 2813]. Cordierite spotting is seen adjacent to metadolerite bodies, indicating that the spots may relate either to the intrusion of the basic bodies, or to contact metamorphism associated with granite intrusion with their distribution reflecting differences in rock geochemistry rather than metamorphic grade.

The intensity of quartz veining is variable across the section. In Piskie's Cove, thin quartz-veins in groups less than a metre thick are concordant with the gently west-dipping foliation. Mineralised lodes are present at Keneggy Sands, where steep southwest-dipping quartz-sphalerite veins form composite bands several metres wide. At Sydney Cove [SW 5738 2802], northwest-southeast striking steep veins cross-cut earlier generations of vein which are folded and attenuated into pods and porphyroclasts.

A granitic dyke several metres wide crops out at Sydney Cove. The feldspar phenocrysts define a strong northwest-southeast trending fabric indicative of magmatic flow rather than tectonic strain. The adjacent slates are indurated and have shiny cleavage planes and prominent weathered cordierite spots.

The Tregonning Godolphin Granite crops out to the east of Praa Sands [SW 585 275], and forms smooth orange-weathering outcrops of a muscovite-rich phenocrystic two-mica granitoid. A shallowly south- to southwest- dipping fabric is defined by variations in grain-size and mineralogy which represent crystallisation fronts between different pulses of magma. Close to the granite-slate contact, the granite fabric parallels S2 cleavage within the slates, whilst away from the contact the magmatic fabric is diffuse and often folded due to magmatic processes.

The roof-zone of the intrusion, exposed at Porthcew [SX 5923 2697], is characterised by a very strong igneous foliation. Marginal pegmatites increase in frequency toward the contact and record late decompression of the stock. Stoped blocks of slate containing at least two foliations are infrequently seen and confirm that the granite was emplaced after the main fabric forming events (compressional and extensional). Immediately above the pluton, the Mylor slates are hornfelsed and spotted with andalusite

blasts, becoming black and glassy within the immediate vicinity of the contact. They are intensely strained by a flaggy, subhorizontal foliation which postdates the S1 slaty cleavage retained in siltstone pods.

Compressional features

A west-dipping, S1 slaty foliation is present to the east of Cudden Point, containing a southwest-plunging L1 intersection lineation (Figure 4.7A; Plate 4.4). Evidence of F1 folding is seen where thin sandstone beds are present (e.g. Sydney Cove) or are inferred from changes in vergence of rootless fold closures within siltstone beds. The dominant fabric is locally a shallowly dipping S2 pressure solution cleavage, with bedding and S1 cleavage picked out by steeply south-dipping planes within lithons. The deformation chronology is clearly seen at the cliff-foot of Little Castle [SW 5624 2791], where a downward- (north) facing F1 synform with axial planar S1 is transected by the S2 cleavage (Plate 4.5). F2 folding of V1 veins here are anomalous, verging to the southeast and thus suggesting that they lie in the inverted limb of a larger D2 structure. Quartz-veins are focused into areas of F2 fold development, locating the positions of D2 fluid conduits (thrust-planes?).

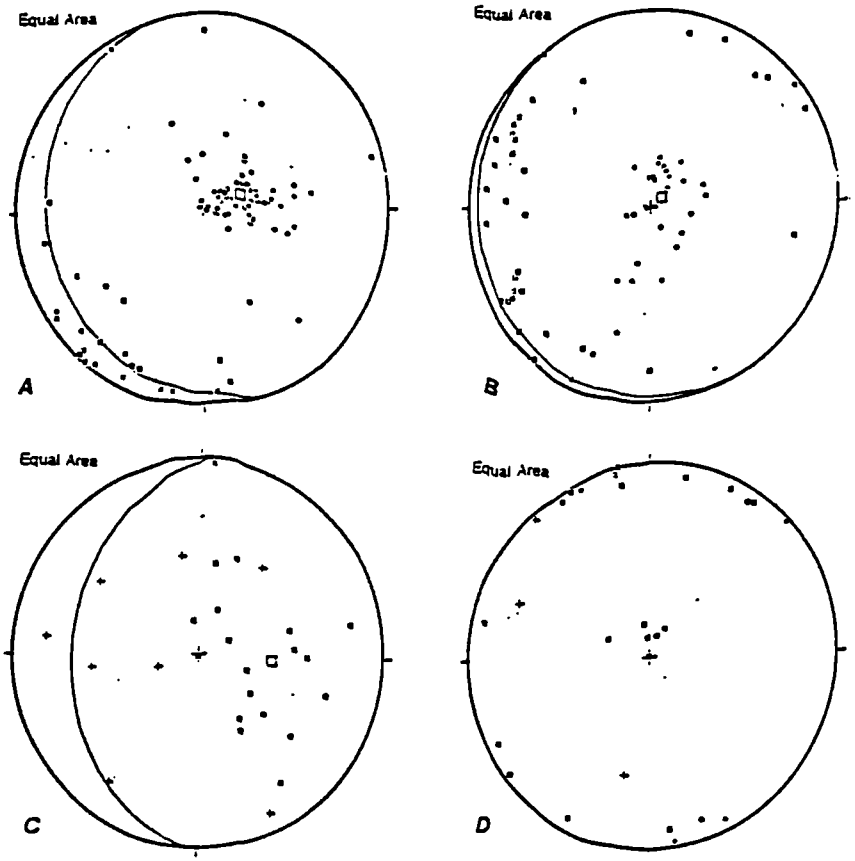

Figure 4.7 Stereoplots of structural orientation data for section 4.2.3; Piskie's Cove to Trewavas Head. (A) Compressional structure (• S0 (2); ○ S0/1/2 (69); ▪ L1/2 (25); *mean compressional foliation* 161/17 W). (B) Extensional fabric elements (• S3 (30); ▫ L3 (34); • kink axial plane (1); ▪ kink axis (4); *mean extensional fabric* 146/6 W). (C) Faults and slickenlines (▪ normal fault (19); + normal slickenlines (8); *mean fault-plane* 183/32 W). (D) Miscellaneous/late structure (• S4 (5); + L4 (3); • vein (10); ▪ joint (6); ○ igneous foliation (14)).

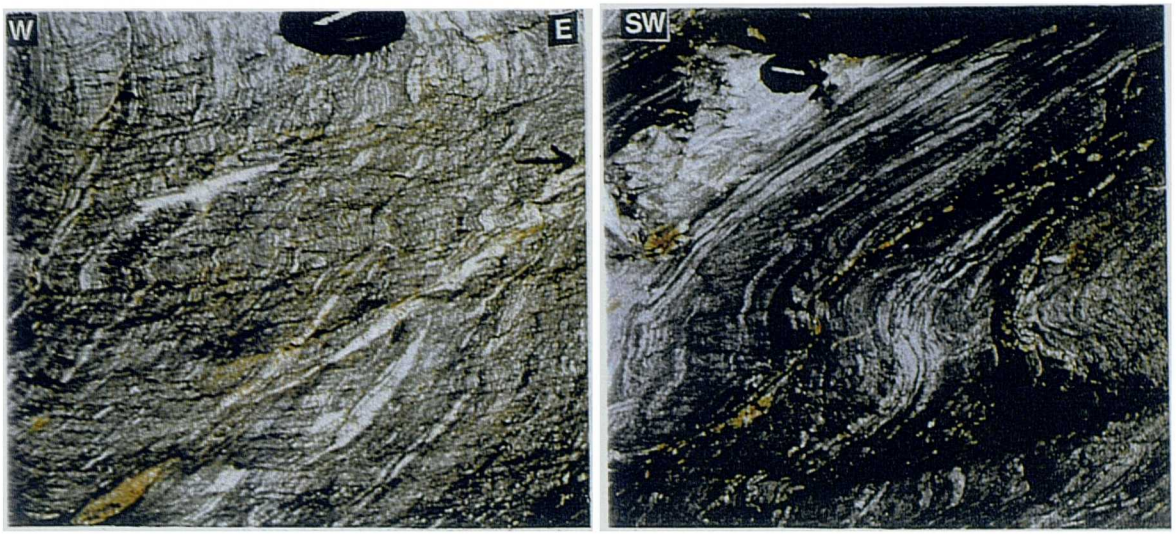

Plate 4.4 Compressional deformation elements, Bessy's Cove. (a) Subhorizontal pressure solution S2 cutting a steeply west-dipping composite S0/1 fabric in olistolithic breccias. (b) F2 z-fold.

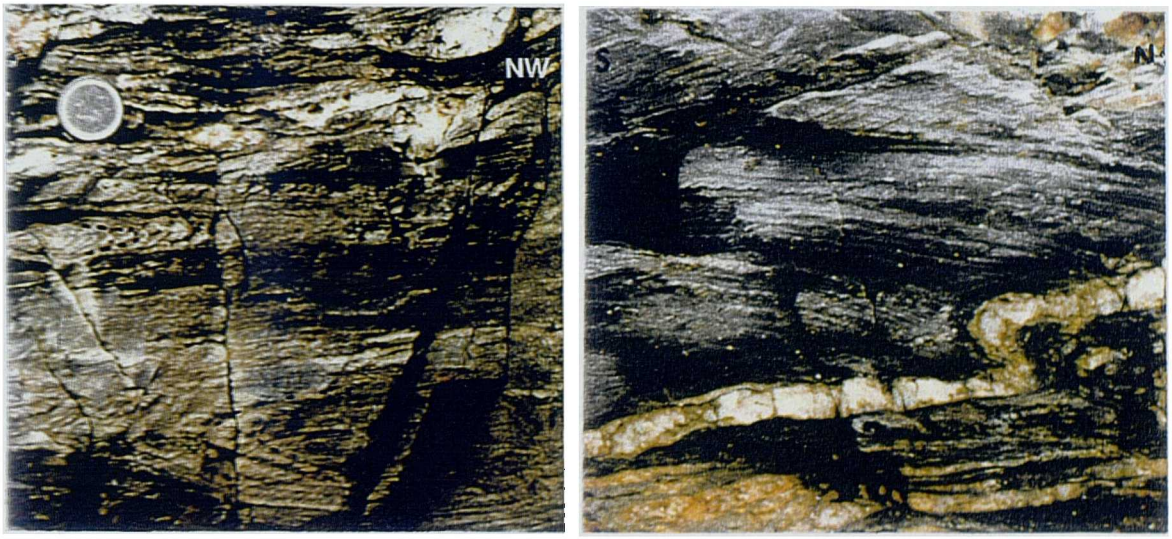

Plate 4.5 Structural elements, Little Castle. (a) Preserved recumbent F1 isocline (lower right), with partial transposition by a pressure solution S2 fabric (apparent shallow southeast-dip). (b) South-vergent F2 fold in V1 quartz vein.

The roof pendant of Mylor Slates exposed at Porthcew show similar structural elements to those of Little Castle, with an intense flat-lying foliation reflecting intense strains above the granite body. The S2 fabric generally dips shallowly to the west, cutting the hinges of tight recumbent F2 folds and transposing earlier structures in discrete bands. Bedding and S1 foliation are subparallel and dip towards the northwest, west or southwest according to the position within F2 folds.

Extensional features

An S3 crenulation cleavage is patchily developed across the area and dips toward the south, east or southwest. The variation in S3 orientation reflects very complex changes in kinematics across a small distance. At Prussia Cove [SW 557 279], F3 folds verge both to the southeast and northwest, their orientations affected an east trending D4 fabric (Figure 4.7). Late (post-D3) kink-bands and σ-porphyroclasts formed from V1 vein-quartz show southeast directed non-coaxial shear within the S2 fabric. Normal faulting is restricted to late conjugate planes which dip both northwest and southeast and is related to a phase of east trending tensile quartz-vein development.

At the western end of Praa Sands [SW 5738 3813], extension is directed towards the northwest as demonstrated by S3 cleavage-vergence, σ-poprhyroclast asymmetry and minor fold vergence within the S2 fabric. D3 strain is again low, but intensifies into zones of quartz-veining. At Porthcew, F3 folds verge south to southeast and are developed above shallowly southeast-dipping normal faults. North-directed D3 deformation overprints the low-angle structures and is seen in domino-faulting and brittle normal faulting. Granite emplacement must postdate the later faulting episode as a steep granite dyke exploits the fault close to the contact.

Thin section analysis

Samples of Mylor slate were collected at Little Castle [SW 5726 2802], Bessy's Cove [SW 5572 2791] and Keneggy Sands [SW 5604 2818], providing sections ranging from slates with thin siltstone stringers to fine sandstones and slumped beds. They typically show a quartz, muscovite and opaque-mineral assemblage with varying amounts of biotite. Cordierite spotting is developed at Little Castle in rocks adjacent to the elvan, and secondary chlorite vein-fill is present.

The style of microfabrics reflects differing rheologies and variations in strain magnitude. Where lithologies are competent and strain is low, bedding and crossbed-foresets are preserved in fine sandstones (e.g. Bessy's Cove), whilst weak rheologies and zones of high strain rarely preserve S0 which is seen as ghost traces in inter-S1 lithons (e.g. Little Castle). The dominant (S1) cleavage is slaty and composed of muscovite and/or biotite, with fine quartz-grains flattened into parallelism with the long-axes of micas. Sandstone bands have a crude pressure solution fabric defined by aligned sericite needles.

The secondary fabrics in each case are crenulation cleavages which locally form pressure solution seams. F3 microfolds produce a chevron effect in S1 cleavage in places, and develops into a discrete crenulation fabric elsewhere (Plate 4.6).

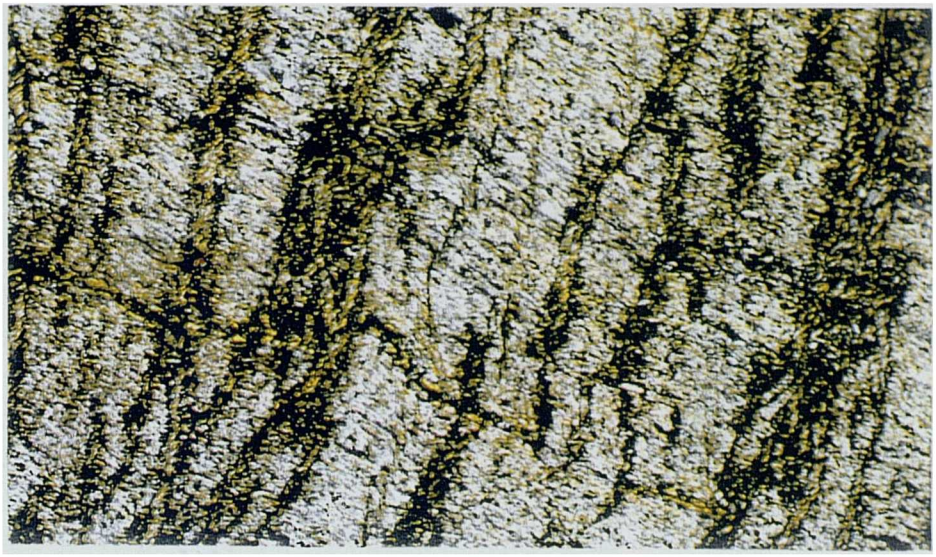

Plate 4.6 Intense development of flat-lying crenulation cleavage, Bessy's Cove (x10, XPL).

Extensional microstructures are identified in most localities, suggesting shear along the slaty or crenulation and pressure solution fabrics. At Little Castle, extension is seen on a range of scales, from cm- wavelength drag-folds verging northeast and developing an S3 pressure solution cleavage, to microscopic S-C fabrics and quartz-biotite σ-porphyroclasts which suggest top to the west shear. A pervasive S3 crenulation is seen at Bessy's Cove and Keneggy Sands, where extension appears to have occurred during a phase of sericite and chlorite growth.

Microstructures preserved in deformed quartz veins are useful indicators of the temperature conditions during deformation. Sedimentary quartz-grains display sweeping undulose extinction suggesting low-temperature deformation. Annealed textures are observed in veins adjacent to the Sydney Cove dyke, suggesting that temperatures of deformation following cessation of deformation were sufficient to allow grain-growth and reordering of grain boundaries (Hirth and Tullis 1992; static recrystallisation).

The granitic dyke exposed on the foreshore at Sydney Cove [SW 5728 2820] has a plagioclase-quartz groundmass which supports aligned sanidine phenocrysts up to 100 mm long. This mineral assemblage is typical of an alkali granite, and the strong marginal megacryst alignment suggests that it quenched very quickly (Blumenfeld and Bouchez 1988).

4.2.4 Legereath Zawn to Porthleven

Lithology

The Mylor slates, which form the bulk of this section, consist of dark-grey to brown weathering pelites containing infrequent metabasite sills up to 2 metres in thickness. Again, intense D2 strain has produced a

subhorizontal pressure solution or crenulation cleavage. Zones of F2 and F3 folding are common, as are quartz-veins of two generations. The first set predate the S2 fabric and are folded into concertina geometries through vertical compression (Plate 4.7D), whereas the second set are subhorizontal within the main foliation.

The western end of the section contains the eastern side of the Tregonning Godolphin granite with granitic to pegmatitic sills intruded along the country rock foliation (Plate 4.7A). The sills reach 3 metres in thickness and have pegmatitic margins and coarse granite cores. Flow-banding is again parallel to the contacts (Figure 4.8D). The slates are spotted within 200 metres of the main contact, and are recrystallised close to the granite sills.

Compressional features

To the east of the Tregonning Godolphin granite, the dominant dip of bedding, S1 and S2 cleavage switches to the southeast (Figure 4.8A). Close to the granite contact, the slates contain a partially transposing sub-horizontal composite S1/2 fabric which obliterates early features, but towards the southeast, this D2 overprint drops and bedding dips shallowly to the southeast. Bedding-cleavage intersection lineations show strong scatter about an anomalous east to southeast plunge which may be explained through rigid rotation of existing lineations during D2 deformation. The L2 intersection lineation plunges gently northeast.

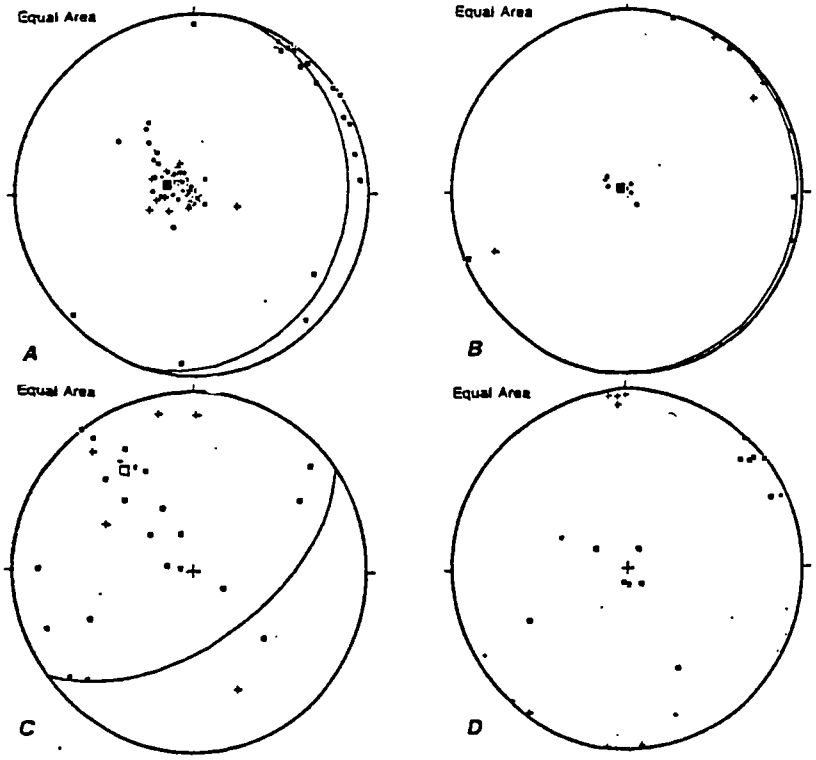

Figure 4.8 Stereoplots of structural orientation data for section 4.2.4; Legereath Zawn to Porthleven. (A) Compressional structure (• S0 (11); ○ S1/2 (36); + S2 (16); ▪ L1 (3); ▫ L1/2 (18); *mean compressional foliation* 019/14 E). (B) Extensional fabric elements (• S3 (8); ▫ L3 (5); + boudin b-axis (5); *mean extensional fabric* 018/4 E). (C) Faults and slickenlines (▪ normal fault (23); + normal slickenlines (5); *mean fault-plane* 055/57 S). (D) Miscellaneous/late structure (+ L4 (8); • vein (6); ▪ joint (7); ▫ igneous foliation (5)).

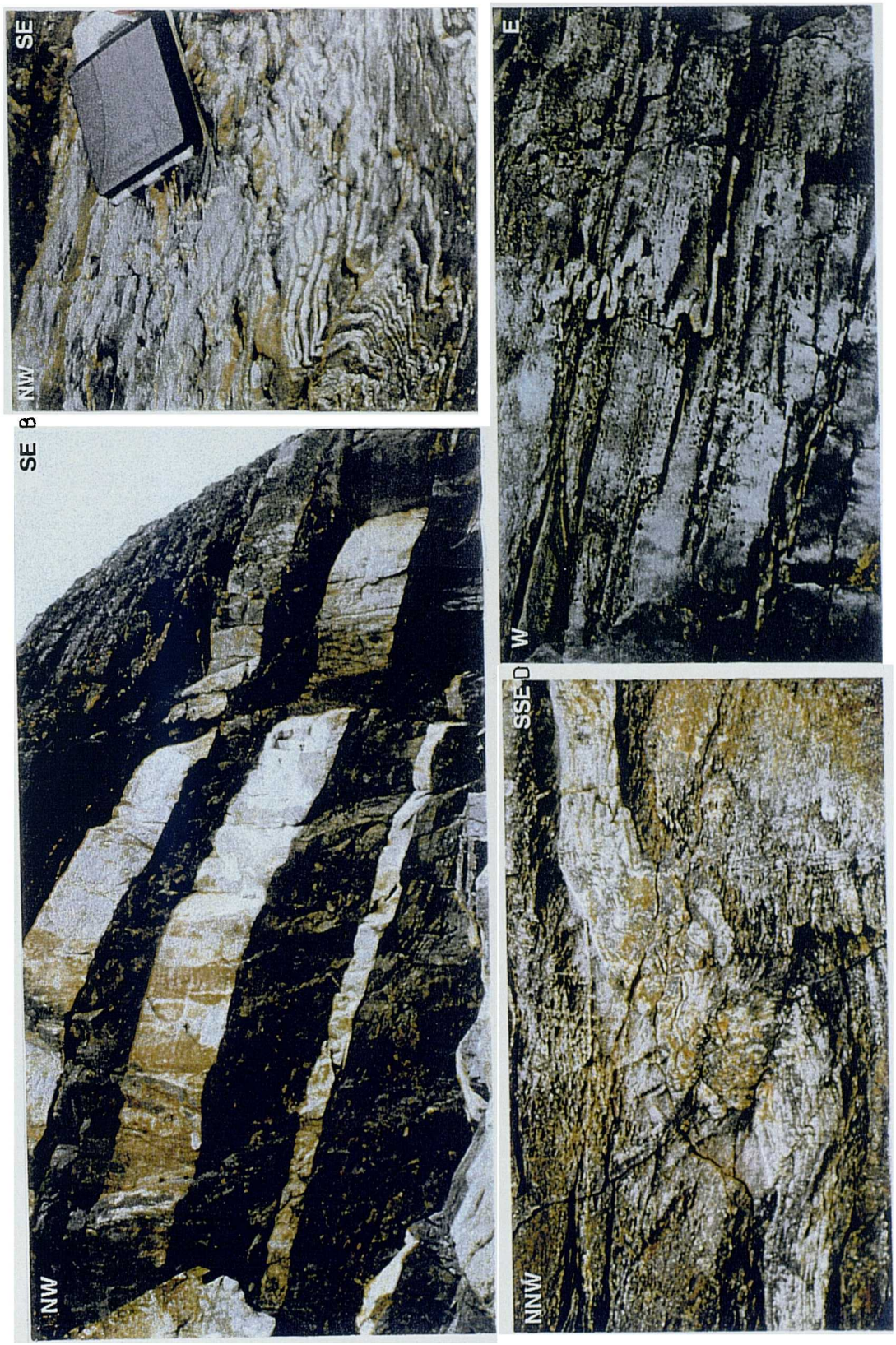

Plate 4.7 Structures exposed between Trequean Zawn and Porthleven Harbour. (A) Granite sheets lying parallel to the main foliation, Megiliggar Rocks. (B) NW-vergent F2 folds of V1 quartz veins, Tremearne Par. (C) North-vergent F2 fold distorting S1 spaced cleavage in psammitic bed and developing an S2 crenulation cleavage. (D) Vertically shortened early veins, Tremearne Par.

A phase of post-extensional east-west compression is recorded in a subvertical north-striking pressure solution fabric (S4) which is patchily developed against dextral wrench faults. The L4 intersection lineation plunges shallowly north and south (Figure 4.8D).

Extensional features

D3 deformation is sometimes seen as folds within the intense main cleavage with a northeast-plunging crenulation lineation and a flat-lying cleavage (Figure 4.8B). Indeed, the presence of non-coaxial shear-generated structures implies that the subhorizontal fabric is intimately related to extension as well as compression. Asymmetric F3 folds occur on a millimetre to decimetre scale and deform both S1 and S2 (Figure 4.9). They verge southeast and have previously been attributed by Turner (D3, 1968) and Leveridge *et al.* (D5, 1985) to the process of doming above the granite batholith. However, the focussing of folding into the hangingwalls of shallowly southeast-dipping normal detachments suggests that they are formed in response to reactivation of S1/2 fabrics and T1/2 thrusts. Towards the southeast end of the section low-angle detachments are cross-cut by steep southeast-dipping faults (Figure 4.8C).

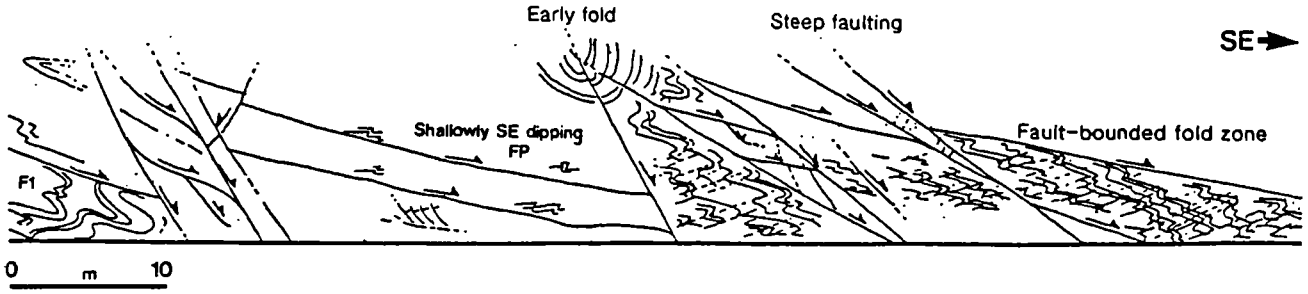

Figure 4.9 Sketch section of Breageside cliffs. Shallowly southeast-dipping normal faults with drag-folds and domino-faults in their wall-rocks are offset by steeply southeast-dipping braided later faults.

Thin section analysis

In the roof region of the Tregonning-Godolphin Granite, slaty lithologies are spotted and iron-stained. Samples from both Porthcew [SW 5928 2698] and east Trequean Zawn [SW 6071 2671] have a muscovite, quartz, clay mineral and cordierite assemblage, with minor development of chlorite. In both cases, bedding is obliterated by a slaty S1/2 foliation which is folded into cm-scale folds verging southeast. Bands of calcareous slate are also sometimes present, and show recrystallisation of calcite grains and formation of a slaty foliation.

Hornfels from the contact region are banded parallel to a pre-existing (S3) fabric of aligned biotite-muscovite laths and flattened quartz grains. Abundant biotite neocrystallisation occurs along discrete layers, whilst elsewhere a phyllonitic fabric of muscovite and to a lesser extent, chlorite is dominant (Plate 4.8). Quartz grains within the banding have slight undulose extinction and straight grain boundaries

suggesting static recrystallisation, whilst post-deformation quartz-veins show no internal strain and have straight grain boundaries.

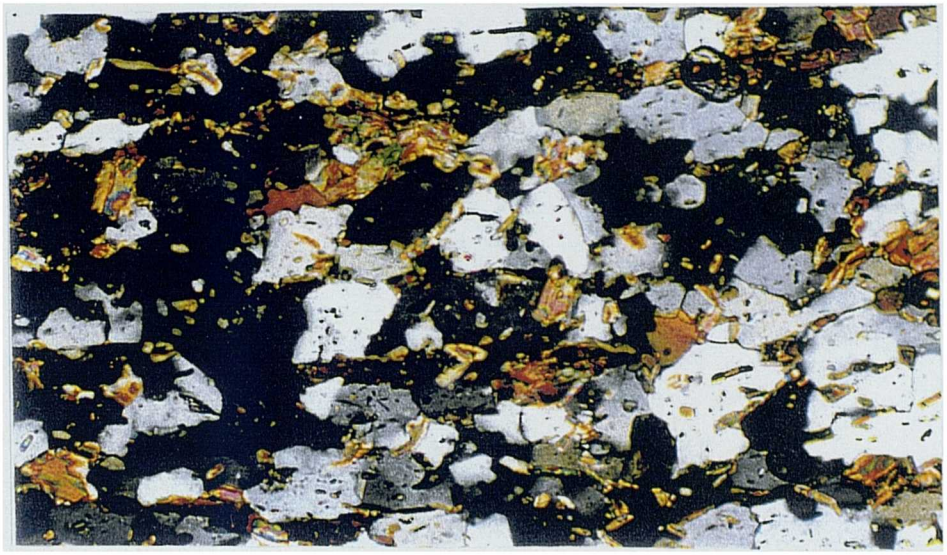

Plate 4.8 Transposed biotite-rich fabric in siltstone, Porthcew (x10, XPL).

A discrete S3 crenulation fabric is present which is associated with a phase of mica formation, overgrowing the slaty cleavage. Quartz-veins show static recrystallisation due to the regional thermal ovcerprint associated with granite emplacement. Progressing away from the granites, evidence for recovery and static recrystallisation diminishes and quartz appears more strained (i.e. shows undulose extinction).

4.2.5 East Porthleven to Gunwalloe Fishing Cove

Lithology

The beach section between Porthleven and Loe Bar [SW 6269 2544 - SW 6428 2429], exposes the southernmost part of the Mylor Slate Formation, as always comprising dark-grey slates interbedded with paler siltstones or fine sandstones. Metadolerite sheets are common within the sequence and reach ten metres thickness on the north side of Tye Rocks [SW 6313 2515]. South Tye Rocks exposes olistrostomic conglomerates of the Porthleven Breccia Member with oblate siltstone clasts. A change in sedimentary facies occurs at Caca Stull Zawn [SW 6358 2479], whereafter purple and green sandstones with a buff-weathering nature become common. The southern margin of the Mylor Slates has traditionally been placed at Loe Bar (Flett 1946), but palynological data presented by Wilkinson and Knight (1989) places the Mylor-Portscatho Boundary at Caca Stull Zawn.

Between Caca Stull Zawn and Blue Rocks [SW 2487 2322], the cliffs comprise pyritous slates, green siltstones and thin sandstone beds in roughly equal proportions corresponding to a Mylor-Portscatho

transitional group. To the southeast of Blue Rocks a typical Portscatho Group lithology comprises pyritous slates and siltstones containing groups of rusty-weathering sandstones which reach several metres in thickness at the southeastern end of the section. On the basis of chronostratigraphic evidence (Wilkinson and Knight 1989). the junctions between each lithofacies are thought to be thrusts with a north-northwest transport direction.

Compressional features

Exposed along Porthleven Sands are a range of structures which record north-northwest directed D1 compression and heterogeneous overprint of coaxial D2 strain (Figure 4.10). F1 folds exposed at Velin Gluz Rocks are fully recumbent and isoclinal, associated with an axial-planar slaty foliation (spaced pressure solution fabric in sandstones) which dips gently or moderately to the southeast, whilst an isolated F1 synform at Little Trigg Rocks [SW 6270 2539] is upright due to refolding within a large F2 monocline and is crenulated by the S3 fabric (Plate 4.9A). The S0/1 intersection lineation is seen throughout the area to plunge gently northeast or southwest. S1-parallel quartz-veining is developed locally, recording late D1 fluid outflux.

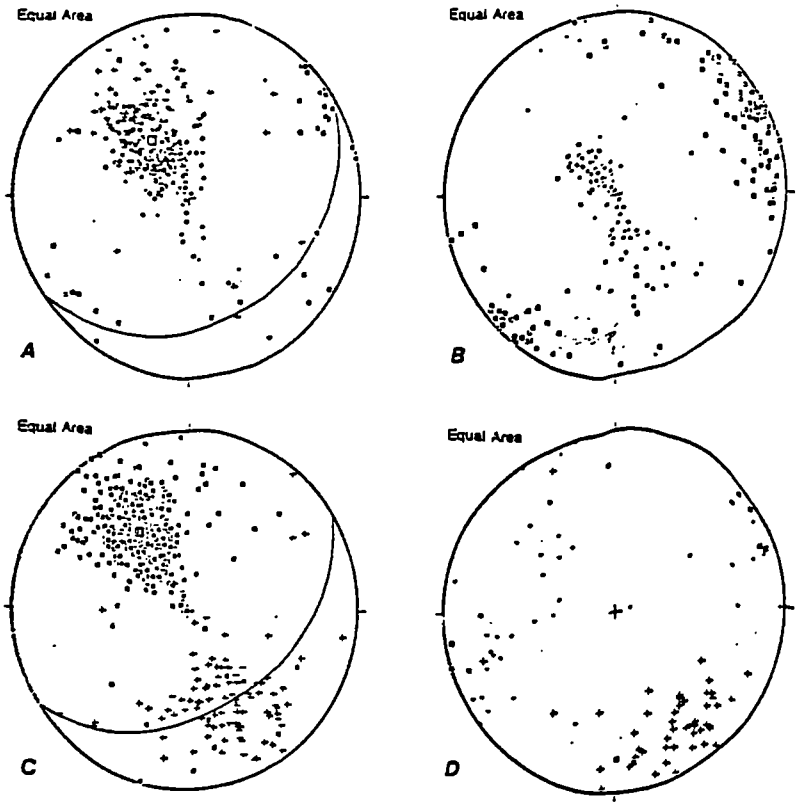

Figure 4.10 Stereoplots of structural orientation data for section 4.2.5; Porthleven to Gunwalloe. (A) Compressional structure (• S0 (78); • S1 (71); ○ S0/1 (78); + S2 (83); ▪ L1 (21); ▫ L2 (13); *mean compressional foliation* 056/31 S). (B) Extensional fabric elements (• S3 (97); ▫ L3 (120); • kink axial plane (13); • kink axis (1); + boudin b-axis (2)). (C) Faults and slickenlines (▪ normal fault (367); + normal slickenlines (94); *mean fault plane* 057/42 S). (D) Miscellaneous/late structure (• S4 (5); + L4 (47); ▫ L5 (4) • vein (35); ▪ joint (4)).

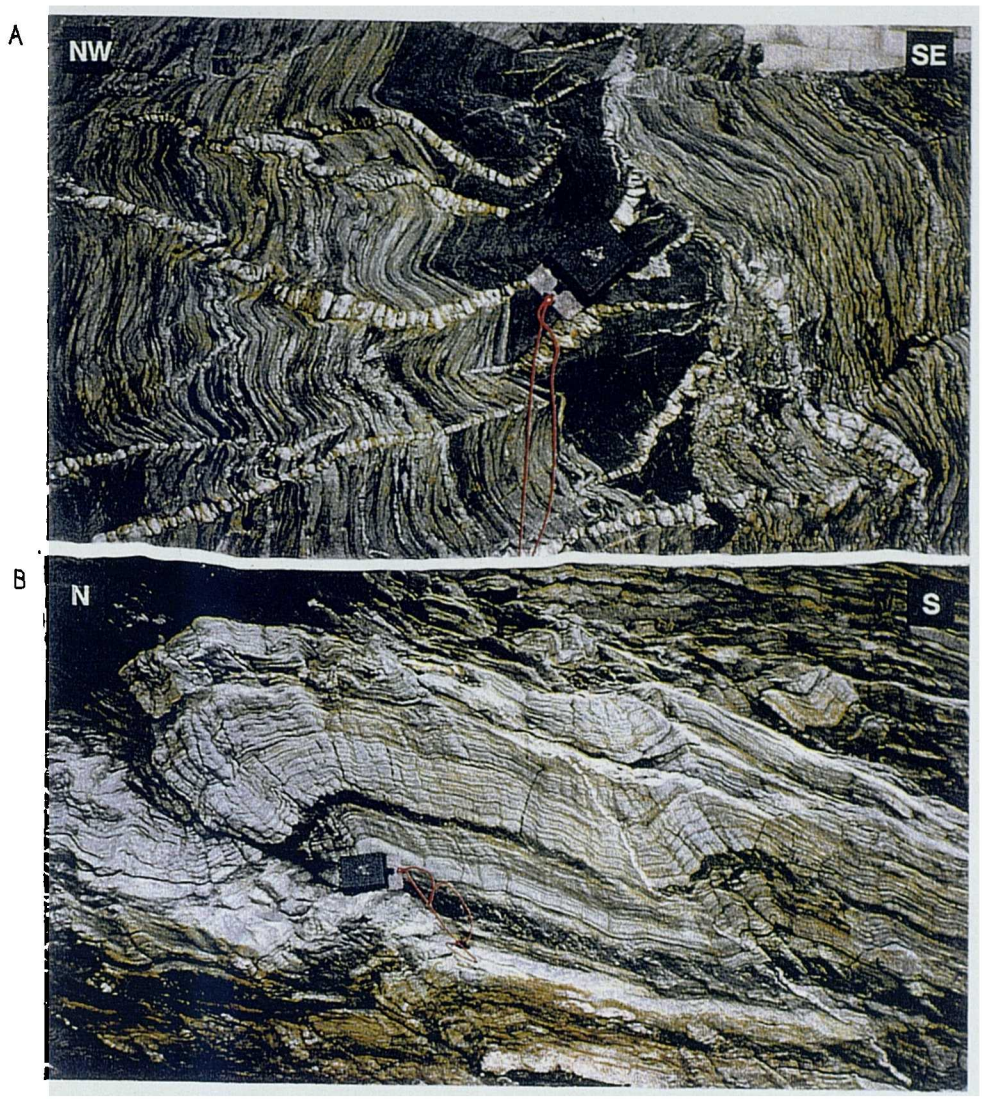

Plate 4.9 Compressive structures, Porthleven Sands. (A) F1 synform with slate core in anomalous upright orientation. V2 quartz veins and the striped S0/1 fabric are folded about subhorizontal F3 folds (verging SE in quartz veins), Little Trigg Rocks. (B) F2 monoclines and spaced S2 cleavage, Velin Gluz Rocks.

The 'Caca Stull Zawn' and 'Blue Rocks' thrusts described by Wilkinson and Knight (1989) exhibit predominantly normal kinematic indicators, consistent with interpretations of reactivation during extension. The main 'Carrick Thrust' (Leveridge *et al.* 1984) which separates the Mylor and Gramscatho Groups is not exposed but is inferred to lie beneath the beach at Loe Bar (Wilkinson and Knight 1989; Shail and Wilkinson 1994). It may be traced offshore on SWAT profiles which reveal a zone of south-southeast dipping reflectors, calculated to intersect the coastline at Porthleven Sands (Section 2.6.1; Day and Edwards 1983; Leveridge *et al.* 1984).

Where present, D2 compression is characterised by open to tight north-vergent folding of the S0/1 fabric, on scales ranging from decimeters to tens of metres. Where folding is tight it is accompanied by a spaced S2 pressure solution cleavage which dips moderately or shallowly to the southwest (Plate 4.9B). The orientation of D2 structural components is therefore similar to that of D1.

Extensional features

The beach section to the southeast of Porthleven exposes southeast to south-southeast vergent asymmetric F3 folds associated with a locally transposing pressure solution cleavage, which deform both D1 and D2 compressional features (Plate 4.10A). Shallowly to moderately southeast-dipping normal faults become increasingly common towards the southeast (Figures 4.10; 4.11; Plates 4.10 B,C). They often have curviplanar or stair-step geometries and are associated with a variety of second-order structures which include domino faults, riedel shears and drag-folds (often in the hangingwall blocks) presenting a structural assemblage which is almost identical to that of Boscastle (Section 3.3.3). All features are consistent with dip-slip displacements toward the southeast ranging from 0.01m to 10+m. The cliff height of <20 metres prevents the identification of larger displacements although such structures are likely on the basis of the intensity of second-order deformation in zones with no clear and correlatable marker bands (Shail and Wilkinson 1994).

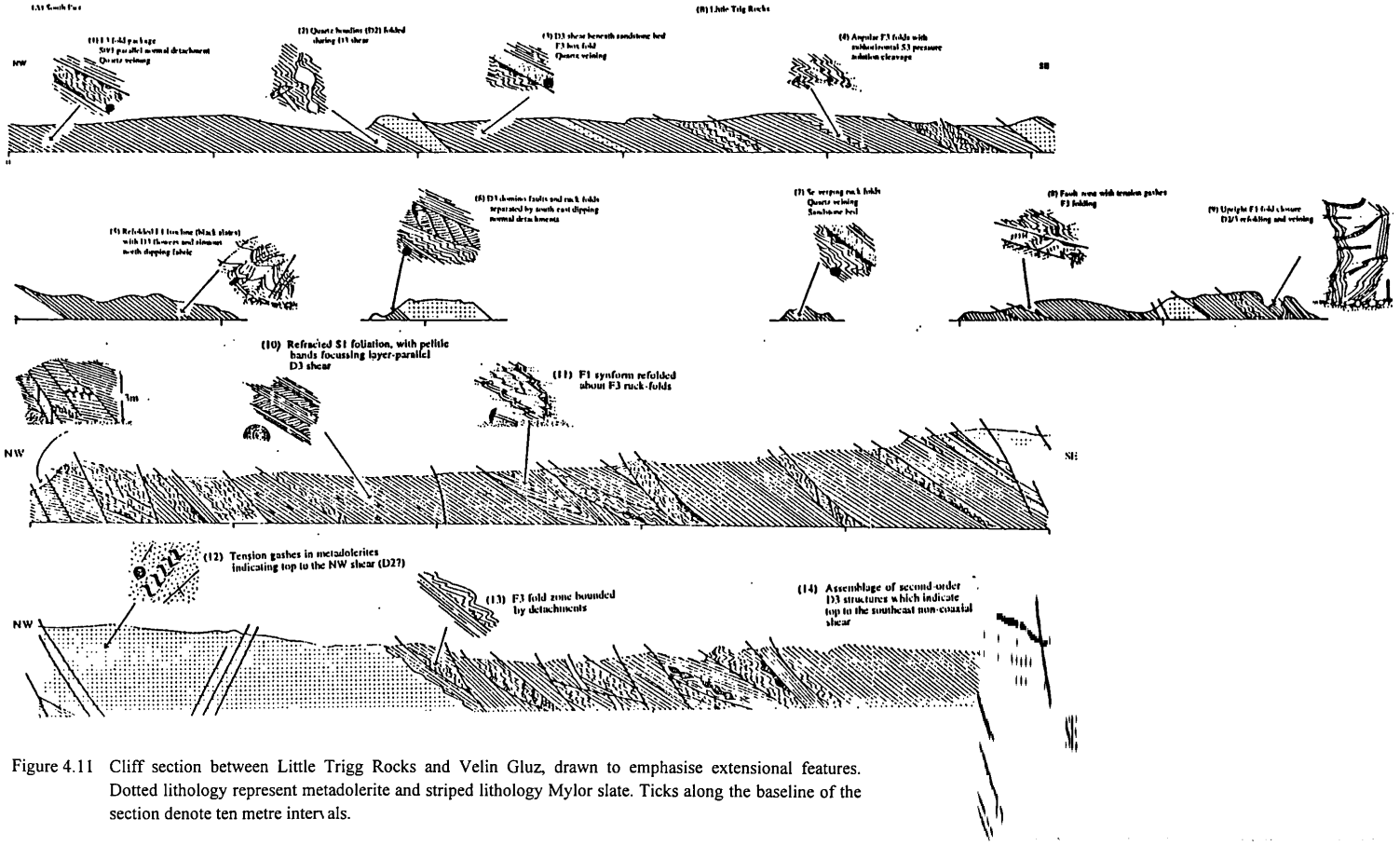

Figure 4.11 Cliff section between Little Trigg Rocks and Velin Gluz, drawn to emphasise extensional features. Dotted lithology represent metadolerite and striped lithology Mylor slate. Ticks along the baseline of the section denote ten metre intervals.

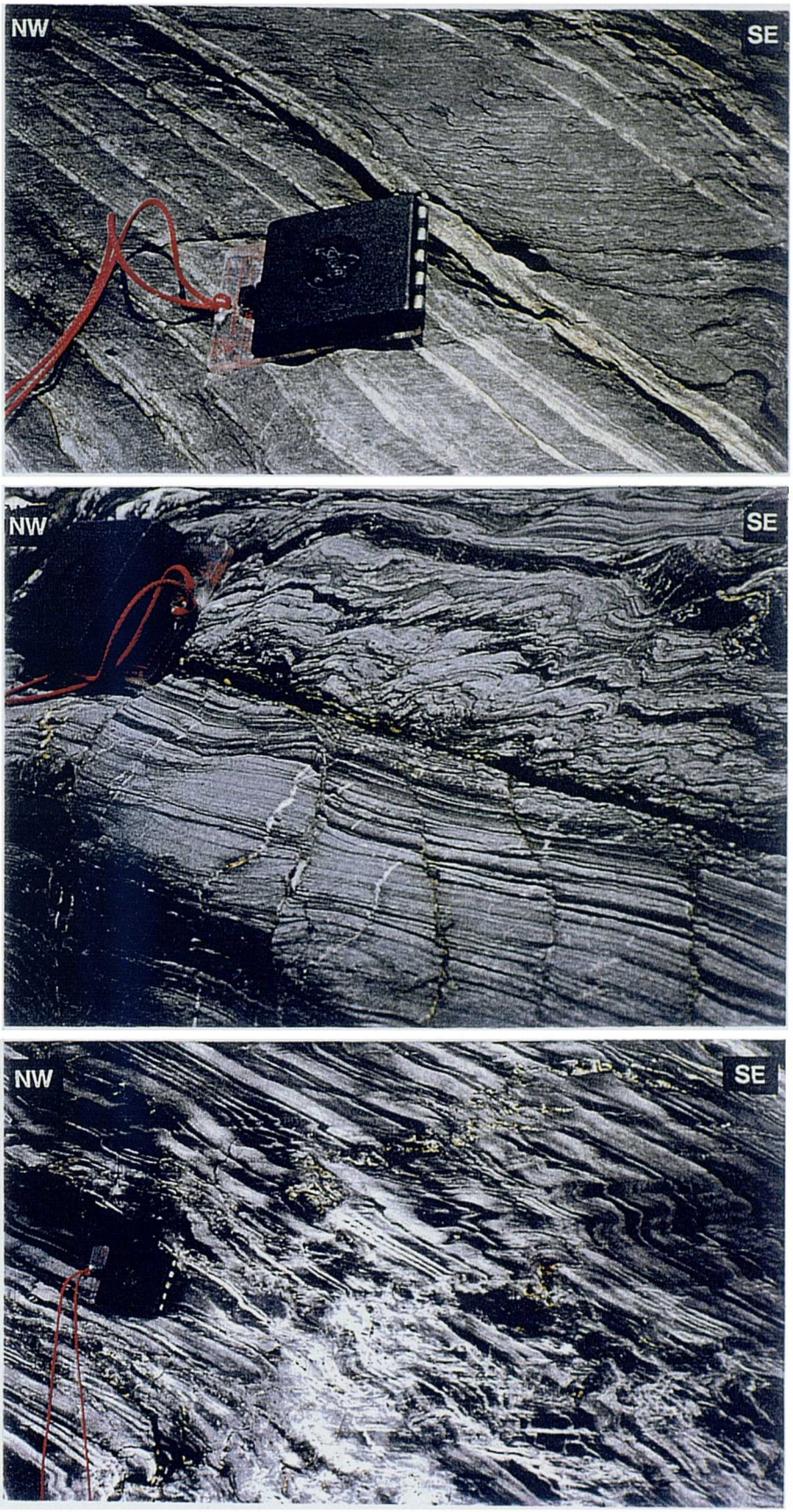

Plate 4.10 Extensional structures, Porthleven Sands. (A) S0/1 striping cross-cut by subhorizontal pressure solution S3 cleavage. (B) Chaotic folding and domino-faulting adjacent to a SSE-dipping normal detachment. (C) SE-vergent small-scale F3 folds and development of the S3 foliation.

The propagation sequence of low-angle detachments is ambiguous, with faults cross-cutting and refolding one another in a seemingly random manner. It appears that they initiated separately and became inactive during a strain-hardening process to be superceded by movement planes with lower rheological resistance. Quartz-veins are localised along movement planes within fault-zones, along the S1 foliation, or within dilational jogs. This is consistent with the presence of large volumes of fluid during deformation. Rotated rigid fault-blocks developed adjacent to faults produce dilational zones which are infilled by the influx of muds and precipitation of vein quartz.

Steep normal faults with a planar geometry occur throughout the section and again strike northeast-southwest and dip southeast. The fault-planes often contain thick quartz breccias (<2 metres) or phyllonitic gouge. Slickenlines and riedel planes indicate dip-slip to slight dextral oblique-slip movement. Such faults are normally observed to cross-cut shallowly dipping detachments. In cases where they appear to have acted as ramp structures during the earlier phase of extension, they have folds, crenulation and domino-faults in adjacent wallrocks which are in keeping with features associated with drag along detachments. Northwest to north-northwest dipping antithetic faults are developed subordinately and cross-cut southeast-dipping faults.

Exposed within the cliffs beneath Loe Bar Lodge is a moderately southeast-dipping normal fault-zone which may represent a cut-out developed during reactivation of the Carrick Thrust (Shail and Wilkinson 1994). A large number of normal faults are present in the immediate hangingwall of the Carrick Thrust (between Caca Stull Zawn and Blue Rocks), and their relationship with the thrust at depth is unknown.

North-northwest striking steep faults with dextral oblique-slip histories are locally observed, and the southeast plunge of slickenlines suggests that they were active during movement of the low-angle normal structures, perhaps acting as transfer-zones between surges in the extension magntiude along detachments. A late north-northwest striking steep cleavage transects all earlier structure (Figure 4.10D).

Thin section analysis

Specimens collected at Little Trigg Rocks [SW 6281 2537], Tye Rocks [SW 6327 2517 - SW 6324 2520] and Velin Gluz Rocks [SW 6376 2456] include banded siltstones, slates with siltstone partings, black slates and poorly sorted sandstones which are composed of quartz, muscovite, clay minerals and sometimes biotite. Within siltstones at Little Trigg Rocks and Tye Rocks, the dominant fabric is a crenulation (S2) which reorients an earlier slaty cleavage. The late crenulation fabric is transposing or forms pressure solution seams in slate bands, with the primary fabric orientation observed in low-strain pods (Plate 4.11a,b). Impure sandstones from Velin Gluz Rocks possess a crude pressure solution fabric and occasional mica fish which demonstrate top-to-the-northwest shear.

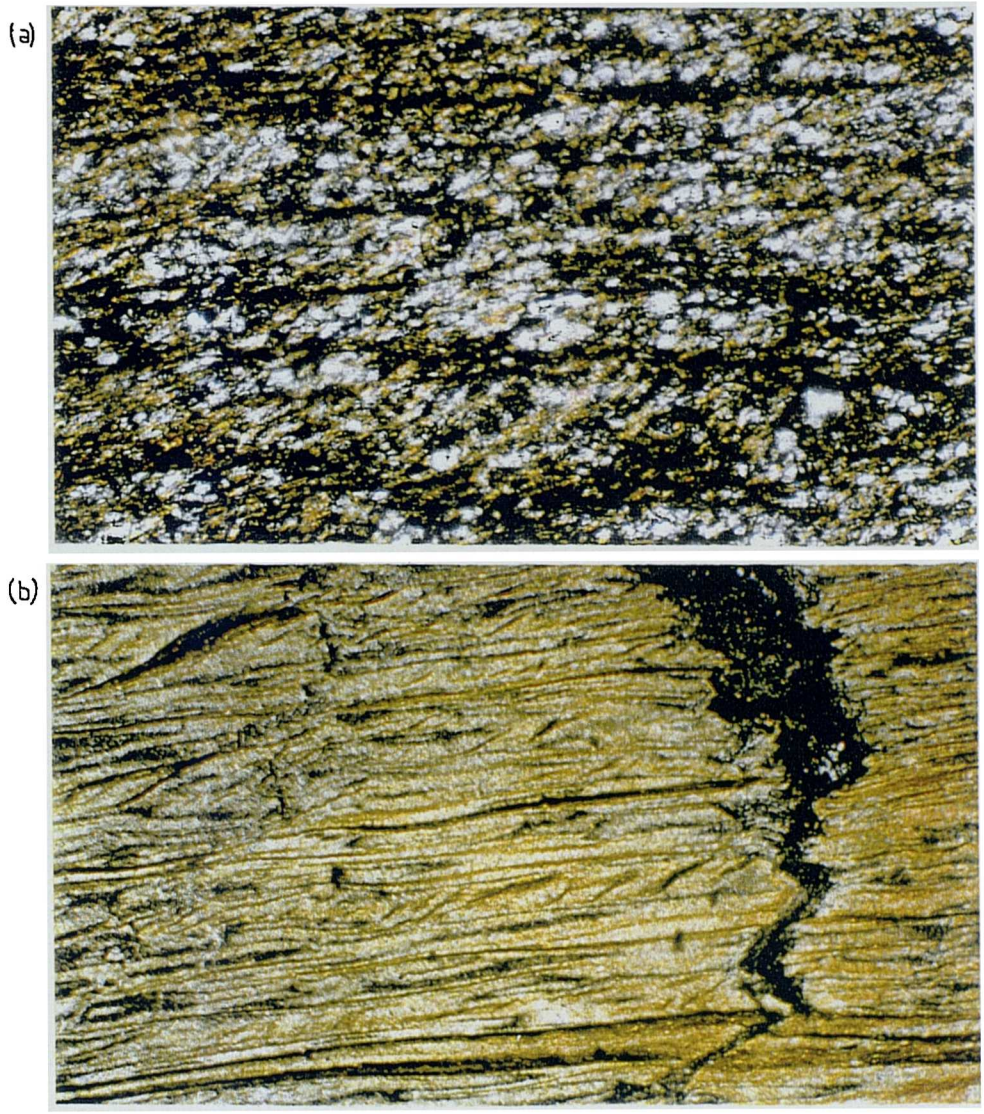

Plate 4.11 (a) Transposing S2 crenulation foliation at low-angles to relict fabric, Little Trigg Rocks (x10, XPL). (b) Sample containing three cleavages, Velin Gluz Rocks (x2, XPL)

A southeast sense of non-coaxial shear is recorded by σ- quartz porphyroclasts and asymmetric microfolds. Quartz-veins relating to D3 faulting have sweeping undulose extinction and interlobate grain boundaries, imply that grain-boundary migration recrystallisation occurred and may indicate temperatures of over 200°C during extension (Wilkinson 1990). The regional geothermal gradient during extension is likely to have been elevated if lamprophyric magmatism occurred soon after, and thus the veins are likely to have developed at depths in excess of 4 kilometers. Alternatively, the abundance of veining suggests that hydrolytic weakening of quartz may have been important during D3, and hence extension may have occurred above 4 kilometers.

At the southern end of Porthleven Sands, quartz-grains within the matrix show brittle intracrystalline fracturing and strained extinction, thus suggesting a progressive decrease in temperature throughout the extensional phase.

4.2.6 Halzephron Cliff to Church Cove

Lithology

The Portscatho Formation crops out along the coast between Portbean Cove and Church Cove [SW 6549 2205 - SW 6614 7230]. It comprises brown-weathering sandstones up to 2 metres thick interbedded with slates and siltstones similar in appearance to the Mylor Slates. The sandstones contain black plant debris at the top of beds (e.g. Gunwalloe Cove). Quartz veining is sometimes present but is generally restricted to the immediate vicinity of normal fault-planes.

Compressional features

With the change in lithology from Mylor Slate to Portscatho Sandstone, the magnitude of extension decreases and D1 structure becomes dominant. Tight to isoclinal F1 folding is common in the cliffs at Gunwalloe, Green Rock and Jangye-Ryn, and individual groups of sandstones may be traced through several closures. Bedding and cleavage thus remain near-parallel and dip moderately south-southeast whilst the L1 intersection lineation plunges shallowly east (Figure 4.12A).

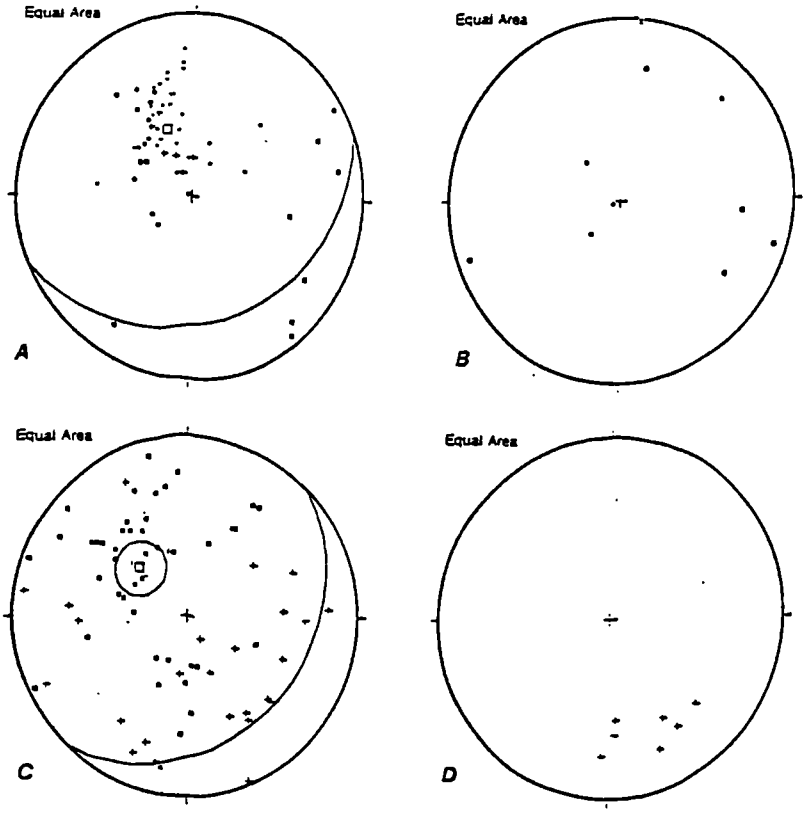

Figure 4.12 Stereoplots of structural orientation data for section 4.2.6; Halzephron Cliff to Church Cove. (A) Compressional structure (• S0 (10); • S1 (30); ○ S0/1 (6); + S2 (7); ▪ L1 (6); ▫ L2 (2); *mean compressional foliation* 068/32 S). (B) Extensional fabric elements (• S3 (3); ▫ L3 (6); • kink axial plane (1); ▪ kink axis (1)). (C) Faults and slickenlines (▪ normal fault (46); + normal slickenlines (29); *mean fault plane* 044/31 E). (D) Miscellaneous/late structure (+ L4(7)).

The foreshore and cliffs at Jangye-ryn [SW 6570 2080] reveals F1 folds developed in thick sandstones which are typical of D1 in this section (Figure 4.18x). F1 folds are tight, angular and seen to face up to the northwest, whilst the S1 cleavage is refracted between lithologies and diverges about fold closures. D2 deformation is not evident, but may relate to the development of occasional recumbent chevron refolds of long F1 limbs.

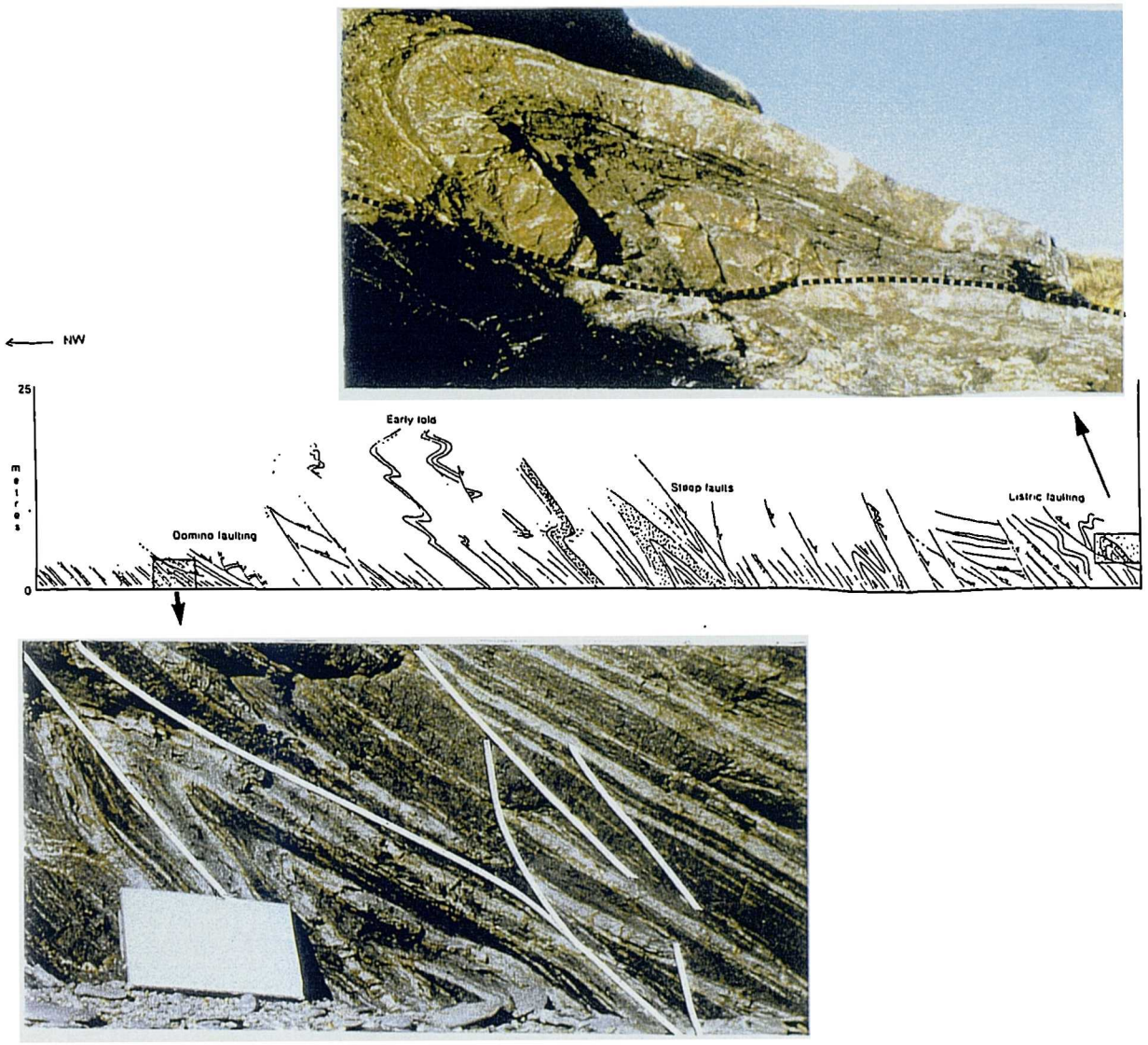

Figure 4.18x Sketch section of the cliffs at Jangye-ryn. Insets; top, NW-vergent F1 antiform overlying T1 thrust. Bottom: smaller-scale tight F1 folds with extensional system developed in normal limb.

Extensional features

Extension is restricted to southeast-dipping normal faults in this section and shows little of the semi-ductile secondary structure displayed to the northwest (Figures 4.12B,C, 4.13). The fault-planes are braided and often listric in profile, splaying into shallow flats into which southeast-dipping domino-faults sole. F3 folds are seen within fault-zones but are intensely veined and are kink-like in style. As the low-angle normal

faults are absent, it appears that pervasive extensional deformation did not extend to the southeast (hangingwall) of the Carrick *(or Blue Rocks)* thrust but rather was focussed into its footwall.

The D4 compressive phase is represented by a moderately south to southeast plunging intersection lineation (L4/0 and L4/1) and upright flexure of all other fabrics, but S4 cleavage planes are not clearly discernible. The cause of these structures is enigmatic as dextral wrench faults are not clearly developed in the section, but some late reactivation of the (locally complex) thrust stack may explain such features.

Thin section analysis

A sample of slate taken at Jangye-ryn [SW 6571 2085] has cordierite spots with pleochroic yellow haloes. The earliest fabric is an intense slaty foliation, whilst cordierites are developed as σ-porphyroblasts within a discrete crenulation at ~30° anticlockwise to the early fabric.

4.2.7 Structural summary and discussion

In common with much of south Cornwall, a four-part deformation chronology is preserved in Mount's Bay. D1 structures are tight to isoclinal and verge/face to the north or north-northwest. Axial planar to the folds, a penetrative S1 foliation dips shallowly to moderately southeast throughout. Within the Lizard Complex to the south, north-northwest verging primary sheath-folds attest to a more ductile environment during thrusting (Vearncombe 1980, Alexander and Shail 1996). Secondary folding is developed sporadically and is well demonstrated at Loe Bar [SW 645 237], where north-northwest vergent folds of the primary foliation with close to tight geometries occur with an axial-planar cleavage, often paralleled by quartz-veins. The S2 foliation also dips to the southeast but at slightly higher angle than the primary cleavage.

Extensional deformation within the bay may be subdivided into three types on the basis of style. (1) To the west of the Tregonning Godolphin Granite, extensional deformation is accommodated by shear along a flat-lying S1/2 foliation. Bedding, S1 and S2 are reorientated by tight F3 ruck-folds ranging in scale from millimetres to metres, producing a flat-lying crenulation or pressure solution overprint which locally forms the dominant fabric. In areas of low to moderate extensional strain a consistent southeast (down-dip) vergence is seen. (2) Between Porthcew and Gunwalloe, low angle detachment systems are observed close to the proposed position of the Carrick Thrust. The detachments reactivate either bedding or the S1 cleavage and are associated with intense folding and domino-faulting. (3) To the southeast of Gunwalloe, extension is largely restricted to brittle faulting which strikes east-northeast and dips east-southeast.

Steeply southeast-dipping normal faults cross-cut earlier structure at the southern end of the section, whilst north-northwest trending steep faults are exposed on the western side of Mount's Bay and host quartz, calcite, prehnite and base-metal ores (Alexander and Shail 1996). North-northwest striking steep fracture

cleavages and quartz-calcite veins with crack-seal textures are frequently observed, post-dating all other structure.

4.3 Central South Coast; Falmouth Bay, Gerrans Bay and Veryan Bay

Stratigraphy

The coastal section to the east of the Lizard Peninsular provides a continuous section through sandstones, slates, limestones, cherts and breccias which dip to the southeast but show increased faunal age in direction of dip (Figure 4.14). Field evidence suggests that the majority of the section is uninverted, leading Leveridge *et al.* (1984) to propose the existence of several major thrust-nappes; the Dodman, Veryan and Carrick Nappes (Section 2.2.3.1).

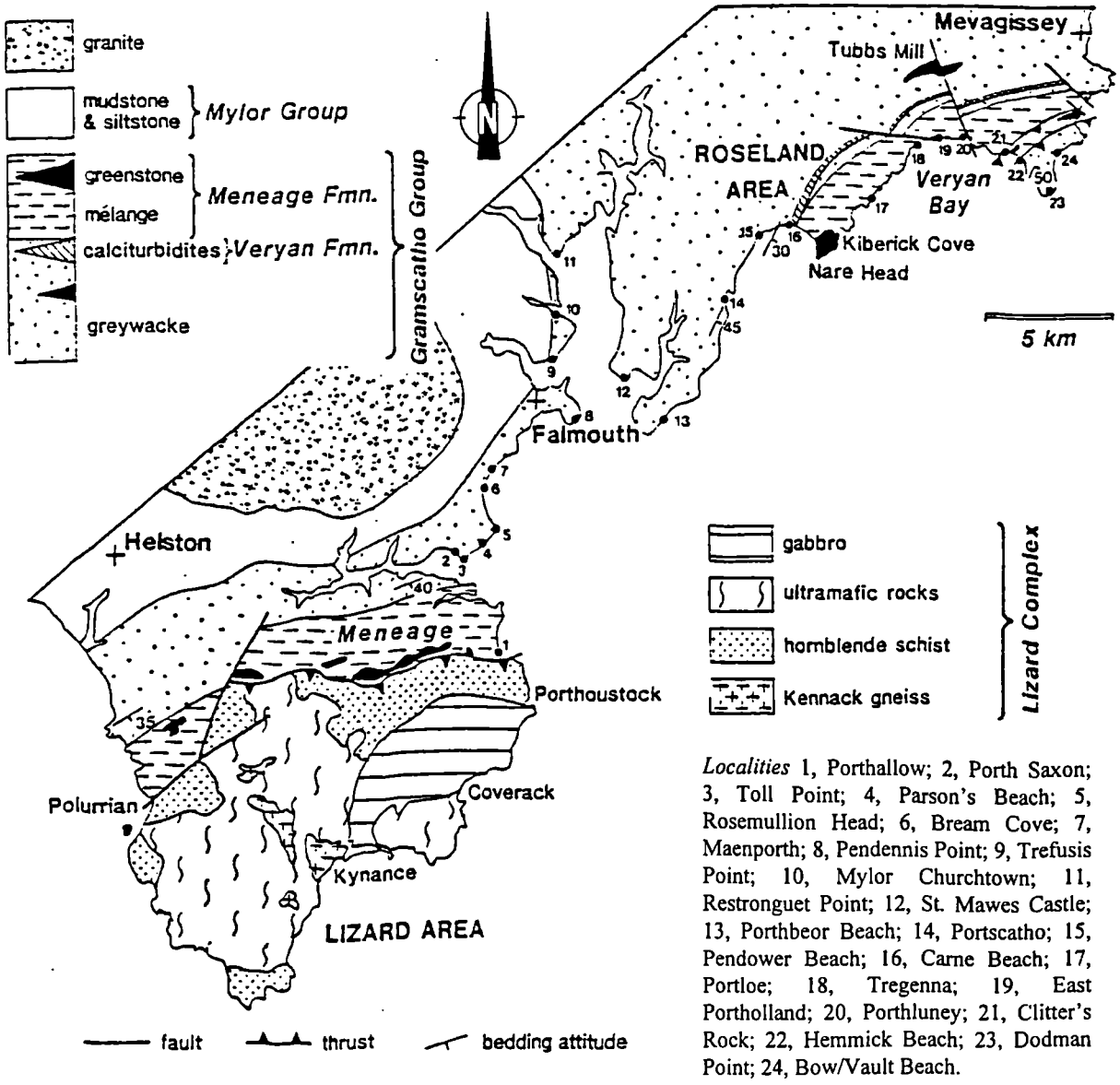

Localities 1, Porthallow; 2, Porth Saxon; 3, Toll Point; 4, Parson's Beach; 5, Rosemullion Head; 6, Bream Cove; 7, Maenporth; 8, Pendennis Point; 9, Trefusis Point; 10, Mylor Churchtown; 11, Restronguet Point; 12, St. Mawes Castle; 13, Porthbeor Beach; 14, Portscatho; 15, Pendower Beach; 16, Carne Beach; 17, Portloe; 18, Tregenna; 19, East Portholland; 20, Porthluney; 21, Clitter's Rock; 22, Hemmick Beach; 23, Dodman Point; 24, Bow/Vault Beach.

Figure 4.14 Generalised geological (and locality) map of central south Cornwall, after Holder and Leveridge (1986).

The *Dodman Phyllites* are a group of intensely veined, pale grey silty slates and phyllites which contain a strong southeast-dipping schistosity. Exposures are restricted to the south of a line drawn between Hemmick Beach [SX 995 406] and Gorran Haven [SX 014 415] across which structural style and lithology changes abruptly (Figure 2.4), marking the position of the Dodman Thrust. The thrust is seen in SWAT deep seismic lines as a prominent SSE-dipping reflector imaged to a depth of approximately 7 kilometers (Leveridge *et al.* 1984; BIRPS).

The *Veryan Nappe* is a WSW/ENE-striking sheet approximately 4 kilometers thick, bounded to the north by the curved Veryan Thrust (Figure 2.4) which is exposed at Pendower Beach [SW 898 382] and Great Perhaver Beach [SX 019 424]. The nappe comprises three formations. The Pendower Formation comprises limestones, sandstones, cherts and slates and forms the southern margin of the nappe, and is succeeded to the north by sandstones and laminar siltstones of the Carne Formation and olistolithic slates and sandstones of the Roseland Breccia Formation.

The *Carrick Nappe* forms the bulk of coastal outcrop to the west of Pendower Beach, comprising turbidites of the Portscatho Formation, similar to those exposed at Jangye-Ryn. The Portscatho sandstones form the Roseland Peninsular, the northern shore of Carrick Roads, a thin swathe along the western side of the River Fal and exposures to the south of Falmouth. The Carrick Thrust forms the base of the formation and is exposed at Pencarrow Point [SW 825 350], Trefusis Point [SW 818 334] and the northern neck of Restronguet Point [SW 811 376]. It cuts up-sequence from north to south, from the basal Porthtowan Formation to the top of the Mylor Slate Formation (the Porthleven Breccia Member). Parautochthonous units of the Mylor Slate Formation and Gramscatho Group are exposed on the western side of Carrick Roads between Falmouth and Feock.

Bulk structure

Both outcrop pattern and structural architecture reflect the action of northwest-transporting (southeast-dipping) T1 thrusts in this region. Bedding and S1 cleavage dip moderately towards the southeast in most areas, but show a strike-swing to the north of Falmouth which closely follows the inferred trace of the Carrick Thrust (Leveridge *et al.* 1984). Primary folds are tight to isoclinal and face up to the northwest, forming zone 11 in the accepted structural scheme (Section 2.3.1; Sanderson and Dearman 1973).

Second-phase deformation products are locally evident as either north-northwest vergent folds or north-northeast displacing extensional shear-bands. The two styles of deformation are observed in close association at Porthbeor Beach [SW 8611 3187], leading Alexander and Shail (1996) to suggest that they formed synchronously.

Low-angle normal faults (D3) are largely restricted to the west of the area along the trace of the Carrick Thrust, showing secondary shear-features consistent with southeast to south-southeast directed hangingwall translation. A later (D4) extensional event is typically recorded by moderately to steeply south-southeast dipping normal faults associated with hangingwall brittle folding or brecciation. The steep faults displace more shallowly-dipping D3 movement planes. Post-orogenic dextral faults are developed at Gorran Haven and on the western side of Carrick Roads (Dearman 1963).

4.3.1 Porth Saxon to Pendennis Point

Lithology

The creeks and northern shore of Helford River expose rusty brown sandstones up to two metres thick separated by buff weathering slates and laminar siltstones. A sheared, olistolithic breccia unit is exposed at Porthallack [SW 7813 2692] and to the south of Mawgan village, containing clasts of pale-grey siltstone and pyritous shale. Thick sandstones, shales and conglomerates crop out along Parson's Beach [SW 788 270], and are repeated across F1 isoclinal closures. A green-brown weathering lamprophyre dyke in the centre of the beach trends northeast-southwest, parallel to the strike of bedding.

On moving north of Rosemullion Head, sandstone beds become less numerous and slates and thin sandstones have a striped appearance. The slaty cleavage becomes more intense in the finer-grained lithology, and has a schistose lustre at Pendennis Point [SW 828 315]. A north striking lamprophyre dyke runs through the point and is offset by east-northeast trending sinistral oblique faults. The dyke is orange-weathering and has a red micaceous groundmass. The margins of the lamprophyre are brecciated and quartz-veined, suggesting that it was intruded along an active fault-plane.

Compressional features

D1 compressional structures are well preserved in the sandstone-rich, thickly-bedded lithology along the northern shore of Helford River. Isoclinal or tight F1 folds dip shallowly southeast and face up to the northwest. The S1 cleavage fans across fold closures but dips shallowly to moderately southeast in shale units (Figure 4.15A). The foreshore between Porthallack and Porth Saxon [SW 7817 2691 - SW 7796 2711] exposes F1 tight folds in a variety of orientations, with axial planes ranging from steep southeasterly dips to more recumbent orientations. Such variation appears to correlate to the positions of T1 thrusts.

D2 compression is heterogeneous and most commonly is recorded by a steeply east-southeast dipping S2 crenulation of the S1 foliation. The strike of S2 cleavage parallels a set of north-northeast trending reverse faults. Primary quartz veins(V1) locally define northwest vergent F2 folds or shallowly northwest-dipping shear-bands. The action of D2 compression upon F1 folds steepens F1 axial planes and produces hook-fold

geometries (e.g. Porthallack, [SW 7811 2698]), where shallowly northwest-dipping shear-bands attenuate fold-limbs. At Maenporth [SW 7912 2951], F2 monoclinal folds verge up the S1 dip towards the northwest and have wavelengths of up to two metres. The folds plunge moderately to the south or southeast at Pendennis Point and show an apparent sinistral shear-couple associated with steep northwest striking faults.

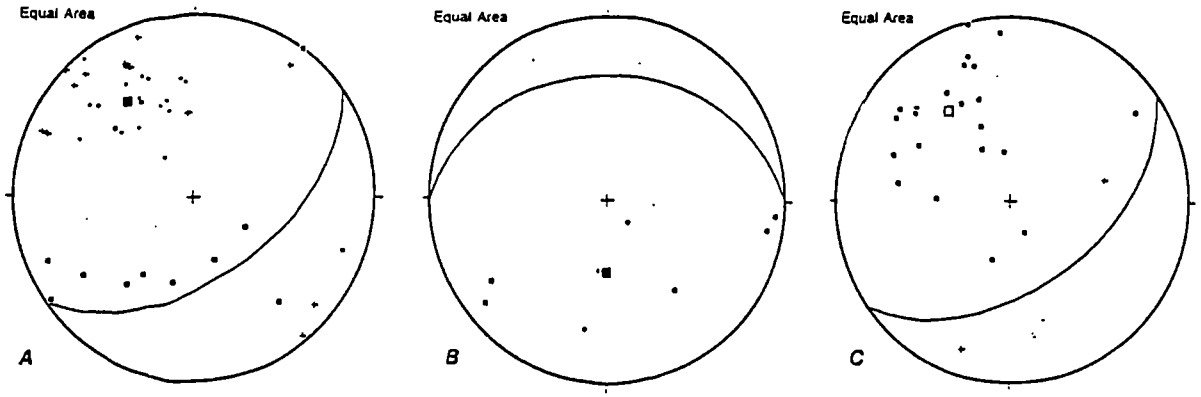

Figure 4.15 Stereoplots of structural orientation data for section 4.3.2; Parson's Beach to Pendennis Point. (A) Compressional structure (• S0 (3); • S1 (17); + S2 (12); ▪ L1 (1); ▫ L2 (9); *mean compressional foliation* 054/53 S). (B) Extensional fabric elements (• S3 (3); ▫ L3 (5); *mean extensional fabric* 270/32 N). (C) Faults and slickenlines (▪ normal fault (22); + normal slickenlines (2); *mean fault plane* 055/50 S).

Extensional features

Post-S2 extensional structures are observed throughout the section in shallowly to moderately southeast-dipping detachments and steeper, curviplanar normal faults. Detachments are developed in laminar siltstones to the west of Toll Point (Figure 4.14), commonly reactivating the normal limbs of F1 folds. Development of an S3 foliation is uncommon with deformation partitioned into the immmediate vicinity of the faults and no evidence for semi-ductile shear along the S1 cleavage. Where present, S3 is a crenulation fabric which dips moderately northwards (Figure 4.15B) and F3 folds verge south or southeast and their axes and L3 crenulations plunge at low angles to the east or southwest.

Steep normal faults dip south or southeast and slickenline orientations imply that they experienced minor oblique sinistral displacement. Such faults are common at Maenporth, where they show SSE-directed brittle extension along braided fault-zones. Listric fault-segments have kink-like F3 folds developed in their hanging-walls which confirm a southeast extension direction.

4.3.2 Flushing to Feock

Lithology

This section consists of two lithologies; the Mylor Slates and the Porthleven Breccia Member. The Mylor slates crop out in the creeks which bound the Flushing and Mylor Bridge peninsulars. Its type-locality at Mylor Creek comprises dark grey slates with pale grey siltstone laminae, the bands commonly displaying grading when greater then 2 centimetres thick. Dark grey and green-grey slates, thin graded sandsones and sedimentary breccias of the Porthleven Breccia Member crop out as a thin north-trending strip of coastline between Flushing and Restronguet Point. Clasts of sandstone reach 2 metres in length on the western side of Restronguet Point (Leveridge *et al.* 1990), whilst centimetre-scale clasts of siltstone and metabasite are intensely deformed into oblate shapes, reflecting high strains along the Carrick Thrust. Metabasic bodies are uncommon within the sequence, but north-south trending granite elvans are seen in the shore at Point [SW 8102 3853] alongside metadoleritic sills.

Compressional features

Low wavecut platforms follow the coast along the western side of Carrick Roads, exposing D1 and D2 fabrics with anomalous moderate or steep easterly dips (Figure 4.16A). At Trefussis Point [SW 817 336] F1 isoclinal folds defined by sandstone beds plunge moderately or steeply to the NNE. The Carrick Thrust is exposed at [SW 8165 3357], juxtaposing folded sandstone beds of the Portscatho Formation against the sheared Porthleven Breccia Member. Exposed fault-planes display stepped slickencrysts and asperities which show downdip asymmetry that suggests a period of normal reactivation during D3 extension. F2 folds plunge moderately east and verge northwards, giving an impression of sinistral shear. S2 pressure solution cleavage is present only in the folded regions and dips steeply east to southeast. To the north at Restronguet Point [SW 8176 3703], a transposing S1/2 cleavage dips variably to the east or northeast. North-vergent F2 folds are tight to isoclinal and again have a sinistral sense of vergence. The magnitude of S2 strain is high in this area, with S1 often only preserved in the microlithons of the spaced S2 pressure solution fabric (Figure 4.17A).

The swing in structural trend of bedding and D1/2 structures coincides with a north-trending section of the Carrick Thrust which formed an oblique or lateral ramp during compression on the basis of kinematic study by Leveridge *et al.* (1990). The sinistral component of shear associated with compression is a consequence of localised strain rotation produced by the obliquity of the thrust-plane to the north-west shortening direction.

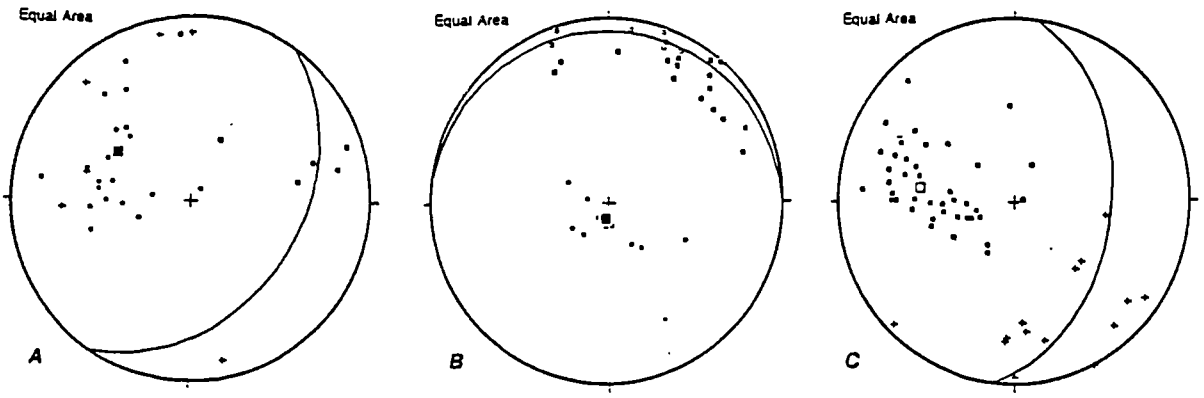

Figure 4.16 Stereoplots of structural orientation data for section 4.3.3; Flushing to Feock. (A) Compressional structure (• S0 (2); ○ S0/1/2 (19); + S2 (6); ▫ L2 (6); *mean compressional foliation* 034/39 E). (B) Extensional fabric elements (• S3 (10); ▫ L3 (23); * kink axial plane (1); ▪ kink axis (1); *mean extensional fabric* 099/7 N). (C) Faults and slickenlines (▪ normal fault (42); + normal slickenlines (14); *mean fault plane* 007/44 E).

Extensional features

The anomalously steep fabrics of the Flushing area are overprinted by a flat-lying S3 crenulation cleavage which is axial planar to southeast- or south- vergent F3 folds. The long to short limb length ratio is small in areas of steep early fabric (c.f. Porthcew concertina folds, Plate 4.4D), but becomes larger where fabrics are more moderately dipping. The folds are often restricted to discrete bands between sandstone beds which have acted as movement planes under vertical D3 compressional strains (Figure 4.17C). Brittle kinks overprint F3 chevrons, again indicating a top sense of shear directed to the southeast.

A shallowly east-dipping S1/2 composite fabric developed at Restronguet Point is parallel to shallowly east to east-southeast dipping normal detachments which partition southeast-vergent F3 folds with shallowly northwest-dipping axial-planar cleavage and gently northeast-plunging axes (Figure 416 B,C; Figure 4.17 B). The deformation chronology is clearly demonstrable on the southern tip of Restronguet Point, where F3 folds of the S2 domainal pressure solution cleavage are seen to deflect an earlier steep fabric preserved within the S2 microlithons. Slickenlines along the detachment surfaces record a slightly dextral component to the slip, allowing southeast directed extension down east-southeast dipping fault planes.

Thin section analysis

A sample of Portscatho Formation slate was taken at East Trefussis Beach, Flushing [SW 8175 3360] at the margin of a D3 shear-zone. It comprises slates of altered white mica and quartz grains cut by anastomosing quartz-veins with fibrous fill elongate north-northwest-south-southeast. Late deformation structures typically occur as an intense crenulation cleavage. Where thick quartz veins predate the extensional deformation their boundaries parallel the slaty cleavage and quartz-grains show mobile grain-boundaries.

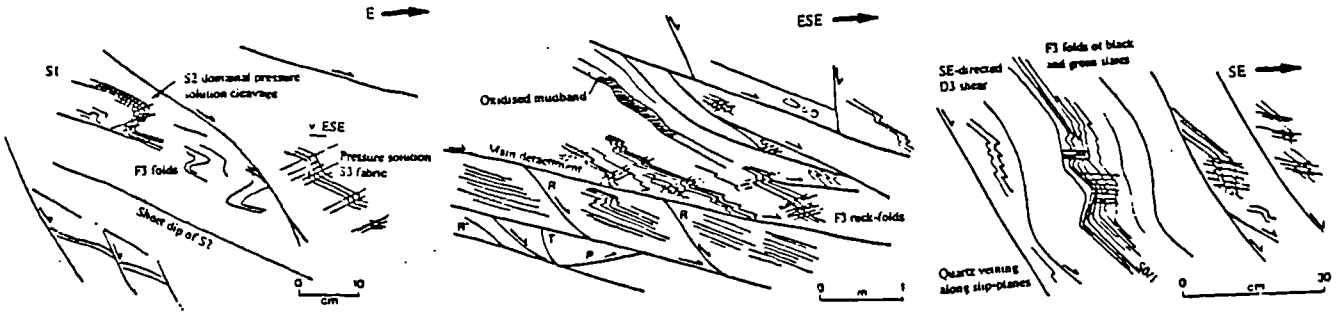

Figure 4.17 Style of D3 extension, western Carrick Roads. (A) D1/2 relationship, Restronguet Point. (B) D3 detachment system, Restronguet Point. (C) D3 vertical shortening of the steep D1/2 fabric, Trefussis Point, Flushing.

4.3.3 Roseland; St Just to Portscatho

Lithology

Between St. Just and Portscatho, the section consists of Portscatho Formation sandstones, siltstones and slates. In general, the sandstones are grey-green and the slates are dark-grey to black, but purple and green intercalations reminiscent of the Dartmouth Slate Formation are seen on the west coast of Roseland. Sandstone beds in the sequence reach a maximum thickness of over a metre at Portscatho, and grade upwards from massive bases to laminar tops. Quartz-veining is developed in the hinges of early folds and along fault-planes.

Compressional features

The orientation of bedding and S1 cleavage returns to a more usual orientation on crossing the River Fal, with moderate southeasterly dips across the region. F1 folds are tight and angular in sandstone units and are generally exposed as northwest-vergent couplets with inverted short limbs. F1 fold axial planes and axes produce a diffuse scatter when plotted stereographically, recording a wide variation in fold attitudes and plunges (Leveridge *et al.* 1990; Figure 4.18A). Leveridge *et al.* (1990) note that the variations in strike to the south of Portscatho could not be accommodated by the N/S-trending and west-facing F4 folds seen across much of south Cornwall (Figure 4.18D), whilst strike swings could not be produced during the coaxial extension which occurs during D3. They hence speculate that the oblique folding zone may reflect the sheath geometry of early folds close to the main Carrick Thrust.

The second compressional event is recorded by north-northwest vergent open to tight folds with attendant pressure solution cleavage(s), north-vergent extensional shear bands and quartz-veining (Alexander and

Shail 1996). Second-phase folds are sometimes sheathed or refolded within the secondary event, due to a progressive north-northwest directed shear couple. The S2 cleavage is commonly developed as steeply southeast- or south- dipping spaced pressure solution seams which locally obliterate earlier fabrics (Figure 4.18A). The L2/1 intersection lineation plunges gently northeast or south, orthogonal to slickenlines preserved on detachment surfaces.

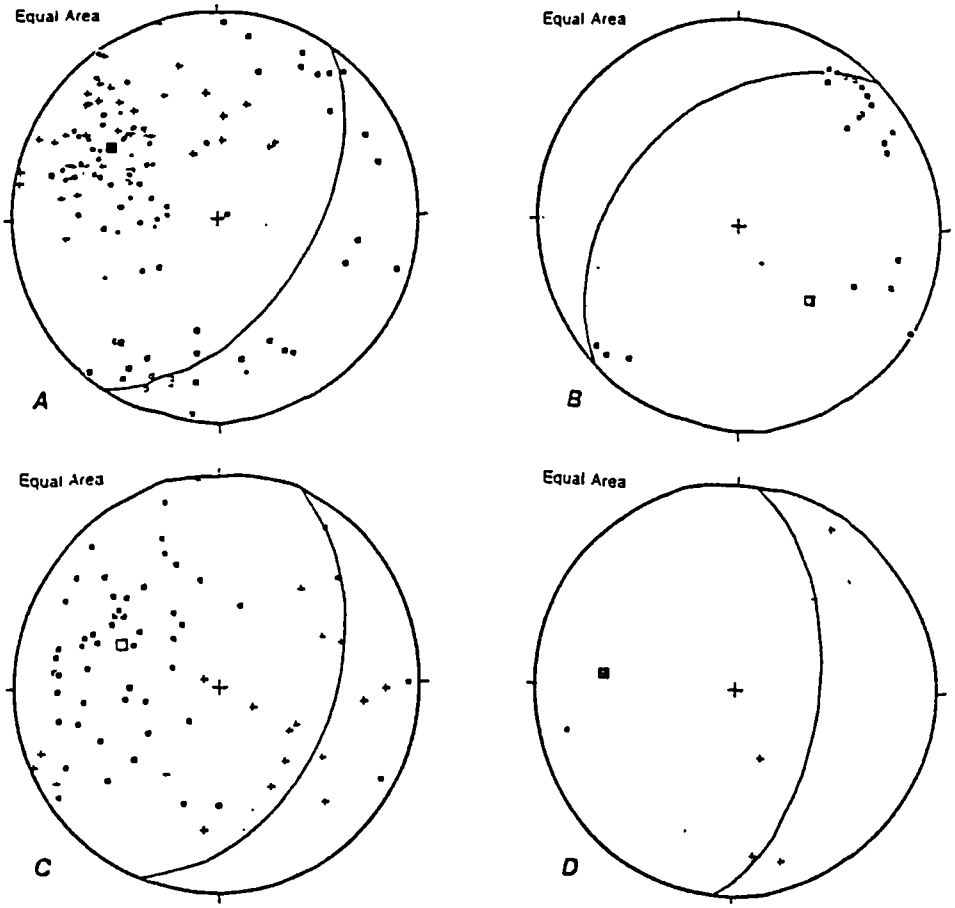

Figure 4.18 Stereoplots of structural orientation data for section 4.3.4; Roseland Peninsular. (A) Compressional structure (• S0 (11); • S1 (11); ○ S0/1 (28); + S2 (38); ▪ L1 (2); ▫ L2 (32); *mean compressional foliation* 034/52 ESE). (B) Extensional fabric elements (• S3 (1); ▫ L3 (20); • kink axial plane (1); ▪ kink axis (3); *mean extensional fabric* 045/41 NW). (C) Faults and slickenlines (• normal fault (54); + normal slickenlines (19); *mean fault plane* 024/43 E). (D) Miscellaneous/late structure (• S4 (1); + L4 (4); *mean S4 fabric* 005/55 E).

Extensional features

The style of extension throughout the area is brittle, mostly restricted to moderate or steeply east, southeast or northeast-dipping normal faults (Figure 4.17C). The faults often reactivate bedding planes and develop thin sulphurous quartz-breccias and packages of brittle folds. At Porthbeor Beach [SW 861 319], southeast-dipping normal faults occur in braided zones up to four metres thick (Plate 4.12A), and accommodate displacements of several metres or perhaps tens of metres.

Away from steep normal faults, a weak D3 impression is seen in gently northeast-plunging crenulations or southeast-vergent monoclinal flexures of the S2 pressure solution cleavage (Plate 4.12). Such structures often occur where V2 quartz-veining is intense, and it appears that they are focussed into zones of high D2 fluid pressure.

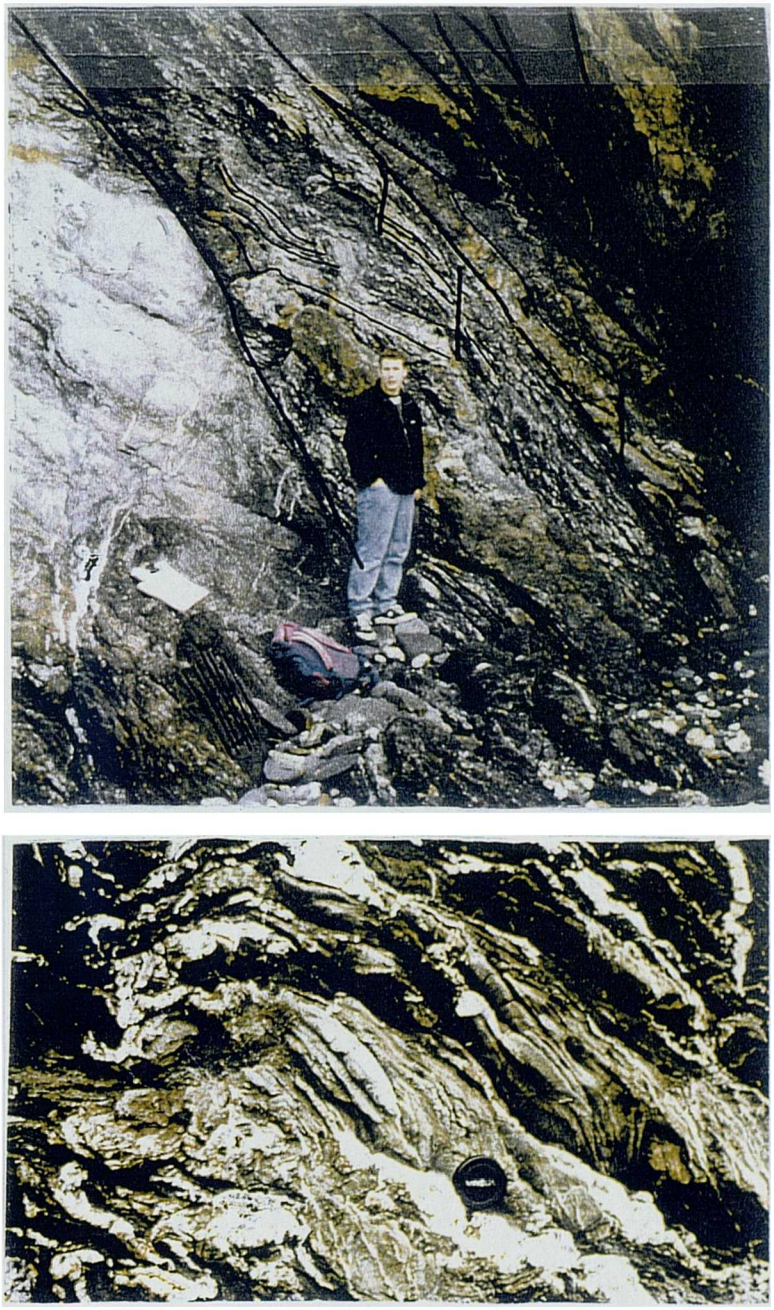

Plate 4.12 Extensional features, Roseland Peninsular. (A) Normal fault-zone with >5 metres displacement, Porthbeor Beach. (B) S2 spaced pressure solution cleavage with S1 traces preserved in lithons. Southeast-verging monoclinal folding is D3 in age.

4.3.4 Gerran's Bay; Rosevine to Nare Head

Lithology

The cliffs and foreshore of Gerran Bay provide a section through the base of the Veryan Nappe. Between Portscatho and Pendower Valley [SW 877 357 - SW 897 381] the Portscatho Sandstones are exposed, with pale grey sandstone beds over 0.3 metres thick separated by layers of black mudstone. Coarse sandstone beds sometimes preserve flute moulds, have traction carpets and contain rip-up clasts or coarse sandstone lenses; all features consistent with proximal turbidite facies (Leveridge *et al.* 1990). The proportion of thick sandstone beds decreases southwards to Creek Stephen [SW 8865 3725] where they more commonly show cross-lamination. The southernmost exposures at Pendower Hotel comprise poorly sorted, conglomeratic sandstones (often with erosional bases)within black mudstones. Detailed sedimentary logs of the succession are included in Leveridge *et al.* 1990 *Figure 6*).

The Pendower Formation at its type section of Pendower Beach [SW 898 382 - SW 905 382] consists of black pyritous and manganiferous slates and cherts at its western extent (Hendriks 1937), interbedded grey to beige slates and buff-weathering coarse sandstones, and green or beige mudstones with purplish brown limestone beds and abundant calcite veining in the upper part of the formation to the east. The base of the Formation is exposed at Pendower [SW 8970 3811] and appears to rest conformably upon the Portscatho Formation, but palaeontological data suggests that it is a thrust (Leveridge *et al.* 1990).

The junction between the Pendower and Carne Formations occurs to the east of Gidley Well [SW 9086 3810], where transitional facies suggest that it is sedimentary in nature. The Carne Formation is dominated by thick quartzite beds separated by black slates. The base of the formation is heavily veined and brecciated by a number of minor thrusts dipping shallowly to the southeast (Reid 1907). The Carne Sandstones pass conformably into the Roseland Breccia Formation to the west of Pennarin Point [SW 9131 3762], again displaying conglomeratic units interbedded with sandstones and intruded by metabasic bodies at Pennarin Point and by the Nare Head metagabbro intrusion to the south of Menanare Point [SW 9147 3741].

Compressional features

F1 folds are well defined in the sandstone-rich lithologies to the west of Pendower, with tight to isoclinal profiles and north-northwest vergence and facing. Leveridge *et al.* (1990) record northeast-verging F1 recumbent isoclines in chert bands of the Pendower Formation [SW 9000 3814], with curvilinear fold axes defining weak sheathed forms. North-northeast vergent isoclinal F1 closures are also preserved towards the top of the Carne Formation to the west of Pennarin Point [SW 9117 3785], where hanging-wall anticlines

occur above east-southeast dipping thrusts. Limestone beds of the Veryan Formation show more typical, northwest-vergent F1 tight folds, their axial planes dipping shallowly southeast.

Bedding and S1 foliation are parallel and shallowly to moderately southeast-dipping regionally, with mineral lineations plunging downdip (Figure 4.19A). The S1 foliation in the Pendower mudstones often wraps pyrite cubes, displaying quartz-calcite strain shadows consistent with top to the northwest shear.

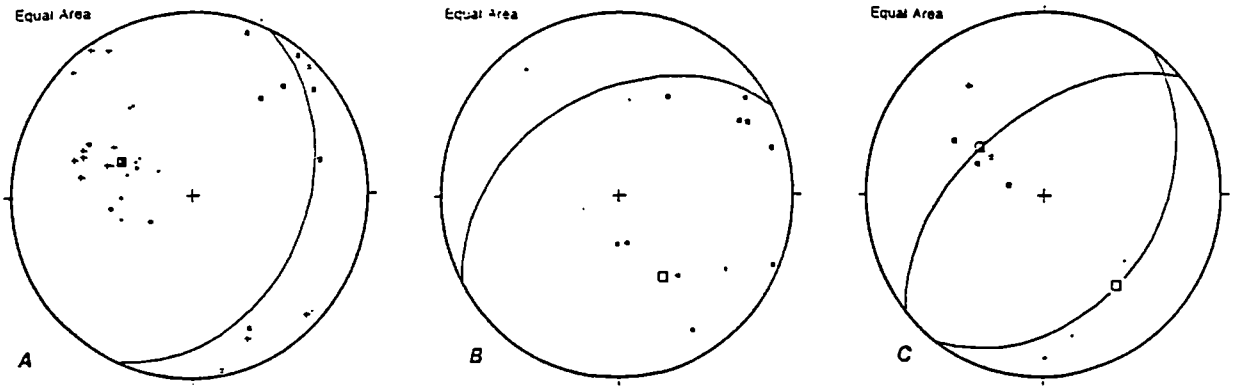

Figure 4.19 Stereoplots of structural orientation data for section 4.3.5; Gerran's Bay. (A) Compressional structure (• S0 (4); • S1 (10); + S2 (11); ▪ L1 (1); ▫ L2 (8) *mean compressional foliation* 026/35 E). (B) Extensional fabric elements (• S3 (4); ▫ L3 (4); • kink axial plane (1); ▪ kink axis (2); *mean extensional fabric* 062/42 NW). (C) Faults and slickenlines (• normal fault (2); + normal slickenlines (1); ▫ thrust/reverse fault (4); ▪ reverse slickenlines (2); *mean fault planes* 037/40 E, 050/55 N).

A D2 overprint is intense in exposures between Pendower and Carne, with northeaststriking open upright F2 folds steepening the S1 slaty cleavage and a discrete S2 crenulation fabric dipping steeply to the southeast (Figure 4.19A) The upright folds are less well developed to the west of Pendower Hotel [SW 9038 3823], appearing to be focused either into Pendower Formation slates or in the hanging-wall of the Veryan Thrust. F2 folding is closely associated with southeast-dipping T2 thrusts at Gidley Well Stream [SW 9085 3825] (Figure 4.19A,C). The fold attitudes steepen into the hanging-walls of the thrusts whilst northwest-dipping D2 extensional shear-bands occur between thrust-planes (Figure 4.19). Quartz-filled tension gashes lie in a similar orientation to the shear-bands and appear to have developed synchronously with them. The style of F2 folding adjacent to the thrust may suggest that the structures exposed along Pendower Beach are themselves underlain at shallow depth by a T2 thrust fault.

Extensional features

D3 is absent or confined to brittle normal faults across much of the section. Brittle drag-folds and Riedel shear plane orientations suggest that southeast-dipping faults accommodated downdip movement of several metres. A subordinate northwest-dipping set of faults are developed locally, emphasising the brittle nature of extension.

An S3 crenulation cleavage dipping moderately northwest is first seen at Pendower Beach, developed patchily in slaty lithologies. The fabric intensifies towards Gidley Well until F3 folds reach 0.01-0.4 metres in wavelength (Figure 4.20). The folds are partitioned into the footwall of T2 thrusts, often forming boxed refolds of F2 features. Fold vergence is towards the east-southeast or southeast, down the dip of T2 thrusts, whilst fold axes plunge at low angles to the ENE (Figure 4.19B).

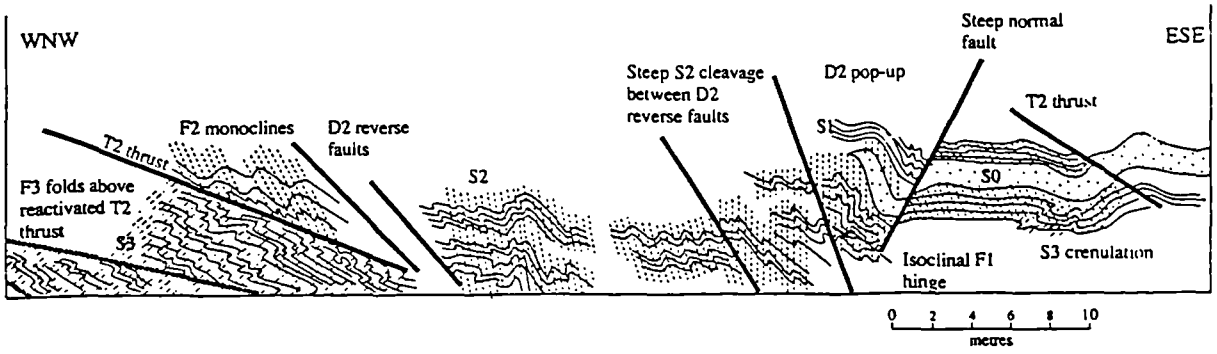

Figure 4.20 Reactivated T2 thrust, Gidley Well Stream [SW 9085 3825]. F3 chevron folds developed above reactivated thrust plane. F2 folds (verging NW) preserved in roof of deformation zone above pristine T2 thrust.

The presence of F3 folds in the footwall of T2 thrusts suggests that such zones were preferentially exploited during layer-parallel extensional shearing and that they acted as weak horizons during extension. This may be a result of fault-sealing and fluid pressure increase beneath the thrusts as D2 ceased, but a lack of intense D3 veining makes this unlikely. Alternatively, the footwalls may have been reactivated due to their relative lack of contortion to the S1 fabric and more continuous planes of weakness suitable for later reactivation.

4.3.5 Veryan Bay; Kiberick Cove to Gorran Haven

Lithology

The Nare Head Greenstone forms the headland south of Paradoe Cove [SW 9131 3768] and west Kiberick Cove [SW 9235 3798], comprising tuffs, flattened pillow lavas and igneous breccias. Its basal contact with the Roseland Breccias is discordant and heavily veined, with serpentinite intruded along D1 fault planes. The occurrence of serpentinite lenses within the breccias at Kiberick Cove suggests that the greenstones represent a large block within the olistostromes (Barnes 1983). To the north, similar igneous bodies crop out at The Blouth, Manare Point, Jacka Point, Portloe Point and Hartriza Point, following a trend parallel to the inferred trace of the Veryan Thrust inland. The igneous bodies may thus form a continuous sheet within the Roseland Breccias or may be discrete olistoliths within the melange.

The western side of Veryan Bay exposes a strike section through the Roseland Breccias, with clasts of mica-schist, limestone, quartzite, amphibolite, granite and arenite contained within dark-grey mudstone. The conglomeratic blocks reach diameters or several metres, and at Jacka Point [SW 9388 3929] *'... is exceptionally coarse, with pebbles sometimes as big as a man's head'* (Reid 1907). The olistostrome is extremely sheared and fine-grained at Portloe [SW 9390 3940], with interbeds of sandstones and mudstone much like the Portscatho Formation explained by Barnes (1983) as a local channel fill sequence.

Between Tregenna and Long Point [SW 9520 4080 - SW 9696 4103] the section comprises bedded greywacke sandstones and slates of the Carne Formation. Olistostromic breccias are sometimes present between Portholland Bay [SW 9602 4119], and Perbean Beach [SX 9640 4112], suggesting a transitional sedimentary contact. The Roseland Breccias are again present between Watchhouse Point [SW 9725 4125] and Cadythew Rock [SW 9921 4059], with sedimentary breccias interbedded with mudstones and thick sandstones. Orange-weathering metabasic rocks occur with thrust offsets on the eastern side of Porthluney Cove, again identified as an amphibolite phacoid within the breccias by Barnes (1983). Bands of breccia to the east yield quartzite clasts which contain Ordovician fauna (Reid 1907), whilst acid tuffs form the headland at Greeb Point [SW 9813 4058].

The thrusted contact between the Dodman phyllites and Roseland Breccias is inferred to run through the beach sands at Hemmick Beach [SW 9941 4052]. To the west, the sequence consists of mudstones, siltstones and fine sandstones, with discontinuous beds of limestone, buff quartzite and green metabasite tens of metres in length. To the southeast, lustrous and platy phyllites and cleaved sandstones are heavily quartz-veined parallel to an intense foliation. The phyllites are often careous and red when weathered, due to the breakdown of micaceous minerals.

Compression features

Compressional structure in Veryan Bay continues the pattern observed in Gerran's Bay to the west, with bedding and slaty S1 cleavage subparallel to one another, dipping moderately to the southeast (Figure 4.21A). The D1 phase is dominant in this area, with clasts within the sedimentary breccias recording intense flattening strains and attenuation. The subparallel S0/1 foliations dip between 45° SE at Portloe and 70°SE at East Portholland [SW 9602 4119] and strikes swing from NE/SW to ENE/WSW on traversing toward the Dodman Thrust.

The S1 foliation seldom reveals primary fold closures or thrusts, and is rather monotonous in the Dodman area. NW-vergent parasitic F1 monoclines are present at Perbean Beach [SW 9640 4112] , to the east of Porthluney Beach [SW 9766 4111], and at Hemmick Beach [SW 9925 4050], but the location of metre to decimetre scale F1 fold-hinges is often clear only from changes in younging direction. The parallelism of bedding and S1 cleavage implies that such folds are tight or isoclinal in form. Southeast-dipping thrusts of

T1 age offset an igneous band to the east of Porthluney Cove by several metres and deflects bedding into hanging-wall anticlines, confirming that compression was directed to the northwest. A large thrust fault is also present at Cadythew Rock [SW 9916 4053], entraining white quartzite phacoids along its heavily veined trace. On entering the Dodman Nappe, a jump in strain magnitude is suggested in the strongly foliated nature of the rocks and the presence of a southeast-dipping mineral stretching lineation.

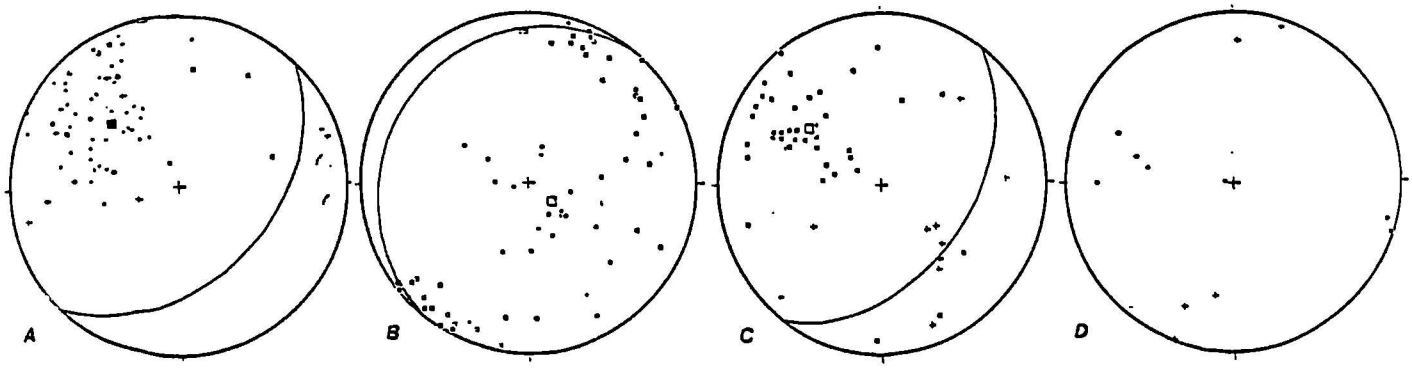

Figure 4.21 Stereoplots of structural orientation data for section 4.3.6; Veryan Bay and Dodman Point. (A) Compressional structure (• S0 (8); * S1 (44); + S2 (10); ▪ L1 (1); ▫ L2 (4); *mean compressional foliation* 045/44 SE). (B) Extensional fabric elements (• S3 (15); ▫ L3 (32); * kink axial plane (7); ▪ kink axis (11); *mean extensional fabric* 039/14 W). (C) Faults and slickenlines (▪ normal fault (39); + normal slickenlines (10); ▫ thrust/reverse fault (2); *mean fault plane* 038/45 E). (D) Miscellaneous/late structure (• S4 (7); + L4 (6)).

The D2 compressional event is patchily developed on the western side of Veryan Bay as a steeply southeast-dipping pressure solution cleavage. Upright F2 folds are well formed in the foreshore at Perbean Beach, and D2 extensional shear-bands with a top to the northwest sense of shear are present at West Watchhouse Point [SW 9710 4110] (Plate 4.13). Northwest-vergent F2 folds are again present on the eastern side of Porthluney Cove, imposing a steep, spaced pressure solution cleavage upon the S1 foliation.

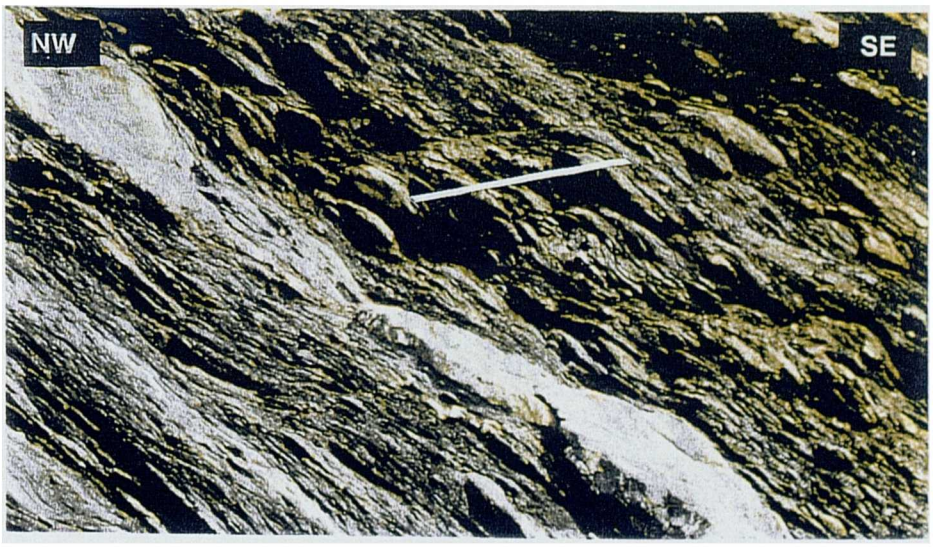

Plate 4.13 D2 extensional shear-bands, Watchhouse Point. Shear-bands dip shallowly to the northwest (parallel to white line), offsetting flattened olistoliths in the moderately southeast-dipping fabric.

A D2 high strain zone occurs at Hemmick Beach [SW 9935 4042], producing the *'strong vertical strain-slip cleavage'* described by Reid (1907). This subvertical or steeply east-southeast dipping pressure solution cleavage is axial planar to upright F2 folds which occur on all scales, from kink-like brittle flexure which verge up the S1 dip to rounded arches (Reid 1907; *Plate 4*). The kinematics of D2 are locally oblique to the usual northwest trend, as the S2 cleavage and F2 folds often verge west. Upright F2 folding is again present within the Dodman phyllites at Vault Beach [0087 4046] and Pen-a-Maen [SX 0181 4125], whilst southeast-dipping D2 shear-bands accommodate northwestward shear at Cadythew Point [SX 0150 4090].

Extensional features

Extension is most commonly recorded by steeply east or southeast dipping normal faults, their slickenlines plunging downdip to the southeast (Figure 4.21C). Fault-planes reactivate bedding in many places (eg. East Portholland [SW 9610 4113]) and are associated with bands of quartz-cemented breccia and muddy gouge up to a metre in thickness. The faults are closely spaced in some areas (e.g. Perbean Beach [SW 9640 4112]), with up to 15 faults demonstrating throws greater than 2 metres present over 100 metres of section. Veining becomes intense into the fault-planes, with anastomosing networks of quartz-calcite veins utilising the S1 foliation.

Shallowly southeast-dipping detachments become more frequent towards the east, developing along slate bed boundaries and S1 cleavage at West Watchhouse Point [SW 9710 4110] and Hemmick Beach (Figure 4.22). The location of detachment faults in the immediate footwall of the Dodman Thrust confirms a genetic relationship between primary thrusts and extension as seen with the Veryan and Carrick Thrusts to the south.

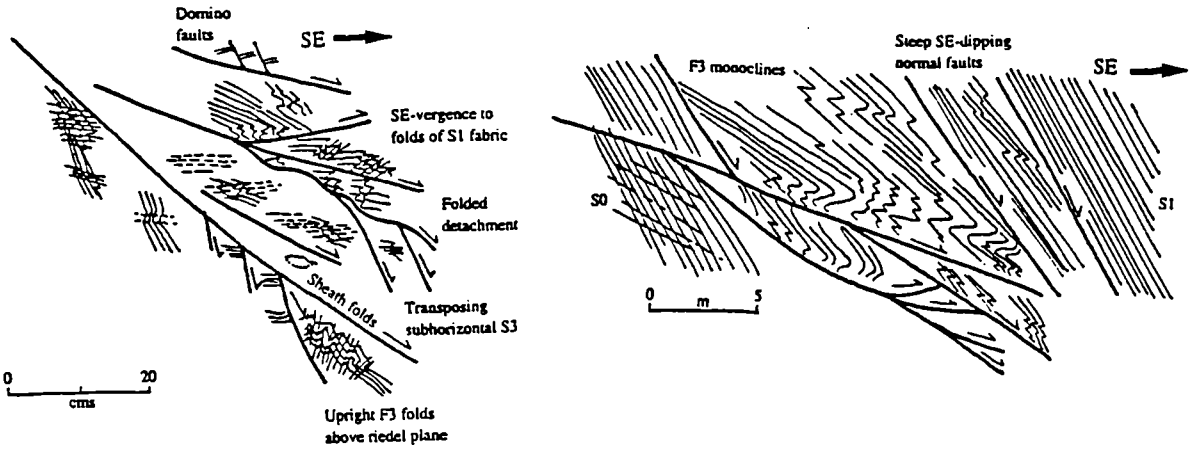

Figure 4.22 Extensional structures associated with normal faulting. (A) Moderately southeast-dipping detachment in the footwall of the Dodman Thrust, Hemmick Beach West [SW 9925 4050]. (B) F3 'mega-kinks' above east-dipping fault-plane, Cadythew Rocks [SW 9910 4055].

F3 folds with gently north-northeast to south-southwest plunging axes and shallowly northwest or southeast dipping axial planes record strain produced by drag along normal faults (Figure 4.21B). In each case, the folds verge down the dip of the adjacent fault-plane. They have a brittle, kink-like style and range in scale from decimetres at Portholland [SW 9602 4119] to over five metres at Cadythew Rocks [SW 9910 4055]. Symmetric, neutrally-verging concertina folds are present in the Dodman phyllites at Vault Beach, imparting a subhorizontal S3 crenulation to the steeply southeast-dipping foliation.

Dextral late faulting is observed along northwest-striking steep structures at West Porthluney [SW 9725 4125], perhaps explaining the strike swings experienced along the section. North-northeast trending upright F4 flexures and a steeply east-dipping late pressure solution is developed in areas with moderate or shallow S0/S1 dip.

Thin section analysis

Lithologies of the Veryan Formation are extremely variable in composition and sedimentology. A conglomerate band sampled at West Carne Beach [SW 9040 3819] contains clasts of quartz-grains and intraclasts of vein quartz and fine-grained volcanic ash within a very fine matrix of quartz and sericite. The primary foliation is seen as aligned muscovite and biotite crystals which wrap the clasts. Where present, porphyroclasts record top to the northwest rotation related to D2 thrusting.

Pale-grey weathering arkosic sandstones are also prevalent within the Formation (sampled at Cadythew Rock [SW 9916 4053]). They typically contain poorly sorted feldspar and quartz clasts within a fine-grained sericitic groundmass. A primary foliation is patchily developed from aligned micas. Extensional deformation is seen in southeast-dipping extensional shear-bands which are exploited by calcite veins.

4.3.6 Structural summary

The compressional architecture of the central south coast of Cornwall reflects the positions and orientations of the Carrick, Veryan and Dodman Thrusts. Primary compression is associated in all areas with a slaty or spaced pressure solution foliation which in most cases dips towards the southeast. A notable exception to this trend is in the sidewall ramp of the Carrick Thrust in the Carrick Roads area, where easterly dips are recorded. Primary thrusts are best observed in areas of low D2 and D3 strain, whilst F1 folds are best preserved in lithologies which contain thick sandstone beds. F1 fold axes and bedding-cleavage intersection lineations plunge at low angles towards the northeast or southwest, swinging to the north-northeast in the Falmouth district (Leveridge *et al.* 1990).

D2 deformation is heterogeneously distributed and records top-to-the-northwest or north-northwest non-coaxial shear in all areas. It produces coaxial refolds of D1 structure in most places, and generates a

pressure solution cleavage which dips steeply to the southeast in the east of the section, and more shallowly in the west of the section. D2 strains are often high in the immediate hanging-wall of T1 thrusts (e.g. Parson's Beach, Carne Beach). Subsequent east-west compression produces a north-northeast trending crenulation lineation upon all fabrics.

Extensional deformation is directed towards the southeast or east-southeast throughout the region, with sinistral transtensile strains recorded where primary structures are oblique (i.e. along the sidewall-ramp of the Carrick Thrust). It is characterised by shallowly-dipping detachments which reactivate bedding or S1 cleavage close to the position of major thrusts (e.g. Flushing, Restronguet Point, Gidley Well, Hemmick Beach), and focuses into the footwalls of T2 thrusts where they are seen at Carne Beach. Away from the major thrust-faults, extension is focused into steep normal faults. Brittle, downdip-vergent F3 folds are seen close to these faults, recording a normal sense of shear.

4.4 The Eastern Margin of the Start-Perranporth Zone; Gorran Haven to Pentewan

Stratigraphy

Between Gorran Haven and Pentewan (Figure 4.23), the eastern strike-equivalent to the East Veryan Bay tectonostratigraphic sequence is exposed. The Dodman Thrust is predicted to run east-northeast through the beach at Gorran Haven, accounting for the change in lithology from silty slates and red-weathering phyllites to the south to olistolithic Roseland Breccia to the north (Holder and Leveridge 1986). A high volcanogenic content to the breccias is accompanied by rafts of black cherty mudstone of apparent Pendower affinity and a large pillowed metabasite body at Great Perhaver Point which looks similar to the Nare Head greenstones.

Poor exposure along Great Perhaver Beach masks the contact between the Roseland Breccia and Carne Formations, although blocks of Carne sandstone become increasingly prevalent to the east of Jobbles Rock. A steep, WNW/ESE-trending normal fault with extensive quartz-veining cuts the beach at [SW 0183 4258], with coarse sandstones interbedded with sandy slates in the footwall to the north (Reid 1907; Holder and Leveridge 1986). The normal fault thus cuts out the eastern exposure of the Veryan thrust and separates the Veryan Nappe from the underlying parautochthonous Gramscatho Group.

The Portscatho Formation comprises of slates, siltstones and coarse sandstones, and extends to the northern margin of the section at Pentewan. Sandstone beds become less dominant towards the north, with banded slates and siltstones cut by an intense steep cleavage and displaying strong quartz-veining.

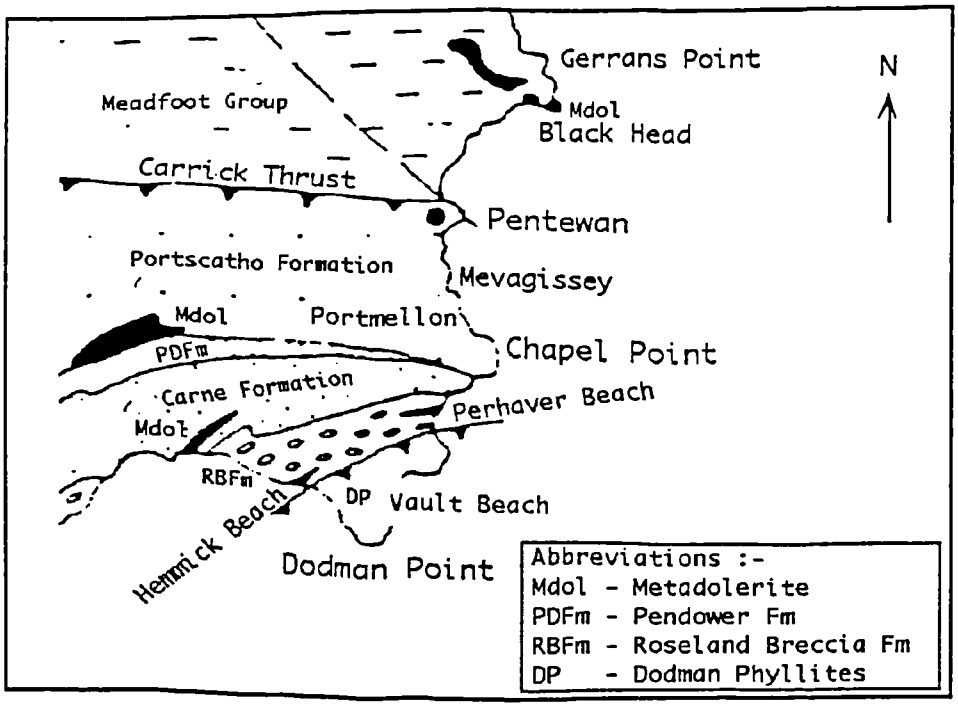

Figure 4.23 Simplified solid geology of the coast between Hemmick Beach and Black Head (amended from Holder & Leveridge 1986). Scale is approximately 1:100,000 (5 cm = 5 kilometers).

Compressive features

A detailed survey of D1 and D2 structure was conducted by Steele (1994) to the north of Turbot Point (Figure 4.24). A steeply north or south-dipping slaty S1 foliation, axial planar to open to tight upright F1 folds characterises D1 deformation regionally. D2 overprint is heterogeneous, seen in crenulations of S0/1, north-verging or steeply plunging dextral F2 folds, dextral shear-bands and a pressure solution S2 fabric.

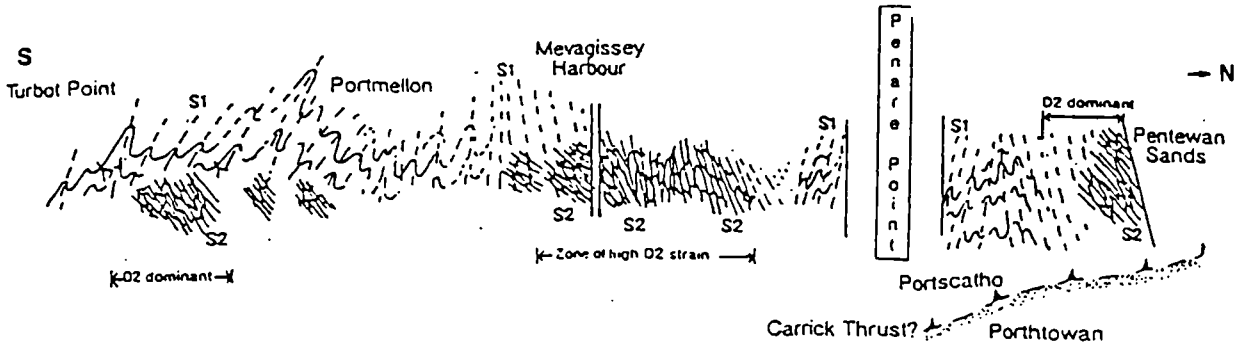

Figure 4.24 - Structural cartoon of the coast from Turbot Point to Pentewan Sands (Steele 1994).

Between Gorran Haven and Great Perhaver Beach [SW 0140 4165 - 0220 4265], S0 and S1 dip 65° towards the southeast and F1 fold closures are not observed. A north-dipping S2 crenulation fabric is often developed in association with shallowly northwest-dipping extensional shear bands. F1 open upright folds of sandstone beds at Turbot Point occur to the south of a zone of tightened, upright, isoclinal F1 folds between Chapel Point and Roward's Quay [SX 0269 4348]. D2 deformation intensifies in the same interval, from minor north-vergent F2 folds and a crenulation S2 fabric at Turbot Point to transposing steep S2 pressure solution fabrics with extensive quartz-veining and abundant dextral shear-bands and folds (Figure 4.25B).

Upright open F1 folds and a moderately to steeply north-dipping S1 fabric are dominant at Portmellon, where D2 strain is sufficiently low for deformed burrows and D1 mineral stretching lineations to be preserved. D2 strain increases northwards across Polkirt Beach [SW 0167 4327], with north-vergent shear-bands and veins exhibiting dextral dilational jogs. Between Polkirt Beach and Mevagissey, S0 and S1 rotate into parallelism and record a tightening of early features into the zone of isoclinal F1 folds reported by Steele (1994) at Cockleridge Beach. D2 strains also increase towards Mevagissey and beyond to Penare Point [SW 0213 4587], where upright north-vergent F2 folds become dominant and the near-vertical S2 cleavage becomes intense to transposing. Dextral shear-bands associated with quartz-veining are seen locally and suggest a dextral shear component.

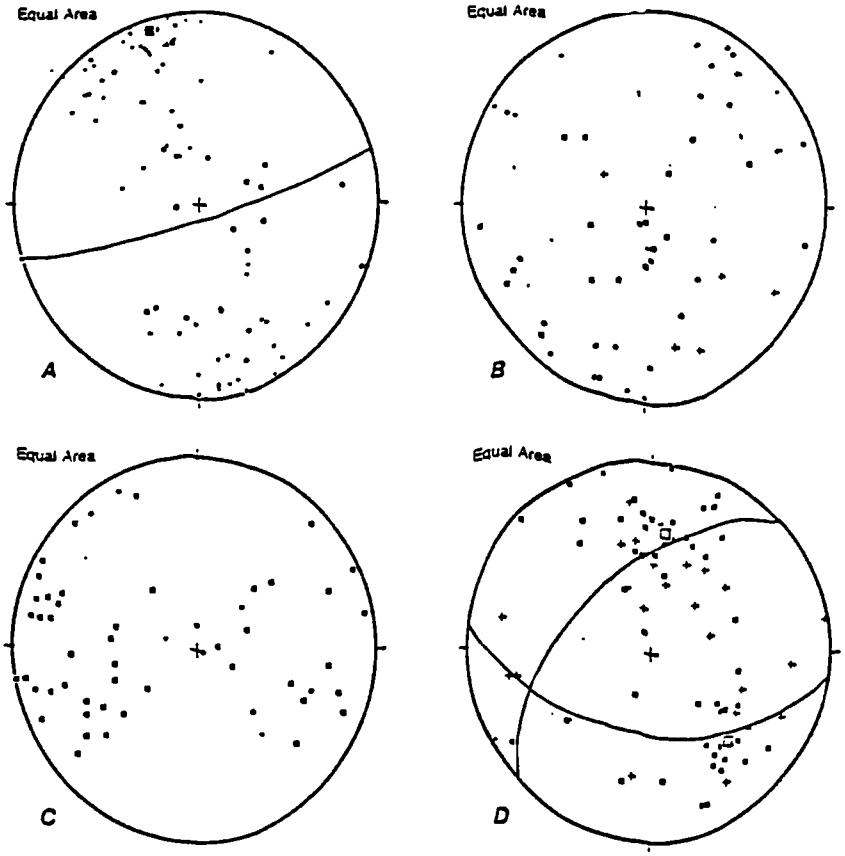

Figure 4.25 Stereoplots of structural orientation data for section 4.4; Gorran Haven to Pentewan. (A) D1 compressional structure (• S0 (25); • S1 (56); ▪ L1 (7); *mean S1 plane* 073/84 S). (B) D2 transpressional structure (+ S2 (7); ▫ L2 (7); • F2 axial plane (5); ▪ F2 axis (11); ○ D2 shear band (22); • shear fibres (4)). (C) Extensional fabric elements (• S3 (7); ▫ L3 (42); • kink axial plane (2); ▪ kink axis (6)). (D) Faults and slickenlines (▪ normal fault (53); + normal slickenlines (22); *mean fault planes* 097/54 S, 046/54 N).

North of Penare Point, F1 isoclinal folds with steep plunges are exposed in the backshore, and a steep S1 fabric is dissected by dextral northeast-dipping shears and patchily overprinted by the S2 pressure solution fabric (Plate 4.14A). Steeply plunging z-folds of the S1 cleavage occur in bands and are clearly cross-cut by a later S3 fabric (see later). A northwest striking steep dextral fault cuts the beach north of Cockaluney, and is surrounded by dextral shears and folds which suggest that the movement plane was utilised during D2 (Plate 4.14B).

Plate 4.14 Compressional Features, Cockaluney Beach [SW 0188 4622]. (A) Steeply NE-vergent F1 fold closure in sandstone bed. S2 fabric developed in hinge, overprinting fanning S1 fabric. (B) Dextral shear-plane with F2 fold on southeast margin.

Extensional features

Steep normal faults parallel to S0/1 typifies extensional structures in this area. Between Gorran Haven and Turbot Point, faults dip steeply to the north-northwest and focus quartz-calcite veining along movement surfaces (Figure 4.25D). North and south-dipping normal faults are extremely common to the north of Turbot Point, with spacings of between 3-25 metres and displacements often in excess of 5 metres. Such faults dissect F1 folds at North Polkirt Beach, and separate steeply and shallowly-dipping S1 fabric domains.

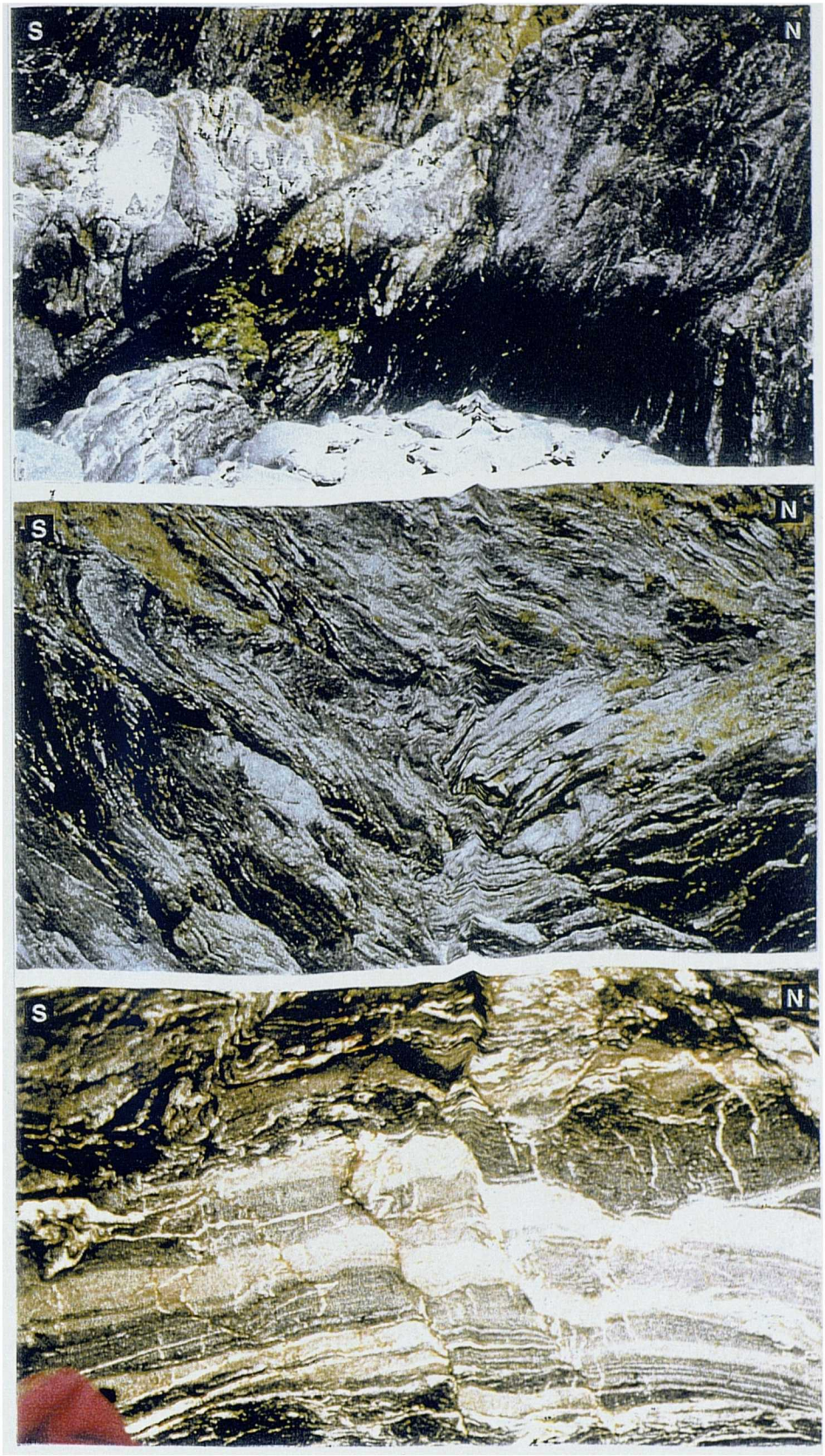

Plate 4.15 Extensional features, Cockaluney Bay. (A) Moderately south-dipping normal fault with sandstone fold hinge in its hanging-wall. Note minor south-dipping F3 flexures in footwall (FOV. 4 m). (B) Moderately north-dipping detachment with large-scale downdip-verging folds in hangingwall (FOV 10 m). (C) North-dipping domino faults in the immediate footwall of a D3 north-transporting normal fault (FOV. 1.2 m).

To the north of Perran Beach moderately north-dipping normal faults are exposed at Cockaluney Bay. The fault-planes are overlain by metre-scale brittle F3 folds which verge downdip, and slickenline and domino-fault orientations which confirm a northward sense of shear (Figure 4.25C; Plate 4.15). The importance of such faults may be great locally if regions of anomalously shallow S1 fabric within the Start-Perranporth Zone represent rotated fault-blocks above normal faults (Steele 1994). Steep conjugate north and south-dipping faults offset their shallower equivalents and show no secondary semi-ductile deformation.

4.5 Lower Devonian; East Pentewan to Plymouth

Stratigraphy

The cliff section between Pentewan and Point of Well [SX 0200 4712 - SX 0255 4736] is fundamental to tectonostratigraphic models of South Cornwall, as it contains the contact between the Gramscatho Group and the Meadfoot Beds which is thought to represent the northern margin of the Gramscatho Basin (Section 2.2.3.1; Figure 4.26). The Carrick Thrust was placed along this boundary by Leveridge *et al.* (1984), but its exact location is somewhat speculative due to the lack of inland exposure. Holder and Leveridge (1986b) describe the boundary as a steep normal fault (cutting out the thrust-plane), with Meadfoot Beds in its hanging-wall and Portscatho sandstones in its footwall. Subsequent work by Shail (1992) and Steele (1994) refutes this model on the basis of sedimentological evidence. A reassessment of sandstones at the contact led Shail (1992) to classify them as Treworgans Sandstones (Porthtowan Formation) rather than Portscatho Formation, and hence no stratigraphic ommission occurs across the junction.

To the east of Gamas Head, Lower Devonian rocks of the Meadfoot and Dartmouth Formations are exposed continuously into south Devon (Section 2.2.2). The dark-grey slates, siltstones and sandstones of the Meadfoot Beds become calcareous and fossilliferous upwards and are underlain conformably by sandstones of the Staddon Grits. They are conformably underlain by purple and green slates, siltstones and sandstones of the Dartmouth Slates. The outcrop pattern of the three subdivisions has traditionally been considered to reflect the position of major fold-structures (e.g. *Dartmouth Antiform*, Section 2.3.1; Hobson 1976a), but subsequent remapping has revealed thrust-faults to the east of the area which may exert a strong control upon the level of exposure (Barton *et al.* 1993; Barton 1994).

Bulk structure

The strike of D1 structure is relatively uniform between Pentewan and Plymouth, the entire section falling into a single tectonic zone in the Sanderson and Dearman scheme (1973; Figure 2.11; Section 2.3.1). The convergence direction as ascertained from mineral stretching lineations is consistently towards the north-northwest (Coward and Smallwood 1984), with folds facing and verging to the north or north-northwest and their axes plunging west-southwest or east-northeast. Uniformity of structural grain coincides with a

zone of consistent K-Ar ages, with 340-320 Myr dates suggesting that D1 deformation was in progress prior to the Tournasian (Dodson and Rex 1971; Coward and Smallwood 1984).

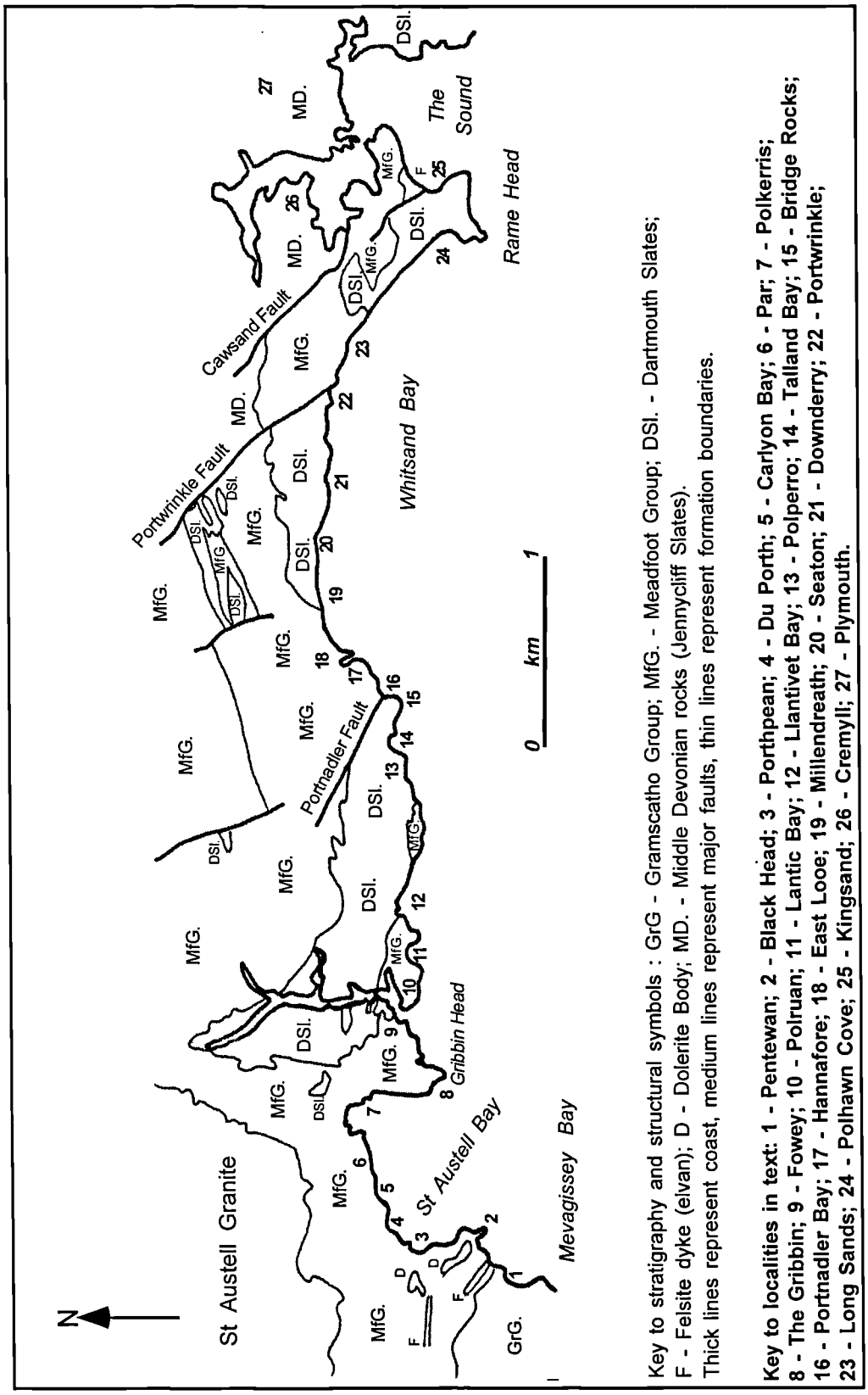

Figure 4.26 Simplified solid geology of the coast between East Pentewan and Plymouth (amended from Holder & Leveridge 1986).

A region of primary facing inversion is preserved from the eastern side of Gribben Head to West Looe, where folds face and verge to the south and slaty S1 cleavage dips moderately northwards. The boundaries to this region are the St Minver to Llantivet and the St Teath to Portnadler faults (Section 2.3.3; Figure 2.14); north-northwest striking dextral wrench faults which extend across the Cornish Peninsular from coast to coast. Lane (1970) suggested that the change in facing and vergence was due to rotation of the original south-dipping fabric elements above a north-northwest transporting decollement. Hobson (1976a) argued that the necessary 80° of rotation required for such reorientation is unlikely, and hypothesised the presence of a large-scale late D1 open monoformal refold of the Dartmouth Antiform, running between southwest Devon and Gribben Head. An alternative suggestion was advanced by Warr (1991), who noted that zones of reversed facing may develop where structural barriers prevent the advance of thrust-sheets. Such buttressing may have occurred against the Gramscatho Basin if it had undergone structural inversion prior to the onset of local T1 thrusting. The dextral faults which bound the zone act as transfers to the anomalous deformation and thus may be inherited basement features (*cf.* Holdsworth 1989b).

East-northeast plunging F2 folds become progressively less common and of lower magnitude to the north of Pentewan, with only a weak crenulation present at Black Head. To the east, D2 compressional fabrics are of local significance only. D4 compressional fabrics as described across much of south Cornwall continue to be present sporadically.

Extensional deformation is accommodated through movement upon slip-planes parallel to S1 foliation, producing downdip-verging angular folds and kinks with a weak S3 crenulation fabric. Non-coaxial D3 shear is distributed through the S1 cleavage or focused into bedding-parallel detachment zones which separate zones of intense crenulation or chevron folding from undeformed S1 domains. Later steep faults are present in zones of intense primary folding. The top sense of extensional shear is directed north or northeast to the west of Portnadler Beach and southeast between Looe and Rame Head, down the dip of the primary cleavage.

4.5.1 St. Austell Bay; East Pentewan to Little Combe Haven

Lithology

The first exposures encountered on the northern side of the St Austell River are thickly bedded (>30 m), gritty sandstones interbedded with silts and shales, identified as the Treworgans Sandstone Member (*Porthtowan Formation*, Shail 1992). The sandstones have basal conglomerates consisting of clasts of sandstone, shale, schist and granite (Steele 1994), and entraining rip-up clasts up to a metre in length. Across the transitional facies, the Meadfoot Beds comprise heavily veined grey and grey-green slates and siltstones with sub-centimetre scale discontinuous sandstone bands. The slates contain grey calcareous

concretions on the northern side of Gamas Point, flattened into the S1 slaty cleavage. Tension gashes and thin veins contain calcite, quartz and siderite minerals.

Black shales bands and pale-grey fossilliferous limestone beds are common between Gerrans Point and Carlyon Bay [SX 0400 4881 - SX 0600 5220], whilst medium-bedded sandstones, shales and basalt-rich debrite beds are reported at Fishing Point [SX 0670 5214] (Shail 1992; Steele 1994). Carbonate and quartz veining is intense a. Bream Rocks [SX 0750 5240], forming anastomosing networks along normal faults. The western shore of Gribben Head exposes grey, brown and black slates interbedded with pale green metadolerite bands. Fine sandstone beds up to 2 cm thick occur in the slates at Polkerris.

Metadolerite intrusions are locally observed, notably at Black Head [SX 040 480] and Carrickowel Point, Du Porth [SX 035 508], and east trending granite elvan dykes intersect the coast at Polrudden Beach [SX 0261 4758] and Phoebes Point [SX 0333 4986].

Compressional features

The section to the east of Pentewan has anomalous D1 orientation, with S1 dipping gently to the north and close F1 folds verging northwards and facing up to the south (Figure 4.27A). This discrepancy between vergence and facing proves problematic. In the absence of intense secondary deformation, it appears most likely that the structural relationships point to the location of the inverted limb of a primary backfold (Steele 1994). If this hypothesis is correct, then the change in S1 from north-dipping at Little Hell, through steep fabrics to the north of Polkerris into moderately south-dipping fabrics at Gribben Head marks a complex geometrical transition from backfolds to forefolds.

The trend of S1 also proves difficult to explain, with the western coast of the bay characterised by moderately north-dipping fabrics (e.g. Gamas Head [SX 0204 4716]), the northern coast displaying east-dipping cleavage with down-dip plunging L1 lineations (e.g. Charleston [SX 0390 5170]) and the eastern coast recording moderately north-dipping cleavage (e.g. Booley Beach [SX 0891 8249]). Over the same interval, L1 lineations and primary fold axes remain constant, trending east-northeast. The swing in trends is best explained as either primary, due to the presence of a lateral ramp at depth causing strain perturbations in the overlying rocks, or secondary, relating to a late north-northwest trending refold. Such structures may have formed in this region as a consequence of emplacement of a ridge of the St. Austell granite at depth, or through extension-related refolding of D4/5 age (Steele 1994).

D2 structures are restricted to shallowly southwest-dipping extensional shear bands around Gamas Head, offsetting beds towards the northeast. Minor T2 thrusts are seen on the northern side of the headland, with calcite-veined movement surfaces and northeast-vergent monoclines in their hangingwalls defined by V1

quartz-veins. To the north, weak D2 shear-bands transporting to the north-northeast are again present at Par Sands and Bream Rocks.

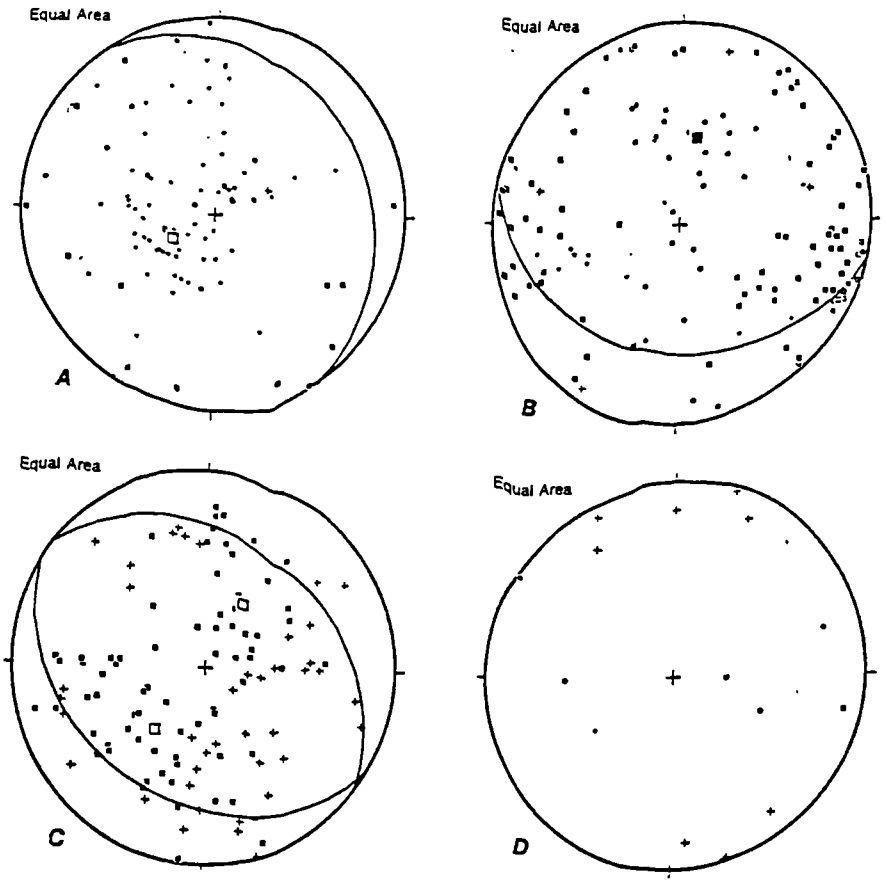

Figure 4.27 Stereoplots of structural orientation data for section 4.5.1; St Austell Bay and Gribben Head West. (A) Compressional structure (• S0 (13); • S1 (64); + S2 (1); ▪ L1 (10); ▫ L2 (3); *mean compressional foliation* 146/20 E). (B) Extensional fabric elements (• S3 (28); ▫ L3 (60); • kink axial plane (12); ▪ kink axis (26); + boudin b-axis (4); *mean extensional fabric* 101/36 S). (C) Faults and slickenlines (▪ normal fault (70); + normal slickenlines (41); ▫ thrust/reverse fault (4); *mean fault planes* 128/34 N, 120/32 S). (D) Miscellaneous/late structure (• S4 (5); + L4 (10); • vein (1); ▪ joint (1)).

Extensional features

Extensional features are extremely common in St Austell Bay, represented by bedding- or S1- parallel detachments, asymmetric folds, domino faults and steep normal faults displaying two dominant kinematic senses; top to the northeast and top to the southwest (Figure 4.27C). The overprinting relationships of both groups of structure are inconsistent and thus it appears that they formed synchronously.

At Gamas Head, shallowly northeast-dipping detachments are developed in mudstone units, with consistent downdip shear evident from domino-faulting and the vergence of asymmetrical F3 drag-folds (Figure 4.27B). The detachments are often listric and splay into steeper normal faults. Southwest-dipping

detachments, again with minor drag folds developed along their planes, displace the northeast-dipping planes and must therefore postdate them. Both groups of detachment are displaced by steep north-dipping normal faults (Plate 4.16B). A more ductile form of the detachment systems is encountered at Robin's Rock [SX 0313 5042], where a shallowly southwest-dipping S3 pressure solution fabric transposes S1 in mudstone units, and detachments with tight hangingwall folds crop out on the headland (Plate 4.16A).

Plate 4.16 Normal fault structures, St. Austell Bay. (A) tight F3 folds above a shallowly northeast-dipping movement surface, Porthpean. (B) Steep north-dipping fault, Gamas Head.

The magnitude of extension increases northwards to Par Sands, about which shallowly- north dipping detachments contort the primary foliation into north-vergent folds with an axial planar south-dipping crenulation fabric (Figure 4.27B). Northeast-dipping steep faults displace the detachments by several metres at Little Hell [SX 0879 5283] and Booley Beach [SX 0885 5246], accommmodating upwards of 15% extension.

The style of F3 folds appears to be closely related to the orientation of S1 planes, as illustrated at Porthpean. Where S1 is steep, D3 produces a subhorizontal crenulation fabric and chevroned concertina folds, whereas shallowly dipping S1 planes are associated with asymmetric drag-folds. The D3 deformation phase thus appears to have initiated in response to vertical compression acting upon planes of weakness, with the complex kinematic pattern controlled overwhelmingly by the dip direction of the S1 foliation. As southwest-dipping fabrics are not observed whilst southeast-vergent extensional deformation bands are observed, a component of extensional shear may relate to reactivation of lateral thrust ramps at depth.

Thin Section Analysis

Muddy sandstones of the basal Meadfoot Group crop out on the northern side of Pentewan Beach [SX 0200 4713], displaying a fine muscovite-chlorite-quartz groundmass and supporting quartz clasts up to 2mm in diameter (Plate 4.17a). A primary foliation is formed of aligned mica whilst quartz grains form σ-porphyroclasts with muscovite-rich tails. Interlayered siltstones and slates sampled on the northern side of Gamas Head [SX 0260 4740] again show a slaty cleavage parallel to bedding.

Extension is recorded in a pressure solution S3 fabric which truncates quartz-grains at Pentewan. At Gamas Head F3 folds occur on all scales. Phyllitic bands are strongly crenulated, whilst siltstone bands are folded in a more brittle style (i.e. they are more angular). The nature of the S3 foliation is thus controlled by the rheology of the host rock. In siltstones a crude fracture cleavage at the fold hinges is infilled by antiaxial quartz-veins and post-deformation chlorite books, whilst in phyllites, a crenulation is observed.

Slates of the Meadfoot Group in the core of a late asymmetric fold were sampled at Porthpean [SX 0313 5061]. The primary slaty cleavage is composed of aligned white mica and flattened quartz-grains, and is crenulated by an S2 cleavage axial planar to the fold-hinge. Infrequent well-formed muscovite crystals overprint the slaty fabric and overgrow the crenulation.

Slates from the eastern side of Par Sands (Bream Rocks [SX 0750 5245], Little Hell [SX 0875 5271] and Booley Beach [SX 0882 5243]) are mottled black and green due to oxidation, and preserve a slaty muscovite schistocity which obliterates bedding. Quartz σ-porphyroclasts with muscovite tails and a top to

the north sense of shear are developed at Bream Rocks, whilst top to the south shear is seen at Little Hell (Plate 4.17b), representing the local D2 phase of back-folding.

The extensional phase is represented by north-vergent micro-kinks with moderately to steeply south-dipping axial planes. A crenulation foliation is variably developed close to fold hinges. Quartz veins parallel to the main fabric show undulose extinction once again and thus imply a low-grade, fluid-rich environment during extension.

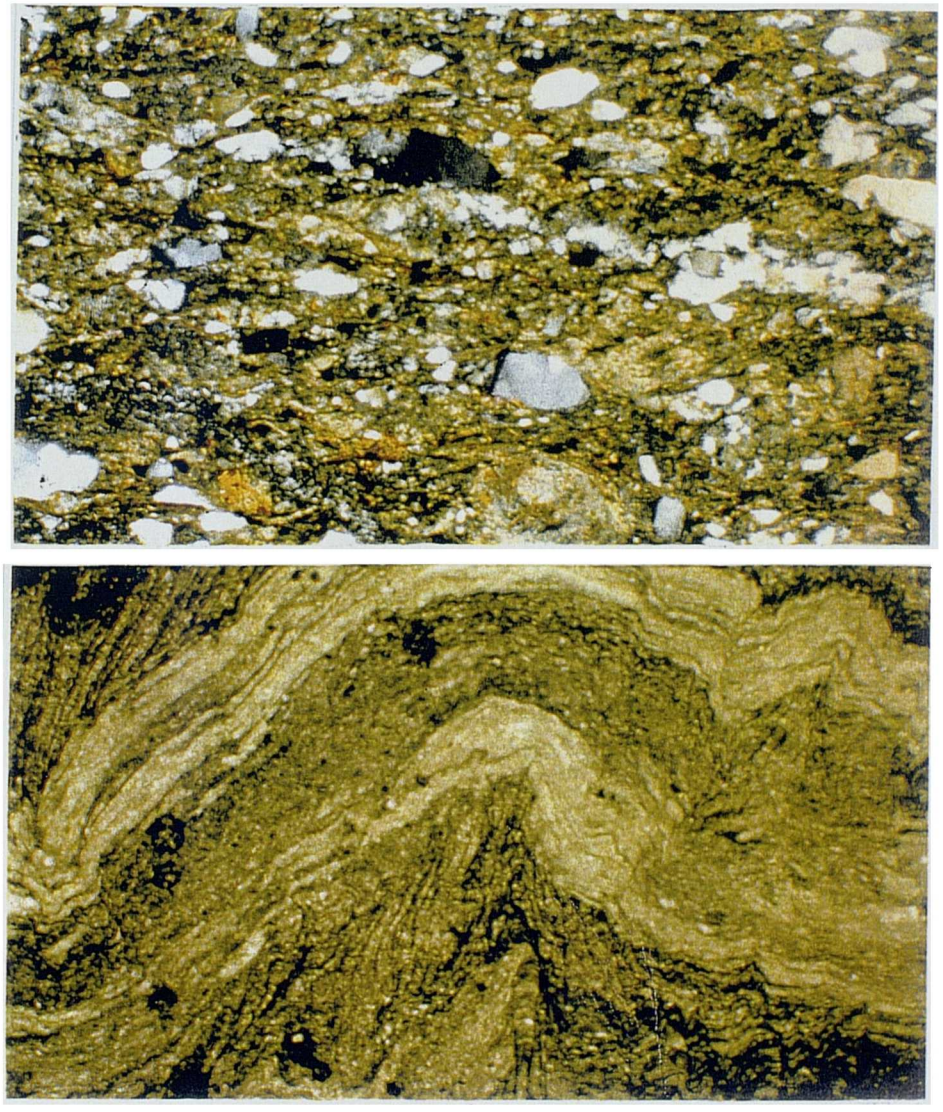

Plate 4.17 (a) Section through the Treworgans Sandstone Member on the northern side of Pentewan Beach (x2, XPL). (b) Development of crenulation cleavage and asymmetric folds in slates, Little Hell (x2, XPL).

4.5.2 Coombe Hawne to Hore Stone

Lithology

The coastline between Gribben Head and Portnadler Bay wholly comprises the Lower Devonian Meadfoot and Dartmouth Groups. The Meadfoot Beds crop out between Gribben Head and Watch House Cove [SX 0983 4931 - SX 1562 5091] and again between Shag Rock and Raphael Spreads [SX 1799 5054 - SX 1574 5088], and typically comprises grey slates with siltstone and limestone interbeds. Local lithological variation includes blue-black slates with brown siltstone laminae (Watch House Cove [SX 1574 5088]), fossilliferous limestone beds (Polruan and Pencarrow Head), and thin sandstone beds (East Lookhouse Cove). Green-weathering sheared metadolerites up to 3 metres thick are exposed in the western area of exposure, with notable examples on the foreshore at Polridmouth.

The Dartmouth Slates are readily identifiable along the remainder of the coast as striped red, grey and green slates. Sandstone beds up to 2 metres thick are locally present, allowing evaluation of F1 fold structures within Lantivet Bay.

Compressional features

West of the Coombe Hawne Fault, bedding and primary slaty cleavage dip moderately to steeply southwards and the bedding-cleavage intersection lineation plunges shallowly west-southwest. The main fault-plane is assumed to run inland along the stream towards Coombe Farm [SX 1104 5110], and is poorly exposed at [SX 1141 5084] as north-northwest trending bands of intense veining. Moderately to steeply northwest-dipping quartz-planes have west-plunging slickenlines which attest to sinistral, top-to-the-west movement.

The section to the east of Coombe Hawne is characterised by a moderately north-dipping slaty cleavage and a west-northwest trending bedding-S1 cleavage intersection lineation (Figure 4.28A). Tight primary folds are exposed at Great Lantic Beach [SX 1482 5086, SX 1460 5083], their axial planes dipping at 5-45°NE. Graded bedding in folded sandstone layers indicates that the folds face up to the southwest. F1 folding on a wavelength of tens of metres is exposed in the wavecut platform at Lantivet Bay [SX 1699 5096]. Folds plunge shallowly towards the east-southeast, verge south-southwest and face up to the south.

A second compressional event is not represented across most of the area. Dextral shears trending north-south are seen at Aesop's Beds [SX 2302 5132], but appear to postdate extensional structures and to relate to the steeply west-dipping S4 crenulation fabric (Figure 4.28D).

Extensional features

To the west of the Coombe Hawne Fault, steep normal faults trending northwest-southeast reactivate steep S1 planes and south-vergent kink-bands are focused into adjacent wallrocks. North-vergent kinks are seen to overprint the south-vergent features. Immediately to the north of the fault at Little Combe Have [SX 1135 5067], bedding and S1 dip steeply east-southeast or southeast whilst kink-bands trend northeast-southwest and verge northwest.

Angular D3 kinks and drag folds verge downdip within the domain of northeast-dipping S0/1 fabric to the east of the Coombe Hawne Fault, the change in vergence coinciding with the fault-zone. Kinking becomes so intense at St. Katherine's Castle [SX 1187 5094] that it gives a herringbone appearance to the S1 cleavage. Their axes consistently trend west-northwest and the resultant crude crenulation cleavage dips moderately to the southeast (Figure 4.28B). When seen in plan view, the folds often show en-echelon offsets and sheath geometries (Plate 4.18A). The weathered S3 (local S2) fabric is well exposed at Washing Rocks [SX 5057 1250], where pressure solution seams are spaced by ~5-20 mm. Slip planes are parallel to the S1 cleavage and planar orange-weathered quartz-veins separate zones of pristine and contorted S1.

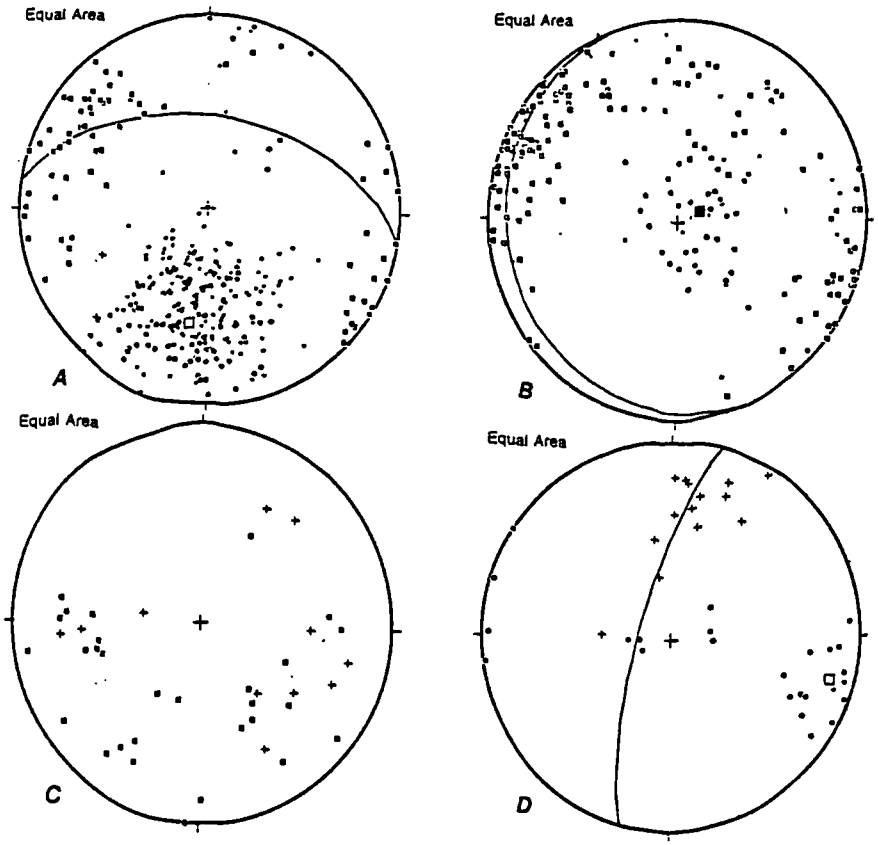

Figure 4.28 Stereoplots of structural orientation data for section 4.5.2; Coombe Hawne to Hore Stone. (A) Compressional structure (• S0 (78); • S1 (178); + S2 (2); ▪ L1 (73); ▫ L2 (2); *mean compressional foliation* 099/50 N). (B) Extensional fabric elements (• S3 (44); ▫ L3 (96); • kink axial plane (20); ▪ kink axis (39); *mean extensional fabric* 158/10 W). (C) Faults and slickenlines (▪ normal fault (29); + normal slickenlines (11)). (D) Miscellaneous/late structure (• S4 (25); + L4 (14); *mean S4 foliation* 015/76 W).

Kinking is largely absent in sandy units exposed at Lantic Bay and Lookhouse Cove [SX 1552 5076], where exposures are dominated by F1 folds. In their place, steep north-striking normal faults with eastward downthrow are evident, often reactivating the bedding in the short limbs of F1 folds. Shallowly northeast to east-dipping normal detachments at the foot of Pencarrow Head [SX 1494 5036] are overlain by northeast- to east- vergent folds with a shallowly west- or southwest- dipping pressure solution cleavage developed in their hinges (Plate 4.18B). Moderately north-dipping faults at Polperro Harbour enclose thick quartz-veined bands suggestive of high pore-fluid pressures (Plate 4.18C).

Northeast-vergent kinks are again the dominant D3 expression to the east of West Coombe, where S1-parallel quartz-veins define northeast-vergent folds. S1-parallel slip must have occurred to allow the features to develop, but the strains are distributed and not focussed into detachments. It appears that this style of deformation is most developed where the lithology is mud-dominated. Green siltstone exposures at northeast Downend Beach [SX 2216 5133] contain calcite σ-porphyroclasts which record downdip shear towards the east.

The Portnadler Fault is exposed at the western end of Samphire Beach [SX 2414 5175]. A steeply northeast-dipping normal fault is seen to separate red slates from buff-coloured slates and siltstones in the backshore. Later dextral movement is recorded in shear-bands, z-folds and in the subhorizontal slickenlines which adorn bedding planes. A late period of post-strike-slip extension is apparent from brittle folding of dextral fault-planes, but may relate to recent cliff processes rather than the imposition of a far-field stress regime.

Thin section analysis

Meadfoot Slates (Washing Rocks [SX 1250 5057]) have a muscovite-defined schistosity which contains wrapped clasts which exhibit ambiguous shear-sense to the southwest and northeast. The extensional phase is recorded in a crenulation cleavage cutting the slaty fabric at high angles. Microfolds verge to the northwest and are focused along bedding planes reactivated in layer-parallel non-coaxial shear.

Samples of Dartmouth Slate show considerable variation in sedimentary style across the area. At Sandheap Point East [SX 1639 5112] the slates contain siltstone laminae and shale rip-up clasts, at East Talland Beach [SX 2476 5141] they are slates interleafed with carbonaceous muds, and at West Looe [SX 2581 5293] they are iron-stained siltstones with a high proportion of altered feldspar. The primary foliation is defined by a muscovite schistosity, changing to one characterised by pressure solution seaming in bands of high quartz content. Extension is expressed by north-vergent microfolds and a steeply south-dipping crenulation cleavage formed axial planar to cm-scale folds (Plate 4.19). At West Looe Harbour, a steeply north-east dipping spaced foliation is exploited by post-tectonic quartz-veins.

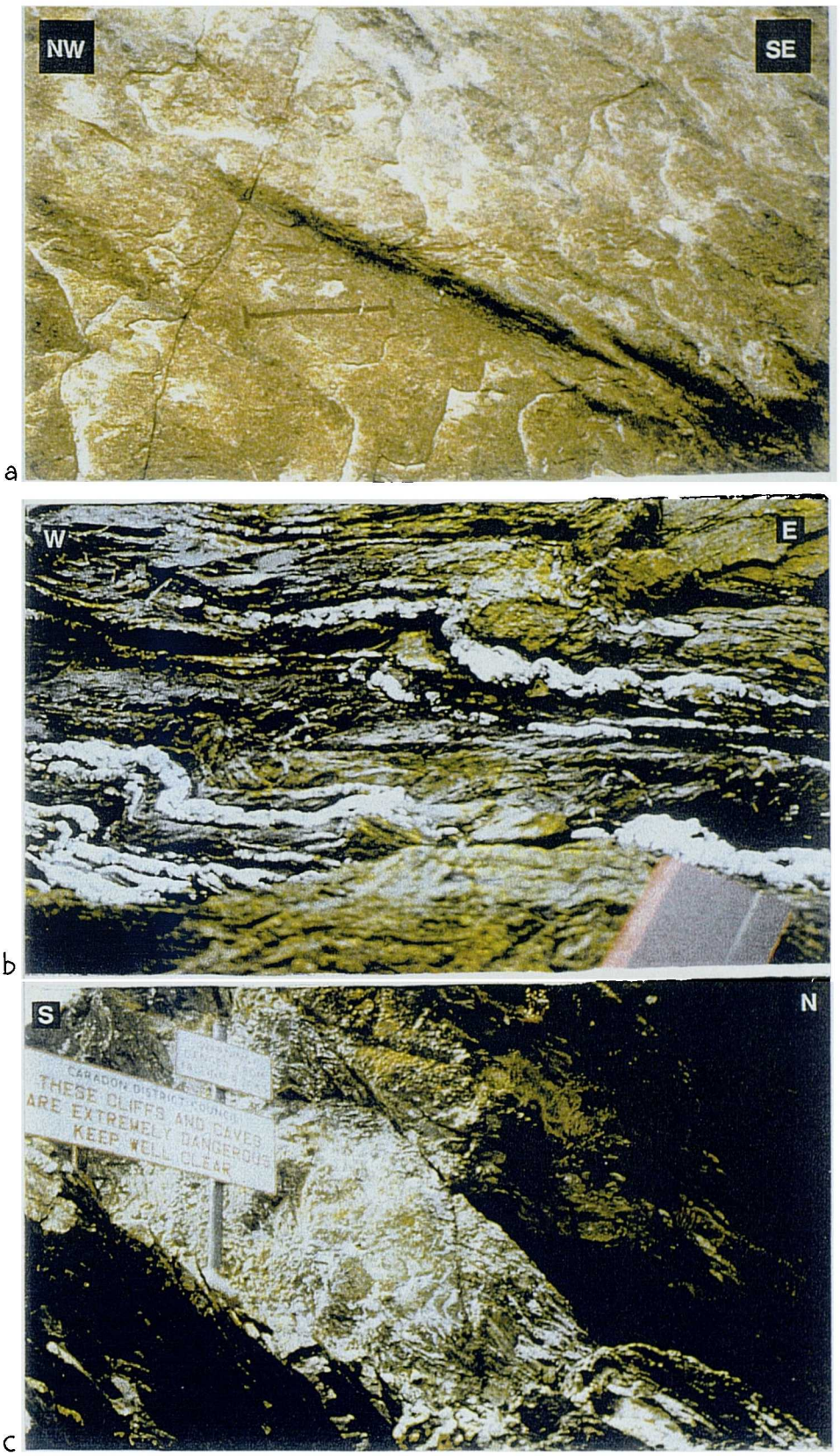

Plate 4.18 Extension-related structures exposed in section 4.5.2. (A) Shallowly southeast-plunging F3 sheath folds with en-echelon offset, St. Katherine's Castle (scale bar 10 cm). The form and geometry of the folds suggest that they relate to top-to-the-north non-coaxial shear. (B) F3 folds formed above shallowly east-dipping, S1-parallel detachments, Pencarrow Head (book width 10 cm). Note folded slickensided detachment-plane at **A**, showing progressive folding of early faults. (C) Heavily veined normal fault-zone (north-dipping), Polperro Harbout (FOV 8 m)

4.5.3 Portnadler Bay to West Looe

Lithology

Between Portnadler Bay and Looe Harbour, exposures consist almost entirely of red and green Dartmouth slates with frequent sandstone beds. The Meadfoot Group is represented by dark-grey slates which crop out over approximately 200 metres of the cliff and are heavily slumped and obscured by vegetation. The junction between the two lithologies appears to be transitional and is folded by F1 isoclines. It trends east-northeast and intersects the shore to the east at Neilsea [SX 2577 5287], where grey-green marly slates occur.

Plate 4.19 Crenulations overprinting slaty cleavage which parallel bedding (colour bands), Talland Bay (x2, PPL).

Compressional features

The anomalous D1 orientation zone ends abruptly at the Portnadler Fault, with bedding and cleavage returning to a moderately southeast-dipping attitude (Figure 4.29A). Primary folding is intense along the Meadfoot-Dartmouth boundary, with tight northwest facing folds of sandstone beds and minor T1 thrusts exposed in the foreshore at Hannafore Beach. A D4, steeply east-northeast dipping spaced pressure solution fabric is seen to crosscut S1 at Hannafore Beach and postdates all other features (Figure 4.29D).

Extensional features

The magnitude of extension is extremely low in this section, again suggesting that the D3 event is preferentially developed in mudstone lithologies and is absent in areas of intense primary folding. Normal faults reactivate bedding to form a conjugate set of late steep features, overprinting a shallowly northwest dipping crenulation fabric (Figure 4.29B,C). Kink bands are again developed in the Dartmouth Slates and plunge subhorizontally northeast-southwest and verge southeast.

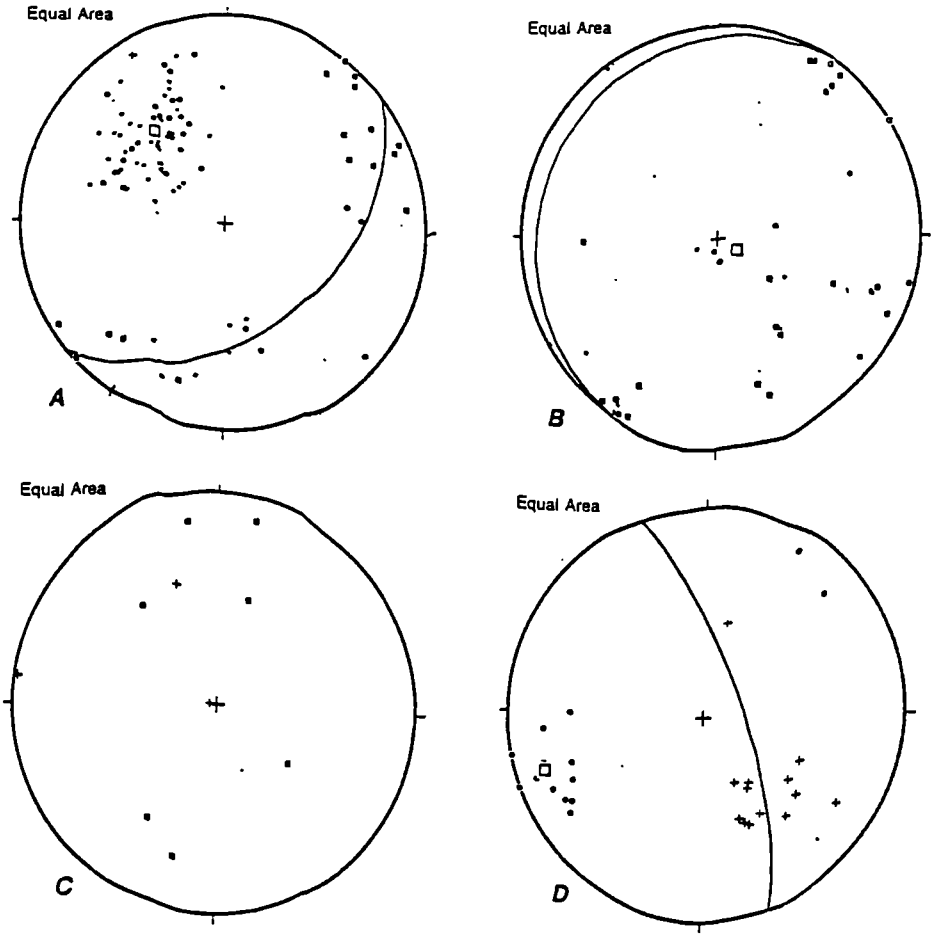

Figure 4.29 Stereoplots of structural orientation data for section 4.5.3; Portnadler Bay to West Looe. (A) Compressional structure (• S0 (33); • S1 (42); + S2 (1); ▪ L1 (15); ▫ L2 (1); *mean compressional fabric* 051/46 S). (B) Extensional fabric elements (• S3 (6); ▫ L3 (12); • kink axial plane (7); ▪ kink axis (13); *mean extensional fabric* 033/9 W). (C) Faults and slickenlines (▪ normal fault (7); + normal slickenlines (3)). (D) Miscellaneous/late structure (• S4 (15); + L4 (13); *mean S4 foliation* 160/74 E)

4.5.4 East Looe to Rame Head

Lithology

The coast between Looe and Rame Head exposes a section through the Lower Devonian, with Dartmouth Beds cropping out between Bodigga Cliff and Portwrinkle [SX 2741 5410 - SX 3590 5380] and again between Tregantle Cliff and Rame Head [SX 3862 5285 - SX 4195 4855], whilst Meadfoot Beds form the intervening section. The outcrop pattern is mainly controlled by the dextral, NW/SE-striking Portwrinkle and Rame Faults which displace the conformable boundary between the two lithologies by approximately 6 kilometers at Long Sands (Figure 4.30). The constituent rock-types of the two formations are outlined in section 2.3.3 and further discussed throughout section 4.5.

Compressional features

Slaty cleavage is the dominant D1 feature throughout the section, dipping moderately southeast and parallel to bedding (Figure 4.31A). It is defined by closely spaced pressure solution seams in most lithologies, and develops as a chlorite shape fabric at the margins of syn-sedimentary metadolerite sheets. Where bedding is distinguishable it dips moderately east-southeast to steeply southeast and is uninverted. The variations in S0/1 orientation along the section appear to be due to late rotation against northwest trending dextral strike-slip faults at Portwrinkle and Rame, across which up to 75° clockwise rotation occurs.

North to northwest upward-facing F1 folds are identified throughout the section, and are often associated with primary thrusts which dip moderately or steeply to the southeast. Fold axes trend northeast-southwest and verge northwest whilst fold-style varies with lithology and D1 strain. For example, isoclinal closures of colour banding in the Dartmouth slates are observed at Salter Rocks West [SX 2807 5417], whilst sandstone-rich Dartmouth Beds at Battern Cliff preserve tight angular F1 chevrons and thrust faults (Figure 4.32). The primary folds and S1 cleavage steepen between Long Stone and Britain Point [SX 3374 5368 - SX 3510 5384], where thick sandstone beds form rounded upright folds with moderate northeast plunges (Plate 4.20A).

D2 strain is heterogeneously distributed and appears related to renewed northwest-directed compression. Shallowly northwest- or southeast- dipping extensional shear-bands are increasingly common towards the southeast (Plate 4.20B), and two orthogonal cleavages trending northwest-southeast and northeast-southwest are present, perhaps recording complex strain expected close to oblique thrust-ramps. Upright angular F2 folds are locally observed (e.g. Salter Rocks). Top-to-the-northwest rotating quartz porphyroclasts are seen at East Murraytown Beach [SX 2918 5428] within S1 cleavage, recording foliation-parallel shear at the thrusted junction between the Dartmouth and Meadfoot Beds.

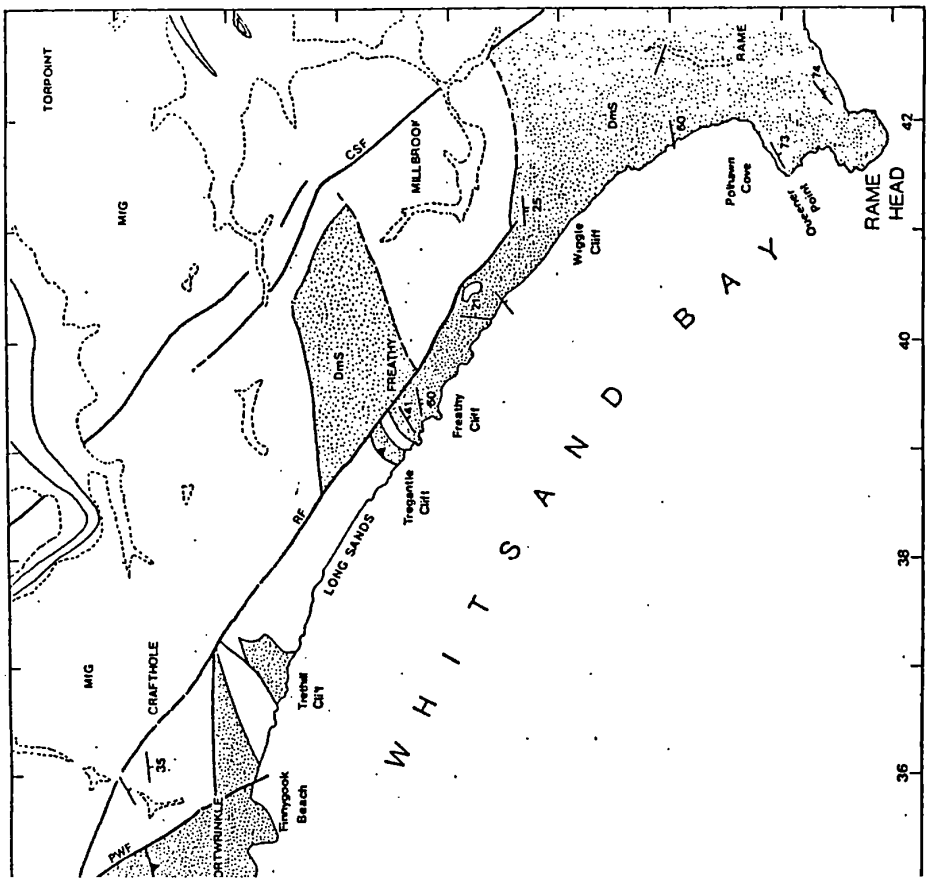

Figure 4.30 Geological map of the coastal section between Looe and Rame Head, adapted from BGS 1:50 000 sheet 348 with reference to Hobson (1978), Barton *et al.* (1993), Barton (1994). Scale ticks denote OS kilometer grid-squares.

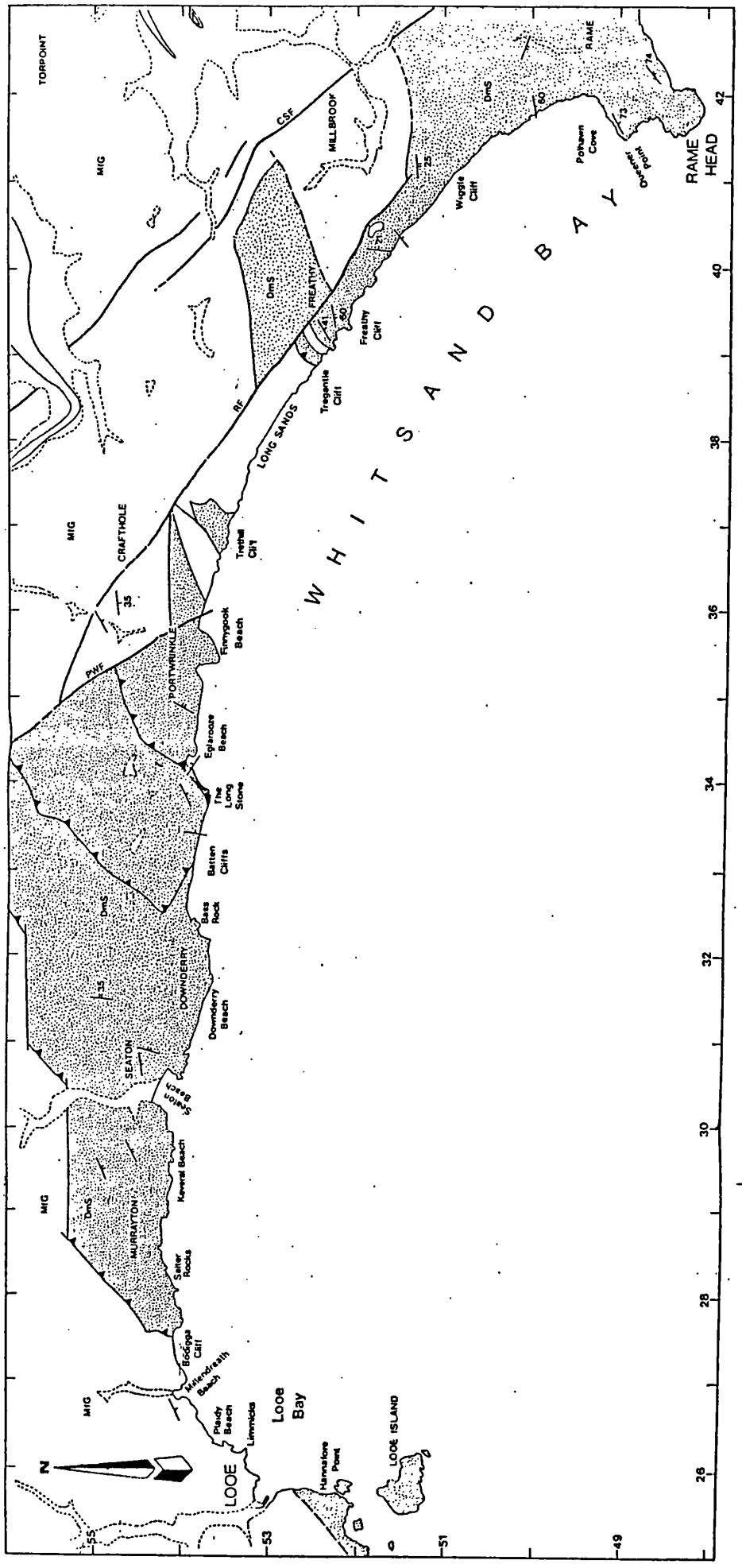

Figure

sheet
e OS

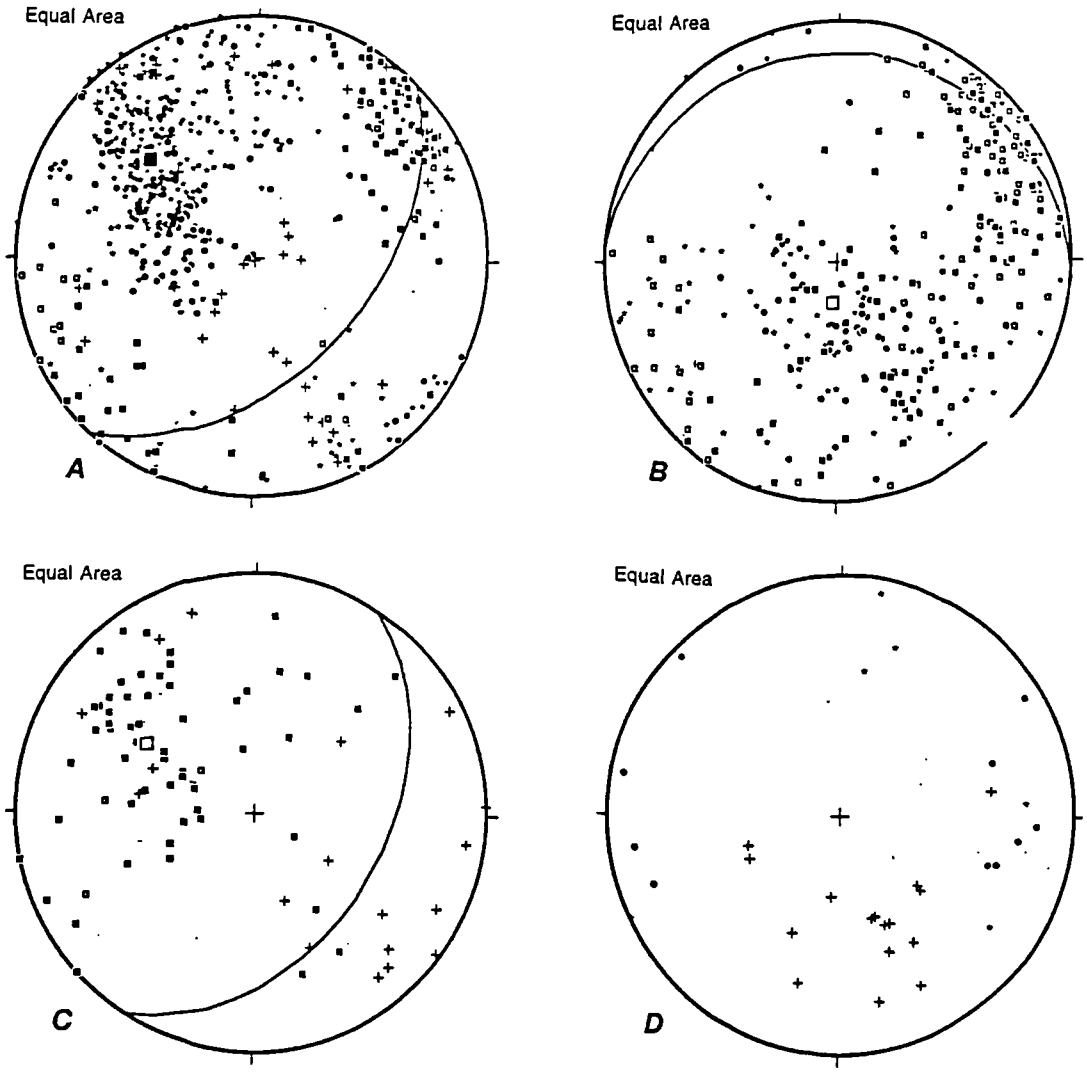

Figure 4.31 Stereoplots of structural orientation data for section 4.5.4; East Looe to Rame Head. (A) Compressional structure (• S0 (135); • S1 (292); + S2 (36); ▪ L1 (95); ▫ L2 (17); *mean compressional foliation* 043/50 E). (B) Extensional fabric elements (• S3 (58); ▫ L3 (79); • kink axial plane (84); ▪ kink axis (94); *mean extensional fabric* 095/14 N). (C) Faults and slickenlines (▪ normal fault (57); ▫ thrust/reverse fault (3); + normal slickenlines (19); *mean fault plane* 032/44 ESE). (D) Miscellaneous/late structure (• S4 (10); + L4 (16); • vein (6)).

Extensional features

Extension is partitioned into detachments developed along the lithological contacts between sandstones and mudstones, with downdip-vergent chevron folds formed through drag or sticking on the movement surfaces (Figures 4.31 B,C; 4.32). A penetrative pressure solution S3 fabric dipping to the northwest is observed at Salter Rocks, and equivalent metre-scale chevron folds are present in zones up to five metres thick in adjacent slates (Plates 4.20 C,D). Quartz-veining increases into the detachments, suggesting that they acted as permeability barriers during the D3 event, and shortening estimates of up to 40% across the F3 folds indicates that extension after nucleation of the folds is in excess of that figure.

Plate 4.20 Structures of the section Plymouth - Rame Head. (A) Upright rounded F1 fold, West Eglarooze Beach. (B) D2 shear-bands transporting top to the northwest, Tregantle Cliff. (C) D3 chevron folds, Salter Rocks (height of photo 3.5 metres). (D) Detail of S3 crenulation cleavage, Salter Rocks.

Shallowly southeast dipping detachments are often seen adjacent to D1/2 thrust-features and thus deformation appears to be partitioned against or reactivate fabrics within thrust-zones as seen elsewhere on the south coast (e.g. Gidley Well). Where T1 thrusting is not seen in the cliffs as at Portwrinkle and Tregantle Cliff, steep southeast-dipping normal faults cut down-section and truncate minor down-dip verging kink-bands. The strength of deformation decreases towards Rame Head, with detachments replaced by steep normal faults with small-scale kinking in the wall-rocks.

Thin section analysis

Samples of red Dartmouth slate and pale-grey sandstones collected at Salter Rocks West [SX 2807 5417], Murraytown Beach [SX 2862 5439] and East Skerrish [SX 3360 5380] contain a slaty S1 cleavage

composed of aligned muscovite laths which forms a braided pressure solution fabric within quartz-rich bands. Localised development of secondary pressure solution fabrics is seen, and a kink-like crenulation fabric records layer-parallel shear during extension (Plate 4.21a). Where present, quartz-veins are deformed by south verging D2 folds.

The Long Stone microgabbro [SX 3396 5380] is internally massive with clots of amphibole, pyroxene and feldspar. The margin of the gabbro is strongly deformed and contains a crude foliation formed from aligned muscovite and chlorite crystals and separating lithons in which feldspars are heavily altered to sericite. Feldspar crystals are attenuated to form pull-aparts infilled with chlorite, fibrous quartz and calcite and are overgrown with calcite, whilst opaque-mineral pull-aparts are infilled with calcite only. Downdip-directed non-coaxial shear is suggested by the geometry of chlorite fish. The microstructures are indicative of fluid-assisted diffusive mass transfer in low-grade metamorphic conditions.

Between Long Stone and Portwrinkle the Dartmouth Group was sampled at Eglarooze Beach [SX 347 538] and Portwrinkle Beach [SX 3572 5381]. Again, the primary slaty or pressure solution cleavage is cross-cut at high-angles by a crenulation cleavage related to folds above low-angle slip planes. The magnitude of extensional shear is variable. At Eglarooze Beach, micro-shears with a crenulation foliation contain σ-porphyroclasts which suggest moderately ductile, S1-parallel shear towards the southeast. Further to the east, twinning in folded calcite veins and undulose extinction in quartz-grains have been observed and are consistent with lower extensional strains.

The Meadfoot Beds exposed at west Trethill Cliffs [SX 3680 5348] contain a slaty S1 cleavage which is distorted about closely spaced, southeast-dipping crenulations. Metabasic layers contain abundant muscovite lathes which form the S1 cleavage and contain porphyroclasts of plagioclase feldspar and pulled-apart opaque minerals separated by quartz-fibres (Plate 4.21c). The extensional phase is recorded by kinks which fold the fabric. In contrast, crinoidal limestones exposed at Blarrick Cliff [SX 3818 5304] show S1 in the alignment of sand-grains and pressure solution seams, and are unaffected by later strain.

Between Tregantle Cliff and Rame Head the Dartmouth Slates again crop out as a series of siltstones. The primary compression event is seen in a crude pressure solution cleavage and crudely aligned muscovite laths whilst the extensional event is not preserved. Quartz and calcite infilling veins show no evidence for crystal plastic deformation, which suggest that the veining may be relatively late or post-extensional. Green indurated siltstones at Penmillard [SX 4204 4970] contains a small amount of muscovite and chlorite, but micas show no kinking and thus appear to have undergone significant post-D1 deformation.

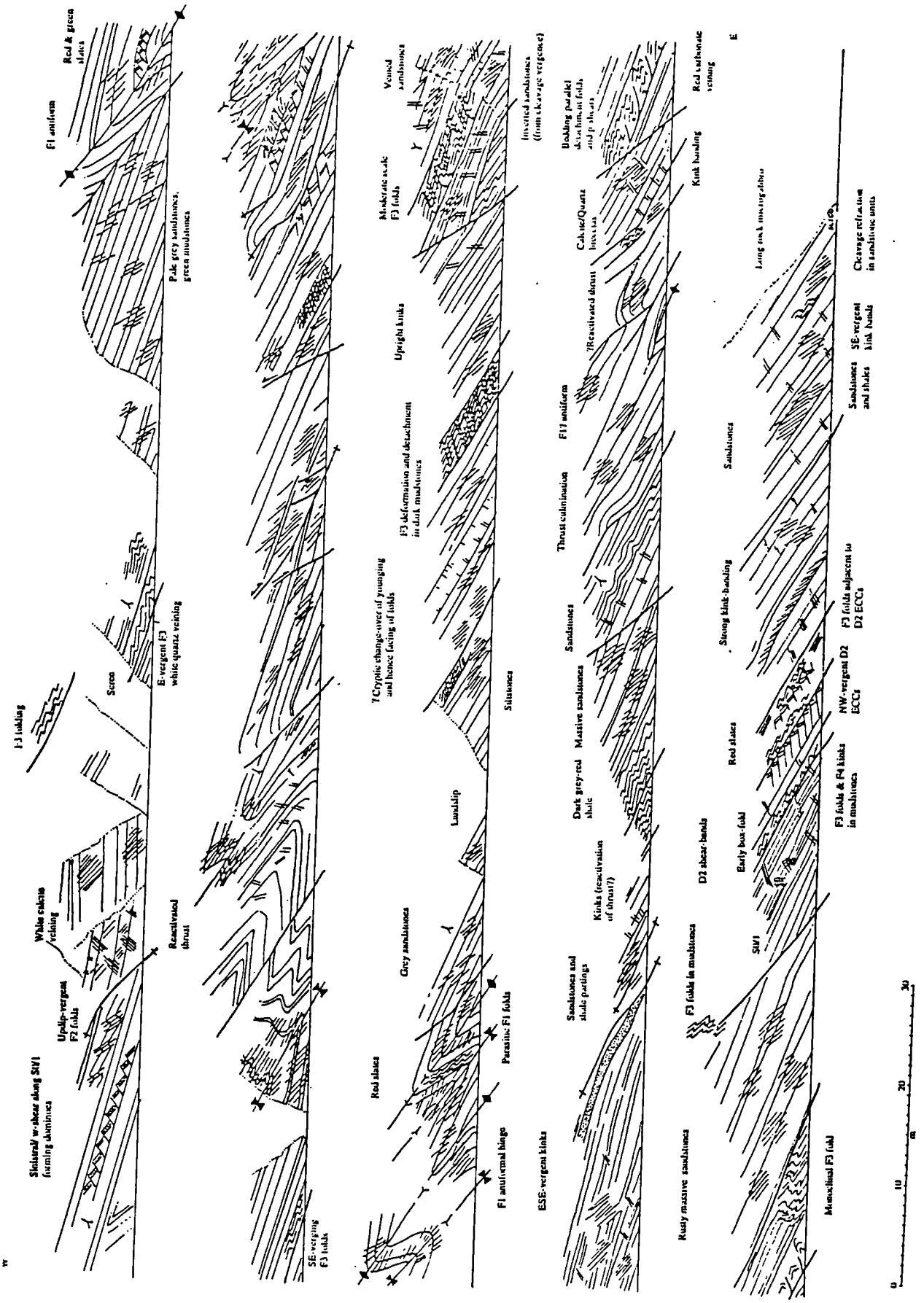

Figure 4.32 - Schematic sketch section, Battern Cliffs, redrawn from field sketches.

Plate 4.21 (a) Brittle kinking of slaty cleavage developed in the hanging wall of a moderately-dipping normal fault, The Skerrish (x2, XPL). (b) Foliated metagabbro from the eastern margin of the Long Stone intrusion (x2, XPL). (c) Foliated metadolerite containing σ- quartz (and untwinned feldspar) porphyroclasts (x10, XPL).

4.5.5 Cawsand Bay

Reconaissance mapping was undertaken along a short section of Cawsand Bay to examine the junction between Permian lava-flows and the underlying Lower Devonian sequence. The flow top orientation is of interest to extension studies, as it forms a palaeohorizontal against which present day orientations of extensional structures may be assessed.

Lithology

Cawsand bay is divided into two sections by a northwest-southeast trending dextral fault zone (the Cawsand Fault), which separates Dartmouth Slates to the west from the Staddon Grits to the east. The Dartmouth Slates at Kingsand Beach comprise interbedded, bleached, purple and green slates and siltstones which dip 60°S and are uninverted (Hobson 1978). Permian rhyolitic lavas with a brick-red coloration and rubbly appearance crop out on the northern side of the beach and display flow banding which defines open upright folds. The composition of the lavas is consistent with their generation as extruded magma from the main granite batholith (Cosgrove and Elliot 1976).

The eastern margin of the lavas is exposed at Sandway Beach [SX 441 511] where a Permian sedimentary breccia comprises angular clasts of sandstone, slate, limestone and rhyolite contained within a red sandstone matrix. The breccia is similar in appearance to Permian conglomerates at Bovisand (Hobson 1978). The Staddon Grits are cleaved red-grey sandstones and siltstones in this locality, with metabasic dykes in the backshore also containing a crude S1 fabric.

The slaty S1 cleavage of the Dartmouth Group is steeply south-inclined close to the Cawsand Fault and primary compressional features are poorly preserved. Northwest trending dextral faults with quartz-breccias cut the early structure. The eastern margin of the lavas at Sandway Point again exhibit a steep south-dipping primary cleavage which shallows to the north. Graded beds are folded into close upright closures which face down to the south and appear to be parasitic upon the inverted limb of a larger F1 fold. NW-vergent T2 thrusts are present within sandstone beds, with S0 and S1 deformed into monoclines in the hanging-walls and a steep late cleavage developed in their hinges.

Extensional deformation is weak and restricted to strong kinking to the west and steep northwest dipping normal faulting to the east. The margins of the Permian lavas are also faulted, cutting out the basal unconformity. The relationship is clearly angular as the lavas and Permian breccias are subhorizontal and uncleaved whilst the Devonian slates are strongly cleaved and dip steeply south. The basal Permian unconformity in this area is thus flat-lying and hence the end Devonian palaeohorizontal appears to be close to the present horizontal. Extensional features in this district thus appear to lie at their original, pre-granite inclination although their dip direction may have been rotated by the dextral faults.

4.5.6 Structural Summary

The compressional architecture of southeast Cornwall is predominantly D1 in genesis, with cleavage and bedding dipping to the southeast and F1 folds facing and verging to the north. A facing reversal occurs to the west of Portnadler Bay, where primary backfolds face and verge south and hence the primary cleavage dips north. The switch in D1 polarity occurs across a northwest-trending dextral fault which acted as a transfer zone during compression. A second phase of northwestwards compression is evident in zones of tightened F1 folds and F2 refolds but is absent over much of the region. North-trending steep pressure solution fabrics of S4 age are also developed to the west of Looe but again appear to be localised in their importance.

Extension is accommodated by a combination of three processes. Most commonly, it is seen in asymmetric folds and kinks of the primary cleavage, with the strain distributed along S1-parallel slip planes. Higher D3 strain is patchily recorded by fault-zones which reactivate bedding and S1 cleavage and bound zones of compressional deformation relating to sticking strains developed during normal movement. Such zones appear to record in excess of 40% lateral movement. A final group of structures are steep normal faults which dip in the same direction as the detachments and locally reactivate the steep limbs of F1 folds. In accordance with the pattern seen across the orogen, they postdate more shallowly dipping extensional features.

The dip of normal faults and vergence of F3 folds is consistently down the dip of the S0 and S1 fabrics, indicating that they record a phase of vertical compression rather than regional extension (i.e. rifting). The kinematics appear to have undergone little post-Carbonferous tilting as the Permian at Kingsand is subhorizontal.

4.6 Discussion of Extensional Features of the South Cornish Coast

4.6.1 Style

Extensional structures exposed along the south Cornish coast exhibit the same geometric range displayed on the north coast (Section 3.7). The most ductile style of extension is displayed to the west of the Tregonning Godolphin granite, where non-coaxial and coaxial strains are recorded along the flat-lying composite compressional foliation. The symmetry of folds reflects a regime of vertical compression which was exerted after the cessation of compression. F3 drag-folds occur on a millimetre to metre scale and produce a flat-lying crenulation or pressure solution fabric. To the southeast of Porthleven, extension is non-coaxial and recorded by a group of semi-ductile features which consistently suggest the generation of shear down the dip of S1 cleavage and bedding. Drag folds and linked extensional fault-systems occur on a centimetre to decimetre scale and are associated with a variety of semi-ductile structures including

porphyroclasts, kink-bands, domino-faults and Riedel arrays. This semi-ductile style of deformation is also recorded around Falmouth Bay, btween Mevagissey and Gribben Head and at Whitsand Bay (Figure 4.33).

Shallowly-dipping detachment systems are exposed at Loe Bar, between Porthsaxon and Restronguet Poin, along the eastern shore of the River Fal, at Hemmick Beach and again at Gidley Well. In each case, extension is focused into S1 ot S0 parallel movement planes which have surface morphologies and slickenlines which support downdip (or oblique dip-slip) non-coaxial shear. The detachments appear to be preferentially developed along the traces of T1 and T2 thrusts, although updip indicators on thrusts surfaces may indicate that the thrust planes are not reactivated in extension but that their wallrocks are utilised as slip surfaces.

Extension is recorded elsewhere by steep normal faults with brittle hangingwall structures. Downdip-vergent angular drag folds with the appearance of slump structures are sometimes present above the fault-planes. The dip of normal faults and vergence of folds is consistently down in the dip-direction of earlier fabrics despite not reactivating the fabrics. They are often curviplanar in profile and only reactivate steep zones of bedding in the steep limbs of F1/2 folds. Post-D3 southeast and north-northwest dipping steep normal faults crosscut all earlier extensional structures.

4.6.2 Kinematic Pattern

The top sense of extensional shear is predominantly directed towards the southeast throughout the region, down the dip of the mean S0/1 foliation (Figure 4.33) Where the primary anisotropy is anomalously orientated the sense of extensional shear is anomalous. For example, bedding and S1 cleavage dip towards the north and northeast between St. Austell Bay and Looe (Section 4.5) and in this section fault striae and drag-folds indicate a top-to-the north or northeast extension direction. The trace of the Carrick Thrust exposed in the shores of the Fal estuary exhibits dextral transpressive features during extension with detachments dipping ESE (down the foliation) but fault surface lineations and drag folds suggesting top-to-the southeast shear. This observation supports the hypothesis that the thrust architecture inherited from D1/2 compression is a control on kinematics and that late-orogenic extension is predominantly away from structural highs.

Coaxial flattening is recorded by structures in western Mount's Bay, Gerran's Bay, Llantivet Bay and Kingsand Bay. In Mount's Bay, the proximity of the upper surface of the granite batholith leads to a model of vertical shortening driven by magmatic buoyancy stresses, but further from the granites coaxial strains may relate to later extension sited to the south in the Plymouth Bay Basin.

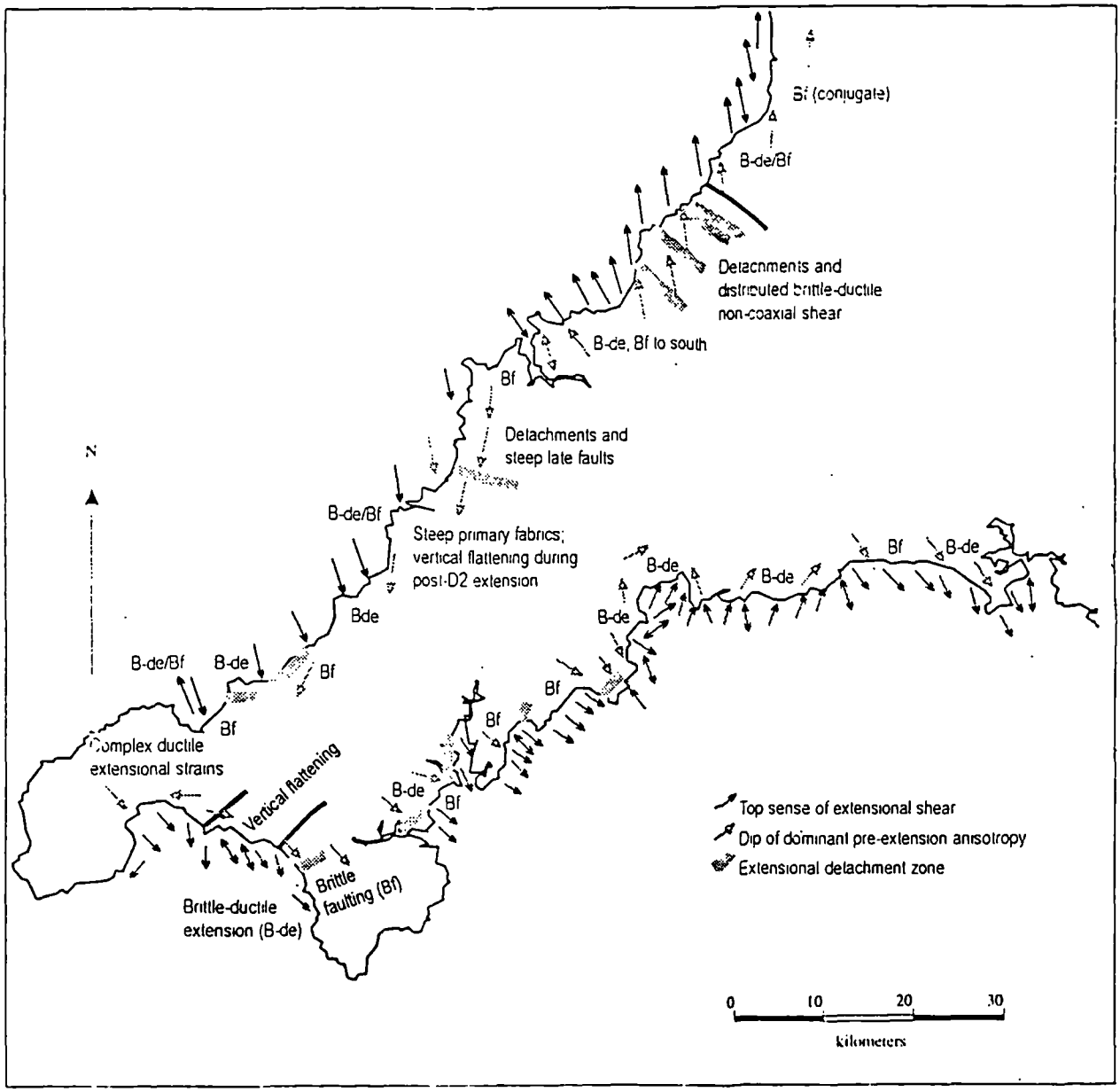

Figure 4.33 Style and kinematics of extensional deformation of the Cornish coast

4.6.3 Magnitude

The highest extensional strains are recorded in zones of shallowly dipping detachments where upwards of 40% horizontal extension is calculated. Extensional strains are generally higher in the southwest than the east, reflecting a transition from the internal to external orogen. The magnitude of strain in the southwesternmost exposures is difficult to determine due to the transposing nature of D3 cleavage and hence a lack of pre-extensional marker bands. The low-angle normal faults described to the east of Mount's Bay occur on an interval of 100s of metres and accommodate considerable extensional strain. The degree of shortening in hangingwall drag structures in Whitsand Bay is locally greater than 50% and thus extension is assumed to exceed this value if the planes experienced sticking after they had accommodated some extensional slip.

4.7 Distribution of Extensional Structures in Cornwall

Mapping of coastal exposures has revealed that extensional features are found throughout southwest England (Figure 4.32). The identification of inland continuity of extensional structures is hampered by a lack of good outcrop, but low-angle faults described along strike of the detachments at Boscastle may be of the same generation as those described in the Tintagel High Strain Zone (Wilson 1951; Freshney *et al.* 1972; Dearman and Butcher 1966). Many of the thrusts identified as tectonostratigraphic boundaries may benefit from re-examination in the light of detachments exposed on the coast.

The style of extension appears closely related to conditions experienced during extension and thus to the compressional nappe stack geometry. Ductile late-orogenic deformation in Mount's Bay, St. Ives Bay and at Perran Bay may have been produced at points of most thickened crust in the nappe pile as vertical compression is a major influence on deformation at the base of thrust sheets (Coward and Potts 1982) due to the action of gravity on the mass of allochthonous rock and progressive rheological weakening related to a rise in temperature. It is therefore no surprise that this style of post-convergent deformation is observed in the most internal parts of the orogen represented in the UK.

Shallowly dipping detachments are noted in several areas, reactivating bedding or S1 cleavage in a normal sense. Significant detachment systems are recorded in the northern Trevone Basin, at Watergate Bay, to the south of Perranporth, in Mount's Bay and at Carne and Hemmick Beach. Each example corresponds to the location of major T1/2 thrusts described in published works (Selwood and Thomas 1986b; Freshney *et al.* 1972; Holder and Leveridge 1986). The detachments may therefore develop along crustal-scale anisotropies developed during compression which cut out the hangingwalls of the thrust. Alternatively, some of the thrusts described previously may, in fact, represent detachments developed in extension which have been mis-interpreted on the basis of the association of compressional features with detachments, produced during sticking or strain hardening of the slip planes.

The style of normal faulting is a consequence of the bulk rheology of the rocks affected and therefore is affected greatly by changes in temperature and pressure and hence burial depth. Extension in the Culm Basin is brittle, and this may reflect thin-skinned deformation and shallow burial depths. Extension in western Mount's Bay is much more ductile and may therefore be interpreted to have occurred at a deeper structural level during thicker-skinned orogenic processes. The consistent overprinting of ductile structures by brittle structures is of great significance to understandings of process and is discussed at length in Chapter 6.

PART III

COMPARISON WITH THE ALPI APUANE, ITALY

Chapter Five - Late-orogenic evolution of the Apuane Alps, Italy

CHAPTER 5 : LATE-OROGENIC EVOLUTION OF THE APUANE ALPS, ITALY

5.1 Introduction

Whilst ancient orogenic belts provide some insight into kinematic evolution of orogens, Cenozoic mountain belts provide a fuller understanding of deformation process for several reasons: (1) They commonly preserve a more complete section through the crust; (2) they have more extreme relief and better exposure; (3) they experience seismicity which provides information on stress orientation; and (4) they have high geothermal gradients and magmatism. The Northern Apennine belt of Italy may consequently provide a Recent analogue to late-Variscan orogenic processes and therefore allow a better interpretation of structures discussed in Chapters 3 and 4.

5.2 Review of published work

The structural setting of the Northern Apennines reflects the eastward migration of two deformation regimes. The first regime records compression relating to plate collision, whilst the second relates to late-orogenic extension through to subsequent rifting. At the present day, a fold and thrust-belt is active in the east whilst extensional faulting occurs in the west. Metamorphic core complexes have developed along the western flank of the chain during extension exposing sections of cover and basement rocks, of which the Alpi Apuane is the largest and best-known (Figure 5.1; Coli 1989; Carmignani and Kligfield 1990).

5.2.1 Plate motions

The Northern Apennine fold- and thrust- belt formed in the Oligocene to Miocene period through collision between three main continental units (Figure 5.2): (1) the Corso-Sardinian block; (2) the Apulian (Adriatic) microcontinent; and (3) the Apenninic orogenic wedge. The continental blocks were separated by the Liguria-Piedmont Ocean; an offshoot of the Tethyan Ocean (Boccaletti and Guazzoni 1975; Ziegler 1990)

Deformation began on the western margin of the Liguria-Piedmont ocean in the late Cretaceous with obduction of ophiolitic sheets onto the East Corsican margin (Carmignani *et al.* 1995), whilst on the eastern margin of the ocean, an accretionary prism developed against a west-dipping subduction zone. Continent-continent collision occurred between late Eocene (Eastern Corsica) and late Oligocene epochs (Northern Apennines) and produced imbricate thrust-stacks on both continental margins. In the Northern Apennine region, the Ligurian accretionary prism was thrust northeastwards over the Apulian continental margin between the late Oligocene and lowermost Miocene. Remnants of Ligurian oceanic crust were thrust over the late Oligocene Macigno Formation and the buoyant continental crust was imbricated, forming an orogenic wedge of Tuscan continental material.

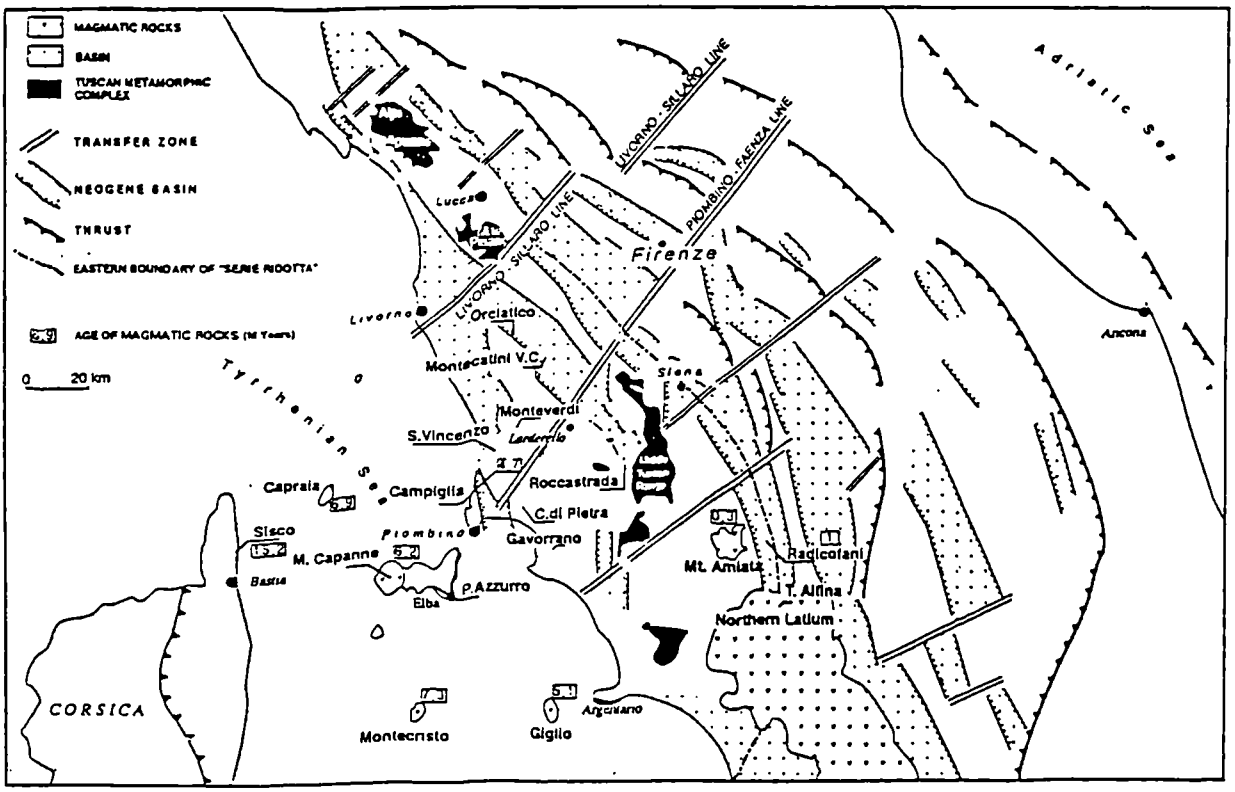

Figure 5.1 Main structural features of the northern Apennines. Magmatic rocks named in bold type and ages indicated in boxes (Carmignani *et al.* 1994).

The Tyrrhenian Sea began to open in the early Miocene in response to asthenospheric diapirism and rotation of the Adriatic microplate (Camelli *et al.* 1993). It originated as a north-south trending rift during late Miocene extension and is floored by Neogene-age oceanic crust in the south and by attenuated continental crust to the north (Chiocci and Orlando 1991). Seismic profiles, marine surveys and core samples in the north Tyrrhenian Sea reveal nappe sheets overlying metamorphic basement (Bartole *et al.* 1991).

Extension in the Northern Apennines is known to have been initiated by the upper Miocene (the age of the oldest sediments deposited in Miocene-Pliocene graben) and omissions of stratigraphy suggest that extension is likely to have been active during the early and middle Miocene (Bertini *et al.* 1991). Early extension is characterised by low-angle normal faults which in part reactivate existing thrusts, producing compressional structures in their hangingwalls (see later). Carmignani and Kligfield (1990) suggest that this phase of crustal attenuation is responsible for the exhumation of metamorphic complexes along the western flank of the chain, and Bertini *et al.* (1991) calculated that over 60% of extension must have occurred to account for this exhumation. From late Miocene times onwards, the western side of the Northern Apennines has been affected by rifting and extension along steep normal faults. A series of northwest-southeast trending graben lacustrine and continental fill developed during the late Miocene and Pliocene, cumulatively recording 10% of horizontal extension (Bertini *et al.* 1991).

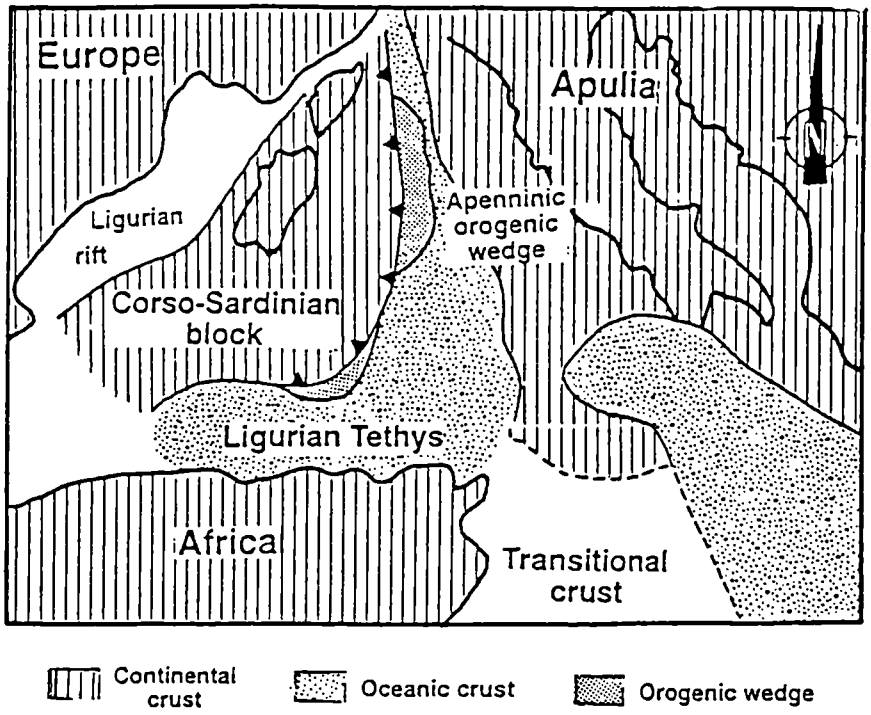

Figure 5.2 Palaeogeographic reconstruction of the Ligurian Tethys immediately prior to continent-continent collision between the Apulian and Corso-Sardinian Plates (Keller *et al.* 1994).

Four models have been proposed to explain this phase of extension. It may: (1) relate to the formation of the Tyrrhenian Sea as a back-arc basin (Boccaletti *et al.* 1974); (2) relate to Tyrrhenian rifting due to an eastwards-migrating asthenospheric lithosphere (Locardi and Nicolich 1988); (3) have been caused by delamination and sinking of the Adriatic lithosphere after collision (Royden *et al.* 1987; Serri *et al.* 1991); (4) reflect transtension and crustal thinning due to anticlockwise rotation of the Adriatic Plate (Lavecchia 1988). Magnetic anomaly data suggests that extension relating to the formation of the Tyrrhenian Sea had begun by 13 Ma, accompanied by a shift in the pole of rotation of the Corso-Sardinian Plate (Dewey *et al.* 1989).

Continental magmatism accompanied extension, its age and composition changing progressively from west to east (Figure 5.1; Serri *et al.* 1991; Lavecchia and Stoppa 1989): Plio-Pleistocene sodic-alkaline volcanics occur in Corsica and Sardinia, calc-alkaline and transitional suites are observed in the Tyrrhenian Sea and Quaternary potassic-alkaline and ultra-alkaline melilitites and carbonatites are present in the Apennines. Granitic bodies also occur in the collision zone and show progressive younging to the east (Alvarez 1972): Elba and Montecristo have grabites dated at 7 Ma, the Giglio pluton is dated at 5 Ma, and Monte Amiata (mainland Italy) has an age of 0.3-0.2 Ma. The magmas show a geochemical evolution which supports generation from melted crustal and mantle rocks derived from the subducted Adriatic plate.

5.2.2 Present day tectonic environment

The Apennine mountains are bordered to the west by the Tyrrhenian Sea, to the east by the Adriatic Sea, and to the north by the main Alpine Chain (Figure 5.3). The east of the chain is being actively underthrusted by the Dinaric plate and earthquake focal solutions indicate that thrusting and transcurrent faulting continue to dominate deformation. The Adriatic Sea represents the active foreland basin of the Apennines and developed in the Pliocene ahead of the advancing Umbro-Marchian fold-belt (Carmignani and Kligfield 1990). Deformation within the basin is controlled by reactivation of pre-Pliocene faults and by movement along weak (evaporitic) strata in the Mesozoic succession (Argnani *et al.* 1991). Its coastline is defined geophysically by a north-northeast trending low Bouguer anomaly which suggests that the MOHO is depressed beneath the Umbro-Marchian fold-belt (Cassinis *et al.* 1991). This is consistent with the occurrence of a west-dipping subduction zone beneath the Po Plain.

To the west of Romagna, extension is occurring along steep normal faults with up to 3 kilometres of displacement which bound graben with Quaternary fill (Capozzi *et al.* 1991). The western flank of the northern Apennines is experiencing mid-crustal seismicity relating to extensional strains, with epicentres of 8-14 km depth in the east and 90 km depth in the west beneath the Tyrrhenian Sea. The progressive westerly deepening of epicentre depths is thought to record the descent of subducted Tethyan crust (Amato and Selvaggi 1991). The extension may be related to roll-back of the Tyrrhenian subduction zone (Camelli *et al.* 1993).

Northwest-southeast trending ridges developed in Tuscany correspond to areas of maximum post-Tortonian extension and hence Pliocene uplift (Mongelli *et al.* 1991). Highly attenuated areas (e.g. Larderello, Alpi Apuane) have the highest heat production and if modelled for simple shear have a β- stretching factor of 3.0 (Mongelli and Zito 1991). This amount of stretching is sufficient to trigger underplating of the thinned crust by asthenospheric melt, and hence may explain zones of anomalous heatflow (Della Vedova *et al.* 1984).

5.2.3 Stratigraphy

5.2.3.1 Northern Apennines

The Northern Apennines are constructed from a number of thrust-sheets which belong to five distinct palaeogeographical domains, distinguished on the basis of provenance and depositional environment: the Ligurian, the Sub-Ligurian, Tuscan, Mt. Cervarola and Umbro-Marchian domains. (Merla 1951; Elter 1960; Kentler 1964; Gianni and Lazzarotto 1975; Conti *et al.* 1991; Table 5.1; Figure 5.4). The style of compressional structures and metamorphic pattern of the each unit suggests that they were stacked in

piggyback fashion with rocks from the most westerly palaeogeographic region uppermost (Carmignani *et al.* 1993).

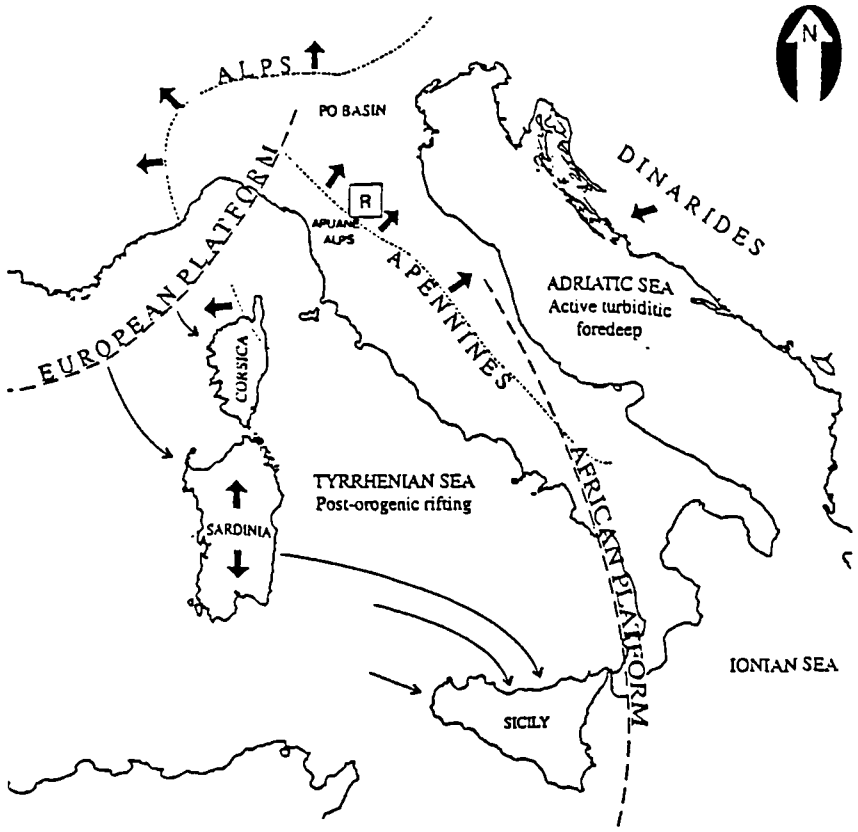

Figure 5.3 Present day tectonics of the Italian region (Adapted from Caire 1971). Wide black arrows indicate vergence directions of compressional structures; thin black arrows indicate post-Cretaceous Plate motions.

Domain		Age Range	Lithologies	Interpretation
Ligurian		Jurassic to Eocene	Basic and ultrabasic igneous rocks, slates, radiolarites, flysch	Oceanic crust and pelagic sediments; ophiolites
Sub-Ligurian		Lower Cretaceous to Oligocene	Sandstones, mudstones, limestones	Transitional crustal setting between Tuscan and Ligurian domains
Tuscan	Internal	Palaeozoic to Tertiary	Greenschist facies: schists, quartzites, phyllites	Continental crust (Hercynian basement) hosting lacustrine, carb-onate platform, pelagic and flysch sedimentation.
	External	Lower Triassic to lower Oligocene	Diagenetic grade: evaporites, carbonates, mudrocks, flysch	As above, detached during early compression and not incorporated as basement unit
Monte Cervarola		Middle Miocene	Arenaceous flysch	Foreland basin to Umbro-March domain
Umbro-Marchian		Permian to upper Miocene	Condensed Tuscan-like sequence	Near craton foreland deposits, continental

Table 5.1 Palaeogeographical domain summary. Information derived from Gianni and Lazzarotto 1975; Carmignani *et al.* 1993, 1994; Camelli *et al.* 1993.

Consistent temporal changes in stratigraphy between domains records the evolution of the Apulian continent as a passive continental margin (Carmignani *et al.* 1993). Between middle Triassic and lower Lias, limestones and dolomites were deposited on a carbonate platform which was progressively block-faulted and finally inundated during the middle Lias. Subsidence of the platform was superceded by generation of oceanic crust in the Ligurian Domain and progressive deepening of facies from early Dogger times onwards (middle Jurassic). Facies variation at this time suggest that fault-movement and differential subsidence exerted a strong influence upon sedimentation. A gradual increase in depth of deposition following the cessation of rifting led to the dissolution of $CaCO_3$, and a homogenisation of limestone facies by the Malm.

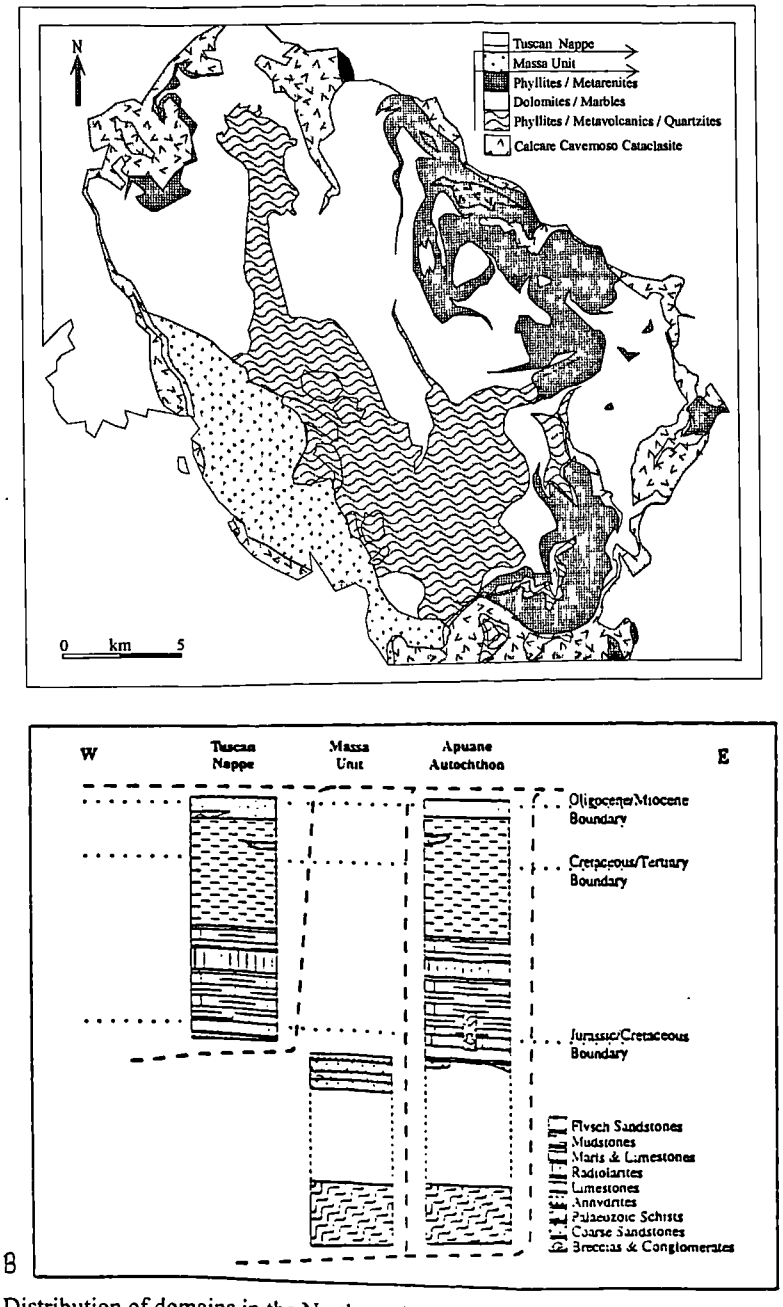

Figure 5.4 (A) Distribution of domains in the Northern Apennines (Carmignani *et al.* 1993). (B) Tectonostratigraphy of the Northern Apennines.

By the end of the lower Cretaceous, the evolution of the Ligurian and Sub-Ligurian Domains diverged from that of domains closer to the continental margin. In the Tuscan Domain, material from the Jurassic carbonate platform was resedimented, with the dominant hemipelagic sedimentation repeatedly punctuated by clastic influxes between the Jurassic and Palaeogene, as carbonaceous and argillaceous flysch passed onto the continental shelf (Carmignani *et al.* 1993).

5.2.3.2 Alpi Apuane

The Alpi Apuane region represents a tectonic window through the Ligurian and Tuscan Nappe and into metamorphic basement rocks (Figure 5.5; Carmignani *et al.* 1994):

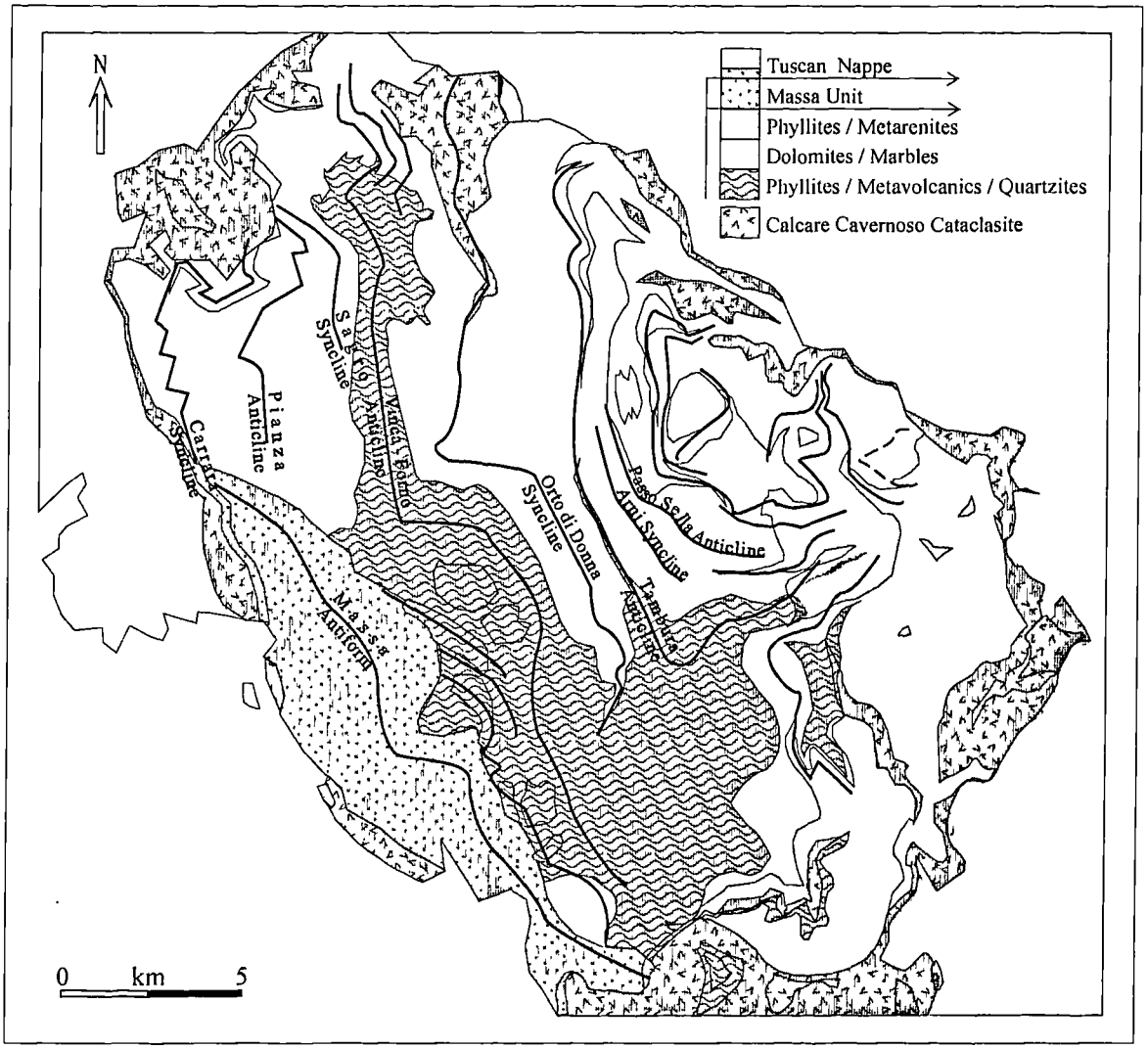

Figure 5.5 Axial trends of F1 isoclines, Apuane Alps (after Carmignani *et al.* 1994).

(1) Palaeozoic - early Mesozoic basement. Sericite ± chlorite quartz-phyllites with lenses of albitic gneiss and porphyritic schists represent metamorphosed Permo-Triassic acid volcanics and sandstones (Giglia 1966) and upper Silurian phyllites and slaty dolomites (Vai 1972). A pre-Alpine deformation phase is recognised in these rocks and is attributed to Hercynian deformation.

(2) Autochthon. Triassic fluvial clastics of the Verrucano and Vinca Formations disconformably overlie metamorphic basement (Cambrian to Triassic). The Verrucano Formation (middle-upper Triassic) consists of conglomerates, coarse sandstones, limestones, mudrocks and muscovitic phyllites (Elter 1966), whilst the Vinca Formation (upper Triassic) comprises feldspathic meta-arenites of variable grainsize interbedded with muscovitic phyllites and grey/red dolomites. Both were deposited within graben during rifting of the Italo-Dinaric margin. Across much of the region, the unconformable boundary between the Verrucano or Vinca and Palaeozoic units represents a time-gap from early Permian to middle Triassic (Cocozza 1965).

(3) Tuscan Basement (Internal Tuscan Domain). Development of a carbonate platform is first seen in upper Triassic strata of the Grezzoni Formation, which crops out widely in the western autochthon and is composed of recrystallised grey dolomites with stromatolitic banding. From a brecciated base, the unit is massive and becomes banded and phyllitic upwards, with its uppermost part characterised by black marbles and tabular shelly dolomites. Limestone facies developed across the Tuscan Domain in the uppermost Triassic and throughout the Jurassic. The upper contact of the Grezzoni is transitional with saccharoidal megalodont marbles which contain bands of muscovite and chlorite. Succeeding them, the Seravezza breccias and chloritic schists are polygenic breccias of marble (and to a lesser extent dolomite), with red-green coloration and a chloritic matrix. They grade laterally into chloritic phyllites with clasts derived from the surrounding carbonates. Lower to middle Liassic dolomitic marbles and crystalline dolomites grade upwards into pure marbles of various colours and faunas, locally containing brecciated horizons. Fine-grained, deep-water sediments characterise the middle Jurassic and upper Cretaceous, reflecting the break-up and inundation of the Jurassic carbonate platform. Carbonaceous phyllites, jasper- and chert-rich marls, polygenic breccias, meta-radiolarites and stratified cherty marls were developed at this time.

The Cretaceous to Eocene period is represented by red and green sericitic schists, muscovitic phyllites, marbles and diaspiric mudstones, and green Cipollini calc-schists with white quartzite nodules. Nummulitic limestones are present at the top of the succession, representing calcareous turbidite influxes into the Tuscan basin. The uppermost unit within the autochthon is the Pseudomacigno Formation; an Upper Oligocene arenaceous flysch unit probably analogous with the Mt. Cervarola sandstones which form part of the nappe cover and recording continental input into the basin from adjacent mountains.

(4) Tuscan Nappe. Upper Triassic to Lower Miocene rocks which have been translated upon an Upper Triassic evaporite horizon; the Calcare Cavernoso Formation (Carmignani and Kligfield 1990). Metamorphic grade is low throughout the sheet reaching anchizone at a maximum, and brittle-ductile

deformation is pervasive. The Calcare Cavernoso Formation is a porous carbonate layer up to 200 metres thick which shows strong brecciation and acted as the dÈcollement. The original lithology of the unit is evident in carbonate-cemented clasts within the cataclasite, displaying dolomite with anhydrite inclusions. The anhydrites form the base to the carbonate platform sequence of upper Triassic to middle Liassic limestones as seen in the autochthon. Rocks of the Jurassic period shows pronounced deepening of facies, with limestones giving way to cherty marls and radiolarian muds. During the period between lower Cretaceous and Oligocene, the Scaglia Toscana was deposited as turbidites and gravity flow deposits within graben. These well-banded, variagated marls and quartzites mark the destruction of the Tuscan basin and its evolution as a foreland trough. The Macigno Formation (upper Oligocene to lower Miocene) at the top of the nappe represents syn-orogenic arenaceous flysch. (Carmignani *et al.* 1994).

(5) Massa Unit. Exposed on the southwestern side of the region, the Massa Unit represents the remnants of a terrane which originated between the Tuscan province and the Adriatic foreland (Carmignani *et al.* 1993). It comprises Palaeozoic greenschists and a Triassic cover sequence which developed during the opening of Tethys in the Triassic. The basement of the unit is very similar to that of the autochthon, being dominated by Cambro-Ordovician muscovite and chlorite schists which were deformed during the Hercynian Orogeny. Cover rocks are middle Triassic in age, and record the transgression of the Italo-Dinaric margin and its 'Verrucano' re-emergence. Calcareous sandstones change upwards into crinoidal limestones and calcareous muscovitic breccias. Middle Triassic albite-basalts are interlayered with a sequence of phyllites, calc-arenites and gravity flow conglomerates. The top of the Massa sheet constitutes fluvial conglomerates and sandstones interlayered with muscovitic meta-pelites (Camelli *et al.* 1993).

5.3 Structural features of the Apuane Alps

5.3.1 Introduction

The Apuane Alps represents a tectonic window through the Liguride and Tuscan Nappes and into polyphase greenschist-grade basement rocks (Table 5.1). Measuring 25 km by 35 km, it has a domal geometry defined by primary cleavage exposing Palaeozoic rocks in its core. The boundary between metamorphic basement and unmetamorphosed cover lies along the Calcare Cavernoso evaporite formation which acted as the master decollément during both compression and extension. Three deformation events have been described from the region by previous workers (Table 5.2).

5.3.2 D1 compression

The Apuane Alps display complex D1 structure (Elter 1960) recording a phase of folding and northeast directed overthrusting (Figure 5.6; Carmignani and Kligfield 1990). A syn-metamorphic schistosity occurs pervasively in basement rocks, axial planar to non-cylindrical isoclinal, recumbent and sometimes

overturned folds, often with sheath-geometries. Fold vergence suggests east to east-northeast overthrusting during the main compressional phase. Carbonaceous and phyllitic rocks record a stretching lineation which trends northeast-southwest, parallel to the vergence of the major folds (Carmignani *et al.* 1993a). The late Triassic Calcare Cavernoso Formation acted as the main décollement during thrusting, and separates very low-grade rocks of the Tuscan Nappe from greenscists of the autochthon and Massa Unit.

Phase	*Age/Epoch*	*Ma*	*Regime*	*Style*
D1	Late Oligocene	34-27	Compression	Brittle thrusting, nappe folding, formation of Apuane antiformal stack.
D2	Mid- Miocene	14-12	Extension	Reactivation of thrusts as low-angle normal faults, asymmetric refolding of D1 structure, phacoidal ductile shear in basement
D3	Post-Tortonian	9-0	Extension	High-angle normal faulting, truncating and reorienting earlier structure, rifting, magmatism and extension in the Tyrrhenian Sea

Table 5.2 Deformation history of the Alpi Apuane region during Alpine orogenesis. (Carmignani and Kligfield 1990).

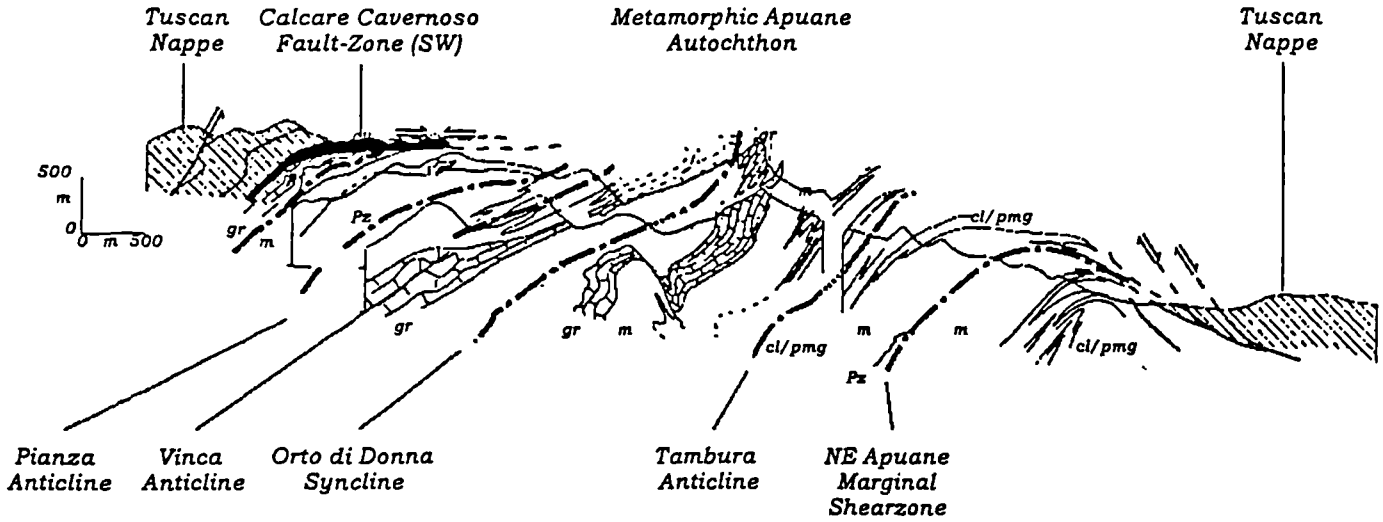

Figure 5.6 Sketch section through the northern Apuane Alps, annotated with F1 axes (solid lines), normal faults (arrows indicate displacement) and lithologies. After Carmignani *et al.* 1993.

5.3.3 D2 extension

D1 structures were refolded during the D2 extensional event, producing complex fold-interference structures and reactivating T1 thrusts as low-angle normal faults. On a regional scale, F2 folds have S-geometries on the southwestern flank of the dome and Z-geometries on its northeastern flank (Figure 5.6; Carmignani and Kligfield 1990). This is corroborated by shear-sense indicators which consistently indicate down to the southwest and down to the northeast top sense of shear on the southwestern and northeastern sides of the dome respectively. The reversal in shear sense occurs across the crest of the D1 dome-

structure. D2 appears to be strongly controlled by the rheology of strata and the orientation and intensity of D1 structures. On the southwestern side of the dome, discrete shear-zones occur along the contacts between competent dolomites and more ductile marbles, whilst on the northeastern side, D1 was more intense and transposed lithological boundaries and subsequently, D2 strain is more evenly distributed (Carmignani and Kligfield 1990).

In the Tuscan Nappe, D2 deformation is mainly brittle, with high- and low-angle normal faults commonly juxtaposing young rocks above old (Carmignani *et al.* 1994). The faults appear listric when reconstructed from outcrop traces and seen to root into the Calcare Cavernoso horizon, effectively isolating the upper crust from lower crust extensional processes. Asymmetrical folds are found but are restricted to specific horizons (immediately above the Calcare Cavernoso, between flysch and Cretaceous rocks and between the Tuscan and Liguride Nappes). Fold vergences are consistent with those of the basement, with conjugate folds seen in areas of F1 culmination.

The Calcare Cavernoso Formation crops out around the perimeter of the dome and appears to have acted as the master décollement during extension as it had during compression, with marls and 'Scaglia' heterolithics focusing additional strain. At its base, it consists of crenulated metamorphic clasts in a cataclastic matrix, with a mylonitic contact locally observed.

The metamorphic basement contains ductile shear-zones formed during the D2 phase and is characterised by folds ranging from kilometre to centimetre scale. Early foliations are crenulated by, transposed by or cut by a second-phase cleavage which produces a NW-SE trending intersection lineation with S0 and S1. The shear-zones are located in weak lithologies and contain a number of shear-sense indicators such as s-c fabrics, σ- and δ- porphyroclast-tail systems, and domino-faults but mainly asymmetric folds. Conjugate shear-zones are encountered in the units of highest metamorphic grade and are though to reflect the style of thinning active in lower levels of the crust (Carmignani *et al.* 1994).

The northeast vergence of D1 nappe-folds is clearly shown, with axial planes dipping ~30 southwest and axes plunging 10-20 north. Post D1 deformation is evident to the south of Mount Grondilice where the hinge of the Orto di Donna / Mount Altissimo Syncline is seen to be refolded and join the Mandriola Fold in the foreground. The major F2 flexure responsible for this type-III interference geometry is located near Resceto. It verges to the southwest, and has an axial plane which plunges ~45 northeast. The inverted limb of the Vinca-Forno Anticline is refolded by a fold-pair in the southeastern slopes of Mount Rasiori (Carmignani *et al.* 1993), the dolomites, marbles and phyllites of which show great structural complexity. Carmignani *et al.* (1993) suggest that this complexity is due to the presence of a ductile transfer zone in the Frigido Valley relating to D3, as is evident from an offset of boundaries in plan view and a 25 strike swing of D2 axis (*16/351* to the southwest and *30/326* to the northeast). The interference structures must thus be considerably more complex than the coaxial style thus far considered.

5.3.4 D3 extension

The third phase of deformation (D3) began during the Messinian (uppermost Miocene), with steep normal faults cutting and reorienting Alpine features and forming the graben which border the region to the east (Serchio Valley) and west (Magra Valley). The faults locally dissect the Calcare Cavernoso Formation, indicating that it was inactive by this time. The Serchio and Magra valleys are filled by Quaternary strata and consequently, deformation must predate this stage. The distribution of post-Miocene graben features is shown in Figure 5.7, the NW-SE trending graben axes running parallel to the structural grain (i.e. strike).

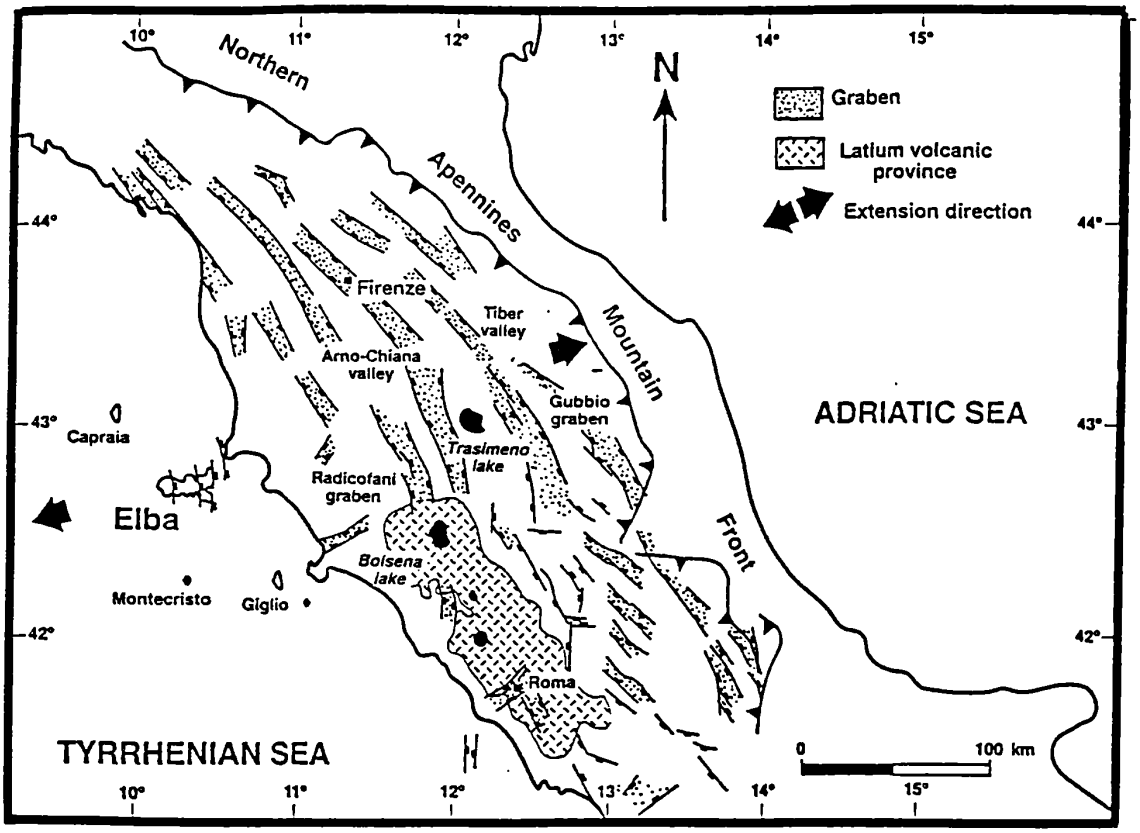

Figure 5.7 Quaternary graben in northern Italy (Keller 1994).

5.4 Observations of late-orogenic extension

The following section records observations made during fieldwork in the Apuane region in May 1995. Localities visited (Figure 5.8) were chosen under the guidance of Prof. L. Carmignani and Dr. M. Meccheri of the University of Siena with reference to the excursion guide '*Tettonica distensiva del Complesso Metamorphico Apuano*' (Carmignani *et al.* 1993). Each section examines the style and magnitude of extension at a variety of structural depths in a separate tectonostratigraphic unit.

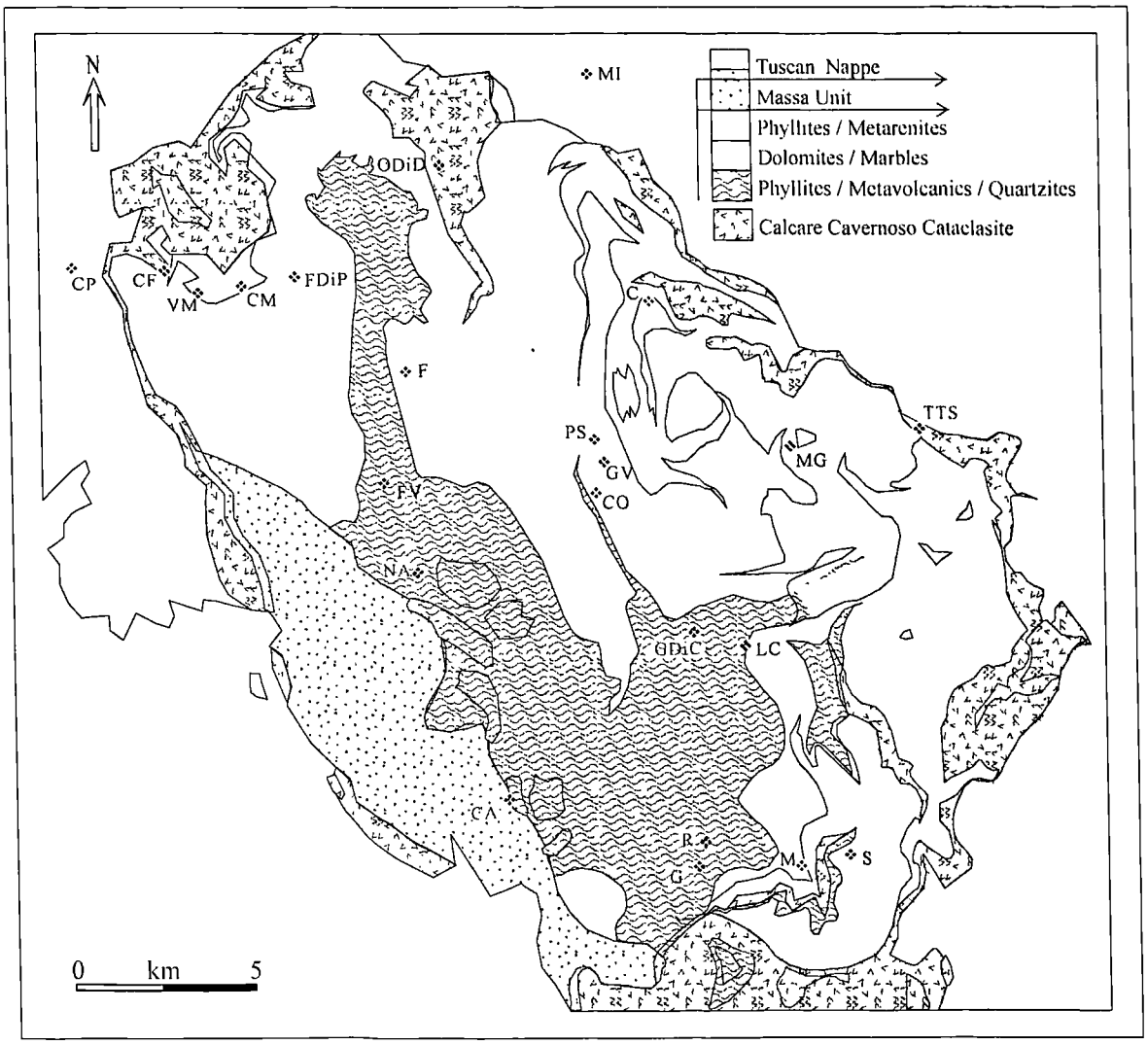

Figure 5.8 Field locality map (geology after Carmignani *et al.* 1993). **Basement** : R - Ruosina; G - Gallena; FV - Frigido Valley; GDiC - Galleria del Cipollaio; F - Forno, Coll dei Botticini; LC - La Croce; CO - Campo dell Orzo, Arni; GV - Galleria di Valsora; PS - Passo Sella; M - Mullina; S - Stazzema; C - Castagnola; MG - Mount Grotti; ODiD - Orto di Donna; FDiP - Foce di Pianza, Campocecina; CM - Cave del Morlungo, Campocecina; VM - Via Martiri della Liberta; NA - Northwest Antona. **Calcare Cavernoso fault-zone** : CF - Capanne Ferrari; TTS - Torrente Turrite Secca. **Massa Unit** : CA - Castello Aghinolfi. **Tuscan Nappe** : CP - Castelpoggio; MI - Minucciano.

5.4.1 Extensional structures within basement rocks

The style of extensional deformation structures is extremely varied in the Tuscan Metamorphic Complex reflecting heterogeneity in bulk rheology generated by lithological variation and changes in metamorphic grade. Localities described are grouped by style of deformation (see Figure 5.8), with zones of highest metamorphic grade considered, followed by areas closer to the basement-cover contact (i.e. the Calcare Cavernoso Formation).

5.4.1.1 Deep basement structures

The deepest structural level exposed in the Apuane Alps is represented by Palaeozoic phyllites, quartzites, metavolcanics and schists exposed at the centre of the metamorphic complex. This structural zone was studied at Ruosina, Gallena, North Antona and Forno. Two distinct styles of extension were observed:

- Conjugate ductile shear-zones separating lozenges of low (extensional) strain, typified by structures exposed in the Ruosina roadcut.
- Non-coaxial ductile shear focused into the primary (S1) cleavage, typified by structures exposed at Gallena, North Antona and in Frigido Valley, Forno.

Ruosina shear-zones

The roadcut at Ruosina was first picked out by Carmignani and Kligfield (1990), who identified two post-S1 fabrics. Deformation within the micaceous schists is intense and ductile in character, with conjugate shear-zones dipping northeast and southwest (Plate 5.1; Figure 5.9). S-C fabrics and porphyroclasts generated by attenuation of V1 veins are identified alongside a slaty late cleavage which locally transposes the S1 fabric. Carmignani and Kligfield (1990) maintain that the shear-zones provide insight into deformation mechanisms in the middle crust during extension, providing meso-scale analogues to the macro-scale structures which have accommodated D2 extension. If this analogue is accurate, opposed extensional transport directions in the upper crust formed synchronously with ductile shear in the middle crust. Seismic refraction studies of Tuscany identify lozenge-shaped featured close to the MOHO and thus support the hypothesis that the deep basement preserves mid to lower crustal textures developed during extensional exhumation and unroofing of the basement.

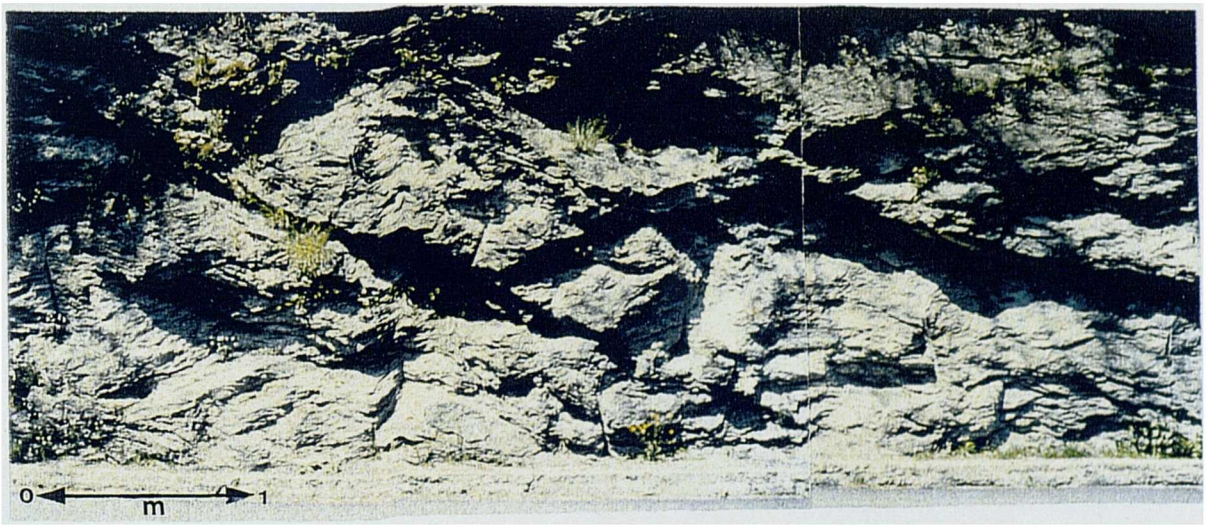

Plate 5.1 Conjugate shear-zones developed in basement phyllites, Ruosina. See Figure 5.9 for sketch and explanation.

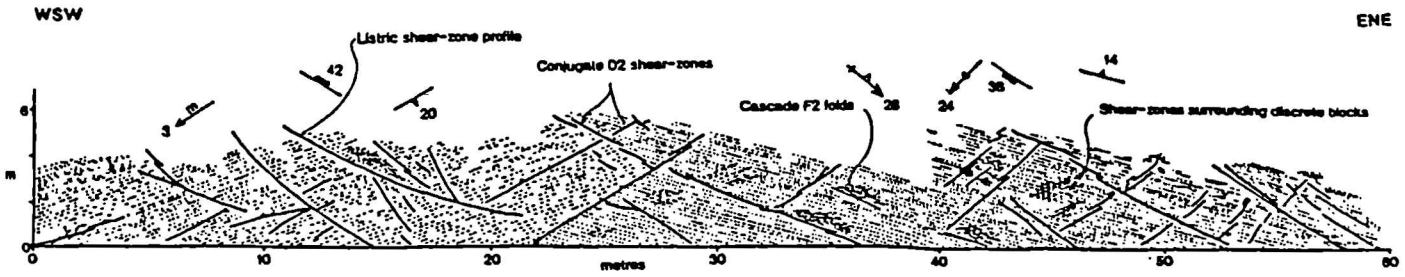

Figure 5.9 Field-sketch of folding in schistosity of Ordovician phyllites, south Forno. Folds verge NE and are thus thought to be D1 in age and overprinting a Hercynian schistosity. Ductile shear-zones cutting long-limbs are thought to be D2 in age.

Thin section analysis of the schists reveals a quartz-calcite-muscovite mineralogy (60%-25%-15%; Plate 5.2). Quartz grains show weak sub-graining, contain calcite/sericite inclusions and have lobate boundaries indicative of grain boundary recrystallisation at 300-400°C, whilst calcite grains (assimilated veins?) are untwinned and again have lobate boundaries. Muscovite occurs in phyllonite bands and defines a type-II extensional crenulation cleavage (Plate 5.2). Only one cleavage phase is seen, suggesting that transposition occurred during shear along an earlier fabric.

Plate 5.2 Type-II S-C fabric indicating top to the left (down S1-dip) shear. Width of view 2 mms.

Close examination of the shear-zones shows that northeast-dipping examples consistently crosscut their conjugate equivalents and therefore appear to have remained active after ductile attenuation had ceased. Furthermore, drag-folds observed within the slaty (S2) cleavage consistently verge northeast. They are therefore unlikely to have been generated concurrently with the conjugate shear-zones which would be

expected to produce folds of both vergence-senses. It is more probable that the folds are slightly younger than the conjugate shears and reflect progressive embrittlement of structures through time accompanied by a switch to non-coaxial shear.

Non-coaxial shear deformation

Gallena: Palaeozoic Phyllites reveal ductile D2 features including S-C fabrics (top to the east shear), porphyroclast-tail systems and S2 crenulation. Asymmetric folds of S1, where seen, have a west-sense of vergence. To the north-northwest at Forno, Ordovician porphyritic schists and Cambro-Ordovician phyllites are pervasively cleaved and strongly contorted by F2 folds. Quartz-veins pick out apparent northeast verging, decimetre scale folds of steeply-dipping (Hercynoid) fabric. Ductile extensional shear-zones cut along the long limbs of the folds and may be responsible for anomalous steepness of the fabric.

Calc-schists exposed at the mouth of the Cipollaio tunnel show evidence of high D2 strain. S1 foliation is again strongly folded by asymmetrical (NW-verging) F2 folds with highly curvilinear axes. Long limbs are characterised by a transposing S2 cleavage and an intense mineral lineation. This fabric is itself cut by shear-bands which again produce top to the northwest offsets. Calcareous bands within the schists show ductile D2 shear in a series of σ-porphyroclasts consistent with top to the north-northwest shear. A dramatic change in structural style occurs over the boundary with the Grezzoni formation. The effects of D2 die out less than two metres into the dolomites, with brittle deformation in the form of northwest-dipping normal faults. Deformation style is thus demonstrated to be lithologically influenced, with ductile strains accommodated by micaceous schists.

Forno: The boundary between Ordovician schists and Grezzoni dolomites is again exposed at Coll dei Botticini, Forno. The unconformity is separated at this locality by a layer of schists and breccias up to 25 metres thick (Seravezza Breccias), consisting of imbricated clasts of dolomite and marble within a matrix of green chloritic phyllites (Plate 5.3A,B). Within the peraluminous schists, a gold-weathering mica is seen to form elongate masses parallel to the long axes of clasts, whilst chloritoid (formed through alteration of lateritic material; Giglia and Trevisan 1967) shows no clear elongation in argillaceous layers. This suggests that the first cleavage event was related to mica growth, and that peak metamorphic conditions (chloritoid formation) occurred after D1 at low strain rates. The Seravezza Breccias (interspersed with black chloritoid schists) contain clasts with aspect ratios of 15:1 which define a subvertical mineral lineation within a north-south trending, subvertical cleavage (Figure 5.10). The plastic deformation of clasts has an orientation which is anomalous to the normal D1-trend, indicating that it has been strongly reoriented through superposition of D2 strain. A subhorizontal crenulation lineation on the S1 fabric indicates the reactivation of early foliation in a downdip (westward) sense. Closer examination of the conglomerates reveals sub-vertically-plunging folds which produce sinistral (west-vergent) cleavage-bedding relationships. This regime is also evident from thin-section analysis of the schists, in which sinistral

porphyroclasts are developed with calcite cores and mica tails. Continuing to the northeast, the lithology changes to massive dolomites, again with no evident internal deformation.

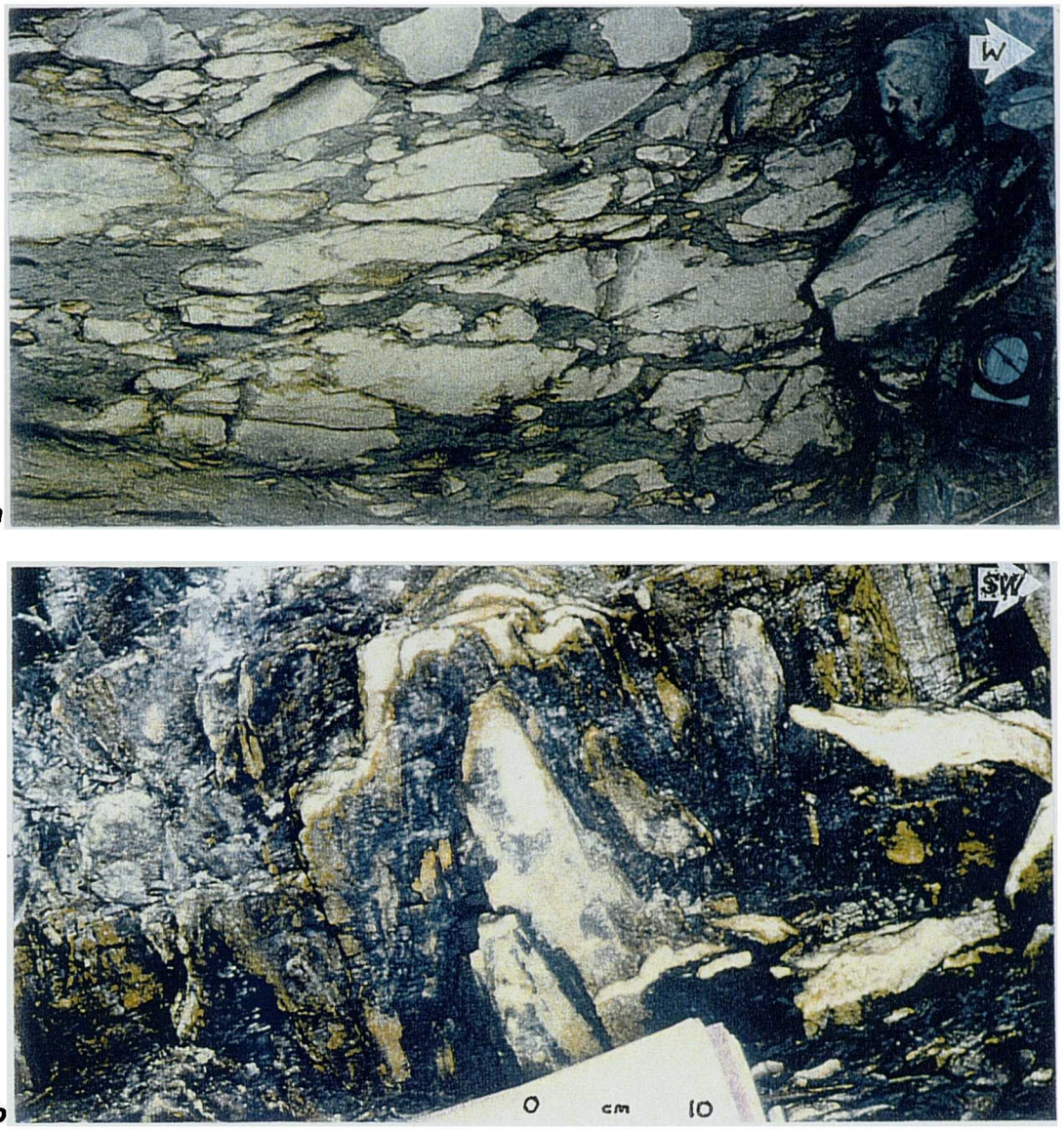

Plate 5.3 Deformed conglomerate, displaying steeply inclined prolate marble ellipsoids in a chloritoid-rich matrix; Coll dei Botticini. (A) XY-plane. (B) YZ-plane.

5.4.1.2 Mid- to upper- basement structures

Extensional structures within the Tuscan basement may be subdivided into three groups on the basis of dominant deformation styles observed:

- Diffuse strain through rocks, producing shape fabrics, exhibited by lithologies with low competence contrast (e.g. marble breccias) and exemplified by structures at Mulina.
- Strain focused along S1/S0 anisotropy, typified by detachment systems exposed at La Croce, Orto di Donna, Passo Sella and Via Martiri della Liberta.

- Intense shear along S0 producing semi-brittle features, exhibited by structures at Monte Grotti, Capanne di Careggine.

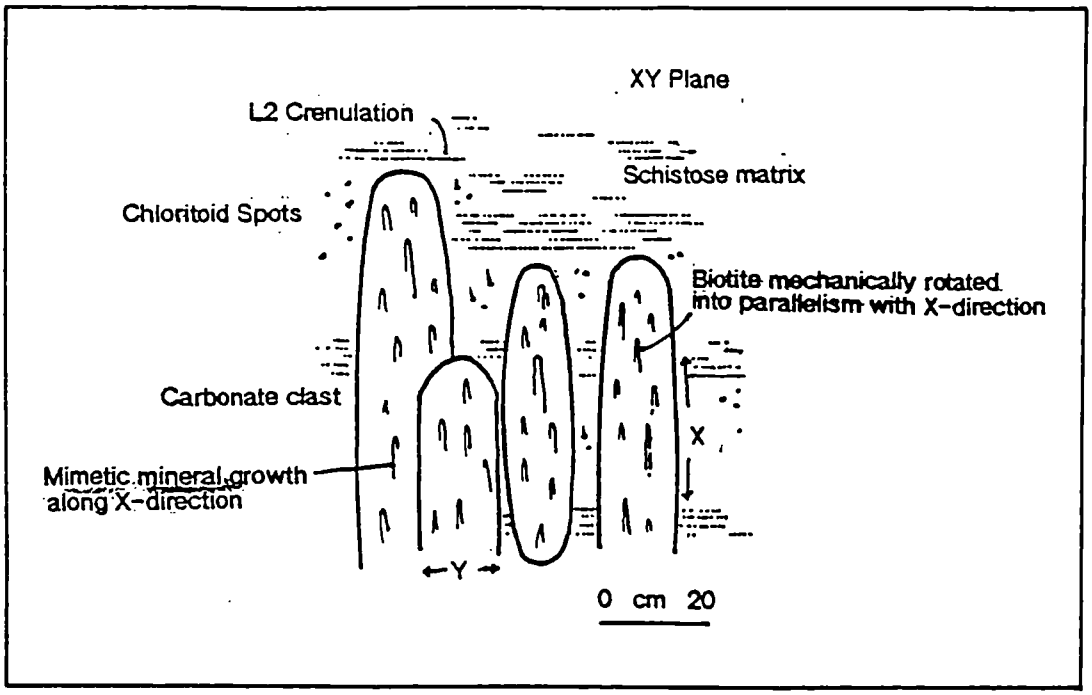

Figure 5.10 Structural elements of the Seravezza Breccias (after field sketch).

Diffuse ductile strains

Mullina: On the banks of the Molina river, Triassic marbles and marble-breccias exhibit a strong shape fabric. Cut faces provide sections through the X:Z and Y:Z planes of the breccias, and it is evident that X:Z ratios reach over 20:1 and Y:Z ratios are approximately 3:1. The XY aspect plane (S2) dips moderately to the southeast, whilst X-axes plunge shallowly to the south-southeast. Non-coaxial prolate strain was directed either down to the south-southeast or up to the north-northwest. Minor asymmetric folds of the marble fabric also verge southeast and deform the marble shape fabric, suggesting that deformation switched from diffuse to layer-parallel through time and was directed down the dip of S1 fabric.

Detachment systems

Where heterolithic units are exposed, extensional strain is commonly partitioned into bed- or S1- parallel detachments evident from drag-folding, Riedel fracture arrays, veins and secondary cleavages developed adjacent to the slip planes.

Monte Corchia: Palaeozoic schists on the western flank of Monte Corchia provide exposures of typical D2 structures developed within rocks with very strong S1 anisotropy. The locality lies on the eastern flank of the S1 cleavage dome close to the base of the Triassic carbonate sequence. D2 deformation is a series of minor asymmetrical folds of S1 schistosity nucleating along foliation-parallel detachments (Figure 5.15).

Close, chevron F2 folds with parasitic monoclines are observed in areas of moderate strain and in competant lithologies whilst chaotic fold packages bounded by detachments are developed in phyllitic media (Plate 5.4). In each case, the folds verge down the dip of minor detachments along the S1 cleavage, with the most intense deformation focused into interbedded strata of high competance contrast. Within higher strain zones, quartz-veins of pre-S2 age show top to the southwest rotation, are domino-faulted and s-c fabrics and s-porphyroclasts (dextral sense, top to the east-southeast) are developed. An S2 cleavage is present in high strain zones and is seen to be axial planar to folds, but is weaker and more patchy in the carbonates.

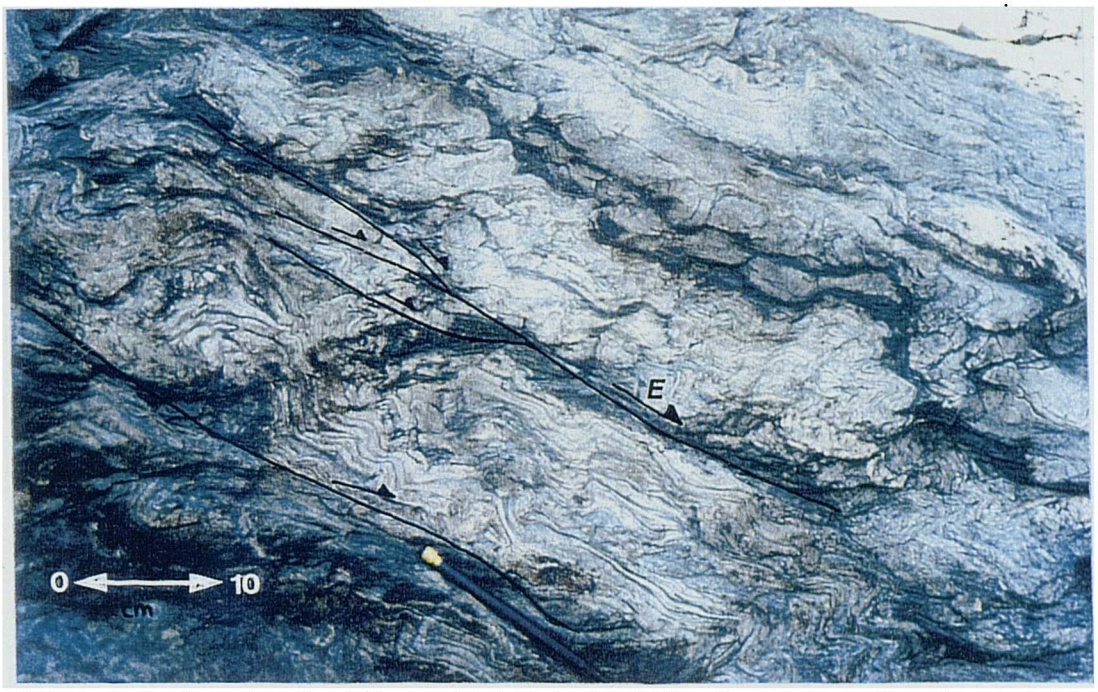

Plate 5.4 Shallowly east-southeast-dipping detachment with folding focused into deformation zone. Note the presence of minor shear-planes and down-dip sense of fold vergence.

Orto di Donna: Very similar D2 structures are exposed within the the core of the Orto di Donna syncline. The lithologies exposed include sericitic schists, cherty limestones, *Diaspirite*, and cherty limestones. Sericitic schists within the hinge of the Orto di Donna syncline show a range of features which are characteristic of late deformation in the basement (Figure 5.11; Plates 5.5A,B). The well developed, moderately west or southwest dipping S1 schistosity has been affected to a varying degree by D2. In low strain regions, the schistosity has been crenulated to form a strong lineation plunging to the west-northwest, whilst in zones of higher strain, F2 folds of S1 fabric with WSW vergence and axes plunging shallowly to the northwest are seen above S1-parallel normal detachments (Plate 5.5). A patchy S2 cleavage is seen and transposes the earlier fabrics in extreme cases, with S1 only identifiable in microlithons.

Moving northwards, the S2-foliation swings round to an E-W strike and northerly dip, with intensification of S2 cleavage and hence of the northwest-dipping intersection lineation, thus defining the closure of the F1 fold. Where sericitic schists are interbedded with limestone and chert, the dominant mode of D2

deformation is ruck-folding and S1-parallel movement (Figure 5.11). These folds have thick short limbs and thin long limbs, with domino-faults in dolomitic bands and shear-bands in the schists (Plate 5.5).

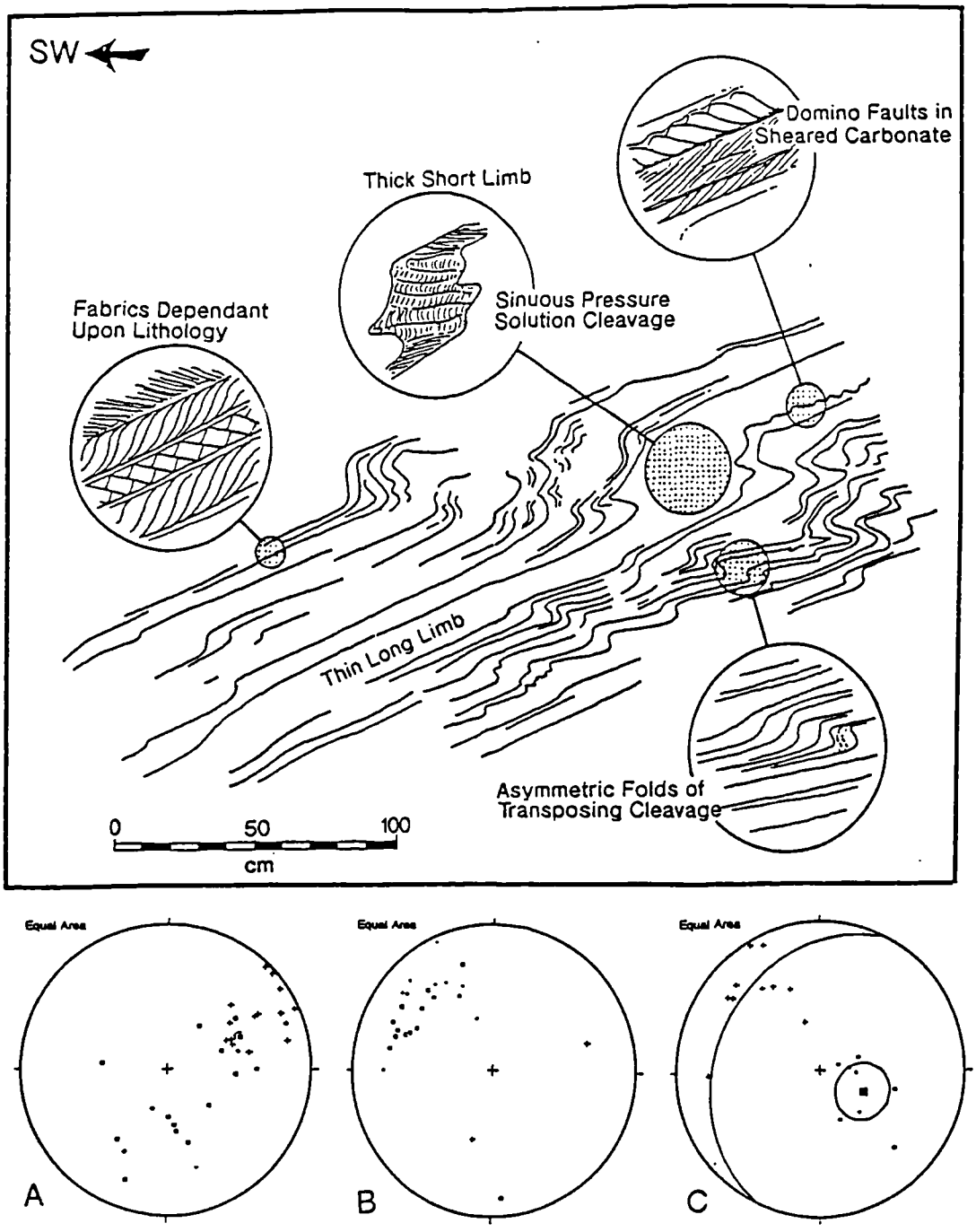

Figure 5.11 Ruck-folding in calc-schists, Orto di Donna. Stereoplot A shows poles to fabrics (dots = S0 (5), crosses = S1 (15), squares = S2 (10)), stereoplot B shows lineations (dots = L1 (2), crosses = ML (2), squares = L2 (11), small dots = F2 axes (9)), stereoplot C shows D2 fold data (dots = poles to F2 axial planes (7), crosses = F2 fold-axes (10)).

a

b

Plate 5.5 Folds developed above shallowly-dipping, S1 cleavage-parallel detachments, Orto di Donna. (A) Folding style in marbles showing thick short limbs and attenuated long limbs. (B) Detail of long fold limb, displaying subhorizontal pressure solution cleavage axial-planar to F2 folds.

Passo Sella: Quarry tracks leading northwards into the high mountains from the village of Arni provide access to a series of exposures which represent deep levels of the basement beneath the Tambura Thrust. Lithologies include marbles, jasper-rich bands, dolostones and Scaglia Toscana, with the dominant S1 cleavage subparallel to stratigraphic layering. This is a consequence of isoclinal F1 folding as is clearly seen in repeated closures of jasper beds seen from Arni village in the southwestern slopes of Mount Sella (Plate 5.6)

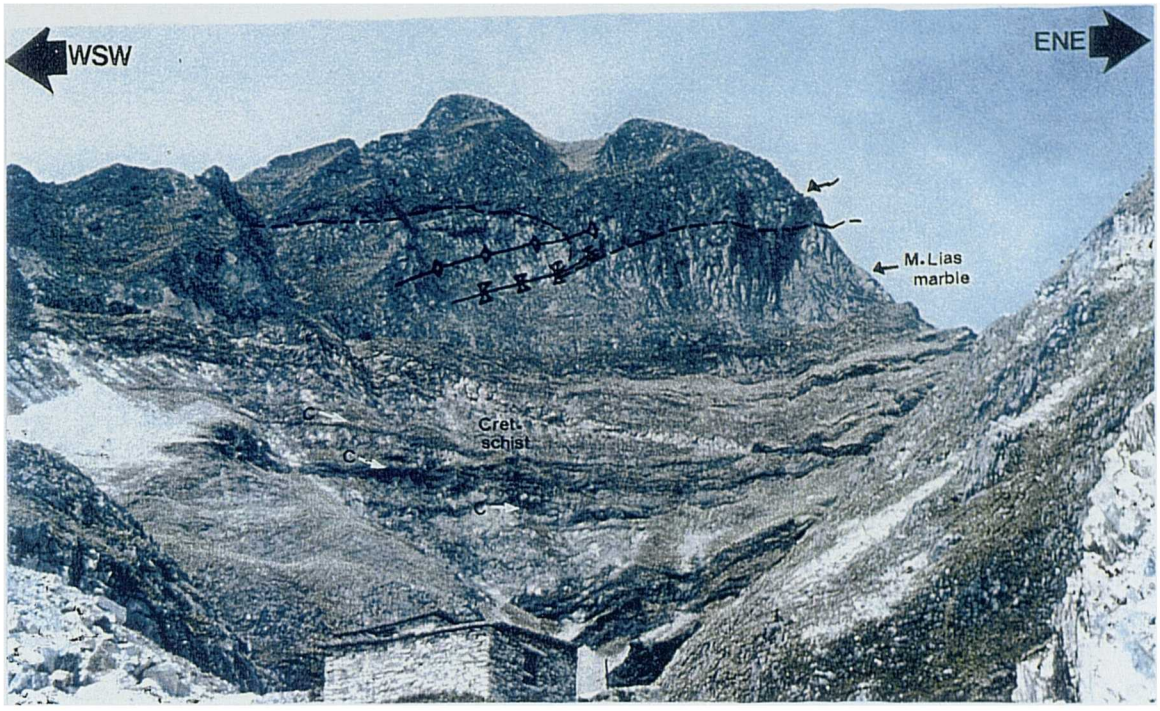

Plate 5.6 View NNW to Monte Sella. Note prominent jasper beds in hillside, terminating in F1 isoclinal hinges.

Stratigraphic repetition of up to 15 times is recorded in the southeastern flanks of Mount Sella (Meccheri *pers. comm.* 1995), with D1 structures refolded by northwest-verging close F2 folds (Figure 5.12; the Arni Syncline and Passo Sella Anticline). The Scaglia units at Passo Sella record the polyphase deformation of the region through a variety of shear criteria including the geometry of porphyroclast systems, the asymmetry of minor folds of S1 cleavage and the sense of offset in bookshelf microfault arrays. The northwest-verging intrafolial folds are most commonly developed in finely interbedded schists and impure marbles and are strongly sheathed, their axes rotating towards parallelism with the regional stretching lineation. This indicates the very high magnitude of ductile strain which occurred during the D2 extensional event.

Via della Liberta: This locality exposes mudstones, siltstones and sandstones of the Scaglia Formation, strongly deformed by D2 structures. The most conspicuous features are a series of asymmetric F2 chevron folds which verge southwest (Figure 5.13), and whilst only one phase of folding is evident at first glance, more careful observation reveals that F1 isoclines are present, and that the dominant fabric is thus a composite S0/S1 schistosity. Layer thickness changes abruptly between F2 fold limbs, with the short limbs being thicker than the long limbs by a ratio of 3:1. Out-of-fold thrusts occur through the hinge regions of the tighter chevrons, where over 35% shortening has occurred with respect to individual sandstone horizons.

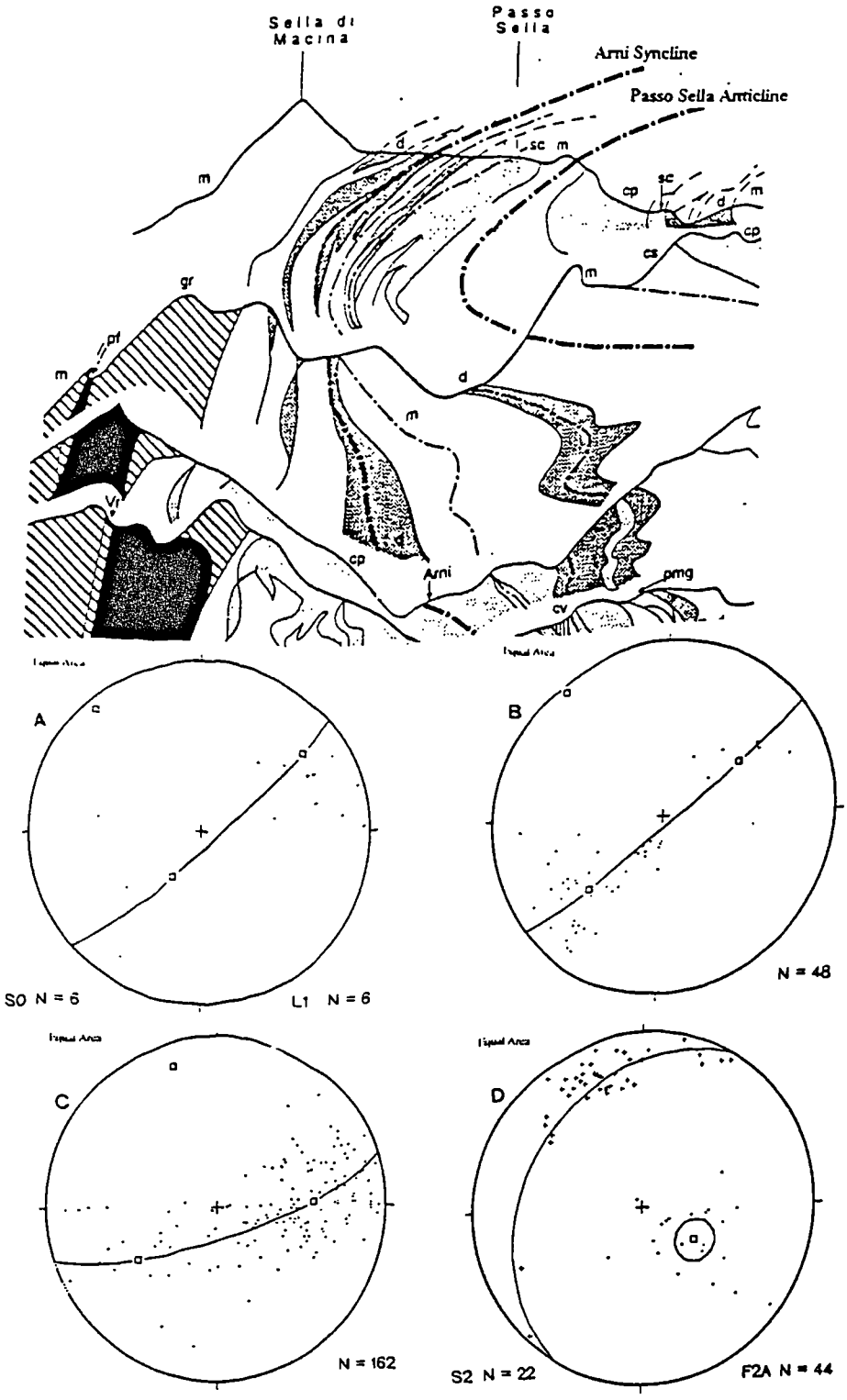

Figure 5.12 Structural data from the Passo Sella area, compiled from field data and measurements by Carmignani *et al.* 1993. Geological panorama from Carmignani *et al.* 1993; m, Marble; pf, Porphyroidal schists; Gr, Grezzoni; Vr, Verrucano; d, Diaspiri; sc, Sericitic schist; cp, Cipollini; cv, Calcare Cavernoso; pmg, Pseudomacigno. (A) Scatter plot of poles to S0 layering (crosses) and of L1 intersection lineation (dots). Girdle shows reorientation of F1 axes during D2. Cleavage is seen to dip uniformly to the WSW, reflecting the isoclinal nature of F1 folds. (B) Scatter plot of mineral lineations (D1), with girdle distribution from F2 refolding. (C) Scatter plot of poles to S1 foliation, again showing a girdle distribution (D2 refolding). (D) Scatter plot of poles to S2 cleavage (dots) and of F2 fold axes (crosses). Great circle marks mean S2 foliation. The diffuse distribution of fold axes is a consequence of their sheath geometries, and the poor clustering of S2 reflects the variation in orientation of F2 fold axial planes.

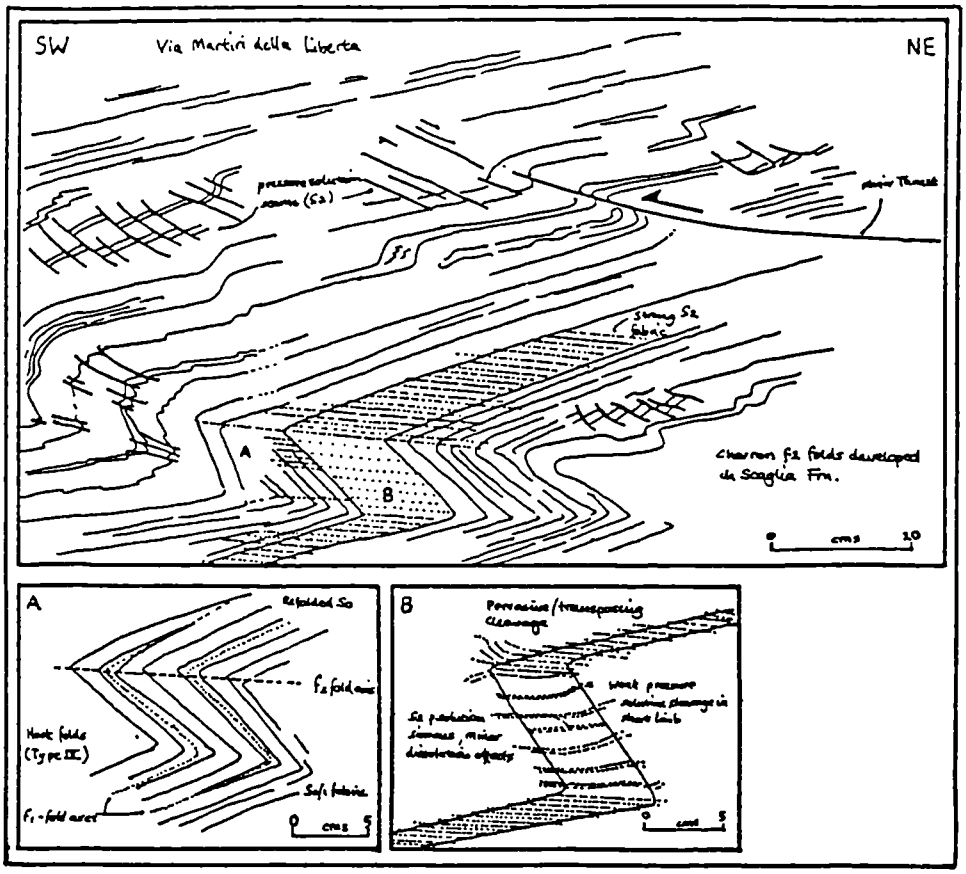

Figure 5.13 F2 chevron folds, Via Martiri Della Liberta. (A) Detail of F1 folds within composite S0/1 fabric. (B) S2 cleavage characteristics across F2 fold limbs.

The folds have a weak, subhorizontal S2 cleavage developed in their short limbs, and a pervasive and locally transposing pressure solution S2 cleavage in their boudinaged long limbs, suggesting that the folds were generated by ductile shear subparallel to S1 and hence the long limbs. The S2 cleavage steepens away from the fold hinges until it dips moderately northeast, and the pressure-solution offsets it produces across chert bands forms the appearance of northeast-extending domino faults (Plate 5.5B).

Bed-parallel semi-brittle deformation zones

D2 deformation within beds of extreme competence contrast is typified by domino-faulting and extensional shear-banding as demonstrated at *Monte Grotti.* Where the prevailing cleavage is inclined at a shallow angle, the impure limestones and marbles reveal flat-lying F1 isoclines, but where the foliation is steeply-dipping, chert bands are boudinaged and offset by domino-faults, cut by dextral calcite tension-gashes and folded by dm-scale flexures, all of which indicate top to the northeast shear (Plate 5.7). Extensional strain is only intense in these steep belts, and they appear therefore to form where bedding is anomalously steep. When traced laterally, the steep zones are seen to have a similar orientation to D2 faults and it is thus likely that they represent the semi-ductile equivalent to these faults. Boudinage within the chert bands, whilst causing attenuation of the primary lamination, is likely to pre-date the D2 shear-event. It is seen across the

steep and shallow cleavage domains and boudin necks appear to have caused the nucleation of D2 folding. The D2 folds have sheath geometries and thus suggest strong ductile shear within the less competent limestones.

Plate 5.7 Rotated rigid chert blocks in calcite matrix developed through shear along steep bedding in extensional shear-zone, Monte Grotti. Right = northeast.

5.4.2 Extensional deformation of the Calcare Cavernoso Formation

The Calcare Cavernoso Formation is of fundamental importance in the regional geology of the Apuane Alps when macro-scale observations of nappe fold geometry, the distribution of metamorphic rocks and dating criteria are considered. Exposure-scale features are not commonly observed due to the extensive dolomitisation which has affected the evaporites. The formation was examined at *Capanne Ferrari* , where roadcuts expose a section through the boundary between greenschist basement rocks and the over-riding Tuscan Nappe. The Calcare Cavernoso Formation contains abundant blocks of dolomite, limestone and anhydrite derived from formations on either side of the fault-zone. The exposure may therefore represent cataclasites generated through movement of the Tuscan Nappe.

Whilst the Calcare Cavernoso was originally an evaporite horizon, subsequent deformation, alteration and erosion has replaced ~85% of the exposures here with a rubbly limestone breccia in a red mud matrix. The matrix colour, imbrication and angular nature of clasts suggests that the formation has been resedimented in caves. The remnant grey breccias of the Calcare Cavernoso are careous weathering angular breccias with a careous weathering nature. A crude foliation is noted in more coherent zones, with grey-white evaporites flattened into a crude S1 foliation. Elsewhere, clasts contain internal foliation and thus must have experienced a compressive phase prior to their cataclasis; i.e. that cataclasis occurred during D2

reactivation. The weathered nature of the outcrop makes kinematic analysis difficult, but high- and low-angle faults are distinguishable in the breccias. Intense brittle deformation appears concentrated into the upper boundary of the breccias, but the extensional nature of the zone as a whole may only be inferred by stratigraphic offset.

The contact between the Tuscan Nappe and the underlying metamorphic complex is visible on a larger-scale from Foce di Pianza, Campocecina. Looking west to Mount Borla, Mount Pessaro and Mount Uccelliera from the tunnel mouth of the Boscacchio marble quarry, a panorama is exposed through the Carrara syncline; a refolded isoclinal F1 fold, facing and verging up to the NE. The core of the structure contains sericitic schists of the Scaglia Tuscana Formation, surrounded by a conspicuous conglomerate band of quartzite clasts in a calcite cement, then a large thickness of marbles and cherty limestones. Small klippes of Calcare Cavernoso evaporite are exposed along the summit ridge of Mount Borla - Zucco del Latte, forming banded, dark-weathering knolls.

The Carrara syncline shows type-III (coaxial) interference folding in the Morlungo area (Figure 5.14; Plate 5.8), where a SW-verging fold-pair refolds the right-way-up limb of a parasitic z-fold to the main syncline. The F2 folds occur within 200 metres of the Calcare Cavernoso fault-zone, and thus may be explained as drag-folds produced during normal faulting within the evaporite horizon. The coaxial nature of refolding implies that normal reactivation of the dÈcollement occurred through movement diametrically opposed to the initial thrust-transport; the Tuscan Nappe slid back down existing thrusts as an extensional regime was exerted. Further evidence for a SW-directed D2 event is seen in faults within the marble units, dipping moderately SSW and with normal slickenlines plunging toward 209 N. Within interbedded limestones, siltstones and quartzites of the Scaglia Formation, F2 folds with sheath-like geometries are developed, verging modally towards 188 N, down the sheet dip of the bedding (211 N).

In thin section, the Liassic marbles are seen to be largely monominerallic and composed of equant calcite crystals with a regular ~ 0.15 mm grain-diameter. The calcite grains contain very fine opaque inclusions along cleavage planes and are strongly twinned. The twinning process appears to be related to crystallisation rather than deformation, as twin planes are regular in form and extend across the full width of each grain. There is no crystal preferred orientation to the crystal lattice or the twin planes, as evidenced by random colours when viewed in cross-polarised light through a sensitive tint plate. Grain boundaries are straight, forming 120° triple junctions and an annealed deformation microstructure. This suggests that the temperature remained elevated at above 300°C for some time after deformation and relates to dynamic recrystallisation with low applied stress, destroying any CPO fabric present following D1 or D2 deformation.

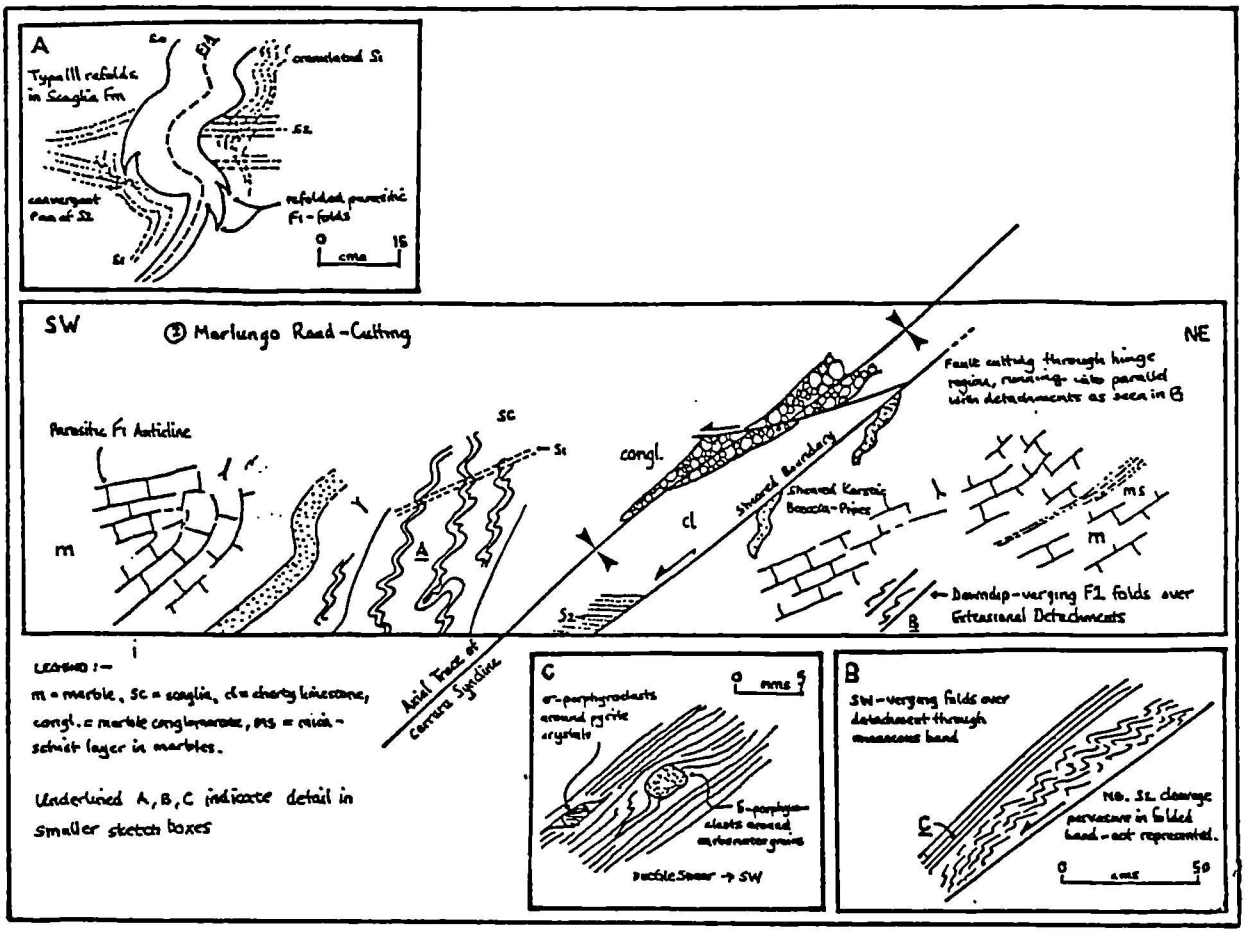

Figure 5.14 Sketch of structures exposed at Morlungo displaying down S0/1 non-coaxial shear-products.

Plate 5.8 Refolded F1 isocline, Morlungo. Fold axes indicated by annotated lines.

5.4.3 Extensional deformation style in allochthon

Massa Unit

Due east of the coll at Castello Aghinolfi, road-cuttings cross the contact between the Massa Unit and the allochthonous Tuscan Nappe. The Massa Unit is largely composed of quartzites containing a schistosity of aligned white micas, defining a steep early foliation dipping to the west. A mineral lineation of stretched quartz aggregates plunges moderately to steeply down the S1 cleavage towards the southwest (226 N). The coarse sandstones show abundant top-to-the west post-D1 shear criteria, with extensional crenulation cleavages, s-porphyroclasts and ductile shear-zones observed. S2 crenulation cleavage is commonly seen, its intersection with S1 subparallel to ML1. The D2 fabric dips shallowly to the west, thus indicating west/southwest cleavage vergence.

Recrystallised calc-rudites are encountered immediately below the contact with the Tuscan Nappe, and despite the intense elongation of clasts, the S1 foliation retains the strong mineral lineation with quartz clasts stretched symmetrically along the main fabric. Bedding planes are preserved as rusty horizons which show up to 35% layer-parallel extension. The base of the Tuscan Nappe consists of careous-weathering brecciated limestones overlain by thickly-bedded white limestones. The contact displays intense extension through both shear-zones and normal faults, with the transport direction again to the southwest.

Tuscan Nappe

Extensional structures exposed in the low-grade Tuscan Nappe show more brittle geometries, with more subtle fabric development and abundant normal faulting. Localities were studied on both the west and the east of the complex (at Castelpoggio and Minucciano; Figure 5.8) as described below:

Castelpoggio: At the roadside to the northeast of Faglia della Foces, the contact between the Diaspiri Cherts and the Scaglia Formation is exposed, showing the interference of D1 and D2 structures. Deformation in the unmetamorphosed Tuscan Nappe often proves more subtle than in basement units as the folds associated with both events occur on a large-scale (l=100s m). In such cases, the general structure is identifiable through analysis of cleavage vergence relationships.

Starting within the *Calcari ad Angulati* Formation, a primary tectonic foliation (S1) is pervasively developed at a low-angle to bedding within fine-grained horizons, whilst it forms a weaker fabric in sandy layers at a higher angle to S0. S0 and S1 consistently dip to the southwest, the more steeply-dipping fabric being S1. This relationship is observed throughout most of the Tuscan Nappe, confirming that tectonic transport was towards the northeast during D1 deformation. A change in cleavage vergence occurs at the first hairpin bend, where the S0/S1 relationship is overturned with S0 horizontal and S1 dipping west. S2 is

represented by a patchy, subhorizontal spaced pressure solution fabric within competent layers and along bedding contacts, producing crenulations within S1. It has a constant orientation, lying parallel to the fold axial plane, and the cleavage vergence suggests southwesterly transport. The Castelpoggio fold is thus D2 in age and refolds uninverted strata.

In addition to the S2 fabric, post-D1 conjugate kink-bands are observed within fine-grained horizons. They appear related to a phase of reverse faulting which has caused layer-parallel extension. The faults show carbonate mineralisation which may derive from material released during formation of the S2 pressure solution cleavage

Minucciano: This locality is situated at a boundary between the *Calcari ad Angulata* limestone formation and *Macigno* carbonaceous flysch sandstones. The contact is tectonic, with normal faulting causing the omission of Lower Liassic to Oligocene strata within the Tuscan Nappe sequence. D1 deformation is seen in folds of the bedding-parallel colour banding within the impure marbles, forming a fold girdle with a pole of 13/132, parallel to F1 *and* F2 fold axes. The poles to compositional banding are evenly spread along the profile plane, indicating that fold-hinges are rounded, in contrast to the exposed large-scale folds seen on the western side of the Apuane region. S1 cleavage is weakly developed in the limestones, dipping shallowly to the west (*174/28W*) and producing a shallowly northwest-plunging intersection lineation (*16/299*). The cleavage-bedding relationship is variable but is regionally consistent with ENE vergence of F1 folds.

Post D1 deformation is apparent only in the normal faulting separating lithologies at this locality. The fault-surface is not exposed and is inferred mainly from stratigraphic omission. Its trace may be mapped as a band of orange-weathering sandstones along the eastern side of the contact surrounded by beige-coloured Macigno sandstones.

5.5 Discussion

5.5.1 Metamorphism

Both D1 and D2 are associated with syntectonic greenschist facies metamorphism in the basement rocks and by very low-grade metamorphism in the Tuscan and Ligurian Nappes. In the basement, D1 thrusting was accompanied by the growth of muscovite, paragonite, biotite, quartz and chlorite, whilst D2 extension prompted the growth of chloritoid, kyanite and epidote, K-feldspars, chlorite and carbonates. Chloritoid and kyanite are seen to have grown during formation of the S2-cleavage, and hence the peak grade appears to have been reached early in the D2 phase. Mica fabrics dated by Ar-Ar ages to 12 Myrs (Kligfield *et al.* 1986; closure temperature) correspond to mid-crustal depths of 8-10 km (Carmignani and Kligfield 1990).

A significant jump in metamorphic grade occurs between the greenschist lower plate and the anchimetamorphic upper plate across the Calcare Cavernoso detachment, and this has led workers to suggest that the upper plate cannot have provided the load required to produce metamorphism of the autochthon (for references see Carmignani and Kligfield 1990). This is explained by Carmignani and Kligfield (1990) through the evaporites acting as a 'glide horizon' during both D1 and D2, and in this interpretation the jump in facies is predicted to occur during low-angle normal faulting (Wheeler and Butler 1994).

Fluid inclusions in quartz in the Calcare Cavernoso cataclasites record a maximum palaeotemperature of 345°C and pressure of 240 MPa which indicate fault activity at 8-10 km depth (Hodgkins and Stewart 1994), whilst Sr^{87}/Sr^{86} isotopic ratios suggest that the horizon acted as a fluid conduit throughout compressional deformation and formed a fluid-barrier between autochthon and allochthon (Carter *et al.* 1994). The partitioning effect of the Calcare Cavernoso is likely to have allowed brittle extension at shallow structural level to occur concomitantly with ductile simple-shear and conjugate pure-shear at depth.

5.5.2 Formation of the Apuane tectonic window

Carmignani and Kligfield (1990) argue that exhumation of basement rocks is a consequence of re-equilibration of the orogenic wedge formed during compression as a metamorphic core complex. They note that the locus of D2 low-angle extension corresponds with the culmination of an antiformal stack which was itself generated above a ramp in the initial passive margin architecture, and note that the Alpi Apuane is analogous to North American Core Complexes of the Basin and Range Province in that it records early compression, followed by extension and then Basin-and-Range-type rifting (Carmignani and Kligfield 1990). In such a model, exhumation of basement rocks in such a short timescale (from 10 km in 8 Myrs) would be facilitated through movement along the Calcare Cavernoso detachment, releasing pressure above the region of opposed extension-directions and hence updoming of the detachment (Coney 1980).

This theory is problematic on two counts. Firstly, structural analysis of the first phase of deformation suggests that the bulk geometry of the basement was little changed by D2, although the form may have been exaggerated by extension. Secondly, fluid inclusion analyses of authogenic quartz in the detachment zone provides evidence for activity at depths below 8 km but not at shallower levels (Hodgkins and Stewart 1994). The fault-system thus appears to have been abandoned prior to exhumation and not to have produced it. The consistent cross-cutting of low-angle by high-angle normal faults indicates that deformation was occurring at progressively rising structural levels, and the cumulative action of both D2 and D3 is thus most likely to have exhumed the Apuane basement.

5.5.3 Kinematics of extension

The kinematics of deformational events may be deduced through examination of shear-sense criteria (as reviewed in section 1.3). In the Alpi Apuane region, shear-sense is most commonly interpreted from fold geometry and the asymmetry of limbs (vergence), shear-zone geometry, geometry of extensional crenulation cleavages (S-C fabrics); geometry of secondary shear planes in fault-zones, relationships between porphyroclasts and their recrystallised tails, and angular relationships between shear-bands and mylonitic foliations (Carmignani and Kligfield 1990)

Composite results indicate that the compressional event relates to a period of consistent northeasterly directed shearing, whilst extension occurred in the upper crust through bimodal shear (illustrated in Figure 5.15), to the southwest on the southwestern side of the region, to the northeast on the northeastern side of the region, and in the middle crust through conjugate ductile shear. The change in shear-direction corresponds to the position of the domed antiformal fold-hinge defined by the Calcare Cavernoso evaporites.

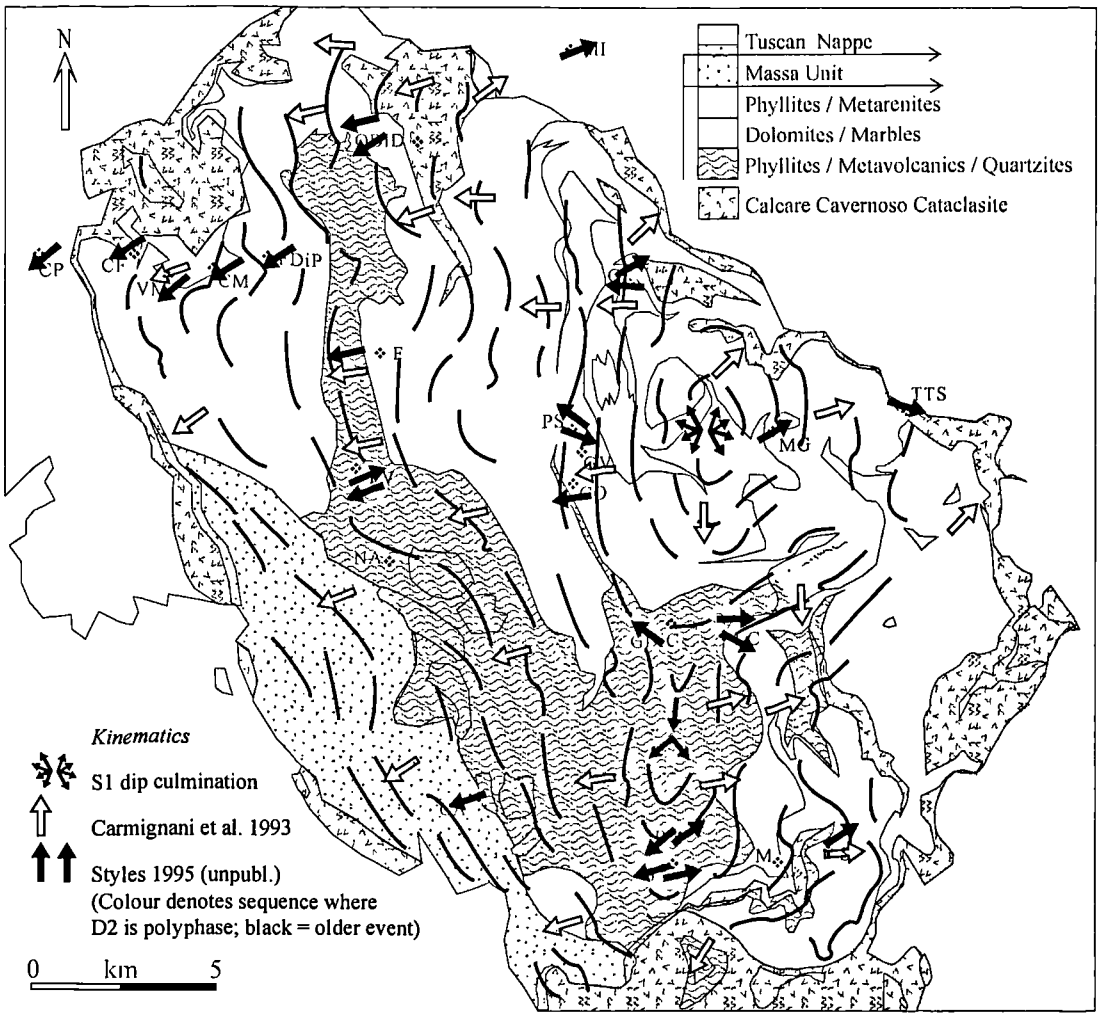

Figure 5.15 Kinematic map of the Apuane Alps, adapted from Carmignani *et al.* 1993. Arrows indicate top sense of extensional shear; muliple arrows indicate culminations in S1 structure (structural highs).

5.6 Summary

The Tuscan Nappe is characterised by low metamorphic grade and distributed compressional deformation, characterised by folding, cleavage development and thrusting. Its extensional history is recorded largely in a series of planar and listric normal faults, the sense of extension of which are known mainly from stratigraphic omission and cut-off. One such fault forms the northeastern margin to the metamorphic complex and is exposed for over 40 kilometers. It soles downwards into the Calcare Cavernoso evaporites and is associated with the development of a roll-over anticline in its hanging wall (Carmignani and Kligfield 1990).

Some minor extensional displacements are observed along the Posidonia Marls and Scaglia Formation on the northeastern side of the complex, suggesting that lithology was a strong control upon deformation style and magnitude (Nardi 1961). D2 brittle-ductile structures reminiscent to those of the Tuscan Nappe are observed in localised glide packages and show shear senses in agreement with those observed in the autochthon.

Within the normal fault population, high-angle faults consistently cross-cut lower angle detachments, often splaying from one another. The Sechio and Magra valleys are located along major listric normal faults which are also thought to sole into Triassic evaporites on the basis of progressive fault-block rotations to either side of the valleys (Carmignani and Kligfield 1990).

The Calcare Cavernoso evaporites represent an inherently weak layer utilised as a glide plane of fundamental importance during both compressive and extensional events. Consistent first-phase shear-sense indicators suggest that it initiated as a major thrust fault during the Oligocene, upon which nappe sheets of Tethyan and Apulian material were translated northeastwards. The curviplanar nature of the detachment is thus likely to have been formed during initial thrusting as part of an antiformal thrust stack system, rather than generated during later unloading of the basement rocks.

The metamorphosed lower plate is characterised by intense interference between D1 (compressional) and D2 (extensional) structures, allowing a wide range of shear-sense indicators to be used to define the kinematic of extension. D2 extensional deformation was partitioned into shear-zones and the contacts between lithologies with marked competence contrasts, generating drag folds on all scales and low-angle detachments which are cross-cut by listric normal faults (Carmignani and Kligfield 1990). This is observed in the localisation of D2 shear-zones and drag-folds into the contacts between dolomites and marbles (e.g. Forno, Passo Sella), Palaeozoic rocks within F1 antiforms (e.g. Ruosina, Frigido Valley), and in Liassic to Cretaceous phyllites at the cores of F1 synforms (e.g. Passo Sella, Via Martiri della Liberta, Orto di Donna). Lithological controls upon D2 deformation is commonly seen in the southwestern portion of the dome where D1 deformation was weakest, but is rarely observed in the northeast of the region where D1

deformation was intense. On this side, the transposition of S0 into S1 introduced a sufficient anisotropy to ensure even D2 deformation.

Late-orogenic extensional structures were observed throughout the Apuane Alps and may be grouped into four suites on the basis of style:

i. *Distributed Ductile Shear.* The deepest basement units at Ruosina contain conjugate shear-zones separating megaboudins of undeformed primary structure. The shear-zones are 10s of metres in width and dip at 15-25° northeast or southwest. This style of deformation appears to be active to the southeast of the Apuane Alps at the present day, as lozenge-shaped features are recognisable at depths of approximately 4 kilometers in seismic refraction profiles (e.g. LAR 12; Cameli *et al.* 1993). On a larger scale the action of such ductile shear-zones is seen in folded F1 axial planes which indicate northeast or southwest-directed top-sense-of-shear (Carmignani *et al.* 1990). Shear-sense is discernible from study of asymmetric boudins, shape fabrics in marble breccias, porphyroclast-tail asymmetry and the closure direction of sheath-fold noses.

ii. *Detachments.* Shallowly-dipping, bed-parallel detachments are common within metamorphic basement rocks dipping to the northeast or southwest by up to 30 . Drag-folds are commonly developed in the hangingwalls of detachments, and crenulation fabrics, micro-faults and porphyroclasts are seen adjacent to the faults. Radiogenic dating of the evaporites (Hodgkins and Stewart 1994, Carter *et al.* 1994) reveals thrusting in the Late Oligocene superceded by low-angle normal faulting. The extensional unroofing of the detachment thus occurred within a timespan of approximately 12 Ma.

iii. *Calcare Cavernoso decollement.* On a regional scale, the Calcare Cavernoso evaporites appear to have acted as a major extensional detachment separating the brittle deformation regime of the Tuscan Nappe from the more ductile regime within the basement. They preserve little evidence of deformation as a consequence of the amount of alteration they have experience during exhumation. Jumps in metamorphic grade and isochron ages for metamorphic minerals strongly suggest that several kilometers of extension occurred along the horizon during extension.

iv. *Brittle normal faults.* Steep normal faults are common within the Tuscan Nappe and characterise late-orogenic extension within the upper plate of the complex. When traced into the internal Apuane Alps, the steep normal faults become more shallowly inclined and appear to root downwards into the Calcare Cavernoso Formation. This model is supported by seismic refraction studies which image listric features splaying from detachments at depth (Buness 1985). Stratigraphic offsets in the Magra and Serchio graben suggest that up to 10% extension has occurred along normal faults dipping 55-80 northeast and southwest (Cameli *et al.* 1993).

The present day distribution of styles of deformation strongly suggests that the depth at which deformation occurred was the major control of their geometries - brittle features are seen in the Tuscan Nappe, brittle-

ductile along Triassic evaporites and ductile in basement rocks. In addition, the consistent cross-cutting of ductile by more brittle structures indicates that extension was accompanied by exhumation of the metamorphic complex. Extension in upper levels of the crust is thought to have caused an unloading effect upon the decollément zone to eccentuate its curved profile and hence increase the gravitation instability of the upper plate. In this manner, the metamorphic basement would have been brought upwards throught the crust and into the brittle extension field.

Carmignani and Kligfield (1990) considered the Alpi Apuane to be a classic core complex of North American type, with listric normal faulting typical of the Basin and Range at high structural levels and distributed ductile shear at mid-crustal levels.

D2 shear is regionally directed down the dip of the dominant foliation and away from the culmination of the D1 antiformal stack, and it thus appears that extension occurred through the reactivation of pre-existing (D1 or sedimentological) architectures. Extension was accommodated within basement rocks through movement along cleavage and bedding planes which acted as D2 shear zones.

PART IV

SYNTHESIS AND CONCLUSION

Chapter Six - Synthesis and discussion

CHAPTER 6 : SYNTHESIS AND DISCUSSION

6.1 Introduction

Interest in late-orogenic extensional structures has increased over the past decade in response to the independant recognition of extensional structure in orogens ranging in age from Precambrian to Recent (Seranne and Malavielle 1994). This study has documented a variety of extensional structures in both SW England and Italy which immediately post-date compressional deformation. Analysis of similarities and contrasts in structural style, kinematics, timing and magnitude of extension provides insight into the latter stages of mountain-building in case-studies separated by over 280 million years of geological time.

6.2 Summary of findings

Until recently, apparently extensional structures observed in fold and thrust belts were generally modelled as perturbations within the compressional system despite the more simple explanation that they are truely extensional structures. For example, shallowly-dipping detachments recording apparently normal hanging-wall translation were often described as reoriented thrusts, nappe-glide structures or localised phenomena accommodating bulk crustal thickening. Such an explanation is perpetuated by the association of compressional second-order structures against slip planes as a consequence of drag or friction during faulting. Detailed cataloguing of putatively extensional structures allows the wide-scale significance of the features to be assessed.

Structures described in Chapters three to five reveal that extensional features overprint compressional features in both regions. Such structures have been widely reported from the Italian peninsular (Chapter 5), but have largely been overlooked in the Variscides of SW England. The findings of chapters three to five are described in the following section and compared in Section 6.2.3.

6.2.1 SW England

Late-orogenic extensional structures are found throughout much of SW England. Four main structural associations are recognised which display differing degrees of discordance, reactivation and embrittlement (Figure 6.1).

i. *Ductile shear-zones.* Zones of distributed ductile deformation in which early planar fabrics (bedding and/or S1 cleavage) accommodate downdip-directed non-coaxial shear and/or vertical shortening (Figure 6.1a). Deformation is confined to metre- or decimetre- thick bands dipping between horizontal and 30° and separated from unextended strata by sharply defined, foliation-parallel slip planes. The

magnitude of extension is difficult to ascertain due to the general lack of recognisable marker horizons across which offset may be guaged, but it appears to locally exceed 50% layer attenuation where on the basis of shear-zone fabric orientation and early (compression-related) vein offsets. A range of structures are developed which appear to be dependant upon strain magnitude and the orientation of pre-existing anisotropy. Typical late structures exposed along western Mount's Bay (where S0/1 fabric is subhorizontal) include subhorizontal pressure solution or crenulation fabrics enclosing boudins of V1 vein material, 'concertina' folds with symmetrical limbs demonstrating vertical shortening and at Boscastle (where S0/1 fabric dips moderately), ductile shear-zones are developed parallel to foliation and contain asymmetric boudins and sygmoidal transposition fabrics. This ductile style of extensional deformation is restricted to areas which display the highest regional metamorphic grade (mid-greenschist) and to pelite-dominated formations with a strong compressional fabric (e.g. Boscastle Formation, Mylor Slate Formation).

ii. *Detachments.* Shallowly-dipping normal faults which partition non-coaxial shear along discrete horizons surrounded by zones of low extensional strain (Figure 6.1b). In excess of 55% layer-parallel extension is locally accommodated by detachments ranging in dip from 0-35 which develop along the dominant pre-extension fabric (S0 or S1) (e.g. Boscastle, Watergate Bay). A range of associated, second-order structures of both extensional and compressional nature are developed adjacent to detachments, including extensional shear-bands, Riedel fractures, tensile veins, bookshelf structures, porphyroclast-tail systems, crenulation cleavages, asymmetric drag folds and kink-bands on a mm- to m- scale. The detachments are distributed along the traces of major thrusts (e.g. Gidley Well, Carrick Thrust) although obviously reactivated thrust-planes are seldom observed. The detachment systems must post-date ductile (type I) deformation as they cross-cut earlier extensional features and sometimes exploit extension-related transposition fabrics.

iii. *Extensional duplexes and curviplanar normal faults.* Interlinked stair-step normal faults which record synchronous movement histories, with curviplanar fault-planes and detachments (dips 0-30) which steepen into brittle normal faults (>30 dip; Figure 6.1c). Duplexes locally accommodate 40% extension (e.g. Port William, Pentargon), whilst curviplanar faults accommodate up to 25% layer attenuation. Curviplanar faults are widely developed and have attendant Riedel fracture arrays and drag-folds which allow kinematic analysis. This style of extension is observed within rocks of intermediate metamorphic grade (low to sub- greenschist) and reactivate bedding and/or S1 cleavage where it is suitably oriented. Cross-cutting relationships suggest that the fault-systems postdate ductile non-coaxial shear (i) and were active in the latter stages of movement along detachments.

iv. *Discrete brittle normal faults.* Steep normal faults (modally 60-80 dip), sometimes conjugate, are developed throughout SW England (Figure 6.1d) in rocks of all metamorphic grades and all lithologies. Drag-folds or Riedel shear arrays are sometimes developed in wallrocks and indicate up to 15% extensional strain. The faults cross-cut all other styles of extensional structure and hence appear to have formed during the latter stages of extension.

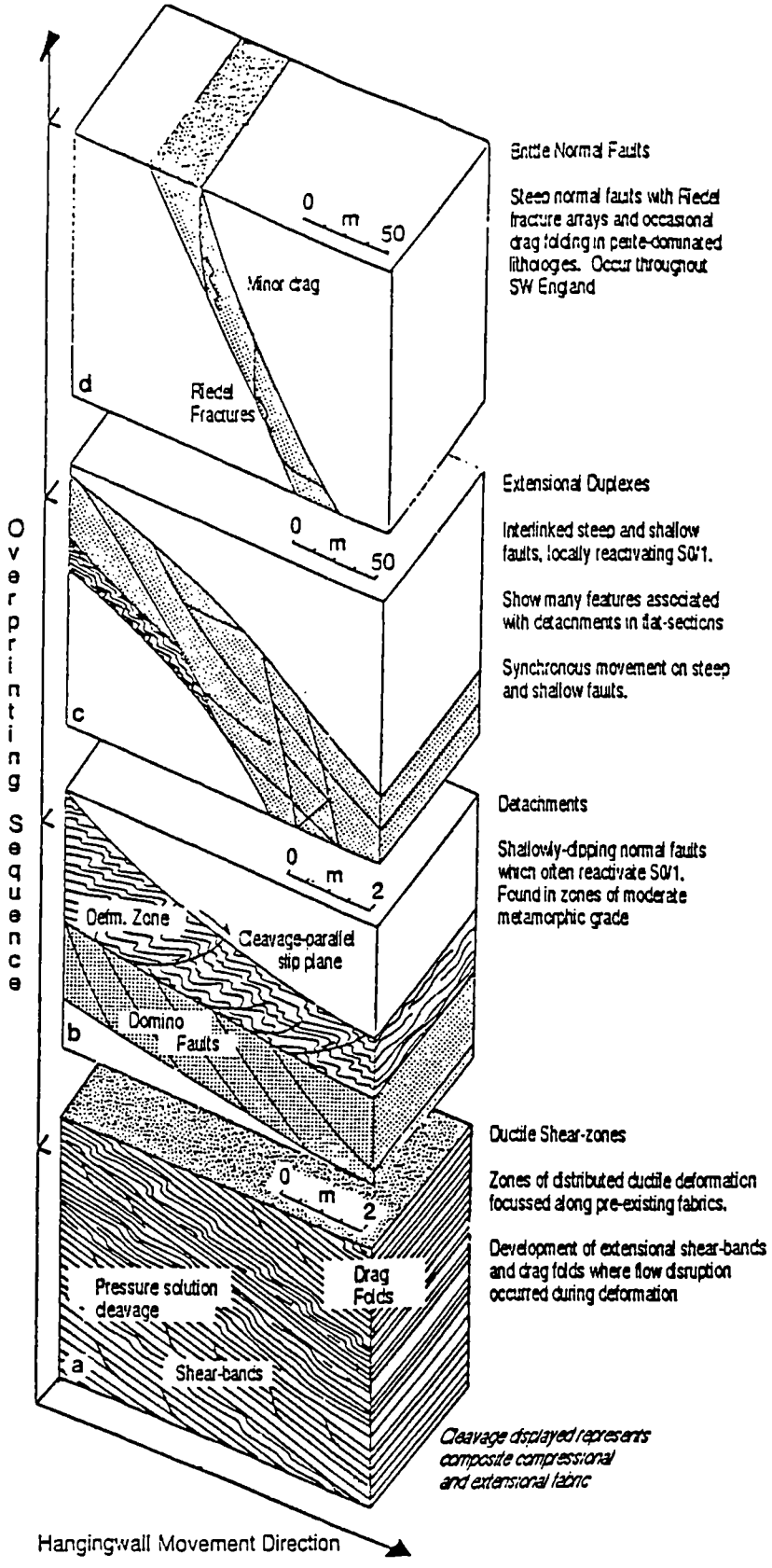

Figure 6.1 Range of structures relating to late-orogenic extension identified in SW England. (a) *Ductile shear-zones; (b) Detachments; (c) Extensional duplexes; (d) Discrete brittle normal fault*

The timing of extensional deformation can be indirectly determined from field relationships, although accurate dating of structures is made difficult by the diachroneity of features across the orogen (See Table 2.3). The dating of structures through radiogenic study of deformation products was outside the scope of this study, but published work has been considered in light of primary observation.

- Extensional structures deform compressional fabrics previously dated to between the late Devonian period (south Cornwall) and Namurian age (central and north Cornwall, mid Devon; Dodson and Rex 1971; Section 2.3.1).
- Shallowly-dipping detachments host granite dykes dated to 280-270 Ma (Darbyshire and Shepherd 1985) and lamprophyres dated to 296-292 Ma (Hawkes 1981; Goode and Taylor 1988), suggesting that low-angle faulting was active by the end Westphalian age to earliest Permian period. Furthermore, the association of potassic dyke intrusion with late-orogenic extensional faults has been noted in the Caledonides of East Greenland (McClay *et al.* 1986).
- Cordierite spotting developed within the aureoles of granite stocks overgrow extensional microstructures which must therefore pre-date granite emplacement (Stephanian to Sakmarian, 274-294 Ma; Chen *et al.* 1993; Clark *et al.* 1993; Alexander and Shail 1996; Section 2.4.1).
- Fluid inclusion analysis from vein material developed along fault-planes in south Cornwall indicates that detachments were active by the late Stephanian and that cross-cutting steep normal faults were active after the uppermost Carboniferous (Shail and Wilkinson 1994).
- Detachments and many steep faults are truncated by the post-Variscan unconformity exposed in south Devon and overlain by the early Permian Exeter volcanics, and must therefore have ceased to be active in that region in the earliest Permian.
- Steep normal faults record reactivation at 220, 170 and 75 Ma in their suite of hydrothermal minerals (Halliday and Mitchell (1976).

The top sense of extensional shear extracted from kinematic analysis of structures on both microscopic and macroscopic scale allows regional kinematic maps to be drawn for the extensional event (Figure 6.2). Structures define domains of consistent tectonic transport which switch across discrete zones. In general, extensional transport is seen to be consistently directed down the dip of the dominant compressional anisotropy, away from structural highs. Forethrust zones thus tend to record top-to-the-southeast shear (e.g. Looe to Plymouth) whilst backthrust zones show top-to-the-northwest shear (e.g. Padstow to Bude). Zones of oblique shear-sense are developed where primary foliation is oblique to the regional trend, such as the transpressive Start-Perranporth Zone and the lateral ramp of the Carrick Thrust inferred to lie along the western shore of the River Fal. Oblique slickenfibres are also noted on detachments which are slightly oblique to the dominant dip and thus may have acted as lateral ramps during extension (e.g. Pentargon Cove).

Transfer zones which compartmentalise extension domains appear to coincide with structural highs and long-lived basement structures which acted during compression or perhaps even sedimentation. For example, a switch in extension vector occurs across the Padstow Facing Confrontation, coinciding with a fundamental culmination in the compressional system (e.g. Roberts and Sanderson 1971; Andrews *et al.* 1988; Pamplin and Andrews 1988), and a further switch is recorded across the NW-SE trending Portnadler Fault; a major steep structure seen in the field to record extensional and dextral motions.

Figure 6.2 Kinematic map of SW England constructed from field data. Arrows illustrate top sense of extensional shear (shaded heads) and dominant pre-extension anisotropy dip-direction (open heads). Note that extension is generally directed down the dip of S1 cleavage.

6.2.2 Apuane Alps, Italy

Late-orogenic extensional structures were mapped across much of the Apuane Alps and may be grouped into three suites on the basis of style:

i. *Distributed Ductile Shear.* Greenschist-grade basement rocks exposed in the central Apuane Alps preserve a range of ductile extensional structures which attenuate convergence-realted structures (Figure 6.3a). In the deepest exhumed basement units at Ruosina, conjugate shear-zones separate boudins of undeformed primary structure. The shear-zones are generally 10s of metres in width and dip 15-25° northeast or southwest. This style of deformation appears to be active to the southeast of the Apuane Alps at the present day, as lozenge-shaped features are recognisable beneath the Larderello geothermal field at depths of approximately 4 kilometers in seismic refraction profiles (e.g. LAR 12; Cameli *et al.* 1993). On a kilometer-scale, the action of such ductile shear-zones may be seen in folded F1 axial planes which indicate northeast or southwest-directed top-sense-of-shear (Carmignani *et al.* 1990). Shear-sense is discernible from study of asymmetric boudins, shape fabrics in marble breccias, porphyroclast-tail asymmetry and the closure direction of sheath-fold noses.

ii. *Detachments.* Shallowly-dipping, bedding parallel detachments are common within metamorphic basement rocks (Figure 6.3b), dipping to the northeast or southwest by up to 30°. Drag-folds are commonly developed in the hangingwalls of detachments, and crenulation fabrics, micro-faults and porphyroclasts are seen adjacent to the faults.

iii. *Calcare Cavernoso decollement.* On a regional scale, the Calcare Cavernoso evaporites appear to have acted as a major extensional detachment separating the brittle deformation regime of the Tuscan Nappe from the more ductile regime within the basement (Figure 6.3c). The evaporites are heavily altered and preserve little kinematic evidence for reactivation, but jumps in metamorphic grade and isochron ages for metamorphic minerals strongly suggest that several kilometers of extension occurred along the horizon during extension.

iv. *Brittle normal faults.* Steep normal faults are common within the Tuscan Nappe and characterise late-orogenic extension within the upper plate of the complex (Figure 6.3d). When traced into the internal Apuane Alps, the steep normal faults become more shallowly inclined and appear to root downwards into the Calcare Cavernoso Formation. This model is supported by seismic refraction studies which image listric features splaying from detachments at depth (Buness 1985). Stratigraphic offsets in the Magra and Serchio graben suggest that up to 10% extension has occurred along normal faults dipping 55-80° northeast and southwest (Cameli *et al.* 1993).

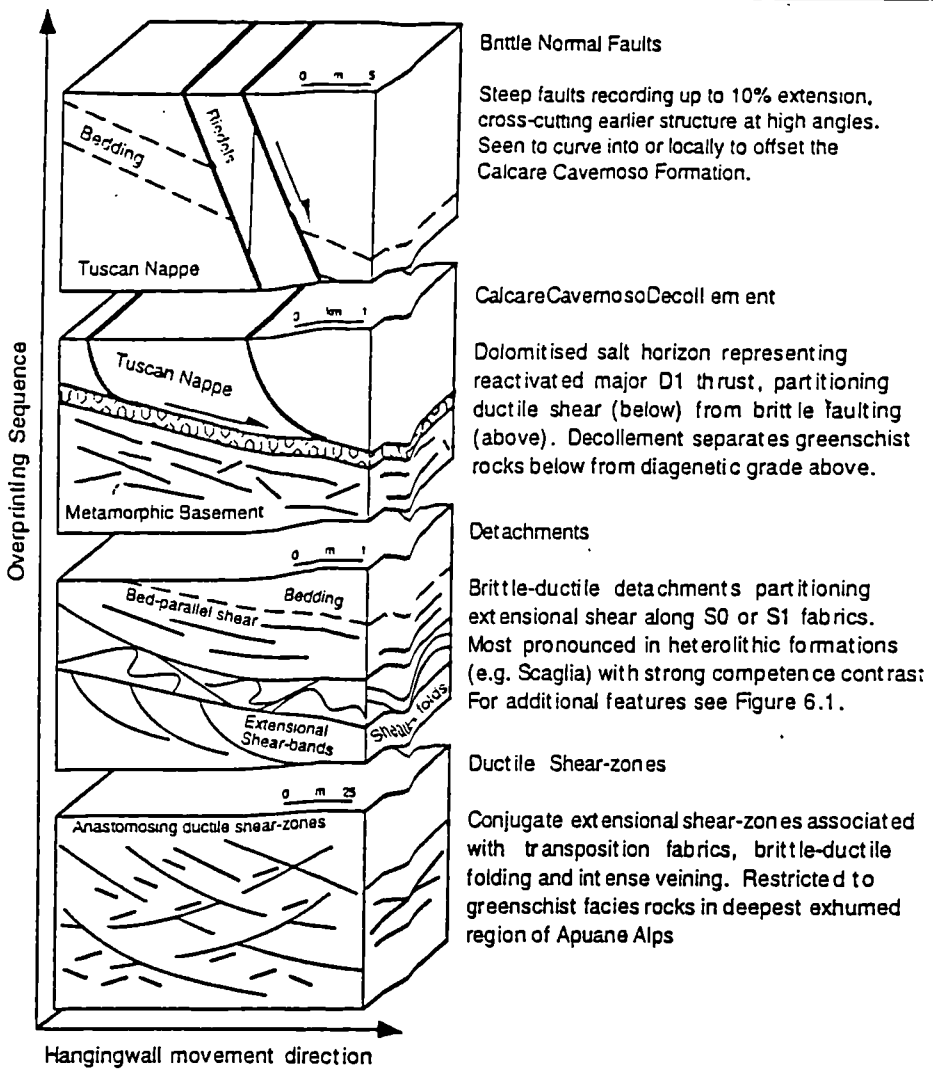

Figure 6.3 Extensional structural styles identified in the Apuane Alps. (a) Conjugate distribute ductile shear. (b) Detachments); (c) Calcare Cavernoso decollément; (d) Brittle normal faults.

The timing of extensional structures in the Apuane Alps is well constrained by a variety of isotopic studies conducted in the region and the increased accuracy possible in Tertiary to Recent rocks. The evidence is:

- Radiogenic dating of the Calcare Cavernoso evaporites (Hodgkins and Stewart 1994, Carter *et al.* 1994) reveals that thrusting took place during the late Oligocene and was superceded by low-angle normal faulting. The extensional unroofing of the detachment thus occurred within a timespan of approximately 12 Ma.
- Extensional structures deform compressional fabrics dated by K-Ar and Ar-Ar techniques to approximately 27 Ma (Kligfield *et al.* 1986), the approximate age derived for the Pseudomacigno Formation (the oldest unfolded sediments; Dallan-Nardi 1977; Carmignani *et al.* 1993).
- Syn-extensional phengite, chlorite, chloritoid and kyanite minerals dated by Ar-Ar technique provide an age of 12-14 Ma (Giglia and Radicati 1970; Kligfield *et al.* 1986). This suggests that ductile

extensional shear was underway by the middle Miocene and that the greenschist-facies minerals have thus undergone over 10 km exhumation since that time.

- Steep normal faults which intersect the Calcare Cavernoso evaporites are associated with graben which contain fill of Upper Miocene age (Carmignani *et al.* 1994), suggesting that the mode of extension changed from bed/cleavage-parallel shear to steep faulting between the late Oligocene and late Tortonian.
- Lamprophyre dykes are exposed approximately 20 km to the southwest of the Apuane Alps at Sisco (Figure 6.4). The dykes are dated to 15 Ma and have a geochemical signature indicating a mixed source of acid (crustal) and basic (sub-crustal) melts (Innocenti *et al.* 1992). This evolutionary trend towards more basic, sub-crustal sources through time and enhanced heatflow suggests increasing involvement of the deep lithosphere since Langhian (middle Miocene) times (Cameli *et al.* 1993). This date coincides with the generation of early oceanic crust in the southern Tyrrhenian Sea and thus may record a regional shift to extensional tectonism.
- Apatite fission track data from the region show that the upper plate passed through the closure temperature of apatite (120°C) at 10 Ma, and the lower plate at 2-5 Ma (Abbate *et al.* 1990). At an average geothermal gradient, this indicates that the basement rocks were exhumed from 4 km depth to the surface in the last 2-5 Ma at rates of ~0.8-2km/Ma (Carmignani *et al.* 1990).

The sense of extensional shear is readily derived in the Apuane Alps due to the development of drag folds (*cascade folds;* Carmignani and Kligfield 1990) within the basement rocks. Extension is down-to-the-southwest or west in the southwestern part of the region and down-to-the-northeast in the northeastern side of the complex (Figure 6.4). The change in shear-sense coincides with the antiformal culmination in compressional structure at the centre of the region, where conjugate northeast- and southwest- dipping ductile shear-zones are developed. In the southwest of the region, extension is almost exclusively directed down the dip of bedding, whilst in the northeast, extension reactivates S1 cleavage where bedding was obliterated during compressional deformation.

6.2.3 Comparison of late-orogenic extension in SW England and the Apuane Alps

Structural analysis of late-orogenic features in SW England and the Apuane Alps reveals similar deformation style and kinematic behaviour following compression. Structural style shows an evolution through time from ductile to brittle on a timescale of approximately 10-20 Ma (Carter *et al.* 1994; Shail and Wilkinson 1994), with strong similarities in structural style at each stage of this evolution.

In both areas, the earliest structures seen to affect compressional fabrics record ductile vertical shortening and regional down-dip shear, refolding convergence-related folds and faults (e.g. Rinsey Cove, S.

Cornwall; Passo Sella, Central Apuane Alps). Deformation is accommodated through the generation of subhorizontal crenulation or pressure solution fabrics and non-coaxial shear along pre-existing cleavages. Such deformation is likely to have occurred as a result of the action of gravity upon nappe stacks during thermal re-equilibration and is known to occur in the latter stages or immediately following lithospheric compression (Glazner and Bartley 1985; Dewey 1988). Published extension estimates for the ductile structures in Italy exceed 120% (including low-angle normal faulting; Carmignani *et al.* 1994) and this study identifies over 60% extension in SW England through ductile shear.

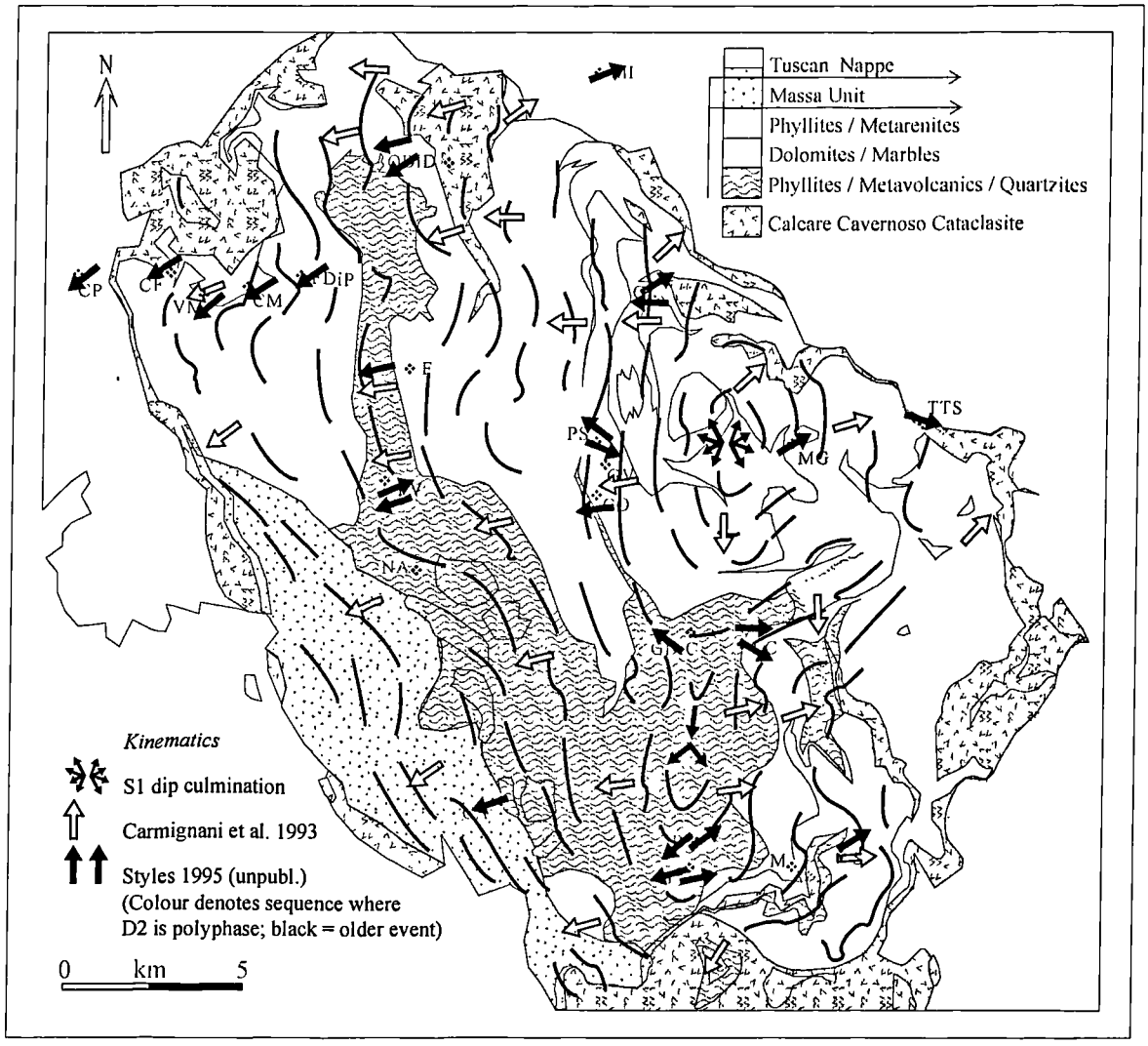

Figure 6.4 Kinematic map of the Apuane Alps, constructed from field data and displaying extensional shear vectors produced by Carmignani *et al.* 1993. Note that the top sense of extension (arrows) is generally perpendicular to the strike of S1 cleavage (black lines), directed down the dip of the dominant anisotropies.

The second stage of extension is recorded by low-angle normal faulting, reactivating bedding and or convergence-related cleavage. In both Italy and Cornwall, detachments are seen along the traces of earlier thrust-faults which mark major structural breaks within the bulk compressional structure. Up to 8 kilometres of exhumation is thought to have occurred through movement along the Calcare Cavernoso evaporite horizon in Italy over a period of approximately 10 Ma (Carmignani and Kligfield 1990; Carter *et al.* 1994; ~16 km of slip along detachment), juxtaposing diagenetic grade rocks of the cover sequence against greenschist-grade basement rocks in its footwall. Such a large metamorphic jump is not observed anywhere in Cornwall, although detachment systems (e.g. Rusey Cliff, Loe Bar) are seen to coincide with minor jumps in metamorphic grade suggesting a lesser degree of exhumation (Wheeler and Butler 1993).

Extensional duplexes described in north Cornwall are not well exposed within the Apuane Alps, although linked normal faults are exposed close to the main extensional detachment at Capanne Ferrari. However, when steep normal faults are mapped across the Apuane Alps they are seen to sole into the Calcare Cavernoso decollement and braid with one another along bedding-parallel flats to form linked extensional fault systems on a kilometer scale. The latter stages of late-orogenic extension occur through steep normal faulting in both areas, offsetting earlier brittle-ductile features.

The main discrepancy between structural style in Italy and Cornwall is the predominance of a master detachment horizon in the Apuane Alps (the Calcare Cavernoso) and the apparent lack of such a detachment in Cornwall. The reason for this may be rheological and related principally to the stratigraphy; in Cornwall, the sequence is made up of sandstones, siltstones and mudstones and there are no major, sharply-defined rheological disparities which could be utilised as a glide zone. In contrast, the carbonate sequence of the Apuane Alps contains a thick salt horizon which is extremely weak and susceptible to deformation. The distribution of detachments along the trace of the major thrusts (e.g. Gidley Well; Capanne Ferrari) suggests that strata adjacent to important thrusts may focus extensional strain where reactivated thrusts-planes are not evident. Such strain-partitioning is noted in other ancient orogens and appears to reflect the inherent weakness of long-lived fault-zones within continental crust (Holdsworth *et al.* 1997; Imber *et al.* 1997).

6.3 True crustal extension?

The recognition of truely extensional structures in polyphase orogenic belts is problematic as such structures must be shown to extend the lithosphere and hence the syn-orogenic surface (Wheeler and Butler 1993). Extension of layering alone does not form a sufficient criterion since earlier deformation can reorient banding into a non-horizontal attitude prior to later deformation. Furthermore, pre-existing compressional faults may be reoriented by later folding and tilting which may be related to displacements on other thrusts (e.g. Butler 1982).

6.3.1 SW England

The structures described from SW England cannot conclusively be proven to have extended the crust because the diagnostic metamorphic and geochronological criteria identified by Wheeler and Butler (1993) cannot be applied (Section 1.2). This is a result of the distributed nature of the putatively extensional strain in the region, with displacements occurring along thousands of detachments rather than being focused along a small number of high-displacement faults across which obvious differences in metamorphic/geochronological history might be identified. In addition, the limited vertical exposure means that it is impossible to assess the orientation of structures relative to the syn-orogenic surface (i.e. palaeohorizontal). Several field observations and the findings of other workers support the extensional generation of the structures :-

- Field observation of the basal unconformity of Permo-Triassic molasse deposits in South Devon suggests that there has been little post-Variscan reorientation of the palaeohorizontal. Furthermore, there is no geological or geophysical evidence for any significant reorientation of the Cornubian batholith.
- Many of the graben-bounding normal faults associated with Permo-Triassic sedimentation are indistinguishable from steep normal faults associated with latest extension in Cornwall.
- Throughout SW England, the hanging walls of detachments consistently display normal senses of movement relative to the present day surface so that the faults cut downwards, away from the Earth's surface. No detachment faults can be traced into thrust faults anywhere in the region.
- Several authors have pointed to the superficial similarity in form of extensional detachments and thrust faults (e.g. Andrews *et al.* 1988; Freshney *et al.* 1972) and have therefore classified them as rotated thrusts. This interpretation requires a phase of fault rotation to have occurred after thrusting to reorient them into their apparent extensional trajectories. This premise is flawed for three main reasons. Firstly, were the faults to be reoriented thrusts, they may be expected to be traced into unambiguous thrusts but this is not observed. Secondly, were the faults to be rotated thrusts, the apparent post-rotational features may be expected to produce scattered orientation datasets showing variable rotation, but data is consistent over tens of kilometers. Finally, were the faults to be rotated thrusts, they should be able to be backrotated into a 'true thrusting' orientation and to lie within an orientation which is consistent with the pre-existing compressional structures such as S1 cleavage or F1 folds. This is not the case as the detachments commonly parallel cleavage planes and so rotation of thrust causes rotation of cleavage and requires more complex explanations for compressional architectures. In the absence of any evidence for the rotation of thrusts (e.g. reorientation of the palaeohorizontal, lateral changes from thrust to normal fault offsets), detachments are most simply explained as extensional features.
- Fluid inclusion data from south Cornwall suggests that extensional detachments predate steep normal faults by several million years and that they were active at temperatures up to 200°C higher than

those experienced during the steep normal faulting (Shail and Wilkinson 1994). This data shows a decrease in temperature through time from thrusting to steep normal faulting which is consistent with exhumation and hence extensional deformation.

- Very similar detachment zones have been described from crystalline Moine rocks in Scotland by Holdsworth (1989b), who points out that they closely resemble structures formed in poorly consolidated sediments due to slumping (Farrell 1984; Elliot and Williams 1988). These structures differ markedly from those found in conventional foreland thrust belts (Holdsworth 1989b) and their form may reflect a common gravitational origin.

6.3.2 Apuane Alps

An extensional genesis for late-orogenic structures described from the Apuane Alps is more firmly demonstrated as a consequence of the younger age of the rocks and the dominance of the Calcare Cavernoso detachment system during deformation. All three main criteria for identifying true crustal extension are satisfied regionally (Section 1.2; Wheeler and Butler 1993).

- Kinematic analysis of shear-sense indicators exposed along the evaporite band record a two-phase movement history; the first in a thrust sense at 27 Ma (hangingwall transport direction points towards the palaeosurface) and the second in a normal sense at 12 Ma (hangingwall transport down from the Earth's surface).
- The pressure-time curve of rocks in the footwall (basement) decreases faster than that recorded in the hangingwall (Carmignani and Kligfield 1990; Carmignani *et al.* 1994). Apatite fission track evidence for exhumation rate suggests 4 kilometres of hangingwall exhumation
- The Calcare Cavernoso detachment juxtaposes rocks with old cooling ages in its hangingwall from rocks with younger cooling ages in its footwall.

The similarities in structural style between detachment structures firmly identified as extensional in Italy and more putative extensional structures discussed from SW England also supports the existence of widespread extensional detachments in the Variscan orogen in the latter region.

6.4 Discussion

6.4.1 Implications of observed structural styles and overprinting sequence

Similarities in the styles of extensional structures and the consistent overprinting sequence through time in both study areas indicates a similar evolution of deformation environment through time. In each case, ductile structures recording vertical shortening and reactivation of bedding and pre-existing cleavages are

superceded by detachment faulting at low-angles to the dominant early anisotropy. Faults progressively initiate at higher angles to anisotropies and to the palaeohorizontal through time.

This progression of geometry may most simply be related to the structural level (i.e. temperature, pressure and pore-fluid pressure) during extension. Increasing embrittlement is consistent with gradual unroofing of structures; a process recognised during compressional thrust breaching (Butler 1982) but more often seen in extensional exhumation systems (Figure 6.5; Platt 1986). This model is supported by available evidence in both areas. Palaeotemperature estimates made from fluid inclusion studies in both areas indicate detachment activity at temperatures of between 350-400 C and thus depths of 10-14km (Shail and Wilkinson 1994; Hodgkins and Stewart 1994), and brittle normal faulting at below 200 C and hence depths of 5-7 km in the crust. Furthermore, lamprophyres derived from subcrustal melts are known to have developed synchronously with detachment motion in Cornwall (Shail and Wilkinson 1994), Italy (Cameli *et al.* 1993) and in other regions of proposed late-orogenic extension (e.g. East Greenland Caledonides; McClay *et al.* 1986).

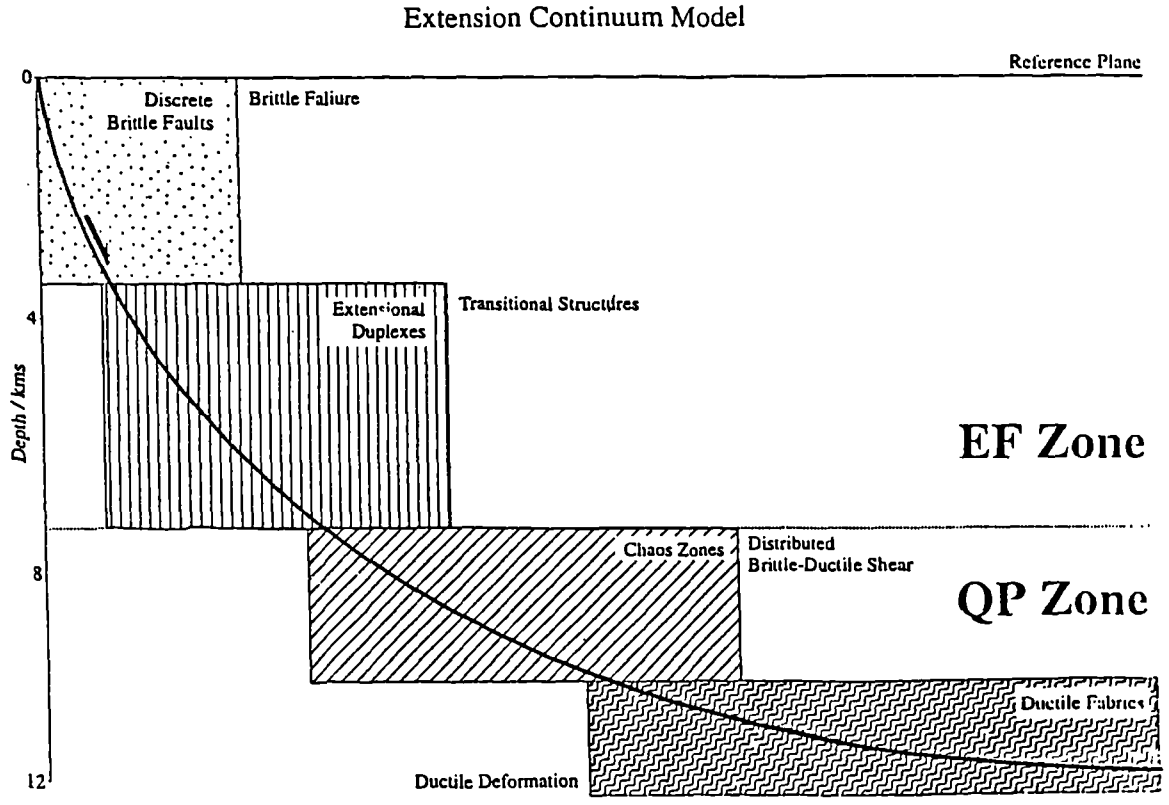

Figure 6.5 Exhumation continuum model for the range of structural styles observed in both study areas. The boundary between the elastofrictional and quaziplastic regions of the crust is taken as the level at which detachments are active.

6.4.2 Proposed driving force of extension

The principal extensional zones of the Earth's continents are orogenic belts (Dewey 1988), indicating that previously thickened crust is more susceptible to extension than undeformed continental crust. The reason for this inherent weakness is that the rheology of continental crust may be approximated to a viscous fluid intersected by planes of harder rheology (Platt 1986; Dewey 1988). The balance of forces at work in an orogen is known from the application of experimental and theoretical studies. Orogens have approximately wedge-shaped profiles resting upon a rigid underthrusting plate and buttressed against the foreland (Figure 6.6; Platt 1986). The geometry of the orogenic wedge results from the dynamic balance between gravitational potential energy exerted upon the overthickened region of crust (influenced by crustal rheology, anisotropies and their orientation), the frictional force acting upon the underlying detachment (influenced by the rheology of the subduction zone, its pore-fluid pressure and slope) and the convergent force supporting the hinterland of the orogen. Extension will occur if there is a decrease in plate-boundary stress magnitude, the rheology of the orogen is weakened through time (i.e. thermal equilibration occurs as relatively cool thrust units heat up within a nappe stack; Seranne and Malavielle 1994), delamination of a dense lower-crustal root-zone (Bird 1979) or a steepening of the underlying thrusts (e.g. through subduction zone roll-back; Tricart *et al.* 1994).

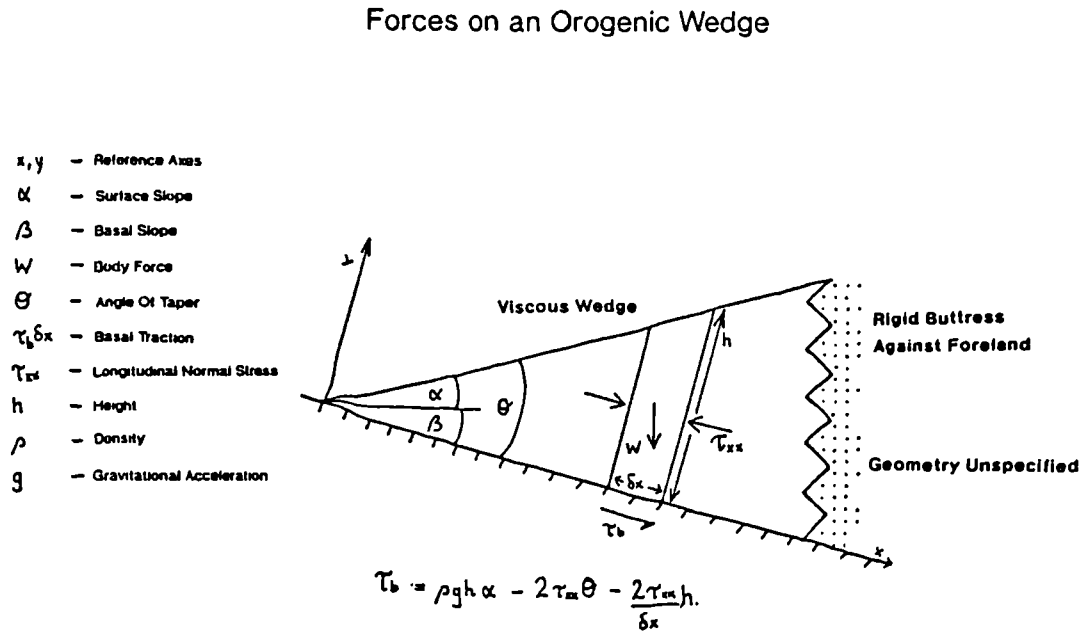

Figure 6.6 Forces acting upon a viscous wedge (Platt 1986).

Glazner and Bartley (1985) noted that the timing of late-orogenic extension is approximately 10-15 Ma after the waning of convergent forces after which orogenic welts have no long-term yield strength. The time-lag between compression and extension corresponds to the predicted period of rheological weakening through thermal equilibration after which gravitational force exceeds the yield strength of the crust and vertical shortening (i.e. horizontal extension) occurs. This model fits age constraints in both study-areas and is supported by the observation that brittle-ductile deformation structures developed during detachment motion share common geometric features with slump folds and deformation products in unlithified sediments.

Early studies of extensional structures in Cornwall suggested radial movements along detachment systems away from granite bodies (e.g. Stone 1966; Turner 1968; Rattey 1980), and thus the granites were invoked as a driving force behing extension. The relationship between granite emplacement and extension is not straightforward and field study is hindered by stoping in the exposed roof zones. The intrusion of granites would produce a major increase in crustal heat flow and in fluid abundance, thus weakening the rheology of the orogenic welt and triggering extension. However, the granites appear always to postdate detachment faulting and locally utilise such planes as conduits. It thus appears that granites are controlled by the location of extension systems rather than vice versa.

6.4.3 Discussion of deformation along shallowly-dipping detachments

In both Variscan and Cenozoic examples, it appears that movement along shallowly-dipping normal faults is a key stage in late-orogenic evolution. The initiation of such structures was first documented in the Basin and Range Province of North America (Hamilton and Myers 1966), but considerable disagreement remains as to the origins of so-called detachment faults (Johnson and Loy 1992). The observation that mid-crustal rocks are sometimes juxtaposed against upper-crustal rocks along subhorizontal movement surfaces necessitates the existence of detachments. The classic Andersonian model for the dynamics of faulting (Anderson 1951) argues that shallowly-dipping faults initiate in compression only and the dynamic implications of transporting several kilometres of crustal rocks in the hangingwall of essentially horizontal normal faults would require such high stresses to overcome friction without faliure of the intact rock.

Subsequent work on low-angle normal faulting has led to a number of models which overcome the problems of friction along such movement planes. Andersonian theory could apply if such structures developed through reorientation of the principal stress axis (e.g. Sibson 1985), if the faults initiated at high-angles and were subsequently rotated into their inclined attitudes (Wernicke and Axen 1988), or if the faults developed in response to high pore-fluid pressures at mid-crustal level, causing decreased friction and changing crustal stress conditions (Axen 1992). Observations from the Basin and Range suggest that detachments do initiate in shallow inclinations (Scott and Lister 1992), although examples of normal

movement along previously initiated low-angle thrusts has been noted elsewhere (West 1992; Carmignani and Kligfield 1990).

Mathematical modelling of stresses required for movement to occur along shallowly-dipping faults in both compression and extension suggests that both are equally possible, although compressional faulting is more likely as more tectonic compression is possible in the crust that extension (Reiter 1996). Jaeger and Cook (1969) demonstrated that a pore-pressure of 125% hydrostatic pressure (achievable in the mid-crust along impermeable layers and through redistribution of stress (Rice 1992)) would allow low-angle fault motion with an average coefficient of friction of below 0.4. Wojtal and Mitra (1986) demonstrate that a fine-grained or rheologically weak fault-layer can accommodate movement at low shear-stress levels through study of the southern Appalachians.

Both field observation of fault-plane shear-sense indicators and analogue modelling indicate that normal faults are unlikely to interact to any great extent with pre-existing, shallowly-dipping thrust-faults (Facenna *et al.* 1995). Sand-box experiments indicate that normal faults branch from pre-existing thrust faults at terminations of décollement horizons when the thrust dip exceeds 41° (Facenna *et al.* 1995), and demonstrate that the dip of normal faults decreases as the dip of thrust faults increases. This critical reactivation angle may be decreased by fault-plane cohesion, pore-pressure friction coefficient and fault-plane geometry (Sibson 1985).

Field observation in SW England confirms that wholesale thrust reactivation is not widespread and that detachments are initiated in extension though they may be focused against major thrust-faults. Detachments commonly have intense veining in their footwalls which suggests that pore-fluid pressures were high during low-angle extension. The development of high pore-fluid pressures may therefore explain the movement of detachments in this area. The partitioning of extensional shear along the Calcare Cavernoso Formation in Italy is clearly controlled by rheology. The evaporite formation is a plane of significant weakness relative to the surrounding sequences and appears to have focussed fluid flow during extension (Hodgkins and Stewart 1994), and thus it has a suitably weak nature to be reactivated. It appears, therefore, that the presence of a weak decollement horizon which may have been exploited during thrusting may be of fundamental importance in later extension, facilitating decoupling of the orogenic wedge along a discrete horizon and forming a core complex. In contrast, where orogens with no weak horizon, they undergo distributed late-orogenic extension through movement along thousands of detachments, as is seen in SW England.

6.5 Conclusions

- Late-orogenic extensional structures have been identified throughout both SW England and the Apuane Alps and appears to represent a distinct stage in orogenic evolution in both areas.
- Structures associated with late-orogenic extension may be grouped on the basis of style and the degree to which they reactivate earlier anisotropies to produce a consistent scheme with constant overprinting sequence in both regions.
- The style and relative age of extensional structures may be incorporated with published geochronological information to invoke the presence of major intracrustal normal faults/shear-zones re-equilibrating crustal thickness soon after the end of plate convergence. Compression estimates of orogenic belts must therefore be treated with caution unless such extension is taken into account.
- Extension magnitudes range from 6-10% in external regions of each orogen to 60-120% in zones of highest metamorphic grade. The coincidence of peak regional metamorphic grade with the zones of highest extension suggests that metamorphic variation in orogens reflects variation in exhumation magnitude, which is itself controlled by pre-extensional structural architecture.
- Extension is accommodated through movement along detachment faults which mark planes of weakness in the compressional system. Extension is partitioned into decollement horizons where suitable rheologies are present and elsewhere occurs through more distributed shear, possibly assisted by high pore-fluid pressures.
- The kinematics of extension record non-coaxial shear away from structural highs through reactivation of planar fabrics generated before extension.

The strong correlation of structural style, timing of extension relative to compression and magnitude of strain strongly suggests that late-orogenic extension is common to many orogens and allows the equilibration of transiently overthickened crustal wedges.

REFERENCES

ABBATE, A. 1991. Sezione geologica dai Monte del Chianti al Passo dei Mandrioli. *In:* PIALLI, G., BARCHI, M., MENICHETTI, M. (EDS). *Studi preliminiari all acquisizione del profilo CROP 03 Punta Ala - Gabicce.* AGIP - CNR - ENEL.

AL-RAWI, F.R.J. 1980. A geophysical study of deep structures in southwest Britain. *PhD Thesis, University of Wales.*

ALEXANDER, A.C. & SHAIL, R.K. 1995. Late-Variscan structures on the coast between Perranporth and St. Ives, Cornwall. *Proceedings of the Ussher Society, 8,* 398-404.

ALEXANDER, A.C. & SHAIL, R.K. 1996. Late- to post- Variscan structures on the coast between Penzance and Pentewan, south Cornwall. *Proceedings of the Ussher Society, 9,* 172-178.

ALLAN, T.D. 1961. A magnetic survey in the western English Channel. *Quarterly Journal of the Geological Society, London, 117,* 157-168.

ALLEN, J.R.L. 1979. Old Red Sandstone facies in external basins with particular reference to southern Britain. *In : House, M.R., Scrutton, C.T. & Bassett, M.G. (eds.) The Devonian System. Special papers in Palaeontology,* 23, 73-167.

ALLEN, P.A., HOMEWOOD, P. & WILLIAMS, G.D. 1986. Foreland basins: an introduction. *Special Publication of the International Association of Sedimentologists, 8,* 3-12.

ALVAREZ, W. 1972. Rotation of the Corsica-Sardinia microplate. *Nature, 235,* 103-105.

ANDERSON, E.M. 1951. The dynamics of faulting. *Oliver and Boyd, Edinburgh,* 206pp

ANDERTON, R., BRIDGES, P., LEEDER, M. & SELWOOD, B.W. 1979. A dynamic stratigraphy of the British Isles. George Allen & Unwin, London.

ANDREWS, J.R., BARKER, A.J. & PAMPLIN, C.F. 1988. A reappraisal of the facing confrontation in north Cornwall: fold or thrust dominated tectonics ? *Journal of the Geological Society of London, 145,* 777.

ANGELIER, J. 1994. Fault slip analysis and palaeostress reconstruction. *In:* HANCOCK, P.L. (ed). *Continental Deformation.* Pergamon Press, Oxford.

ARTHAUD, F. & MATTE, P. 1977. Late Paleozoic strike-slip faulting in southern Europe and northern Africa: Result of a right-lateral shear zone between the Appalachians and the Urals. *Bulletin of the Geological Society of America, 88,* 1305-1320.

ASHWIN, D.P. 1958. The coastal outcrop of the Culm sediments between Boscastle and Bideford, north Devon. *PhD Thesis, London*

AVEDIK, A. 1975. Seismic refraction survey in the Western Approaches to the English Channel : preliminary results. *Philosophical Transactions of the Royal Society, London, A279,* 29-39.

AXEN , G.J. 1992. Pore fluid stress increase and fault weakening in low-angle normal faults. *Journal of Geophysical Research, 97,* 8989.

BACON, M. 1975. A gravity survey of the eastern English Channel between Lyme Bay and St Brieuc Bay. *Philosophical transactions of the Royal Society, London, A279,* 69-78.

BADHAM, J.P.N. & HALLS, C. 1975. Microplate tectonics, oblique collisions and the evolution of orogenic systems. *Geology, 3,* 373-376.

BADHAM, J.P.N. 1982. Strike-slip orogens - an explanation for the Hercynides. *Journal of the Geological Society of London, 139,* 495-507.

BARKER, A. & GAYER, R. 1985. Evolution of the pre-Variscan basement of SW England. *Proceedings of the Ussher Society, 6,* 120-124.

BARNES, R.P. 1993. The stratigraphy of a sedimentary melange and associated deposits in south Cornwall, England. *Proceedings of the Geologist's Assoiation, 94,* 37-39.

BARNES, R.P. & ANDREWS, J.R. 1981. Pumpellyite-actinolite grade regional metamorphism in south Cornwall. *Proceedings of the Ussher Society, 5,* 139-146.

BARNES, R.P. & ANDREWS, J.R. 1986. Upper Palaeozoic ophiolite generation and obduction in south Cornwall. *Journal of the Geological Society of London, 143,* 117-124.

BARNES, R.P. & ANDREWS, J.R. 1984. Hot or cold emplacement of the Lizard Complex ? *Journal of the Geological Society of London,* ***141,*** 37-39.

BARNES, R.P. 1982. The geology of south Cornish melanges. *Unpubl. PhD Thesis.* University of Southampton.

BARNES, R.P. 1983. The stratigraphy of a sedimentary melange and associated deposits in south Cornwall, England. *Proceedings of the Geologists' Association,* ***94,*** 217-229.

BARTON, C.M. 1994. Geology of the Liskeard District 1:10 000 scale sheet SX26SE. *Technical report of the British Geological Survey, Onshore Geology Series, WA/94/30. British Geological Survey, Exeter.*

BARTON, C.M., GOODE, A.J.J. & LEVERIDGE, B.E. 1993. Geology of the St. Germans district (Cornwall). 1:10 000 sheets SX35NW, SX35SW, AND SX35SE. *Technical report of the British Geological Survey, Onshore Geology Series, WA/93/93.* British Geological Survey, Exeter.

BATHER, F.A. 1907. The discovery in west Cornwall of a Silurian crinoid characteristic of Bohemia. *Transactions of the Royal Geological Society of Cornwall, 13,* 191-197.

BELL, A. M. 1981. Vergence: an evaluation. *Journal of Structural Geology, 3,* 197-202.

BERTHE, D., CHOUKROUNE, P. & JEGOUZO, P. 1979. Orthogneiss, mylonite and non-coaxial deformation of granites: the example of the south Armorican Shear Zone. *Journal of Structural Geology, 1,* 31-42.

BERTINI, G., CAMELLI, G.M. & CONSTANTINI, A. 1991. Strutura geologica fra i monti di Campighia e Rapalano Terme (toscana Mendiaule). *Struturi Geologica Camerti, 1,* 155-178.

BIRD, P. & KANG, X. 1994. Computer simulations of California tectonics confirm the very low strength of major faults. *Bulletin of the Geological Society of America,* ***106,*** 159-174.

BIRD, P. 1979. Continental delamination of the Colorado Plateau. *Journal of Geophysical research,* ***84,*** 7561-7571.

BIRPS & ECORPS 1986. Deep seismic profiling between England, France and Ireland. *Journal of the Geological Society of London,* ***143,*** *45-52.*

BLUCK, B.J., HAUGHTON, P.D.W., HOUSE, M.R., SELWOOD, E.B. & TUNBRIDGE, I.P. 1988. Devonian of England, Wales and Scotland. *In: Devonian of the World.* Canadian Society of Petroleum Geologists Memoirs, **14,** 305-324.

BOCCALETTI, M. & GUAZZONI, G. 1975. Remnant arcs and marginal basins in the Cenozoic development of the Mediterranean. *Nature,* ***255,*** 54-78.

BOCCALETTI, M. & GUAZZONE, G. 1975. Plate tectonics in the Mediterranean region. In: SQUYES, C.H. (ed). *The Geology of Italy.* Earth Sciences Society of the Libyan Arab Republic, Tripoli, LAR, 143-163.

BOTT, M.H.P. & SCOTT, P. 1964. Recent geophysical studies in southwest England. *In:* HOSKING, K.F.G. & SHRIMPTON, G.J.,(eds), *Present views on some aspects of the geology of Cornwall,* Royal Geological Society of Cornwall, 25-44.

BOTT, M.H.P. 1982. Origin of lithospheric tension causing basin formation. *Philosophical Transactions of the Royal Society of London, Series A,* ***305,*** 319-324.

BOTT, M.H.P., DAY, A.A. & MASSON-SMITH, D. 1958. The geological interpretations of gravity and magnetic surveys in Devon and Cornwall. *Philosophical Transactions of the Royal Society of London,* ***251,*** 161-191.

BOTT, M.P.H., HOLDER, A.P., LONG, R.E. & LUCAS, A.L. 1970. Crustal structure beneath the granites of southwest England. *In:* NEWALL, G. & RAST, N. (eds.). *Mechanisms of Igneous Intrusion. Geological Journal Special Issue 2,* 93-102.

BROOKS, M. & LE GALL, B. 1992. Discussion on the crustal evolutionary model for the Variscides of England and Wales from SWAT seismic data. *Journal of the Geological Society, London,* ***149,*** 681-682.

BROOKS, M. & THOMPSON, M.S. 1973. The geological interpretation of a gravity survey of the Bristol Channel. *Journal of the Geological Society, London,* ***129,*** 245-274.

BROOKS, M., DOODY, J.J. & AL-RAWY, F.R.J. 1984. Major crustal reflectors beneath SW England. *Journal of the Geological Society of London,* ***141,*** 97-103.

BROOKS, M., MECHIE, J., LLEWELLYN, D.J. 1983. Geophysical investigations in the Variscides of southwest Britain. *In:* HANCOCK, P.L. *The Variscan fold-belt in the British Isles.* Adam Hilger Ltd. 186-198.

BULLARD, E.C, & GASKELL, T.F. 1941. Submarine seismic investigations. *Proceedings of the Royal Society, A177,* 476-499.

BURTON, C.G. & TANNER, P.W.G. 1986. The stratigraphy and structure of the Devonian rocks around Liskeard, east Cornwall, with regional implications. *Journal of the Geological Society of London, 143,* 95-105.

BUTLER, C.A. 1995. Basement fault reactivation: the kinematic evolution of the Outer Hebrides Fault Zone, Scotland. *Unpublished PhD thesis,* University of Durham.

BUTLER, R.W.H. 1982. The terminology of structures in thrust belts. *Journal of Structural Geology, 4,* 239-245.

BUTLER, R.W.H. 1989. The influence of pre-existing basin structure on thrust system evolution in the western Alps. *In:* COOPER, M.A., WILLIAMS, G.D. (eds) , 1989. *Inversion tectonics.* Special Publications of the Geological Society of London, **44**, 105-122.

CAMELLI, G.M., DUI, I. & LIOTTA, D. 1993. Upper crustal structure of the Larderello Geothermal Field as a feature of post-collisional extensional tectonics (southern Tuscany, Italy). *Tectonophysics, 224,* 413-423.

CARMIGNANI, L., & KLIGFIELD, R. 1990. Crustal extension in the northern Appennines: the transition from compression to extension in the Alpi Apuane core complex. *Tectonics, 9,* 2715.

CARMIGNANI, L., DECANDI, A.F., FANTOZZI, P.L., LAZZAROTTO, A., LIOTTA, D. & MECCHERI, M. 1994. Tertiary extensional tectonics in Tuscany. *Tectonophysics, 238,* 295-315.

CARMIGNANI, L., DECANDI, A.F., DISPERATI, L., FANTOZZI, L.P., LAZZAROTTO, A., LIOTTA, D. & OGGIANO, G. 1995. Relationships between the Sardinia-Corsica Provencal domain and the northern Apennines. *Terra Nova, 7,* 412-419.

CARTER, K.E., DWORKIN, S.I., CARMIGNANI, L., MECCHERI, M. & FANTOZZI, L.P. 1994. Dating thrust events using Sr 87/86: an example from the Apuane Alps, northern Apennines, Italy. *Tectonophysics, 191,* 335-346.

CHADWICK, R.A. 1993. Aspects of basin inversion in southern Britain. *Journal of the Geological Society of London, 150,* 311-322.

CHADWICK, R.A., KENOLTY, N. & WHITTAKER, A. 1983. Crustal structure beneath southern England from deep seismic reflection profiles. *Journal of the Geological Society of London, 140,* 893-911.

CHAPMAN, T.J. 1986. The Variscan structure of southwest England and related areas: conference report and introduction to published papers. *Journal of the Geological Society of London, 143,* 41-43.

CHAPMAN, T.J., FRY, R.L., HEAVEY, P.T. 1984. A structural cross-section through SW Devon. *In*: Hutton, D.H.W., Sanderson, D.J. (eds) *Variscan Tectonics of the north Atlantic region.* Special Publications of the Geological Society of London, **14**, 113-118.

CHAROY, B. 1986. The genesis of the Cornubian batholith (south-west England): the example of the Carnmenellis Pluton. *Journal of Petrology, 27,* 571-604.

CHEN, Y., CLARK, A.H., FARRAR, E., WASTENEYS, H.A.H.P., HODGSON, M.J. & BROMLEY, A.V. 1993. Diachronous and independent histories of plutonism and mineralisation in the Cornubian Batholith, southwest England. *Journal of the Geological Society of London, 150,* 1183-1191.

CHEN, Y., ZENTILLI, M.A., CLARK, A.H., FARRAR, E., GRIST, A.M. & WILLIS-RICHARDS, J. 1996. Geochronological evidence for post-Variscan cooling and uplift of the Carnmenellis granite, SW England. *Journal of the Geological Society of London, 153,* 191-196.

CHESLEY, J.T., HALLIDAY, A.N., SNEE, L.W., MEZGER, K., SHEPHERD, T.J. & SCRIVENOR, R.C. 1993. Thermochronology of the Cornubian Batholith : implications for pluton emplacement and protracted episodic hydrothermal mineralisation. *Geochimica et Cosmochimica Acta, 57,* 1817-1835.

CHIOCCI & ORLANDO 1991. Considerazione sulla sismostratigrafia ad altissima risoluzione dei depositi constituenti lat plattaforma continentale tra L'Isola Elba e la Toscana. *In:* PIALLI, G., BARCHI,

M. & MENICHETTI, M. (eds). *Studi preliminari all'acquisitione del profilo CROP 03 Punta Ala-Gabicce.* AGIP-C.N.R.-E.N.E.L.

COLI, A. 1989. Times and mode of uplift of the Apuane Alps Metamorphic Complex. *Atti. Tic. Sc. Terra, 32,* 47-56.

CONEY, P.J. 1980. Cordilleran metamorphic core complexes: an overview. *Memoirs of the Geological Society of America, 153,* 7-12.

CONTI, P., GATTAGLIO, M. & MECCHERI, M. 1991. The overprint of the Alpine tectonometamorphic evolution of the Hercynian Orogen: an example from the Apuane Alps (northern Apennines, Italy). *Tectonophysics, 191,* 335-346.

COOKE, A.C., MURCHISON, D.G. & SCOTT, E. 1972. A British meta-anthracitic coal of Devonian age. *Geological Journal, 8,* 83-94.

COOPER, M.A. & WILLIAMS, G.D. 1989. Inversion tectonics. *Special Publication of the Geological Society of London, 44.*

CORNFORD, C., YARNELL, L. & MURCHISON, D.G. 1987. Initial vitrinite reflectance results from the Carboniferous of north Devon and north Cornwall. *Proceedings of the Ussher Society, 6,* 461-467.

COWARD, M.P. & MCCLAY, K.R., 1983. Thrust Tectonics of south Devon. *Journal of the Geological Society of London, 140,* 215-228.

COWARD, M.P. & POTTS, G.J., 1983. Complex strain patterns developed at the frontal and lateral tips to shear zones and thrust zones. *Journal of Structural Geology, 5,* 383-399.

COWARD, M.P. & SMALLWOOD, S., 1984. An interpretation of the Variscan tectonics of southwest Britain. *In:* HUTTON, D.H.W., SANDERSON, D.J. (eds) *Variscan Tectonics of the north Atlantic region.* Special Publications of the Geological Society of London, **14,** 89-102.

DALLAN NARDI, L. 1977. Segnalaziane di lepidocycline nella porte basale dello 'pseudomargino' della Alpi Apuane. *Bulletin di Societi Geologico Italia, 95,* 459-477.

DARBYSHIRE, D.P.F. & SHEPHERD, T.J. 1985. Chronology of granite magmatism and associated mineralisation, SW England. *Journal of the Geological Society of London, 142,* 1159-1177.

DAVIES, G.R. 1984. Isotopic evolution of the Lizard Complex. *Journal of the Geological Society of London, 141,* 3-14.

DAVIS, J. & COTT, B. 1980. Structural characteristics of metamorphic core complexes of southern Arizona. *Memoirs of the Geological Society of America, 153,* 35-39.

DAVIS, P.G. 1990. A late Gedinnian - early Siegenian palynomorph assemblage from the Dartmouth Beds of north Cornwall. *Proceedings of the Ussher Society, 7,* 307.

DAY, G.A. & EDWARDS, J.W.F. 1983. Variscan thrusting in the basement of the English Channel and SW Approaches. *Proceedings of the Ussher Society, 4,* 432-436.

DAY, G.A. & WILLIAMS, C.A. 1970. Gravity compliation in the N.E. Atlantic and interpretation of Gravity in the Celtic Sea. *Earth and Science Planetary Letters, 8,* 205-213.

DE LA BECHE, H.T. 1839. Report on the geology of Cornwall, Devon and West Somerset. *Memoir of the Geological Survey of Great Britain.*

DE SITTER, L.U. 1965. Structural Geology. Mc-Graw-Hill, New York & London.

DEARMAN, W.R. & BUTCHER, N.E. 1959. The geology of the Devonian and Carboniferous rocks of the northwest border of the Dartmouth Granite. *Proceedings of the Geologists Association, 70,* 51-92.

DEARMAN, W.R. 1962. Structure of the southern Culm Basin. *Proceedings of the Ussher Society, 1,* 25-27.

DEARMAN, W.R. 1963. Wrench faulting in Cornwall and Devon. *Proceedings of the Geologist's Association, 74,* 265-285.

DEARMAN, W.R. 1969. Refolded folds in the Dartmouth Slates at Portwrinkle, south Cornwall. *Proceedings of the Ussher Society, 1,* 265-285.

DEARMAN, W.R. 1971. A general view of the structure of Cornubia. *Proceedings of the Ussher Society, 2,* 220-236.

DEARMAN, W.R. & FRESHNEY, E.C. 1966. Repeated folding at Boscastle, north Cornwall. *Proceedings of the Geologists Association, 77,* 199-215.

DEARMAN, W.R., FRESHNEY, E.C. & McLEAN, M. 1964. Early folds and cross-lineation at Tintagel, Cornwall. *Nature, 203,* 933-935.

DELLA VEDOVA, B., PELLIS, B., FOUCHER, G. & REHAULT, J.B. 1984. Geothermal structure of the Tyrrhenian Sea. *Marine Geology, 55,* 271-289.

DEWEY, J.F. 1982. Plate tectonics and the evolution of the British Isles. *Journal of the Geological Society, London, 139,* 371-412.

DEWEY, J.F. 1988. Extensional collapse of orogens. *Tectonics, 7,* 1123-1139.

DINELEY, D.L. 1986. Cornubian Quarter-Century : Advances in the geology of southwest England, 1960-1985. *Proceedings of the Ussher Society, 6,* 275-290.

DODSON, M.H. & REX, D.C. 1971. Potassium-argon ages of slates and phyllites from south-west England. *Quarterly Journal of the Geological Society, London, 126,* 469-499.

DOODY, J.J. & BROOKS, M. 1986. Seismic refraction investigation of the structural setting of the Lizard and Start Complexes, SW England. *Journal of the Geological Society, London, 143,* 135-140.

DURRANCE, E.M. 1985. A possible major Variscan thrust along the southern margin of the Bude Formation, southwest England. *Proceedings of the Ussher Society, 6,* 173-179.

EDMONDS, E.A. 1974. Classification of the Carboniferous rocks of south-west Engalnd. *Report of the Institute of Geological Sciences, 74/13,* 7pp.

EDMONDS, E.A., WILLIAMS, B.J. & TAYLOR, R.T. 1979. Geology of Bideford and Lundy Island. *Memoir of the Geological Survey of Great Britain.*

EDWARDS, J.W.F. 1986. Interpretations of seismic and gravity surveys over the eastern part of the Cornubian platform. *In:* HUTTON, D.H.W., SANDERSON, D.J. *(eds) Variscan Tectonics of the north Atlantic region.* Special Publications of the Geological Society of London, **14,** 119-124.

EDWARDS, J.W.F., DAY, G.A. & LEVERIDGE, B.E. 1989. Thrusts under Mount's Bay and Plymouth Bay. *Proceedings of the Ussher Society, 7,* 131-135.

ELLIOT, C.G. & WILLIAMS, P.F. 1988. Sediment slump structures: a review of diagnostic criteria and application to an example from Newfoundland. *Journal of Structural Geology, 10,* 171-182.

ELLIOT, T. 1976. Upper Carboniferous sedimentary cycles produced by river-dominated, elongate deltas. *Journal of the Geological Society, London, 132,* 199-208.

EVANS, C.D.R. 1990. The geology of the western English Channel and its western Approaches. *United Kingdom Offshore Regional Report, British Geological Survey, London.*

EVANS, K.M., 1981. A marine fauna from the Dartmouth Beds (Lower Devonian) of Cornwall. *Geological Magazine, 118,* 517-523.

EVANS, K.M., 1985. The brachiopod fauna of the Meadfoot Group (Lower Devonian) of the Torbay area, south Devon. *Geological Journal, 20,* 81-90.

EXLEY, C.S. & STONE, M. 1982. Chapters 20, 21 & 22; Hercynian intrusive rocks. *In*: SUTHERLAND, D.E. *(ed.) Igneous Rocks of the British Isles.* John Wiley, Chichester. 287-300.

FACENNA, C., NALPAS, T. & BOSI, V. 1995. The influence of pre-existing thrust faults on normal fault geometry in nature and in experiments. *Journal of Structural Geology, 17,* 1139-1149.

FARRELL , S.G. 1984. A dislocation model applied to slump structures, Ainsa Basin, south-central Pyrrhenees. *Journal of Structural Geology, 6,* 727-736.

FEAR, M. 1984. Geology of the Tintagel area. *Unpublished MSc Thesis,* University of Brimingham.

FLOYD, P.A. 1982. Chemical variations in Hercynian basalts relative to plate tectonics. *Journal of the Geological Society of London, 139,* 505-520.

FLOYD, P.A. 1983. Composition and petrogenesis in the Lizard Complex and pre-orogenic basaltic rocks in southwest England. *In :* HANCOCK, P.L. (ed.). The Variscan Foldbelt in the British Isles. 130-152.

FLOYD, P.A. 1984. Geochemical characteristics and comparison of the basic igneous rocks of the Lizard Complex and the basaltic lavas within the Hercynian troughs of SW England. *Journal of the Geological Society of London, 141,* 61-70.

FLOYD, P.A. & LEVERIDGE, B.E. 1987. Tectonic environment of the Devonian Gramscatho basin, south Cornwall: framework mode and geochemical evidence from turbiditic sandstones. *Journal of the Geological Society of London, **144**,* 1-12.

FLOYD, P.A., HOLDSWORTH, R.E. & STEELE, S.A. 1993. Geochemistry of the Start Complex greenschists. *Geological Magazine, **130**,* 345-352.

FOSSEN, H. & RYKKELID, E. 1992. Postcollisional extension of the Caledonian orogen in Scandinavia - structural expressions and tectonic significance. *Geology, **20**,* 737-740.

FOSSEN, H. 1992. The role of extensional tectonics in the Caledonides of south Norway. *Journal of Structural Geology, **14**,* 1033-1046.

FRESHNEY, E.C. 1965. Low-angle faulting in the Boscastle area. *Proceedings of the Ussher Society, **1**,* 175-178.

FRESHNEY, E.C., WILLIAMS, M. & McKEOWN, M.C. 1966. Structure of the Boscastle-Tintagel region. *Proceedings of the Ussher Society, **1**,* 308-310.

FRESHNEY, E.C. & TAYLOR, R.T. 1972. The Upper Carboniferous stratigraphy of north Cornwall and west Devon. *Proceedings of the Ussher Society, **5**,* 464-471.

FRESHNEY, E.C., McKEOWN, M.C., WILLIAMS, M. 1972. Geology of the coast between Bude and St Agnes. *NERC Special Publication.*

GAUSS, G.A. 1973. The structure of the Padstow area, north Cornwall. *Proceedings of the Geologists Association, **84**,* 283-313.

GAYER, R. & JONES, J. 1989. The Variscan foreland in south Wales. *Proceedings of the Ussher Society, **7**,* 177-179.

GIANNI, E. & LAZZAROTTO, A. 1975. Tectonic evolution of the northertn Apennines. In: SQUYRES, C.H. (ed). *The geology of Italy.* Earth Sciences Society of the Libyan Arab republic, Tripoli, LAR. 237-287.

GIBBONS, W. & THOMPSON, L. 1991. Ophiolitic mylonites in the Lizard Complex: ductile extension in the lower oceanic crust. *Geology, **19**,* 1009-1012.

GIGLIA, G. 1966. Geologica dell Alta Versilia Settentiale. *Memoirs of the Geological Society of Italy, **6**,* 67-95.

GIGLIA, G. & RADICATI, R. 1970. K/Ar age of melting in the Apuane Alps (northern Tuscany). *Bulletin of the Italian Geology Society, **89**,* 485-497.

GLAZNER, A. & BARTLEY, R. 1985. Evolution of lithospheric strength after thrusting. *Geology, **13**, 42.*

GOODE, A.J.J. & MERRIMAN, R.J. 1987. Evidence of crystalline basement west of the Land's End granite. *Proceedings of the Geologists' Association, **98**,* 39-43.

GOODE, A.J.J. & TAYLOR, R.T. 1988. Geology of the country around Penzance. *Memoir of the British Geological Survey,* Sheets 351 and 359 (England and Wales).

HALLIDAY, A.N. & MITCHELL, J.G. 1976. Structural K-Ar and Sr-Ar age studies of adularia K-feldspars from the Lizard Complex, England. *Earth and Planetary Science Letters, **29**,* 227-237.

HALLS, R. 1971. A mechanistic approach to the paragenetic interpretation of mineral lodes in Cornwall. *Proceedings of the Ussher Society, **6**,* 548-554.

HANDY, M.R. 1990. The solid-state flow of polymineralic rocks. *Journal of Geophysical Research, **95**,* 8674-8661.

HANMER, S. & PASSCHIER, C. 1991. Shear-sense indicators : a review. *Geological Survey of America Special Paper, **90-17**.*

HARTLEY, A.J. & WARR, L.N. 1990. Upper Carboniferous foreland basin evolution in SW Britain. *Proceedings of the Ussher Society, **7**,* 212-216.

HARTLEY, A.J. 1993. Silesian sedimentation in south-west Britain. *In : Gayer, R.A. & Grieling, R. The Rhenohercynian and Sub-Variscan Fold Belts.* Earth Evolution Series, Vieweg, 159-196.

HAWKES, J.R. 1981. A tectonic 'watershed' of fundamental consequence in the post-Westphalian evolution of Cornubia. *Proceedings of the Ussher Society, **5**,* 128-131.

HENDRIKS, E.M.L. 1937. Rock succession and structure in south Cornwall, a revision. With notes on the Central European facies and Variscan folding there present. *Quarterly Journal of the Geological Society, London, **93**,* 322-360.

HENDRIKS, E.M.L. 1971. Facies variations in relation to tectonic evolution in Cornwall. *Transactions of the Royal Geological Society of Cornwall, **20**,* 114-150.

HENLEY, S. 1970. The geology and geochemistry of an area around Perranporth, Cornwall. *Unpublished PhD Thesis,* University of Nottingham.

HENLEY, S. 1973. The structure of the Perranporth area, Cornwall. *Proceedings of the Ussher Society, **2**,* 521-524..

HIGGS, R. 1991. The Bude Formation (Lower Westphalian), SW England: siliciclastic shelf sedimentation in a large equatorial lake. *Sedimentology, **38**,* 445-469.

HILLIS, R.R. & CHAPMAN, T.J. 1992. Variscan structure and its influence on post-Carboniferous basin development, Western Approaches Basin, SW UK continental shelf. *Journal of the Geological Society of London, **149**,* 413-417.

HIRTH, G. & TULLIS, J. 1992. Dislocation creep regimes in quartz aggregates. *Journal of Structural Geology, **14**,* 145-159.

HOBSON, D.M. & SANDERSON, D.J. 1975. Major early folds at the southern margin of the Culm Synclinorium. *Journal of the Geological Society of London, **131**,* 337-352.

HOBSON, D.M. & SANDERSON, D.J. 1983. Variscan deformation in southwest England. *In:* HANCOCK, P.L. *(ed.) The Variscan Fold Belt in the British Isles.* Hilger, Bristol, 108-129.

HOBSON, D.M. 1976. The structure of the Dartmouth Antiform. *Proceedings of the Ussher Society, **2**,* 320-331.

HOBSON, D.M. 1978. The Plymouth Area. *Geological Association Guide, **38**.*

HODGKINS, M.A. & STEWART, K.G. 1994. The use of fluid inclusions to constrain F2 pressure, temperature and kinematic history – an example from the Alpi Apuane, Italy. *Journal of Structural Geology, **16**,* 85-96.

HOLDER, A.P. & BOTT, M.H.P. 1971. Crustal structure in the vicinity of southwest England. *Geophysical Journal of the Royal Astronomical Society, **23**,* 465-489.

HOLDER, M.T. & LEVERIDGE, B.E. 1986a. A model for the tectonic evolution of south Cornwall. *Journal of the Geological Society of London, **143**,* 125-134.

HOLDER, M.T. & LEVERIDGE, B.E. 1986b. Correlation of the Rhenohercynian Variscides. *Journal of the Geological Society of London, **143**,* 141-147.

HOLDSWORTH, R.E. 1989a. Short Paper : The Start-Perranporth Line : a Devonian terrane boundary in the Variscan orogen of southwest England? *Journal of the Geological Society of London, **146**,* 419-421.

HOLDSWORTH, R.E. 1989b. Late brittle deformation in a Caledonian ductile thrust wedge: new evidence for gravitational collapse in the Moine thrust sheet, Sutherland, Scotland. *Tectonophysics, **170**,* 17-28.

HOLDSWORTH, R.E., BUTLER, C.A. & ROBERTS, A.M. 1997. The recognition of reactivation during continental deformation. *Journal of the Geoogical Society of London, **154**,* 73-76.

HOUSE, M.R. 1963. Devonian ammonoid successions and facies in Devon and Cornwall. *Quarterly Journal of the Geological Society of London, **70**,* 315-321.

HOUSE, M.R., RICHARDSON, J.B., CHALONER, W.G., ALLEN, J.R.L., HOLLAND, C.H. & WESTOLL, T.S. 1977. A correlation of Devonian rocks of the British Isles. *Special report of the Geological Society of London, **8**.*

IMBER, J., HOLDSWORTH, R.E., BUTLER, C.A. & LLOYD, G.E. 1997. Fault zone weakening processes along the reactivated Outer Hebrides Fault Zone, Scotland. *Journal of the Geological Society of London, **154**,* 105-110.

INNOCENTI, F., SERRI, G., FERRARA, G., MANETTI, P. & TONORINNI, S. 1992. Genesis and classification of the rocks of the Tuscan Magmatic Province: 30 years after Marinelli's model. *Acta Volcanilogica, 2,*247-265.

INSTITUTE OF GEOLOGICAL SCIENCES 1965. Aeromagnetic map of Great Britain - sheet 2.

ISAAC, K.P., TURNER, P.J. & STEWART, I.J. 1982. The evolution of the Hercynides in central SW England. *Journal of the Geological Society, London, **139**,* 523-531.

ISAAC, K.P., SELWOOD, E.B. & SHAIL, R.K. 1996. The Devonian. *In:* SELWOOD, E.B., DURRANCE, E.N. & BRISTOW, C.N. *The Geology of Cornwall.* University Press, Exeter.

JACKSON, N.J., HALLIDAY, A.N., SHEPPARD, S.M.F. & MITCHELL, J.G. 1982. Hydrothermal activity in the St. Just mining district. *In :* EVANS, A.M. *(ed.) Metalisation associated with acid magmatism.* Wiley, Chichester.

KELLING, G. 1988. Silesian sedimentation and tectonics in the South Wales Basin : a brief review. *In :* BESLEY, B. & KELLING G. (eds.) *Sedimentation in a synorogenic basin complex : Upper Carboniferous of north-west Europe.* Blackie, Glasgow and London, 38-42.

KENOLTY, N., CHADWICK, R.A., BLUNDELL, D.J. & BACON, M. 1981. Deep seismic reflection survey across the Variscan Front of southern England. *Nature, **293**,* 451-453.

KIRBY, G.A. 1978. Layered gabbros in the eastern Lizard, Cornwall, and their significance. *Geological Magazine, **115**,* 345-354.

KIRBY, G.A. 1984. The petrology and geochemistry of dykes of the Lizard ophiolite complexes, Cornwall. *Journal of the Geological Society of London, **141**,* 53-59.

KLIGFIELD, R., HUUZIKER, J., PALLMEYER, R.D. & SCANNEL, S. 1986. Dating of deformation using K-Ar and Ar-Rb techniques: results from the northern Apennines. *Journal of Structural Geology, **8**,* 781-798.

LAKE, S.D. & KARNER, G.D. 1987. The structure and evolution of the Wessex Basin, southern England : an example of inversion tectonics. *Tectonophysics, **137**,* 347-378.

LANE, A.N. 1970. Possible Tertiary deformation of Armorican structures in southeast Cornwall. *Proceedings of the Ussher Society, **3**,* 197-204.

LARSON, P.H. & BENGAARD, H.J. 1991. Devonian basin initiation in east Greenland - a result of sinistral wrench faulting and Caledonian extensional collapse. *Journal of the Geological Society of London, **148**,* 355-368.

LAVECCHIA, G. 1988. The Tyrrhenian-Apennine system: structural setting and seismotectogenesis. *Tectonophysics, **147**,* 263-296.

LE GALL, LE HERISSE, A., DEUNFF, J. 1985. New palynological data from the Gramscatho Group at the Lizard front (Cornwall) : palaeogeographical and geodynamical implications. *Proceedings of the Geologists' Association, **96**,* 237-253.

LEAT, P.T., THOMPSON, R.M., MORRISON, M.A., HENDRY, G.L. & TRAYHORN, S.C. 1987. Geodynamic significance of basaltic and ultrapotassic Permian lavas and minette dykes in SW England. *Journal of the Geological Society of London, **144**,* 532-538.

LEVERIDGE, B.E., HOLDER, M.T. & DAY, G.A. 1984. Thrust nappe tectonics in the Devonian of south Cornwall and the western English Channel. *In :* HUTTON, D.H.W. & SANDERSON, D.J. *(eds.) Variscan tectonics of the North Atlantic region.* Special Publication of the Geological Society of London, **14**, 103-112.

LEVERIDGE, B.E., HOLDER, M.T. & GOODE, A.J.J. 1990. Geology of the country around Falmouth. *Memoir of the British Geological Survey, Sheet 352 (England and Wales).*

LISLE, R.J. 1992. Strain estimation from flattened buckle folds. *Journal of Structural Geology, **14**,* 369-371.

LISLE, R.J. 1994. Palaeostrain analysis. *In :* HANCOCK, P.L. (ed.) Continental deformation. Pergamon Press, Oxford.

LISTER, G.S. & SNOKE, A.W. 1984. S-C mylonites. *Journal of Structural Geology, **6**,* 617-638.

LLOYD, G.E. & WHALLEY, J.S. 1986. The modification of chevron folds by simple shear: examples from north Cornwall and Devon. *Journal of the Geological Society of London, **143**,* 89-94.

MATTHEWS, S.C. 1977. The Variscan fold-belt in southwest England. *Neues Jahrbüch fur Geologie und Palaeontologie Abhandlungen, **154**,* 94-127.

Mc CLAY, K.R. 1987. Analogue models in inversion tectonics. *In:* COOPER, M.A. & WILLIAMS, G.D. (eds). *Inversion Tectonics.* Special Publication of the Geological Society of London, ***44***, 41-49.

MECHIE, J. & BROOKS, M. 1984. A seismic study of the deep geological structure in the Bristol Channel. *Geophysical Journal of the Royal Astronomical Society, **78**,* 661-689.

MEISSNER, R., BARTELSEN, H. & MURAWSKI, H. 1981. Thin-skinned tectonics in the northern Rhenish Massif, Germany. *Nature, **290**,* 399-401.

MELVIN, J. 1986. Upper Carboniferous fine-grained turbiditic sandstones from south-west England : a model for growth in an ancient, delta-fed subsea fan. *Journal of Sedimentary Petrology, **56**,* 19-34.

MERLA, G. 1951. Geologica dell'Appennino Settentriane. *Society of Italian Geologists' Bulletin, **70**,* 295-382.

OWEN, D.A. 1934. The Carboniferous rocks of the Cornish coast and their structures. *Proceedings of the Geologists Association, **45**,* 451-471.

OWEN, T.R. & WEAVER, J.D. 1983. The structure of the main South Wales Coalfield and its margins. *In :* HANCOCK, P.L. *(ed.) The Variscan Fold Belt in the British Isles.* Hilger, Bristol, 74-87.

PAMPLIN, C.F. & ANDREWS, J.R. 1988.Timing and sense of shear in the Padstow Facing Confrontation, Cornwall. *Proceedings of the Ussher Society, 7,* 73-76.

PAMPLIN, C.F. 1988. A re-examination of the Tintagel High Strain Zone and the Padstow Facing Confrontation, north Cornwall. *PhD Thesis, Southampton.*

PASSCHIER, C.W. & SIMPSON, C. 1985. Porphyroclast systems as kinematic indicators. *Journal of Structural Geology, **8**,* 831-843.

PASSCHIER, C.W. & TROUW, R.A.J. 1996. Microtectonics. Springer-Verlag, Heidelberg.

PEARCE, J.A., HARRIS, N.B.W. & TINDLE, A.G. 1984. Trace element discrimination diagrams for the tectonic interpretation of granitic rocks. *Journal of Petrology, **25**,* 956-983.

PETIT, J.P. 1987. Criteria for the sense of movement on fault surfaces in brittle rocks. *Journal of Structural Geology, **9**,* 567-608.

PHILLIPS, F.C. 1964. Metamorphism in south-west England. *In:* HOSKING, K.F.G. & SHRIMPTON, G.J. *(eds.) Present views on some aspects of the geology of Cornwall and Devon.* Royal Geological Society of Cornwall. Blackford, Truro.

PHILLIPS, S.R. 1928. Metamorphism in the Upper Devonian of north Cornwall. *Geological Magazine, **65**,* 541-556.

PHILLIPS, W.J. 1966. Hydraulic fracturing and mineralisation. *Journal of the Geological Society of London, **128**,* 337-359.

PLATT, J.P. 1986. Dynamics of orogenic wedges and uplift of high pressure metamorphic rocks. *Bulletin of the Geological Society of America, **97**,* 1037-1053.

POUND, C.J. 1983. The sedimentology of the Lower - Middle Devonian Staddon Grits Jennycliff Slates on the east side of Plymouth Sound. *Proceedings of the Ussher Society, **5**,* 465-472.

POWELL, C.M. 1989. Structural controls on Palaeozoic basin evolution and inversion in southwest Wales. *Journal of the Geological Society of London, **146**,* 439-446.

POWER, M.R. & SCOTT, P.W. 1994. Talc-carbonate alteration of some basic and ultrabasic intrusions in Cornwall. *Proceedings of the Ussher Society, **8**,* 392-397.

PRIMMER, T.J. 1985a. A transition from diagenesis to greenschist facies within a major Variscan fold/thrust complex in south-west England. *Mineralogical Magazine, **49**,* 365-374.

PRIMMER, T.J. 1985b. Low-grade Variscan regional metamorphism in southwest England. *PhD Thesis, Bristol.*

PRIMMER, T.J. 1985c. The pressure-temperature history of the Tintagel district, Cornwall : metamorphic evidence on the evolution of the area. *Proceedings of the Ussher Society, **6**,* 218-223.

RAMSAY, J.G. & HUBER, M.I. 1987. The techniques of modern structural geology. Volume 2, Folds and fractures. Academic Press Ltd., London.

RATTEY, R.P. 1980. Deformation in south Cornwall. *Proceedings of the Ussher Society, **5**,* 39-43.

RATTEY, R.P. & SANDERSON, D.J. 1982. Patterns of folding within nappes and thrust sheets : examples from the Variscides of southwest England. *Tectonophysics, **88**,* 247-267.

REID, C. 1907. The geology of the country around Mevagissey. *Memoirs of the Geological Survey.*

RICHTER, D. 1965. Observations on vulcanicity and tectonics of the Torquay area. *Proceedings of the Ussher Society, **1**,* 44.

RICHTER, D. 1967. Sedimentology and facies of the Meadfoot Beds (Lower Devonian) in south-west Devon (England). *Geologische Rundschau, **56**,* 543-561.

RICHTER, D. 1969. Structures and metamorphism of the Devonian rocks south of Torquay, southeast Devon (England). *Geologie Mittschaft, **9**,* 109-178.

ROBERTS, J.L. & SANDERSON, D.J. 1971. Polyphase development of slaty cleavage and the confrontation of facing directions in the Devonian rocks of north Cornwall. *Nature, **230**,* 87-89.

ROBINSON, D. & REID, D. 1981. Metamorphism and mineral chemistry of greenschists from Trebarwith Strand, Cornwall. *Proceedings of the Ussher Society, **5**,* 132-138.

ROYDEN, L., PATACA, E. & SCANDONE, P. 1987. Segmentation and configuration of subducted lithosphere in Italy: an important control upon thrust belt and foredeep basin evolution. *Geology, **15**,* 714-717.

SADLER, P.M. 1973. An interpretation of new stratigraphic evidence from south Cornwall. *Proceedings of the Ussher Society, **3**,* 535-550.

SANDERSON, D.J. 1971. Superimposed folding at the northern margin of the Gramscatho and Mylor Beds, Perranporth, Cornwall. *Proceedings of the Ussher Society, **2**,* 266-269.

SANDERSON, D.J. 1973. Correlation of fold-phases in SW England. *Proceedings of the Ussher Society, **2**,* 525-528.

SANDERSON, D.J. 1974. Chevron folding in the Upper Carboniferous rocks of northern Cornwall. *Proceedings of the Ussher Society, **3**,* 96-103.

SANDERSON, D.J. 1979. The transition from upright to recumbent folding in the Variscan fold-belt of southwest England : a model based on the kinematics of simple shear. *Journal of Structural Geology, **1**,* 171-180.

SANDERSON, D.J. 1984. Structural variations across the northern margin of the Variscan in NW Europe. *In :* HUTTON, D.H.W. & SANDERSON, D.J. (eds.) *Variscan tectonics of the North Atlantic region.* Special Publication of the Geological Society, London, **14**, 149-165.

SANDERSON, D.J. & DEARMAN, W.R. 1973. Structural zones of the Variscan foldbelt in SW England; their location and development. *Journal of the Geological Society of London, **129**,* 527-536.

SCOTESE, C., BAMBACH, R.K., BARTON, C., VAN DER VOO, R. & ZIEGLER, P.A. 1979. Palaeozoic base maps. *Journal of Geology, **87**,* 217-278.

SCOTESE, C.R. & MCKERROW, W.S. 1990. Revised world maps and introduction. *In: Palaeozoic palaeogeography and biogeography.* Special Publication of the Geological Society of London, **12**, 1-12.

SCRUTTON, C.T. 1977a. Reef facies in the Devonian of eastern South Devon, England. *Mem. Bur. Rech. geol. minier., **89**,* 125-135.

SCRUTTON, C.T. 1977b. Facies variations in the Devonian limestones of eastern South Devon. *Geological Magazine, **114**,* 165-193.

SELWOOD, E.B. & DURRANCE, E.M. 1982. The Devonian rocks. *In:* DURRANCE, E.M. & LAMING, D.J.C. (eds.) *The geology of Devon.* University of Exeter, 15-41.

SELWOOD, E.B. & THOMAS, J.M. 1986a. Upper Palaeozoic successions and nappe structures in north Cornwall. *Journal of the Geological Society of London, **143**,* 75-82.

SELWOOD, E.B. & THOMAS, J.M. 1986b. Variscan facies and structure in central south-west England. *Journal of the Geological Society of London, **143**,* 199-207.

SELWOOD, E.B. & THOMAS, J.M. 1988. The Padstow Confrontation, north Cornwall: a reappraisal. *Journal of the Geological Society of London, **145**,* 801-807.

SELWOOD, E.B. 1990. A review of basin development in central southwest England. *Proceedings of the Ussher Society, **7**,* 199-205.

SELWOOD, E.B., STEWART, I.J. & THOMAS, J.M. 1985. Upper Palaeozoic sediments and structure in north Cornwall - a reinterpretation. *Proceedings of the Geologists' Association, **96**,* 129-141.

SERANNE, M. & MALAVIELLE, J. 1994. Preface. *Tectonophysics, **238**,* vii-ix.

SERRI, G., INNOCENTI, F. & MANETTI, P. 1991. U magmatisimo Neogenico-Quatenario dell'area Tosco-Laziale-Umbra. *Studi Geologico Camerti,* 429-463.

SHACKLETON, R.M. 1984. Thin-skinned tectonics, basement control and the Variscan Front. *In :* HUTTON, D.H.W. & SANDERSON, D.J. *(eds.) Variscan tectonics of the North Atlantic region.* Special Publication of the Geological Society of London, **14**, 148-165.

SHACKLETON, R.M., RIES, A.C. & COWARD, M.P. 1982. An interpretation of the Variscan structures in southwest England. *Journal of the Geological Society of London, **139**,* 533-541.

SHAIL, R.K. 1989. Gramscatho-Mylor facies relationships, Hayle, south Cornwall. *Proceedings of the Ussher Society, 7,* 125-130.

SHAIL, R.K. 1992. The provenance of the Gramscatho Group, south Cornwall. *PhD Thesis, Keele.*

SHAIL, R.K. & WILKINSON, J.J. 1994. Late- to post- Variscan extensional tectonics in south Cornwall. *Proceedings of the Ussher Society, **8**,* 262-270.

SHEPHERD, T.J. & SCRIVENOR, R.C. 1987. Role of basinal brines in the genesis of polymetallic vein deposits, Kit Hill - Gunnislake area, SW England. *Proceedings of the Ussher Society, **6**,* 491-497.

SIBSON, R.H. 1985. A note on fault reactivation. *Journal of Structural Geology, 7,* 751-754.

SIMPSON, R.H. & SCHMIDT, S. 1983. An evaluation of criteria to deduce the sense of movement in sheared rocks. *Bulletin of the Geological Society of America, **94**,* 1281-1288.

SIMPSON, S. 1979. Geology of Exeter and its region. BARLOW, F. *(ed.), University of Exeter.*

SMYTHE, D.K. 1984. Discussion on thrust tectonics of south Devon. *Journal of the Geological Society of London, **141**,* 593-594.

SOPER, N.J. & HUTTON, D.H.W. 1984. Late Caledonian sinsitral displacements in Britain : implications for a three-plate collision model. *Tectonics, 3,* 781-794.

SOPER, N.J. & WOODCOCK, N.H. 1990. Silurian collision and sediment dispersion patterns in southern Britain. *Geological Magazine, 127,* 527-542.

SOPER, N.J., STRACHAN, R.A., HOLDSWORTH, R.E., GAYER, R.A. & GREILING, R.O. 1992. Sinistral transpression and the Silurian closure of Iapetus. *Journal of the Geological Society of London, **149**,* 871-880.

SOPER, N.J., WEBB, N.C., WOODCOCK, N.H., 1987. Late Caledonian (Acadian) transpression in northwest England: timing, geometry and geotectonic significance. *Proceedings of the Yorkshire Geologists' Association, 97,* 175-192.

STEELE, S.A. 1994. The Start-Perranporth Zone – transpressional reactivation across a major basement fault in the Variscan orogen of SW England. *Unpublished PhD Thesis,* University of Durham.

STEMPROK, M. 1995. A comparison of the KruŠné Hory-Erzgebirge (Czech Republic - Germany) and Cornish (UK) granites and their related mineralisation. *Proceedings of the Ussher Society, **8**,* 347-356.

STONE, M. 1966. Vertical flattening in the Mylor Beds near Portleven, Cornwall. *Proceedings of the Ussher Society, 1,* 301.

STONELEY, R. 1982. The structural development of the Wessex Basin. *Journal of the Geological Society of London, **139**,* 543-554.

STOREDVEDT, K.M., PEDERSEN, S., LØVLIE, R. & HALVORSEN, E. 1978. Palaeomagnetism in the Oslo Rift zone. *In* : RAMBERG, I.B. & NEUMANN, E.-R. *(eds.) Tectonics and Geophysics of Continental Rifts. N.A.T.O. Advanced Study Institute.* Series C, Maths and Physical Sciences, **37**, Riedel Publishing Company, Dordrecht, 289-296.

STYLES, M.T. & KIRBY, G.A. 1980. New investigations of the Lizard Complex, Cornwall, England, and a discussion of an ophiolite model. *In :* PANAYIOTON, A. *(ed.) Proceedings of the international Symposium, Cyprus.* Cyprus Geological Survey, 519-526.

STYLES, M.T. & RUNDLE, C.C. 1984. The Rb-Sr isochron age of the Kennack Gneiss and its bearing on the age of the Lizard Complex, Cornwall. *Journal of the Geological Society of London, **141**,* 15-19.

SWANSON 1988. Fracture nomenclature. *Journal of Structural Geology, **10**, 320-324.*

THORPE, R.S., COSGROVE, M.E. & VAN CALSTEREN, P.W.C. 1986. Rare element, Sr- and Nd-isotope evidence for petrogenesis of Permian basaltic and K-rich volcanic rocks from south-west England. *Mineralogical Magazine, **50**,* 481-489.

TILLEY, C.E. 1925. Petrographical notes on some chloritoid rocks. *Geological Magazine, **62**,* 309-314.

TRICART, P., TORELLI, L., ARGNANI, A., REKHISS, F. & ZITELLINI, N. 1994. Extensional collapse related to compressional uplift in the Alpine Chain of northern Tunisia (central Mediterranean). *Tectonophysics, **238**,* 317-329.

TUNBRIDGE, I.P. 1986. Mid-Devonian tectonics and sedimentation in the Bristol Channel area. *Journal of the Geological Society of London, **143**,* 107-116.

TURNER, P.J. 1986. Stratigraphical and structural variations in central SW England: a critical appraisal. *Proceedings of the Geologists Association, **97**,* 331-345.

TURNER, R.E. 1984. Hercynian high-angle fault-zones between Dartmoor and Bodmin Moor. *Proceedings of the Ussher Society, **6**,* 60-67.

TURNER, R.G. 1968. The influence of granite emplacement on structures in southwest England. *PhD Thesis,* Newcastle-upon-Tyne.

TWISS, R.J. & MOORES, E.M. 1992. Structural Geology. WH Freeman, New York.

VAI, G.B. 1972. Evidence of Silurian in the Apuane Alps (Tuscany, Italy). *Corn. Geol., **38**,* 349-372.

VEARNCOMBE, J.R. 1980. The Lizard ophiolite and two phases of suboceanic deformation. *In :* PANAYIOTON, A. *(ed.) Proceedings of the international Symposium, Cyprus.* Cyprus Geological Survey, 527-537.

WARR, L.N. 1988. The deformation history of the area northwest of the Bodmin Moor Granite, north Cornwall. *Proceedings of the Ussher Society, 7,* 67-74.

WARR, L.N. 1989. The structural evolution of the Davidstow Anticline and its relationship to the Southern Culm Overfold, north Cornwall. *Proceedings of the Ussher Society, 7,* 136-140.

WARR, L.N. 1991a. Basin inversion in the external Variscan of SW England. *Unpublished PhD Thesis,* University of Exeter.

WARR, L.N. 1991b. Basin inversion and foreland basin development in the Rhenohercynian of southwest England. *In:* GAYER, R.A. & GRIELING, R. *The Rhenohercynian and Sub-Variscan Fold Belts.* Earth Evolution Series, Vieweg, 197-224.

WARR, L.N. 1994. A reconnaissance study of very low-grade metamorphism in south Devon. *Proceedings of the Ussher Society, **8**,* 405-410.

WARR, T.N., PRIMMER, T.J. & ROBINSON, D. 1991. Variscan very low-grade metamorphism in southwest England: a diastathermal and thrust-related origin. *Journal of Metamorphic Geology, **9**,* 751-764.

WATSON, J.V., FOWLER, M.B., PLANT, J.A. & SIMPSON, P.R. 1984. Variscan-Caledonian comparisons: late orogenic granites. *Proceedings of the Ussher Society, **6**,* 2-12.

WHEELER, J. & BUTLER, R.W.H., 1994. Brevia: short notes. Criteria for identifying structures related to true crustal extension in orogens. *Journal of Structural Geology, **16**,* 1023-1027.

WHITE, S.H., BRETAN, P.G. & RUTTER, E.H., 1986. Fault-zone reactivation: kinematics and mechanisms. *Philosophical Transactions of the Royal Society of London, **317**,* 81-97.

WILKINSON, J.J. 1990. The Mylor-Gramscatho transition, Porthleven Sand, south Cornwall. *Excursion Guide, Variscan Workshop.*

WILKINSON, J.J. & KNIGHT, R. 1989. Extensional structures of Mounts' Bay, south Cornwall. *Field excursion guide, Variscan Workshop.*

WILLIAMS, P.F., GOODWIN, L.B. & RALSER, S., 1994. Ductile deformation processes. *In:* HANCOCK, P.L. (ed.). *Continental deformation.* Pergamon Press, Oxford, 1-27.

WILLIS-RICHARDS, J. & JACKSON, N.J. 1989. Evolution of the Cornubian Ore Field, Southwest England : Part I. Batholith modelling and ore distribution. *Economic Geology, **84**,* 1078-1100.

ZHANG, G.J., DAVIS, D.M. & WONG, T.F. 1993. The brittle-ductile transition in porous sedimentary rocks: geological implications for acretionary wedge aseismicity. *Journal of Structural Geology, **15**,* 819.

ZIEGLER, P.A. 1982. Geological atlas of Western and Central Europe. *Shell International Petroleum,* 130pp.

ZIEGLER, P.A. 1990. Geological atlas of Western and Central Europe (2nd ed). *Shell International Petroleum,* 239pp.

ZWART, H.J. 1967. The duality of orogenic belts. *Geologie Mijnbouw, **46**,* 283-309.